ELSEVIER

World Journal of Gastroenterology®

Supported by NSFC 2005-2006

Volume 11 Number 8
February 28, 2005

National Journal Award

Contents

World Journal of Gastroenterology®
Volume 11 **Number** 8 **February** 28, 2005

Contents

World Journal of Gastroenterology®
Volume 11 **Number** 8 **February** 28, 2005

Contents

World Journal of Gastroenterology (*World J Gastroenterol , WJG*), a leading international journal in gastroenterology and hepatology, has an established reputation for publishing first class research on esophageal cancer, gastric cancer, liver cancer, viral hepatitis, colorectal cancer, and *Helicobacter pylori* infection, providing a forum for both clinicians and scientists, and has been indexed and abstracted in Index Medicus, MEDLINE, PubMed, Chemical Abstracts, EMBASE, Abstracts Journals, Nature Clinical Practice Gastroenterology and Hepatology, CAB Abstracts and Global Health. Impact factor of ISI JCR during 2000-2003 is 0.993, 1.445, 2.532 and 3.318, respectively. *WJG* is a weekly journal published jointly by The *WJG* Press and Elsevier Inc.. The publication date is on 7th, 14th, 21st, and 28th every month. The *WJG* is supported by the National Natural Science Foundation of China, No. 30224801 and No.30424812, which was founded with a name of *China National Journal of New Gastroenterology* on October 1,1995, and renamed as *WJG* on January 25, 1998.

PUBLISHED JOINTLY BY
The WJG Press and Elsevier Inc

PRINTING GROUP
Printed in Beijing on acid-free paper by Beijing Kexin Printing House

 Print ISSN 1007-9327
CN 14-1219/R.

EDITORIAL OFFICE
Editor: *World Journal of Gastroenterology*,
The WJG Press, Apartment 1066 Yishou Garden, 58 North Langxinzhuang Road, PO Box 2345, Beijing 100023, China
Telephone: +86-(0)10-85381901-1013
Fax: +86-10-85381893
E-mail: wjg@wjgnet.com
http://www.wjgnet.com

Public Relationship Manager
Shi-Yu Guo
The WJG Press, Apartment 1066 Yishou Garden, 58 North Langxinzhuang Road, PO Box 2345, Beijing 100023, China
Telephone: +86-(0)10-8538 1901-1023
Fax: +86-10-8538 1893
E-mail: s.y.guo@wjgnet.com
http://www.wjgnet.com

SUBSCRIPTION INFORMATION
Foreign
Elsevier (Singapore) Pte Ltd, 3 Killiney Road #08-01, Winsland House I, Singapore 239519
Telephone: +65-6349 0200
Fax: +65-6733 1817
E-mail: r.garcia@elsevier.com
http://asia.elsevierhealth.com
Institutional Rates Print-2005 rates: USD1 500.00
Personal Rates Print-2005 rates: USD700.00

Domestic
Local Post Offices Code No. BM 82-261

Author Reprints and Commercial Reprints
The WJG Press, Apartment 1066 Yishou Garden, 58 North Langxinzhuang Road, PO Box 2345, Beijing 100023, China
Telephone: +86-(0)10-85381901-1013
Fax: +86-10-85381893
E-mail: wjg@wjgnet.com
http://www.wjgnet.com

ADVERTISING
Rosalia Da Carcia
Elsevier Science
Journals Marketing & Society Relations Health Science Asia
3 Killiney Road #08-01, Winsland House 1
Singapore 239519
Telephone: +65-6349 0200
Fax +65- 6733 1817
E-mail: r.garcia@elsevier.com
http://asia.elsevierhealth.com

INSTRUCTIONS TO AUTHORS
Full instructions are available online at http://www.wjgnet.com/wjg/help/instructions.jsp If you do not have web access please contact the editorial office.

World Journal of Gastroenterology®

Editorial Board

2004-2006

Published by The WJG Press and Elsevier Inc., PO Box 2345, Beijing 100023, China
Fax: +86-(0)10-85381893 E-mail: wjg@wjgnet.com http://www.wjgnet.com

Bulgaria
Zahariy Alexandrov Krastev, *Sofia*

Canada
Wang-Xue Chen, *Ottawa*
Richard N Fedorak, *Edmonton*
Hugh James Freeman, *Vancouver*
Samuel S Lee, *Calgary*
Philip Martin Sherman, *Toronto*
Alan BR Thomson, *Edmonton*
Eric M Yoshida, *Vancouver*

China
Francis KL Chan, *Hong Kong*
Xiao-Ping Chen, *Wuhan*
Jun Cheng, *Beijing*
Chi-Hin Cho, *Hong Kong*
Zong-Jie Cui, *Beijing*
Da-Jun Deng, *Beijing*
Er-Dan Dong, *Beijing*
Sheung-Tat Fan, *Hong Kong*
Xue-Gong Fan, *Changsha*
Jin Gu, *Beijing*
De-Wu Han, *Taiyuan*
Shao-Heng He, *Shantou*
Fu-Lian Hu, *Beijing*
Wayne HC Hu, *Hong Kong*
Ching Lung Lai, *Hong Kong*
Kam Chuen Lai, *Hong Kong*
Wai-Keung Leung, *Hong Kong*
Zhi-Hua Liu, *Beijing*
Ai- Ping Lu, *Beijing*
Jing-Yun Ma, *Beijing*
Lun-Xiu Qin, *Shanghai*
Yu-Gang Song, *Guangzhou*
Peng Shang, *Xi'an*
Qin Su, *Beijing*
Yuan Wang, *Shanghai*
Benjamin Wong, *Hong Kong*
Wai-Man Wong, *Hong Kong*
Hong Xiao, *Shanghai*
Dong-Liang Yang, *Wuhan*
Xue-Biao Yao, *Hefei*
Yuan Yuan, *Shenyang*
Man-Fung Yuen, *Hong Kong*
Jian-Zhong Zhang, *Beijing*
Zhi-Rong Zhang, *Chengdu*
Xiao-Hang Zhao, *Beijing*
Shu Zheng, *Hangzhou*

Costa Rica
Edgar M Izquierdo, *San José*

Croatia
Marko Duvnjak, *Zagreb*

Denmark
Flemming Burcharth, *Herlev*
Peter Bytzer, *Copenhagen*
Hans Gregersen, *Aalborg*
Jens H Henriksen, *Hvidovre*
Fin Stolze Larsen, *Copenhagen*
Søren Møller, *Hvidovre*

Egypt
Abdel-Rahman El-Zayadi, *Giza*

Finland
Pentti Sipponen, *Espoo*

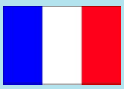

France
Charles Paul Balabaud, *Bordeaux*
Jacques Belghiti, *Clichy*
Pierre Brissot, *Rennes*
Franck Carbonnel, *Besancon*
Bruno Clément, *Rennes*
Jacques Cosnes, *Paris*
Francoise Degos, *Clichy*
Francoise Lunel Fabian, *Angers*
Gérard Feldmann, *Paris*
Jean Fioramonti, *Toulouse*
Rene Lambert, *Lyon*
Didier Lebrec, *Clichy*
Francis Mégraud, *Bordeaux*
Richard Moreau, *Clichy*
Jose Sahel, *Marseille*
Jean-Yves Scoazec, *Lyon*
Jean-Pierre Henri Zarski, *Grenoble*

Germany
HD Allescher, *Garmisch-Partenkirchen*
Rudolf Arnold, *Marburg*
Hubert Blum, *Freiburg*
Peter Born, *Muchen*
Heinz J Buhr, *Berlin*
Haussinger Dieter, *Düsseldorf*
Dietrich CF, *Bad Mergentheim*
Wolfram W Domschke, *Muenster*
Ulrich Robert Fölsch, *Kiel*
Peter R Galle, *Mainz*
Burkhard Göke, *Munich*
Axel M Gressner, *Aachen*
Eckhart Georg Hahn, *Erlangen*
Werner Hohenberger, *Erlangen*
RG Jakobs, *Ludwigshafen*
Joachim Labenz, *Siegen*
Ansgar W Lohse, *Hamburg*
Peter Malfertheiner, *Magdeburg*
Andrea Dinah May, *Wiesbaden*
Stephan Miehlke, *Dresden*
Gustav Paumgartner, *Munich*
Ulrich Ks Peitz, *Magdeburg*
Giuliano Ramadori, *Göttingen*
Tilman Sauerbruch, *Bonn*
Hans Seifert, *Oldenburg*
J Ruediger Siewert, *Munich*
Manfred V Singer, *Mannheim*
Jurgen M Stein, *Frankfurt*
Manfred Stolte, *Bayreuth*
Wolfgang R Stremmel, *Heidelberg*
Hans Ludger Tillmann, *Leipzig*
Siegfried Wagner, *Deggendorf*
Bertram Wiedenmann, *Berlin*

Greece
Arvanitakis C, *Thessaloniki*
Elias A Kouroumalis, *Heraklion*

Hungary
Simon A László, *Szekszárd*
János Papp, *Budapest*

Iceland
Hallgrimur Gudjonsson, *Reykjavik*

India
Sujit Kumar Bhattacharya, *Kolkata*
Chawla YK, *Chandigarh*
Radha Dhiman K, *Chandigarh*
Sri Prakash Misra, *Allahabad*
Kartar Singh, *Lucknow*

Iran
Reza Malekzadeh, *Tehran*

Israel
Abraham Rami Eliakim, *Haifa*
Yaron Niv, *Pardesia*

Italy
Giovanni Addolorato, *Roma*
Alfredo Alberti, *Padova*
Annese V, *San Giovanni Rotondo*
Giovanni Barbara, *Bologna*
Gabrio Bassotti, *Perugia*
Franco Bazzoli, *Bologna*
Adolfo Francesco Attili, *Roma*
Antomio Benedetti, *Ancona*
Giovanni Cammarota, *Roma*
Antonino Cavallari, *Bologna*
Dario Conte, *Milano*
Gino Roberto Corazza, *Pavia*
Guido Costamagua, *Roma*
Antonio Craxi, *Palermo*
Fabio Farinati, *Padua*
Giovanni Gasbarrini, *Roma*
Paolo Gentilini, *Florence*
Edoardo G Giannini, *Genoa*

Paolo Gionchetti, *Bologna*
Roberto De Giorgio, Bologna
Mario Guslandi, *Milano*
Giovanni Maconi, *Milan*
Giulio Marchesini, *Bologna*
Giuseppe Montalto, *Palermo*
Luisi Pagliaro, *Palermo*
Fabrizio R Parente, *Milan*
Perri F, *San Giovanni Rotondo*
Raffaele Pezzilli, *Bologna*
Pilotto A, *San Giovanni Rotondo*
Massimo Pinzani, *Firenze*
Gabriele Bianchi Porro, *Milano*
Piero Portincasa, *Bari*
Giacomo Laffi, *Firenze*
Enrico Roda, *Bologna*
Massimo Rugge, *Padova*
Vincenzo Savarino, *Genova*
Vincenzo Stanghellini, *Bologna*
Calogero Surrenti, *Florence*
Roberto Testa, *Genoa*
Dino Vaira, *Bologna*

Japan

Kyoichi Adachi, *Izumo*
Takashi Aikou, *Kagoshima*
Taiji Akamatsu, *Matsumoto*
Takafumi Ando, *Nagoya*
Akira Andoh, *Otsu*
Taku Aoki, *Tokyo*
Masahiro Arai, *Tokyo*
Tetsuo Arakawa, *Osaka*
Yasuji Arase, *Tokyo*
Masahiro Asaka, *Sapporo*
Hitoshi Asakura, *Tokyo*
Yutaka Atomi, *Tokyo*
Takeshi Azuma, *Fukui*
Nobuyuki Enomoto, *Yamanashi*
Kazuma Fujimoto, *Saga*
Toshio Fujioka, *Oita*
Yoshihide Fujiyama, *Otsu*
Hiroyuki Hanai, *Hamamatsu*
Kazuhiro Hanazaki, *Nagano*
Naohiko Harada, *Fukuoka*
Makoto Hashizume, *Fukuoka,*
Tetsuo Hayakawa, *Nagoya*
Kazuhide Higuchi, *Osaka*
Ichiro Hirata, *Osaka*
Keiji Hirata, *Kitakyushu*
Takafumi Ichida, *Shizuoka*
Kenji Ikeda, *Tokyo*
Kohzoh Imai, *Sapporo*
Fumio Imazeki, *Chiba*
Masayasu Inoue, *Osaka*
Hiromi Ishibashi, *Nagasaki*
Shunji Ishihara, *Izumo*
Toru Ishikawa, *Niigata*
Kei Ito, *Sendai*
Masayoshi Ito, *Tokyo*
Hiroaki Itoh, *Akita*
Hiroshi Kaneko, *Aichi-Gun*
Shuichi Kaneko, *Kanazawa*
Takashi Kanematsu, *Nagasaki*
Junji Kato, *Sapporo*
Mototsugu Kato, *Sapporo*
Shinzo Kato, *Tokyo*
Sunao Kawano, *Osaka*
Yoshikazu Kinoshita, *Izumo*
Masaki Kitajima, *Tokyo*
Tsuneo Kitamura, *Chiba*
Seigo Kitano, *Oita*
Hironori Koga, *Kurume*
Satoshi Kondo, *Sapporo*
Shoji Kubo, *Osaka*
Shigeki Kuriyama, *Kagawa*
Masato Kusunoki, *Mie*
Takashi Maeda, *Fukuoka*
Shin Maeda, *Tokyo*
Osamu Matsui, *Kanazawa*
Yasushi Matsuzaki, *Tsukuba*
Hiroto Miwa, *Hyogo*
Masashi Mizokami, *Nagoya*
Motowo Mizuno, *Hiroshima*
Morito Monden, *Suita*
Hisataka S Moriwaki, *Gifu*
Yoshiharu Motoo, *Kanazawa*
Akihiro Munakata, *Hirosaki*
Kazunari Murakami, *Oita*
Kunihiko Murase, *Tusima*
Masato Nagino, *Nagoya*
Yujl Naito, *Kyoto*
Hisato Nakajima, *Tokyo*
Hiroki Nakamura, *Yamaguchi*
Shotaro Nakamura, *Fukuoka*
Akimasa Nakao, *Nagoya*
Mikio Nishioka, *Niihama*
Susumu Ohmada, *Maebashi*
Masayuki Ohta, *Oita*
Tetsuo Ohta, *Kanazawa*
Susumu Okabe, *Kyoto*
Katsuhisa Omagari, *Nagasaki*
Saburo Onishi, *Nankoku*
Morikazu Onji, *Ehime*
Hiromitsu Saisho, *Chiba*
Hidetsugu Saito, *Tokyo*
Takafumi Saito, *Yamagata*
Isao Sakaida, *Yamaguchi*
Michiie Sakamoto, *Tokyo*
Iwao Sasaki, *Sendai*
Motoko Sasaki, *Kanazawa*
Chifumi Sato, *Tokyo*
Shuichi Seki, *Osaka*
Hiroshi Shimada, *Yokohama*
Mitsuo Shimada, *Tokushima*
Hiroaki Shimizu, *Chiba*
Tooru Shimosegawa, *Sendai*
Tadashi Shimoyama, *Hirosaki*
Ken Shirabe, *Iizuka City*
Yoshio Shirai, *Niigata*
Katsuya Shiraki, *Mie*
Yasushi Shiratori, *Okayama*
Yasuhiko Sugawara, *Tokyo*
Toshiro Sugiyama, *Toyama*
Kazuyuki Suzuki, *Morioka*
Hidekazu Suzuki, *Tokyo*
Tadatoshi Takayama, *Tokyo*
Tadashi Takeda, *Osaka*
Koji Takeuchi, *Kyoto*
Kiichi Tamada, *Tochigi*
Akira Tanaka, *Kyoto*
Eiji Tanaka, *Matsumoto*
Noriaki Tanaka, *Okayama*
Shinji Tanaka, *Hiroshima*
Kyuichi Tanikawa, *Kurume*
Tadashi Terada, *Shizuoka*
Akira Terano, *Shimotsugagun*
Kazunari Tominaga, *Osaka*
Hidenori Toyoda, *Ogaki*
Akihito Tsubota, *Chiba*
Shingo Tsuji, *Osaka*
Takato Ueno, *Kurume*
Shinichi Wada, *Tochigi*
Hiroyuki Watanabe, *Kanazawa*
Sumio Watanabe, *Akita*
Toshio Watanabe, *Osaka*
Yuji Watanabe, *Ehime*
Chun-Yang Wen, *Nagasaki*
Koji Yamaguchi, *Fukuoka*
Takayuki Yamamoto, *Yokkaichi*
Takashi Yao, *Fukuoka*
Hiroshi Yoshida, *Tokyo*
Masashi Yoshida, *Tokyo*
Norimasa Yoshida, *Kyoto*
Kentaro Yoshika, *Toyoake*
Masahide Yoshikawa, *Kashihara*

Lithuania

Sasa Markovic, *Japljeva*

Macedonia

Vladimir Cirko Serafimoski, *Skopje*

Malaysia

Andrew Seng Boon Chua, *Ipoh*
Jayaram Menon, *Sabah*
Khean-Lee Goh, *Kuala Lumpur*

Monaco

Patrick Rampal, *Monaco*

Netherlands

Louis MA Akkermans, *Utrecht*
Karel Van Erpecum, *Utrecht*
Albert K Groen, *Amsterdam*
Dirk Joan Gouma, *Amsterdam*
Jan BMJ Jansen, *Nijmegen*
Evan Anthony Jones, *Abcoude*
Ernst Johan Kuipers, *Rotterdam*
Chris JJ Mulder, *Amsterdam*
Michael Müller, *Wageningen*

Pena AS, *Amsterdam*
Andreas Smout, *Utrecht*
RW Stockbrugger, *Maastricht*
GP Vanberge-Henegouwen, *Utrecht*

New Zealand
Ian David Wallace, *Auckland*

Norway
Trond Berg, *Oslo*
Helge Lyder Waldum, *Trondheim*

Pakistan
Muhammad S Khokhar, *Lahore*

Philippines
Eulenia Rasco Nolasco, *Manila*

Poland
Tomasz Brzozowski, *Cracow*
Andrzej Nowak, *Katowice*

Portugal
Miguel Carneiro De Moura, *Lisbon*

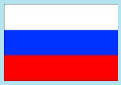

Russia
Vladimir T Ivashkin, *Moscow*
Leonid Lazebnik, *Moscow*
Vasiliy I Reshetnyak, *Moscow*

Singapore
Bow Ho, *Kent Ridge*
Francis Seow-Choen, *Singapore*

Slovakia
Anton Vavrecka, *Bratislava*

South Africa
Michael C Kew, *Parktown*

South Korea
Jin-Hong Kim, *Suwon*
Myung-Hwan Kim, *Seoul*
Yun-Soo Kim, *Seoul*
Yung-Il Min, *Seoul*
Jae-Gahb Park, *Seoul*
Dong Wan Seo, *Seoul*

Spain
Abraldes JG, *Barcelona*
Fernando Azpiroz, *Barcelona*
Ramon Bataller, *Barcelona*
Josep M Bordas, *Barcelona*
Maria Buti, *Barcelon*
Xavier Calvet, *Sabadell*
Antoni Castells, *Barcelona*
Manuel Daz-Rubio, *Madrid*
Juan C Garcia-Pagán, *Barcelona*
Genover JB, *Barcelona*
Javier P Gisbert, *Madrid*
Jaime Guardia, *Barcelona*
Angel Lanas, *Zaragoza*
Ricardo Moreno-Otero, *Madrid*
Julian Panes, *Barcelona*
Miguel Perez-Mateo, *Alicante*
Josep M Pique, *Barcelona*
Jesus Prieto, *Pamplona*
Luis Rodrigo, *Oviedo*

Sri Lanka
Janaka De Silva, *Ragama*

Swaziland
Gerd Kullak-Ublick, *Zurich*

Sweden
Lars Christer Olbe, *Molndal*
Curt Einarsson, *Huddinge*
Lars R Lundell, *Stockholm*
Xiao-Feng Sun, *Linkoping*

Switzerland
Christoph Beglinger, *Basel*
Michael W Fried, *Zurich*
Bruno Stieger, *Zurich*
Arthur Zimmermann, *Berne*

Turkey
Yusuf Bayraktar, *Ankara*
Figen Gurakan, *Ankara*
Cihan Yurdaydin, *Ankara*

United Kingdom
Axon ATR, *Leeds*
Paul Jonathan Ciclitira, *London*
Amar Paul Dhillon, *London*
Stuarts Forbes
Subrata Ghosh, *London*
Brian T Johnston, *Belfast*
David EJ Jones, *Newcastle*
Michael A Kamm, *Harrow*
Hong-Xiang Liu, Cambridge
Giorgina Mieli-Vergani, *London*
Nikolai V Naoumov, *London*
John P Neoptolemos, *Liverpool*
James Neuberger, *Birmingham*
Colm Antoine O'Morain, *Dublin*
Simon D Taylor-Robinson, *London*
Frank Ivor Tovey, *Basingstoke*
Min Zhao, *Foresterhill*

United States
Firas H Ac-Kawas, *Washington*
Gianfranco D Alpini, *Temple*
Paul Angulo, *Rochester*
Jamie S Barkin, *Miami Beach*
Todd Baron, *Rochester*
Kim Elaine Barrett, *San Diego*
Jennifer D Black, *Buffalo*
Xu Cao, *Birmingham*
David L Carr-Locke, *Boston*
Marc F Catalano, *Milwaukee*
Xian-Ming Chen, *Rochester*
James M Church, *Cleveland*
Vincent Coghlan, *Beaverton*
James R Connor, *Hershey*
Pelayo Correa, *New Orleans*
John Cuppoletti, *Cincinnati*
Peter V Danenberg, *Los Angeles*
Kiron Moy Das, *New Brunswick*
Hala El-Zimaity, *Houston*
Ronnie Fass, *Tucson*
Emma E Furth, *Pennsylvania*
John Geibel, *New Haven*
Graham DY, *Houston*
Joel S Greenberger, *Pittsburgh*
Anna S Gukovskaya, *Los Angeles*
Gavin Harewood, *Rochester*
Atif Iqbal, *Omaha*
Hajime Isomoto, *Rochester*
Dennis M Jensen, *Los Angeles*
Leonard R Johnson, *Memphis*
Peter James Kahrilas, *Chicago*
Anthony Nicholas Kalloo, *Baltimore*
Neil Kaplowitz, *Los Angeles*
Emmet B Keeffe, *Palo Alto*
Joseph B Kirsner, *Chicago*
Burton I Korelitz, *New York*
Robert J Korst, *New York*
Richard A Kozarek, *Seattle*
Shiu-Ming Kuo, *Buffalo*
Frederick H Leibach, *Augusta*
Andreas Leodolter, *La Jolla*
Ming Li, *New Orleans*
Lenard M Lichtenberger, *Houston*
Gary R Lichtenstein, *Philadelphia*
Josep M Llovet, *New York*
Martin Lipkin, *New York*

Manuscript reviewers of *World Journal of Gastroenterology*

PO Box 2345, Beijing 100023, China
www.wjgnet.com
wjg@wjgnet.com

ELSEVIER

World J Gastroenterol 2005;11(8):1091-1095
World Journal of Gastroenterology ISSN 1007-9327

Initial experience from a combination of systemic and regional chemotherapy in the treatment of patients with nonresectable cholangiocellular carcinoma in the liver

Timm Kirchhoff, Lars Zender, Sonja Merkesdal, Bernd Frericks, Nisar Malek, Joerg Bleck, Stefan Kubicka, Stefan Baus, Ajay Chavan, Michael P. Manns, Michael Galanski

Timm Kirchhoff, Stefan Baus, Michael Galanski, Department of Diagnostic Radiology, Hannover Medical School, Germany
Lars Zender, Nisar Malek, Joerg Bleck, Stefan Kubicka, Michael P. Manns, Department of Gastroenterology, Hepatology, and Endocrinology, Hannover Medical School, Germany
Sonja Merkesdal, Division of Rheumatology, Hannover Medical School, Germany
Bernd Frericks, Department of Radiology and Nuclear Medicine, Campus B.F-Charité-University Medicine, Berlin, Germany
Ajay Chavan, Department of Radiology and Nuclear Medicine, Klinikum Oldenburg, Germany
Correspondence to: Timm Kirchhoff, M.D., Department of Diagnostic Radiology, OE 8220, Hannover Medical School, Carl-Neuberg Str.1, D-30625 Hannover, Germany. kirchhoff.timm@mh-hannover.de
Telephone: +49-511-5323421 Fax: +49-511-5328262
Received: 2004-07-31 Accepted: 2004-09-19

Abstract

AIM: In nonresectable cholangiocellular carcinoma (CCC) therapeutic options are limited. Recently, systemic chemotherapy has shown response rates of up to 30%. Additional regional therapy of the arterially hyper vascularized hepatic tumors might represent a rational approach in an attempt to further improve response and palliation. Hence, a protocol combining transarterial chemoembolization and systemic chemotherapy was applied in patients with CCC limited to the liver.

METHODS: Eight patients (6 women, 2 men, mean age 62 years) with nonresectable CCC received systemic chemotherapy (gemcitabine 1 000 mg/m^2) and additional transarterial chemoembolization procedures (50 mg/m^2 cisplatin, 50 mg/m^2 doxorubicin, up to 600 mg degradable starch microspheres). Clinical follow-up of patients, tumor markers, CT and ultrasound were performed to evaluate maximum response and toxicity.

RESULTS: Both systemic and regional therapies were tolerated well; no severe toxicity (WHO III/IV) was encountered. Nausea and fever were the most commonly observed side effects. A progressive rarefication of the intrahepatic arteries limited the maximum number of chemoembolization procedures in 4 patients. A median of 2 chemoembolization cycles (range, 1-3) and a median of 6.5 gemcitabine cycles (range, 4-11) were administered. Complete responses were not achieved. As maximum response, partial responses were achieved in 3 cases, stable diseases in 5 cases. Two patients died from progressive disease after 9 and 10 mo. Six patients are still alive. The current median survival is 12 mo (range, 9-18); the median time to tumor progression is 7 mo (range, 3-18). Seven patients suffered from tumor-related symptoms prior to therapy, 3 of these experienced a treatment-related clinical relief. In one patient the tumor became resectable under therapy and was successfully removed after 10 mo.

CONCLUSION: The present results indicate that a combination of systemic gemcitabine therapy and repeated regional chemoembolizations is well tolerated and may enhance the effect of palliation in a selected group of patients with intrahepatic nonresectable CCC.

Key words: Cholangiocellular carcinoma; Gemcitabine; Intraarterial chemoembolization

Kirchhoff T, Zender L, Merkesdal S, Frericks B, Malek N, Bleck J, Kubicka S, Baus S, Chavan A, Manns MP, Galanski M. Initial experience from a combination of systemic and regional chemotherapy in the treatment of patients with nonresectable cholangiocellular carcinoma in the liver. *World J Gastroenterol* 2005; 11(8): 1091-1095
http://www.wjgnet.com/1007-9327/11/1091.asp

INTRODUCTION

Intrahepatic cholangiocellular carcinoma (CCC) is a rare entity associated with chronic inflammatory bile duct disorders. Diagnosis often occurs in patients having large tumors at nonresectable stages[1,2]. In the past, systemic chemotherapy has shown limited success in terms of objective responses or prolonged survival especially in single agent therapy using 5-FU. Response rates of about 25% were the most to be expected[3]. Gemcitabine (2, 2-dideoxy-fluorocytidine) has gained importance in the palliative treatment of solid tumors. The substance demonstrated activity against breast, bladder, ovarian, pancreatic and non-small cell lung cancer while having a low toxicity profile[4,5]. A large phase III trial on pancreatic cancer revealed a higher activity of gemcitabine compared to 5-FU in terms of patient survival and improvement of symptoms[6]. In a recent phase II study on nonresectable CCC of our institution systemic gemcitabine monotherapy achieved objective response rates of 30%[3]. Furthermore, a majority of the patients experienced

a chemotherapy-related relief of symptoms.

Regional intraarterial therapies of the liver have shown efficacy and safety in hypervascularized hepatic tumors or metastases[7]. The rationale for this approach is further increased antitumoral activity in the liver by inducing a temporary local ischemia and increasing local chemotherapy concentrations while reducing the systemic side effects[8]. Hence, in an attempt to improve palliation a combination therapy of systemic gemcitabine with repeated intraarterial chemoembolization appears promising in those patients with CCC limited to the liver in order to further enhance response rates and symptom relief while maintaining low toxicity. Based on this hypothesis a selected group of patients with nonresectable intrahepatic CCC was included in a study to investigate this combination regime.

MATERIALS AND METHODS

From June 2002 to February 2004 eight patients (6 women, 2 men, mean age 62 years) with histologically proven nonresectable CCC were included to the study (Table 1). Inclusion criteria were (1) measurable, unresectable intrahepatic tumors; (2) >18 years of age, a life expectancy of >3 mo; (3) no prior chemotherapy; (4) technically feasible catheterization of the hepatic artery; (5) adequate functional, hematological and biochemical parameters (i.e., cardiac ejection fraction >50%, leukocytes >3 000/μL, thrombocytes >90 000/μL, creatinine-clearance >60 mL/min, bilirubin <3 mg/dL, cholinesterase >2 mU/mL (21 ℃), bilirubin <3 mg/mL, prothrombin time >50%); and (6) informed consent. Patient characteristics are shown in Table 1.

Systemic gemcitabine therapy

Systemic gemcitabine was administered on an out-patient basis. 1 000 mg/m^2 were given once a week intravenously over 30 min for 3 consecutive weeks followed by a pause of one week. One therapy cycle was defined as one 4-wk period. During the first cycle gemcitabine was also given during the fourth week. Prophylaxis against nausea consisted of metoclopramide orally.

Intraarterial chemoembolization

Intraarterial chemoembolization was performed on an in-patient basis after 2 systemic gemcitabine cycles had been given and was tolerated in terms of toxicity and clinical response. Chemoembolizations were repeated in case of stable disease or remission after an interval of at least 8 wk.

Antiemetics (5 mg tropisetron) and steroids (24 mg dexamethasone) were injected intravenously prior to each procedure. Also, intravenous antibiotic prophylaxis (3×200 mg ciprofloxacin/d, 3×500 mg metronidazole/d) against biliary infections was administered before and for 7 d after the procedure.

During arterial angiography using the femoral approach, an aortography and a selective mesenteric portography were performed to show vascular anatomy and the patency of the portal vein. Then, a selective hepatography was done using a standard diagnostic catheter or, if necessary, a coaxial catheter system. Intra-arterial analgesia (50-100 mg pethidine) was applied to control possible local pain. According to tumor vascularization a mixture of doxorubicin (50 mg/m^2) and cisplatin (50 mg/m^2) and 300-600 mg degradable starch microspheres (DSM, Spherex™, Pharmacia, Erlangen, Germany) was administered via hand injection under fluoroscopic control to check for stasis or reflux. In case of stasis, the injection was stopped until the arterial flow resumed. Finally, a control hepatography was performed. After the chemoembolization procedure the patient remained on the ward for at least five days. Systemic gemcitabine treatment was continued under laboratory controls for therapy-related toxicity after an interval of 3 to 4 wk.

Evaluation of response and toxicity

Pretreatment evaluation included physical examinations, evaluation of tumor markers, hematological and biochemical parameters. For tumor staging transabdominal ultrasound and a CT scan of thorax and abdomen were performed. The imaging modality and technique showing the best visibility at the start of treatment were used for baseline and follow-up tumor measurements (Figure 1). The sizes of measurable lesions were determined as the products of the two greatest perpendicular diameters. The following definitions were used: complete response (CR) for the disappearance of all clinical evidence of tumor for a minimum of 4 wk, partial response (PR) for a decrease of more than 50% in the measurable disease for a minimum of 4 wk, progressive disease (PD) for an increase in tumor size of more than 25%, the appearance of new lesions, or a deterioration of clinical status consistent with disease progression. Patients who did not meet criteria of CR, PR or PD were defined as having a stable disease (SD). Time to tumor progression was defined as the time between administration of the first chemotherapy and the time PD was diagnosed.

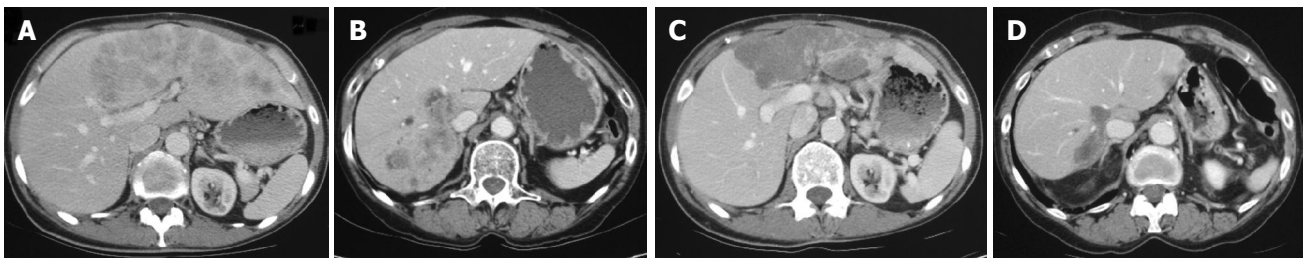

Figure 1 A: Axial CT shows a large hyper vascularized CCC in the left liver lobe of patient 4 before therapy; B: In patient 3 axial CT shows hyper vascularized CCC nodules in the lateral right liver; C: After 7 mo of therapy there is marked shrinkage and hypodense transformation of the tumor in PR in patient 4; D: In patient 3 the same changes are apparent in the right liver in PR after 7 mo of therapy.

Table 1 Patient characteristics, maximum toxicity, maximum response, adverse events, and arterial hypovascularisation under therapy

Patient number	Age (yr)	Gender	Maximum number of gemcitabine cycles	Maximum number of chemo-occlusion cycles	Maximum response	Neutropenia acc. to WHO	Thrombopenia acc. to WHO	Anemia acc. to WHO	Cholestasis acc. to WHO	Nausea acc. to WHO	Flush symptoms acc. to WHO	Tumor-related disease	Clinical therapy related benefit	Progressive arterial hypovascularization
1	60	M	5	2	SD	2	2	2	2	2	1	yes	-	-
2	71	F	4	1	SD	2	2	1	2	2	1	yes	-	-
3	67	F	11	3	PR	1	1	1	2	0	1	-	-	yes
4	47	F	7	3 (+1[1])	PR	1	0	1	1	2	2	yes	-	yes
5	63	F	9	2 (+1[1])	PR	0	0	1	2	1	1	yes	yes	yes
6	76	F	6	2 (+1[1])	SD	0	0	0	0	1	1	yes	yes	yes
7	53	F	9	2	SD	0	1	1	2	2	2	yes	yes	-
8	56	M	4	1	SD	0	0	2	2	1	2	yes	-	-

[1]Single chemoperfusion without DSM because of early vascular stasis due to progressive arterial hypovascularization.

Table 2 Present status, chemotherapy-related response and changes of tumor markers

Patient number	Observervation period (mo)	Maximum response	Highest tumor markers before therapy	Lowest tumor marker under therapy (%)	Time to tumor progression (mo)	Survival (mo)
1	10	SD	None	-	7	Dead (10)
2	14	SD	Ca15-3:48	47 (-2[1])	5	Alive
3	18	PR	Ca19-9:1 442	34 (-98[1])	18	Alive
4	12	PR	Ca19-9:89	19 (-77[1])	NA (still PR)	Alive
			AFP:35	6 (-83[1])		
5	10	PR	Ca19-9:786	139 (-82[1])	NA resected after 10	Alive
6	16	SD	Ca15-3:54	43 (-20[1])	7	Alive
			Ca19-9:88	115 (+31[1])		
7	12	SD	Ca19-9:845 200	435 (-99[1])	7	
			CEA:285	2 (-99[1])		Alive
8	9	SD	Ca15-3:435	204 (-53[1])	3	
			Ca19-9:117	84 (-28[1])		Dead (9)

[1]Change of tumor marker in percent compared to highest value before therapy NA: not assessable.

Therapy-related toxicity was assessed once weekly during treatment by investigations of serum liver enzymes, bilirubin, creatinine, and complete blood counts. Clinical relief was defined as a chemotherapy-related relief of tumor symptoms or weight gain (including third-space fluid) of >7% from baseline for at least 4 wk without deterioration in any other parameters.

Evaluation of quality of life (QOL)

QOL was assessed prior to each chemoembolization procedure using the SF-36 Health Survey[9]. As components of QOL, the SF-36 questionnaire comprises the distinct aspects physical functioning, physical role, emotional role, social functioning, mental health index, general health, vitality, and bodily pain. A score for each category was calculated (0-100). Based on these scores a bodily sum score was determined. The sum scores before and during chemotherapy were compared.

RESULTS

A median of 2 chemoembolization cycles (range, 1-3) and a median of 6.5 gemcitabine cycles (range, 4-11) were applied (Table 1).

Response

In terms of maximum response, there were five patients with SD and 3 patients with PR; CR was not achieved (Table 1, 2). The median time to tumor progression was 7 mo (range, 3-18). Six patients are still alive, 2 patients died from tumor progression after 9 and 10 mo. The current median survival is 12 mo (range, 9-18).

Seven patients suffered from tumor-related symptoms, 3 of these experienced a treatment-related clinical relief (Table 1). The tumor of patient 5 became resectable during PR and was successfully removed by hemi-hepatectomy 10 mo after onset of therapy.

Six patients had elevated tumor marker Ca19-9 serum levels. Four patients showed a chemotherapy-related decrease of more than 75% compared to the baseline value further indicating response to therapy (Table 2).

Toxicity

Both systemic and regional therapies were tolerated well, no severe toxicity (WHO III/IV) was encountered (Table 1). Nausea and fever were the most commonly observed side effects. In patients 3, 4, 5, and 6 repeated chemoembolization led to a progressive rarefication of the intrahepatic arteries limiting the maximum applicable number of interventions (Table 1, Figure 2). In patient 3, the left hepatic artery remained permanently occluded after the second procedure. Further chemoembolization cycles were attempted in patients 4, 5, and 6. However, due to the progressive arterial hypovascularization the application of DSM had become

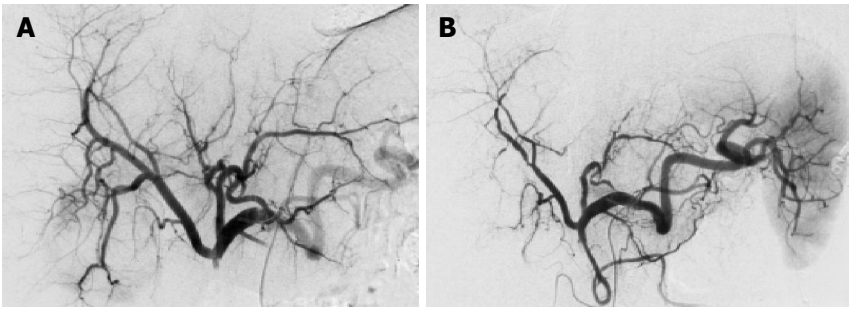

Figure 2 A: The arteriogram of patient 4 shows a beginning rarefication of the intrahepatic arteries after one chemoembolization; B: After three chemoembolizations the arteriogram of the same patient shows a progressive arterial rarefication with irregular stenoses and occlusions of peripheral branches.

impossible. The chemotherapeutics were finally administrated once in the course of a regional chemoperfusion before further regional therapy was considered impossible in these patients (Table 1).

Quality of life (QOL)

Patients 1, 2, 4, 5, and 6 were evaluable in terms of QOL follow-up using the SF-36; the remaining three patients did not provide follow-up data. The bodily sum scale remained stable under therapy in 4 patients (46/45, 39/31, 49/47, and 48/50). Patient 4 showed a gradual decrease from 53 to 38.

DISCUSSION

The overall prognosis of patients with nonresectable CCC remains dismal[10]. At present, only palliative therapeutical options are available. In addition to the improvement of the prognosis, chemotherapy has to be tolerable and should maintain the quality of life. The combination of 5-FU and leucovorin improved survival and QOL compared to best supportive care; however, the effect was limited[11]. In the search for improved systemic chemotherapy gemcitabine demonstrated tolerability and good QOL for patients with solid tumors[12]. In advanced pancreatic tumors, a phase III study revealed a better survival and symptom control compared to 5-FU[6]. Due to a common developmental origin of the pancreas and the biliary tract, CCC and pancreatic cancer share similarities in terms of tumor markers and resistance to chemotherapy. Hence, gemcitabine was administered in a phase II study to patients with unresectable CCC showing an objective response rate of 30%, a median time to progression of 27 wk and a median survival time of 9.3 mo[3].

Regional intraarterial therapies of the liver have shown efficacy in hyper vascularized hepatic malignancies[7,13,14]. While normal liver parenchyma receives more than two-thirds of its blood supply from the portal vein, hepatic tumors derive their blood supply almost completely from the hepatic artery[15]. The rationale for a regional intraarterial approach is a further increased anti tumoral activity induced by a temporary local ischemia and increasing local chemotherapy concentrations while reducing the systemic side effects[8].

Only limited data is available in terms of regional treatment of nonresectable CCC[16,17]. Cisplatin and doxorubicin have been applied successfully in the regional chemotherapy of hepatocellular carcinoma (HCC). The combination with lipiodol yielded anti-tumoral efficacy at a low systemic toxicity[18]. These observations led to the assumption that additional intraarterial chemoembolization of hypervascularized CCC might further enhance intrahepatic tumor response while maintaining the efficacy of systemic gemcitabine therapy.

In the course of the present study 8 patients with intrahepatic CCC received a combination of systemic chemotherapy and regional intraarterial chemoembolization. Maximum response was PR in 3 patients and SD in 5 patients. Six patients are still alive after a mean observation period of 14 mo. Three of the 7 patients who suffered from tumor-related disease symptoms experienced a clinical relief under therapy. Furthermore, from the 6 patients with elevated Ca19-9 levels, 4 patients showed a therapy-related decrease of more than 75%; among those the 3 patients with PR. QOL remained stable under therapy in those patients evaluable. These data are well in line and even exceed those from the gemcitabine monotherapy study from Kubicka *et al* showing objective responses in 30%, a therapy-related decrease in CA19-9 levels in 11 of 14 patients and a chemotherapy-related clinical relief in 7 of 11 patients with tumor symptoms[3].

One patient of our study showed a partial tumor remission under the combined therapy. The initially unresectable tumor became resectable after 10 mo. Whether a neoadjuvant intention might improve the prognosis in terms of secondary resectability will have to be determined by future observations. However, secondary resectability does not necessarily represent cure. Valverde and coworkers observed a 3-year-survival rate of only 22% after extensive surgical resection of intrahepatic CCC mainly related to the presence of intrahepatic satellite nodules and/or regional lymph node metastasis[2].

In spite of careful technique and the regular application of dexamethasone before the chemoembolization procedure, the number of cycles became limited to a maximum of three due to a progressive rarefication of the intrahepatic arteries. Incidents of regional therapy-related arteritis have been reported[19-21]. While a mechanical trauma may be responsible in some instances, toxic chemotherapy-related arteritis or ischemic reactions appear to be the more probable explanation in our situation for there is a progressive character of the changes. Interestingly, these phenomena

occurred in 4 of our 8 patients with CCC in non-cirrhotic livers. In contrast, we rarely encountered it after regional therapies of our patients with HCC in cirrhotic livers. Demachi and colleagues suggested that hypertrophy of peribiliary capillary plexus in cirrhosis could act as a portoarterial shunt thereby acting protective during decreased arterial flow[22]. In CCC there is a constant risk of focal cholestasis. The biliary structures are mainly dependent on the arterial perfusion. Hence, arterial hypoperfusion during chemoembolization is associated with an increased risk of biliary complications and infections[23]. These vascular and biliary side effects of regional chemoembolization are also reported by other investigators to be more pronounced in the non-cirrhotic liver with a good organ function than in the cirrhotic liver[24]. In our set of patients we did not encounter a clinically obvious complication such as cholangitis or biloma; however, the administration of antibiotics during the chemoembolization therapy and careful catheter management seems mandatory to avoid these instances.

Our results suggest that in patients with nonresectable hepatic CCC being in a good physical condition regional chemoembolization in addition to systemic gemcitabine is well tolerated and may further enhance the palliative effect of systemic gemcitabine therapy. It is, however, too early to demonstrate a clear advantage towards systemic therapy alone. One should be aware of the potentially progressive arterial hypo vascularization after repeated chemoembolization cycles possibly limiting the maximum number of procedures.

ACKNOWLEDGEMENTS

The outstanding support and assistance of Sabine Tegtmeier, Frank Socko, Monique Horning, and Heike Steinlandt are greatfully acknowledged.

REFERENCES

1 **Pichlmayr R,** Lamesch P, Weimann A, Tusch G, Ringe B. Surgical treatment of cholangiocellular carcinoma. *World J Surg* 1995; **19:** 83-88
2 **Valverde A,** Bonhomme N, Farges O, Sauvanet A, Flejou JF, Belghiti J. Resection of intrahepatic cholangiocarcinoma; a Western experience. *J Hepatobiliary Pancreat Surg* 1999; **6:** 122-127
3 **Kubicka S,** Rudolph KL, Tietze MK, Lorenz M, Manns M. Phase II study of systemic gemcitabine chemotherapy for advanced unresectable hepatobiliary carcinomas. *Hepatogastroenterology* 2001; **48:** 783-789
4 **Barton-Burke M.** Gemcitabine: a pharmacologic and clinical overview. *Cancer Nurs* 1999; **22:** 176-183
5 **Kuhn R,** Hribaschek A, Eichelmann K, Rudolph S, Fahlke J, Ridwelski K. Outpatient therapy with gemcitabine and docetaxel for gallbladder, biliary, and cholangio-carcinomas. *Invest New Drugs* 2002; **20:** 351-356
6 **Burris HA,** Moore MJ, Andersen J, Green MR, Rothenberg ML, Modiano MR, Cripps MC, Portenoy RK, Storniolo AM, Tarassoff P, Nelson R, Dorr FA, Stephens CD, Von Hoff DD. Improvements in survival and clinical benefit with gemcitabine as first-line therapy for patients with advanced pancreas cancer: a randomized trial. *J Clin Oncol* 1997; **15:** 2403-2413
7 **Lopez RR,** Pan SH, Lois JF, McMonigle ME, Hoffman AL, Sher LS, Lugo D, Makowka L. Transarterial chemoembolization is a safe treatment for unresectable hepatic malignancies. *Am Surg* 1997; **63:** 923-926
8 **Chen HS,** Gross JF. Intra-arterial infusion of anticancer drugs: theoretic aspects of drug delivery and review of responses. *Cancer Treat Rep* 1980; **64:** 31-40
9 **McHorney CA,** Ware JE, Raczek AE. The MOS 36-Item Short-Form Health Survey (SF-36): II. Psychometric and clinical tests of validity in measuring physical and mental health constructs. *Med Care* 1993; **31:** 247-263
10 **Kaczynski J,** Hansson G, Wallerstedt S. Incidence, etiologic aspects and clinicopathologic features in intrahepatic cholangiocellular carcinoma-a study of 51 cases from a low-endemicity area. *Acta Oncol* 1998; **37:** 77-83
11 **Glimelius B,** Hoffman K, Sjoden PO, Jacobsson G, Sellstrom H, Enander LK, Linne T, Svensson C. Chemotherapy improves survival and quality of life in advanced pancreatic and biliary cancer. *Ann Oncol* 1996; **7:** 593-600
12 **Carmichael J,** Fink U, Russell RC, Spittle MF, Harris AL, Spiessi G, Blatter J. Phase II study of gemcitabine in patients with advanced pancreatic cancer. *Br J Cancer* 1996; **73:** 101-105
13 **Cammà C,** Schepis F, Orlando A, Albanese M, Shahied L, Trevisani F, Andreone P, Craxì A, Cottone M. Transarterial chemoembolization for unresectable hepatocellular carcinoma: meta-analysis of randomized controlled trials. *Radiology* 2002; **224:** 47-54
14 **Tellez C,** Benson AB, Lyster MT, Talamonti M, Shaw J, Braun MA, Nemcek AA, Vogelzang RL. Phase II trial of chemoembolization for the treatment of metastatic colorectal carcinoma to the liver and review of the literature. *Cancer* 1998; **82:** 1250-1259
15 **Breedis C,** Young G. The blood supply of neoplasms in the liver. *Am J Pathol* 1954; **30:** 969-977
16 **Melichar B,** Cerman J, Dvorak J, Jandik P, Mergancova J, Melicharova K, Touskova M, Krajina A, Voboril Z. Regional chemotherapy in biliary tract cancers – a single institution experience. *Hepatogastroenterology* 2002; **49:** 900-906
17 **Tanaka N,** Yamakado K, Nakatsuka A, Fujii A, Matsumura K, Takeda K. Arterial chemoinfusion therapy through an implanted port system for patients with unresectable intrahepatic cholangiocarcinoma-initial experience. *Eur J Radiol* 2002; **41:** 42-48
18 **Inoue H,** Miyazono N, Hori A, Miyake S, Satake M, Kanetsuki I, Nishida H, Ikeda K, Nakajo M. Treatment of hepatocellular carcinoma by intraarterial injection of adriamycin/mitomycin C oil suspension (ADMOS) alone or combined with cis-diaminodichloroplatinum (CDDP). *Acta Radiol* 1993; **34:** 388-391
19 **Belli L,** Magistretti G, Puricelli GP, Damiani G, Colombo E, Cornalba GP. Arteritis following intra-arterial chemotherapy for liver tumors. *Eur Radiol* 1997; **7:** 323-326
20 **Forsberg L,** Hafstrom L, Lunderquist A, Sundqvist K. Arterial changes during treatment with intrahepatic arterial infusion of 5-fluorouracil. *Radiology* 1978; **126:** 49-52
21 **Bledin AG,** Kim EE, Chuang VP, Wallace S, Haynie TP. Changes of arterial blood flow patterns during infusion chemotherapy, as monitored by intra-arterially injected technetium 99m macroaggregated albumin. *Br J Radiol* 1984; **57:** 197-203
22 **Demachi H,** Matsui O, Kawamori Y, Ueda K, Takashima T. The protective effect of portoarterial shunts after experimental hepatic artery embolization in rats with liver cirrhosis. *Cardiovasc Intervent Radiol* 1995; **18:** 97-101
23 **Kim HK,** Chung YH, Song BC, Yang SH, Yoon HK, Yu E, Sung KB, Lee YS, Lee SG, Suh DJ. Ischemic bile duct injury as a serious complication after transarterial chemoembolization in patients with hepatocellular carcinoma. *J Clin Gastroenterol* 2001; **32:** 423-427
24 **Yu JS,** Kim KW, Jeong MG, Lee DH, Park MS, Yoon SW. Predisposing factors of bile duct injury after transcatheter arterial chemoembolization (TACE) for hepatic malignancy. *Cardiovasc Intervent Radiol* 2002; **25:** 270-274

PO Box 2345, Beijing 100023, China
www.wjgnet.com
wjg@wjgnet.com

ELSEVIER

World J Gastroenterol 2005;11(8):1096-1104
World Journal of Gastroenterology ISSN 1007-9327

Enhanced migration of tissue inhibitor of metalloproteinase overexpressing hepatoma cells is attributed to gelatinases: Relevance to intracellular signaling pathways

Elke Roeb, Anja-Katrin Bosserhoff, Sabine Hamacher, Bettina Jansen, Judith Dahmen, Sandra Wagner, Siegfried Matern

Elke Roeb, Sabine Hamacher, Bettina Jansen, Judith Dahmen, Sandra Wagner, Siegfried Matern, Department of Internal Medicine III, University Hospital RWTH Aachen, Germany
Anja-Katrin Bosserhoff, Institute of Pathology, University of Regensburg, Germany
Supported by grants from the Federal Ministry of Education and Research of Germany, Deutsche Forschungsgemeinschaft (DFG), and Aachen University
Correspondence to: Professor Elke Roeb, Department of Internal Medicine III, University Hospital RWTH Aachen, Pauwelsstr. 30, 52057 Aachen, Germany. eroeb@ukaachen.de
Telephone: +49-241-8089200 Fax: +49-241-8082455
Received: 2004-06-24 Accepted: 2004-08-22

Abstract

AIM: To study the effect of gelatinases (especially MMP-9) on migration of tissue inhibitor of metalloproteinase (TIMP-1) overexpressing hepatoma cells.

METHODS: Wild type HepG2 cells, cells stably transfected with TIMP-1 and TIMP-1 antagonist (MMP-9-H401A, a catalytically inactive matrix metalloproteinase (MMP) which still binds and neutralizes TIMP-1) were incubated in Boyden chambers either with or without Galardin (a synthetic inhibitor of MMP-1, -2, -3, -8, -9) or a specific inhibitor of gelatinases.

RESULTS: Compared to wild type HepG2 cells, the cells overexpressing TIMP-1 showed 115% migration ($P<0.05$) and the cells overexpressing MMP-9-H401A showed 62% migration ($P<0.01$). Galardin reduced cell migration dose dependently in all cases. The gelatinase inhibitor reduced migration in TIMP-1 overexpressing cells predominantly. Furthermore, we examined intracellular signal transduction pathways of TIMP-1-dependent HepG2 cells. TIMP-1 deactivates cell signaling pathways of MMP-2 and MMP-9 involving p38 mitogen-activated protein kinase. Specific blockade of the ERK pathway suppresses gelatinase expression either in the presence or absence of TIMP-1.

CONCLUSION: Overexpressing functional TIMP-1-enhanced migration of HepG2-TIMP-1 cells depends on enhanced MMP-activity, especially MMP-9.

Key words: HepG2; MMP-2; MMP-9; p38MAPK; Galardin; Genistein

Roeb E, Bosserhoff AK, Hamacher S, Jansen B, Dahmen J, Wagner S, Matern S. Enhanced migration of tissue inhibitor of metalloproteinase overexpressing hepatoma cells is attributed to gelatinases: Relevance to intracellular signaling pathways. *World J Gastroenterol* 2005; 11(8): 1096-1104
http://www.wjgnet.com/1007-9327/11/1096.asp

INTRODUCTION

Proteins of the matrix metalloproteinases (MMPs), a family of structurally related zinc-dependent enzymes, are involved in the breakdown of extracellular matrix (ECM) in normal physiological processes, such as embryonic development, reproduction, and tissue remodeling as well as in disease processes, such as arthritis, tumor cell invasion, migration, and metastasis[1-3]. Most MMPs are secreted as inactive proteins, which are activated when cleaved by extracellular proteinases. MMPs may be expressed on the surface of cells, thus allowing a precise and localized proteolysis[4]. The gelatinases MMP-2 and MMP-9 are necessary for the migration of Langerhans cells and dermal dendritic cells from human and murine skin[5]. MMP-2 (gene ID 4313 on chromosome 16q13-q21) e.g., is involved in cell migration of human lung carcinoma cells[6]. MMP-9 (gene ID 4318, chromosome 20, q11.2-q13.1) is a major secretion product of macrophages and a component of cytoplasmic granules of neutrophils[7]. The enzyme is also secreted by lymphocytes and stromal cells upon stimulation by inflammatory cytokines, or upon delivery of bidirectional activation signals following integrin-mediated cell-cell or cell-matrix contacts[8]. MMP-9 plays an important role in tumor invasion and angiogenesis. Secretion has been reported in various cancer types including lung, colon, and breast cancer. The activity of MMPs is tightly controlled by endogenous specific inhibitors, the tissue inhibitors of metalloproteinases (TIMPs). The balance between activated MMPs and their free inhibitors determines the net MMP activity and seems to be of great importance for matrix protein turnover associated with tumor cell invasion and metastasis. A striking phenotypic characteristic of fibrotic liver is a dramatic up-regulation of TIMP-1 (GenBank number NM 003254.1, chromosome X, Xp11.3-p11.23), which seems to be a functional promotor of hepatic fibrosis[9,10]. But there is also evidence that TIMPs are associated with suppression of programed cell death, tissue remodeling during tumor progression and mitogenic activity[11,12]. TIMP-1 has been shown to suppress apoptosis in a series of Burkitt's lymphoma

cell lines[13] and to act as a survival factor blocking apoptosis in B cells[14,15]. TIMP-1 must, therefore, be regarded as a multifunctional protein[16,17]. Recently, evidence has been provided that TIMP-1 induces specific signaling pathways[18]. TIMP-1 is able to activate Ras involving the Tyk/mitogen-activated protein kinase (MAPK) pathway[19]. A specific blockade of the ERK pathway suppresses the expression of MMP-9 and inhibits markedly the invasiveness of tumor cells[20]. The PKC-dependent NFK kappa B activation is absolute for MMP-9 induction and PKC-dependent ERC activation devotes to increase the expression level of MMP-9 in hepatocellular carcinoma cells[21,22]. St-Pierre *et al*[8] have given an overview of recent developments in the field of MMP-9 gene expression in different cell types, from the triggering of cell-surface receptors to the activation of cytoplasmic mediators and transcription factors responsible for the activation of MMP-9 promotor. Fibronectin up-regulates MMP-9 and induces coordinated expression of MMP-2 and its activator, the membrane-type MT1-MMP (MMP-14) by human T-lymphocyte cell lines, a process repressed through Ras/MAP kinase signaling pathways[23]. Accordingly, transfection of T-cell lines with dominant negative mutant of Ha-Ras strongly increases fibronectin-induced expression of MMP-2 and MMP-9[23]. In human glioma cells, angiopoietin-2 induces tumor cell infiltration by activation of MMP-2. MMP-2 is associated with tumor size, invasiveness, and survival in breast cancer[24]. SB203580, a p38 MAP kinase inhibitor, reduces MMP-2 expression in melanoma cells[25]. Non-steroidal anti-inflammatory drugs inhibit MMP-2 via suppression of ERK/Sp1-mediated transcription[26].

Recently, we demonstrated an increased expression of MMP-2 and MMP-9 protein as a result of increased TIMP-1 expression in human hepatoma cells[27]. Beyond that TIMP-1 overexpressing HepG2 cells could grow in nests and keep in contact with each other[27,28]. This striking phenotype could be abrogated by a TIMP-1 antagonist, the mutant MMP-9-H401A[28]. Three histidine residues constitute the active site of MMP-9 by binding to the catalytic zinc. A MMP-9 mutant has been generated in which the histidine residue at position 401 is replaced by alanine. The mutant is enzymatically inactive but is still able to bind to TIMP-1. Furthermore, MMP-9-H401A is able to neutralize the ability of TIMP-1 to inhibit MMP-9 activity[28]. With the help of this TIMP-1 antagonist the influence of TIMP-1 e.g., on cell migration and invasion might be demonstrated much more clearly. Recent discoveries regarding the main functions of TIMP-1 (inhibition of tumor growth, invasion, angiogenesis, and metastasis; exhibition of growth factor-like activity and suppression of programmed cell death independent of the MMP inhibitory activity) have complicated the understanding of this protease inhibitor. Presently TIMP-1 can no longer be regarded uniquely as a tissue inhibitor of metalloproteinases. We decided to study in more detail the role of TIMP-1 and MMPs in the migration and signal transduction of human hepatoma cells by using an established cell motility assay with clear and defined conditions. We showed here that TIMP-1 overexpressing cells exhibit increased migration by chemotaxis, which could be reduced by MMP inhibition, especially inhibition of gelatinases. Following this discovery, we further investigated the signal transduction pathways of MMP-2 and MMP-9 in the event of TIMP-1 overexpression and demonstrated that TIMP-1 deactivates specific cell signaling pathways of MMPs.

MATERIALS AND METHODS

Materials

Culture reagents were from Sigma (Steinheim, Germany), Gibco (Eggenstein, Germany), or Sarstedt (Berlin, Germany). All chemicals were purchased from Sigma (Germany), Pharmacia (Freiburg, Germany), or ICN (Meckenheim, Germany). Galardin (GM 6001), a broad spectrum inhibitor of MMPs, genistein (4,5,7-trihydroxyisoflavone), an inhibitor of tyrosine kinases, SB 202190 (FHPI; 4-(4-fluorophenyl)-2-(4-hydroxyphenyl)-5-(4-pyridyl)1H-imidazol), an inhibitor of p38 MAP kinase, UO126 (1,4-diamino-2,3-dicyano-1,4-bis(2-aminophenylthio) butadien), an inhibitor of MEK1/2, and MMP-2/MMP-9 inhibitor I (2R,2,4-biphenylylsulfonylamino-3-phenylpropionic acid) were obtained from CalBiochem (Bad Soden, Germany). Preparation of a rabbit polyclonal anti-murine-TIMP-1 antiserum was described elsewhere[29]. Boyden chambers were purchased from Neuroprobe (Gaithersburg, US) and membranes from Merck (Darmstadt, Germany). Recombinant murine TIMP-1 was obtained from R&D Systems (Wiesbaden-Nordenstadt, Germany). A semi-quantitative PCR detection kit was purchased from BioSource International (Camarillo, CA).

Construction of a TIMP-1 antagonist

The MMP-9 mutant MMP-9-H401A was cloned as previously described[28]. To introduce a point mutation at amino acid 401 of murine MMP-9 (MMP-9-H401A), PCR-aided mutagenesis was performed using the following primers: 5'-TGG CAG CGG CCG AGT TCG GCC ATG-3' sense and 5'-CGA ACT CGG CCG CTG CCA CCA GG-3' antisense.

Cells and cell treatment

Human hepatoma cells (HepG2) were maintained in Dulbecco's modified Eagle's medium (DMEM) supplemented with 50 mL/L fetal calf serum (FCS), 100 mg/L streptomycin and 60 mg/L penicillin. Cells were grown at 37 ℃ in a water-saturated atmosphere in air/CO_2 (19∶1). Cells were assessed for the expression of TIMP-1 by Western blotting after incubation under serum-free conditions for 24 h. Selection of HepG2 clones stably transfected with murine TIMP-1 cDNA or murine MMP-9-H401A cDNA was previously described[27,28]. For stable expression, HepG2 cells were transfected with the expression vector pcDNA3.1-mTIMP-1 or pcDNA3.1-MMP-9-mut containing the neomycin resistance gene. Colonies resistant to 500 μg/mL neomycin were isolated, several clones were established and assessed for the expression of murine TIMP-1 or mutant MMP-9 by Northern and Western blotting. Expression by these cells was maintained for more than 20 passages. Three positive clones for each plasmid were used for further analyses.

Western blot

Serum-free cell supernatants of HepG2 cells and HepG2

cell clones were separated by SDS-polyacrylamide gel electrophoresis separating gels of 12.5% polyacrylamide and stacking gels of 3% polyacrylamide. Lanes were loaded with 2 μg of total protein each. Following electrophoresis at 30 V the proteins from serum-free cell supernatants were transferred to nitrocellulose membrane. Protein bands were localized by staining Ponceau S. Blots were blocked with TBS-N (pH 7.6) containing 10% BSA, 20 mmol/L Tris, 137 mmol/L NaCl, 0.1% Nonidet P40, washed and incubated with antibodies against TIMP-1 (dilution 1:1 000). Signals were visualized by enhanced chemiluminescence according to the manufacturer's instructions (Amersham). Experiments were done in triplicate.

Boyden chamber experiments

Transwell 0.64-cm^2 filter inserts (8-μm pores) coated with a thin layer of gelatin (125 $\mu g/cm^2$) were re-hydrated according to the customer's instructions essentially as described previously[30]. Prior to seeding into the transwell inserts, cells were released using trypsin-EDTA and sequentially rinsed with DMEM containing 10% FCS and serum-free DMEM. The rinsed cells were re-suspended in serum-free DMEM (2.5×10^5 cells/mL) and 800 μL was added to the upper chambers. Galardin (2 μmol/L), MMP-2/MMP-9 inhibitor I (20 μmol/L) or 0.1% DMSO as control were added. In the lower compartment, fetal calf serum was used as chemoattractant. Chambers were incubated in a humified tissue incubator, containing 50 mL/L CO_2 for 4 h at 37 ℃. The cells on the upper surface of the filters were then removed using a cotton swab and those remaining on the lower surface of the filter were fixed with 10% methanol and stained with hematoxylin and eosin. The filters were rinsed with deionized water, dried and examined using light microscopy. The number of cells in five random optical fields (×400 magnification) from triplicate filters was averaged to obtain the number of migrating cells.

Attachment assay

Attachment assays were performed in 96-well plates. The wells were coated with gelatin solutions at a concentration of 10 μg/mL at 4 ℃ for 18 h. Unspecific binding of cells was blocked by pre-incubation of the wells with 3% BSA/PBS for 2 h. Hepatoma cell clones were harvested by trypsin incubation for 2 min, resuspended in DMEM without FCS at a density of 2×10^5 cells/mL and placed in the respective wells. For 4 h cells remaining in suspension were counted every 15 min. The assays were carried out in triplicate. Numerical data were analyzed by analysis of variance and Tukey's multiple range tests at 5 and 1% levels. Data were presented as mean±SD.

RT-PCR

RNA was isolated from whole cells by Ultraspec™ phenol chloroform extraction procedure (Biotecx Laboratories Inc., Houston, TX) according to the instruction manual, quantified spectrophotometrically at 260 nm and stored at -70 ℃. Five micrograms of RNA were heated to 65 ℃ for 10 min in 50% formamide, 20 mmol/L 3-[N-morpholino] propane sulfonic acid (MOPS), 5 mmol/L sodium acetate, 1 mmol/L EDTA, and 2.2 mol/L formaldehyde before gel electrophoresis in 1% agarose containing 2.2 mol/L formaldehyde, 20 mmol/L MOPS, 5 mmol/L sodium acetate, and 1 mmol/L EDTA. After electrophoresis, integrity of the RNA was controlled by ethidium bromide staining of 18S and 28S ribosomal RNA. First-strand complementary DNA (cDNA) was synthesized from 1 μg of DNA-free total RNA with a T-primed first-strand kit (Pharmacia Biotech, Freiburg, Germany) according to the manufacturer's instructions. A 1:100 final dilution of the reaction was used as template for PCR. In preliminary experiments, we determined the optimal number of cycles within the linearity of reactions for each PCR product. The cycle number was 35 cycles for MMP-9, MMP-14, and human TIMP-1, and 25 cycles for MMP-2 and GAPDH. The primers for PCR were as follows: human MMP-2 (756-1682 nt, GenBankTM accession no. AL832088), forward (5'-CCA CGC TGC GGC AAC CCA GAT GTG GCC AAC-3') and backward (5'-GGC GTG GCC AAA CTC GTG GGC TGC CAC-3'); human GAPDH (292-885 nt, GenBankTM J04038), forward (5'-CCC ATC ACC ATC TTC CAG) and backward (5'-CCT GCT TCA CCA CCT TCT); human MMP-9 (1512-2120 nt, GenBankTM BC006093), forward (5'-ACG GCC ACT ACT GTG CCT TTG-3') and backward (5'-AGG GCA CTG CAG GAT GTC ATA GG-3'); human MMP-14 (1247–1766 nt, GenBankTM NM 031056), forward (5'-GCC CAT TGG CCA GTT CTG GCG GG-3') and backward (5'-CCT CGT CCA CCT CAA TGA TGA TC-3'); human TIMP-1 (169-494 nt, GenBankTM NM003254), forward (5'-GCA ATT CCG ACC TCG TCA TC-3') and backward (5'-AGT GTA GGT CTT GGT GAA GC-3'). Using these primers, PCR was performed by the expand high fidelity PCR system (Roche Diagnostics) at 94 ℃ for 4 min followed by individual cycles at 94 ℃ for 30 s, at 58 ℃ for 30 s, and at 72 ℃ for 1 min with an extension step at 72 ℃ for 7 min at the end of the last cycle. The products were resolved in agarose gel (1.8%), followed by staining with ethidium bromide, and recorded by digital camera. The relative density of the products was quantitated by the Bio-Rad Gel-Doc system. The predicted PCR product size for MMP-2 and MMP-9 was 926 and 608 bp, respectively. For glyceraldehyde 3-phosphate dehydrogenase (GAPDH) the product size is 593 bp, for MMP-14 519 bp, and for human TIMP-1, 325 bp. Identity of the PCR product for MMP-2, MMP-9, MMP-14, and human TIMP-1 was confirmed by DNA sequencing. The values were depicted as the ratio to those of GAPDH.

Semi-quantitative multiplexPCR detection

The expression of human MMP-1, -3, -7, -2, -9, and GAPDH were detected by a multiplexPCR kit (BioSource International) according to the supplier's instructions. The primers were selected with similar Tm such that highly stringent conditions for all primers could be utilized for RT-multiplexPCR. Buffers used were formulated to decrease competition among amplicons and to enhance the amplification of longer DNA fragments during multiplexPCR. Following PCR, the amplicons were analyzed by gel electrophoresis. Since the amplification efficiency of each primer pair was equivalent, the intensity of each

amplicon band was proportional to their relative concentration in the cDNA sample. Agarose gel electrophoresis bands were scanned by computer analysis, and the optical density was plotted by histogram. The Bio-Rad Gel-Doc system was used to quantify PCR data. Data from MMP-cDNA were normalized to the respective content of GAPDH.

RESULTS

Effect of TIMP-1 and TIMP-1 antagonist on TIMP-1 expression

HepG2 wild type cells were compared with HepG2 cell clones overexpressing murine TIMP-1 (#T1, #T2, #T3) and HepG2 cells overexpressing the TIMP-1 antagonist MMP-9-H401A (#M1, #M2, #M3). Western blot analysis was performed for serum-free supernatants from HepG2 cells, HepG2-TIMP-1, (Figure 1, Lane 3) and HepG2-MMP-9-H401A. Using a specific polyclonal antiserum against murine TIMP-1 that did not detect human TIMP-1, amounts of murine TIMP-1 could be detected in HepG2-TIMP-1 cells. The supernatants of three different clones for HepG2-TIMP-1 (Figure 1, lane 2) and three different clones for MMP-9-H401A (Figure 1, lane 1), respectively, were pooled.

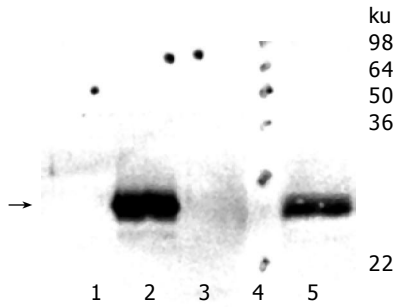

Figure 1 TIMP-1 protein expression of hepatoma cells overexpressing murine TIMP-1 and those overexpressing the TIMP-1 antagonist MMP-9-H401A. The arrow indicates the position of murine TIMP-1. TIMP-1 protein could be detected in HepG2-TIMP-1 cells only.

Effect of TIMP-1 and TIMP-1 antagonist on expression of MMP-1, -3, -7, -2, -9, and MMP-13

Semi-quantitative multiplexPCR was used to investigate the expression of MMP-1, -3, -2, -9, and -14 simultaneously in HepG2 cells, HepG2-TIMP-1 cells and HepG2 cells overexpressing MMP-9-H401A. The average values of three different clones for each cell line are indicated in Figure 2. Expression values of HepG2 cells were set to 100%. There were no significant changes in the expression levels of MMP-1, MMP-3, and MMP-14 between wild type HepG2 (white columns), TIMP-1 overexpressing HepG2 cells (black columns), and HepG2 overexpressing MMP-9-H401A (halftone columns). We observed a significant increase in the expression of MMP-9 (HepG2-TIMP-1: $P = 0.003$; HepG2-MMP-9-H401A: $P = 0.05$) in both HepG2-TIMP-1 and HepG2-MMP-9-H401A cells (Figure 2). MMP-9 primers did not differ between endogenous human MMP-9 and the transgene MMP-9-H401A with a single point mutation on DNA level. MMP-2 expression increased in HepG2-TIMP-1 in comparison to HepG2 cells but values did not reach the level of significance. MMP-2 expression levels in HepG2-MMP-9-H401A, however, decreased (Figure 2). There were no changes in the expression of the endogenous TIMP-1 between all cell clones examined (Figure 2, right panel).

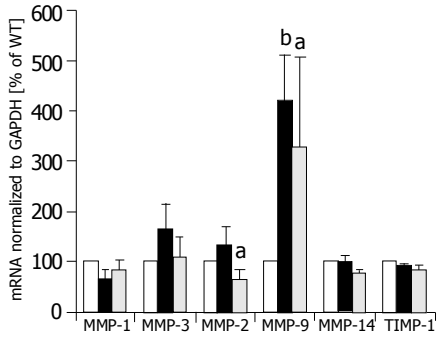

Figure 2 MMP mRNA expression of HepG2 (white columns), HepG2-TIMP-1 clones (black columns), and HepG2 cells overexpressing the TIMP-1 antagonist MMP-9-H401A (halftone columns). [a]$P<0.05$; [b]$P<0.01$.

Migration of human hepatoma cells was influenced by endogenous TIMP-1

To investigate whether TIMP-1 or TIMP-1 antagonism contributed to differences in cell migration, HepG2-TIMP-1 and HepG2-MMP-9-H401A cells were incubated in Boyden chambers. Fetal calf serum was used as chemoattractant. After incubated for 4 h, migrated cells were numbered on the undersite of the permeable membrane coated with gelatin. Data were normalized by setting the number of HepG2 wild type cells to 100% (Figure 3, white column, lane 1) and were presented as mean±SD. Compared with wild type HepG2 cells, the cells overexpressing TIMP-1 showed 114.6±10.7% ($P = 0.039$) migration (Figure 3, black column, lane 2) and the cells overexpressing the TIMP-1 antagonist showed 62.2±16% ($P = 0.0196$) migration (Figure 3, halftone column, lane 3). The difference between TIMP-1 clones and clones overexpressing the TIMP-1 antagonist was highly significant ($P = 0.0057$). Thus, TIMP-1 overexpression associated with increased expression of MMP-9 and MMP-2 favors migration in contrast to TIMP-1 inhibition by MMP-9H401A.

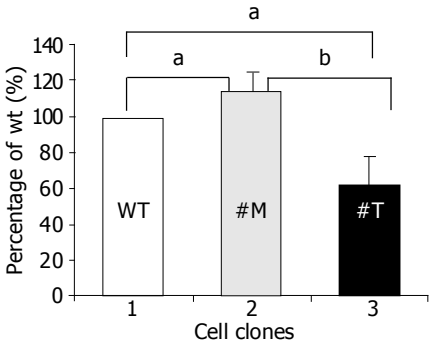

Figure 3 TIMP-1 and TIMP-1 antagonist contribute to differences in cell migration. [a]$P<0.05$; [b]$P<0.01$.

Migration of hepatoma cells overexpressing TIMP-1 was inhibited by a broad spectrum inhibitor of MMPs and a specific inhibitor of MMP-2 and MMP-9

To investigate whether MMPs were responsible for the different migration rates of HepG2 cells overexpressing TIMP-1 or MMP-9-H401A, cells were incubated with the broad spectrum MMP-inhibitor Galardin (Figure 4, lanes 2, 5, 8, 11, 14, 17, 20; few points) and a specific inhibitor of MMP-2/MMP-9 (Figure 4, lanes 3, 6, 9, 12, 15, 18, 21; many points). HepG2, HepG2-TIMP-1, and HepG2-MMP-9-H401A cells were incubated in Boyden chambers either with or without 2 μmol/L Galardin (GM 6001, inhibitor of MMP-1, -2, -3, -8, -9) and 20 μmol/L MMP-2/MMP-9 inhibitor. Fetal calf serum was used as chemoattractant. After 4 h of incubation migrated cells were numbered on the bottom of the permeable membrane coated with gelatin. Incubation with 2 μmol/L Galardin and 20 μmol/L gelatinase inhibitor reduced cell migration from 27.7±15.6 to 22.2±10.3 (P = 0.038) and 25.1±15.7 in HepG2 wild type cells (Figure 4, column 1-3). In the case of HepG2-MMP-9-H401A, incubation with Galardin reduced cell migration significantly from 21.5 to 16.1 (P = 0.02, #M1), 17.6 to 4.8 (P = 0.0016, #M2), and 12.6 to 6.9 (P = 0.03, #M3) for all clones analyzed separately. Gelatinase inhibitor was not able to reduce cell migration significantly in wild type cells and two of three cell clones overexpressing the TIMP-1 antagonist MMP-9-H401A (Figure 4, lanes 3, 6, and 12; many points). In the case of HepG2-TIMP-1, incubation with Galardin reduced cell migration from 33.9 to 25.8 (P = 0.02, #T1), 30.8 to 24.6 (P = 0.018, #T2), and 28.1 to 14.5 (P<0.0001, #T3). In the presence of MMP-2/-9 inhibitor a reduced migration was observed in all TIMP-1 overexpressing cell clones (Figure 4, lane 15, 18, and 21: many points), although reduction did not achieve significance in all cases (Figure 4, lane 18). Incubation of HepG2-TIMP-1 (#T1) with the specific MMP-2/-9 inhibitor reduced cell migration from 33.9±18.9 to 15.4±10.7 (P = 0.000003) beyond the number achieved by incubation with Galardin.

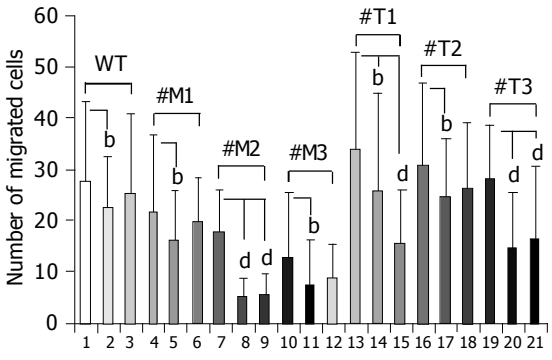

Figure 4 Effect of a broad spectrum MMP inhibitor and a specific MMP-2/MMP-9 inhibitor on the migration of HepG2, HepG2-TIMP-1 and HepG2-MMP-9-H401A cells. ^{b}P<0.01; ^{d}P<0.001.

Effect of TIMP-1 overexpression and TIMP-1 antagonism on cell attachment

We examined the attachment of all cell clones used to gelatin-coated membranes as shown in Figure 5. Three different clones of HepG2-TIMP-1 (#T1, #T2, #T3) and HepG2-MMP-9-H401A (#M1, #M2, #M3) behaved similarly to wild type HepG2 cells and showed a comparable attachment (Figure 5).

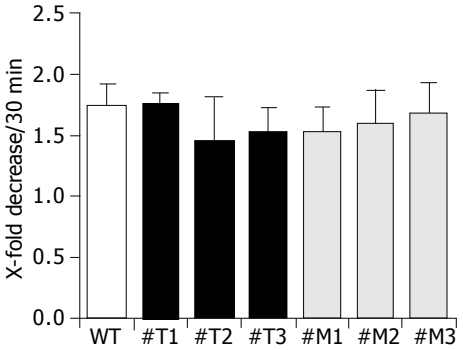

Figure 5 TIMP-1 and TIMP-1 antagonist do not influence cell attachment.

Signaling pathways required for expression of MMP-2 and MMP-9 in TIMP-1 overexpressing cells

To test which signaling pathways were involved in the expression of MMP-2 and MMP-9 in wild type HepG2 and TIMP-1 overexpressing HepG2, cells were incubated with different kinase inhibitors. Ras proteins are key molecular switches that mediate transmembrane signaling through the activation of multiple downstream pathways, which include the MAPK kinase pathways[31]. A series of pharmacological inhibitors were used to test the potential contribution of one or more signaling pathways that might regulate the steady-state transcription of the MMP-2 and the MMP-9 gene in wild-type or TIMP-1 overexpressing HepG2 cells: genistein (25 and 50 μmol/L; tyrosine kinase inhibitor), SB 202190 (2.5 μmol/L; potent inhibitor of p38 MAP kinase), and UO126 (1 μmol/L; potent and specific inhibitor of MEK1 and MEK2).

UO126 and genistein treatment at a dose of 50 μmol/L inhibited the secretion of MMP-2 in wild type and TIMP-1 overexpressing hepatoma cells (Figures 6A, B and columns 3, and 5). There was also a less pronounced but reproducible effect using the general tyrosin kinase inhibitor genistein at a dose of 25 μmol/L (Figure 6A, B and column 2). The specific p38 MAP kinase inhibitor SB 202190 was effective in blocking MMP-2 expression in HepG2 wild-type cells only, suggesting that the MMP-2 expression was not regulated through p38 MAPK in the case of TIMP-1 overexpression. These data all supported the hypothesis that constitutive MMP-2 expression is regulated through a steady-state signaling event, passing through Ras, MEK1/2, and p38 MAP kinases (Figure 6A). All TIMP-1 overexpressing cell clones (#T1, #T2, #T3) behaved similar (Figure 6 B).

Genistein at a dose of 25 and 50 μmol/L inhibited the secretion of MMP-9 in wild-type and TIMP-1 overexpressing hepatoma cells (Figure 6C, D and columns 2, 3). There was also a less-pronounced but reproducible effect using the specific MEK1/2 inhibitor UO126 at a dose of 1 μmol/L

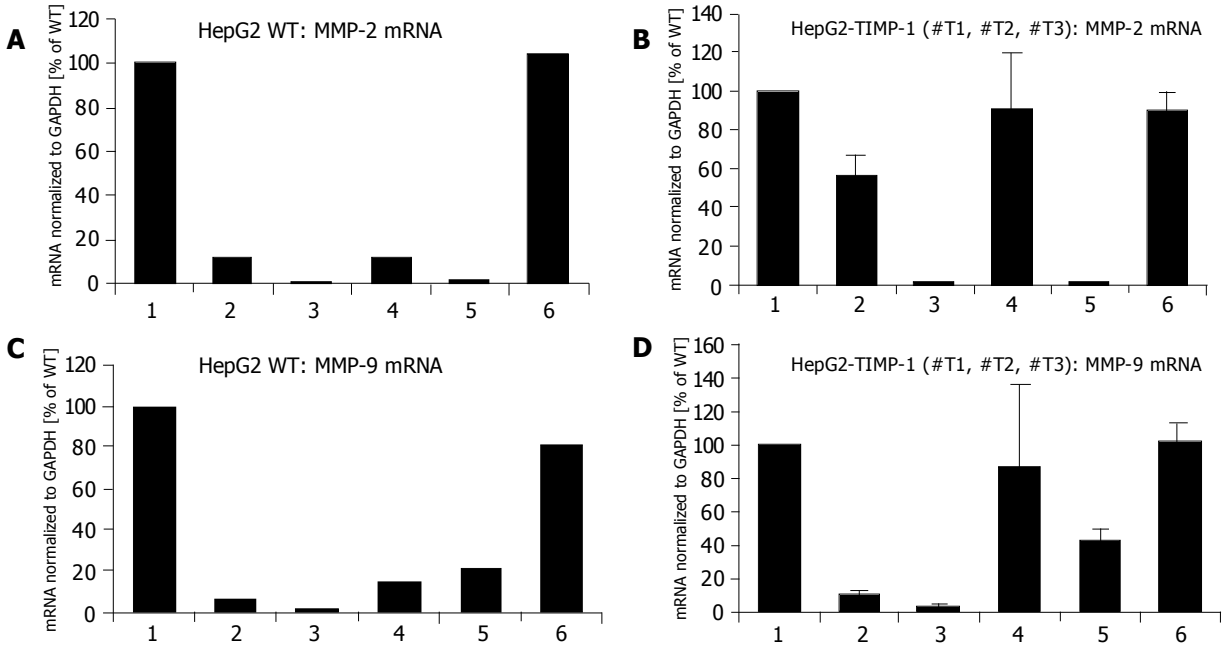

Figure 6 Effect of genistein, p38 MAPK inhibitor (SB 202190), and UO126 on the induction of MMP-2 and MMP-9 mRNA expression in HepG2 (A and C) and HepG2 TIMP-1 overexpressing cell clones (B and D). Cells were treated with Genistein 25 μM (2), Genistein 50 μM (3), SB202190 (4), and UO126 (5). mRNA expression of untreated cells (1) were set to 100%. Incubation with DMSO served as control (6).

(Figure 6C, D and column 5). The specific p38 MAP kinase inhibitor SB 202190 was effective in blocking MMP-9 expression in HepG2 wild-type cells and less pronounced in one (#T1) of the TIMP-1 overexpressing clones (individual data not shown) whereas MMP-9 expression could not be influenced by p38 MAK inhibition in other TIMP-1 overexpressing clones (#T2, #T3) (individual data not shown). These data suggested that TIMP-1 overexpression attenuates MMP-9 expression through p38 MAPK. Similar to MMP-2 constitutive MMP-9 expression is regulated through a steady-state signaling event passing through Ras, MEK1/2, and p38 MAP kinases (Figure 6C).

DISCUSSION

A critical involvement of TIMP-1 and MMPs, in the extent of migration of human hepatoma cells, is shown here. It has previously been reported that TIMP-1 may play an important role in growth and migration, especially of hepatocellular and cholangiocellular carcinomas[32]. In this report, we extend these data in several ways. The migration of human hepatoma cells is characterized by the presence of TIMP-1 and a novel TIMP-1 antagonist. The influence of MMPs in the presence of high TIMP-1 levels can be determined by the application of a broad spectrum MMP inhibitor (Galardin GM6001) and a specific inhibitor of MMP-2, and MMP-9. MMP-2 and MMP-9 were critical for the migration of hepatoma cells in the presence of TIMP-1 (Figure 4). The action of TIMP-1 on the migration of hepatoma cells is functionally different from the MMP-inhibitors indicating other functions of TIMP-1 besides its MMP inhibitory capacity. The influence of cell attachment on the extent of migration is excluded by defining the attachment of all cell clones used. Signal transduction pathways responsible for the gene expression of MMP-2 and MMP-9 are analyzed either in the presence or absence of TIMP-1 and differences are elaborated concerning p38 MAPK.

TIMP-1 overexpression leads to increased migration of hepatoma cells (Figure 2). This phenomenon linked to TIMP-1 is confirmed by the use of the novel TIMP-1 antagonist MMP-9-H401-A[28]. This MMP-9 mutant has the opposite effect of TIMP-1 and reduces migration in our system. Although both TIMP-1 and the synthetic MMP-inhibitor GM6001 are able to inhibit MMPs, TIMP-1 increases and GM6001 decreases migration. Thus, the action of TIMP-1 on migration of hepatoma cells is functionally different from GM6001. Since TIMP-1 enhances migration in hepatoma cells, the influence of TIMP-1 on migration seems to be at least partly independent of its MMP inhibitory activity and indicates other functions of TIMP-1 besides its MMP inhibitory capacity. Recent studies showed that apoptotic effects of TIMP-1, especially the inhibition of apoptosis in tumor cells, are independent of MMP inhibition[11,33]. However, apoptosis would hardly be the reason for increased migration in our experiments because we measured migration over 4 h, too short for significant effects of programed cell death. Furthermore, we measured apoptosis in all cell clones used *vs* HepG2 wild-type cells by a cell death detection (nuclear matrix protein) but ELISA and apoptotic DNA Ladder kit could not detect any significant differences (data not shown). Further biological functions of TIMP-1, mitogenic activity, and cell-growth promoting activity, can be mainly excluded for the short period of time selected[11,34-36]. The effect of TIMP-1 on hepatoma cell migration might be cell tissue specific because in B16-F10 melanoma cells a specific up-regulation of murine TIMP-1 expression directly suppresses the invasive

ability in a matrigel transwell invasion assay[37]. Recently the modulation of cell morphology has been reported to have a function for TIMP-1[11,38]. In smooth muscle cells a minimum expression of the contractile proteins and a maximal proliferation rate are correlated with the highest levels of both MMP-1 and TIMP-1[38]. TIMP-1 overexpressing HepG2 cells actually have a characteristic phenotype; they grow in nests and lie on top of each other[27]. It might be possible that this specific phenotype enables the cells to enhance migration through the gelatin-coated transwell filters. Whether the modulation of cell morphology by TIMP-1 takes place by changing the expression pattern of contractile proteins is the subject of our current investigation.

MMP-2 and -9 are necessary for the migration of many cell types and tumor cells, e.g., Langerhans cells and dermal dendritic cells from human and murine skin[5]. The migration of the latter cells, however, is inhibited by TIMP-1 and TIMP-2. We also demonstrated that MMPs are critical for the migration of hepatoma cells either in the presence or absence of TIMP-1 (Figure 4). Overexpressing functional TIMP-1 seems to depend on enhanced MMP-activity. Since Galardin is able to inhibit MMP-1, -2, -3, -8 and -9, one or more of these MMPs might be responsible for migration in HepG2 cells in our system. Overexpression of MMP-9 in HepG2-TIMP-1 cells has been demonstrated earlier[27]. Actually, we observed a reduced migration of all cell clones used in the presence of MMP-2/MMP-9 inhibitor. In some cases (Figure 4), however, reduction of migration did not achieve significance.

Migration of cells through a coated membrane involves not only ECM degradation but also requires the ability of adhesive interactions between cells and matrix. Cell migration can be viewed as a process regulated by counter-balanced forces or activities. Strength of cell adhesion and inhibitory degrees of cell adhesion can regulate the speed of motility[6,39]. In the present study, however, decreased and increased migration did not correlate with different adhesion (Figure 5).

MAPK activities exert a crucial role in cellular migration, and their implication in this process has been highlighted by the use of specific inhibitors (indicated in Figure 7).

Several reports have shown that SAPK2/p38 is involved in chemokine-induced chemotaxis of cells[40-42]. For this reason, we examined the migration potential of TIMP-1 overexpressing cells in the presence of specific signal transduction inhibitors (Figure 7) and our study presents evidence that p38 but not ERK, intervenes in the control of hepatoma cell migration. Signal transduction has traditionally been examined by short-term stimulation of cells with agents that induce mitogenesis, differentiation, or apoptosis[43]. Recent work showed that maintenance of basal cell function also requires "steady-state" signal transduction[44]. In this specific instance, the steady-state production of MMP-2 and MMP-9 involved in cell attachment, detachment, and migration was examined in our study. Constitutive MMP-2 and MMP-9 expression is regulated through a steady-state signaling event passing through tyrosine kinases, MEK1/2, and p38 MAP kinases (Figures 6, 7). Our results are in accordance with others[42-44,48]. For head and neck cancer cells, it has already been reported that the general tyrosine kinase inhibitor genistein induces several specific molecular changes, such as down-regulation of c-erbB-2 expression, down-regulation of MMP-2 and MMP-9 secretion, inhibition of tumor cell invasion and down-regulation of nuclear factor-kappaB DNA binding activity[45]. In human keratinocytes, the inhibition of MAPK pathway is correlated with down-regulation of MMP-9 secretion induced by TNF-alpha[46]. In brain cells, ERK and p38 MAP kinases are up-regulated after mechanical injury, and mediate the secretion of MMP-9[47]. Recently, it has been shown that inhibition of monocyte migration occurs via inhibiting crucial signaling pathways, like SAPK2/p38 (Figure 7) and MMP-2 activities[48].

Given the data presented in this manuscript, we could now predict that expression of MMP-2 and MMP-9 in

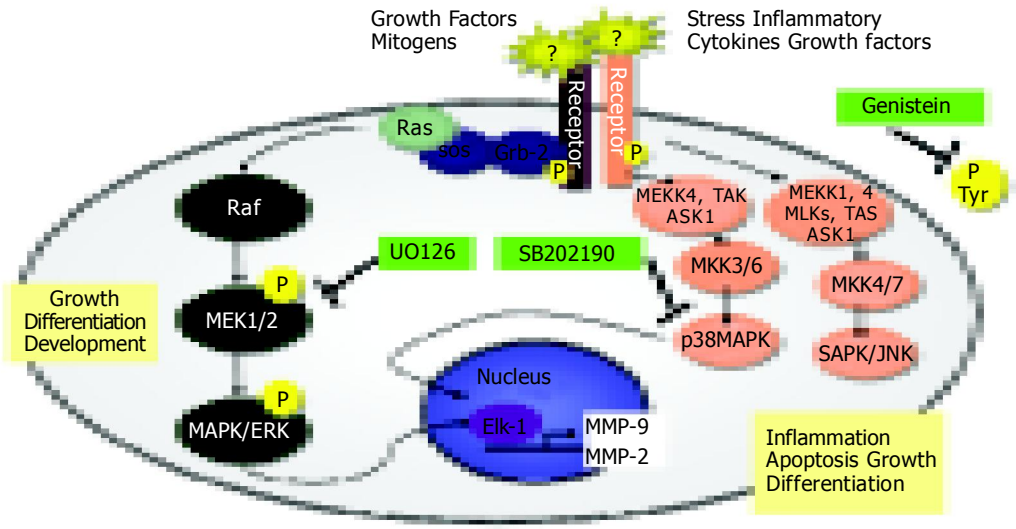

Figure 7 Signal transduction pathways and MAP kinase signaling cascades in mammalian cells shown in schematic form.

liver tumors containing high TIMP-1 activity cannot be influenced by inhibition of p38 MAK (Figure 7). This should result in a higher metastatic potential and probably a poorer overall prognosis.

Our data add new insights in the complex function of TIMP-1 and control of MMP activity in human liver cells. Thus, the suggested role of TIMP-1 in tumor cell migration has substantially changed from the initial focus on MMP inhibition to a broader focus including modulation of MMP secretion, cell morphology, and cell migration. With regard to the treatment of inflammatory disorders and metastasis, it might be useful to target the signaling pathways regulating these MMPs in more detail.

ACKNOWLEDGEMENTS

A part of the data has been presented as a plenary talk on the Single Topic Conference Liver Fibrosis of the EASL in Florence, 2001.

REFERENCES

1 **Stetler-Stevenson WG**, Aznavoorian S, Liotta LA. Tumor cell interactions with the extracellular matrix during invasion and metastasis. *Annu Rev Cell Biol* 1993; **9**: 541–573
2 **Coussens LM**, Werb Z. Matrix metalloproteinases and the development of cancer. *Chem Biol* 1996; **3**: 895–904
3 **Shapiro SD**. Matrix metalloproteinase degradation of extracellular matrix: biological consequences. *Curr Opin Cell Biol* 1998; **10**: 602–608
4 **Yu Q**, Stamenkovic I. Cell surface-localized matrix metalloproteinase-9 proteolytically activates TGF-beta and promotes tumor invasion and angiogenesis. *Genes Dev* 2000; **14**: 163-176
5 **Ratzinger G**, Stoitzner P, Ebner S, Lutz MB, Layton GT, Rainer C, Senior RM, Shipley JM, Fritsch P, Schuler G, Romani N. Matrix metalloproteinases 9 and 2 are necessary for the migration of Langerhans cells and dermal dendritic cells from human and murine skin. *J Immunol* 2002; **168**: 4361–4371
6 **Gu J**, Nishiuchi R, Sekiguchi K. Matrix metalloproteinase-2 is involved in A549 cell migration on laminin-10/11. *Biochem Biophys Res Commun* 2002; **296**: 73–77
7 **Kang T**, Yi J, Guo A, Wang X, Overall CM, Jiang W, Elde R, Borregaard N, Pei D. Subcellular distribution and cytokine- and chemokine-regulated secretion of leukolysin/MT6-MMP/MMP-25 in neutrophils. *J Biol Chem* 2001; **276**: 21960–21968
8 **St-Pierre Y**, Van Themsche C, Esteve PO. Emerging features in the regulation of MMP-9 gene expression for the development of novel molecular targets and therapeutic strategies. *Curr Drug Targets Inflamm Allergy* 2003; **2**: 206–215
9 **Arthur MJ**. Collagenases and liver fibrosis. *J Hepatol* 1995; **22**: 43–48
10 **McCrudden R**, Iredale JP. Liver fibrosis, the hepatic stellate cell and tissue inhibitors of metalloproteinases. *Histol Histopathol* 2000; **15**: 1159–1168
11 **Mannello F**, Gazzanelli G. Tissue inhibitors of metalloproteinases and programmed cell death: conundrums, controversies and potential implications. *Apoptosis* 2001; **6**: 479–482
12 **Murphy FR**, Issa R, Zhou X, Ratnarajah S, Nagase H, Arthur MJ, Benyon C, Iredale JP. Inhibition of apoptosis of activated hepatic stellate cells by tissue inhibitor of metalloproteinase-1 is mediated via effects on matrix metalloproteinase inhibition: implications for reversibility of liver fibrosis. *J Biol Chem* 2002; **277**: 11069–11076
13 **Guedez L**, Courtemanch L, Stetler-Stevenson M. Tissue inhibitor of metalloproteinase (TIMP)-1 induces differentiation and an antiapoptotic phenotype in germinal center B cells. *Blood* 1998; **92**: 1342-1349
14 **Guedez L**, Stetler-Stevenson WG, Wolff L, Wang J, Fukushima P, Mansoor A, Stetler-Stevenson M. *In vitro* suppression of programmed cell death of B cells by tissue inhibitor of metalloproteinases-1. *J Clin Invest* 1998; **102**: 2002–2010
15 **Gaudin P**, Trocme C, Berthier S, Kieffer S, Boutonnat J, Lamy C, Surla A, Garin J, Morel F. TIMP-1/MMP-9 imbalance in an EBV-immortalized B lymphocyte cellular model: evidence for TIMP-1 multifunctional properties. *Biochim Biophys Acta* 2000; **1499**: 19–33
16 **Lambert E**, Boudot C, Kadri Z, Soula-Rothhut M, Sowa ML, Mayeux P, Hornebeck W, Haye B, Petitfrere E. Tissue inhibitor of metalloproteinases-1 signalling pathway leading to erythroid cell survival. *Biochem J* 2003; **372**: 767–774
17 **Ikenaka Y**, Yoshiji H, Kuriyama S, Yoshii J, Noguchi R, Tsujinoue H, Yanase K, Namisaki T, Imazu H, Masaki T, Fukui H. Tissue inhibitor of metalloproteinases-1 (TIMP-1) inhibits tumor growth and angiogenesis in the TIMP-1 transgenic mouse model. *Int J Cancer* 2003; **105**: 340–346
18 **Alexander JP**, Acott TS. Involvement of the Erk-MAP kinase pathway in TNFalpha regulation of trabecular matrix metalloproteinases and TIMPs. *Invest Ophthalmol Vis Sci* 2003; **44**: 164–169
19 **Wang T**, Yamashita K, Iwata K, Hayakawa T. Both tissue inhibitors of metalloproteinases-1 (TIMP-1) and TIMP-2 activate Ras but through different pathways. *Biochem Biophys Res Commun* 2002; **296**: 201–205
20 **Tanimura S**, Asato K, Fujishiro SH, Kohno M. Specific blockade of the ERK pathway inhibits the invasiveness of tumor cells: down-regulation of matrix metalloproteinase-3/-9/-14 and CD44. *Biochem Biophys Res Commun* 2003; **304**: 801–806
21 **Woo JH**, Park JW, Lee SH, Kim YH, Lee IK, Gabrielson E, Lee SH, Lee HJ, Kho YH, Kwon TK. Dykellic acid inhibits phorbol myristate acetate-induced matrix metalloproteinase-9 expression by inhibiting nuclear factor kappa B transcriptional activity. *Cancer Res* 2003; **63**: 3430–3434
22 **Hah N**, Lee ST. An absolute role of the PKC-dependent NF-kappaB activation for induction of MMP-9 in hepatocellular carcinoma cells. *Biochem Biophys Res Commun* 2003; **305**: 428–433
23 **Esparza J**, Vilardell C, Calvo J, Juan M, Vives J, Urbano-Marquez A, Yague J, Cid MC. Fibronectin upregulates gelatinase B (MMP-9) and induces coordinated expression of gelatinase A (MMP-2) and its activator MT1-MMP (MMP-14) by human T lymphocyte cell lines. A process repressed through RAS/MAP kinase signaling pathways. *Blood* 1999; **94**: 2754–2766
24 **Nakopoulou L**, Tsirmpa I, Alexandrou P, Louvrou A, Ampela C, Markaki S, Davaris PS. MMP-2 protein in invasive breast cancer and the impact of MMP-2/TIMP-2 phenotype on overall survival. *Breast Cancer Res Treat* 2003; **77**: 145–155
25 **Denkert C**, Siegert A, Leclere A, Turzynski A, Hauptmann S. An inhibitor of stress-activated MAP-kinases reduces invasion and MMP-2 expression of malignant melanoma cells. *Clin Exp Metastasis* 2002; **19**: 79–85
26 **Pan MR**, Hung WC. Nonsteroidal anti-inflammatory drugs inhibit matrix metalloproteinase-2 via suppression of the ERK/Sp1-mediated transcription. *J Biol Chem* 2002; **277**: 32775–32780
27 **Roeb E**, Winograd R, Breuer B, Nguyen H, Matern S. Increased TIMP-1 activity results in increased expression of gelatinases and altered cell motility. *J Cell Biochem* 1999; **75**: 346–355
28 **Roeb E**, Behrmann I, Grötzinger J, Breuer B, Matern S. An MMP-9 mutant without gelatinolytic activity as a novel TIMP-1-antagonist. *FASEB J* 2000; **14**: 1671–1673
29 **Roeb E**, Graeve L, Müllberg J, Matern S, Rose-John S. TIMP-1 protein expression is stimulated by IL-1 beta and IL-6 in primary rat hepatocytes. *FEBS Lett* 1994; **349**: 45–49
30 **Wach F**, Eyrich AM, Wustrow T, Krieg T, Hein R. Comparison of migration and invasiveness of epithelial tumor and melanoma cells *in vitro*. *J Dermatol Sci* 1996; **12**: 118–126

31 **Campbell SL**, Khosravi-Far R, Rossman KL, Clark GJ, Der CJ. Increasing complexity of Ras signaling. *Oncogene* 1998; **17**: 1395–1413

32 **Nakatsukasa H**, Ashida K, Higashi T, Ohguchi S, Tsuboi S, Hino N, Nouso K, Urabe Y, Kinugasa N, Yoshida K, Uematsu S, Ishizaki M, Kobayashi Y, Tsuji T. Cellular distribution of transcripts for tissue inhibitor of metalloproteinases 1 and 2 in human hepatocellular carcinomas. *Hepatology* 1996; **24**: 82–88

33 **Li G**, Fridman R, Kim HR. Tissue inhibitor of metalloproteinase-1 inhibits apoptosis of human breast epithelial cells. *Cancer Res* 1999; **59**: 6267–6275

34 **Gomez DE**, Alonso DF, Yoshiji H, Thorgeirsson UP. Tissue inhibitors of metalloproteinases: structure, regulation and biological functions. *Eur J Cell Biol* 1997; **74**: 111–122

35 **Murphy G**, Willenbrock F. Tissue inhibitors of matrix metalloendopeptidases. *Methods Enzymol* 1995; **248**: 496–510

36 **Nagase H**, Woessner JF. Matrix metalloproteinases. *J Biol Chem* 1999; **274**: 21491–21494

37 **Khokha R**, Zimmer MJ, Graham CH, Lala PK, Waterhouse P. Suppression of invasion by inducible expression of tissue inhibitor of metalloproteinase-1 (TIMP-1) in B16-F10 melanoma cells. *J Natl Cancer Inst* 1992; **84**: 1017–1022

38 **Kato S**, Yasukawa H, Fujii T, Yamaguchi M, Miyagi N, Okamoto K, Wada Y, Miyamoto T, Morimatsu M, Fox JC. Coordinate regulation of matrix metalloproteinase-1 and tissue inhibitor of metalloproteinase-1 expression in human vascular smooth muscle cells. *Connect Tissue Res* 2000; **41**: 143–153

39 **Palecek SP**, Loftus JC, Ginsberg MH, Lauffenburger DA, Horwitz AF. Integrin-ligand binding properties govern cell migration speed through cell-substratum adhesiveness. *Nature* 1997; **385**: 537–540

40 **Ashida N**, Arai H, Yamasaki M, Kita T. Distinct signaling pathways for MCP-1-dependent integrin activation and chemotaxis. *J Biol Chem* 2001; **276**: 16555–16560

41 **Sun Y**, Cheng Z, Ma L, Pei G. Beta-arrestin2 is critically involved in CXCR4-mediated chemotaxis, and this is mediated by its enhancement of p38 MAPK activation. *J Biol Chem* 2002; **277**: 49212–49219

42 **Cara DC**, Kaur J, Forster M, McCafferty DM, Kubes P. Role of p38 mitogen-activated protein kinase in chemokine-induced emigration and chemotaxis *in vivo*. *J Immunol* 2001; **167**: 6552–6558

43 **Kerkhoff E**, Rapp UR. Cell cycle targets of Ras/Raf signalling. *Oncogene* 1998; **17**: 1457–1462

44 **Liao J**, Wolfman JC, Wolfman A. K-ras regulates the steady-state expression of matrix metalloproteinase 2 in fibroblasts. *J Biol Chem* 2003; **278**: 31871–31878

45 **Alhasan SA**, Aranha O, Sarkar FH. Genistein elicits pleiotropic molecular effects on head and neck cancer cells. *Clin Cancer Res* 2001; **7**: 4174–4181

46 **Holvoet S**, Vincent C, Schmitt D, Serres M. The inhibition of MAPK pathway is correlated with down-regulation of MMP-9 secretion induced by TNF-alpha in human keratinocytes. *Exp Cell Res* 2003; **290**: 108–119

47 **Wang X**, Mori T, Jung JC, Fini ME, Lo EH. Secretion of matrix metalloproteinase-2 and -9 after mechanical trauma injury in rat cortical cultures and involvement of MAP kinase. *J Neurotrauma* 2002; **19**: 615–625

48 **Vitale S**, Schmid-Alliana A, Breuil V, Pomeranz M, Millet MA, Rossi B, Schmid-Antomarchi H. Soluble fractalkine prevents monocyte chemoattractant protein-1-induced monocyte migration via inhibition of stress-activated protein kinase 2/p38 and matrix metalloproteinase activities. *J Immunol* 2004; **172**: 585–592

PO Box 2345, Beijing 100023, China
www.wjgnet.com
wjg@wjgnet.com

ELSEVIER

World J Gastroenterol 2005;11(8):1105-1108
World Journal of Gastroenterology ISSN 1007-9327

Expression of cyclooxygenase-2 in colorectal cancer and its clinical significance

Bin Xiong, Tao-Jiao Sun, Wei-Dong Hu, Fu-Lin Cheng, Min Mao, Yun-Feng Zhou

Bin Xiong, Tao-Jiao Sun, Wei-Dong Hu, Fu-Lin Cheng, Min Mao, Yun-Feng Zhou, Department of Oncology, Affiliated Zhongnan Hospital of Wuhan University, Wuhan 430071, Hubei Province, China
Supported by Hubei Province Natural Science Foundation, No. 2000J054
Correspondence to: Dr. Yun-Feng Zhou, Affiliated Zhongnan Hospital of Wuhan University, Wuhan 430071, Hubei Province, China. binxiong88@yahoo.com
Telephone: +86-27-67813358
Received: 2004-02-06 Accepted: 2004-04-05

Abstract

AIM: To clarify the clinicopathologic significance of COX-2 expression in human colorectal cancer.

METHODS: A total of 128 surgically resected colorectal cancer specimens were immunohistochemically analyzed with the use of anti-COX-2, anti-VEGF and anti-MMP-2 antibodies. The relationship between the cyclooxygenase-2 expression in primary lesions of colorectal cancer and clinicopathologic parameters was evaluated by chi-square test.

RESULTS: Among 128 cases of colorectal cancer, 87 (67.9%) were positive for cyclooxygenase-2. The expression of cyclooxygenase-2 was significantly correlated with the depth of invasion, stage of disease, and metastasis (lymph node and liver). Patients in T3-T4, stages III-IV and with metastasis had much higher expression of cyclooxygenase-2 than ones in T1-T2, stages I-II and without metastasis ($P<0.05$). Among 45 cases of colorectal cancer with lymph node metastasis, the COX-2-positive rate was 86.7% (39/45) for primary lesions and diffuse cytoplasmic staining for COX-2 protein was detected in cancer cells in 100% of metastatic lesions of the lymph nodes. VEGF expression was detected in 49 tumors (38.3%), and VEGF expression was closely correlated with COX-2 expression. The positive expression rate of VEGF (81.6%) in the cyclooxygenase-2-positive group was higher than that in the cyclooxygenase-2-negative group (18.4%, $P<0.05$). MMP-2 expression was detected in 88 tumors (68.8%), and MMP-2 expression was closely correlated with COX-2 expression. The positive expression rate of MMP-2 (79.6%) in the positive COX-2 group was higher than that in the negative COX-2 group (20.4%, $P<0.05$).

CONCLUSION: Cyclooxygenase-2 may be associated with tumor progression by modulating the angiogenesis and cancer cell motility and invasive potential in colorectal cancer and it can be used as a possible biomarker.

Key words: Cyclooxygenase-2; Colorectal cancer; Immunohistochemical

Xiong B, Sun TJ, Hu WD, Cheng FL, Mao M, Zhou YF. Expression of cyclooxygenase-2 in colorectal cancer and its clinical significance. *World J Gastroenterol* 2005; 11(8): 1105-1108

http://www.wjgnet.com/1007-9327/11/1105.asp

INTRODUCTION

Cancer has been described as a disease of aberrant signal transduction. Carcinogenesis is a multistep process characterized by progressive changes in the amounts or activity of proteins that regulate cellular proliferation, differentiation, and survival. These changes can be mediated through both genetic and epigenetic mechanisms. Cyclooxygenase (COX) is a rate-limiting enzyme in prostaglandin biosynthesis[1]. Evidence suggests that nonsteroidal anti-inflammatory drugs reduce the risk of colorectal cancer and that this effect is mediated through COX inhibition[2-4]. Two COX isoforms, COX-1 and COX-2, have been identified. COX-1 is constitutively expressed and involved in general cell functions, whereas COX-2 is an inducible enzyme that is up-regulated in response to various stimuli, including growth factors and mitogens[5-8]. An enhanced expression of COX-2 has been found in many tumors, such as the lung, breast, esophageal, and colon cancers[2-4,9-11]. Recent studies have demonstrated that COX-2 could affect carcinogenesis via several different mechanisms[1,12-15]. Overexpression of COX-2 leads to phenotypic changes involving increased adhesion to the extracellular matrix and inhibition of apoptosis in rat intestinal epithelial cell, which could enhance their tumorigenic potential[3,8,10,15-18]. Constitutive expression of COX-2 can also lead to alterations in the invasive potential of colorectal cancer cells, and COX-2 may be involved in tumor angiogenesis[1,11,13,17-20]. COX-2 may be related to the development of colorectal cancer, but the precise role of COX-2 in colorectal cancer is not yet fully known.

In this study we compared COX-2 expression in primary and metastatic lesions by immunohistochemical staining in a group of colorectal cancer patients. Our objective was to

determine the clinical significance of COX-2 in advance of colorectal cancer.

MATERIALS AND METHODS

Patients

A total of 128 cases of colorectal adenocarcinoma that had undergone surgical resection were collected in the Affiliated Zhongnan Hospital of Wuhan University (Wuhan, China) from January 1999 to September 2002, and COX-2, VEGF and MMP-2 immunohistochemical staining were performed. There were 73 men and 55 women, and their age ranged from 23 to 74 years (mean, 56±11 years). Among 128 patients, 26 were well-differentiated adenocarcinoma, 57 moderately differentiated adenocarcinoma and 45 poorly differentiated adenocarcinoma. According to Dukes' staging criteria, 37 cases were stage I, 41 stage II, 39 stage III and 11 stage IV.

Methods

Immunohistochemical staining All the tissue specimens were fixed in 100 mol/L neutral formalin and embedded in paraffin. Five-μm thick sections were dewaxed in xylene and dehydrated in ethanol. Tissue sections were washed three times in 0.05 mol/L PBS, and incubated in endogenous peroxidase blocking solution. Non-specific antibody binding was blocked by pretreatment with PBS containing 5 g/L bovine serum albumin. Sections were then rinsed in PBS and incubated overnight at 4 ℃ with diluted anti-COX-2 (Santa Cruz), anti-VEGF (Bosden, Wuhan, China) and anti-MMP-2 (Santa Cruz) antibodies. The steps were performed using S-P detection kit (Maxin, Fuzhou, China) according to the manufacturer's instructions. PBS was used as substitutes of antibody for negative control. The sections were examined under light microscope.

Evaluation of the staining Evaluation for COX-2 was performed according to the following scoring system[1]: staining intensity was graded as weak (1), moderate (2), or strong (3), and area of staining positivity as <10% (0) of all cells stained in the cytoplasm, 10-40% (1), 40-70% (2), or ⩾70% (3). Total scores for grade and area of three or more was defined as positive expression and less than three as negative. Positive signal for VEGF and MMP-2 was located in the cytoplasm or/and cell membrane[11,21-24]. Immunoreactivity was graded as follows: +, ⩾10% stained tumor cells; and −, <10% stained tumor cells[18,25-28].

Statistical analysis

The difference between each group was analyzed by χ^2 test. $P<0.05$ was considered significant.

RESULTS

COX-2 expression in colorectal cancer and clinicopathologic findings

COX-2 was expressed in the cytoplasm of cancer cells (Figure 1A) and the expression in primary tumor was noted in 67.9% (87/128). The correlation between COX-2 expression and the clinicopathologic findings is shown in Table 1. The expression of COX-2 was significantly correlated with depth of invasion, stage of disease and metastasis (lymph node and liver). Patients in T3-T4, stages III-IV and metastasis had much higher COX-2 expression than ones in T1-T2, stages I-II and without metastasis ($P<0.05$). The expression of COX-2 was not correlated with age, gender and differentiation degree of the tumor ($P>0.05$).

Table 1 Clinicopathologic characteristics of colorectal cancer with expression of COX-2

Variable	*n*	COX-2 positive *n* (%)	COX-2 negative *n* (%)
Sex			
Male	73	50 (68.5)	23 (31.5)
Female	55	37 (67.3)	18 (32.7)
Age (yr)		54±12	56±15
Histological differentiation			
Well	26	17 (65.4)	9 (34.6)
Moderate	57	40 (70.2)	17 (29.8)
Poor	45	30 (66.7)	15 (33.3)
Depth of invasion			
T1-T2	81	48 (59.3)	33 (40.7)
T3-T4	47	39 (83.0)	8 (17.0)[a]
Metastasis			
Present	50	42 (84.0)	8 (16.0)
Absent	78	45 (57.7)	33 (42.3)[a]
Dukes stage			
I	37	15 (40.5)	22 (59.5)
II	41	28 (68.3)	13 (31.7)
III+IV	50	44 (88.0)	6 (12.0)[a]
VEGF expression			
Positive	49	40 (81.6)	9 (18.4)
Negative	79	47 (59.5)	32 (40.5)[a]
MMP-2 expression			
Positive	88	70 (79.6)	18 (20.4)
Negative	40	17 (42.5)	23 (57.5)[a]

[a]$P<0.05$ *vs* positive.

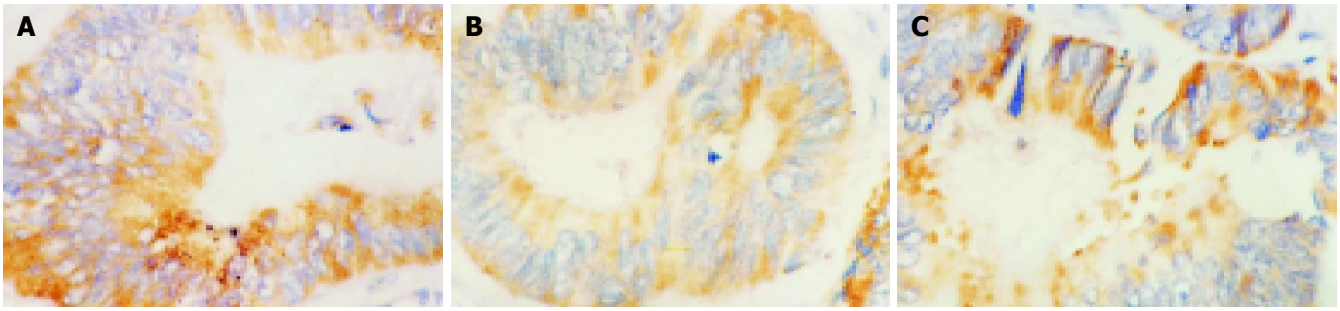

Figure 1 Expression of COX-2, VEGF and MMP-2 in well-differentiated colon adenocarcinoma. A: The staining of COX-2 is mainly in the cytoplasm of tumor cells. S-P, ×400; B: The staining of VEGF is mainly in the cytoplasm and membrane of tumor cells. S-P, ×400; C: The staining of MMP-2 is mainly in cytoplasm and membrane of tumor cells. S-P, ×400.

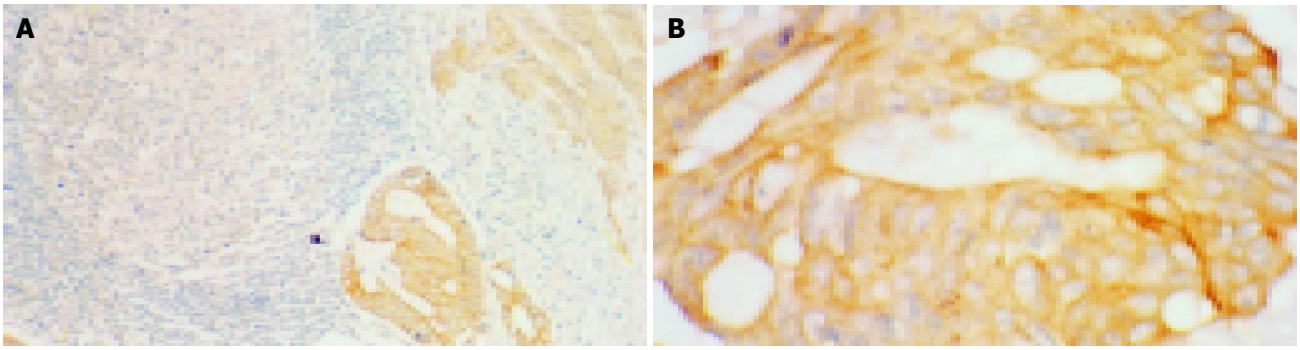

Figure 2 COX-2 expression in lymph node metastatic lesions. A: The staining is mainly in cytoplasm of tumor cells. S-P, ×200; B: The staining is mainly in cytoplasm of tumor cells. S-P, ×400.

Relationship between COX-2, VEGF and MMP-2 expression

VEGF was mainly localized in the cytoplasm and cell membrane of the tumor cells (Figure 1B). VEGF expression was detected in 49 tumors (38.3%), and VEGF expression was closely correlated with COX-2 expression (Table 1). The positive expression rate of VEGF (81.6%) in the positive COX-2 group was higher than that in the negative COX-2 group (18.4%, $P<0.05$).

MMP-2 was mainly localized in the cytoplasm and cell membrane of the tumor cells (Figure 1C). MMP-2 expression was detected in 88 tumors (68.8%), and MMP-2 expression was closely correlated with COX-2 expression (Table 1). The positive expression rate of MMP-2 (79.6%) in the positive COX-2 group was higher than that in the negative COX-2 group (20.4%, $P<0.05$).

Relationship of COX-2 expression between primary and lymph node metastatic lesions

Among 45 cases of colorectal cancer with lymph node metastasis, the COX-2 positive rate was 86.7% (39/45) for primary lesions and 100% for metastatic lesions in the lymph nodes. All cases with no staining in the primary lesion showed COX-2 staining in the metastatic lesion in the lymph nodes (Figures 2A, B).

DISCUSSION

Epidemiological and experimental studies have demonstrated the effect of non-steroidal anti-inflammatory drugs in the prevention of human cancers[1,5-7,16-18]. These drugs block endogenous prostaglandin synthesis through inhibition of COX enzymatic activity[17,20,23-26]. COX-2 is an inducible enzyme that catalyzes the conversion of arachidonic acid to biologically active prostanoids. COX-2 modulates the growth and function of many cells, including those with malignant transformation. The over-expression of COX-2 has been reported in tissues from patients with different carcinoma, and is believed to play a role in tumor transformation and progression, as well as in tumor regression[1,4-7,18,29-32]. Recent experimental studies showed that COX-2 inhibits cell apoptosis, regulates angiogenesis, and is associated with matrix metalloproteinases (MMP)[16,26,33-35].

COX-2 was over-expressed in approximate 80% of colorectal cancer cases[1,18,30,36], and may be related to the development of colorectal cancer. However, the precise role of COX-2 in colorectal cancer is not yet fully known. Yamauchi *et al*[1] reported that COX-2 expression correlated significantly with histologic type, depth of invasion, pathologic stage, and metachronous liver metastasis of colorectal cancer. Multivariate analysis for factors associated with metachronous liver metastasis of colorectal cancer showed that COX-2 expression was one of the independent risk factors, second only to lymph node metastasis[1]. COX-2 expression in the primary lesion may be a useful marker for evaluating prognosis and liver metastasis in patients with colorectal cancer[1]. In our study, COX-2 expression was detected in 87 tumors (67.9%). The expression of COX-2 was significantly correlated with the depth of invasion, stage of disease and metastasis (lymph node and liver). Patients in T3-T4, stages III-IV and with metastasis had much higher expression of COX-2 than ones in T1-T2, stages I-II and without metastasis ($P<0.05$). Among 45 cases of colorectal cancer with lymph node metastasis, the COX-2-positive rate was 86.7% (39/45) for primary lesions and diffuse cytoplasmic staining for COX-2 protein was detected in cancer cells in 100% of metastatic lesions in the lymph nodes. The preferential expression of COX-2 in lymph node metastases suggests a clonal selection of tumor cells with COX-2 expression, specific for the higher potential of lymph node metastasis in tumor advance, and COX-2 plays a role related to the malignant progression of colorectal cancer.

Masferrer *et al*[31] reported that COX-2 stimulates endothelial cell migration and vessel tube formation, which are inhibited by NSAIDs. They also reported that COX-2 affects MMP-2 and activated collagenase levels. This study found that the expression of VEGF and MMP-2 in COX-2-positive group is significantly higher than that in COX-2-negative group. The expression of COX-2 is significantly correlated with the expression of VEGF. It demonstrated that COX-2 might be indirectly correlated with angiogenesis through an up-regulation of the expression of VEGF. The expression of COX-2 is also significantly correlated with MMP-2 in colorectal cancer. It indicates that COX-2 can also lead to alterations in the invasive potential of colorectal cancer cells through an up-regulation of the expression of MMP-2. It suggests that COX-2 is closely related to the invasion and metastasis of colorectal cancer and it may be used as a possible biomarker.

REFERENCES

1 **Yamauchi T**, Watanabe M, Kubota T, Hasegawa H, Ishii Y, Endo T, Kabeshima Y, Yorozuya K, Yamamoto K, Mukai M, Kitajima M. Cyclooxygenase-2 expression as a new marker for patients with colorectal cancer. *Dis Colon Rectum* 2002; **45**: 98–103
2 **Qiu DK**, Ma X, Peng YS, Chen XY. Significance of cyclooxygenase-2 expression in human primary hepatocellular carcinoma. *World J Gastroenterol* 2002; **8**: 815–817
3 **Wu QM**, Li SB, Wang Q, Wang DH, Li XB, Liu CZ. The expression of COX-2 in esophageal carcinoma and its relation to clinicopathologic characteristics. *Shijie Huaren Xiaohua Zazhi* 2001; **9**: 11–14
4 **Wu HP**, Wu KC, Li L, Yao LP, Lan M, Wang X, Fan DM. Cloning of human cyclooxygenase-2 (COX-2) encoding gene and study of gastric cancer cell transfected with its antisense vector. *Shijie Huaren Xiaohua Zazhi* 2000; **8**: 1211-1217
5 **Cao Y**, Prescott SM. Many actions of cyclooxygenase-2 in cellular dynamics and in cancer. *J Cell Physiol* 2002; **190**: 279–286
6 **Koki AT**, Masferrer JL. Celecoxib: a specific COX-2 inhibitor with anticancer properties. *Cancer Control* 2002; **9**: 28-35
7 **Kakiuchi Y**, Tsuji S, Tsujii M, Murata H, Kawai N, Yasumaru M, Kimura A, Komori M, Irie T, Miyoshi E, Sasaki Y, Hayashi N, Kawano S, Hori M. Cyclooxygenase-2 activity altered the cell-surface carbohydrate antigens on colon cancer cells and enhanced liver metastasis. *Cancer Res* 2002; **62**: 1567-1572
8 **Hida T**, Kozaki K, Ito H, Miyaishi O, Tatematsu Y, Suzuki T, Matsuo K, Sugiura T, Ogawa M, Takahashi T, Takahashi T. Significant growth inhibition of human lung cancer cells both *in vitro* and *in vivo* by the combined use of a selective cyclooxygenase2 inhibitor, JTE-522, and conventional anticancer agents. *Clin Cancer Res* 2002; **8**: 2443–2447
9 **Yamada H**, Kuroda E, Matsumoto S, Matsumoto T, Yamada T, Yamashita U. Prostaglandin E2 down-regulates viable Bacille Calmette-Guerin-induced macrophage cytotoxicity against murine bladder cancer cell MBT-2 *in vitro*. *Clin Exp Immunol* 2002; **128**: 52-58
10 **Harizi H**, Juzan M, Pitard V, Moreau JF, Gualde N. Cyclooxygenase-2-issued prostaglandin e(2) enhances the production of endogenous IL-10, which down-regulates dendritic cell functions. *J Immunol* 2002; **168**: 2255-2263
11 **Kundu N**, Fulton AM. Selective cyclooxygenase (COX)-1 or COX-2 inhibitors control metastatic disease in a murine model of breast cancer. *Cancer Res* 2002; **62**: 2343–2346
12 **Leahy KM**, Ornberg RL, Wang Y, Zweifel BS, Koki AT, Masferrer JL. Cyclooxygenase-2 inhibition by celecoxib reduces proliferation and induces apoptosis in angiogenic endothelial cells *in vivo*. *Cancer Res* 2002; **62**: 625–631
13 **Hansen-Petrik MB**, McEntee MF, Jull B, Shi H, Zemel MB, Whelan J. Prostaglandin E(2) protects intestinal tumors from nonsteroidal anti-inflammatory drug-induced regression in Apc(Min/+) mice. *Cancer Res* 2002; **62**: 403–408
14 **Waskewich C**, Blumenthal RD, Li H, Stein R, Goldenberg DM, Burton J. Celecoxib exhibits the greatest potency amongst cyclooxygenase (COX) inhibitors for growth inhibition of COX-2-negative hematopoietic and epithelial cell lines. *Cancer Res* 2002; **62**: 2029–2033
15 **Jones MK**, Szabo IL, Kawanaka H, Husain SS, Tarnawski AS. von Hippel Lindau tumor suppressor and HIF-1alpha: new targets of NSAIDs inhibition of hypoxia-induced angiogenesis. *FASEB J* 2002; **16**: 264–266
16 **Kvirkvelia N**, Vojnovic I, Warner TD, Athie-Morales V, Free P, Rayment N, Chain BM, Rademacher TW, Lund T, Roitt IM, Delves PJ. Placentally derived prostaglandin E2 acts via the EP4 receptor to inhibit IL-2-dependent proliferation of CTLL-2 T cells. *Clin Exp Immunol* 2002; **127**: 263–269
17 **Adam L**, Mazumdar A, Sharma T, Jones TR, Kumar R. A three-dimensional and temporo-spatial model to study invasiveness of cancer cells by heregulin and prostaglandin E2. *Cancer Res* 2001; **61**: 81–87
18 **Dannhardt G**, Ulbrich H. *In-vitro* test system for the evaluation of cyclooxygenase-1 (COX-1) and cyclooxygenase-2 (COX-2) inhibitors based on a single HPLC run with UV detection using bovine aortic coronary endothelial cells (BAECs). *Inflamm Res* 2001; **50**: 262–269
19 **Bae SH**, Jung ES, Park YM, Kim BS, Kim BK, Kim DG, Ryu WS. Expression of cyclooxygenase-2 (COX-2) in hepatocellular carcinoma and growth inhibition of hepatoma cell lines by a COX-2 inhibitor, NS-398. *Clin Cancer Res* 2001; **7**: 1410–1418
20 **Yang WL**, Frucht H. Activation of the PPAR pathway induces apoptosis and COX-2 inhibition in HT-29 human colon cancer cells. *Carcinogenesis* 2001; **22**: 1379–1383
21 **Dohadwala M**, Luo J, Zhu L, Lin Y, Dougherty GJ, Sharma S, Huang M, Pold M, Batra RK, Dubinett SM. Non-small cell lung cancer cyclooxygenase-2 dependent invasion is mediated by CD44. *J Biol Chem* 2001; **276**: 20809-20812
22 **Dempke W**, Rie C, Grothey A, Schmoll HJ. Cyclooxygenase-2: a novel target for cancer chemotherapy? *J Cancer Res Clin Oncol* 2001; **127**: 411-417
23 **Gilroy DW**, Saunders MA, Wu KK. COX-2 expression and cell cycle progression in human fibroblasts. *Am J Physiol Cell Physiol* 2001; **281**: C188–C194
24 **Chen WS**, Wei SJ, Liu JM, Hsiao M, Kou-Lin J, Yang WK. Tumor invasiveness and liver metastasis of colon cancer cells correlated with cyclooxygenase-2 (COX-2) expression and inhibited by a COX-2-selective inhibitor, etodolac. *Int J Cancer* 2001; **91**: 894–899
25 **Rozic JG**, Chakraborty C, Lala PK. Cyclooxygenase inhibitors retard murine mammary tumor progression by reducing tumor cell migration, invasiveness and angiogenesis. *Int J Cancer* 2001; **93**: 497–506
26 **Williams CS**, Tsujii M, Reese J, Dey SK, DuBois RN. Host cyclooxygenase-2 modulates carcinoma growth. *J Clin Invest* 2000; **105**: 1589–1594
27 **Marrogi A**, Pass HI, Khan M, Metheny-Barlow LJ, Harris CC, Gerwin BI. Human mesothelioma samples overexpress both cyclooxygenase-2 (COX-2) and inducible nitric oxide synthase(NOS2): *in vitro* antiproliferative effects of a COX-2 inhibitor. *Cancer Res* 2000; **60**: 3696–3700
28 **Uefuji K**, Ichikura T, Mochizuki H. Cyclooxygenase-2 expression is related to prostaglandin biosynthesis and angiogenesis in human gastric cancer. *Clin Cancer Res* 2000; **6**: 135–138
29 **Attiga FA**, Fernandez PM, Weeraratna AT, Manyak MJ, Patierno SR. Inhibitors of prostaglandin synthesis inhibit human prostate tumor cell invasiveness and reduce the release of matrix metalloproteinases. *Cancer Res* 2000; **60**: 4629–4637
30 **Shao J**, Sheng H, Inoue H, Morrow JD, DuBois RN. Regulation of constitutive cyclooxygenase-2 expression in colon carcinoma cells. *J Biol Chem* 2000; **275**: 33951–33956
31 **Masferrer JL**, Leahy KM, Koki AT, Zweifel BS, Settle SL, Woerner BM, Edwards DA, Flickinger AG, Moore RJ, Seibert K. Antiangiogenic and antitumor activities of cyclooxygenase-2 inhibitors. *Cancer Res* 2000; **60**: 1306–1311
32 **Reddy BS**, Hirose Y, Lubet R, Steele V, Kelloff G, Paulson S, Seibert K, Rao CV. Chemoprevention of colon cancer by specific cyclooxygenase-2 inhibitor, celecoxib, administered during different stages of carcinogenesis. *Cancer Res* 2000; **60**: 293–297
33 **Hsueh CT**, Chiu CF, Kelsen DP, Schwartz GK. Selective inhibition of cyclooxygenase-2 enhances mitomycin-C-induced apoptosis. *Cancer Chemother Pharmacol* 2000; **45**: 389–396
34 **Hida T**, Kozaki K, Muramatsu H, Masuda A, Shimizu S, Mitsudomi T, Sugiura T, Ogawa M, Takahashi T. Cyclooxygenase-2 inhibitor induces apoptosis and enhances cytotoxicity of various anticancer agents in non-small cell lung cancer cell lines. *Clin Cancer Res* 2000; **6**: 2006–2011
35 **Hull MA**, Fenwick SW, Chapple KS, Scott N, Toogood GJ, Lodge JP. Cyclooxygenase-2 expression in colorectal cancer liver metastases. *Clin Exp Metastasis* 2000; **18**: 21–27
36 **Ferrario A**, Von Tiehl K, Wong S, Luna M, Gomer CJ. Cyclooxygenase-2 inhibitor treatment enhances photodynamic therapy-mediated tumor response. *Cancer Res* 2002; **62**: 3956–3961

PO Box 2345, Beijing 100023, China
www.wjgnet.com
wjg@wjgnet.com

ELSEVIER

World J Gastroenterol 2005;11(8):1109-1114
World Journal of Gastroenterology ISSN 1007-9327

Importance of adequate immunosuppressive therapy for the recovery of patients with "life-threatening" severe exacerbation of chronic hepatitis B

Keiichi Fujiwara, Osamu Yokosuka, Hiroshige Kojima, Tatsuo Kanda, Hiromitsu Saisho, Hiroyuki Hirasawa, Hiroshi Suzuki

Keiichi Fujiwara, Osamu Yokosuka, Hiroshige Kojima, Tatsuo Kanda, Hiromitsu Saisho, Department of Medicine and Clinical Oncology, Graduate School of Medicine, Chiba University, Chiba 260-8670, Japan
Hiroyuki Hirasawa, Department of Emergency and Critical Care Medicine, Graduate School of Medicine, Chiba University, Chiba 260-8670, Japan
Hiroshi Suzuki, Department of Surgery, Takushinkai Tatsumi Hospital, Ichihara, Chiba 290-0003, Japan
Correspondence to: Osamu Yokosuka, M.D., Department of Medicine and Clinical Oncology, Graduate School of Medicine, Chiba University, 1-8-1 Inohana, Chuo-ku, Chiba 260-8670, Japan. yokosukao@faculty.chiba-u.jp
Telephone: +81-43-226-2083 Fax: +81-43-226-2088
Received: 2004-07-31 Accepted: 2004-09-09

Abstract

AIM: Hepatitis B virus (HBV) re-activation often occurs spontaneously or after withdrawal of immunosuppressive therapy in patients with chronic hepatitis B. Severe exacerbation, sometimes developing into fulminant hepatic failure, is at high risk of mortality. The efficacy of corticosteroid therapy in "clinically severe" exacerbation of chronic hepatitis B has not been well demonstrated. In this study we evaluated the efficacy of early introduction of high-dose corticosteroid therapy in patients with life-threatening severe exacerbation of chronic hepatitis B.

METHODS: Twenty-two patients, 14 men and 8 women, were defined as "severe" exacerbation of chronic hepatitis B using uniform criteria and enrolled in this study. Eleven patients were treated with corticosteroids at 60 mg or more daily with or without anti-viral drugs within 10 d after the diagnosis of severe disease ("early high-dose" group) and 11 patients were either treated more than 10 d or untreated with corticosteroids ("non-early high-dose" group).

RESULTS: Mean age, male-to-female ratio, mean prothrombin time (PT) activity, alanine transaminase (ALT) level, total bilirubin level, positivity of HBeAg, mean IgM-HBc titer, and mean HBV DNA polymerase activity did not differ between the two groups. Ten of 11 patients of the "early high-dose" group survived, while only 2 of 11 patients of the "non-early high-dose" group survived ($P<0.001$). During the first 2 wk after the introduction of corticosteroids, improvements in PT activities and total bilirubin levels were observed in the "early high-dose" group. Both ALT levels and HBV DNA polymerase levels fell in both groups.

CONCLUSION: The introduction of high-dose corticosteroid can reverse deterioration in patients with "clinically life-threatening" severe exacerbation of chronic hepatitis B, when used in the early stage of illness.

Key words: Chronic hepatitis B; Severe exacerbation; Immunosuppressive therapy

Fujiwara K, Yokosuka O, Kojima H, Kanda T, Saisho H, Hirasawa H, Suzuki H. Importance of adequate immunosuppressive therapy for the recovery of patients with "life-threatening" severe exacerbation of chronic hepatitis B. *World J Gastroenterol* 2005; 11(8): 1109-1114
http://www.wjgnet.com/1007-9327/11/1109.asp

INTRODUCTION

It is well recognized that exacerbation of hepatitis B may occur in chronic hepatitis B virus (HBV) carriers spontaneously or in relation to cytotoxic or immunosuppressive therapy. A clinical picture of acute hepatitis, and even severe exacerbation, sometimes fulminant hepatic failure, may develop and is associated with high mortality[1]. In a retrospective survey in Japan, a 53% incidence of severe hepatitis with a 24% mortality rate (mortality rate of 45% in severe hepatitis) is reported in relation to chemotherapy in HBV carriers with hematologic malignancies[2]. For the treatment of patients with severe exacerbation without malignancies who progressed to serious deterioration, liver transplantation may be considered. However, the problems of the shortage of donor- livers and the high cost of liver transplantation still remain in Japan. Thus, therapies other than transplantation must be further investigated for the hepatitis B patients with severe exacerbation.

In HBV infection, liver injury is considered to be induced mainly by CTL-mediated cytolytic pathways of infected hepatocytes[3]. Examination of B and T lymphocyte functions in patients with chronic hepatitis B revealed that serum alanine transaminase (ALT) level is closely correlated with suppressor T lymphocyte activity[4]. Sjogren *et al*[5] suggested that corticosteroids modulate the activity of chronic hepatitis B by suppressing the host-immune response to HBV antigens. Nouri-Aria *et al*[6] have shown the defects in suppressor T lymphocyte activity in chronic hepatitis B. Therefore, it must

be reasonable to treat chronic hepatitis B patients with corticosteroids in order to inhibit excessive immune response and prevent cytolysis of infected hepatocytes.

Corticosteroids have been used in the treatment of chronic active hepatitis B since the 1970s. However, in recent years corticosteroids have not been used for the routine management of chronic hepatitis B since the advantage of their use was not confirmed by control studies. For example, Lam *et al*[7] reported that long-term low-dose prednisolone treatment delays remission and increases relapse, complications, and death in a pair-randomized study, indicating that prednisolone has a deleterious effect on chronic active hepatitis B. Hoofnagle *et al*[8] showed that 4 wk of pre-dnisolone treatment produces no benefit in patients with chronic hepatitis B and is even harmful because of worsening of histopathological features. Scullard *et al*[9] showed that immunosuppressive therapy has a potentiating effect on hepatitis B viral replication in patients with chronic active hepatitis. However, these studies mainly dealt with cases of clinically "non-severe" hepatitis that is not urgently life-threatening and the effects of corticosteroid treatment for "potentially life-threatening" severe exacerbation of chronic hepatitis B as well as the timing and dose of treatment have not been well demonstrated. Lau *et al*[10] reported that the re-introduction of long-term high-dose corticosteroids in the early phase of reactivation after the withdrawal of immunosuppressive therapy prevents both progressive clinical deterioration and the potential need for orthotopic liver transplantation.

In this study, we investigated the clinicopathological features of chronic hepatitis B patients with severe exacerbation selected by uniform criteria, and treated with early introduction or reintroduction of sufficient doses of corticosteroids, in order to clarify the benefits and limitations of the effects of corticosteroids for amelioration of clinically severe exacerbation of chronic hepatitis B.

MATERIALS AND METHODS

Patients

Twenty-two chronic hepatitis B patients with severe exacerbation, who were admitted to our liver unit (Chiba University Hospital and related hospitals) during the last decade, were studied. The diagnosis of chronic hepatitis B viral carriers was made, based on either the positivity of hepatitis B surface antigen (HBsAg) for at least 6 mo before entry, or the positivity of hepatitis B surface antigen, anti-hepatitis B core antibody (HBcAb) at high titer and negativity or low titer of IgM anti-hepatitis B core antibody (IgM-HBc) in patients with follow-up periods less than 6 mo before entry. The patients, fulfilling the following three criteria during the course, were defined as having severe exacerbation: prothrombin time (PT) activity less than 60% of normal control, total bilirubin (T-bili) greater than 3.0 mg/dL, and ALT greater than 300 IU/L. All patients had a poor general condition, manifested as general malaise, fatigue, jaundice, edema, ascites and encephalopathy. Histological examination was performed in the convalescent phase or after death in 16 patients.

All patients were negative for IgM anti-HAV antibody, anti-hepatitis D antibody, anti-HCV antibody, HCV RNA, IgM anti-Epstein-Barr virus antibody (IgM-EBV), IgM anti-herpes simplex virus antibody (IgM-HSV), IgM anti-cytomegalovirus antibody (IgM-CMV), anti-nuclear antibody, anti-smooth muscle antibody, liver kidney microsomal antibody-1 and anti-mitochondrial antibody. Patients with a history of recent exposure to drugs and chemical agents and histories of recent heavy alcohol in-take were ruled out. None of the patients had clinical and laboratory evidence of acquired immune deficiency syndrome.

Protocols for treatment

Eleven patients were treated with "early high-dose" of corticosteroids (Table 1). Informed consent was obtained from patients or their appropriate family members. Corticosteroids, 60 mg or more prednisolone daily, was administered within 10 d after the diagnosis of severe disease using the above-mentioned criteria. The dosage of prednisolone was maintained at least for 4 d. When the patients showed a trend toward remission in PT[11], the dosage was reduced by 10 mg at least every 4 d to 30 mg. Then, the dosage was reduced by 2.5 or 5 mg every 2 wk or longer, depending on the decreasing trend of the ALT level.

The remaining 11 patients were not treated with "early high-dose" corticosteroids (Table 1), because it was already 10 d before they were admitted to our unit.

Two patients (patients 1 and 17) with marked prolongation of PT were treated with 1 000 mg of methylprednisolone daily for 3 d followed by the same pre-dnisolone therapy as described above. Two patients with deep hepatic coma at admission (patients 12 and 17) were treated with a combination therapy of corticosteroid and interferon. Interferon-β was administered at 3 million units/d. Afterwards, lamivudine, a nucleoside analogue with significant inhibition of HBV DNA polymerase, which could be used safely in patients with severe disease[12-17] was administered, in addition to prednisolone, at a daily dose of 150 mg in 3 patients, 2 in the "early high-dose" group (patients 6 and 7) and 1 in the "non-early high-dose" group (patient 14).

Four patients were treated with intravenous glycyrrhizin (stronger neominophagen C) at 60 mL/d, an aqueous extract of licorice root which is reported to have anti-inflammatory activity and has been used for the treatment of chronic viral hepatitis in Japan[18].

Serological markers

HBsAg, hepatitis B e antigen (HBeAg), anti-HBe antibody (HBeAb), HBcAb, IgM-HBc, IgM anti-HAV antibody, and anti-hepatitis D antibody were detected by commercial radioimmunoassay (Abbott Laboratories, Chicago, IL), and HCV RNA was measured by nested RT-PCR[19]. The second generation of anti-HCV anti-body was measured by enzyme immunoassay (Ortho Diagnostics, Tokyo, Japan). IgM-EBV, IgM-CMV, and IgM-HSV were examined by enzyme-linked immunosorbent assays. Anti-nuclear antibody, anti-smooth muscle antibody, anti-mitochondrial antibody, and anti-liver kidney microsomal-1 antibody were detected by fluorescent antibody method. HBV DNA polymerase was assayed according to the method of Kaplan *et al*[20]. HBV DNA level was measured by hybridization assay (Abbott) or branched DNA hybridization assay (Chiron, Emeryville, CA).

Table 1 Clinical features of patients

Pt	Age (yr)	Sex	Therapy drug	Duration (d)[1]	Condition	History of immunosuppresive or cytotoxic therapy	Outcome
Patients who received early introduction of high-dose corticosteroids							
1.	27	M	MPSL/PSL	1	Ulcerative colitis	+	Death
2.	36	M	PSL	2		-	Recovery
3.	41	F	PSL	3		-	Recovery
4.	27	M	PSL	4		-	Recovery
5.	41	F	PSL	4	Schizophrenia	-	Recovery
6.	33	M	PSL+Lam	4		-	Recovery
7.	68	F	PSL+Lam	4	Non-Hodgkin's lymphoma	+	Recovery
8.	56	M	PSL	5		-	Recovery
9.	57	F	PSL	5		-	Recovery
10.	39	M	PSL	5	Acute lymphocytic leukemia	+	Recovery
11.	43	M	PSL	10		-	Recovery
Patients who did not receive early introduction of high-dose corticosteroids							
12.	49	F	PSL+IFN	14	Non-Hodgkin's lymphoma	+	Death
13.	59	F	PSL	14		-	Death
14.	47	M	PSL+Lam	14	Ulcerative colitis	+	Death
15.	58	M	PSL	15		-	Death
16.	59	M	PSL	17		-	Death
17.	36	F	MPSL/PSL+IFN	28	Breast cancer	+	Death
18.	68	F	PSL	120	Pemphigoid	+	Death
19.	41	M	glycyrrhizin			-	Recovery
20.	55	M	glycyrrhizin			-	Recovery
21.	59	M	glycyrrhizin			-	Death
22.	28	M	glycyrrhizin		Mental retardation	-	Death

PSL: prednisolone, MPSL: methylprednisolone, IFN: interferon, Lam: lamivudine. [1]Duration between the diagnosis of severe disease and introduction of immunosuppressive drugs.

Statistical analysis

Differences among the groups were compared by Fisher's exact probability test, Student's *t* and Welch's *t*.

RESULTS

Clinicopathological features of severe chronic hepatitis B patients at admission

Of the 22 patients fulfilling the criteria of "severe" exacerbation, 14 were men and 8 women. The mean age at the time of admission was 46.7±12.9 years. HBeAg/HBeAb status was +/- in 7, -/+ in 12, +/+ in 2, and -/- in 1. Seven patients had primary diseases (2 non-Hodgkin's lymphoma, 2 ulcerative colitis, 1 acute lymphocytic leukemia, 1 breast cancer, and 1 pemphigoid), and all 7 had been treated with immunosuppressive or cytotoxic drugs, suffering exacerbations after their withdrawal. Two patients had primary conditions, 1 with schizophrenia, and the other with mental retardation. Eleven patients were treated with "early high-dose" corticosteroids and 11 were not. The clinical, biochemical, and histological features of all patients at admission are provided in Tables 1 and 2.

The clinicopathological features of the "early high-dose" and "non-early high-dose" groups of patients at admission stage were compared (Table 2). There were no differences in mean age, male-to-female ratio, mean PT activity, mean ALT level, mean T-bili level, positivity of HBeAg, mean IgM-HBc titer and HBV DNA polymerase activity between two groups. Serum HBV DNA was positive in 4 of 7 "early high-dose" patients and in 4 of 8 "non-early high-dose" patients. The duration between the diagnosis of severe exacerbation and the introduction of corticosteroids or immunosuppressive drugs was 4.3±2.3 d in the "early high-dose" group, and 31.7±39.3 d in the "non-early high-dose" group ($P = 0.11$).

Responses to corticosteroids and clinical outcomes

Ten of 11 patients were alive and well after treatment in the "early high-dose" group. Ten alive patients were free of hepatic encephalopathy during the course. One patient died of sepsis. In the "non-early high-dose" group, 2 patients recovered and 9 patients died ($P<0.001$). Eight patients died of hepatic failure and 1 (patient 22) of sepsis. Two patients (patients 12 and 17) had deep coma at admission, and neither responded to therapies including artificial liver support such as plasma exchange and hemodiafiltration. None of the remaining 9 patients had encephalopathy at admission, but 7 of them failed to respond to therapies and gradually developed hepatic failure.

Changes in PT activities, ALT levels, T-bili levels, and HBV DNA polymerase activities after the introduction of corticosteroid therapy are shown in Figure 1. Improvement of PT activities was found in all but one (patient 7) of the "early high-dose" group. In patient 7 treated with corticosteroid and lamivudine, PT activities fluctuated and improvement was delayed by some months (Figure 2). In the "non-early high-dose" group, improved PT activities were obtained in 2 patients but not in the others, although some of them showed transient rise after infusions of fresh frozen plasma. The elevation of PT activities in the first 2 wk was significant ($P = 0.006$) in the "early high-dose" group, but not in the "non-early high-dose" group (Figure 1A).

The ALT levels fell in all 22 patients during the course, with the decline in the first 2 wk being significant ($P<0.001$)

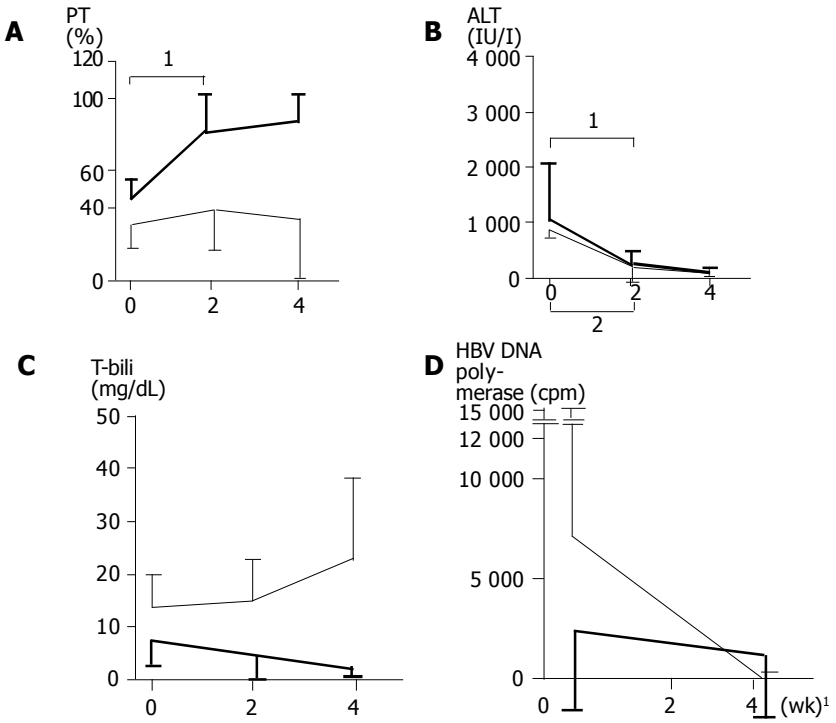

Figure 1 Prothrombin time activities (A), alanine transaminase levels (B), total bilirubin levels (C), and HBV DNA polymerase activities (D) before and after the administration of corticosteroids in 11 "early high-dose" and 11 "non-early high-dose" patients. Thick and thin lines denote those of "early high-dose" and "non-early high-dose", respectively. A: The mean activity at each point was 41±13, 77±23 and 81±19% in "early high-dose" and 29±13, 37±22 and 32±32% in "non-early high-dose", respectively. [1]Statistically significant (P = 0.006); B: The mean level at each point was 976±990, 225±200 and 100±53 IU/L in "early high-dose" and 816±1 072, 191±292 and 97±67 IU/L in "non-early high-dose", respectively. [2]Statistically significant (P<0.001); C: The mean activity at each point was 6.7±4.3, 3.8±4.4 and 1.5±0.7 mg/dL in "early high-dose" and 12.8±6.8, 14.2±8.3 and 22.2±14.9 mg/dL in "non-early high-dose", respectively; D: The mean level at each point was 2 325±3 879 and 1 282±3 022 cpm in "early high-dose", and 6 866±1 6981 and 44±86 cpm in "non-early high-dose", respectively.

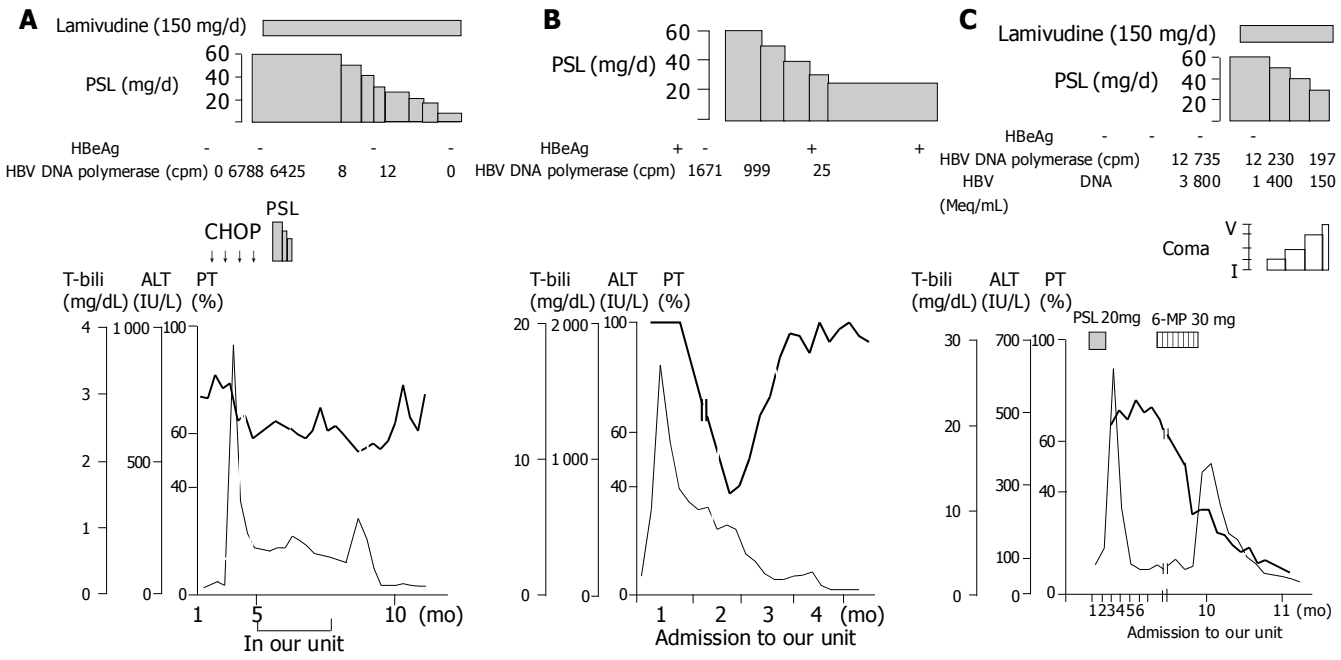

Figure 2 Clinical courses of patient 7 (A), patient 4 (B), and patient 14 (C). A: Clinical course of a 68-year-old female patient (patient 7). She suffered from non-Hodgkin's lymphoma and was found to be an HBV carrier with normal ALT, anti-HBe and no HBV DNA polymerase activity. After four cycles of chemotherapy (CHOP therapy), hematologic examination of her bone marrow showed complete remission, but reactivation of HBV occurred. High-dose corticosteroid was administered in combination with lamivudine because her serum HBV DNA titer was high. She gradually responded to the therapy. Thick solid, thin solid and dashed lines denote prothrombin time (PT), alanine transaminase (ALT) and total bilirubin (T-bili), respectively; B: Clinical course of a 27-year-old male patient (patient 4). He had natural reactivation of chronic hepatitis B and responded to corticosteroid therapy with transient HBeAg seroconversion; C: Clinical course of a 47-year-old male patient (patient 14). He suffered from chronic hepatitis B with anti-HBe and ulcerative colitis. He had HBV reactivation and convalesced spontaneously after the withdrawal of prednisolone. Six months later, he had repeated reactivation of HBV with marked prolonged PT and high level of viremia after the withdrawal of 6-mercaptopurine for ulcerative colitis, and was treated with corticosteroid and lamivudine, but did not respond to the combination therapy.

Table 2 Biochemical and histological features of patients at admission

Pt	PT (%)	ALT (IU/L)	T-bili (mg/dL)	HBeAg/HBeAb	IgM-HBc (cut-off index)	HBV DNA polymerase (cpm)	HBV DNA (Meq/mL)	Liver histology
Patients who received early introduction of high-dose corticosteroids								
1.	16	1 698	9.5	-/+	2.6	10	ND	ND
2.	31	2 689	3.0	+/-	0.3	3 517	ND	ND
3.	57	474	15.2	-/+	0.2	50	<0.70	ND
4.	37	495	12.0	+/-	0.3	999	920 pg/mL	CAH (F2, severe)
5.	37	155	8.0	-/-	0.5	ND	1+	ND
6.	56	2 080	4.2	+/+	1.8	595	<0.70	CAH (F2, severe)
7.	57	167	3.1	-/+	ND	6 425	ND	ND
8.	37	2 257	3.7	-/+	2.3	28	20	CAH (F3, severe)
9.	34	224	7.3	+/-	1.4	25	1.2	ND
10.	56	399	3.8	-/+	3.7	11 600	ND	Submassive necrosis
11.	46	101	6.4	-/+	0.3	10	<0.70	LC, submassive necrosis
Patients who did not receive early introduction of high-dose corticosteroids								
12.	29	254	12.6	-/+	1.1	0	<0.70	ND
13.	34	2 643	19.3	+/-	1.6	0	<0.70	ND
14.	32	240	2.9	-/+	0.5	12 735	3 800	ND
15.	28	228	13.3	-/+	3.3	16	1.1	Submassive necrosis
16.	29	150	13.3	-/+	0.2	53 856	>10 000	Submassive necrosis
17.	19	549	11.1	+/-	7.6	2	1.9	LC, submassive necrosis
18.	28	954	6.3	-/+	ND	ND	ND	Submassive necrosis
19.	59	214	12.9	+/+	0.4	5	ND	CAH (F3, moderate)
20.	38	3 620	7.7	-/+	0.2	0	<0.70	CAH (F3, moderate)
21.	33	164	8.9	+/-	ND	7 576	ND	LC, submassive necrosis
22.	21	49	8.0	+/-	1.0	0	<0.70	Submassive necrosis

CAH: chronic active hepatitis; LC: liver cirrhosis; ND: not done.

in both groups (Figure 1B). T-bili levels fell during the course in the "early high-dose" group, but rose in the "non-early high-dose" group (Figure 1C). HBV DNA polymerase activities fell in all the patients examined (Figure 1D). These results might indicate that the "early high-dose" introduction of corticosteroids could suppress the host immunologic reaction to HBV and inhibit significant liver cell degeneration.

Liver histology of 5 "early high-dose" patients showed submassive necrosis in 1, liver cirrhosis with submassive necrosis in 1, chronic hepatitis (F2, severe) in 2, and chronic hepatitis (F3, severe) in 1. Liver histology of 8 "non-early high-dose" patients showed submassive necrosis in 4, liver cirrhosis with submassive necrosis in 2, and chronic hepatitis (F3, moderate) in 2 (Table 2).

DISCUSSION

The prognosis of severe exacerbation of chronic hepatitis B is poor if signs of liver failure appear[1,2,21]. The mortality rate of chronic hepatitis B patients with severe exacerbation related to chemotherapy is reported to be 45% from Japan[2], and 60% from Slovenia[21]. If effective therapeutic approaches are available, they must be beneficial for these patients. In the current study, only one of the 11 (9%) "early high-dose" corticosteroid-treated patients died, whereas 9 of 11 (82%) "non-early high-dose" patients died ($P<0.001$), suggesting that "early high-dose" corticosteroid treatment is beneficial for clinically severe exacerbation of chronic hepatitis B. Representatively, clinical course of one patient (patient 4) who recovered after treatment with only corticosteroid is demonstrated in Figure 2B.

Regarding the timing of corticosteroid treatment, Gregory *et al*[22] reported that methyl prednisolone cannot enhance survival in patients with severe "acute" viral hepatitis when used later, but they conceived that steroid would have likely proved beneficial if treatment had started "much earlier". Actually, in our study, all the 7 patients died when high-dose corticosteroid was given more than 10 d after the diagnosis of severe disease, indicating the importance of the "early" usage of corticosteroid. When the start of treatment is delayed, quite a large number of hepatocytes would probably already have been destroyed and inhibition of the inflammatory reaction would not be effective.

Regarding the corticosteroid dosage, Schalm *et al*[23] demonstrated that histologically severe chronic active hepatitis B patients failing treatment with conventional doses of prednisone often improved with higher doses, suggesting that higher doses of steroid might be more efficacious. One of the reasons, for not using corticosteroids in the treatment of chronic hepatitis B, is that it might enhance the replication of HBV through a steroid-responsive element in the HBV genome[24]. In our study, serum HBV DNA at admission was negative in about half of our patients. Moreover, none of the patients, given high doses of corticosteroids, showed increments of HBV. Because of the rapid and aggressive immune clearance of virus-infected hepatocytes by CTL-mediated cytolytic pathways, patients developing a rapid course of liver- failure might not show evidence of HBV replication during the short-term observation period of the present study.

Our results indicate the importance of immunosuppressive therapy for preventing the progression of liver failure. If HBV proteins are not produced in hepatocytes, CTL will not recognize and destroy the HBV-infected hepatocytes. Therefore, suppression of the production of HBV-related proteins by preventing HBV replication must also be important in the treatment of severe exacerbation of chronic hepatitis B.

In a couple of cases, we administered lamivudine, an

antiviral agent, in combination with corticosteroids. Lamivudine is a nucleoside analogue that has recently been used for the treatment of chronic hepatitis B, demonstrating a strong inhibitory effect on HBV replication. Several recent studies have reported that lamivudine appears to be effective in advanced and decompensated chronic liver disease and acute hepatic failure due to hepatitis B[12-17]. Therefore, lamivudine may be effective in the treatment of severe exacerbation of chronic hepatitis B.

With the administration of lamivudine, HBV DNA is reduced rapidly, but the improvement in liver-function is delayed by a few weeks to a few months[14]. During the time- lag phase, excessive immunological reaction may continue and liver cell injury may progress. We observed in a patient (patient 7) who needed more than 3 mo before the improvement of liver function became evident (Figure 2A), and a patient (patient 14) who died despite the usage of lamivudine (Figure 2C). The latter patient was an asymptomatic carrier of HBV with anti-HBe, and severe exacerbation of hepatitis occurred after the withdrawal of immunosuppressive drugs for ulcerative colitis. When admitted to our hospital, PT was already markedly prolonged (Figure 2C). It seems that anti-viral therapy is not enough to stop progressive deterioration, and additional therapy to suppress liver cell degeneration may be required. Combination treatment with "early high-dose" corticosteroids and lamivudine might be effective in suppressing the excessive host immune response in the early period. Additionally, lamivudine may make it possible to shorten the term of corticosteroid therapy. The efficacy of this combination therapy needs to be examined as soon as possible.

In summary, our study demonstrates that the early introduction of high-dose corticosteroid treatment is useful for "clinically severe" acute exacerbation of chronic hepatitis B; we did not include placebo-controlled patients, considering the current knowledge of the poor prognosis of such patients. The combination of corticosteroids with lamivudine may be a beneficial option for the treatment of such patients. Nevertheless, delay in the treatment may result in fatal liver-failure even though these treatment protocols are used, suggesting the requirement of early diagnosis of such patients, at the first sign of a biochemical trend of liver failure, before the appearance of clinical symptoms.

ACKNOWLEDGEMENTS

We thank Dr. Toshiki Ehata (Ehata Clinic, Unakami, Chiba) for clinical contributions.

REFERENCES

1 Chemotherapy and hepatitis B. *Lancet* 1989; **2:** 1136–1137
2 **Nakamura Y,** Motokura T, Fujita A, Yamashita T, Ogata E. Severe hepatitis related to chemotherapy in hepatitis B virus carriers with hematologic malignancies. Survey in Japan, 1987-1991. *Cancer* 1996; **78:** 2210–2215
3 **Chisari FV,** Ferrari C. Hepatitis B virus immunopathogenesis. *Annu Rev Immunol* 1995; **13:** 29–60
4 **Hanson RG,** Peters MG, Hoofnagle JH. Effects of immunosuppressive therapy with prednisolone on B and T lymphocyte function in patients with chronic type B hepatitis. *Hepatology* 1986; **6:** 173–179
5 **Sjogren MH,** Hoofnagle JH, Waggoner JG. Effect of corticosteroid therapy on levels of antibody to hepatitis B core antigen in patients with chronic type B hepatitis. *Hepatology* 1987; **7:** 582–585
6 **Nouri-Aria KT,** Hegarty JE, Alexander GJ, Eddleston AL, Williams R. Effect of corticosteroids on suppressor-cell activity in "autoimmune" and viral chronic active hepatitis. *N Engl J Med* 1982; **307:** 1301–1304
7 **Lam KC,** Lai CL, Trepo C, Wu PC. Deleterious effect of prednisolone in HBsAg-positive chronic active hepatitis. *N Engl J Med* 1981; **304:** 380–386
8 **Hoofnagle JH,** Davis GL, Pappas SC, Hanson RG, Peters M, Avigan MI, Waggoner JG, Jones EA, Seeff LB. A short course of prednisolone in chronic type B hepatitis. Report of a randomized, double-blind, placebo-controlled trial. *Ann Intern Med* 1986; **104:** 12–17
9 **Scullard GH,** Smith CI, Merigan TC, Robinson WS, Gregory PB. Effects of immunosuppressive therapy on viral markers in chronic active hepatitis B. *Gastroenterology* 1981; **81:** 987–991
10 **Lau JY,** Bird GL, Gimson AE, Alexander GJ, Williams R. Treatment of HBV reactivation after withdrawal of immunosuppression. *Lancet* 1991; **337:** 802
11 **Katz R,** Velasco M, Klinger J, Alessandri H. Corticosteroids in the treatment of acute hepatitis in coma. *Gastroenterology* 1962; **42:** 258–265
12 **Santantonio T,** Mazzola M, Pastore G. Lamivudine is safe and effective in fulminant hepatitis B. *J Hepatol* 1999; **30:** 551
13 **Van Thiel DH,** Friedlander L, Kania RJ, Molloy PJ, Hassanein T, Wahlstrom E, Faruki H. Lamivudine treatment of advanced and decompensated liver disease due to hepatitis B. *Hepatogastroenterology* 1997; **44:** 808–812
14 **Chan TM,** Wu PC, Li FK, Lai CL, Cheng IK, Lai KN. Treatment of fibrosing cholestatic hepatitis with lamivudine. *Gastroenterology* 1998; **115:** 177–181
15 **ter Borg F,** Smorenburg S, de Man RA, Rietbroek RC, Chamuleau RA, Jones EA. Recovery from life-threatening, corticosteroid-unresponsive, chemotherapy-related reactivation of hepatitis B associated with lamivudine therapy. *Dig Dis Sci* 1998; **43:** 2267–2270
16 **Ahmed A,** Keeffe EB. Lamivudine therapy for chemotherapy-induced reactivation of hepatitis B virus infection. *Am J Gastroenterol* 1999; **94:** 249–251
17 **Villeneuve JP,** Condreay LD, Willems B, Pomier-Layrargues G, Fenyves D, Bilodeau M, Leduc R, Peltekian K, Wong F, Margulies M, Heathcote EJ. Lamivudine treatment for decompensated cirrhosis resulting from chronic hepatitis B. *Hepatology* 2000; **31:** 207–210
18 **Iino S,** Tango T, Matsushima T, Toda G, Miyake K, Hino K, Kumada H, Yasuda K, Kuroki T, Hirayama C, Suzuki H. Therapeutic effects of stronger neo-minophagen C at different doses on chronic hepatitis and liver cirrhosis. *Hepatol Res* 2001; **19:** 31–40
19 **Okamoto H,** Okada S, Sugiyama Y, Tanaka T, Sugai Y, Akahane Y, Machida A, Mishiro S, Yoshizawa H, Miyakawa Y. Detection of hepatitis C virus RNA by a two-stage polymerase chain reaction with two pairs of primers deduced from the 5'-noncoding region. *Jpn J Exp Med* 1990; **60:** 215–222
20 **Kaplan PM,** Greenman RL, Gerin JL, Purcell RH, Robinson WS. DNA polymerase associated with human hepatitis B antigen. *J Virol* 1973; **12:** 995–1005
21 **Markovic S,** Drozina G, Vovk M, Fidler-Jenko M. Reactivation of hepatitis B but not hepatitis C in patients with malignant lymphoma and immunosuppressive therapy. A prospective study in 305 patients. *Hepatogastroenterology* 1999; **46:** 2925–2930
22 **Gregory PB,** Knauer CM, Kempson RL, Miller R. Steroid therapy in severe viral hepatitis. A double-blind, randomized trial of methyl-prednisolone versus placebo. *N Engl J Med* 1976; **294:** 681–687
23 **Schalm SW,** Summerskill WH, Gitnick GL, Elveback LR. Contrasting features and responses to treatment of severe chronic active liver disease with and without hepatitis BS antigen. *Gut* 1976; **17:** 781–786
24 **Tur-Kaspa R,** Burk RD, Shaul Y, Shafritz DA. Hepatitis B virus DNA contains a glucocorticoid-responsive element. *Proc Natl Acad Sci USA* 1986; **83:** 1627–1631

PO Box 2345, Beijing 100023, China
www.wjgnet.com
wjg@wjgnet.com

ELSEVIER

World J Gastroenterol 2005;11(8):1115-1121
World Journal of Gastroenterology ISSN 1007-9327

• *BASIC RESEARCH* •

Effect of endothelin-1 receptor antagonists on histological and ultrastructural changes in the pancreas and trypsinogen activation in the early course of caerulein-induced acute pancreatitis in rats

Anna Andrzejewska, Jan W. Dlugosz, Albert Augustynowicz

Anna Andrzejewska, Albert Augustynowicz, Department of Medical Pathomorphology, Medical University of Bialystok, Bialystok, Poland
Jan W. Dlugosz, Department of Gastroenterology and Internal Medicine, Medical University of Bialystok, Bialystok, Poland
Supported by the Medical University of Bialystok within the Project # 3-12770
Co-first-authors: Anna Andrzejewska and Jan W. Dlugosz
Correspondence to: Professor Anna Andrzejewska M.D., Department of Medical Pathomorphology, Medical University of Bialystok, Waszygton Str. 13, 15-269 Bialystok, Poland. anna.andrzejewska@poczta.fm
Telephone: +48-85-7485989 Fax: +48-85-7485989
Received: 2004-07-17 Accepted: 2004-09-19

Abstract

AIM: To assess the effect of non-selective $ET_{A/B}$ (LU 302872) and selective ET_A (LU 302146) antagonist on pancreatic histology and ultrastructure of acinar cells in connection with trypsinogen activation in early caerulein-induced AP.

METHODS: Male Wistar rats with caerulein-induced AP, lasting 4 h, were treated *i.p.* with 10 and 20 mg/kg b.w. of each antagonist. Edema, inflammatory infiltration, necrosis and vacuolization of acinar cells in the pancreas were scored at 0-3 scale. Free active trypsin (FAT), total potential trypsin (TPT) after activation with enterokinase, and index of trypsinogen activation (%FAT/TPT) were assayed in pancreatic homogenates.

RESULTS: In untreated AP, the edema, inflammatory infiltration, necrosis and vacuolization increased as compared to control healthy rats ($P<0.01$). None of the treatment exerted any meaningful effect on the edema and inflammatory infiltration. The selective antagonist increased slightly the necrosis score to 0.82±0.06 at higher dose ($P<0.05$) *vs* 0.58±0.06 in untreated AP. The non-selective antagonist increased slightly the vacuolization score to 2.41±0.07 at higher dose ($P<0.01$) *vs* 1.88±0.08 in untreated AP. The decrease in the number of zymogen granules, disorganization of endoplasmic reticulum, autophagosomes and cytoplasmic vacuoles were more prominent in treated AP than in untreated AP groups. %FAT/TPT in untreated AP increased about four times (18.4±3.8 *vs* 4.8±1.3 in control group without AP, $P<0.001$). Treatment of AP with both antagonists did not affect significantly augmented trypsinogen activation.

CONCLUSION: The treatment with endothelin-1 receptors (non-selective $ET_{A/B}$ and selective ET_A) antagonists has essential effect neither on the edema and inflammatory infiltration nor on trypsinogen activation observed in the early course of caerulein-induced AP. Nevertheless a slight increase of the necrosis and vacuolization score and some of the ultrastructural data could suggest the possibility of their undesired effects in caerulein-induced AP at investigated doses.

Key words: Acute pancreatitis; Caerulein; Endothelin-1 receptors antagonists; Ultrastructure; Trypsin

Andrzejewska A, Dlugosz JW, Augustynowicz A. Effect of endothelin-1 receptor antagonists on histological and ultrastructural changes in the pancreas and trypsinogen activation in the early course of caerulein-induced acute pancreatitis in rats. *World J Gastroenterol* 2005; 11(8): 1115-1121
http://www.wjgnet.com/1007-9327/11/1115.asp

INTRODUCTION

The role of endothelin-1 (ET-1), as a potent vasoconstrictor polypeptide, and its receptor antagonists in acute pancreatitis (AP) has been an intensively studied issue recently. The experimental studies have brought varied results and evoked a number of controversies. In many experiments, the application of selective and non-selective ET-1 receptor A and B antagonists caused a significant improvement in pancreatic capillary blood flow, a decrease in capillary permeability and a reduction in leukocyte rolling in mild and severe AP[1-5]. A beneficial effect of the ET-1 receptor antagonists was also evidenced by less pronounced morphological changes in AP, including necrosis and vacuolization of acinar cells, hemorrhagic changes and granulocytic infiltration of pancreatic parenchyma[3,6-9]. Foitzik *et al*[10] found a considerable drop in the mortality rate of rats after the application of the selective ET-1 receptor A antagonist, LU 135252, in severe AP.

However, not all researchers have confirmed the beneficial effects of ET-1 receptor antagonists in AP. The results of Martignoni *et al*[11] clearly indicated that selective ET-1 receptor A (ET_A) antagonist (LU 135252) did not decrease but showed a tendency to increase mortality in animals with taurocholate-induced pancreatitis. A study by Fiedler *et al*[12] revealed no effect of non-selective ET-1

receptor A and B ($ET_{A/B}$) antagonist, bosentan, on the survival rate of rats or on the morphological and biochemical changes in severe taurocholate AP. Todd *et al*[9] observed no decrease in the mortality rate of animals in acute hemorrhagic pancreatitis after the application of non-selective ET-1 receptor A and B antagonist PD 145065, despite decreased severity of inflammation. Also recent studies have not confirmed the advantageous effect of non-selective ($ET_{A/B}$) and selective (ET_A) blockade in necrotic or edematous AP[11].

On the other hand, Kogire *et al*[13] found a significant improvement in the course of caerulein-induced pancreatitis following systemic infusion of ET-1 by evaluating serum α-amylase level, dry/wet weight ratio, and histological changes. In contrast, endothelin receptor blockade with BQ 123, a potent selective ET_A receptor antagonist, augmented pancreatic edema and the extent of inflammatory cell infiltration. The above data indicate that the role of ET-1 and ET-1 receptors antagonists in AP remains controversial and not fully elucidated.

Therefore, the aim of the present study was to evaluate and compare the effect of non-selective ET-1 A and B receptors ($ET_{A/B}$) antagonist, LU 302872, and selective receptor A (ET_A) antagonist, LU 302146, on the morphological and ultrastructural changes and trypsinogen activation in the pancreas in early caerulein-induced edematous, AP in rats.

MATERIALS AND METHODS

Animals

The experiments were carried out on 40 male Wistar rats, 240-280 g of body weight, housed individually in wire bottomed cages, at a room temperature of 21±1 ℃ using a 12-h light-dark cycle. They were fed with a laboratory chow diet and fasted overnight, before the experiment, with free access to water. Care was provided in accordance with the current procedures for the care and use of laboratory animals. The protocol has been approved by the local Bioethical Commission.

Induction of acute pancreatitis

Acute pancreatitis was induced according to the method of Yamaguchi *et al*[14]. The rats were injected with caerulein (Sigma Chemical Co., St. Louis, MO, USA) at a dose of 40 μg/kg of body weight intraperitoneally (*i.p.*) twice, at 1 h interval. In control rats, only vehiculum of caerulein (saline solution) was given *i.p.* In the treated rats, the solution of respective ET-1 receptor antagonist in vehiculum was given *i.p.* simultaneously with the first injection of caerulein.

Experimental design

Rats were subdivided into six groups as follows:

Group 1. Control group (C), received only saline solution *i.p.* at 0 and 1 h ($n = 6$).

Group 2. Rats with untreated caerulein-induced AP, received only saline solution *i.p.* as in the control group ($n = 10$).

Group 3. Rats with caerulein-induced AP treated with the non-selective antagonist of ET-1 A and B receptors: LU 302872 ($ET_{A/B}$ antagonist) at a dose of 10 mg/kg b.w. *i.p.* given at the beginning of the experiment , at the same time as the first injection of caerulein ($n = 6$).

Group 4. Rats with caerulein-induced AP treated with LU 302872 at a dose of 20 mg/kg b.w., *i.p.* given at the beginning of the experiment, at the same time as the first injection of caerulein ($n = 6$).

Group 5. Rats with caerulein-induced AP treated with selective ET-1 A receptor antagonist LU 302146 (ET_A antagonist), at a dose of 10 mg/kg b.w. *i.p.*, at the beginning of the experiment, at the same time as the first injection of caerulein ($n = 6$).

Group 6. Rats with caerulein-induced AP treated with LU 302146, at a dose of 20 mg/kg b.w. *i.p.*, at the beginning of the experiment, at the same time as the first injection of caerulein ($n = 6$).

The volume of saline as a vehiculum was equilibrated in all groups to 2×2 mL/kg b.w. The ET-1 receptor antagonists were generously donated by Knoll AG, Ludwigshafen, Germany (Dr. M. Kirchengast).

The animals were killed by quick decapitation after 4 h after the first injection of caerulein, in general anesthesia induced with *i.p.* ketamine 40 mg/kg b.w. and pentobarbital 20 mg/kg b.w. The pancreases were quickly excised, freed from the peripancreatic tissues and weighed. The specimens for histological and ultrastructural examinations were taken. The remaining portion of the pancreas was processed for biochemical assays.

Histological examination

The representative specimen of the pancreatic tissue from each rat was fixed in 10% neutral-buffered formalin. Sections of the samples were stained with H&E and examined under light microscope at ×200 magnification - intermediate power field (IPF) by a blinded observer in a hundred fields from each group. Histological changes were evaluated according to Kyogoku *et al*[15]. Interstitial edema was scored as follows: 0 = absent, 1 = expanded interlobular septa, 2 = expanded intralobular septa, 3 = separated individual acini. Polymorphonuclear neutrophils (PMNs) infiltration was scored as 0 = absent, 1 = less than 20 PMNs per IPF, 2 = 20-50 PMNs per IPF and 3 = more than 50 PMNs per IPF. Parenchymal necrosis was scored as the percentage involvement of the examined area: 0 = absent, 1 = less than 5% IPF, 2 = 5-20% IPF, 3 = more than 20% IPF. The grading of vacuolization was based on the percentage of acinar cells with cytoplasmic vacuoles per IPF: 0 = absent, 1 = less than 20%, 2 = 20-50%, 3 = more than 50%. Hemorrhagic changes were absent and therefore not scored.

Ultrastructural examination

Small specimens (about 1 mm^3) of pancreatic tissue (three from each animal) were immediately fixed in 3.6% glutaraldehyde in 0.1 mol/L cacodylate buffer (pH 7.4) for 3 h and after washing in a buffer, postfixed in 2% osmium tetroxide for 1 h. The samples were dehydrated in alcohol and propylene oxide and then embedded in Epon 812. The ultrathin sections were cut from each block on a Reichert ultramicrotome, stained with lead citrate and uranyl acetate, and studied under an Opton 900 PC transmission electron microscope field by field. Fifty to 60 electron micrographs

of the most characteristic changes from each group were made. The determination of pathology was made blind.

Biochemical assays

The remaining pancreatic tissue was homogenized in ice-cold four volumes of 50 mmol/L Tris-HCl buffer (pH 8.0), containing nonorganic detergent Triton X-100, 5 mL/L during 1 min by three full up and down strokes using a motor-driven glass-Teflon homogenizer (Thomas Scientific, Swedesboro, NJ, USA) cooled with ice. The resulting homogenate was sonified for 20 s in an ice bath using Vibra cell, model VC 50, Sonics and Materials Inc., Danbury, CT (frequency 20 kHz and amplitude 70). The volumes were then adjusted giving 10% homogenates placed on ice.

Free active trypsin (FAT) and total potential trypsin (TPT) in whole homogenate were assayed according to Yamaguchi *et al*[14] with the exception that N_{α}-p-tosyl-L-arginine methyl ester hydrochloride (TAME) 1 mmol/L was used as a substrate and the absorbance of released product was estimated at 247 nm wave length in an automatic spectrophotometer Pye Unicam SP 505 (Cambridge, UK), as in our previous studies[16, 17].

TPT in whole homogenate was estimated after the activation of trypsinogen with enterokinase in 1:1 dilution in 50 mmoL Tris-HCl buffer, pH 8.0 for 30 min at 37 ℃. The freshly prepared working solution of enterokinase contained 2 mg of enzyme/mL of the same buffer. The time of activation proved to be sufficient for complete activation. The activity was expressed in μg of trypsin/mg of protein by comparison with the calibration curve of increasing concentrations of bovine trypsin, type I. The %FAT/TPT ratio served as an index of trypsinogen activation[14].

All reagents for biochemical assays were purchased from Sigma Chemical Co., St. Louis, MO, USA.

Statistical analysis

Histologic data were expressed as the range of the scores and mean±SE and compared using non-parametric tests: the Mann-Whitney for two groups and the Kruskal-Wallis for multiple groups. The results of biochemical assays were reported as mean±SE and after performing an F test for the equality of variances, the means were compared using the t test for unpaired data. The differences with $P<0.05$ were considered statistically significant. SPSS 8.OPL statistical program was used (SPSS Inc., Chicago, IL).

RESULTS

Light microscopy

The microscopic picture of the pancreas in the control group (C) showed only negligible swelling of pancreatic interstitial tissue with the presence of single neutrophils. Rats with untreated AP displayed moderate edema and inflammatory infiltration of neutrophils. Moreover, a necrosis of some of the acinar cells and their marked vacuolization were found. The changes in all AP animals were significantly more pronounced ($P<0.001$) than in healthy animals. Assuming the increase of score from 0 to 3 points as 100%, the treatment of AP with ET-1 receptor antagonists did not reduce the pancreatic edema and even a slight increase (<10%) of its score after higher dose of non-selective $ET_{A/B}$ receptor antagonist was noted. Only slight reduction of PMNs infiltration (<10%) after higher dose of the selective antagonist compared to untreated AP or treated with the non-selective antagonist was noted. The necrosis of acinar cells was slightly more pronounced (6-13%) after the application of both doses of the selective receptor A antagonist than in the untreated group or in the groups treated with both doses of non-selective $ET_{A/B}$ antagonist. Mean vacuolization score was slightly increased after both doses of non-selective (12-18%) and after higher dose of selective ET-1 receptors antagonists (10%) as compared to untreated AP. The mean scores of histological changes are reported in Table 1.

Table 1 Histological changes in the pancreas of rats with caerulein-induced acute pancreatitis (AP) in comparison to control group (C), SE range of scores in brackets

No.	Group	Edema	PMNs infiltration	Necrosis	Vacuolization
1	Control (C)	(0–1)	(0–1)	(0)	(0–1)
	(n = 6)	0.12±0.03	0.06±0.02	0.00±0.00	0.08±0.03
2	Untreated AP	(1–3)	(0–3)	(0–2)	(1–3)
	(n = 10)	2.04±0.07[b]	1.61±0.08[b]	0.58±0.06[b]	1.88±0.08[b]
3	AP + LU 302872	(1–3)	(0–3)	(0–1)	(1–3)
	10 mg/kg (n = 6)	2.02±0.07[b]	1.66±0.07[b]	0.48±0.05[b]	2.24±0.08[b,d]
4	AP + LU 302872	(1–3)	(0–3)	(0–2)	(1–3)
	20 mg/kg (n = 6)	2.30±0.06[b,d,h]	1.68±0.08[b]	0.50±0.05[b]	2.41±0.07[b,d]
5	AP + LU 302146	(0–3)	(0–3)	(0–2)	(1–3)
	10 mg/kg (n = 6)	1.96±0.09[b]	1.43±0.09[b,e]	0.86±0.07[b,d,f]	1.91±0.09[b,f]
6	AP + LU 302146	(0–3)	(0–3)	(0–2)	(1–3)
	20 mg/kg (n = 6)	2.14±0.07[b]	1.41±0.07[b,c,e]	0.82±0.06[b,d,f]	2.19±0.07[b,d,e,g]

LU 302872 (non-selective ET-1 receptor A and B antagonist) or LU 302146 (selective ET-1 receptor A antagonist) were given *i.p.* at the indicated dosage at the beginning of the experiment, at 0 time, simultaneously with the first *i.p.* injection of caerulein. *Statistical significance of differences*: [a]$P<0.05$, [b]$P<0.01$ *vs* control [c]$P<0.05$, [d]$P<0.01$ *vs* AP untreated [e]$P<0.05$, [f]$P<0.01$ *vs* non-selective antagonist [g]$P<0.05$, [h]$P<0.01$ *vs* lower dose of antagonist.

Electron microscopy

Group 1 (control group) The ultrastructural picture of acinar cells did not show any deviations from the norm (Figure 1). The interstitial tissue displayed slight swelling and sporadic neutrophils and erythrocytes. Blood vessels were normal in appearance.

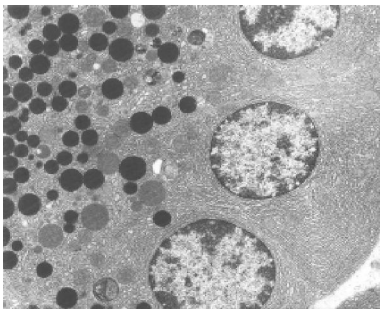

Figure 1 Normal ultrastructural appearance of pancreatic acinar cells. Control group (C). Original magnification ×3 000, bar = 2.5 μm.

Group 2 (untreated AP) Acinar cells of the pancreas displayed features of damage of varied intensity. Many of them had dilated, disorganized, and partially degranulated rough endoplasmic reticulum (RER) channels (Figure 2A). The cisternae of the Golgi apparatus were sometimes distended and filled with flocculent material. Zymogen granules were rare, varying in size and electron density (Figure 2B) and frequently migrated to the basolateral parts of the cell. Some of the mitochondria showed increased matrix translucence and destruction of their cristae. The majority of pancreatic acinar cells contained vacuoles, which sometimes reached large sizes and occupied a considerable area of the cell. Moreover, the cytoplasm contained autophagosomes with fragments of cellular organelles or sometimes zymogen granules. A necrosis of acinar cells was only sporadically observed.

The interstitial tissue showed marked edema and quite numerous inflammatory cells. Some of endothelial cells were swollen, with features of destruction of their organelles.

Groups 3 and 4 (AP treated with $ET_{A/B}$ antagonist) In both groups treated with non-selective $ET_{A/B}$ antagonist at a dose of 10 and 20 mg/kg, pancreatic acinar cells displayed slightly higher degree of damage than in the untreated AP. The cytoplasm contained quite numerous vacuoles some of them migrated to the base of the cells as if opening to the interstitial space (Figure 3A). These vacuoles were usually empty or contained membranous structures. Moreover, typical autophagous vacuoles were quite common and they

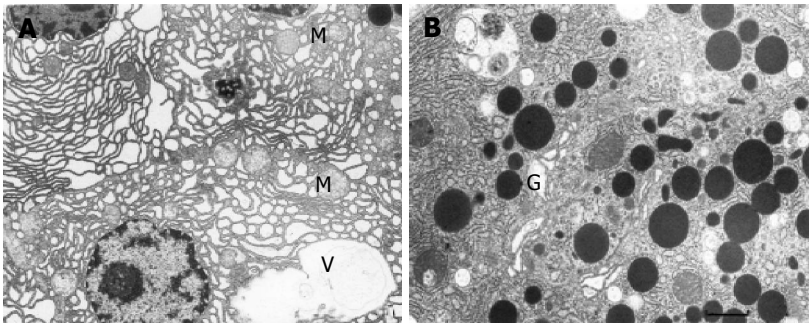

Figure 2 Ultrastructural changes in the pancreatic acinar cells in untreated caerulein-induced AP. A: Dilated channels of rough endoplasmic reticulum and slightly damaged mitochondria (M) in the cytoplasm of the acinar cells. In the vicinity of nucleus, a vacuole (V) is seen. Original magnification ×3 000, bar = 2.5 μm; B: Zymogen granules of different shape and size and dilated cisternae of the Golgi apparatus (G). Original magnification ×7 000, bar = 1.1 μm.

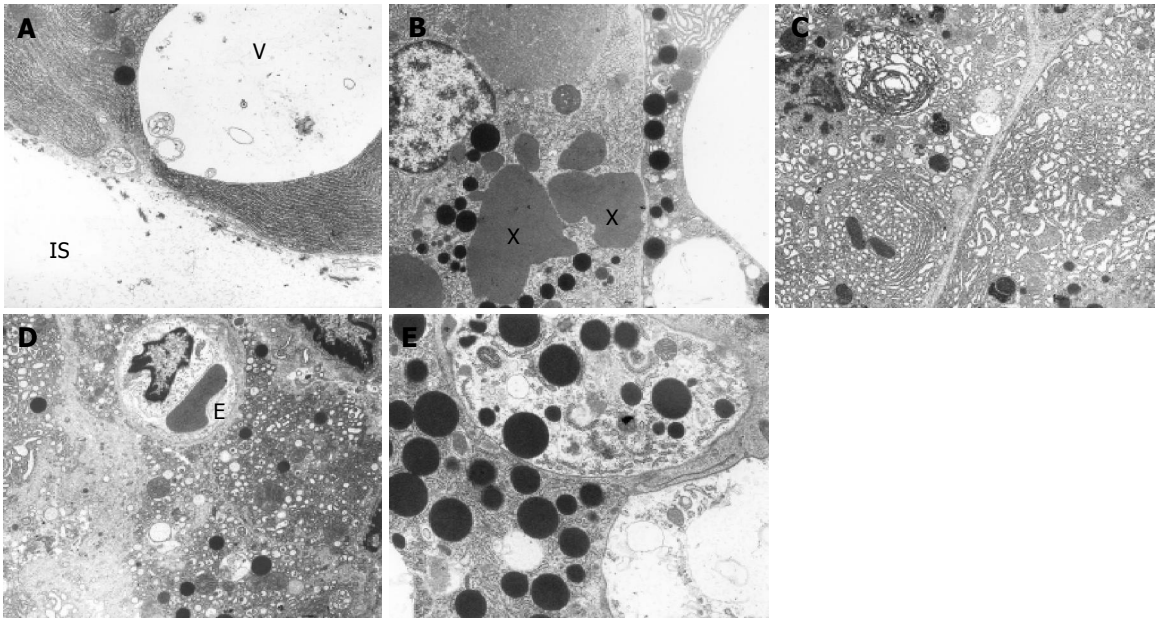

Figure 3 Ultrastructural changes in the pancreatic acinar cells in caerulein-induced AP treated with non-selective ($ET_{A/B}$) or selective (ET_A) ET-1 receptors antagonists. A: Large vacuole (V) at the base of acinar cell opening into the interstitial space (IS). Group 3 – AP treated with LU 302872 ($ET_{A/B}$ antagonist) at a dose of 10 mg/kg b.w. Original magnification ×4 400, bar=1.7 μm; B: Irregular "lakes" of zymogen material (*), large vacuoles and zymogen granules at the base of two acinar cells. Group 3 – AP treated with LU 302872 ($ET_{A/B}$ antagonist) at a dose of 10 mg/kg b.w. Original magnification ×3 000, bar=2.5 μm; C: Concentric arrangement, vesicular transformation and disorganization of endoplasmic reticulum. Note some phagosomes (Ph) in the cytoplasm. Group 4 – AP treated with LU 302872 ($ET_{A/B}$ antagonist) at a dose of 20 mg/kg b.w. Original magnification ×3 000, bar = 2.5 μm; D: Total disintegration of the acinar cell – its fragments in the interstitial space are seen. The endothelial cells (E) of capillary are swollen. Group 6 – caerulein-induced AP treated with LU 302146 (ET_A antagonist) at a dose of 20 mg/kg b.w. Original magnification ×3 000, bar = 2.5 μm; E: Autophagous vacuoles containing zymogen granules, fragments of endoplasmic reticulum and other acinar cell organelles. Group 6 – caerulein-induced AP treated with LU 302146 (ET_A antagonist) at a dose of 20 mg/kg b.w. Original magnification ×7 000, bar = 1.1 μm.

contained RER fragments, damaged mitochondria, sometimes zymogen granules and amorphous or membranous structures. Zymogen granules were rare, varying in size and electron density, sometimes fused together to form irregular "lakes" (Figure 3B). Channels of RER were usually dilated and showed vesicular transformation, concentric arrangement, partial degranulation and focal total disorganization (Figure 3C). The cisternae of the Golgi apparatus were frequently dilated. Some mitochondria showed features of swelling. Necrosis of acinar cells was sporadic.

The interstitial tissue displayed distinct swelling, fibrin strands, inflammatory cells and features of damage in some endothelial cells. Generally the ultrastructural changes were similar after both doses of $ET_{A/B}$ antagonist and they were a bit more prominent than in the untreated group with AP.

Group 5 and 6 (AP treated with ET_A antagonist).

Ultrastructural changes after treatment with lower dose of selective ET_A antagonist resembled those observed in animals treated with both doses of non-selective $ET_{A/B}$ antagonist.

However, after treatment with higher dose, the ultrastructural alterations were more pronounced. Many acinar cells showed features of total disintegration and their fragments could be seen in the interstitial space (Figure 3D). The cytoplasm contained numerous vacuoles varying in size. Zymogen granules had varied electron density, frequently migrated to the base of the cell, and sporadically merged to form large irregular "lakes". Sometimes they were found in autophagous vacuoles (Figure 3E) or were lying loosely in the interstitial space. Changes in RER, Golgi apparatus, mitochondria and in the interstitial tissue were similar to those noted in the previous groups.

Trypsinogen activation index (%FAT/TPT)

In pancreatic homogenate (Table 2) in untreated AP this index was over four times as high as in control group ($P<0.01$). Treatment with non-selective $ET_{A/B}$ antagonist and selective ET_A antagonist at both doses did not affect significantly the augmented trypsinogen activation index, compared to the untreated AP group.

Table 2 Free active trypsin (FAT), total potential trypsin (TPT) activity and index of trypsinogen activation (%FAT/TPT) in whole homogenate of the rat pancreas in caerulein-induced acute pancreatitis (AP) in rats in comparison to control group (C) (mean±SE)

Group	FAT (μg/mg protein)	TPT (μg/mg protein)	FAT/TPT (%)
Control ($n=6$)	0.394±0.094	8.90±1.14	4.8±1.3
Untreated AP ($n=10$)	1.542±0.249	9.77±0.94	18.4±3.8[b]
AP+LU302872 10 mg/kg ($n=6$)	1.543±0.134	10.56±1.04	14.9±1.2[b]
AP+LU302872 20 mg/kg ($n=6$)	1.245±0.176	9.06±2.18	16.7±2.6[b]
AP+LU302146 10 mg/kg ($n=6$)	0.969±0.08	6.61±0.98	16.0±2.6[b]
AP+LU302146 20 mg/kg ($n=6$)	1.869±0.52	8.11±1.55	21.8±3.0[b]

LU 302872 (non-selective ET-1 receptor A and B antagonist) or LU 302146 (selective ET-1 receptor A antagonist) was given *i.p.* at the indicated dosage at the beginning of the experiment, at 0 time, simultaneously with the first *i.p.* injection of caerulein. *Statistical significance of differences in %FAT/TPT:* [b]$P<0.01$ *vs* control.

DISCUSSION

Caerulein-induced pancreatitis is a well established and commonly used model of mild, edematous pancreatitis[13,18-21]. In the light microscopy, it displayed features of swelling, inflammatory infiltration composed mainly of neurophils, distinct vacuolization of acinar cells and sporadically necrosis. In our study, the treatment with ET-1 receptor antagonists (non-selective $ET_{A/B}$ and selective ET_A) increased slightly the vacuolization of acinar cells but did not affect meaningfully the edema. ET-1 receptor antagonists did not diminish the score of necrosis and it was even slightly increased after both ET_A antagonist doses. Parallel, ET_A antagonist decreased PMNs infiltration of pancreatic tissue in histological examination. The ultrastructural changes such as decreased number of zymogen granules, disorganization of endoplasmic reticulum, autophagosomes and cytoplasmic vacuoles were even more prominent in treated groups than in rats with untreated AP. The simultaneous biochemical assays revealed that the treatment with non-selective $ET_{A/B}$ and selective ET_A antagonists did not affect the increased trypsinogen activation index in pancreatic homogenate as compared to untreated AP.

The overall outcome of the present study was rather surprising for us. In our previous study[8], the same ET-1 receptor antagonists considerably reduced the extent of morphological changes in the pancreas, evaluated by light and electron microscopy in the model of severe AP induced by sodium taurocholate retrograde injection lasting 24 h. Our previous results also suggested a significant role of the antagonism of ET-1 receptors, mainly of the receptor A, which is blocked by the two antagonists, in the inhibition of trypsinogen activation[8]. However, actually in a mild caerulein-induced pancreatitis, we observed no beneficial effects of the same antagonists of ET-1 receptor. This leads us to thinking that the endothelin-1 receptor antagonists may act in different ways in different models of AP. The reason for this is not clear, but can be at least partly explained by differences in pancreatic microcirculation disorders between necrohemorrhagic and edematous AP[9,22]. In severe necrotic pancreatitis, the pancreatic blood flow decreases to 47% of baseline within 6 h[23], and plasma ET-1 level significantly increases[24]. In this situation, application of ET-1 receptor antagonists could considerably improve the circulatory parameters[2-4,10,24] preventing the development of more advanced morphological and biochemical changes. However, the pancreatic capillary flow in edematous, caerulein-induced AP rapidly increases to 188% of baseline and remains elevated up to 6 h of experiment[23], and ET-1 plasma level does not increase[13]. Complete capillary stasis develops in 38% of capillaries in severe AP and is absent in edematous AP[23]. Thus, both the vasoconstrictive action of ET-1 and the blockade of its receptors may be of less importance in the course of edematous AP than in the severe, necrotic one. These differences could be crucial for the explanation of the controversial role of ET-1 receptor antagonists in AP reported in the literature.

Acinar cell vacuolization is a major morphological change in caerulein-induced AP. Watanabe *et al*[20] have shown that in some developmental stages of this model of disease, vacuoles contain digestive and lysosomal enzymes, which

may lead to intracellular activation of trypsinogen by lysosomal cathepsin B and may be an important step in the development of AP. Simultaneous blockade of apical secretion is a prerequisite to basolateral output of partially activated zymogens into the interstitial space with a consecutive release of cytokines and vasoactive mediators, causing edema and chemoattraction of inflammatory cells and activation of vascular endothelium[25]. In our study, we found almost four-fold increase in trypsinogen activation index in pancreatic homogenate in the untreated AP group, compared to control animals. Application of endothelin-1 receptors antagonists had no significant effect on this augmented trypsinogen activation index, as compared to untreated AP nor did it affect meaningfully the edema score. However, the treatment with the selective receptor A antagonist at a dose of 20 mg/kg, slightly but significantly, decreased inflammatory infiltration. According to Plusczyk *et al*[7], the selective inhibition of the ET_A receptor prevents migration of leukocytes in acute experimental pancreatitis. This is consistent with the finding that ET_A receptor antagonists inhibit ET-1-mediated adhesion and migration of leukocytes[13,26,27]. Martignoni *et al*[11] revealed that after the application of selective ET_A antagonist (LU 135252), pancreatic edema in animals with caerulein-induced pancreatitis, was similar to that observed in non-treated animals. An increase in edema and in inflammatory infiltration after the administration of BQ-123, a potent ET_A receptor antagonist was observed by Kogire *et al*[13] in caerulein-induced AP. Also Liu *et al*[6] found no advantageous effect of BQ-123 on swelling and inflammatory infiltration in caerulein+stress-induced pancreatitis, although this antagonist was found to decrease vacuolization and necrosis of acinar cells.

Except for our previous work[8], no reports are available on the ultrastructural changes in pancreatic acinar cells in association with the application of endothelins or ET-1 receptor antagonists in AP. In the group of animals with untreated AP, we observed degenerated acinar cells with vacuoles, dilated rough endoplasmic reticulum, decreased number of zymogen granules and necrosis of some acinar cells. These findings are in accordance with observations of other authors[13,18-20,28,29]. The application of $ET_{A/B}$ and ET_A receptors antagonists did not improve the ultrastructural picture; on the contrary, it intensified to some degree the changes, especially in the group treated with higher dose of selective ET_A antagonist many acinar cells displayed numerous autophagous vacuoles and total cytoplasm disintegration, leading to cell degradation. This group showed the highest trypsinogen activation index, which may confirm the involvement of trypsin in the development and intensification of cellular changes in AP.

Thus, our present examinations, i.e., light microscopy, ultrastructural visualizing of cell organelles and measurement of trypsinogen activation index in pancreatic homogenate, reveal that the treatment with ET-1 receptor antagonists (non-selective $ET_{A/B}$ and selective ET_A) does not affect essentially either the edema and inflammatory infiltration or trypsinogen activation observed in the early course of caerulein-induced AP. Nevertheless, a slight increase of the necrosis and vacuolization score and some of the ultrastructural data could suggest the possibility of their undesired effects in caerulein-induced AP at investigated doses. Therefore, it is tempting to suggest that some intracellular effects mediated by ET-1 receptors could be protective in caerulein-induced AP.

LU 302872 is a derivative of endothelin A selective receptor antagonist LU 135252, which retains affinity for ET_A but exhibits substantial ET_B affinity as well. It antagonises the big ET-induced blood pressure increase in rats and big ET-induced bronchospasm in guinea pigs at the dose of 10 mg/kg[30,31]. LU 302146 is a derivative of LU 135252 with a higher ET-A receptor specificity[32]. Both antagonists have been used at the dose of 30 mg/kg daily *p.o.*, to prevent experimental uremic cardiomyopathy[33]. There are no dates on the doses of used antagonists to be sufficient for complete blockade of ET-1 receptors. The doses of both antagonists chosen in this study are comparable to that in other studies[30,31]. Nevertheless, similar effects of both investigated doses suggest that lower dose (10 mg/kg) is sufficient for the suturing of ET-1 receptors. Different potency or specificity of the endothelin receptor antagonists, dosing differences, the type of animals used and variation in pancreatitis model might be an explanation for the contradictory results reported in the literature.

In conclusion, we are of the opinion that the beneficial effect of endothelin-1 receptor blockade in early, edematous AP could be questioned and the attempts intending to introduce endothelin receptor antagonists to prevent the development of edematous pancreatitis (i.e., socalled post-ERCP pancreatitis) or its transition into necrotic one, should be treated with considerable caution.

REFERENCES

1 **Eibl G,** Hotz HG, Faulhaber J, Kirchengast M, Buhr HJ, Foitzik T. Effect of endothelin and endothelin receptor blockade on capillary permeability in experimental pancreatitis. *Gut* 2000; **46:** 390-394

2 **Eibl G,** Buhr HJ, Foitzik T. Therapy of microcirculatory disorders in severe acute pancreatitis: what mediators should we block? *Intensive Care Med* 2002; **28:** 139-146

3 **Foitzik T,** Eibl G, Buhr HJ. Therapy for microcirculatory disorders in severe acute pancreatitis: comparison of delayed therapy with ICAM-1 antibodies and a specific endothelin A receptor antagonist. *J Gastrointest Surg* 2000; **4:** 240-246; discussion 247

4 **Foitzik T,** Faulhaber J, Hotz HG, Kirchengast M, Buhr HJ. Endothelin mediates local and systemic disease sequelae in severe experimental pancreatitis. *Pancreas* 2001; **22:** 248-254

5 **Foitzik T,** Hotz HG, Eibl G, Hotz B, Kirchengast M, Buhr HJ. Therapy for microcirculatory disorders in severe acute pancreatitis: effectiveness of platelet activating factor receptor blockade *vs* endothelin receptor blockade. *J Gastrointest Surg* 1999; **3:** 244-251

6 **Liu X,** Nakano I, Ito T, Kimura T, Nawata H. Is endothelin-1 an aggravating factor in the development of acute pancreatitis? *Chin Med J (Engl)* 1999; **112:** 603-607

7 **Plusczyk T,** Witzel B, Menger MD, Schilling M. ET_A and ET_B receptor function in pancreatitis-associated microcirculatory failure, inflammation, and parenchymal injury. *Am J Physiol Gastrointest Liver Physiol* 2003; **285:** G145-G153

8 **Andrzejewska A,** Dlugosz JW. The endothelin-1 receptor antagonists ameliorate histology and ultrastructural alterations in the pancreas and decrease trypsinogen activation in severe taurocholate pancreatitis in rats. *Int J Exp Pathol* 2003; **84:** 221-229

9 **Todd KE,** Lewis MP, Gloor B, Lane JS, Ashley SW, Reber HA. An ETa/ETb endothelin antagonist ameliorates systemic inflammation in a murine model of acute hemorrhagic pancreatitis. *Surgery* 1997; **122:** 443-449; discussion 449-450

10 **Foitzik T,** Eibl G, Hotz HG, Faulhaber J, Kirchengast M, Buhr HJ. Endothelin receptor blockade in severe acute pancreatitis leads to systemic enhancement of microcirculation, stabilization of capillary permeability, and improved survival rates. *Surgery* 2000; **128:** 399-407

11 **Martignoni ME,** Ceyhan GO, Ayuni E, Kondo Y, Zimmermann A, Büchler MW, Friess H. Endothelin receptor antagonists are not beneficial in the therapy of acute experimental pancreatitis. *Langenbeck's Arch Surg* 2004; **389:** 184-192

12 **Fiedler F,** Ayasse D, Rohmeiss P, Gretz N, Rehbein C, Keim V. The endothelin antagonist bosentan does not improve survival in severe experimental pancreatitis in rats. *Int J Pancreatol* 1999; **26:** 147-154

13 **Kogire M,** Inoue K, Higashide S, Takaori K, Echigo Y, Gu YJ, Sumi S, Uchida K, Imamura M. Protective effects of endothelin-1 on acute pancreatitis in rats. *Dig Dis Sci* 1995; **40:** 1207-1212

14 **Yamaguchi H,** Kimura T, Mimura K, Nawata H. Activation of proteases in cerulein-induced pancreatitis. *Pancreas* 1989; **4:** 565-571

15 **Kyogoku T,** Manabe T, Tobe T. Role of ischemia in acute pancreatitis. Hemorrhagic shock converts edematous pancreatitis to hemorrhagic pancreatitis in rats. *Dig Dis Sci* 1992; **37:** 1409-1417

16 **Dlugosz JW,** Wroblewski E, Poplawski C, Gabryelewicz A, Andrzejewska A. Does antecedent ethanol intake affect course of taurocholate pancreatitis in rats? *Dig Dis Sci* 1997; **42:** 944-952

17 **Andrzejewska A,** Dlugosz JW, Jurkowska G. The effect of antecedent acute ethanol ingestion on the pancreas ultrastructure in taurocholate pancreatitis in rats. *Exp Mol Pathol* 1998; **65:** 64-77

18 **Lampel M,** Kern HF. Acute interstitial pancreatitis in the rat induced by excessive doses of a pancreatic secretagogue. *Virchows Arch A Pathol Anat Histol* 1977; **373:** 97-117

19 **Takano S,** Kimura T, Kawabuchi M, Yamaguchi H, Kinjo M, Nawata H. Ultrastructural study of the effects of stress on the pancreas in rats. *Pancreas* 1994; **9:** 249-257

20 **Watanabe O,** Baccino FM, Steer ML, Meldolesi J. Supramaximal caerulein stimulation and ultrastructure of rat pancreatic acinar cell: early morphological changes during development of experimental pancreatitis. *Am J Physiol* 1984; **246:** G457-G467

21 **Zhou ZG,** Chen YD, Sun W, Chen Z. Pancreatic microcirculatory impairment in experimental acute pancreatitis in rats. *World J Gastroenterol* 2002; **8:** 933-936

22 **Klar E,** Schratt W, Foitzik T, Buhr H, Herfarth C, Messmer K. Impact of microcirculatory flow pattern changes on the development of acute edematous and necrotizing pancreatitis in rabbit pancreas. *Dig Dis Sci* 1994; **39:** 2639-2644

23 **Schmidt J,** Ebeling D, Ryschich E, Werner J, Gebhard MM, Klar E. Pancreatic capillary blood flow in an improved model of necrotizing pancreatitis in the rat. *J Surg Res* 2002; **106:** 335-341

24 **Foitzik T,** Faulhaber J, Hotz HG, Kirchengast M, Buhr HJ. Endothelin receptor blockade improves fluid sequestration, pancreatic capillary blood flow, and survival in severe experimental pancreatitis. *Ann Surg* 1998; **228:** 670-675

25 **Klar E,** Werner J. New pathophysiologic knowledge about acute pancreatitis. *Chirurg* 2000; **71:** 253-264

26 **Cui P,** Tani K, Kitamura H, Okumura Y, Yano M, Inui D, Tamaki T, Sone S, Kido H. A novel bioactive 31-amino acid endothelin-1 is a potent chemotactic peptide for human neutrophils and monocytes. *J Leukoc Biol* 2001; **70:** 306-312

27 **Zouki C,** Baron C, Fournier A, Filep JG. Endothelin-1 enhances neutrophil adhesion to human coronary artery endothelial cells: role of ET(A) receptors and platelet-activating factor. *Br J Pharmacol* 1999; **127:** 969-979

28 **Brunelli A,** Scutti G. An ultrastructural study to investigate the effect of allopurinol on cerulein-induced damage to pancreatic acinar cells in rat. *Int J Pancreatol* 1998; **23:** 25-29

29 **Grönroos JM,** Aho HJ, Hietaranta AJ, Nevalainen TJ. Early acinar cell changes in caerulein-induced interstitial acute pancreatitis in the rat. *Exp Pathol* 1991; **41:** 21-30

30 **Amberg W,** Hergenroder S, Hillen H, Jansen R, Kettschau G, Kling A, Klinge D, Raschack M, Riechers H, Unger L. Discovery and synthesis of (*S*)-3-[2-(3, 4-dimethoxyphenyl)ethoxy]-2-(4,6-dimethylpyrimidin-2-yloxy)-3, 3-diphenylpropionic acid (LU 302872), a novel orally active mixed ET (A)/ET (B) receptor antagonist. *J Med Chem* 1999; **42:** 3026-3032

31 **Raschack M,** Gock S, Unger L, Hahn A, Amberg W, Jansen R, Alken P, Weber A, Hergenroder S. LU 302 872 and its racemate (LU 224 332) show balanced endothelin-A/B receptor affinity, high oral activity, and inhibit human prostate tissue contractions. *J Cardiovasc Pharmacol* 1998; **31** Suppl 1: S241-S244

32 **Knoll T,** Oltersdorf J, Gottmann U, Schaub M, Michel MS, Kirchengast M, van der Woude FJ, Rohmeiss P, Braun C. Influence of acute selective endothelin-receptor-A blockade on renal hemodynamics in a rat model of chronic allograft rejection. *Transpl Int* 2003; **16:** 425-429

33 **Wolf SC,** Amend T, Risler T, Amann K, Brehm BR. Influence of endothelin receptor antagonists on myocardial protein kinase C isoforms in uraemic cardiomyopathy. *Clin Sci (Lond)* 2002; **103** Suppl 48: 276S-279S

PO Box 2345, Beijing 100023, China
www.wjgnet.com
wjg@wjgnet.com

ELSEVIER

World J Gastroenterol 2005;11(8):1122-1130
World Journal of Gastroenterology ISSN 1007-9327

• *BASIC RESEARCH* •

Antidiabetic thiazolidinediones induce ductal differentiation but not apoptosis in pancreatic cancer cells

Elisabetta Ceni, Tommaso Mello, Mirko Tarocchi, David W Crabb, Anna Caldini, Pietro Invernizzi, Calogero Surrenti, Stefano Milani, Andrea Galli

Elisabetta Ceni, Stefano Milani, Mirko Tarocchi, Calogero Surrenti, Andrea Galli, Gastroenterology Unit, Department of Clinical Pathophysiology, University of Florence, Florence, Italy
David W Crabb, Departments of Medicine and of Biochemistry and Molecular Biology, Indiana University School of Medicine, IN, USA
Anna Caldini, Clinical Chemistry Laboratories, Careggi Hospital, Florence, Italy
Pietro Invernizzi, Department of Medicine Ospedale San Paolo, University of Milan, Milan, Italy
Tommaso Mello, Farmacogenomic Foundation FiorGen, Florence, Italy
Supported by Ministero dell'Università, della Ricerca Scientifica e Tecnologica, (MURST)
Correspondence to: Andrea Galli, M.D., Ph.D., Gastroenterology Unit, Department of Clinical Pathophysiology, University of Florence, Viale Morgani 85, 50134 Firenze Italy. a.galli@dfc.unifi.it
Telephone: +39-554271294 Fax: +39-554271297
Received: 2004-07-09 Accepted: 2004-10-13

Abstract

AIM: Thiazolidinediones (TZD) are a new class of oral antidiabetic drugs that have been shown to inhibit growth of same epithelial cancer cells. Although TZD were found to be ligands for peroxisome proliferator-activated receptor γ (PPARγ), the mechanism by which TZD exert their anticancer effect is presently unclear. In this study, we analyzed the mechanism by which TZD inhibit growth of human pancreatic carcinoma cell lines in order to evaluate the potential therapeutic use of these drugs in pancreatic adenocarcinoma.

METHODS: The effects of TZD in pancreatic cancer cells were assessed in anchorage-independent growth assay. Expression of PPARγ was measured by reverse-transcription polymerase chain reaction and confirmed by Western blot analysis. PPARγ activity was evaluated by transient reporter gene assay. Flow cytometry and DNA fragmentation assay were used to determine the effect of TZD on cell cycle progression and apoptosis respectively. The effect of TZD on ductal differentiation markers was performed by Western blot.

RESULTS: Exposure to TZD inhibited colony formation in a PPARγ-dependent manner. Growth inhibition was linked to G1 phase cell cycle arrest through induction of the ductal differentiation program without any increase of the apoptotic rate.

CONCLUSION: TZD treatment in pancreatic cancer cells has potent inhibitory effects on growth by a PPAR-dependent induction of pacreatic ductal differentiation.

Key words: Thiazolidinediones; Pancreatic cancer; PPARγ; Cancer growth; Differentiation

Ceni E, Mello T, Tarocchi M, Crabb DW, Caldini A, Invernizzi P, Surrenti C, Milani S, Galli A. Antidiabetic thiazolidinediones induce ductal differentiation but not apoptosis in pancreatic cancer cells. *World J Gastroenterol* 2005; 11(8): 1122-1130
http://www.wjgnet.com/1007-9327/11/1122.asp

INTRODUCTION

Pancreatic cancer is a devastating disease characterized by an increased incidence in western industrialized countries, an extremely poor median survival of 4-6 mo after diagnosis[1], and limited therapeutic options[2].

The majority of pancreatic cancers arises from the pancreatic duct cells and is characterized by uncontrolled growth, inability to express the differentiated features of normal duct cells and progressive accumulation of multiple genetic abnormalities[3].

It has been suggested that the pharmacological induction of cellular differentiation might be an alternative to conventional tumor chemotherapy. The activation of the terminal differentiation program in genetically abnormal tumor cells is strictly associated with irreversible growth arrest[4]. In pancreatic cancer cells, retinoids, for example, induce differentiation and inhibit growth by activation of their specific nuclear receptors[5,6] suggesting that other nuclear receptors involved in the regulation of cellular differentiation might be targets for novel therapeutic strategies of pancreatic cancer.

Thiazolidinediones (TZD) such as pioglitazone (PGZ) and rosiglitazone (RGZ) are a new class of antidiabetic drugs, which attenuate the insulin resistance associated with obesity, hypertension and impaired glucose tolerance in humans as well as in several animal models of non-insulin-dependent diabetes mellitus[7]. TZD were found to be ligands for peroxisome proliferator-activated receptor γ (PPARγ), a member of the nuclear receptor superfamily of ligand-dependent transcription factors that is predominantly expressed in adipose tissue although it is also expressed in other tissue at much lower levels[8-10]. In adipose tissue PPARγ functions as a master regulator of adipogenesis and

its ligand-mediated activation in fibroblasts induces adipocyte differentiation and lipid storage[11,12]. TZD activate PPARγ and promote association with 9-cis retinoic acid receptor (RXR) to form functional heterodimers, which recognize their cognate response element at the level of target genes[13,14].

Several recent studies have indicated that TZD may have anticancer properties in a variety of different epithelial malignancies including breast, prostate and gastrointestinal cancers[15-17]. Treatment of cultured breast and colon cancer cells with TZD resulted in a reduction in growth rate and induction of apoptosis[18,19]. Furthermore, human colorectal cancer cells implanted in nude mice were shown to grow more slowly in mice treated with TZD, with a 50% reduction of tumor volume[20]. In addition loss-of-function mutation of the PPARγ gene has been found in some human colon and thyroid carcinomas[21,22]. As a consequence, PPARγ has become a molecular target for anticancer drug development, and TZD have been proposed for therapy of PPARγ-expressing tumors.

Although preliminary evidence has shown that, troglitazone, the first TZD marketed for use in humans, inhibited pancreatic cell proliferation[23,24], the mechanism by which these drugs inhibit cell growth in these cells has not been conclusively established.

In this study we demonstrated that exposure of pancreatic cancer cells to TZD inhibited anchorage-independent growth with a PPARγ-dependent differentiation-inducing mechanism. Surprisingly the ductal pro-differentiation program induced by PPARγ activation was not associated with apoptosis in these cells.

MATERIALS AND METHODS

Materials

Most chemicals and supplies were purchased from Sigma Chemical Company (St. Luis, MO). Nitrocellulose and Nytran were from Schleicher and Schuell, Inc., (Keene, NH). Agarose, trypsin, all restriction endonucleases, DNA-modifying enzymes, and tissue culture media were purchased from Gibco BRL (New Brunswick, NJ). Fetal bovine serum (FBS) was from HyClone Laboratories (Logan, UT). D-threo-[dichloroacetyl-1,2-^{14}C]-chloramphenicol was purchased from New England Nuclear (Boston, MA). Rosiglitazone and pioglitazone were from SmithKline Beecham Pharmaceuticals (Welwyn, UK) and Takeda Chemicals (Tokyo, Japan) respectively.

Tissue sample and cell cultures

The pancreatic adenocarcinoma cell lines PANC-1, CAPAN-2, and HPAC were obtained from the American Type Culture Collection (ATCC, Rockville, MD). Cells were maintained in Dulbecco's modified Eagles medium (DMEM; GIBCO Laboratories, Grand Island, NY) containing 10% fetal bovine serum (FBS, Gibco). Culture medium was supplemented with 50 U/mL penicillin and 50 μg/mL streptomycin. All experiments were performed in phenol red-free medium.

Tumor clonogenic assay

Pancreatic cancer cells were trypsinized and disaggregated through a 19-gauge needle into a single-cell suspension, as evaluated by microscopy. Cells 2×10^4 were mixed with DMEM/5% dialyzed FBS containing 0.3% agarose and TZD at the concentration indicated. Cells were then layered over a solid base of 0.5% agarose in the same medium, in 60-mm dishes. The cultures were incubated in humidified 50 mL/L CO_2/95% air at 37 ℃. After 14 d the colonies were counted by an Omnicon 3 600 Colony Counter and photographed.

Cell cycle analysis

Cells (4×10^5) were exposed to TDZ for 4 d in medium supplemented with 5% dialyzed FBS. Total cells both in suspension and adherent, were collected, washed, suspended in cold PBS, and stained in trypan blue. Both blue and non-blue cells were counted. The cells were adjusted to 1×10^6 viable cells/mL and fixed in 2:1 ratio (v/v) in methanol overnight before staining with propidium iodide. Cell cycle status was analyzed with Becton Dickinson Flow Cytometer and CellFIT Cell-Cycle Analysis software.

Protein extract and Western blot

Whole-cell proteins were extracted from the different adenocarcinoma cell lines. Cells were cultured in the presence or absence of test agents and were homogenized in Laemmli buffer[25]. Nuclear proteins were isolated from treated and untreated cells based on micro preparation methods[26]. The nuclear extracts were suspended in 20 mmol/L HEPES (pH 7.9), 40 mmol/L NaCl, 1.5 $MgCl_2$, 0.2 mmol/L ethylenediaminetetraacetic acid, 25% glycerol, 0.5 mmol/L dithiothreitol, and 0.2 mmol/L phenylmethylsulfonyl fluoride. Lysates were centrifuged at 20 000 g for 10 min at 4 ℃ and supernatants were frozen in liquid nitrogen and stored at -80 ℃ until use. Nuclear and whole-cell extracts (40 μg protein) were fractionated in 12% sodium dodecyl sulfate-polyacrylamide gel electrophoresis and electro blotted onto nitrocellulose filters. Proteins were detected by incubating the filters with the following primary antibody: mouse anti-human PPARγ (1:500) (Santa Cruz Biotechnology, Santa Cruz, CA, USA), sheep anti-human carbonic anhydrase II (1:500)[27] cytokeratin 7 (1:1 500) (Novocastra Lab, Newcastle UK), p21 (1:1 000) (Santa Cruz Biotechnology, Santa Cruz, CA) and p27 (1:1 000) (Santa Cruz Biotechnology, Santa Cruz, CA), mouse anti-human bcl-2, bax, and bcl-xl (1:1 000) (Transduction, Laboratories, San Diego CA) mouse anti human bax (1:1 000), and mouse anti-human bak (1:1 000) (CalBiochem, San Diego CA). Detection of the protein bands was performed using the Amersham ECL kit (Arlington Heights, IL).

RNA extraction and RT-PCR

Total RNA was extracted from cultured cells and by guanidinium-phenol-chloroform methods of Chomczynski and Sacchi[28] with minor modifications[29]. One mg of RNA from tumor cells was reverse transcribed with Molony murine leukemia virus (MMLV) reverse transcriptase (Life Technologies Inc., Paisley, UK) at 42 ℃ for 60 min in a 20-μL mixture in the presence of random hexamers. The nucleotide bases used for human PPARγ were 5'-TCTGGCCCACC-AACTTTGGG-3' and 5'-CTTCACAAGCATGA-

ACTCCA-3'. Two μL of a reverse-transcribed mixture was subjected to PCR in a 20-μL reaction solution [10 mmol/L Tris-HCl (pH 8.3), 50 mmol/L KCl, 2.0 mmol/L $MgCl_2$, 0.01% gelatin, 20 mmol/L deoxynucleotide triphosphate, 0.5 units of Taq polymerase (Life Technologies Inc., Paisley, UK), and 0.25 pmoL of primers]. Twenty-five cycles of reaction at 94 ℃ for 50 s, 60 ℃ for 45 s, and 72 ℃ for 90 s were carried out by DNA thermal cycler (Perkin-Elmer Cetus Norwalk, CT). Efficiency of RT was controlled in each sample by PCR amplification of human β_2-microglobulin (5'-GCAAAAGATGAGTATGCCTG-3', 5'-TTCACTCAATCCAAATGCGG-3').

Transient transfection of culture cells

Cells were transfected at the density of 5×10^5 cells/60 mm dish with 2.5 μg of peroxisome proliferator response element $(ARE)_3$-tk-luciferase reporter plasmid (containing 3 copies of the PPRE from the adipocyte lipid-binding protein (aP2) gene ligated to a herpes simplex thymidine kinase promoter upstream of a luciferase gene)[30,31], and 5 μg of pSV_2CAT (vector containing SV40 early promoter and enhancer sequences that drives a chimeric chloramphenicol acetyl transferase [CAT] gene) as an internal control by calcium phosphate precipitation. Total amount of DNA transfected was normalized with a carrier DNA (pcDNA3.1; Invitrogen Corporation, Carlsbad, CA). Four hours later the cells were exposed to PBS containing 15% glycerol for 3 min. The cells were rinsed twice with PBS and fresh serum supplemented with 5% dialyzed FBS was added. Twenty four hours after transfection cells were treated with TZD. Twenty four hours later, the cells were harvested, washed twice with PBS, and lysed in 150 μL of buffer containing 25 mmol/L Tris, pH 7.8, 2 mmol/L ethylenediaminetetraacetic acid, 20 mmol/L dithiothreitol, 10% glycerol, and 1% Triton X-100. Fifty microliters of cell extract were incubated with luciferase assay reagent based on the original protocol of de Wet *et al*[32]. The number of relative light units with a 3-s delay and 30-s incubation were measured by Sirius1 luminometer (Berthold Detection System, Pforzheim/ Germany). CAT activity was measured as described previously[33]. The conversion of chloramphenicol to its acetylated products was quantified on Ambis beta scanner (Ambis System, San Diego, CA).

Generation of the PPARγ-expressing cell line

Human PPARγ cDNA was cloned into pLNCX, a retroviral vector driving expression of the cloned cDNA from the cytomegalovirus promoter and conferring resistance to G418. Retrovirus plasmid was transfected into a packaging cell line, PA317, and used to transduce HPAC cells as previously described[34]. In brief, PA317 were transfected with 10 μg of the cloned construct (PPARγ-pLNCX) or the empty retroviral vector, using calcium phosphate precipitation followed by glycerol stock as described above. Twenty four hours after transfection the virus-containing supernatant was removed, filtered through a 45-μm filter, and stored at -70 ℃. A total of 5×10^5 HPAC cells were infected with 10^6 cfu/mL virus in the presence of 6 μg/mL polybrene. Twenty four hours later the cells were replated in duplicate and selected with 600 μg/mL of the antibiotic G418. After selection of G418-resistant cells, the clones were expanded and screened for PPARγ expression by Western blotting.

Apoptosis assay

Following the indicated treatments, apoptosis was measured by a DNA fragmentation assay (Apo-Direct) as recommended by the manufacturer (PharMingen, San Diego, CA). Briefly, cells (adherent and floating) were fixed in 1% formaldehyde in PBS overnight. After washing, 10^6 fixed cells were incubated with terminal deoxynucleotidyl transferase enzyme (TdT) and FITC-dUTP for 90 min at 37 ℃ to label DNA breaks. Cells were rinsed, incubated in RNaseA/propidium iodide in the dark for 30 min at room temperature to stain total DNA, and then analyzed by flow cytometry. Cells doublets and clumps were eliminated from the analysis by gating.

Statistical analysis

Data was expressed as mean±SD. Statistical correlation of data was checked for significance by ANOVA and paired Student's *t* test. The corresponding probability (*P*) is given.

RESULTS

TZD inhibited anchorage-independent growth of human pancreatic cancer cells with a PPARγ-dependent mechanism

We initially investigated the effect of TZD on pancreatic cancer cell growth. The effect of TZD on anchorage-independent growth was assessed by cloning cancer cells in soft agarose. Treatment with both TZD at the concentration of 10 μmol/L resulted in a significant inhibition of colony formation by Panc-1 and Capan-2 cell lines, whereas drug treatment was ineffective in the PPARγ non-expressing HPAC cells (Figure 1A, B). Clofibric acid was used as a negative control. The dose dependency for the anchorage-independent growth inhibition was further characterized in Panc-1 cells. PGZ inhibited colony formation in a dose-dependent manner in Panc-1 cell line (Figure 1C). Moreover, the size of the colonies was significantly smaller in the RGZ-treated cells compared to cells treated with vehicle alone.

To confirm the role of PPARγ in TDZ-induced growth arrest, we generated a PPARγ-expressing HPAC cells using transducing retroviruses. Four isolated HPAC clones showed selective overexpression of PPARγ protein compared to parental wild type and mock-transfected controls (Figure 2A). Of the selected clones, number 3 (P3-HPAC) was used for further studies. In these cells, PGZ induced the activity of the ARE-7_3-tk-luc reporter in a dose-dependent manner (Figure 2B) and this effect was correlated to a significant inhibition of anchorage-independent growth (Figure 2C).

PPARγ activation by TZD alters cell cycle progression but does not induce apoptosis in pancreatic cancer cells

Preliminary experiments evaluating trypan blue exclusion and lactate dehydrogenase leakage from pancreatic cancer cells into the culture medium showed that both TZD induced growth inhibition rather than cytotoxicity, because the number of vitally stained cells was higher than 90% in all experiments at any given time point. Based on this observation,

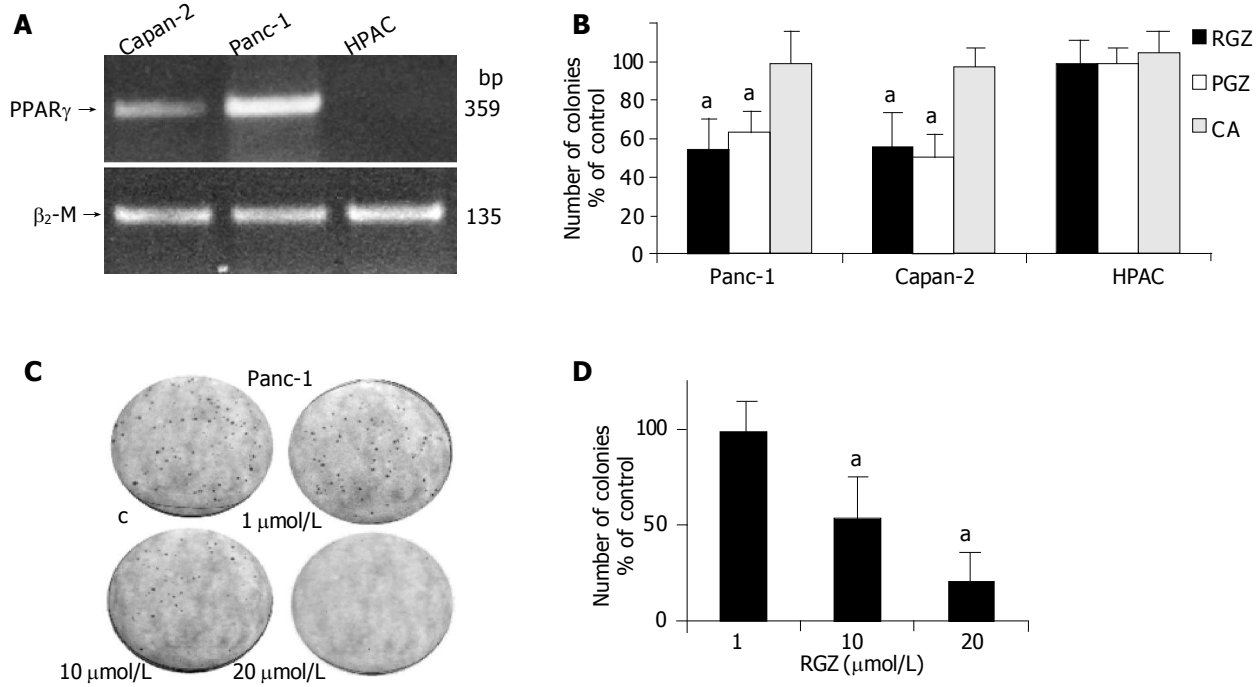

Figure 1 Effect of TZD on anchorage-independent growth in human pancreatic adenocarcinoma cells. A: PPARγ expression in human pancreatic adenocarcinoma. One microgram of total RNA extracted from three pancreatic cancer cell lines (Capan-2, Panc-1, and HPAC) was reverse transcribed using random hexamers and amplified by polymerase chain reaction using specific primers for PPARγ and for β_2-microglobulin (β_2-M) as described in Methods. The reverse-transcription polymerase chain reaction products were electrophoresed on ethidium bromide-containing agarose gel; B: TZD inhibit anchorage-independent growth. 2x10^4 cells were plated into media containing 0.3% agarose, supplemented with either 10 μmol/L of TZD (RGZ o PGZ), or 1 mmol/L clofibrate (CA). After 14 d the number of colonies was determined and then expressed as the percentage of control cells treated with vehicle (DMSO) alone. The mean±SD of six independent experiments performed for each cell line in triplicate are shown. $^aP<0.05$ (or higher degree of significance) *vs* control; C: Dose-dependent inhibition of anchorage-independent growth by TZD in Panc-1 cells. Clonogenic assay of Panc-1 cells treated with the indicated concentrations of RGZ was performed as described in Methods. The number of colonies was then given as the percentage of control cells treated with vehicle alone. The mean±SD of five independent experiments performed for each in triplicate are shown. $^aP<0.05$ (or higher degree of significance) *vs* control.

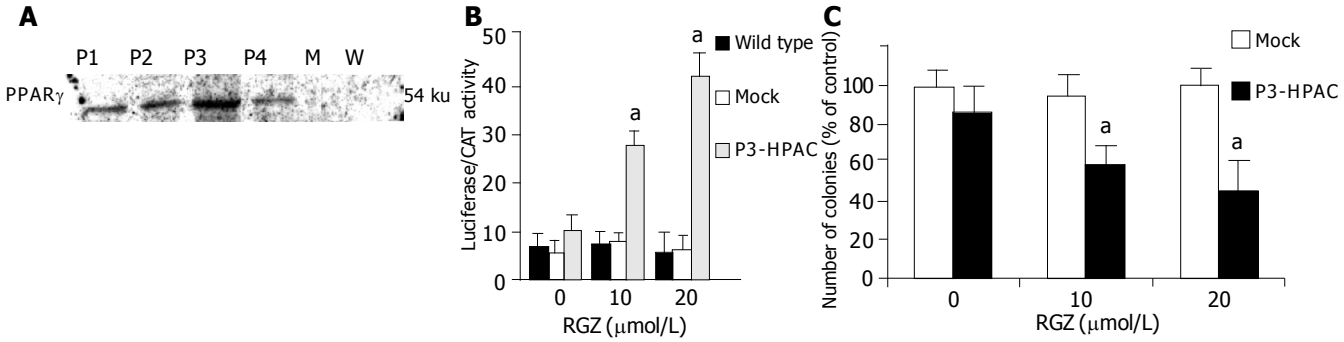

Figure 2 PPARγ expression and transcriptional activity in HPAC cells transduced with PPARγ-expressing retrovirus. A: HPAC cells were stable transduced by retrovirus driving expression of human PPARγ (hPPARγ-pLNCX) as described in methods. After selection with G418 four resistant clones were expanded and screened for hPPARγ expression. The cell extracts were fractionated by sodium dodecyl sulfate-polyacrylamide gel electrophoresis and blotted to nitrocellulose. The proteins (40 μg) were detected with antibody raised against human PPARγ. P1-P4 represent nuclear protein extracted from G418-resistant HPAC cell clones; M represents nuclear proteins from mock (pLNCX) transduced HPAC cells; W (wild type) represents nuclear proteins from untransduced, parental HPAC cells; B: After overnight attachment cells were transfected with ARE-7$_3$-tk-luciferase reporter plasmid and pSV$_2$-CAT as internal control for transfection efficiency. Twenty-four hours after transfection cells were treated with RGZ at the indicated concentration. Twenty-four hours after treatment the cells were harvested for luciferase and CAT assay as described in Methods. The data is expressed as mean±SD for 4 replicate experiments performed in triplicate; $^aP<0.05$ *vs* control; C: Effect of TDZ treatment on anchorage-independent growth of HPAC cells transduced with PPARγ-expressing retrovirus. Clonogenic assay of P3-HPAC cells treated with the indicated concentration of RGZ was performed as described in materials and methods. The number of colonies was then given as the percentage of control cells treated with vehicle alone. The mean±SD of five independent experiments performed for each in triplicate are shown. $^aP<0.05$ *vs* Mock transduced cells.

we assessed the effect of RGZ and PGZ on cell cycle progression. Little change in cell distribution was observed at 12 h with 20 μmol/L of TZD in all cell lines (not shown). In PPARγ-expressing cells both RGZ and PGZ increased the proportion of cells in G_0/G_1 phase at 24 h and the arrest persisted at later time points (Figure 3). The Increased number of cells in G_0/G_1 phase was mirrored by a proportional decrease of cells in S phase. No effect was

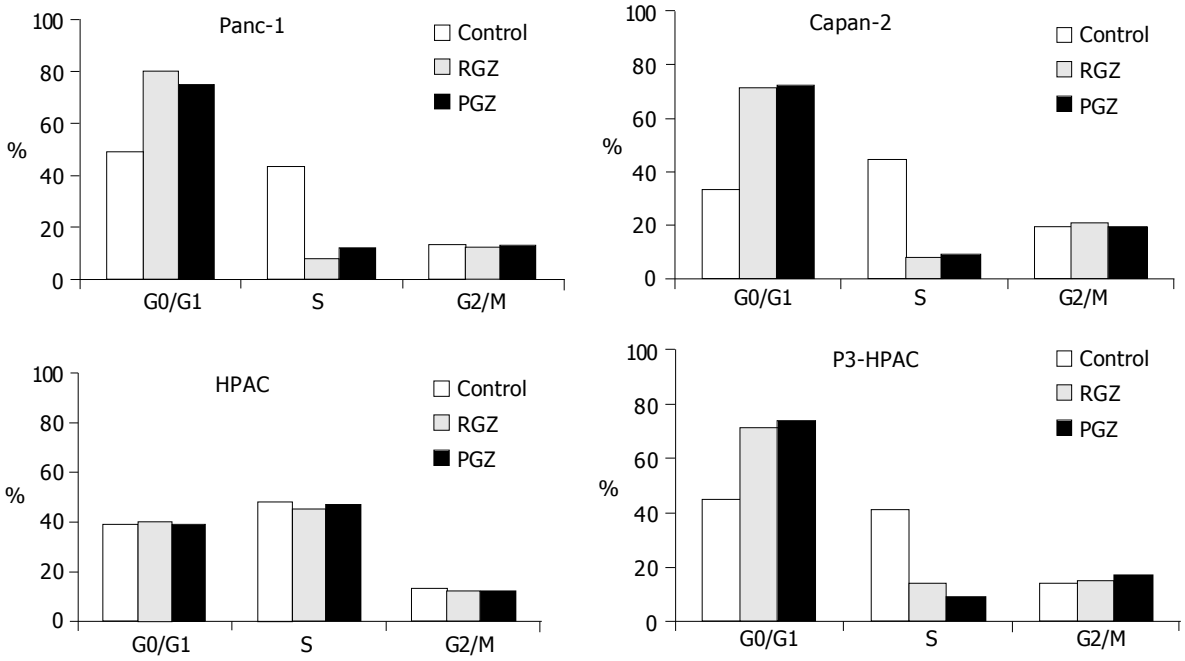

Figure 3 Cell cycle phase distribution of pancreatic tumor cells treated with TZD. After overnight attachment cells were treated with 20 μmol/L of TZD (RGZ or PGZ) for 72 h, followed by staining with propidium iodide and flow cytometric analysis of DNA content. The percentage of cells in each cell cycle phase was determined by analysis of the DNA content histograms using Modfit software as described in Methods. Data show the percentage of cells in each phase of cell cycle in a representative experiment. Similar results were obtained in at least three independent experiments.

documented in the PPARγ-deficient HPAC line, whereas the inhibition of cell cycle progression by TZD was restored in P3-HPAC cells. To determine whether the inhibitory effect of TZD was in part mediated by inducing apoptosis, cells were treated with RGZ or PGZ for 72 h before the analysis. The extent of apoptosis was measured by incorporation of FITC dUTP in the presence of TdT enzyme to detect DNA fragmentation. Both compounds had negligible effect on the extent of apoptosis at the higher concentration used (Table 1). In addition, the expression of the bcl-2 family members involved in regulating apoptosis was also determined in PANC-1, Capan-2 and P3-HPAC cells following treatment with RGZ or PGZ. After 24-h incubation with TZD, no change in the expression of the inducers of apoptosis, bax or bak, or inhibitors of apoptosis such as bcl-2 and its close homologue bcl-xL was detected (Figure 4). These results suggest that pancreatic tumor cells are relatively resistant to apoptosis induced by TZD.

Table 1 Effect of TZD on apoptosis in pancreatic tumor cells. Extent of apoptosis following treatment of pancreatic cancer cell lines with 20 μmol/L of TZD (RGZ or PGZ) for three days was measured by the incorporation of FITC-dUTP in the presence of TdT enzyme to detect DNA fragmentation as described in Methods. Cells were stained with RNase A/PI and analyzed by flow cytometry. The mean±SD of five independent experiments each performed in triplicate are shown

Treatment	Apoptosis (%)			
	Panc-1	Capan-2	HPAC	P3-HPAC
Control (DMSO)	1.16±0.15	0.88±014	0.46±0.19	0.66±017
RGZ	1.20±0.17	0.90±0.22	0.38±0.17	0.58±0.19
PGZ	1.19±0.14	0.93±0.17	0.40±0.18	0.57±0.13

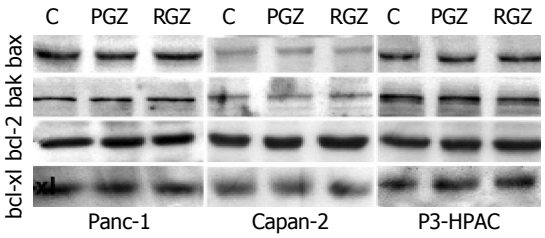

Figure 4 Expression of apoptotic proteins in cells treated with TZD. Sub-confluent cells were treated with 20 μmol/L of TZD (RGZ or PGZ) for 24 h. Cells were then harvested, and whole-cell protein extracts were fractionated by sodium dodecyl sulfate-polyacrylamide electrophoresis and transferred to nitrocellulose paper as described in Methods. Different proteins were detected by incubating the filter with specific antibodies.

TZD promoted differentiation and reversal of the transformed phenotype in PPARγ-expressing cells

In the PPARγ-expressing cell line, PANC-1, 72-h incubation with RGZ resulted in morphological changes with more abundant, flattened cytoplasm, and increased cytoplasmic/nuclear ratio, as is consistent with a more mature phenotype (Figure 5B). To determine whether morphological changes and growth arrest were accompanied by differentiation, analysis of markers of the differentiated state was performed.

Treatment with 20 μmol/L of RGZ resulted in a time-dependent increased expression of ductal specific markers such as carbonic anhydrase II (CA II)[5] and cytokeratin 7[35] as well as "general" differentiation markers such as the cell cycle inhibitors p21 and p27 (Figure 5A). Expression of

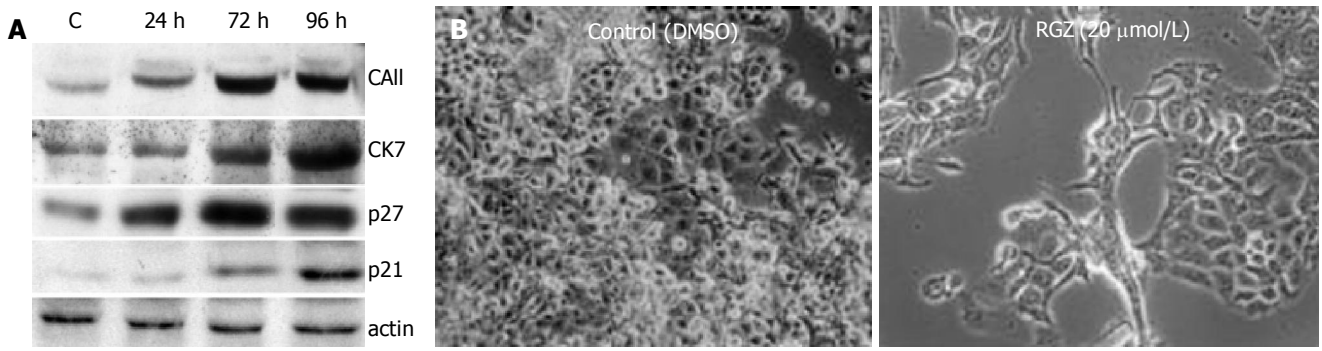

Figure 5 TZD-induced ductal differentiation in pancreatic adenocarcinoma cells. A: Effect of RGZ on the expression of differentiation markers in Panc-1 cells. After 24 h of plating, cells were incubated with 20 μmol/L of RGZ for the indicated time intervals. Protein extracts were then extracted and separated by Western blotting as described in Methods. Immunoreactive proteins were detected by incubating the filters with the specific primary antibodies. A representative of three independent experiments, yielding similar results, is shown; B: Effect of RGZ on tumor cells morphology. Panc-1 cells were plated onto sterile culture chambers and then treated with 20 μmol/L of RGZ for 96 h. After the incubation period cells were photographed with Axiovert 200 Image System (Zeiss, Gottingen, Germany). Original magnification ×200.

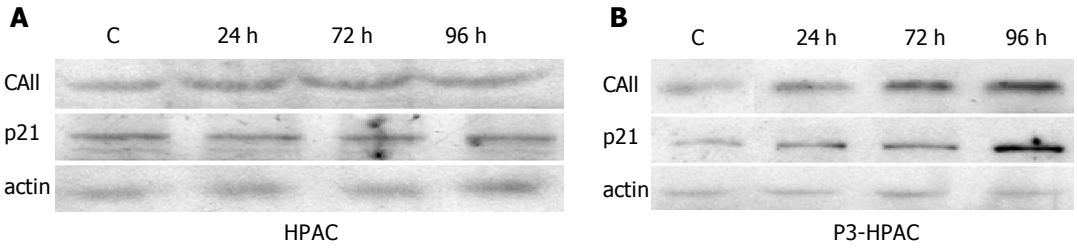

Figure 6 Effect of TZD on expression of differentiation markers in HPAC cells transduced with PPARγ-expressing retrovirus. Untransduced parental HPAC cells. A: or PPARγ-overexpressing P3-HPAC cells; B: were incubated with 20 μmol/L of RGZ for the indicated time intervals. Protein extracts were then extracted and separated by Western blotting as described in Methods. Immunoreactive proteins were detected by incubating the filters with the specific primary antibodies. A representative of three independent experiments, yielding similar results, is shown.

β-actin, used as an internal control, did not change under any experimental condition. Treatment with PGZ had similar effect (not shown). In contrast, HPAC cells did not show any induction of differentiation markers (Figure 6A). TZD induced p21 and CA II expression in the P3-HPAC clone (Figure 6B), thus supporting the role of PPARγ in the acquisition of a more differentiated state.

Because PPARγ activation can enhance adipocyte differentiation[11], we examined the lipid accumulation in PANC-1 and in Capan-2 cells. Oil Red O staining revealed no lipid accumulation after PGZ or RGZ treatment for 4 d (not shown).

DISCUSSION

Here we studied the effects of two TZD, pioglitazone (PGZ) and rosiglitazone (RGZ), on pancreatic cancer cell growth, and we characterized the relationship between PPARγ expression and their anticancer properties. The two TZD similarly induced a strong inhibition of anchorage-independent growth on PPARγ-expressing cell lines but they had no effect on colony formation of the PPARγ-deficient cells, HPAC (Figure 1B). The role of PPARγ in the antiproliferative effect of TZD in pancreatic cancer cells was confirmed by overexpression of the receptor in HPAC cells. Expression of PPARγ in HPAC cells, obtained by transducing retrovirus, restored the growth inhibitory effect of TZD in parallel with a significant induction of PPRE reporter activity (Figure 2B, C). We therefore, conclude that PPARγ expression determines TZD sensitivity in pancreatic carcinoma cells. Confirming our result, the reduction of DNA accumulation by RGZ in glioma cells is strictly dependent on PPARγ expression[36]. In addition RGZ exclusively inhibits anchorage-independent growth in human colorectal cancer cells that express a transcriptionally active PPARγ[18]. This data is, however, partially in contrast with the observation that the anticancer effects of TZD are independent of PPARγ and mediated by inhibition of translation initiation[37]. In fact, in PPARγ ES cells troglitazone induced cell cycle arrest by partial depletion of intracellular Ca^{2+} stores, activation of the double-stranded RNA-dependent protein kinase (PKR), and phosphorylation of the eukaryotic initiation factor 2α (eIF2α). Furthermore, Abe *et al* have indicated that troglitazone suppressed cell growth and histamine secretion by a PPARγ-independent mechanism in the human basophilic leukemia cell line KU812[38]. A possible explanation of this controversy may be due to the different chemical structure of the various members of TZD family. Only troglitazone, for instance, has the chroman structure of vitamin E, suggesting that this TZD could regulate signal pathways by mimicking the effects of vitamin E and independently of PPARγ transcriptional

activation[39].

To define the mechanisms by which TZD inhibit the growth of pancreatic carcinoma cells, we analyzed the cell cycle profile of cells treated with RGZ and PGZ. Both TZD increased the population of cells in G_1/G_0 phase and reduced the population of cells in S phase in PPARγ-expressing cells (Figure 3). These results support recent observations in other growing cells, such as colon cancer cells and myeloid leukemia cells, showing that PPARγ activation induce G_1 cell cycle arrest[18,40]. These cycle alterations were achieved at TZD concentrations that repressed pancreatic cell growth, indicating that cell-cycle arrest is one of the primary mechanisms responsible for the anti-proliferative action of TZD in pancreatic cancer cell *in vitro*.

Apoptosis and cell differentiation are tightly linked to cell cycle control mechanisms, particularly those that regulate the transit through G_1 phase[41,42]. Thus, the induction of G_1 arrest by TZD-activation of PPARγ may be the precipitating molecular events for subsequent cell differentiation or death. We did not find any pro-apoptotic effects in PPARγ-expressing and non-expressing cells after TZD treatment at the highest concentration used (Table 1 and Figure 4), whereas a significant time-dependent induction of both general and ductal-specific differentiation markers was observed after TZD treatment in PANC-1 cells and in the PPARγ overexpressing clone, P3-HPAC. This suggests that the *in vitro* anti-proliferative effects of TZD in pancreatic tumor cells are not primarily mediated by the induction of apoptotic cell death. Our findings are consistent with the apoptotic-resistant phenotype characteristic of pancreatic tumor cells that are resistant to undergoing apoptosis induced by chemotherapeutic agents, activation of surface receptors such as CD 95 or by serum and growth factor withdrawal[43,44]. Similarly to TZD, non-steroidal anti-inflammatory drugs (NSAID) such as indomethacin and sulindac inhibit pancreatic cell growth by cell-cycle arrest without apoptosis via a COX_2-independent mechanism[45]. Interestingly, it has been shown that NSAID are PPARγ activators and their growth-inhibitory effect in pancreatic cells could be mediated, at least in part, by this receptor[46]. Furthermore, Wick *et al*, have recently demonstrated that PPARγ is one of the molecular targets of NSAID mediating COX-independent inhibition of lung cancer cell growth[47]. In contrast, the natural PPARγ ligand, 15d-PGJ_2, induced substantial apoptosis in pancreatic cancer cells[48]. These discrepancies could be explained assuming that the effect of 15d-PGJ_2 may be partially PPARγ-independent. Indeed, cyclopentenone prostaglandins have been shown to induce apoptotic cell death of human hepatic myofibroblasts, which do not express PPARγ, by a mechanism involving the production of reactive oxygen species[49]. Furthermore, specific inhibition of PPARγ does not prevent 15d-PGJ_2-induced apoptosis in breast cancer cells, suggesting that this ecosanoid requires mechanisms others than activation of PPARγ to induce apoptosis[50].

Although inhibition of cloning efficiency is generally considered the hallmark of differentiation, we investigated additional characteristics that would point towards a more differentiated phenotype of ductal carcinoma cells. Whereas much is known about PPARγ and its role in adipocytic differentiation[11], in part because of the identification of well-established markers of the terminally differentiated adipocyte[12], the pancreatic ductal epithelium represents a more complex and challenging system. We found that TZD treatment induced the expression of differentiated ductal cells markers such as CK-7[35] and CAII[5] in parallel with a significant up-regulation of the cell cycle inhibitors p21 and p27 in Panc-1 cells (Figure 5A). By light microscopy, we observed elongation and flattening of cells with extending cellular process after TZD treatment (Figure 5B). These morphological changes are strikingly similar to the ones observed after butyrate and retinoid induced differentiation in the same cell lines[5,51] and represented a more differentiated and less malignant state. In agreement with the negligible effect of TZD on growth of PPARγ non-expressing cells, these drugs have no effect on the expression of CAII and p21 in HPAC cells (Figure 6A). Ectopic expression of PPARγ completely restored the ability of TZD to induce ductal differentiation in HPAC cells, suggesting that the expression and activation of PPARγ pathway is a key step in pancreatic-specific differentiation (Figure 6B). Chang *et al*, have recently reported growth inhibition and increased expression of markers of bronchoalveolar progenitor cells in non-small cell lung cancer after treatment with PPARγ agonists[52]. Similarly to our results, they did not document either lipid accumulation or adipocyte-specific gene expression, thus excluding adipocytic transdifferentiation of these cell lines. The signaling events evoked by PPARγ activation in epithelial cancer cells remain unclear. The ability of TZD to establish various lineage-specific differentiated states that differ according to the cellular type would suggest that the PPARγ pathway functions early in the induction of differentiation, before lineage-specific events occur.

Overall, our study demonstrates that TZD inhibits growth of pancreatic cancer cells via a PPARγ-dependent induction of ductal differentiation. Given the favorable toxicity profile of these drugs and the limited treatment options that are currently available for patients with pancreatic malignancies, TZD might be a new effective approach to complement conventional chemotherapeutic regimens for pancreatic cancer therapy.

ACKNOWLEDGEMENTS

We are indebted to Dr. Mizukami for human PPARγ expression plasmid. The authors express their appreciation to Professor M. Serio and M. Mannelli for many helpful comments and suggestion.

REFERENCES

1 National Cancer: Annual cancer statistic review 1973-1988. bethesda, Department of health and human service 1991, NIH publication No 91-2789

2 **Washaw AL,** Fernandez-Del Castillo C. Pancreatic carcinoma. *N Engl J* Med 1992; **326:** 455-465

3 **Hohne MW,** Halatsch ME, Kahl GF, Weinel RJ. Frequent loss of expression of the potential tumor suppressor gene DCC in ductal pancreatic adenocarcinoma. *Cancer Res* 1992; **52:** 2616-2619

4 **Leszczyniecka M,** Roberts T, Dent P, Grant S, Fisher PB. Differentiation therapy of human cancer: basic science and

clinical applications. *Pharmacol Ther* 2001; **90:** 105-156
5 **Rosewicz S,** Stier U, Brembeck F, Kaiser A, Papadimitriou CA, Berdel WE, Wiedenmann B, Riecken EO. Retinoids: effects on growth, differentiation, and nuclear receptor expression in human pancreatic carcinoma cell lines. *Gastroenterology* 1995; **109:** 1646-1660
6 **Rosewicz S,** Wollbergs K, Von Lampe B, Matthes H, Kaiser A, Riecken EO. Retinoids inhibit adhesion to laminin in human pancreatic carcinoma cells via the alpha 6 beta 1-integrin receptor. *Gastroenterology* 1997; **112:** 532-542
7 **Olefsky JM.** Treatment of insulin resistance with peroxisome-proliferator-activated receptor gamma agonists. *J Clin Invest* 2000; **106:** 467-472
8 **Braissant O,** Foufelle F, Scotto C, Dauca M, Wahli W. Differential expression of peroxisome proliferator-activated receptors (PPARs): tissue distribution of PPAR-alpha, -beta, and -gamma in the adult rat. *Endocrinology* 1996; **137:** 354-366
9 **Kliewer SA,** Forman BM, Blumberg B, Ong ES, Borgmeyer U, Mangelsdorf DJ, Umesono K, Evans RM. Differential expression and activation of a family of murine peroxisome proliferator-activated receptors. *Proc Natl Acad Sci USA* 1994; **91:** 7355-7359
10 **Roberts-Thomson SJ.** Peroxisome proliferator-activated receptors in tumorigenesis: targets of tumour promotion and treatment. *Immunol Cell Biol* 2000; **78:** 436-441
11 **Tontonoz P,** Hu E, Spiegelman BM. Regulation of adipocyte gene expression and differentiation by peroxisome proliferator-activated receptor gamma. *Curr Opin Genet Dev* 1995; **5:** 571-576
12 **Tontonoz P,** Hu E, Spiegelman BM. Stimulation of adipogenesis in fibroblasts by PPAR gamma 2, a lipid activated transcription factor. *Cell* 1994; **79:** 1147-1156
13 **Reginato MJ,** Bailey ST, Krakow SL, Minami C, Ishii S, Tanaka H, Lazar MA. A potent antidiabetic thiazolidinedione with unique peroxisome proliferator-activated receptor gamma-activating properties. *J Biol Chem* 1998; **273:** 32679-32684
14 **Juge-Aubry C,** Pernin A, Favez T, Burger AG, Wahli W, Meier CA, Desvergne B. DNA binding properties of peroxisome proliferator-activated receptor subtypes on various natural peroxisome proliferator response elements. Importance of the 5'-flanking region. *J Biol Chem* 1997; **272:** 25252-25259
15 **Pignatelli M,** Cortes-Canteli M, Lai C, Santos A, Perez-Castillo A. The peroxisome proliferator-activated receptor gamma is an inhibitor of ErbBs activity in human breast cancer cells. *J Cell Sci* 2001; **114**: 4117-4126
16 **Kubota T,** Koshizuka K, Williamson EA, Asou H, Said JW, Holden S, Miyoshi I, Koeffler HP. Ligand for peroxisome proliferator-activated receptor gamma (troglitazone) has potent antitumor effect against human prostate cancer both in vitro and in vivo. *Cancer Res* 1998; **58:** 3344-3352
17 **Tsujie M,** Nakamori S, Okami J, Hayashi N, Hiraoka N, Nagano H, Dono K, Umeshita K, Sakon M, Monden M. Thiazolidinediones inhibit growth of gastrointestinal, biliary, and pancreatic adenocarcinoma cells through activation of the peroxisome proliferator-activated receptor gamma/retinoid X receptor alpha pathway. *Exp Cell Res* 2003; **289:** 143-151
18 **Brockman JA,** Gupta RA, Dubois RN. Activation of PPARgamma leads to inhibition of anchorage-independent growth of human colorectal cancer cells. *Gastroenterology* 115: 1049-1055
19 **Elstner E,** Muller C, Koshizuka K, Williamson EA, Park D, Asou H, Shintaku P, Said JW, Heber D, Koeffler HP. Ligands for peroxisome proliferator-activated receptorgamma and retinoic acid receptor inhibit growth and induce apoptosis of human breast cancer cells in vitro and in BNX mice. *Proc Natl Acad Sci USA* 1998; **95:** 8806-8811
20 **Sarraf P,** Mueller E, Jones D, King FJ, DeAngelo DJ, Partridge JB, Holden SA, Chen LB, Singer S, Fletcher C, Spiegelman BM. Differentiation and reversal of malignant changes in colon cancer through PPARgamma. *Nat Med* 1998; **4:** 1046-1052
21 **Kroll TG,** Sarraf P, Pecciarini L, Chen CJ, Mueller E, Spiegelman BM, Fletcher JA. PAX8-PPARgamma1 fusion oncogene in human thyroid carcinoma [corrected]. *Science* 2000; **289:** 1357-1360
22 **Sarraf P,** Mueller E, Smith WM, Wright HM, Kum JB, Aaltonen LA, de la Chapelle A, Spiegelman BM, Eng C. Loss-of-function mutations in PPAR gamma associated with human colon cancer. *Mol Cell* 1999; **3:** 799-804
23 **Motomura W,** Okumura T, Takahashi N, Obara T, Kohgo Y. Activation of peroxisome proliferator-activated receptor gamma by troglitazone inhibits cell growth through the increase of p27KiP1 in human. Pancreatic carcinoma cells. *Cancer Res* 2000; **60:** 5558-5564
24 **Kawa S,** Nikaido T, Unno H, Usuda N, Nakayama K, Kiyosawa K. Growth inhibition and differentiation of pancreatic cancer cell lines by PPAR gamma ligand troglitazone. *Pancreas* 2002; **24:** 1-7
25 **Laemmli UK.** Cleavage of structural proteins during the assembly of the head of bacteriophage T4. *Nature* 1970; **227:** 680-685
26 **Andrews NC,** Faller DV. A rapid micropreparation technique for extraction of DNA-binding proteins from limiting numbers of mammalian cells. *Nucleic Acids Res* 1991; **19:** 2499
27 **Invernizzi P,** Battezzati PM, Crosignani A, Zermiani P, Bignotto M, Del Papa N, Zuin M, Podda M. Antibody to carbonic anhydrase II is present in primary biliary cirrhosis (PBC) irrespective of antimitochondrial antibody status. *Clin Exp Immunol* 1998; **114:** 448-454
28 **Chomczynski P,** Sacchi N. Single-step method of RNA isolation by acid guanidinium thiocyanate-phenol-chloroform extraction. *Anal Biochem* 1987; **162:** 156-159
29 **Casini A,** Pinzani M, Milani S, Grappone C, Galli G, Jezequel AM, Schuppan D, Rotella CM, Surrenti C. Regulation of extracellular matrix synthesis by transforming growth factor beta1 in human fat-storing cells. *Gastroenterology* 1993; **105:** 245-253
30 **Galli A,** Stewart M, Dorris R, Crabb D. High-level expression of RXRalpha and the presence of endogenous ligands contribute to expression of a peroxisome proliferator-activated receptor-responsive gene in hepatoma cells. *Arch Biochem Biophys* 1998; **354:** 288-294
31 **Camp HS,** Li O, Wise SC, Hong YH, Frankowski CL, Shen X, Vanbogelen R, Leff T. Differential activation of peroxisome proliferator-activated receptor-gamma by troglitazone and rosiglitazone. *Diabetes* 2000; **49:** 539-547
32 **de Wet JR,** Wood KV, DeLuca M, Helinski DR, Subramani S. Firefly luciferase gene: structure and expression in mammalian cells. *Mol Cell Biol* 1987; **7:** 725-737
33 **Crabb DW,** Dixon JE. A method for increasing the sensitivity of chloramphenicol acetyltransferase assays in extracts of transfected cultured cells. *Anal Biochem* 1987; **163:** 88-92
34 **Galli A,** Price D, Crabb D. High-level expression of rat class I alcohol dehydrogenase is sufficient for ethanol-induced fat accumulation in transduced HeLa cells. *Hepatology* 1999; **29:** 1164-1170
35 **Schussler MH,** Skoudy A, Ramaekers F, Real FX. Intermediate filaments as differentiation markers of normal pancreas and pancreas cancer. *Am J Pathol* 1992; **140:** 559-568
36 **Berge K,** Tronstad KJ, Flindt EN, Rasmussen TH, Madsen L, Kristiansen K, Berge RK. Tetradecylthioacetic acid inhibits growth of rat glioma cells ex vivo and *in vivo* via PPARγ-dependent and PPARγ-independent pathways. *Carcinogenesis* 2001; **22:** 1747-1755
37 **Palakurthi SS,** Aktas H, Grubissich LM, Mortensen RM, Halperin JA. Anticancer effects of thiazolidinediones are independent of peroxisome proliferator-activated receptor gamma and mediated by inhibition of translation initiation. *Cancer Res* 2001; **61:** 6213-6218
38 **Abe A,** Kiriyama Y, Hirano M, Miura T, Kamiya H, Harashima H, Tokumitsu Y. Troglitazone suppresses cell growth of KU812 cells independently of PPARgamma. *Eur J Pharmacol* 2002; **436:** 7-13
39 **Inoue I,** Katayama S, Takahashi K, Negishi K, Miyazaki T, Sonoda M, Komoda T. Troglitazone has a scavenging effect

on reactive oxygen species. *Biochem Biophys Res Commun* 1997; **235:** 113-116

40 **Zhu L,** Gong B, Bisgaier CL, Aviram M, Newton RS. Induction of PPARgamma1 expression in human THP-1 monocytic leukemia cells by 9-cis-retinoic acid is associated with cellular growth suppression. *Biochem Biophys Res Commun* 1998; **251:** 842-848

41 **King KL,** Cidlowski JA. Cell cycle regulation and apoptosis. *Annu Rev Physiol* 1998; **60:** 601-617

42 **Gao CY,** Zelenka PS. Cyclins, cyclin-dependent kinases and differentiation. *Bioessays* 1997; **19:** 307-315

43 **Ungefroren H,** Voss M, Jansen M, Roeder C, Henne-Bruns D, Kremer B, Kalthoff H. Human pancreatic adenocarcinomas express Fas and Fas ligand yet are resistant to Fas-mediated apoptosis. *Cancer Res* 1998; **58:** 1741-1749

44 **Raitano AB,** Scuderi P, Korc M. Binding and biological effects of tumor necrosis factor and gamma interferon in human pancreatic carcinoma cells. *Pancreas* 1990; **5:** 267-277

45 **Yip-Schneider MT,** Sweeney CJ, Jung SH, Crowell PL, Marshall MS. Cell cycle effects of nonsteroidal anti-inflammatory drugs and enhanced growth inhibition in combination with gemcitabine in pancreatic carcinoma cells. *J Pharmacol Exp Ther* 2001; **298:** 976-985

46 **Lehmann JM,** Lenhard JM, Oliver BB, Ringold GM, Kliewer SA. Peroxisome proliferator-activated receptors alpha and gamma are activated by indomethacin and other non-steroidal anti-inflammatory drugs. *J Biol Chem* 1997; **272:** 3406-3410

47 **Wick M,** Hurteau G, Dessev C, Chan D, Geraci MW, Winn RA, Heasley LE, Nemenoff RA. Peroxisome proliferator-activated receptor-gamma is a target of nonsteroidal anti-inflammatory drugs mediating cyclooxygenase-independent inhibition of lung cancer cell growth. *Mol Pharmacol* 2002; **62:** 1207-1214

48 **Eibl G,** Wente MN, Reber HA, Hines OJ. Peroxisome proliferator-activated receptor gamma induces pancreatic cancer cell apoptosis. *Biochem Biophys Res Commun* 2001; **287:** 522-529

49 **Li L,** Tao J, Davaille J, Feral C, Mallat A, Rieusset J, Vidal H, Lotersztajn S. 15-deoxy-Delta 12,14-prostaglandin J2 induces apoptosis of human hepatic myofibroblasts. A pathway involving oxidative stress independently of peroxisome-proliferator-activated receptors. *J Biol Chem* 2001; **276:** 38152-38158

50 **Clay CE,** Monjazeb A, Thorburn J, Chilton FH, High KP. 15-Deoxy-delta12,14-prostaglandin J2-induced apoptosis does not require PPARgamma in breast cancer cells. *J Lipid Res* 2002; **43:** 1818-1828

51 **el-Deriny SE,** O'Brien MJ, Christensen TG, Kupchik HZ. Ultrastructural differentiation and CEA expression of butyrate-treated human pancreatic carcinoma cells. *Pancreas* 1987; **2:** 25-33

52 **Chang TH,** Szabo E. Induction of differentiation and apoptosis by ligands of peroxisome proliferator-activated receptor gamma in non-small cell lung cancer. *Cancer Res* 2000; **60:** 1129-1138

PO Box 2345, Beijing 100023, China
www.wjgnet.com
wjg@wjgnet.com

ELSEVIER

World J Gastroenterol 2005;11(8):1131-1140
World Journal of Gastroenterology ISSN 1007-9327

• *BASIC RESEARCH* •

Spatial organization of bacterial flora in normal and inflamed intestine: A fluorescence *in situ* hybridization study in mice

Alexander Swidsinski, Vera Loening-Baucke, Herbert Lochs, Laura P. Hale

Alexander Swidsinski, Vera Loening-Baucke, Herbert Lochs, Innere Klinik, Gastroenterologie, Charité Humboldt Universität 10098 Berlin, Germany
Laura P. Hale, Department of Pathology, Duke University Medical Center, Durham, NC 27710, USA
Supported by Broad Medical Research Program of the Eli and Edy the L. Broad foundation
Correspondence to: Alexander Swidsinski, Innere Klinik, Gastroenterologie, Charité 10098 Berlin, Germany. alexander.swidsinski@charite.de
Telephone: +49-30-45051410 Fax: +49-30-450514923
Received: 2004-07-30 Accepted: 2004-09-19

Abstract

AIM: To study the role of intestinal flora in inflammatory bowel disease (IBD).

METHODS: The spatial organization of intestinal flora was investigated in normal mice and in two models of murine colitis using fluorescence *in situ* hybridization.

RESULTS: The murine small intestine was nearly bacteria-free. The normal colonic flora was organized in three distinct compartments (crypt, interlaced, and fecal), each with different bacterial compositions. Crypt bacteria were present in the cecum and proximal colon. The fecal compartment was composed of homogeneously mixed bacterial groups that directly contacted the colonic wall in the cecum but were separated from the proximal colonic wall by a dense interlaced layer. Beginning in the middle colon, a mucus gap of growing thickness physically separated all intestinal bacteria from contact with the epithelium. Colonic inflammation was accompanied with a depletion of bacteria within the fecal compartment, a reduced surface area in which feces had direct contact with the colonic wall, increased thickness and spread of the mucus gap, and massive increases of bacterial concentrations in the crypt and interlaced compartments. Adhesive and infiltrative bacteria were observed in inflamed colon only, with dominant *Bacteroides* species.

CONCLUSION: The proximal and distal colons are functionally different organs with respect to the intestinal flora, representing a bioreactor and a segregation device. The highly organized structure of the colonic flora, its specific arrangement in different colonic segments, and its specialized response to inflammatory stimuli indicate that the intestinal flora is an innate part of host immunity that is under complex control.

Key words: Intestinal flora; IBD

Swidsinski A, Loening-Baucke V, Lochs H, Hale LP. Spatial organization of bacterial flora in normal and inflamed intestine: A fluorescence *in situ* hybridization study in mice. *World J Gastroenterol* 2005; 11(8): 1131-1140
http://www.wjgnet.com/1007-9327/11/1131.asp

INTRODUCTION

The general consensus that the intestinal flora is important in the pathogenesis of chronic bowel inflammation is based on solid clinical and experimental evidence[1]. Despite this, all attempts to identify specific changes of the intestinal flora that are associated with chronic inflammation have either failed or are inconsistent[2]. Previous investigations of bacterial involvement in inflammatory bowel disease (IBD) have mainly been based on comparative studies of bacterial isolates. It is likely however, that the intestinal flora is structurally organized[3]. Sampling of the intestinal contents prior to culture or gene-based identification disrupts the structural organization of bacteria within the gut and may disguise the complex interactions between intestinal flora and the host.

The aim of this work was to study the composition and spatial organization of the intestinal flora in normal mice and in two commonly used models of murine colonic inflammation, using fluorescence *in situ* hybridization (FISH) with rRNA-targeted, fluorescent Cy3/Cy5 (carbocyanine) labeled oligonucleotide probes[4].

MATERIALS AND METHODS

Animals

Three different groups of mice were investigated: wild-type mice without colitis (WT group, $n = 3$), wild-type mice with acute chemically-induced colitis (DSS group, $n = 3$), IL-10 knockout mice without colitis (IL-10 C- group, $n = 2$) and IL-10 knockout mice with manifest colitis (IL-10 C+ group, $n = 3$). All mice studied were of C57BL/6J background and obtained from Jackson Laboratories (Bar Harbor, ME). Mice were housed in micro-isolator racks and allowed access to food and water *ad libitum*. Colitis was induced in 5 to 8-wk-old wild type mice (WT) by adding 3% dextran sulfate sodium (DSS, 40 kDa MW; obtained from ICN, Costa Mesa, CA) to the drinking water for 5 d. Acute colitis developed in all treated animals by d 4 of DSS exposure.

Symptoms included diarrhea, gross or occult blood in stool (measured by Hemoccult II Sensa cards; Beckman Coulter, Palo Alto, CA), and weight loss. DSS-treated mice were sacrificed on d 7 after first exposure to DSS. The spontaneous development of colitis in mice genetically deficient in IL-10 was monitored by daily weight measurements and weekly stool occult blood tests. Animals were sacrificed by CO_2 asphyxiation. A portion of the midjejunum, the terminal ileum and the whole colon were obtained. The colon was divided into 5 parts representing the cecum, proximal, mid, distal colon, and the rectum. Each colon part was analyzed separately. Intestinal segments were fixed in Carnoy's solution[5] for 3 h, then processed into paraffin blocks using standard techniques, cut into 4-10 μm sections and placed on SuperFrost slides (R. Langenbrinck, Emmendingen, Germany) for pathologic examination and FISH studies.

The studies were conducted under protocols approved by the Institutional Animal Care and Use Committee of Duke University Medical Center.

Fluorescence in situ hybridization

Oligonucleotide probes were synthesized with a Cy3 or Cy5 reactive fluorescent dye at the 5' end (MWG Biotech, Ebersberg, Germany). Forty domain, group and species-specific FISH probes (Table 1) were applied to murine colon sections. The Eub338 universal bacterial probe was used to detect virtually all relevant bacteria. The nonsense probe Non338 was used to test for nonspecific binding of oligonucleotide probes. Formamide concentration and hybridization temperature were used as described to achieve the optimal stringency[6-30]. Additional hybridizations using a permeation step with lysozyme were performed in parallel for detection of Gram-positive bacteria.

***In situ* quantification of fecal bacteria** Bacteria were visualized by FISH and 4, 6-diamidino-2-phenylindole stain (DAPI) under a Nikon e600 fluorescence microscope (Nikon, Tokyo, Japan) and photo-documented with a Nikon DXM1200 camera and software (Nikon). The enumeration of bacteria was performed only when hybridization signals were clear and morphologically distinguishable as bacterial

Table 1 FISH probes

Name	Target	Reference
Eub338	Virtually all *Bacteria*, Kingdom *Eubacteria*	6
Alf1b	Alpha group of *Proteobacteria: Rhodobacter, Acetobacter, Paracoccus*	7
Beta42a	Beta subclass of *Proteobacteria: Rhodocyclus, Bordetella, Neisseria,Thiobacillus, Alcaligenes* and other	7
Gam42a	Gamma subclass of *Proteobacteria: Enterobacteriaceae, Proteus, Legionella, Azotobacter*	7
Ebac	*Enterobacteriaceae*	8
Ec1531	*Escherichia coli*	9
Y16s-69	*Yersinia* species	10
Srb385	Sulfate reducing bacteria	11
Sgd	*Desulfotomaculum* subgroup	12
Hpy-1	*Helicobacter pylori* epsilon subclass of *Proteobacteria*	13
Arc1430	*Arcobacter* ssp. epsilon subclass of *Proteobacteria*	14
HGC	Gram-positive bacteria with high G+C content: *Actinobacteria*	15
LGC	Gram-positive bacteria with low G+C content: *Firmicutes*	16
Sfb	*Segmented filamentous bacteria*	17
Erec	*Clostridium coccoides - Eubacterium rectale* group	18
Lach	Subgroup of Erec	19
Ehal	Subgroup of Erec	19
Chis150	*Clostridium histolyticum* group (Incl. *Clostridium perfringens* and *Clostridium botulinum*)	18
Clit135	*Clostridium lituseburense* group (incl. *Clostridium difficile*)	18
Lab158	*Lactobacillus* and *Enterococcus* group	20
Strc493	*Streptococcus* group	18
Enc131	*Enterococcus* spp and other	21
Efaec	*Enterococcus faecalis*, *Enterococcus sulfuricus*	22
Ato291	*Atopobium, Coriobacterium, Eggerthella and Collinsella* spp	23
Cor653	*Coriobacterium* group	23
Ecyl	*Eubacterium cylindroides*, *Clostridium innocuum, Eubacterium biforme*, *Eubacterium tortuosum and other*	19
Phasco	*Phascolarctobacterium faecium, Acidaminococcus fermentans*, and *Succiniclasticum ruminis*	19
Veil	*Veillonella* group	19
Rbro, Rfla	*Clostridium sporosphaeroides*, *Ruminococcus bromii*, and *Clostridium leptum, Ruminococcus albus* and *Ruminococcus flavefaciens*	19
UroA, UroB	*Ruminococcus obeum*-like bacteria (subgroup of Erec)	24
Ser1410	Genus *Brachyspira*	25
Bif164	*Bifidobacterium*	26
CF319a	*Cytophaga-Flavobacteria* group	27
Bac303	*Bacteroides/Prevotella* group	27
Bfra602	*Bacteroides fragilis* group	18
Bdis656	*Bacteroides distasonis* group	18
Fprau	*Fusobacterium prausnitzii* group	28
Dss658	Sulfate reducing bacteria subgroup of delta proteobacteria	29
Arch915	*Archaea*	30
Non338	Nonsense probe used to test for nonspecific binding	7

cells by triple identification with universal and group-specific FISH probes and DAPI stain, in absence of cross-hybridization or hybridization with the Non338 nonsense probe.

For each group-specific FISH probe, high power (×1 000 magnification) photographs were made of three different microscopic fields within the intestinal lumen at the widest, narrowest, and median diameters of each colonic segment. The estimation of bacterial concentrations was made based on the assumption that a 10-μL sample with a cell concentration of 10^7 cells per mL brings 40 cells per average microscopic field at magnification of 1 000[4]. Two investigators independently counted bacteria within a 50 μm^2 area of the microscopic field (about 1 cm^2 of the 100% scale photographic image). The mean number of bacteria was recorded for each colonic segment. In cases where single bacterial cells were morphologically indistinguishable due to high bacterial concentrations and the fluorescence was confluent to a homogeneously fluorescent mass, no enumeration was attempted and the bacterial concentration was assigned a value of $>10^{12}$ per mL. If single bacterial cells were not distinguishable within the bacterial carpet but some empty gaps could be recognized, the bacterial concentration was assigned a value of $>10^{11}$ per mL.

Evaluation of spatial interrelationship of bacteria and assessment of cross-hybridization The spatial organization of bacteria was evaluated in three steps. Group or species-specific signals (green-orange fluorescence Cy3) were visualized simultaneously with a Eub338 probe universal for all relevant bacteria (dark red fluorescence Cy5). All probes positively hybridizing with more than 1% of bacteria were further combined with each other in pairs, in a two-color analysis (Cy3 *vs* Cy5). This allowed us to characterize the position of different bacterial groups relative to each other within the intestine and to assess potential cross-hybridization. Although probes chosen for this study were designed for definite bacterial groups and extensively tested (Table 1)[6-30], the specificity of each probe is relative. In these experiments, multiple observations were made to determine whether bacteria that hybridized with one probe gave a positive hybridization signal with a probe representing other bacterial groups, rather than to rely on results obtained with a single probe. When probes of unrelated bacterial groups hybridized with the same bacteria, the hybridization stringency was adjusted until a clear differentiation was possible. Otherwise the results achieved with cross-hybridizing probes were excluded.

Quantification of dynamic compartments The quantification of the dynamic structures, such as bacterial populations of crypts, bacteria organized in layers adjacent to the mucosa, and the width and spread of the mucus, was based on the mean values of at least ten photographs of different microscopic fields made within each bowel segment at a magnification of ×400 for layers and ×1 000 for crypts.

Statistical analysis

Mean values and standard deviations were calculated for bacteria concentrations and measurements of layer (e.g., mucus or interlaced) thickness. Using *t*-tests, $P<0.05$ was considered statistically significant.

RESULTS

Distribution of bacteria within bowel based on hybridization with universal bacterial probes

Healthy wild type mice The ileum was narrow. The few microorganisms found were heterogeneously composed, random, and without signs of adhesion or contact with the intestinal wall (Figure 1).

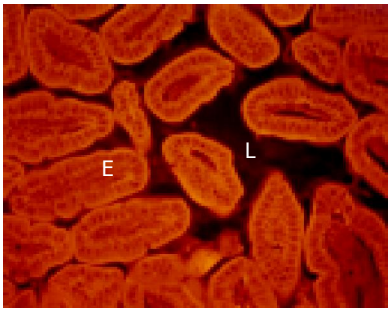

Figure 1 I = ileum of a wild type normal mouse narrow and free of bacteria in most parts. E = epithelium; L = lumen.

The cecum was wide and contained a highly concentrated mass of bacteria. The exact enumeration of bacteria was impossible since single bacteria could not be distinguished within the confluent fluorescent carpet (Figure 2A). Luminal bacteria were in direct contact with the wall of the cecum. Despite this contact, the bacteria lining the cecal mucosa were probably non-adherent. Shrinkage caused by fixation sometimes led to dissection of feces from the cecal wall. In

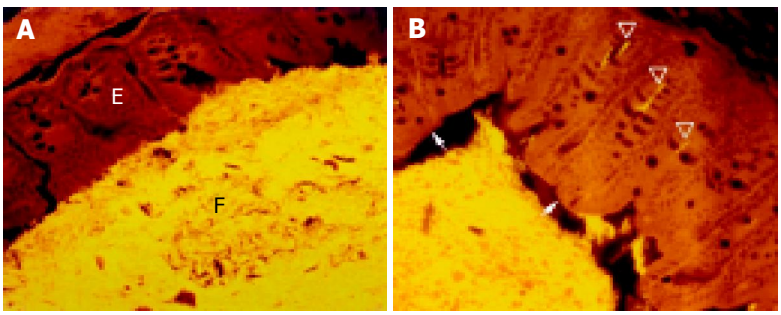

Figure 2 Concentrated bacterial mass in direct contact with the mucosal surface (A) and non-adherent bacteria (B) in cecum of a healthy wild type mouse. E = epithelium; F = feces. Arrow indicates the shrinkage of feces, arrowheads indicate bacteria in crypts.

all regions where this dissection took place, no bacteria adhered to the mucosal surface (Figure 2B). Abundant bacteria were observed within crypts (Figure 2B, arrowheads).

The proximal colon was wide initially, and narrows distally. Fecal bacteria were present in high numbers and contacted the colonic wall along most of its length. Numerous bacteria were seen in nearly half of all intestinal crypts, even very deep within the wall. The number of crypts containing bacteria and the number of bacteria within these crypts were even higher in the proximal colon than in the cecum.

A thin but dense band of homogeneous bacteria was present in the distal part of the colon. Because this band of bacteria was interlaced between the epithelial wall and the unorganized fecal masses, it was termed the interlaced layer (Figure 3).

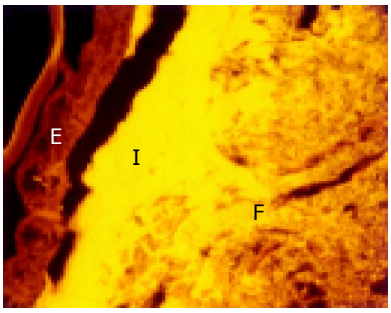

Figure 3 Interlaced layer in the distal portion of the proximal colon.

The mid-colon was narrow, and generally contained little feces. If present, fecal material was restricted to a fine tube-like structure located centrally within the intestinal lumen and separated from the epithelial surface by mucus. Bacteria were seen less often within crypts (Figure 4).

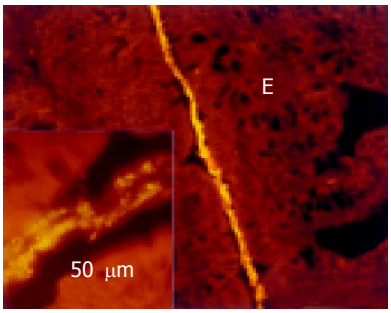

Figure 4 Middle colon in a normal mouse.

The colon lumen widened in the distal colon and was filled with masses of feces containing a high concentration of bacteria. A growing mucus gap devoid of bacteria completely separated the colonic wall from this fecal biomass. Nearly no bacteria was found in crypts and no interlaced layer was seen.

The lumen of rectum was wide. The mucus layer separating the bacteria from the mucosa continuously thickened (Figure 5). No bacteria were found within crypts in the rectum.

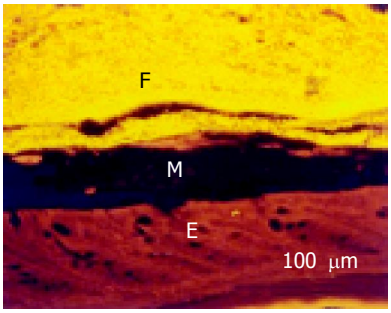

Figure 5 Rectal mucosa covered with thick mucus (M). E = epithelium, F = feces.

IL-10 knockout mice without colitis The bacterial concentrations in the ileum of IL-10 knockout mice without colitis were similar to findings in healthy WT mice. However, the concentrations and occurrence of bacteria in crypts, the thickness of the interlaced layer, and the overall concentrations of fecal bacteria were noticeably less compared to healthy WT mice (Table 2).

DSS-treated wild-type mice and IL-10 knockout mice with colitis Five striking changes were observed both in mice with colitis due to DSS exposure and in IL-10 knockout mice with spontaneous severe colitis (Table 2). First, there was a massive reduction of bacterial concentrations within the fecal masses in all colonic segments compared to healthy WT mice. Second, in inflamed colon, the middle colon lost its dividing function. The narrowing observed in normal WT mice was not observed in the colitis groups. The area where fecal masses had direct contact with the mucosal surface was reduced. The mucus gap separating the colonic wall from the fecal biomass began more proximally than in healthy WT mice. In mice with colitis, the mucus layer was evident in the distal cecum and became broad and complete in the proximal colon. Third, the number and occurrence of bacteria within crypts increased manifold compared to mice without colitis. Bacteria could be regularly seen even in crypts of the inflamed distal colon, while bacteria were seen only in the crypts of cecum and proximal colon in healthy WT mice. Fourth, the interlaced layer became extremely thick in the proximal and middle colon of mice with colitis, and reached thicknesses of >300 μm in some locations. The interlaced layer could be observed separating feces from mucosa, beginning in the distal cecum and continuing to the proximal portion of the distal colon. Fifth, in addition to these gradual changes, bacteria adhering to the mucosa or invading mucosal epithelial cells were seen in mice with colitis, but not in healthy WT mice.

Compartment-specific composition of bacterial communities in different colonic segments

Intestinal bacteria were organized in crypt, interlaced, fecal, adhesive, and invasive compartments. Crypt, interlaced, and fecal compartments were observed in all groups; however, adhesive and invasive bacteria were seen only in animals with colitis. The bacterial groups found in different compartments are summarized in Table 3. Generally all bacterial groups that were observed within the crypt compartment could also be found in the interlaced and fecal compartments. However, not all bacterial groups found in feces had access to the interlaced

Table 2 Spatial organization of intestinal bacteria based on FISH with Eub338 universal bacterial probe

	Group	Ileum	Cecum	Proximal	Middle	Distal	Rectum
Mean lumen width in	WT	Narrow 0.2	Broad 6.4	Narrowing 2.9	Narrow <0.1	Widening 2.4	Broad 2.5
microscopic fields	DSS	Narrow 0.1	Broad 3.0	Irregular 0.9	Irregular 0.8	Irregular 0.6	Irregular 0.6
(×10 00) between	IL-10 C-	Narrow 0.1	Broad 2.1	Irregular 0.6	Irregular 0.5	Irregular 0.7	Irregular 1.2
opposite walls	IL-10 C+	Narrow 0.3	Broad 2.0	Irregular 0.6	Irregular 0.5	Irregular 0.5	Narrow 0.2
Min -max	WT	$0.2\text{-}2.5\times10^{7}$	$>10^{12}$	$>10^{12}$	-	$>10^{12}$	$>10^{12}$
concentrations of	DSS	$<10^{7}$	$1.3\text{-}6.7\times10^{9}$	$1.2\text{-}4.0\times10^{9}$	$2.1\text{-}6.6\times10^{9}$	$1.8\text{-}2.2\times10^{9}$	$1.1\text{-}2.2\times10^{9}$
bacteria per mL	IL-10 C-	$<10^{7}$	$1.0\text{-}5.3\times10^{10}$	$1.0\text{-}5.2\times10^{10}$	$0.6\text{-}3.4\times10^{10}$	$1.2\text{-}1.9\times10^{10}$	$1.4\text{-}2.3\times10^{10}$
of feces	IL-10 C+	$<10^{7}$	$1.7\text{-}5.0\times10^{9}$	$0.7\text{-}4.2\times10^{9}$	$0.7\text{-}4.2\times10^{9}$	$4.7\text{-}7.1\times10^{9}$	$4.7\text{-}9.2\times10^{9}$
Min -max. length	WT	None	None	8-10%	80-90%	Complete	Complete
of mucus gap	DSS	None	8-20%	40-50%	Complete	Complete	Exudate
separating feces	IL-10 C-	None	5-10%	70-80%	Complete	Complete	Complete
from epithelium	IL-10 C+	None	10-20%	50-80%	Complete	Complete	Exudate
Min-max width	WT	-	0	0- 5	0-20	20-50	30-100
of the mucus in	DSS	-	0- 5	0-10	10-50	40-75	60-150
µm between	IL-10 C-	-	0-10	0-10	15-50	40-100	60-200
epithelium and feces	IL-10 C+	-	0-20	0-20	5-50	60-200	Infiltrate
Mean percent of	WT	-	10% (3-12)	16% (6-16)	5% (single)	<1% (single)	0
crypts with bacteria	DSS	-	22% (4-25)	44% (9-30)	27% (4-15)	16% (2-9)	<1%
(mean-max number of	IL-10 C-	-	1% single	5% (1-3)	2% (single)	1% (single)	No
bacteria within each)	IL-10 C+		28% (3-20)	34% (8-34)	27% (2-20)	16% (3-12)	<1%
Min-max thickness	WT	-	0	5-25	0-10	0	0
of the interlaced	DSS	-	0-100	80-400	8-40	0-2	0-2
layer (µm)	IL-10 C-	-	2-10	<5	0	0-2	0
	IL-10 C+		0-120	200-500	80-150	0-15	Infiltrate

Mean number of bacteria within crypts were counted in two different microscopic fields. Only crypts with bacteria were evaluated when mean number of bacteria within crypts was determined.

compartment. In addition, some bacterial groups seen in both fecal and interlaced compartments were never seen in the crypt compartment (Table 3).

Table 3 Bacterial groups identified within defined compartments

FISHProbe	Feces	Interlaced	Crypt
Erec	+	+	+
Alf1b	+	+	+
Lach	+	+	+
Phasco	+	+	+
Cor653	+	+	+
Lab158	+	+/-[1]	+
Rbro	+	+	-
Rfla	+	+	-
Ehal	+	+/-[1]	-
Bdis	+	+/-[1]	-
Bac303	+	-	-
LGC	+	-	-
Clit135	+	-	-
Chis150	+	-	-
Ecyl	+	-	-
Bif164	+	-	-
Veil	+	-	-
UroB	+	-	-
UroA	+	-	-
HGC	+	-	-
Strc493	+	-	-
Ebac	+	-	-
Arc1430	+	-	-
Enc131	+	-	-
Ato291	+	-	-

[1]Composed of different morphotypes one of which could be found within and one outside of the interlaced layer.

The composition of the bacterial populations within single compartments (feces, interlaced, crypt) was the same in all investigated groups of animals. However, the spread, extent, and volume of these different compartments within different colonic segments differed markedly between groups with and without colitis, irrespective of the etiology of the inflammation.

Fecal compartment The composition of the bacterial community in the lumen of ileum could not be reliably evaluated in all groups of mice due to low bacterial concentrations and their irregular distribution within the lumen. Different bacterial groups found in the ileum appeared to be at random and varied from animal to animal in an unpredictable manner.

All bacterial groups that were positively hybridized with FISH probes were homogeneously mixed within the feces, without a gradient in distribution between regions adjacent to the mucosa and distant regions (Figure 6). The Arch915, Gam42a, Beta42a, Srb385, Bfra602, CF319a probes demonstrated a high grade of cross-hybridization and were excluded from the evaluation. The Erec, Lach, Alf1b, Phasco, Lab158 and Bac303 probes hybridized with more than 10% of the fecal population at least in one of the animals tested. The Rbro, Chis150, Clit135, Ehal, Ecyl, LGC, Cor653, Bdis659 probes hybridized with more than 1% of the fecal population. The Bif164, HGC, Rfla, Enc131, Veil, Ato291, UroB, UroA, Strc493, Ebac, Arc1430 probes hybridized with less than 1% of the population. Despite this low overall proportion, the absolute number of these bacterial groups was higher than 10^{7} cells/mL and therefore, easy to distinguish from the non-specific background. The Ec1531, Y16s-69, Sgd, Fprau, Sfb, Hpy-1, Efaec, Ser1410, Dss658 probes failed to give signals that were different from the background fluorescence seen with the nonsense probe.

Changes in bacterial concentrations within the fecal compartment from the cecum to the rectum The types of bacteria present in the fecal compartment were constant

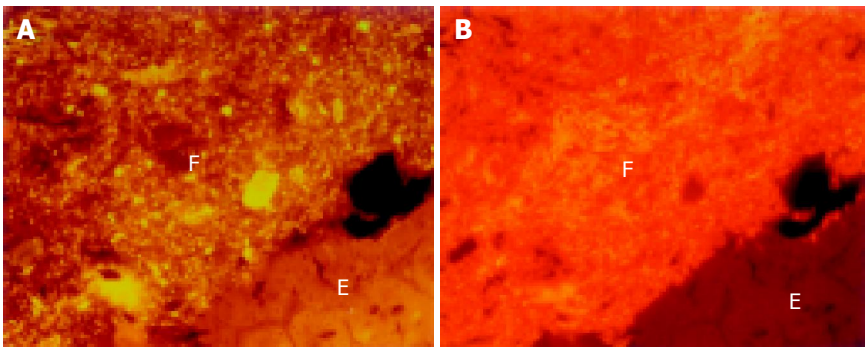

Figure 6 Fecal bacteria hybridized with *Bacteroides* (Cy3 green-orange, 6A) and Erec (Cy5 red, 6B) probes, cecum of healthy WT mice.

in all colonic segments and animal groups; however, the concentrations differed markedly. This was illustrated by the changes in mean concentrations of bacteria that hybridized with Erec and Bac303 probes, the two most abundant bacterial groups within the fecal compartment, during the transition from cecum to rectum (Table 4).

Table 4 Mean concentrations of selected bacterial groups comprising more than 10% of the population within the fecal compartment of cecum and rectum

Probe	Group	Cecum	Rectum
Erec	WT	80×10^9	0.8×10^9
	DSS	13×10^8	0.3×10^8
	IL-10 C-	15×10^8	25×10^8
	IL-10 C+	8×10^8	12×10^8
Bac	WT	2.8×10^8	2.1×10^8
	DSS	1×10^8	0.5×10^8
	IL-10 C-	5×10^8	2×10^8
	IL-10 C+ 28 wk	11×10^8	5×10^8

Bacterial groups found both in the crypt and fecal compartments (e.g., Erec, Alpf1b, Phasco, *etc.*; Table 3) were predominant in the cecum of healthy WT mice and their concentrations declined distally. The concentrations of bacterial groups found mainly in feces (e.g., *Bacteroides*, Clit135, Chis150, *etc.* Table 3) remained relatively stable throughout the colon. Thus their concentrations increased relative to the Erec-like groups.

Crypt bacterial communities Crypt bacteria were mainly found in the cecum and proximal colon of healthy WT mice (Table 2). Starting with the middle colon, bacteria could be only sporadically observed within the crypts. No bacteria were found within crypts of the distal colon and rectum. The occurrence and number of crypt bacteria were significantly reduced in IL-10 knockout mice without colitis. In contrast, in both DSS mice with colitis and IL-10 knockout mice with spontaneous colitis, the crypt population was amplified and crypt bacteria could be seen sporadically even in the rectum (Table 2). Despite this significant difference in the extent and the distribution of crypt communities, the composition of the crypt population was the same in all investigated animal groups. Groups hybridizing with the Alf1b, Erec (Lach), Phasco and Lab158 probes were detected within crypts in different combinations. In the cecum, crypt bacteria directly contacted fecal masses and these bacteria were the main constituents of the fecal compartment. Bacteria positively hybridizing with Bac303 (*Bacteroides)*, Chis150 (*Clostridium histolyticum*), and Clit135 (including *Clostridium difficile*) probes were never identified within crypts of any of the groups investigated (Table 3), although they were homogeneously intermixed within the fecal compartment and directly contacted the mucosa and crypt mouths in the cecum. In the proximal colon, the groups of bacteria that were present within crypts formed the interlaced layer before they mixed with the fecal compartment.

Interlaced layer The interlaced layer was mainly composed of the same bacterial groups that were present within the crypts (Table 3). These bacteria were condensed in extremely dense mats adjacent to the mucosa, which were clearly demarcated from the rest of the feces. This layer was relatively thin in WT mice and in IL-10 knockout mice without colitis. However, the interlaced layer was markedly amplified in all mice with colitis.

The concentration of bacteria into the interlaced layer was not simply numerical. The interlaced layer prevented the mucosa from contact with bacterial groups hybridizing with Bac303 (*Bacteroides*) and Clit135 (*Clostridium difficile*) probes which were observed in the cecum and initial parts of the proximal colon in healthy WT mice (Figure 6). The blocking role of the interlaced layer was especially well seen when pairs of probes representing all (Eub338)/interlaced (Erec, Alf1b, Phasco, Lab158, *etc.*) and exclusively fecal (e.g., Bac303, Clit135) bacterial population were simultaneously used (Figures 7, 8).

Adhesive bacteria Bacteria had direct contact with the cecal wall in healthy WT mice. These bacteria were separated completely from the wall when the fecal masses shrank during fixation without that bacteria adhered to the colonic surface (Figure 2B). Bacterial-mucosal contact in the cecum was therefore not adhesive.

True adhesion was observed in all animals with colitis. This was characterized by bacteria, which lined the mucosal surface and were located beneath the mucus layer. This true adhesion was found in at least one location in all animals with colitis, but was observed mainly in the distal portion of the colon (Figure 9). Sixty percent of adhesive bacteria were *Bacteroides*.

Invading bacteria Bacteria invading the mucosa were found exclusively in the rectum and distal colon of DSS and IL-10 knockout mice with colitis (Figure 10). The types of invading bacteria were heterogeneous but mainly represented bacteria of the *Bacteroides* and Erec groups. The proportion of *Bacteroides* to Erec was more than three to one.

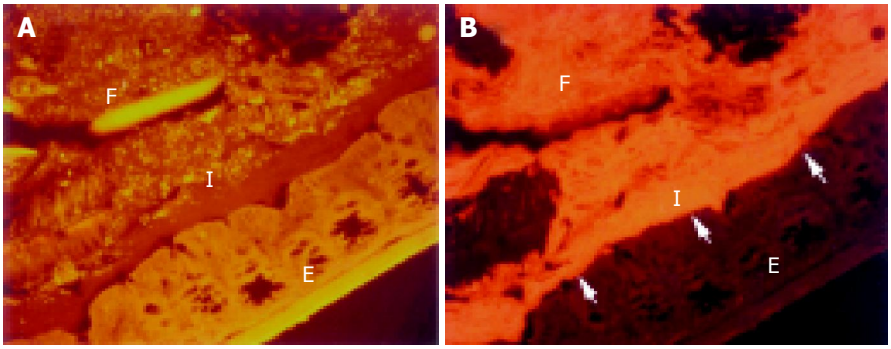

Figure 7 Interlaced layer in the proximal colon of IL-10 mice with colitis visualized simultaneously by hybridization with Bac303 (Cy3 green-orange, 7A) and Eub338 probes (Cy5 red, 7B).

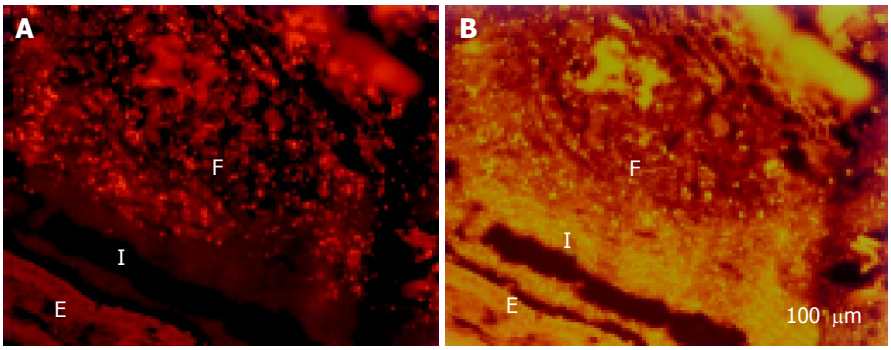

Figure 8 Interlaced layer in proximal colon of DSS mice visualized simultaneously by hybridization with Clit135 (Cy5 red, 8A) and Lab158 probes (Cy3 green-orange, 8B). I = interlaced layer, E = epithelium, F = feces.

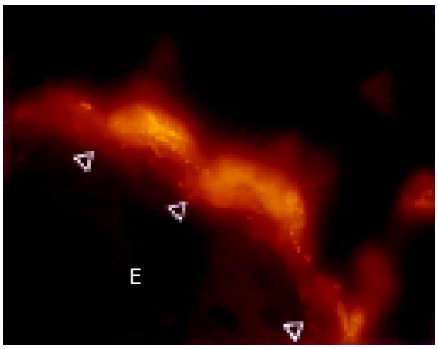

Figure 9 Bacteria location below the intact mucus layer (arrowheads) and adherence to the colonic mucosa in DSS-exposed mice.

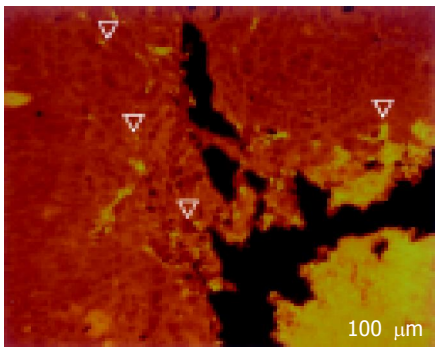

Figure 10 Bacteria infiltrating the mucosa in distal colon of IL-10 mice with colitis (arrowheads).

DISCUSSION

In the present study we described a novel approach for the characterization of biofilm in the murine intestine. The utilization of the broad *in situ* typing methodology, described herein, allowed for the first time to visualize the spatial complexity of murine intestinal microbiota in health and disease. Our results clearly show that normal murine intestinal flora is highly differentiated, organized in structurally definitive, distinctively composed compartments, which are typical for each colonic segment and closely interrelated to colonic function. Finally, we report, for the first time, that intestinal inflammation is associated with spatial re-distribution of specific groups of bacteria in the large intestine of mice.

In recent years a large amount of data has emerged that point out the importance of biofilm in environmental microbiology in such diverse settings as implantable medical devices[31] and dental plaque[32,33]. In regards to the intestinal microbiota, however, detailed investigations are clearly lacking. The limited number of studies that incorporated FISH technology to investigate microorganisms in histologic material of human or animal intestines has dealt for the most part with the detection and enumeration of bacteria[34-36]. In contrast, in the present study, we modified the existing methodology to achieve better characterization of the spatial association between intestinal bacteria and the mucosal environment. First, to accomplish optimal resolution of the spatial structures, our technique included probes, which have

been shown to express low bacterial specificity taking into account some level of uncertainty in regard to the specificity of identification of bacteria and the sensitivity of enumeration studies. Second, we hybridized all probes that generated positive signals in multiple combinations to each other. Probes, which cross-hybridized with a subset of bacteria even when high stringency conditions were applied, were subsequently excluded from the evaluation.

A major finding of our study is the clear diversity observed between different intestinal segments in regards to the number of intraluminal bacteria and the localization of microorganisms in relation to intestinal wall. Specifically, in our study, bacteria were rare in the small intestine. On the contrary, with the exception of middle colon, all colonic segments were found to contain a large number of bacteria within the fecal mass. Striking differences, however, were observed between proximal and distal colonic areas regarding the position of microorganisms in relation to the bowel wall. Indeed, not only were the cecum and proximal colon tightly filled with high concentrations of bacteria, but direct contact of all involved bacterial groups with the bowel wall was observed as well. More importantly, abundant bacteria within colonic crypts were a uniform characteristic of proximal large intestinal segments. On the other hand, in the distal colon and rectum intraluminal bacteria were prohibited from contact to the bowel wall, whereas no microorganisms were detected in the colonic crypts.

We hypothesize that the differences in the spatial association between commensal bacteria and murine colonic wall replicate functional differences between individual colonic segments. First, our data indicate that the cecum and proximal colon, where direct contact of bacteria and bowel wall takes place, are involved in the proper fermentation reactor of the large bowel in mice. In addition, the rich bacterial population found within the crypts of proximal colonic segments of WT mice contradicts the previous assumption that such localization of bacteria indicates the presence of disturbed mucosal barrier[38]. A more plausible explanation is that these bacteria represent inocula used by the host to boost and maintain the stability of fermentation. This notion is strongly supported by the fact that intracryptic bacteria are devoid of potentially harmful species such as *Bacteroides* (Bac303) or *Clostridium difficile* (Clit135). Second, our findings support the concept that, different from the proximal colon, the distal colon functions mainly as a segregation device. In fact, the waste product segregation is managed by a mucus layer that normally starts in the middle colon and becomes fully developed in the distal colon, where the number of crypt bacteria continuously declines. The composition of mucins in the proximal and distal colonic segments in mice and men has been extensively studied and marked differences were previously described[37]. The lack of detection of a mucus layer by *in situ* hybridization in the cecum and proximal colon of WT mice does not indicate that mucin production by the cecal epithelium does not occur. It is more probable that mucus secreted in the murine cecum is penetrable by bacteria and does not lead to the development of the mucus layer, which physically separates the fecal masses from the epithelium. The "physiological" contact that takes place between bacteria and proximal large intestinal wall may underlie the tolerance of the colonic epithelium towards commensal flora that characterizes the healthy state. More importantly it offers an attractive explanation as to why colitis very often originates in the distal colon, where the bacteria are separated from the mucosa and tolerance does not develop. The functional differences between proximal and distal colon in healthy WT mice are further emphasized during peristalsis. The proximal and distal parts of the healthy WT mouse colon are dilated and filled with feces and divided by a narrow middle colon, which prevents the intermixing of the two reservoirs.

A unique finding in our study is the identification of the interlaced bacterial layer. This represents a bacterial sheet that is composed of selected microbial groups, which grow in dense mats between feces and mucosa and are impenetrable for most fecal bacteria. The interlaced layer is an entirely new entity observed in the transition zone between proximal and distal colon. The reason why previous studies failed to detect this distinctive layer may lie in the fact that the interlaced layer is relatively thin in healthy WT mice and poorly contrasts against the bright fluorescence of highly concentrated dense fecal compartment when universal probes or single group-specific probes are used. It can be definitively recognized only when pairs of probes specific for strictly fecal bacteria such as *Bacteroides* along with crypt-specific bacterial probes such as Erec are concomitantly applied, an approach that has not been practiced until now. The functional peculiarities of the interlaced layer indicate that it could be nature's solution for preventing the spoiling of the fermentation by overgrowth of contaminants or facultative pathogens.

Our studies in DSS-treated and IL-10 knockout mice clearly demonstrate that, in the setting of intestinal inflammation, the described complex cooperative work of macro and microorganisms within the intestinal lumen was deranged. The development of colitis introduced changes that can be interpreted as increasing host intolerance to the fecal flora. First, in the inflamed colon the formation of the mucus layer that prevents contact of feces with the colonic wall moved proximally and became detectable in the cecum. Second, the spread and width of the mucus layer significantly increased throughout the colon. Third, redistribution of the intestinal microorganisms occurred that was highly selective and compartment-specific. Indeed, the concentrations of bacteria in the fecal compartment dropped dramatically. Nevertheless, while microorganisms were suppressed within the fecal compartment, the intra-cryptic bacterial groups recognized by the Alf1b, Erec, Phasco and Lab158 probes as well as the interlaced bacterial layer were enhanced in their growth. Both the number of crypts containing bacteria and the number of bacteria within single crypts significantly increased in mice with colitis. Furthermore, intra-cryptic bacteria were regularly found even in the distal colon. The interlaced layer got especially dense and thick in the inflamed proximal and middle colon and spread up into the cecum. Although these results indicate an activation of intestinal defense mechanisms in mice with colitis, as expressed by the wider spread and increased thickness of mucus and the interlaced layer, fecal bacteria

are able to overcome the defense lines. In fact a definite discriminatory characteristic between healthy and colitic mice is the presence of invasive bacteria and bacteria that were adhesive to the mucosa below the mucus in the latter group. Specification analysis revealed that *Eubacterium rectale* group was most numerous in crypts, feces and the interlaced layer. On the other hand, *Bacteroides* species dominated the adhesive and invasive populations documenting the changing spectrum of bacteria involved in the inflammatory process.

In conclusion, the present study indicates that the proximal, middle and distal colonic segments appear to be physiologically distinct with respect to their interactions with bacteria. On the other hand, bacterial attachment to the mucosa can follow one of three principally different processes: fermentation (facilitated by direct contact to the proximal colonic wall), protection (through the formation of an isolating interlaced layer), and inflammation (adhesion and invasion). These processes are differently expressed throughout the colon and have opposite meanings in each case and position. The first is reduced, whereas the last two are enhanced in colitis. As an end result, the interrelation between bacteria and colonic epithelium and the state that predominates (tolerance *vs*. inflammation) is constantly defined by the mode of bacterial attachment and the colonic segment where this attachment takes place. The spatial, segment-specific structure and differential response of specific bacterial groups and compartments to inflammatory stimuli may be pivotal for the clarification of many past inconsistencies of experimental and clinical research regarding the pathogenic role of bacteria in IBD[38-41] and is a promising goal for future studies.

REFERENCES

1 **Sartor RB**. Pathogenesis and immune mechanisms of chronic inflammatory bowel diseases. *Am J Gastroenterol* 1997; **92**: 5S-11S
2 **Wilson M**. Bacterial biofilms and human disease. *Sci Prog* 2001; **84**: 235–254
3 **Podolsky DK**. Inflammatory bowel disease. *N Engl J Med* 2002; **347**: 417-429
4 **Amann RI**, Ludwig W, Schleifer KH. Phylogenetic identification and *in situ* detection of individual microbial cells without cultivation. *Microbiol Rev* 1995; **59**: 143-169
5 **Matsuo K**, Ota H, Akamatsu T, Sugiyama A, Katsuyama T. Histochemistry of the surface mucous gel layer of the human colon. *Gut* 1997; **40**: 782-789
6 **Amann RI**, Krumholz L, Stahl DA. Fluorescent-oligonucleotide probing of whole cells for determinative, phylogenetic, and environmental studies in microbiology. *J Bacteriol* 1990; **172**: 762-770
7 **Manz W**, Amann R, Ludwig W, Wagner M, Schleifer KH. Phylogenetic oligodeoxynucleotide probes for the major subclasses of Proteobacteria: Problems and solutions. *System Appl Microbiol* 1992; **15**: 593-600
8 **Bohnert J**, Hübner B, Botzenhart K. Rapid identification of Enterobacteriaceae using a novel 23S rRNA-targeted oligonucleotide probe. *Int J Hyg Environ Health* 2000; **203**: 77-82
9 **Poulsen LK**, Licht TR, Rang C, Krogfelt KA, Molin S. Physiological state of Escherichia coli BJ4 growing in the large intestines of streptomycin-treated mice. *J Bacteriol* 1995; **177**: 5840-5845
10 **Trebesius K**, Harmsen D, Rakin A, Schmelz J, Heesemann J. Development of rRNA-targeted PCR and in situ hybridization with fluorescently labelled oligonucleotides for detection of Yersinia species. *J Clin Microbiol* 1998; **36**: 2557-2564
11 **Amann RI**, Stromley J, Devereux R, Key R, Stahl DA. Molecular and microscopic identification of sulfate-reducing bacteria in multispecies biofilms. *Appl Environ Microbiol* 1992; **58**: 614-623
12 **Hristova KR**, Mau M, Zheng D, Aminov RI, Mackie RI, Gaskins HR, Raskin L. Desulfotomaculum genus- and subgenus-specific 16S rRNA hybridization probes for environmental studies. *Environ Microbiol* 2000; **2**: 143-159
13 **Feydt-Schmidt A**, Rüssmann H, Lehn N, Fischer A, Antoni I, Störk D, Koletzko S. Fluorescence *in situ* hybridization *vs* epsilometer test for detection of clarithromycin-susceptible and clarithromycin-resistant *Helicobacter pylori* strains in gastric biopsies from children. *Aliment Pharmacol Ther* 2002; **16**: 2073-2079
14 **Snaidr J**, Amann R, Huber I, Ludwig W, Schleifer KH. Phylogenetic analysis and *in-situ* identification of bacteria in activated sludge. *Appl Environ Microbiol* 1997; **63**: 2884-2896
15 **Roller C**, Wagner M, Amann R, Ludwig W, Schleifer KH. *In situ* probing of gram-positive bacteria with high DNA G + C content using 23S rRNA-targeted oligonucleotides. *Microbiology* 1994; **140(Pt 10)**: 2849-2858
16 **Meier H**, Amann R, Ludwig W, Schleifer KH. Specific oligonucleotide probes for *in situ* detection of a major group of gram-positive bacteria with low DNA G + C content. *Syst Appl Microbiol* 1999; **22**: 186-196
17 **Urdaci MC**, Regnault B, Grimont PA. Identification by *in situ* hybridization of segmented filamentous bacteria in the intestine of diarrheic rainbow trout (Oncorhynchus mykiss). *Res Microbiol* 2001; **152**: 67-73
18 **Franks AH**, Harmsen HJ, Raangs GC, Jansen GJ, Schut F, Welling GW. Variations of bacterial populations in human feces measured by fluorescent *in situ* hybridization with group-specific 16S rRNA-targeted oligonucleotide probes. *Appl Environ Microbiol* 1998; **64**: 3336-3345
19 **Harmsen HJ**, Raangs GC, He T, Degener JE, Welling GW. Extensive set of 16S rRNA-based probes for detection of bacteria in human feces. *Appl Environ Microbiol* 2002; **68**: 2982-2990
20 **Harmsen HJ**, Elfferich P, Schut F, Welling GW. A 16S rRNA-targeted probe for detection of lactobacilli and enterococci in fecal samples by fluorescent *in situ* hybridization. *Microbiol Ecol Health Dis* 1999; **11**: 3–12
21 **Frahm E**, Heiber I, Hoffmann S, Koob C, Meier H, Ludwig W, Amann R, Schleifer KH, Obst U. Application of 23S rDNA-targeted oligonucleotide probes specific for enterococci to water hygiene control. *Syst Appl Microbiol* 1998; **21**: 450–453
22 **Jansen GJ**, Mooibroek M, Idema J, Harmsen HJ, Welling GW, Degener JE. Rapid identification of bacteria in blood cultures by using fluorescently labeled oligonucleotide probes. *J Clin Microbiol* 2000; **38**: 814-817
23 **Harmsen HJ**, Wildeboer-Veloo AC, Grijpstra J, Knol J, Degener JE, Welling GW. Development of 16S rRNA-based probes for the Coriobacterium group and the Atopobium cluster and their application for enumeration of Coriobacteriaceae in human feces from volunteers of different age groups. *Appl Environ Microbiol* 2000; **66**: 4523-4527
24 **Zoetendal EG**, Ben-Amor K, Harmsen HJ, Schut F, Akkermans AD, de Vos WM. Quantification of uncultured Ruminococcus obeum-like bacteria in human fecal samples by fluorescent *in situ* hybridization and flow cytometry using 16S rRNA-targeted probes. *Appl Environ Microbiol* 2002; **68**: 4225-4232
25 **Jensen TK**, Boye M, Ahrens P, Korsager B, Teglbjaerg PS, Lindboe CF, Moller K. Diagnostic examination of human intestinal spirochetosis by fluorescent *in situ* hybridization for Brachyspira aalborgi, Brachyspira pilosicoli, and other species of the genus Brachyspira (Serpulina). *J Clin Microbiol* 2001; **39**: 4111-4118
26 **Langendijk PS**, Schut F, Jansen GJ, Raangs GC, Kamphuis GR, Wilkinson MH, Welling GW. Quantitative fluorescence *in situ* hybridization of Bifidobacterium spp. with genus-specific 16S rRNA-targeted probes and its application in fecal

samples. *Appl Environ Microbiol* 1995; **61**: 3069-3075

27 **Manz W**, Amann R, Ludwig W, Vancanneyt M, Schleifer KH. Application of a suite of 16S rRNA-specific oligonucleotide probes designed to investigate bacteria of the phylum cytophaga-flavobacter-bacteroides in the natural environment. *Microbiology* 1996; **142(Pt 5)**: 1097-1106

28 **Suau A**, Rochet V, Sghir A, Gramet G, Brewaeys S, Sutren M, Rigottier-Gois L, Dore J. Fusobacterium prausnitzii and related species represent a dominant group within the human fecal flora. *Syst Appl Microbiol* 2001; **24**: 139-145

29 **Manz W**, Eisenbrecher M, Neu TR, Szewzyk U. Abundance and spatial organization of gram-negative sulfatereducing bacteria in activated sludge investigated by *in situ* probing with specific 16S rRNA targeted oligonucleotides. *FEMS Microbiol Ecol* 1998; **25**: 43-61

30 **Stahl DA**, Amann R. Development and application of nucleic acid probes in bacterial systematics. *In* E. Stackebrandt and M.Goodfellow (ed.), Nucleic acid techniques in bacterial systematics. Chichester, England: John Wiley Sons Ltd. Pub 1991: 205–248

31 **Costerton W**, Veeh R, Shirtliff M, Pasmore M, Post C, Ehrlich G. The application of biofilm science to the study and control of chronic bacterial infections. *J Clin Invest* 2003; 1**12**: 1466-1477

32 **Kolenbrander PE**. Oral microbial communities: biofilms, interactions, and genetic systems. *Annu Rev Microbiol* 2000; **54**: 413–437

33 **Marsh PD**, Bradshaw DJ. Dental plaque as a biofilm. *J Ind Microbiol* 1995; **15**: 169–175

34 **Schultsz C**, Van Den Berg FM, Ten Kate FW, Tytgat GN, Dankert J. The intestinal mucus layer from patients with inflammatory bowel disease harbors high numbers of bacteria compared with controls. *Gastroenterology* 1999; **117**: 1089–1097

35 **Kleessen B**, Kroesen AJ, Buhr HJ, Blaut M. Mucosal and invading bacteria in patients with inflammatory bowel disease compared with controls. *Scand J Gastroenterol* 2002; **37**: 1034-1041

36 **Kleessen B**, Hartmann L, Blaut M. Fructans in the diet cause alterations of intestinal mucosal architecture, released mucins and mucosa-associated bifidobacteria in gnotobiotic rats. *Br J Nutr* 2003; **89**: 597-606

37 **Einerhand AW**, Renes IB, Makkink MK, van der Sluis M, Buller HA, Dekker J. Role of mucins in inflammatory bowel disease: important lessons from experimental models. *Eur J Gastroenterol Hepatol* 2002; **14**: 757-765

38 **Campieri M**, Gionchetti P. Bacteria as the cause of ulcerative colitis. *Gut* 2001; **48**: 132–135

39 **Sartor RB**. Microbial factors in the pathogenesis of Crohn's disease, ulcerative colitis, and experimental intestinal inflammation. In: Kirsner JB (editor) *Inflammatory Bowel Disease*. Philadelphia: *Saunders Pub* 2000: 153-178

40 **Guarner F**, Malagelada JR. Role of bacteria in experimental colitis. *Best Pract Res Clin Gastroenterol* 2003; **17**: 793-804

41 **Shanahan F**. Inflammatory bowel disease: immunodiagnostics, immunotherapeutics, and ecotherapeutics. *Gastroenterology* 2001; **120**: 622-635

PO Box 2345, Beijing 100023, China
www.wjgnet.com
wjg@wjgnet.com

ELSEVIER

World J Gastroenterol 2005;11(8):1141-1148
World Journal of Gastroenterology ISSN 1007-9327

• *BASIC RESEARCH* •

Alterations of mast cells and TGF-β1 on the silymarin treatment for CCl_4-induced hepatic fibrosis

Da-Hee Jeong, Gi-Ppeum Lee, Won-Il Jeong, Sun-Hee Do, Hai-Jie Yang, Dong-Wei Yuan, Ho-Yong Park, Kyu-Jong Kim, Kyu-Shik Jeong

Da-Hee Jeong, Gi-Ppeum Lee, Won-Il Jeong, Sun-Hee Do, Hai-Jie Yang, Dong-Wei Yuan, Kyu-Shik Jeong, Department of Pathology, College of Veterinary Medicine, Kyungpook National University, Daegu 702-701, Republic of Korea
Ho-Yong Park, Korea Research Institute of Bioscience and Biotechnology, Daejon, Republic of Korea
Kyu-Jong Kim, Dr. Kim Medicos Clinics, JungGu, SamdeokDong 3-21, Daegu 702-701, Republic of Korea
Supported by the Brain Korea 21 project in 2004 and the Ministry of Agriculture and Forestry project, No. 202059032WTO11
Correspondence to: Professor, Kyu-Shik Jeong, D.V.M., Ph.D., College of Veterinary Medicine, Kyungpook National University, Daegu 702-701, Republic of Korea. jeongks@knu.ac.kr
Telephone: +82-53-950-5975 Fax: +82-53-950-5955
Received: 2004-07-26 Accepted: 2004-09-09

Abstract

AIM: Silymarin is a potent antioxidant, antiinflammatory and anti-fibrogenic agent in the liver, which is mediated by alteration of hepatic Kupffer cell function, lipid peroxidation, and collagen production. Especially, in hepatic fibrogenesis, mast cells are expressed in chronic inflammatory conditions, and promote fibroblast growth and stimulate production of the extracellular matrix by hepatic stellate cells.

METHODS: We examined the inhibitory mechanism of silymarin on CCl_4-induced hepatic cirrhosis in rats. At 4, 8, and 12 wk, liver tissues were examined histopathologically for fibrotic changes produced by silymarin treatment.

RESULTS: In the silymarin with CCl_4-treated group, increase of hepatic stellate cells and TGF-β1 production were lower than in the CCl_4-treated group at early stages. Additionally, at the late fibrogenic stage, expressions of TGF-β1 were weaker and especially not expressed in hepatocytes located in peripheral areas. Moreover, the number of mast cell in portal areas gradually increased and was dependent on the fibrogenic stage, but those of CCl_4+silymarin-treated group decreased significantly.

CONCLUSION: Anti-fibrotic and antiinflammatory effects of silymarin were associated with activation of hepatic stellate cells through the expression of TGF-β1 and stabilization of mast cells. These results suggest that silymarin prevent hepatic fibrosis through suppression of inflammation and hypoxia in the hepatic fibrogenesis.

Key words: Silymarin; TGF-β1; Mast cell; Hepatic fibrosis

Jeong DH, Lee GP, Jeong WI, Do SH, Yang HJ, Yuan DW, Park HY, Kim KJ, Jeong KS. Alterations of mast cells and TGF-β1 on the silymarin treatment for CCl_4-induced hepatic fibrosis. *World J Gastroenterol* 2005; 11(8): 1141-1148
http://www.wjgnet.com/1007-9327/11/1141.asp

INTRODUCTION

Silymarin, a standardized extract of the milk thistle (*Silybum marianum* [L.] Gaertner) has a long tradition as an herbal remedy[1]. The flavonoid silymarin was introduced as a "hepatoprotective" agent a few years ago and is used clinically in Europe and Asia for the treatment of liver diseases[2]. The protective action of silymarin is explicable in terms of its capacity for trapping free radicals and has a stabilizing effect on the cytoplasmic membranes. In experimental animals, this flavonoid has a protective action on the liver, which is particularly vulnerable to poisoning by several hepatotoxic substances such as carbon tetrachloride (CCl_4), thioacetamide, and D-galactosamine[3]. Silymarin is a potent antioxidant that inhibits lipid peroxide formation in the liver cells[4], and possesses antiinflammatory properties mediated by alteration of hepatic Kupffer cell function[5].

Hepatic fibrosis has been noted in chronic liver disease, and is characterized by increased production and deposition of collagen, glycoproteins, and proteoglycans that compose the extracellular matrix (ECM)[6]. Availability of animal models is crucial for the study of liver fibrosis and/or cirrhosis. It is well known that hepatic cirrhosis animal models for chronic liver damage induced by CCl_4 in rats produce liver fibrosis and biochemical and histological patterns that resemble human liver cirrhosis[7]. Thus, the rat model of liver cirrhosis has been useful in studying the effects of hepatoprotective drugs with therapeutic potential to be used in humans[8]. In hepatic fibrogenesis, myofibroblasts (MFBs) such as hepatic stellate cells (HSCs) are the major source of increased ECM[6]. When they are exposed to soluble factors from damaged hepatocytes and from activated Kupffer cells, MFBs will lose Vitamin A and their lipid contents and undergo activation. The activated MFBs migrate and proliferate at the site of liver injury, playing a pivotal role in the formation of fibrous tissue[9]. Among the various cytokines, TGF-β1 plays an important role as a profibrogenic factor in chronic liver disease, triggering the expression of procollagen-I and tissue inhibitor of metalloproteinases-1 (TIMP-1), key effectors of

fibrogenesis. TGF-β1 is also the most potent mast cell chemo-attractant so far identified and induces mast cell migration at femtomolar (fM) concentrations. Various other cell types, e.g., monocytes, neutrophils, and fibroblasts also migrate towards TGF-β1[10].

Mast cells, which are derived from hematopoietic progenitors, leave the bone marrow and migrate to areas of inflammation. A number of factors responsible for this directional migration and tissue maturation of mast cells have been identified. These include the CXC family of chemokines, stem cell factor (also known as kit-ligand, steel factor, and mast cell growth factor), and TGF-β1[11]. Thus, the activation of mast cells and the subsequent exocytosis of granules are followed by production and secretion of cytokines and other factors that lead to leukocyte infiltration and local inflammation. Mast cell hyperplasia in the liver has also been observed in a variety of experimental models of rat liver fibrosis, such as that induced by CCl_4, diethylnitrosamine, radiation, porcine serum, and bile duct resection[12]. In addition, silymarin acts to stabilize hepatocyte membranes and block receptor binding of various toxins and drugs. Antioxidant activity is also hepatoprotective *in vivo* and *in vitro* studies, showing that silymarin has free radical scavenging activity and enhances superoxide dismutase action in erythrocytes and lymphocytes[13]. Silymarin also protects against glutathione depletion and increases protein synthesis by hepatocytes when there is damage to parenchymatous tissue[14].

In this study, we examined the inhibitory mechanism of silymarin on CCl_4-induced hepatic cirrhosis in rats. The objective of the present study was to observe the alteration of MFBs, TGF-β1, and mast cells histopathologically on the silymarin treatment and to elucidate the correlation between these changes and the antifibrotic effect of silymarin.

MATERIALS AND METHODS

Animals and treatments

Studies were performed on thirty male Wistar rats weighing 130-150 g. They were housed in a room at 22±2 ℃ and a 12-h light-dark cycle. Feed (PMI Nutrition International, USA) and water were supplied *ad libitum*.

Hepatic fibrosis was induced experimentally by intraperitoneal injection (IP) of 1.0 mL/kg body weight of 10% CCl_4 (Sigma, USA) dissolved in olive oil (Sigma, USA), three times a week for 12 wk. Two groups of fifteen animals each were used. These groups are schematically shown in Table 1. The first (CCl_4) group received CCl_4, 1.0 mL/kg IP three times a week and 0.25% carboxymethylcellulose (CMC, Sigma, USA), 1.0 mL/kg per oral, 5 d a week for 12 wk. The second (CCl_4+Sily) group received CCl_4, 1.0 mg/kg IP and a daily oral dose of 50 mg/kg silymarin 5 times a week. Silymarin was given as a suspension in 0.25% CMC. Five rats of each group were sacrificed at wk 4, 8, and 12 respectively.

Serum biochemical measurements

Serum was collected and assayed for alanine aminotransferase (ALT) and aspartate aminotransferase (AST) using standard enzymatic assay kits. Each assay is a colorimetric assay with detection of a highly colored end product measured at 490-520 nm using autoanalyzer - UV/V is spectrophotometer (Hitachi 736-10, Hitachi, Japan). The absorbance of each end product is proportional to the enzyme's activity.

Table 1 Experimental designs used in this study

Group ID	Number of animal	Treatment	Sacrificed time
CCl_4	15	CCl_4, 1.0 mg/(kg·d), IP 3 times a wk 0.25% CMC, 1 mL/(kg·d), PO 5 times a wk	4, 8, 12 wk
CCl_4 + Sily	15	CCl_4, 1.0 mg/(kg·d), IP 3 times a wk Silymarin, 50 mg/(kg·d), PO 5 times a wk	4, 8, 12 wk

Determination of hepatic hydroxyproline content

Hydroxyproline (HYP) was determinated colorimetrically in duplicates from 0.2 g of liver tissue using a modified method of Jamall *et al*[15]. Briefly, the frozen tissue was homogenized in 4 mL of 6N HCl and hydrolyzed at 110 ℃ for 16 h. The hydrolysate was filtered, and then 30 μL aliquot of these samples was evaporated under vacuum. The sediment was dissolved in 1.2 mL of isopropanol and incubated with 0.2 mL of 0.84% chloramines-T in acetate-citrate buffer (pH 6.0) for 10 min at room temperature. Then, 1.0 mL of Ehrlich's reagent was added and the mixture was incubated at 60 ℃ for 25 min. The absorbance of the sample solution was measured at 560 nm wavelength (Hitachi 736-10, Hitachi, Japan). Next, the hydroxyproline content in 100 mg of liver was calculated from the standard curve of 4-hydroxy-L-proline (Sigma, USA) (μg/100 mg liver weight).

Histopathological analysis

Liver tissues from each rat were rapidly removed, fixed in 10% neutral-buffered formalin, and processed routinely. Paraffin-embedded sections were cut into 4 μm thick sections. The sections were stained with hematoxylin and eosin (HE) and with special Azan stain, for collagen fibers. In there experiments, the degree of fibrosis in each section of liver was classified as a grade 0-4[16].

Immunohistochemistry

Liver sections were deparaffinized in xylene, dehydrated in graded alcohol series, and for the block of endogenous peroxidase, sections were incubated in a solution of 3% hydrogen peroxide (H_2O_2) in methanol for 10 min. Tissue sections were washed with PBS containing 0.03% non-fat milk and 0.01% Tween 20, and then immunostained with primary antibodies for alpha-smooth muscle actin (alpha-SMA) and TGF-β1. The antigen-antibody complex was visualized by a labeled streptavidin-biotin method using a Histostatin-PLUS Bulk Kit (Zymed Laboratories Inc., USA) and followed by diaminobenzidine (DAB) as a chromogen. After washing, slides were counter-stained with Meyer's hematoxylin and washed with tap water. The primary antibodies used were monoclonal anti α-SMA at a dilution of 1:800 (clone 1A4, Sigma, USA) and polygonal rabbit LC[1-30] antibody to mature TGF-β1 (kindly provided by Dr. Seong-Jin Kim) at a dilution of 1:100 respectively. Non-

immunized goat sera, which were used instead of the primary antibody, served as the negative control.

Number of mast cells in liver tissue

Toluidine blue staining for mast cells was performed by immersion of liver sections in 0.1% toluidine blue (Sigma, USA) for 1 min at room temperature. The number of mast cells was quantified in 25 randomly selected, non-overlapping fields and expressed as the number of mast cells/mm^2.

Statistical analysis

All results were expressed as mean and standard deviation (SD). Statistical analysis of the data was done using InStat program (GraphPad Software Inc.). A Mann-Whitney *U*-test was conducted and the data that were considered to be significantly different were reported at probability levels of $P<0.05$ or $P<0.005$, as indicated.

RESULTS

Serum biochemistry

Serum ALT and AST levels of all CCl_4-tested animals increased in a time-dependent fashion during the whole of experimental period (Figure 1). These changes indicated that liver damage and inflammation were induced successfully by injection of CCl_4 and were similar to previous results. However, in the CCl_4+silymarin treatment group, increases of serum ALT and AST levels were lower than those of the CCl_4 control group. The reduced ALT and AST activities of the silymarin-treated group were 30%, 72% and 33% compared to increases of 8%, 55% and 34% in the CCl_4-treated groups, at 4, 8, and 12 wk.

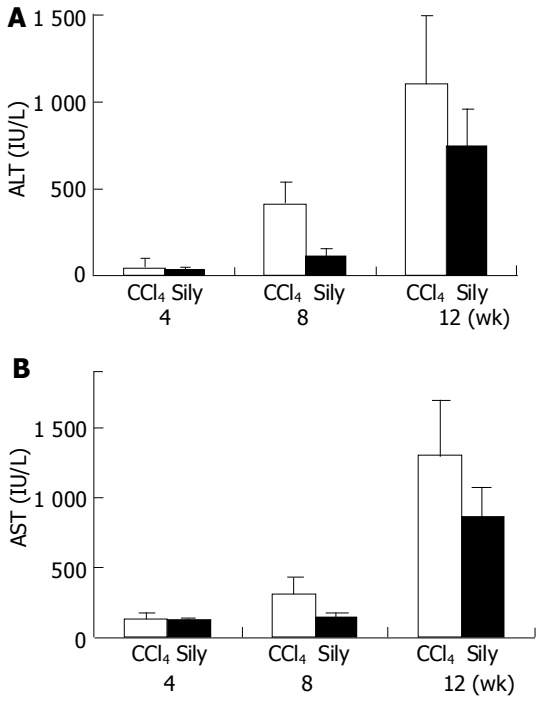

Figure 1 Serum ALT and AST levels in the CCl_4- or CCl_4 with silymarin-treated groups. A: Serum ALT levels were detected at 4, 8, and 12 wk; B: Serum AST levels were detected at 4, 8, and 12 wk. In the CCl_4 with silymarin-treated group (black bar), increase of serum ALT and AST levels were lower than those of CCl_4-treated group (open bar).

Collagen accumulation

Collagen contents of liver tissue were quantified by determination of the hydroxyproline content (Figure 2). In the CCl_4-treated group, hydroxyproline contents at 4, 8, and 12 wk increased 21.81±3.37, 24.31±0.91, and 43.26±1.41 μg/100 mg liver weight respectively. However, in the CCl_4+silymarin-treated group, the HYP contents at 4, 8, and 12 wk were 18.05±1.89, 20.5±1.92, and 27.5±0.69 μg/100 mg liver weight respectively. At 4, 8, and 12 wk, these HYP contents of CCl_4+silymarin-treated group were reduced by 17%, 16%, and 36% respectively compared to those of control group. Reduced HYP contents of 8 and 12 wk in the CCl_4+silymarin-treated group were statistically significant, $P<0.05$ and <0.005 respectively.

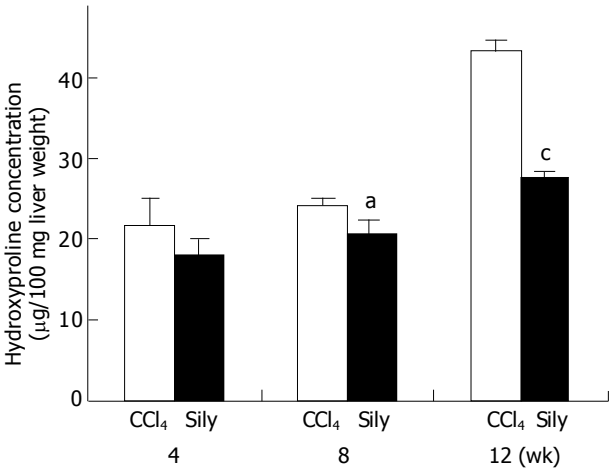

Figure 2 Hydroxyproline content determinated in the livers of CCl_4- or CCl_4 with silymarin-treated groups. At 4, 8 and 12 wk, HYP contents of CCl_4 with silymarin-treated group (black bar) reduced compared to those of control group (open bar). Data are expressed as the mean±SD (n = 5). [a]$P<0.05$ means significant compared to that of CCl_4-treated groups. [c]$P<0.005$ means significant compared to that of CCl_4-treated groups.

Histopathological observations

During the process of cirrhosis, the grade of hepatic fibrosis changed from grade 0 to grade 4 (Table 2). At 4 wk, centrilobular necrosis and moderate fatty change of liver were found in the CCl_4-only-treated group. In this group, there was collagen accumulation around the blood vessels (Figure 3A, G). At 8 wk, fatty change was rarely observed, but collagen fibers were more abundant in the centrilobular area and neighboring central veins were bridged by fibrous septa. Then, pseudolobuli were formed by thin fibrous septa (Figure 3B, H). At 12 wk, pseudolobuli were formed and macrovesicular lipid droplets were detected. The collagenous septa were much thicker, and pseudolobuli were subdivided into smaller lobuli (Figure 3C, I).

In the silymarin with CCl_4 injection group, at 4 wk, the presence of connective tissue was almost normal around the central veins (Figure 3D, J). At wk 8, moderate to severe fatty change was detected around the periportal area and central vein. A slight accumulation and spread of collagen fibers around central veins was observed too (Figure 3E, K). At wk 12, large lipid accumulation was detected more than

Table 2 Histopathological findings of liver tissue in the CCl_4- or CCl_4 with silymarin-treated groups

Group	4 wk		8 wk		12 wk	
	Grade[1]	Lesion	Grade	Lesion	Grade	Lesion
CCl_4	2	Mild fibrosis	3	Severe fibrosis	4	Cirrhosis
CCl_4+Sily	0-1	Mild fatty change	1-2	Mild fatty change and fibrosis	2-3	Severe fatty change and fibrosis

[1]Fibrotic grade classified by Fujiwara *et al*., Grade 0: none, Grade 1: short collagen extended from central veins, Grade 2: slender septa link the central veins but lobular architecture is preserved, Grade 3: pseudolobuli are formed thin septa, Grade 4: parenchyma is subdivided into pseudolobuli by thin septa.

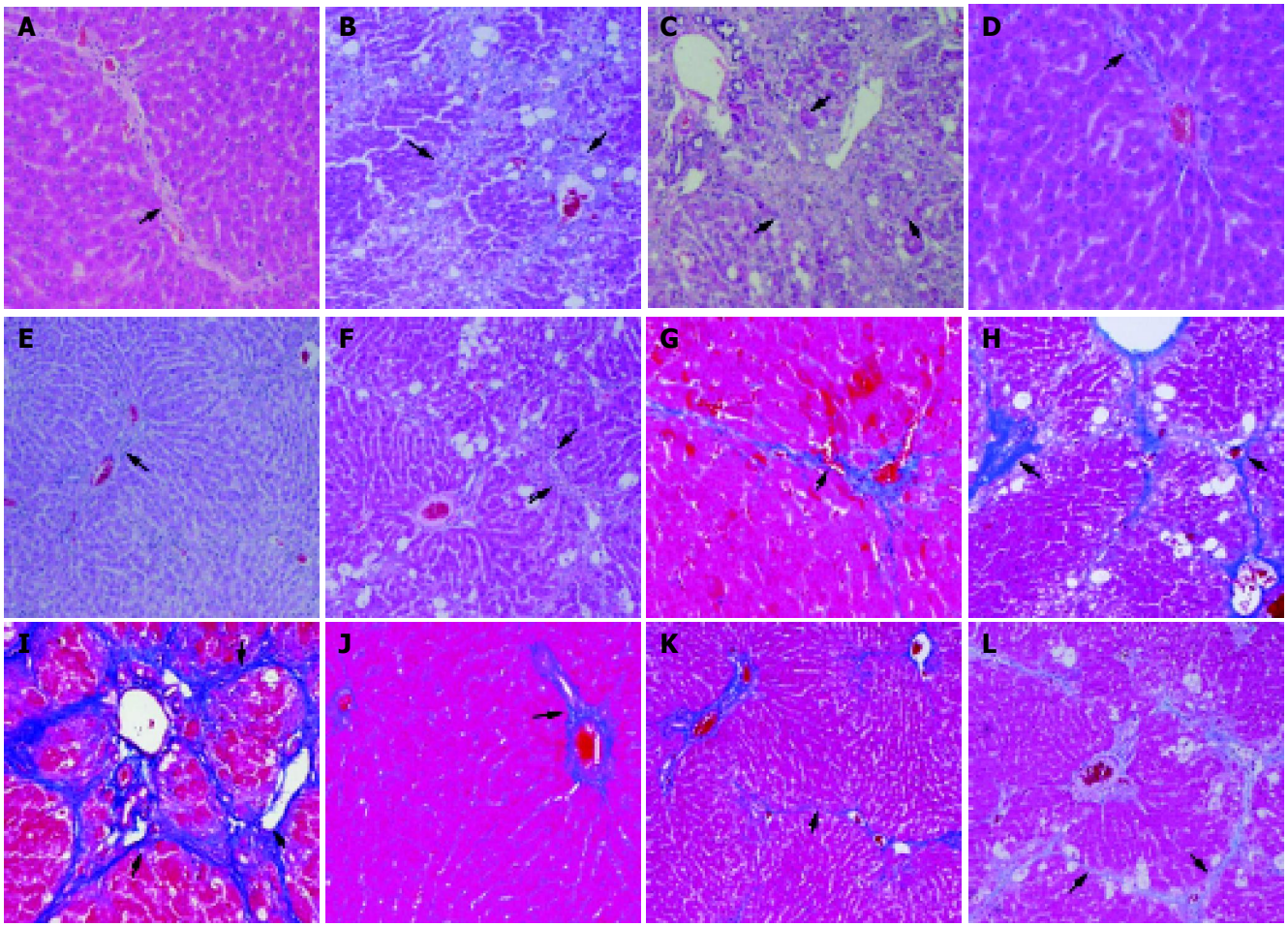

Figure 3 Hepatic fibrosis and accumulation of collagen in only CCl_4- or CCl_4 with silymarin-treated groups. In only CCl_4-treated group - A and G: At 4 wk, collagen (arrowhead) accumulation around the blood vessels; B and H: At 8 wk, collagen fiber (arrowhead) was more abundant in the centrilobular area and neighboring central veins were bridged by fibrous septa; C and I: At 12 wk, pseudolobuli were formed actively and macrovesicular lipid droplets were detected. The collagenous septa (arrowhead) were much thicker, and pseudolobuli were subdivided into smaller lobuli. In CCl_4 with silymarin-treated groups - D and J: At 4 wk, connective tissue was almost normal around the areas of central veins; E and K: At 8 wk, the slight accumulation and spread of collagen fibers around central veins was observed; F and L: At 12 wk, large lipid accumulation was detected more than that of CCl_4-treated group and pseudolobuli were formed by thin collagenous septa. HE stain, A-F; Azan stain, G-L. Original magnification: ×33, A-L.

that of the CCl_4-treated group and pseudolobuli were formed by thin collagenous septa (Figure 3F, L). The presence of collagenous fibers, as demonstrated by Azan stain, was confirmed too.

Immunohistochemical analysis

Normal expression of myofibroblasts (MFBs) (e.g., hepatic stellate cells, HSCs, *etc*.) was identified by α-SMA-positive staining and was limited to the central veins and portal triad. As liver damage, progressed α-SMA-positive cells markedly increased around blood vessels and fibrotic tissue in the CCl_4-only-treated group at wk 4, 8, and 12 (Figure 4A-C). In the silymarin with CCl_4-treated group, at 4 wk, α-SMA-positive cells were slightly detected around central and portal veins, the same as in the control group (Figure 4D), and then at wk 8 increasing α-SMA-positive MFBs exhibited the same pattern of collagen fiber spread from the central veins (Figure 4E). However, the numbers of α-SMA-positive cells in the silymarin with CCl_4-treated group was lower than in the CCl_4-only-treated group at wk 8 (Figure 4B, E). At

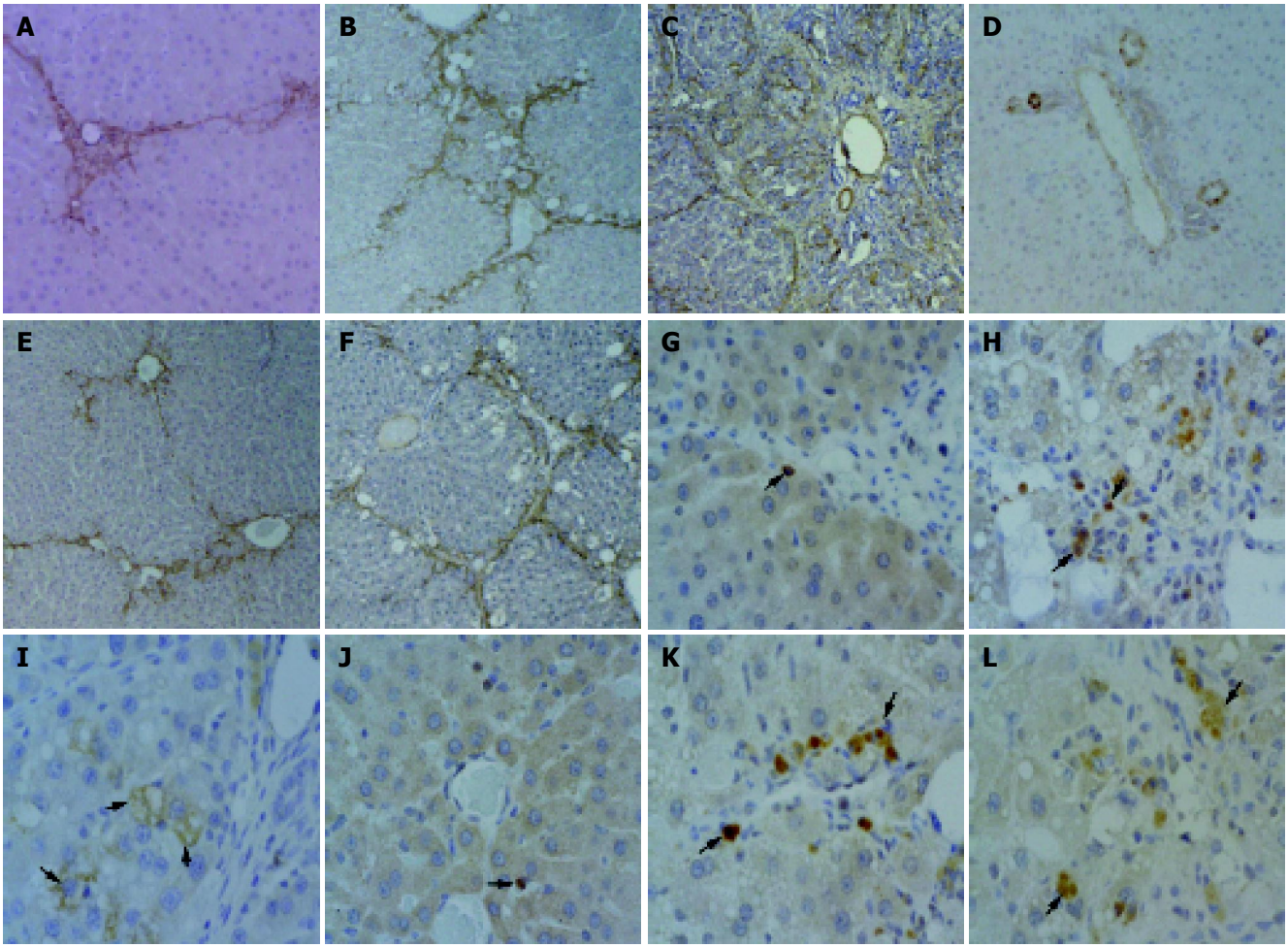

Figure 4 Positive reactive cells for α-SMA, TGF-β1 in only CCl_4- or CCl_4 with silymarin-treated groups. In only CCl_4-treated group - A: Weak positive reaction for α-SMA was detected at 4 wk; B: At 8 wk, increasing positive reaction for α-SMA was observed around fibrous septa; C: At 12 wk, α-SMA-positive cells observed a little decreasing along to the thick collagenous septa. In CCl_4 with silymarin-treated group -D: positive reaction for α-SMA was slightly detected at 4 wk; E: At 8 wk, α-SMA-positive cells were lower than that of CCl_4-only-treated group; F: At 12 wk, positive expression of α-SMA was shown the same pattern with result of CCl_4-treated group at 8 wk. In only CCl_4-treated group -G: Weak positive reaction for TGF-β1 (arrowhead) was detected in portal triad at wk 4; H: At 8 wk, increasing positive reaction for TGF-β1 (arrowhead) was observed in macrophage and around fibrous septa; I: At 12 wk, several hepatocytes (open arrowhead), located peripherally within pseudolobules, were observed TGFbeta1-positive immunoreaction. In CCl_4 with silymarin-treated group - J: At 4 wk, positive reaction for TGF-β1 (arrowhead) was slightly detected in macrophages; K: At 8 wk, positive reactive cells for TGF-β1 (arrowhead) were lower than that of CCl_4-only-treated group; L: At 12 wk, expressions of TGFbeta1 (arrowhead) were seen weaker than those of CCl_4-treated group and not detected in hepatocytes. Immunostaining for α-SMA (A-F) and TGF-β1 (G-L) with hematoxylin counterstain. Original magnifications: ×33 (A-F); ×132 (G-L).

wk 12, the CCl_4-treated group developed into a cirrhotic stage, and α-SMA-positive MFBs were observed mild along to the thick collagenous septa (Figure 4C), compared to 8 wk. This indicated expression of the collagen matrix in the hepatocytes against activation of myofibroblasts, which disappeared at the stage of cirrhosis. However, at 12 wk, MFBs of the CCl_4+silymarin-treated group showed positive expression of α-SMA identical to the pattern in fibrosis (Figure 4F).

During hepatic fibrogenesis in CCl_4-treated group, expression of TGF-β1 was detected in bile ductular epithelial cells and macrophages at 4 and 8 wk (Figure 4G, H). As the fibrotic grade increased, the positive reaction of TGF-β1 was predominantly expressed in the macrophages and MFBs. Significantly, at 12 wk several hepatocytes showed TGF-β1-positive immunoreaction. These hepatocytes were located peripherally within the pseudolobules (Figure 4I). However, in the CCl_4+silymarin-treated group, the expression of TGF-β1 was weaker than in the CCl_4-treated group (Figure 4J-L).

Recruitment of mast cells in liver tissue

In toluidine blue stained liver sections from the CCl_4-treated group mast cells were oval in shape with metachromatic granules in portal areas (Figure 5). At 4, 8, and 12 wk, the number of mast cells of the CCl_4-treated group increased gradually: 12.43±2.38, 18.17±2.12 and 21.8±4.92 cells/mm^2 respectively. However, in the CCl_4+silymarin-treated group, the number of mast cell were 10±3.33, 12.42±2.35, and 12.17±3.07 cells/mm^2 respectively (Figure 6). These numbers for the CCl_4+silymarin-treated group decreased significantly by 19%, 32%, and 44% compared to those of CCl_4-treated group, indicating a silymarin-mediated protective mechanism.

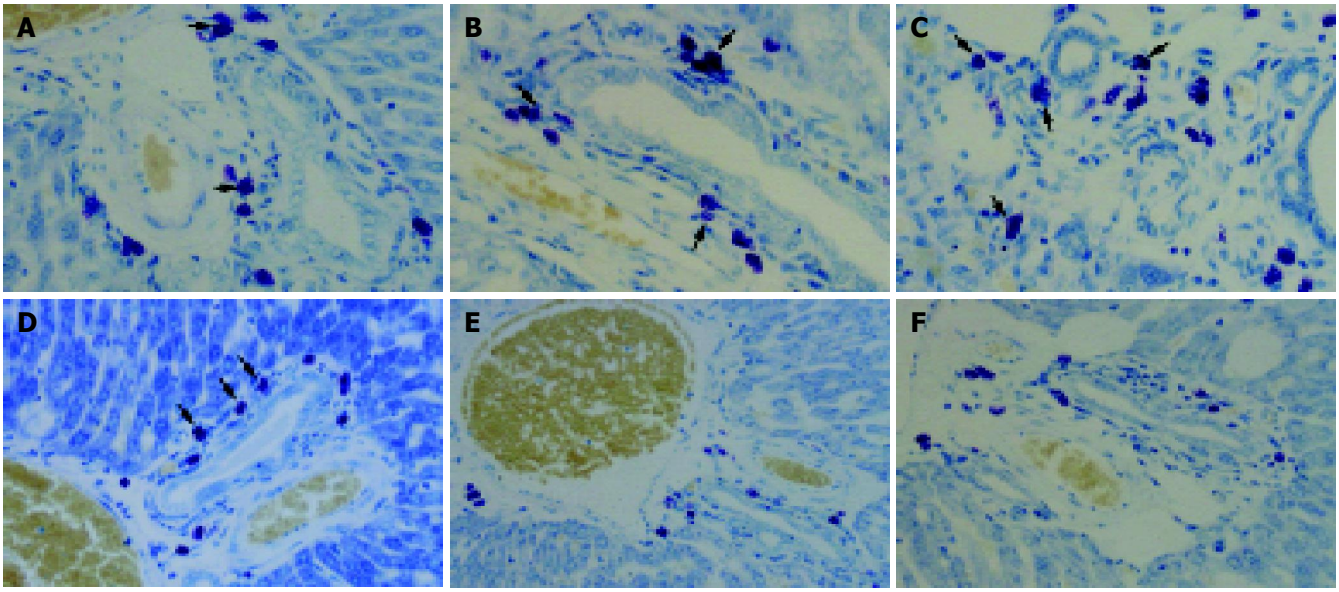

Figure 5 Toluidine blue-stained liver tissue of only CCl_4- or CCl_4 with silymarin-treated groups. In only CCl_4-treated group - A: At 4 wk, specific toluidine blue-stained mast cells (arrowhead) were detected in periportal region; B: At 8 wk, the number of mast cell increased; C: At 12 wk, mast cells increased along the thick collagenous septa. In CCl_4 with silymarin-treated group - D: Positive reaction for toluidine blue (arrowhead) was slightly detected at 4 wk; E: At 8 wk, α-SMA-positive cells were lower than that of CCl_4-only-treated group; F: At 12 wk, positive expression of α-SMA was shown in the same pattern as with the result of CCl_4-treated group at 8 wk. Toluidine blue stain, A-F. Original magnification: ×132, A-F.

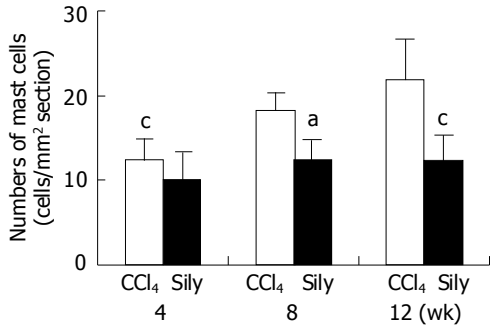

Figure 6 Recruitment of mast cell numbers in only CCl_4- or CCl_4 with silymarin-treated groups. At 4, 8 and 12 wk, mast cell numbers of CCl_4 with silymarin-treated group (black bar) significantly reduced compared to those of control group (open bar). Data are expressed as the mean±SD. $^aP<0.05$ means significant compared to that of CCl_4-treated groups. $^cP<0.005$ smeans significant compared to that of CCl_4-treated groups.

DISCUSSION

Silymarin is well known to be a protective agent against various hepatotoxins, such as acetaminophen, alcohol, carbon tetrachloride, tetrachloromethane, and toluene[17]. Pretreating rats and mice with silymarin before exposure to these chemical hepatotoxins significantly reduced lipid peroxidation and hepatotoxicity[3]. Additionally, the pharmacological effects of silymarin include regulation of cell membrane permeability, leukotriene inhibition, reactive oxygen species scavenging, and suppression of NF-kappaB DNA binding activity[18].

In animal studies, silymarin is as effective as colchicine in reversing hepatic fibrosis due to CCl_4-induced damage[1]. A CCl_4-induced hepatic cirrhosis rat model has been useful in studying the effects of hepatoprotective drugs with therapeutic potential to be used in humans[8]. In the current study, hepatic fibrosis/cirrhosis was successfully induced by CCl_4 injection in rats and flavorous results were obtained similar to previous study. Total hepatic collagen contents determined by hydroxyproline content increased gradually during experimental period and histopathological findings of fibrosis/cirrhosis were observed in H&E and the Azan-stained section. In the present study, the hepatoprotective effect of silymarin was determined in CCl_4-induced liver cirrhosis of rats. In the CCl_4 with silymarin-treated group, total hepatic collagen contents were significantly lower than in the CCl_4-treated group especially at 8 and 12 wk. Additionally histopathological findings of fibrosis/cirrhosis were revealed a significant reduction in the CCl_4-treated group. Similar experiments by Favari *et al* reported the reduction of lipid peroxidation, Na^+, K^+, and Ca^{2+}-ATPase levels and increases of collagen content[3,19].

In hepatic fibrogenesis, myofibroblasts (MFBs) are the major source of increased ECM. The activated MFBs migrate and proliferate at the site of liver injury and play a pivotal role in the formation of fibrous tissue. Therefore, activated MFBs are considered the major cellular target to prevent the progression of liver fibrosis during the new drug development[9]. In addition, transforming growth factor beta (TGF-β) is a potent fibrogenic cytokine produced by Kupffer cells and HSCs. There is a prolonged increase of TGF-β1 expression during hepatic fibrosis in CCl_4- and diethylnitrosamine-induced models[20] and in patients with cirrhosis induced by alcohol or viral hepatitis[21].

In the current study, as liver damage progressed in the CCl_4-only-treated group, α-SMA-positive cells markedly increased around fibrous septa. The number of these cells increased from wk 4 to 8, but slightly decreased along the

thick collagenous septa at 12 wk, developed into the cirrhotic stage. Characteristically, in immunohistochemical analysis for TGF-β1, positive reactions were mainly expressed by HSC and macrophages around the portal region, at early (4 wk) and middle (8 wk) stages of the fibrotic processes, but they were predominantly observed in hepatocytes located in pseudolobules peripherally, at the cirrhosis-occurred stage (12 wk). The mechanism of TGF-β1 expression in hepatocytes has been studied by several researchers, but is still unclear. Furthermore, these alterations of TGF-β1 expression were already reported by our laboratory and we suggested that hypoxia might be associated with fibrogenesis in the liver[22]. However, in the silymarin+CCl_4-treated group of our study, there was increase of α-SMA-positive cells such as MFBs, lower than that of CCl_4-only-treated group, at 4, 8, and 12 wk. Additionally, expressions of TGF-β1 were weaker than those of CCl_4-treated group, during all experimental periods, especially at 12 wk not expressed in hepatocyte located in peripheral areas of pseudolobules. Thus, based on the results of the current study, it is concluded that silymarin has protective effect of proliferation and TGF-β1 production in MFBs.

Fuchs *et al*[23] reported on the basis of *in vitro* studies that the potential antifibrotic properties of silymarin might be the inhibition of hepatic stellate cell proliferation and transformation. Jia *et al*[24] observed that silymarin suppresses expression of profibrogenic procollagen alpha1 (I) and TIMP-1 most likely via down-regulation of TGF-β1 mRNA in rats with biliary fibrosis. However, *in vivo* studies of the anti-fibrotic activities of silymarin have not yet elucidated histopathologically the preventive mechanism of activation or proliferation of MFBs by silymarin during the CCl_4-induced hepatic fibrogenesis. These results suggest that alterations of the numbers of MFBs and TGF-β1 expression in the liver may be involved in the hepatoprotective effects of silymarin observed in other studies. Another study of silymarin explained the antifibrotic action through the effects on TGF-β1 expression[24]. Silymarin has been noted to regenerate cells and enhance RNA synthesis in the rat liver[25].

In liver fibrosis and/or cirrhosis, several studies have reported a relationship between mast cell density, hepatocellular damage, mRNA encoding TGF-β1, hepatic stellate cell activation, and collagen levels[26-28]. Mast cells have been implicated in chronic inflammatory conditions resulting in fibrosis, such as Crohn's disease, and have been identified in human liver. The number of mast cells are reported to increase in chronic liver diseases associated with fibrosis[12]. Armbrust *et al*[29] demonstrated that in the late stage of liver fibrogenesis, mast cells may be involved by displaying protease inhibitory activity in the fibrotic septa. In our previous study, the chronic injection of CCl_4 induced rat liver cirrhosis concomitant with a marked increase of mast cells[30]. In this study, the number of mast cells in portal areas gradually increased in the fibrogenic stage, but the number of mast cells in the CCl_4+silymarin-treated group decreased significantly compared to those of CCl_4-treated group. In the study of Fantozzi *et al*, there was inhibition of neutrophil-mediated histamine release dose-dependently. These results further stress the concept of a neutrophil-mast cell interaction, which may be involved in inflammatory processes[31]. Moreover, mast cells secrete various mediators, which promote fibroblast growth, stimulate production of the extracellular matrix by fibroblasts of hepatic stellate cells, and produce components of the extramedullary matrix themselves[32,33]. However, it is unclear whether they play a central role in its development.

The anti-inflammatory effects of silymarin are also based on multiple activities including mast cell stabilization, inhibition of neutrophil migration, Kupffer cell inhibition, inhibition of leukotrienes, and prostaglandin formation. However, results of earlier studies have not histopathologically shown expression of mast cells in fibrotic liver tissue after silymarin treatment. Thus, silymarin has been histopathologically shown to have significant antiinflammatory effect on hepatic tissue, including mast cell stabilization. In addition, it is likely that the hepatoprotective effect of silymarin is related to prevention of hypoxia in hepatic fibrogenesis.

In conclusion, the anti-fibrotic and antiinflammatory effects of silymarin were histopathologically observed in the hepatic fibrogenesis of chronic liver damage induced by CCl_4 treatment. Furthermore, these effects were associated with activation of MFBs, expression of TGF-β1, and stabilization of mast cells. These results suggest that silymarin prevents hepatic fibrosis through the suppression of inflammation and hypoxia in CCl_4-induced rat liver cirrhosis.

REFERENCES

1 **Valenzuela A**, Garrido A. Biochemical bases of the pharmacological action of the flavonoid silymarin and of its structural isomer silibinin. *Biol Res* 1994; **27**: 105-112
2 **Down WH**, Chasseaud LF, Grundy RK. Effect of silybin on the hepaticmicrosomal drug metabolizing enzyme system in the rat. Arzneim-Forsch. *Drug Res* 1974; **24**: 1986-1988
3 **Mourelle M**, Muriel P, Favari L, Franco T. Prevention of CCL_4-induced liver cirrhosis by silymarin. *Fundam Clin Pharmacol* 1989; **3**: 183-191
4 **Muriel P**, Garcia-pina T, Perez-Alvarez V, Mourelle M. Silymarin protects against paracetamol-induced lipid peroxidation and liver damage. *J Appl Toxicol* 1992; **12**: 439-442
5 **Dehmlow C**, Erhard J, de Groot H. Inhibition of Kupffer cell functions as an explanation for the hepatoprotective properties of silibinin. *Hepatology* 1996; **23**: 749-754
6 **Akiyoshi H**, Terada T. Mast cell, myofibroblast and nerve terminal complexes in carbon tetrachloride-induced cirrhotic rat livers. *J Hepatol* 1998; **29**: 112-119
7 **Perez-Tamayo R**. Is cirrhosis of the liver experimentally produced by CCl_4 and adequate model of human cirrhosis? *Hepatology* 1983; **3**: 112-120
8 **Paquet KJ**, Kamphausen U. The carbon-tetrachloride-hepatotoxicity as a model of liver damage. First report: Long-time biochemical changes. *Acta Hepatogastroenterol (Stuttg)* 1975; **22**: 84-88
9 **Wu J**, Zern MA. Hepatic stellate cells: a target for the treatment of liver fibrosis. *J Gastroenterol* 2000; **35**: 665-672
10 **Olsson N**, Piek E, ten Dijke P, Nilsson G. Human mast cell migration in response to members of the transforming growth factor-beta family. *J Leukoc Biol* 2000; **67**: 350-356
11 **Jones SE**, Kelly DJ, Cox AJ, Zhang Y, Gow RM, Gilbert RE. Mast cell infiltration and chemokine expression in progressive renal disease. *Kidney Int* 2003; **64**: 906-913
12 **Sugihara A**, Tsujimura T, Fujita Y, Nakata Y, Terada N. Evaluation of role of mast cells in the development of liver fibrosis using mast cell-deficient rats and mice. *J Hepatol* 1999; **30**: 859-867

13 **Altorjay I**, Dalmi L, Sari B, Imre S, Balla G. The effect of silibinin (Legalon) on the the free radical scavenger mechanisms of human erythrocytes *in vitro*. *Acta Physiol Hung* 1992; **80**: 375-380
14 **Galisteo M**, Rissel M, Sergent O, Chevanne M, Cillard J, Guillouzo A, Lagadic-Gossmann D. Hepatotoxicity of tacrine: occurrence of membrane fluidity alterations without involvement of lipid peroxidation. *J Pharmacol Exp Ther* 2000; **294**: 160-167
15 **Jamall IS**, Finelli VN, Que Hee SS. A simple method to determine nanogram levels of 4-hydroxyproline in biological tissues. *Anal Biochem* 1981; **112**: 70-75
16 **Fujiwara K**, Ogata I, Ohta Y, Hayashi S, Mishiro S, Takatsuki K, Sato Y, Yamada S, Hirata K, Oka H. Decreased collagen accumulation by a prolyl hydroxylase inhibitor in pig serum-induced fibrotic rat liver. *Hepatology* 1988; **8**: 804-807
17 **Saller R**, Meier R, Brignoli R. The use of silymarin in the treatment of liver diseases. *Drugs* 2001; **61**: 2035-2063
18 **Schumann J**, Prockl J, Kiemer AK, Vollmar AM, Bang R, Tiegs G. Silibinin protects mice from T cell-dependent liver injury. *J Hepatol* 2003; **39**: 333-340
19 **Favari L**, Perez-Alvarez V. Comparative effects of colchicine and silymarin on CCl_4-chronic liver damage in rats. *Arch Med Res* 1997; **28**: 11-17
20 **Nakatsukasa H**, Nagy P, Evarts RP, Hsia CC, Marsden E, Thorgeirsson SS. Cellular distribution of transforming growth factor-beta 1 and procollagen types I, III, and IV transcripts in carbon tetrachloride-induced rat liver fibrosis. *J Clin Invest* 1990; **85**: 1833-1843
21 **Annoni G**, Weiner FR, Zern MA. Increased transforming growth factor-beta 1 gene expression in human liver disease. *J Hepatol* 1992; **14**: 259-264
22 **Jeong WI**, Do SH, Yun HS, Song BJ, Kim SJ, Kwak WJ, Yoo SE, Park HY, Jeong KS. Hypoxia potentiates transforming growth factor-beta expression of hepatocyte during the cirrhotic condition in rat liver. *Liver Int* 2004; **24**: 658-668
23 **Fuchs EC**, Weyhenmeyer R, Weiner OH. Effects of silibinin and of a synthetic analogue on isolated rat hepatic stellate cells and myofibroblasts. *Arzneimittelforschung* 1997; **47**: 1383-1387
24 **Jia JD**, Bauer M, Cho JJ, Ruehl M, Milani S, Boigk G, Riecken EO, Schuppan D. Antifibrotic effect of silymarin in rat secondary biliary fibrosis is mediated by downregulation of procollagen alpha1(I) and TIMP-1. *J Hepatol* 2001; **35**: 392-398
25 **Sonnenbichler J,** Zetl I. Mechanism of action of silibinin. V. Effect of silibinin on the synthesis of ribosomal RNA, mRNA and tRNA in rat liver in vivo. *Hoppe Seylers Z Physiol Chem* 1984; **365**: 555-566
26 **Grizzi F**, Franceschini B, Gagliano N, Moscheni C, Annoni G, Vergani C, Hermonat PL, Chiriva-Internati M, Dioguardi N. Mast cell density, hepatic stellate cell activation and TGF-beta1 transcripts in the aging Sprague-Dawley rat during early acute liver injury. *Toxicol Pathol* 2003; **31**: 173-178
27 **Li CY**, Baek JY. Mastocytosis and fibrosis: role of cytokines. *Int Arch Allergy Immunol* 2002; **127**: 123-126
28 **Zheng M**, Ruan Y, Wu Z. Correlation study of TGF beta expression in diethylnitrosamine-induced rat liver cancer and mast cells in its vicinity. *Zhonghua Zhongliu Zazhi* 2000; **22**: 463-465
29 **Armbrust T**, Batusic D, Ringe B, Ramadori G. Mast cells distribution in human liver disease and experimental rat liver fibrosis. Indications for mast cell participation in development of liver fibrosis. *J Hepatol* 1997; **26**: 1042-1054
30 **Jeong WI**, Lee CS, Park SJ, Chung JY, Jeong KS. Kinetics of macrophages, myofibroblasts and mast cells in carbon tetrachloride-induced rat liver cirrhosis. *Anticancer Res* 2002; **22**: 869-877
31 **Fantozzi R**, Brunelleschi S, Rubino A, Tarli S, Masini E, Mannaioni PF. FMLP-activated neutrophils evoke histamine release from mast cells. *Agents Actions* 1986; **18**: 155-158
32 **Hatamochi A**, Fujiwara K, Ueki H. Effects of histamine on collagen synthesis by cultured fibroblasts derived from guinea pig skin. *Arch Dermatol Res* 1985; **277**: 60-64
33 **Weber S**, Kruger-Krasagakes S, Grabbe J, Zuberbier T, Czarnetzki BM. Mast cells. *Int J Dermatol* 1995; **34**: 1-10

PO Box 2345, Beijing 100023, China
www.wjgnet.com
wjg@wjgnet.com

ELSEVIER

World J Gastroenterol 2005;11(8):1149-1154
World Journal of Gastroenterology ISSN 1007-9327

• *BASIC RESEARCH* •

Up-regulation of intestinal nuclear factor kappa B and intercellular adhesion molecule-1 following traumatic brain injury in rats

Chun-Hua Hang, Ji-Xin Shi, Jie-Shou Li, Wei-Qin Li, Hong-Xia Yin

Chun-Hua Hang, Ji-Xin Shi, Hong-Xia Yin, Department of Neurosurgery, Jinling Hospital, Clinical School of Medicine, Nanjing University, Nanjing 210002, Jiangsu Province, China
Jie-Shou Li, Wei-Qin Li, Research Institute of General Surgery, Jinling Hospital, Clinical School of Medicine, Nanjing University, Nanjing 210002, Jiangsu Province, China
Supported by Scientific Research Foundation of the Chinese PLA Key Medical Programs During the 10th Five-Year Plan Period, No. 01Z011
Correspondence to: Chun-Hua Hang, Department of Neurosurgery, Jinling Hospital, 305 East Zhongshan Road, Nanjing 210002, Jiangsu Province, China. hang1965@public1.ptt.js.cn
Telephone: +86-25-80860010 Fax: +86-25-84810987
Received: 2004-06-29 Accepted: 2004-07-15

Abstract

AIM: Nuclear factor kappa B (NF-κB) regulates a large number of genes involved in the inflammatory response to critical illnesses, but it is not known if and how NF-κB is activated and intercellular adhesion molecule-1 (ICAM-1) expressed in the gut following traumatic brain injury (TBI). The aim of current study was to investigate the temporal pattern of intestinal NF-κB activation and ICAM-1 expression following TBI.

METHODS: Male Wistar rats were randomly divided into six groups (6 rats in each group) including controls with sham operation and TBI groups at hours 3, 12, 24, and 72, and on d 7. Parietal brain contusion was adopted using weight-dropping method. All rats were decapitated at corresponding time point and mid-jejunum samples were taken. NF-κB binding activity in jejunal tissue was measured using EMSA. Immunohistochemistry was used for detection of ICAM-1 expression in jejunal samples.

RESULTS: There was a very low NF-κB binding activity and little ICAM-1 expression in the gut of control rats after sham surgery. NF-κB binding activity in jejunum significantly increased by 160% at 3 h following TBI ($P<0.05$ *vs* control), peaked at 72 h (500% increase) and remained elevated on d 7 post-injury by 390% increase. Compared to controls, ICAM-1 was significantly up-regulated on the endothelia of microvessels in villous interstitium and lamina propria by 24 h following TBI and maximally expressed at 72 h post-injury ($P<0.001$). The endothelial ICAM-1 immunoreactivity in jejunal mucosa still remained strong on d 7 post-injury. The peak of NF-κB activation and endothelial ICAM-1 expression coincided in time with the period during which secondary mucosal injury of the gut was also at their culmination following TBI.

CONCLUSION: TBI could induce an immediate and persistent up-regulation of NF-κB activity and subsequent up-regulation of ICAM-1 expression in the intestine. Inflammatory response mediated by increased NF-κB activation and ICAM-1 expression may play an important role in the pathogenesis of acute gut mucosal injury following TBI.

Key words: Traumatic brain injury; Intestine; Nuclear factor kappa B; Intercellular adhesion molecule-1; Inflammatory response

Hang CH, Shi JX, Li JS, Li WQ, Yin HX. Up-regulation of intestinal nuclear factor kappa B and intercellular adhesion molecule-1 following traumatic brain injury in rats. *World J Gastroenterol* 2005; 11(8): 1149-1154
http://www.wjgnet.com/1007-9327/11/1149.asp

INTRODUCTION

The importance of the intestinal mucosa in the inflammatory and metabolic responses to sepsis, trauma and other critical illnesses is increasingly recognized. Major trauma and shock may initiate a cascade of intestinal events such as intestinal cytokine overproduction[1-3], increased intestinal permeability[4-6], translocation of intestinal bacteria and endotoxins[7]. These events may not only influence the intestinal mucosa itself, but also may affect the function and integrity of remote organs and tissues[8], leading to systemic inflammatory response syndrome (SIRS) and multiple organ dysfunction syndrome (MODS)[9]. Indeed, the gut has been proposed to be the "motor" of MODS in critical illnesses[4,7,10], mainly through the inflammatory response mediated by nuclear factor kappa B (NF-κB) and proinflammatory cytokines[1]. Our previous study demonstrated that traumatic brain injury (TBI) could induce marked damage of intestinal mucosal structure and barrier function[5]. However, the underlying mechanism for the acute gut mucosal injury induced by TBI remains unclear.

NF-κB is a transcription factor that plays a key role in the activation of genes involved in immune and acute phase responses[11,12]. NF-κB can be activated by lesion-induced oxidative stress, bacterial endotoxin or cytokines, and subsequently increases transcriptionally the expression of the genes for many cytokines[13,14], enzymes[15] and adhesion molecules[16], which have been believed to be involved in the acute inflammatory response. Adhesion molecules can

recruit inflammatory cells, such as neutrophils, eosinophils, and T lymphocytes, from the circulation to the site of inflammation to release inflammatory mediators responsible for the gut mucosal damage. NF-κB regulates the expression of several genes that encode these adhesion molecules, including intercellular adhesion molecule-1 (ICAM-1) and E-selectin[16-18], which mediates the initial attachment and rolling of neutrophils, and vascular-cell adhesion molecule-1 (VCAM-1)[19], which mediates the recruitment of monocytes and lymphocytes. Several studies have shown that NF-κB and ICAM-1 play an important role in the pathogenesis of chronic inflammatory bowel disease (IBD)[13,14,20,21]. Taken together, the activation of intestinal NF-κB could induce the up-regulation of ICAM-1, leading to the recruitment of inflammatory cells and exacerbating intestinal inflammation. Intestinal inflammation has been viewed as a process in which gut-derived effector immune cells cause the destruction of other mucosal cells[1,20,22].

To date, there has been no study on intestinal NF-κB binding activity and ICAM-1 expression induced by TBI. Insight into these cellular and molecular events occurring in the gut might contribute to the understanding of inflammatory response and potential mechanisms involved in the acute intestinal mucosal injury following TBI. In this regard, the aim of current study was to evaluate the temporal pattern of intestinal NF-κB activation and ICAM-1 expression following TBI.

MATERIALS AND METHODS

Rat models of TBI

Male Wistar rats (220 to 250 g) were purchased from Animal Center of Chinese Academy of Sciences, Shanghai, China. The rats were housed in temperature- and humidity-controlled animal quarters with a 12 h light/dark cycle, room temperature (RT) at 23±1 ℃ and free access to water. Physiological parameters and eating behaviors were monitored to avoid the confounding variable of different food intakes between the groups on mucosal responses throughout the experiments. All procedures were approved by the Institutional Animal Care Committee, and were in accordance with the guidelines of the National Institutes of Health on the care and use of animals.

The rats were randomly divided into six groups (6 rats in each group) including control group with sham operation and traumatic brain injury groups at hours 3, 12, 24, and 72, and on d 7 respectively. Following intraperitoneal anesthesia with urethane (1 000 mg/kg), the animal head was fixed in the stereotactic device. A right parietal bone window of 5 mm in diameter was made under aseptic conditions with dental drill just behind the cranial coronal suture and beside midline. The dura was kept intact. Right parietal brain contusion was adopted using the weight-dropping method described by Feeney *et al*[23] and severe traumatic brain injury was made by letting a steel rod weighing 40 g with a flat end diameter of 4 mm fall onto a piston resting on the dura from a height of 25 cm. The piston was allowed to compress the brain tissue a maximum of 5 mm. Our preliminary study showed that there was no significant difference between all control rats at various time points from 3 h to 7 d. Therefore, we chose the rats with sham surgery for 72 h as the control group. The control animals were killed for sample collection at 72 h, and TBI group rats were decapitated at their corresponding time points. A 3 cm segment of the midjejunum was taken, flushed with ice-cold saline, opened longitudinally and stored in liquid nitrogen immediately until use.

Nuclear protein extracts and EMSA

NF-κB was examined using electrophoretic mobility shift assay (EMSA). Nuclear extracts of intestinal tissue were prepared by hypotonic lyses followed by high salt extraction[24]. In brief, about 0.1 g of frozen jejunal tissue was homogenized in 0.8 mL ice-cold buffer A, composed of 10 mmol/L HEPES (pH 7.9), 10 mmol/L KCl, 2 mmol/L $MgCl_2$, 0.1 mmol/L EDTA, 1.0 mmol/L dithiothreitol (DTT), and 0.5 mmol/L phenylmethylsulfonyl fluoride (PMSF) (all from Sigma Chemical Co.). The homogenate was incubated on ice for 20 min, and then 50 μL of 10% Nonidet P-40 solution was added (Sigma Chemical Co.); the mixture was vortexed for 30 s and spun by centrifugation for 1 min at 5 000 *g*, 4 ℃. The crude nuclear pellet was resuspended in 200 μL of buffer B, containing 20 mmol/L HEPES (pH 7.9), 420 mmol/L NaCl, 1.5 mmol/L $MgCl_2$, 0.1 mmol/L EDTA, 1 mmol/L DTT, 0.5 mmol/L PMSF, 250 mL/L glycerol, and incubated on ice for 30 min with intermittent mixing. The suspension was spun by centrifugation at 12 000 *g*, 4 ℃ for 15 min. The supernatant containing nuclear proteins was collected and stored at -70 ℃ for further analysis. Protein concentration was determined using a bicinchoninic acid assay kit with bovine serum albumin as the standard (Pierce Biochemicals, Rockford, IL).

EMSA was performed using a commercial kit (Gel Shift Assay System, Promega, Madison, WI). NF-κB consensus oligonucleotide probe (5'-AGTTGAGGGGACTTTCC CAGGC-3') was end-labeled with [γ-^{32}P] ATP (Free Biotech, Beijing, China) and T4-polynucleotide kinase. Nuclear protein (20 μg) was pre-incubated in a total volume of 9 μL in a binding buffer, consisting of 10 mmol/L Tris-Cl, pH 7.5, 1 mmol/L $MgCl_2$, 50 mmol/L NaCl, 0.5 mmol/L EDTA, 0.5 mmol/L DTT, 4% glycerol, and 0.05 g/L of polydeoxyinosinic deoxycytidylic acid (dI-dC) for 15 min at room temperature. After addition of the ^{32}P-labeled oligonucleotide probe, the incubation was continued for 20 min at room temperature. Reaction was stopped by addition of 1 μL of gel loading buffer and the mixture was subjected to non-denaturing 4% polyacrylamide gel electrophoresis in a TBE buffer (Tris-borate-EDTA). The gel was vacuum-dried and exposed to x-ray (Fuji Hyperfilm) at -70 ℃ till an intensifying screen. Levels of NF-κB DNA binding activity was quantified by computer-assisted densitometric scanning and expressed as an arbitrary densitometric unit (ADU).

Detection of ICAM-1 expression in jejunal tissue

The 10% buffered formalin-fixed jejunal tissue was embedded in paraffin, sectioned in 4 μm thickness with a microtome and stained with hematoxylin and eosin (H-E). The H-E stained sections were examined under a microscope for any alteration in histopathology. Rabbit anti CD54

(ICAM-1) primary antibody was purchased from Boster Biotechnology Co., Ltd, China and the working dilutions for these antibodies were 1∶100. For immunohistochemistry, sections were incubated in phosphate-buffered saline (PBS) with 5% normal horse serum and 0.3% Triton X-100 for 1 h at RT. Sections were washed three times with PBS and incubated with primary antibody to ICAM-1 for 2 h at RT. After washing with PBS, sections were incubated with biotinylated second antibodies for 1 h at RT. Sections incubated in the absence of primary antibody were used as negative controls. Microscopy of the immunohistochemically stained tissue sections was performed by an experienced pathologist blinded to the experimental condition. Evaluation of sections was, therefore undertaken by assessing the intensity of staining (5 grades). "0" indicates that there were no detectable positive cells; "1" indicates very low density of positive cells; "2" indicates a moderate density of positive cells; "3" indicates the higher, but not maximal density of positive cells; and "4" indicates the highest density of positive cells.

Statistical analysis

Software SPSS 11.0 was used in the statistical analysis. Each parameter was presented as mean±SD, and compared using one-way ANOVA analysis of variance, followed by Dunnett T3 *post hoc* test. The level of significance was set at $P<0.05$.

RESULTS

NF-κB binding activity in the jejunal tissue

There was a very low NF-κB binding activity in the rats of control group, which showed almost undetectable band intensity in EMSA autoradiograph. Compared to control group, NF-κB binding activity in the jejunum following TBI significantly increased (about 160%) by 3 h after TBI, being highest (about 500% increase) at 72 h post-injury, and remained elevated (about 390% increase) at 7 d post-injury (Figure 1). The specificity of the DNA/protein was determined by competition reactions in which a 100-fold molar excess of unlabeled NF-κB oligonucleotide (specific competitor) or unlabeled AP2 oligonucleotide (nonspecific competitor) was added to the binding reaction 10 min before the addition of radiolabeled probe using Hela nuclear extract (Figure 2).

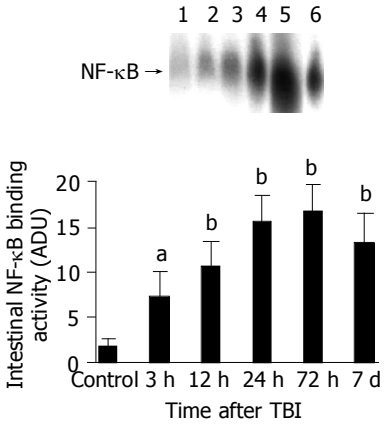

Figure 1 Jejunal NF-κB binding activity following TBI. As compared with control group, NF-κB binding activity in the jejunal tissue following TBI significantly increased at 3 h after TBI, being highest at 72 h postinjury, and remained elevated by 7 d postinjury. Upper: EMSA autoradiogram. Lane 1, control; lane 2, 3 h postinjury; lane 3, 12 h postinjury; lane 4, 24 h postinjury; lane 5, 72 h postinjury; lane 6, 7 d postinjury. Lower: bar graph showing the mean band intensity of EMSA autoradiograph in the jejunal tissue of control, 3, 12, 24, 72 h and 7 d postinjury. $^aP<0.05$, $^bP<0.01$. mean±SD of six animals in each group.

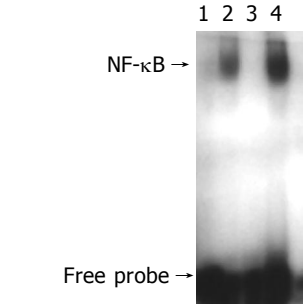

Figure 2 Results of competitive electrophoretic mobility shift assay for NF-κB activity. Lane 1, negative control, no Hela nuclear extract; lane 2, positive control, Hela nuclear extract; lane 3, Hela nuclear extract plus 100-fold molar excess of unlabeled NF-κB consensus oligo (specific competitor); lane 4, Hela nuclear extract plus 100-fold molar excess of unlabeled AP2 consensus oligo (nonspecific competitor). This autoradiograph is representative of 2 independent experiments.

Expression of ICAM-1 in jejunum

The endothelial ICAM-1 expression in jejunum was not significantly different among groups of control, TBI 3 h and 12 h, in which there were few ICAM-1-positive microvessels (Figures 3, 4A). Compared to controls, ICAM-1 was significantly up-regulated in the endothelia of microvessels in villous interstitium and lamina propria by 24 h following TBI (Figure 4B) and maximally expressed at 72 h post-injury (Figure 3, 4C), with marked destruction of villous structure. The endothelial ICAM-1 immunoreactivity in jejunal mucosa still remained strong on d 7 post-injury (Figures 3, 4D), accompanied by mucosal atrophy and villous fusion[5]. The ICAM-1-positive endothelial cells were shown as nigger-brown granules.

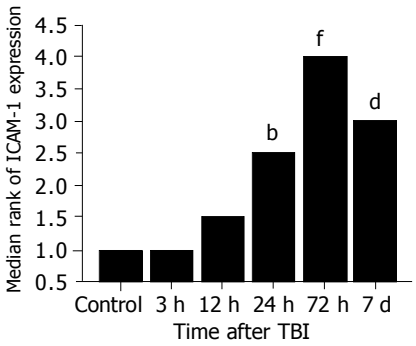

Figure 3 Expression intensity of ICAM-1 in jejunum, manifested as median rank. There was no significant difference in the ICAM-1 positive cells among the rats of control group, TBI 3 h and 12 h. As compared to controls, ICAM-1 immunoreactivity was significantly up-regulated on the endothelia of microvessels in villous interstitium and lamina propria by 24 h following TBI and maximally expressed at 72 h postinjury. The endothelial ICAM-1 expression in jejunal interstitium still remained high at 7 d postinjury. $^bP = 0.01$ *vs* control, $^dP = 0.001$ *vs* control, $^fP<0.001$ *vs* control.

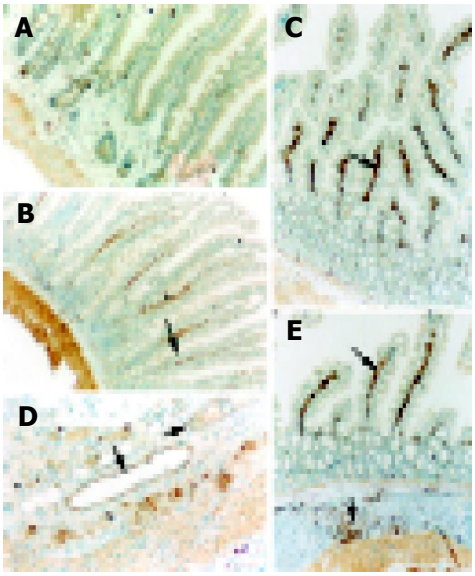

Figure 4 ICAM-1 immunohistochemical staining of jejunal tissue, indicated by the arrows. A: almost undetectable ICAM-1 expression in the villi from control rats; B: moderate ICAM-1 immunoreactivity in the villous interstitium at 24 h postinjury, with the villi well defined; C: strong ICAM-1 immunoreactivity in the villous interstitium at 72 h postinjury, with the villi disarranged and the ICAM-1 positive endothelial cells shown as nigger-brown granules; D: marked ICAM-1 immunohistochemical staining of microvessels in the intestinal lamina propria at 72 h postinjury; E: high ICAM-1 immunoreactivity in the villous interstitium at 7 d postinjury, with the villi atrophic and sparse.

DISCUSSION

The most important finding of the present study is that TBI might induce a significant up-regulation of NF-κB activity and ICAM-1 immunoreactivity in the intestine. The activation of NF-κB significantly increased by 3 h following TBI, peaked at 72 h and remained elevated on d 7 post-injury. Otherwise, the expression of ICAM-1 was significantly up-regulated in the intestine by 24 h following TBI and peaked at 72 h post-injury. The peak of NF-κB activation and ICAM-1 expression coincided in time with the period during which secondary mucosal injury of the gut was also at its culmination following TBI[5], indicating that intestinal inflammatory response mediated by NF-κB and ICAM-1 might play an important role in the acute gut mucosal damage induced by TBI.

NF-κB is a protein transcription factor that functions to enhance the transcription of a variety of genes, including cytokines, growth factors, intercellular adhesion molecules, immunoreceptors and acute-phase proteins[12-14]. Under normal conditions, NF-κB is complexed in the cytoplasm, where it is inactive, through an interaction of the p65 or c-Rel subunit with inhibitory proteins termed inhibitory kappa B (IκB)[11]. In response to a variety of extracellular stimuli such as proinflammatory cytokines (e.g., IL-1β, TNF-α), lipopolysaccharides (LPS), mitogens, viral proteins, ionizing radiation and certain chemical agents[12], at least two of the IκB proteins (IκBα and IκBβ) are rapidly phosphorylated by the recently identified IκB kinase complex at two conserved N-terminal residues. Phosphorylated IκBα is then rapidly polyubiquitinated, and targeted for degradation through proteasome. Once IκBα is degraded, the nuclear localization sequence of NF-κB is exposed, allowing its translocation to the nucleus and activation of gene transcription.

To the best of our knowledge, till now no study has been found in the literature on the intestinal NF-κB activation after trauma. Information about the intestinal activation and regulation of NF-κB induced by trauma is not well understood. Concerning the importance of NF-κB in the inflammatory response[13,14] and gut in MODS[4,7,10], it is necessary to explore the temporal pattern of intestinal NF-κB activation under the condition of trauma. Although current study has shown that TBI could lead to an immediate and persistent NF-κB activation in the gut, the potential mechanism underlying the initial and subsequent activation of intestinal NF-κB following TBI remains unclear. De Plaen[25] have previously shown that NF-κB was constitutively active at low levels in the small intestine of rats, mainly as p50 homodimers, and could be activated by PAF *in vivo* within 30 min and was localized in both epithelial cells and lamina propria cells by immunohistochemical studies. Several factors might promote the activation of intestinal NF-κB, including ischemia-reperfusion, cytokines and reactive oxygen species[26] in the gut. Splanchnic hypoperfusion is a common phenomenon in trauma due to sympathetic response and adaptive regulation of blood supply to vital organs. Therefore, it is highly suggested that gut ischemia and subsequent reactive oxygen species might initiate the NF-κB activation, which can be persistently up-regulated by overproduction of intestinal proinflammatory cytokines following TBI.

Under normal physiological condition, there is no NF-κB activation. After trauma and other pathological stimuli, NF-κB is activated and required for maximal transcription of many cytokines and adhesion molecules[13,14], including TNF-α, IL-6 and ICAM-1, which are thought to be important in the generation of acute inflammatory responses[21,27] and chronic inflammatory bowel disease[13,21]. Several animal models have been developed to evaluate the role of NF-κB in the production of inflammatory events[27-29]. Activation of NF-κB correlates with the expression of mRNA for cytokine-induced neutrophil chemoattractant (CINC), a neutrophil chemotactic chemokine, and these events are followed by an influx of neutrophils into the inflamed site[29]. Neurath[27] recently reported an interesting study in which experimental colitis in mice was effectively blocked by the administration of anti-sense oligonucleotides to the Rel A subunit of NF-κB. These findings support the concept that NF-κB plays a pivotal role in the inflammatory response and regulating NF-κB activation can alter inflammatory events.

The intestinal inflammatory response following trauma is characterized by intestinal recruitments of neutrophils and monocytes by releasing proinflammatory cytokines, elastase and superoxide, which can lead to gut mucosal injury[30]. The adhesion to vascular endothelium and infiltration into the gut mucosa of leukocytes are orchestrated by specific adhesion proteins on both endothelial cells and leukocytes. Up-regulation of adhesion molecule is the basis of priming and activation of leukocytes. ICAM-1 is a member of the immunoglobulin superfamily, which is inducible by NF-κB and inflammatory cytokines such as IL-1β and TNF-α.

ICAM-1 might be up-regulated to involve in the adhesion and infiltration of leukocytes into the injured site[31,32]. There is a low expression of ICAM-1 in normal intestinal epithelium. In this study, increased ICAM-1 immunoreactivity was observed in intestinal villi and lamina propria following TBI. Increased induction of ICAM-1 immunoreactivity in jejunal vessels might promote leukocyte adhesion to the intestinal vascular endothelia and the infiltration of leukocytes by interactions between ICAM-1 and a group of CD11/CD18 glycoproteins on leukocytes, and further support the local accumulation and activation of immunocompetent cells, leading to the gut mucosal damage.

Because of the central role of NF-κB in the inflammatory response, many researches are presently focused on different methods by which NF-κB activation can be reduced. Recent studies suggested that NF-κB DNA-binding activity in intestinal mucosa during endotoxemia was reduced by induction of the stress response[33], antioxidants[34,35], some anti-inflammatory compounds including glucocorticoids and salicylates[36]. In addition, local or systemic administration of anti-sense oligonucleotides to the NF-κB subunit p65 decreased intestinal inflammation in murine experimental colitis[27]. This may be a brand-new direction for further research on the control of inflammatory response induced by TBI.

In summary, we have shown that TBI could induce a significant up-regulation of intestinal NF-κB activation and ICAM-1 immunoreactivity. The peak of NF-κB activation and ICAM-1 immunoreactivity coincides in time with the period during which secondary mucosal injury of the gut is also at its culmination following TBI. Inflammatory response mediated mainly by NF-κB and ICAM-1 may play an important role in the pathogenesis of acute gut mucosal damage following TBI.

ACKNOWLEDGEMENTS

We thank Dr. Genbao Feng and Bo Wu for their technical assistance.

REFERENCES

1 **Grotz MR**, Deitch EA, Ding J, Xu D, Huang Q, Regel G. Intestinal cytokine response after gut ischemia: role of gut barrier failure. *Ann Surg* 1999; **229**: 478-486
2 **Huang L**, Tan X, Crawford SE, Hsueh W. Platelet-activating factor and endotoxin induce tumour necrosis factor gene expression in rat intestine and liver. *Immunology* 1994; **83**: 65-69
3 **Meyer TA**, Wang J, Tiao GM, Ogle CK, Fischer JE, Hasselgren PO. Sepsis and endotoxemia stimulate intestinal interleukin-6 production. *Surgery* 1995; **118**: 336-342
4 **Langkamp-Henken B**, Donovan TB, Pate LM, Maull CD, Kudsk KA. Increased intestinal permeability following blunt and penetrating trauma. *Crit Care Med* 1995; **23**: 660-664
5 **Hang CH**, Shi JX, Li JS, Wu W, Yin HX. Alterations of intestinal mucosa structure and barrier function following traumatic brain injury in rats. *World J Gastroenterol* 2003; **9**: 2776-2781
6 **Faries PL**, Simon RJ, Martella AT, Lee MJ, Machiedo GW. Intestinal permeability correlates with severity of injury in trauma patients. *J Trauma* 1998; **44**: 1031-1035; discussion 1035-1036
7 **Swank GM**, Deitch EA. Role of the gut in multiple organ failure: bacterial translocation and permeability changes. *World J Surg* 1996; **20**: 411-417
8 **Magnotti LJ**, Upperman JS, Xu DZ, Lu Q, Deitch EA. Gut-derived mesenteric lymph but not portal blood increases endothelial cell permeability and promotes lung injury after hemorrhagic shock. *Ann Surg* 1998; **228**: 518-527
9 **Doig CJ**, Sutherland LR, Sandham JD, Fick GH, Verhoef M, Meddings JB. Increased intestinal permeability is associated with the development of multiple organ dysfunction syndrome in critically ill ICU patients. *Am J Respir Crit Care Med* 1998; **158**: 444-451
10 **Wang P**, Ba ZF, Cioffi WG, Bland KI, Chaudry IH. Is gut the "motor" for producing hepatocellular dysfunction after trauma and hemorrhagic shock? *J Surg Res* 1998; **74**: 141-148
11 **Baldwin AS**. The NF-kappa B and I kappa B proteins: new discoveries and insights. *Annu Rev Immunol* 1996; **14**: 649–683
12 **Siebenlist U**, Franzoso G, Brown K. Structure, regulation and function of NF-kappa B. *Annu Rev Cell Biol* 1994; **10**: 405–455
13 **Schottelius AJ**, Baldwin AS. A role for transcription factor NF-kappa B in intestinal inflammation. *Int J Colorectal Dis* 1999; **14**: 18–28
14 **Barnes PJ**, Karin M. Nuclear factor-kappaB: a pivotal transcription factor in chronic inflammatory diseases. *N Engl J Med* 1997; **336**: 1066–1071
15 **Yamamoto K**, Arakawa T, Ueda N, Yamamoto S. Transcriptional roles of nuclear factor kappa B and nuclear factor-interleukin-6 in the tumor necrosis factor-alpha-dependent induction of cyclooxygenase-2 in MC3T3-E1 cells. *J Biol Chem* 1995; **270**:31315-31320
16 **Ledebur HC**, Parks TP. Transcriptional regulation of the intercellular adhesion molecule-1 gene by inflammatory cytokines in human endothelial cells. Essential roles of a variant NF-kappa B site and p65 homodimers. *J Biol Chem* 1995; **270**: 933–943
17 **Chen CC**, Manning AM. Transcriptional regulation of endothelial cell adhesion molecules: a dominant role for NF-kappa B. *Agents Actions Suppl* 1995; **47**: 135–141
18 **Hou J**, Baichwal V, Cao Z. Regulatory elements and transcription factors controlling basal and cytokine-induced expression of the gene encoding intercellular adhesion molecule 1. *Proc Natl Acad Sci USA* 1994; **91**: 11641–11645
19 **Neish AS**, Read MA, Thanos D, Pine R, Maniatis T, Collins T. Endothelial interferon regulatory factor 1 cooperates with NF-kappa B as a transcriptional activator of vascular cell adhesion molecule 1. *Mol Cell Biol* 1995; **15**: 2558–2569
20 **Fiocchi C**. Intestinal inflammation: a complex interplay of immune and nonimmune cell interactions. *Am J Physiol* 1997; **273**: G769-G775
21 **Neurath MF**, Pettersson S. Predominant role of NF-kappa B p65 in the pathogenesis of chronic intestinal inflammation. *Immunobiology* 1997; **198**: 91-98
22 **Spies M**, Chappell VL, Dasu MR, Herndon DN, Thompson JC, Wolf SE. Role of TNF-alpha in gut mucosal changes after severe burn. *Am J Physiol Gastrointest Liver Physiol* 2002; **283**: G703-G708
23 **Feeney DM**, Boyeson MG, Linn RT, Murray HM, Dail WG. Responses to cortical injury: I. Methodology and local effects of contusions in the rat. *Brain Res* 1981; **211**: 67-77
24 **Shimada T**, Watanabe N, Ohtsuka Y, Endoh M, Kojima K, Hiraishi H, Terano A. Polaprezinc down-regulates proinflammatory cytokine-induced nuclear factor-kappaB activiation and interleukin-8 expression in gastric epithelial cells. *J Pharmacol Exp Ther* 1999; **291**: 345-352
25 **De Plaen IG**, Tan XD, Chang H, Qu XW, Liu QP, Hsueh W. Intestinal NF-kappaB is activated, mainly as p50 homodimers, by platelet-activating factor. *Biochim Biophys Acta* 1998; **1392**: 185-192
26 **Lush CW**, Cepinskas G, Kvietys PR. Regulation of intestinal nuclear factor-kappaB activity and E-selectin expression dur-

ing sepsis: a role for peroxynitrite. *Gastroenterology* 2003; **124**: 118-128

27 **Neurath MF**, Pettersson S, Meyer zum Buschenfelde KH, Strober W. Local administration of antisense phosphorothioate oligonucleotides to the p65 subunit of NF-kappa B abrogates established experimental colitis in mice. *Nat Med* 1996; **2**: 998–1004

28 **Shenkar R**, Schwartz MD, Terada LS, Repine JE, McCord J, Abraham E. Hemorrhage activates NF-kappa B in murine lung mononuclear cells *in vivo*. *Am J Physiol* 1996; **270**: L729–L735

29 **Blackwell TS**, Holden EP, Blackwell TR, DeLarco JE, Christman JW. Cytokine-induced neutrophil chemoattractant mediates neutrophilic alveolitis in rats: association with nuclear factor kappa B activation. *Am J Respir Cell Mol Biol* 1994; **11**: 464–472

30 **Partrick DA**, Moore EE, Moore FA, Barnett CC, Silliman CC. Lipid mediators up-regulate CD11b and prime for concordant superoxide and elastase release in human neutrophils. *J Trauma* 1997; **43**: 297-302; discussion 302-303

31 **Frossard JL**, Saluja A, Bhagat L, Lee HS, Bhatia M, Hofbauer B, Steer ML. The role of intercellular adhesion molecule 1 and neutrophils in acute pancreatitis and pancreatitis-associated lung injury. *Gastroenterology* 1999; **116**: 694-701

32 **Molla M**, Gironella M, Miquel R, Tovar V, Engel P, Biete A, Pique JM, Panes J. Relative roles of ICAM-1 and VCAM-1 in the pathogenesis of experimental radiation-induced intestinal inflammation. *Int J Radiat Oncol Biol Phys* 2003; **57**: 264-273

33 **Pritts TA**, Wang Q, Sun X, Moon MR, Fischer DR, Fischer JE, Wong HR, Hasselgren PO. Induction of the stress response *in vivo* decreases nuclear factor-kappa B activity in jejunal mucosa of endotoxemic mice. *Arch Surg* 2000; **135**: 860-866

34 **Essani NA**, Fisher MA, Jaeschke H. Inhibition of NF-kappa B activation by dimethyl sulfoxide correlates with suppression of TNF-alpha formation, reduced ICAM-1 gene transcription, and protection against endotoxin-induced liver injury. *Shock* 1997; **7**: 90-96

35 **Liu SF**, Ye X, Malik AB. *In vivo* inhibition of nuclear factor-kappa B activation prevents inducible nitric oxide synthase expression and systemic hypotension in a rat model of septic shock. *J Immunol* 1997; **159**: 3976-3983

36 **Yin MJ**, Yamamoto Y, Gaynor RB. The anti-inflammatory agents aspirin and salicylate inhibit the activity of I(kappa)B kinase-beta. *Nature* 1998; **396**: 77-80

PO Box 2345, Beijing 100023, China
www.wjgnet.com
wjg@wjgnet.com

ELSEVIER

World J Gastroenterol 2005;11(8):1155-1160
World Journal of Gastroenterology ISSN 1007-9327

• *BASIC RESEARCH* •

Effects of Guiyuanfang and autologous transplantation of bone marrow stem cells on rats with liver fibrosis

Li-Mao Wu, Lian-Da Li, Hong Liu, Ke-Yong Ning, Yi-Kui Li

Li-Mao Wu, Lecturer, Institute of Traditional Chinese Materia Medica, College of Pharmaceutical Science, Zhejiang University, Hangzhou 310031, Zhejiang Province, China
Lian-Da Li, Academician, Affiliated Xiyuan Hospital, China Academy of Traditional Chinese Medicine, Beijing 100091, China
Hong Liu, Postdoctoral, Guangzhou University of Traditional Chinese Medicine, Guangzhou 501405, Guangdong Province, China
Ke-Yong Ning, Doctoral Student, Basic Medicine Group, Affiliated Xiyuan Hospital, China Academy of Traditional Chinese Medicine, Beijing 100091, China
Yi-Kui Li, Doctoral Student, Basic Medicine Group, Affiliated Xiyuan Hospital, China Academy of Traditional Chinese Medicine, Beijing 100091, China
Supported by the National Natural Science Foundation of China, No. 30271663
Correspondence to: Dr. Li-Mao Wu, Institute of Traditional Chinese Materia Medica, College of Pharmaceutical Science, Zhejiang University, Hangzhou 310031, Zhejiang Province, China. wulimao@yahoo.com.cn
Telephone: +86-571-87217250 Fax: +86-571-87217212
Received: 2004-07-17 Accepted: 2004-08-25

Abstract

AIM: To investigate the therapeutic effects of Guiyuanfang and bone marrow stem cells (BMSCs) on rats with liver fibrosis.

METHODS: Liver fibrosis model was induced by carbon tetrachloride, ethanol, high lipid and assessed biochemically and histologically. Liver function and hydroxyproline contents of liver tissue were determined. Serum hyaluronic acid (HA) level and procollagen III level were performed by radioimmunoassay. The VG staining was used to evaluate the collagen deposit in the liver. Immunohistochemical SABC methods were used to detect transplanted BMSCs and expression of urokinase plasminogen activator (uPA).

RESULTS: Serum transaminase level and liver fibrosis in rats were markedly reduced by Guiyuanfang and BMSCs. HA level and procollagen III level were also reduced obviously, compared to model rats (HA: 47.18±10.97 ng/mL, 48.96±14.79 ng/mL; PCIII: 22.48±5.46 ng/mL, 26.90±3.35 ng/mL; $P<0.05$). Hydroxyproline contents of liver tissue in both BMSCs group and Guiyuanfang group were far lower than that of model group (1 227.2±43.1 μg/g liver tissue, 1390.8±156.3 μg/g liver tissue; $P<0.01$). After treatment fibrosis scores were also reduced. Both Guiyuanfang and BMSCs could increase the expression of uPA. The transplanted BMSCs could engraft, survive, and proliferate in the liver.

CONCLUSION: Guiyuanfang protects against liver fibrosis. Transplanted BMSCs may engraft, survive, and proliferate in the fibrosis livers indefinitely. Guiyuanfang may synergize with BMSCs to improve recovery from liver fibrosis.

Key words: Liver fibrosis; Guiyuanfang; Bone marrow stem cells; Transplantation

Wu LM, Li LD, Liu H, Ning KY, Li YK. Effects of Guiyuanfang and autologous transplantation of bone marrow stem cells on rats with liver fibrosis. *World J Gastroenterol* 2005; 11 (8): 1155-1160
http://www.wjgnet.com/1007-9327/11/1155.asp

INTRODUCTION

China has a high incidence of hepatic injury and fibrosis. Current therapeutic options for liver fibrosis, unfortunately, remain inadequate and as a result, the social economic burden remains high. Until now, effective drugs are still lacking, so it is most urgent that some novel effective therapies be developed. In near future, targeting of stellate cells, gene therapy, cytokine antagonist, and fibrogenic mediators will be a mainstay of antifibrotic therapy. Natural extracts with putative antifibrotic activity have gained increasing attention[1]. TCM could lead to new prospects for the therapy of fibrosis. A lot of Traditional Chinese Materia Medica, such as Danshen, Danggui, Gancao[2], Xiaocaihu Tang, Fufang 861, Fuzhenghuayufang, and so on, have been documented effective. Our previous study showed that the Guiyuanfang was very effective for liver injury.

Severe liver dysfunction on terminal liver failure can be reversed by orthotopic liver transplantation, but with the necessity for chronic immunosuppression of the recipient and with the need to wait for a donor liver, sometimes for years, due to paucity of liver donors. A variety of technical, financial, and logistic issues, however, limits its application to a relatively small percentage of patients with liver disease.

Hepatocyte transplantation is emerging as a potential treatment to augment cell number in diseased liver, and to show early promising[3,4]. Hepatocyte transplantation is now being done successfully to sustain liver function in patients awaiting liver transplantation[5]. It not only provides temporary liver function in patients but has also shown to be curative in certain metabolic conditions[6,7]. This procedure may be even

an alternative to orthotopic liver transplantation. Theoretically, hepatocyte transplantation would be less invasive and technically less demanding than whole organ transplantation and, if the procedure could be performed percutaneously, recipients would not require prolonged hospitalization. Isolated liver cells can be cryopreserved for emergency use[8,9].

The major limitation to this form of therapy is the availability of human livers as a source of hepatocytes. Others were immune allograft rejection and proliferative capacity of liver cells. The bone marrow may be a possible adult reservoir of totipotent stem cells or a novel location for various types of determined stem cells[10-12]. Bone marrow cells can be easily obtained from adult marrow opening the possibility of autologous transplantation. Autologous stem cell transplantation for the treatment of diseased liver is becoming an increasingly promising strategy. We propose to alleviate or overcome the liver problem by developing novel therapies using autologous bone marrow stem cells (BMSCs) and TCM. We attempt to confirm the anti-fibrotic activities of TCM and autologous BMSCs. Could the BMSCs survive, proliferate, and differentiate in the fibrotic environment? Could TCM synergize with the BMSCs to improve the diseased liver?

MATERIALS AND METHODS

Animals

Normal Sprague-Dawley rats weighing 180-220 g were obtained from Beijing Tonglihua Experimental Animal Center (China). All animals received care in compliance with the guidelines of China Ministry of Health.

Reagents

The Guiyuanfang consists of four Traditional Chinese Materia Medica purchased from Beijing Tongrentang Pharmaceutical Co., Ltd (Beijing, China), all the herbal was identified by Professor Li JS in the Beijing University of Traditional Chinese Medicine (TCM). ALT Kit, AST Kit, Albumin Kit, and Total Protein kit were all purchased from ZhongShan Biotechnology Co. Ltd (Beijing, China). 5-Bromide-2'-deoxygen-uridine (BrdU) was purchased from Boehringer Co., Ltd (Germany). SABC kit, DSABC kit, and antibody were purchased from Boster Company (Wuhan, China). Hydroxyproline kit was purchased from Jiancheng Biotechnology Co., Ltd (Nanjing, China). All other reagents used were of analytical grade.

Preparation and culture of BMSCs of rats

Bone marrow cells were collected from the femora of Sprague-Dawley rats. Mononuclear cells were obtained by a Percoll-separation step. The mononuclear cells were inoculated at a density of $1\times10^5/cm^2$ into 6-well plates. These plates were pre-coated with 0.1% Matrigel (BD). Basal media used were α-MEM supplemented with 10 ng/mL EGF (BD) and 5% fetal bovine serum (Hyclone). EGF was freshly added when the medium was changed every 3 d. Each culture was labeled according to the animal numbers. After 4 wk the cultures were transplanted to the liver of the same rats. Before the transplantation the 5 μL BrdU solution (50 mg BrdU dissolved in 0.8 mL DMSO, added 1.2 mL ddH_2O) was added into the cultures.

Complex factors (carbon tetrachloride, ethanol, and high lipid) induced hepatic fibrosis and treatment

Fibrosis was induced using carbon tetrachloride, alcohol, and high lipid diet. Briefly, rats were given alcohol (diluted 1:9 in water) added to the drinking water. CCl_4 (diluted 4:6 in olive oil) was given subcutaneously twice a week. The initial dose was 0.5 mL/kg body weight, but subsequent dose was adjusted weekly based on the changes in body weight. When there was no change or an increase in body weight, CCl_4 was given at 0.3 mL/kg. When body weight decreased by 1-10 g, CCl_4 was given at 0.15 mL/kg. When body weight decreased by more than 10 g, CCl_4 was not given and the CCl_4 dose was reassessed 1 wk later. During the fibrotic model replicated, the rats were fed a high-lipid diet (corn powder 79.5%, lard 20%, 0.5% cholesterol). Eight weeks later, rats were randomly allocated to the different groups. For BMSCs transplantation, a small surgical incision was made in the flank and the portal vein was exposed. Five million BMSCs, suspended in 0.5 mL αMEM medium, were injected into the portal vein in 5 min. At the end of the experiment all rats were killed, blood samples were drawn from celiac artery, and the sera were isolated and stored at -20 ℃, a portion of the liver was flash frozen in liquid nitrogen and stored at -70 ℃ until assayed or fixed in 10% neutral buffered formalin for 18-24 h and paraffin embedded.

Assay for liver function and hydroxyproline levels

Sera were analyzed for alanine transaminase (ALT), aspartate transaminase (AST), albumin (ALB), and total protein (TP), and hydroxyproline contents of liver tissue were determined by a biochemical kit according to the manufacturer's instructions. The assay of serum hyaluronic acid (HA) level and procollagen III level was performed with specific radioimmunoassay kit.

Tissue analysis

Samples were obtained from the same liver lobe in all animals and fixed in 10% buffered formalin, embedded in paraffin, sectioned, and stained with hematoxylin-eosin or Van Gieson solutions. Fibrosis was scored according to the following scoring system modified from HAI System[13]; I = thickened perivenular collagen and a few thin collagen septa; II = thin septa with incomplete bridging between portal regions; III = thin septa and extensive bridging; IV = thickened septa with complete bridging of portal regions and a nodular appearance.

Immunohistochemistry

Indirect immunohistochemistry analysis of urokinase plasminogen activators (uPAs) expression was performed on liver sections. Briefly, tissue sections were deparaffinized, and endogenous peroxidase activity was blocked by incubation of tissue in 3% H_2O_2 for 10 min. Primary anti-uPA antibody was applied at 4 ℃ for overnight; rabbit IgG was used as a negative control. Then they were incubated with second antibody, biotin-labeled goat anti-rabbit IgG

Table 1 Effects of Guiyuanfang and BMSCs transplantation on serum ALT, AST, ALB, TP, and A/G levels

Group	*n*	ALT (U/mL)	AST (U/mL)	TP (g/L)	ALB (g/L)	A/G
Control	10	38.3±5.1[b]	127.9±16.3[b]	62.6±5.9	28.8±3.5[b]	0.85±0.06[b]
Model	10	325.9±101.7	697.5±215.8	53.2±10.5	21.6±3.0	0.70±0.09
Guiyuanfang	10	56.8±11.5[b]	149.5±31.7[b]	64.0±7.0	28.3±2.6[b]	0.80±0.07[b]
BMSCs	8	67.3±22.0[b]	133.3±33.8[b]	60.6±8.8	26.1±2.2[a]	0.75±0.03[a]
Guiyuanfang plus BMSCs	8	40.4±9.5[b]	123.1±27.9[b]	57.7±5.1	26.9±4.2[b]	0.83±0.02[b]

[a]$P<0.05$, [b]$P<0.01$ *vs* model group.

antibody (1∶400 dilution), at 37 ℃ for 2 h, followed by incubation with SABC complex (1∶400 dilution), at room temperature for 1 h. Finally, diaminobenzedine was used for color developing, and then the slides were counterstained by hematoxylin.

Dual immunohistochemistry was used to detect the BMSCs in the liver parenchyma and their differentiating state. Monoclonal antibodies against BrdU were used to localize the transplanted bone marrow cells. Briefly, samples were serially rehydrated with 100, 95, and 70% ethanol after deparaffinization with toluene. Endogenous peroxidase in the sample was blocked using 3% hydrogen peroxide for 10 min at room temperature. The sample was treated with pepsin for 5 min at 42 ℃ and 2 N HCl for 30 min at room temperature. After rinsing with PBS three times, the sample was incubated with antibodies against BrdU in a moist chamber for 16 h at 4 ℃. Then they were incubated with second antibody, biotin-labeled goat anti-rabbit IgG antibody (1∶400 dilution), at 37 ℃ for 2 h, followed by incubation with SABC-AP complex (1∶400 dilution) at room temperature for 1 h. BCIP/NBT was used for color developing. After rinsing, monoclonal antibodies against cytokeratin-18 were applied to the slides, the other procedures were similar, except that the SABC-POD was used to replace the SABC-AP, and the AEC solutions to replace BCIP/NBT. Negative control samples were incubated in PBS (without the primary antibodies) under similar conditions.

Statistical analysis

The data are presented as mean±SD. The significance of differences was analyzed with the Student's *t*, Mann-Whitney rank sum, χ^2 tests or analysis of variance (ANOVA) with the pairwise multiple comparison method of *q* test using SPSS 10.0 software. $P<0.05$ was considered significant.

RESULTS

Effects of Guiyuanfang and BMSCs transplantation on liver function

Laboratory measures of liver function remained abnormal in model animals but significantly improved toward normal in animals that received treatment. Administration of Guiyuanfang or BMSC transplantation reduced the elevated serum ALT and AST levels significantly ($P<0.01$), and serum TP, ALB, A/G levels increased in all animals receiving treatment ($P<0.01$ or 0.05), compared to model rats (Table 1).

The serum PCIII, and HA levels were often used as indicators of hepatic fibrosis clinically. As shown in Table 2, the serum PCIII, HA levels of the model rats maintained high level during the period of the study (respectively 91.73, 34.32 ng/mL). However, in the treatment group, the serum PCIII, HA levels were far lower than that of the model rat ($P<0.01$).

Determination of liver tissue hydroxyproline content confirmed the histological studies, showing a net reduction in total collagen levels. Total liver hydroxyproline levels at model group were 2123.1±218.9 μg/g wet weight, which represent a 10-fold increase, compared to normal livers ($P<0.01$), and decreased to about 1 000 μg/g wet weight in Guiyuanfang or BMSCs group (Figure 1).

Table 2 Effects of Guiyuanfang and BMSCs transplantation on serum PCIII and HA levels

Group	*n*	HA (ng/mL)	PCIII (ng/mL)
Control	10	54.61±17.04[b]	23.35±2.70[b]
Model	10	91.73±22.77	34.32±5.21
Guiyuanfang	10	47.18±10.97[b]	22.48±5.46[b]
BMSCs	8	48.96±14.79[b]	26.90±3.35[b]
Guiyuanfang plus BMSCs	8	38.24±10.34[b]	20.15±4.04[b]

[a]$P<0.05$, [b]$P<0.01$ *vs* model group.

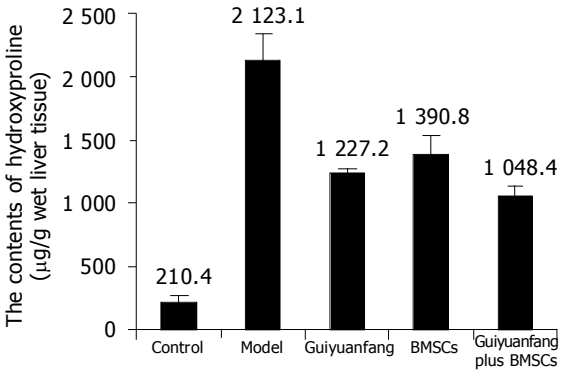

Figure 1 Effects of Guiyuan fang and BMSCs on hydroxyproline levels of liver fibrosis tissue (μg/g wet liver).

Effects of Guiyuanfang and BMSCs transplantation on liver pathology

In normal livers, only minimal collagen staining was present; no fibrosis was detected in the group. In model rats, there was obvious nodular fibrosis with deposition of well-delineated fibrosis septa, extensive collagen deposition, which were continuous and extended throughout each section, with mature collagen fibrils bridging portal regions and vascular

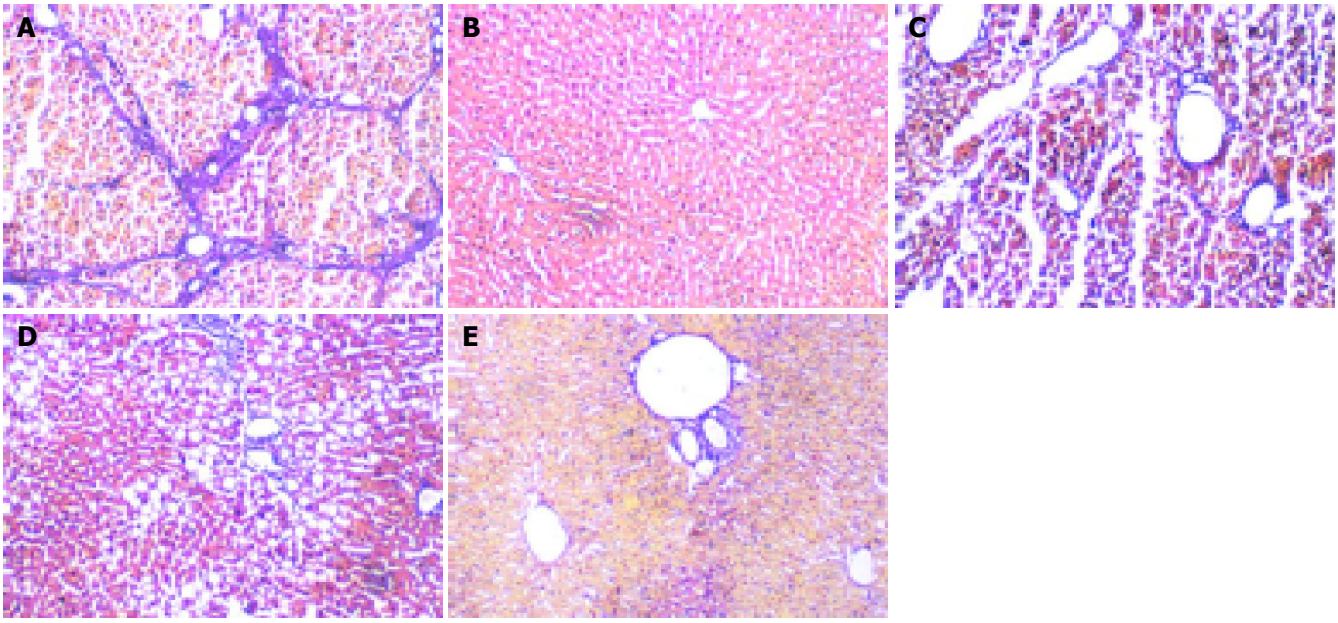

Figure 2 VG staining showing fibrin in liver tissue (100×). A: In model rats, there was obvious nodular fibrosis with deposition of well-delineated fibrosis septa, extensive collagen deposition, which were continuous and extended throughout each section, with mature collagen fibrils bridging portal regions and vascular structures, including perivenular ballooning degeneration of hepatocytes; B: In control livers, only minimal collagen staining was present; no fibrosis was detected in this group; C: In Guiyuanfang group, collagen deposition decreased; D: In BMSCs group, few collagen deposition. E: The appearance of bridging collagen fibers was prevented almost completely in rats treated with Guiyuanfang plus BMSCs. Only occasional short fibril fragments could be visualized. Most liver tissues were restored to normal organization.

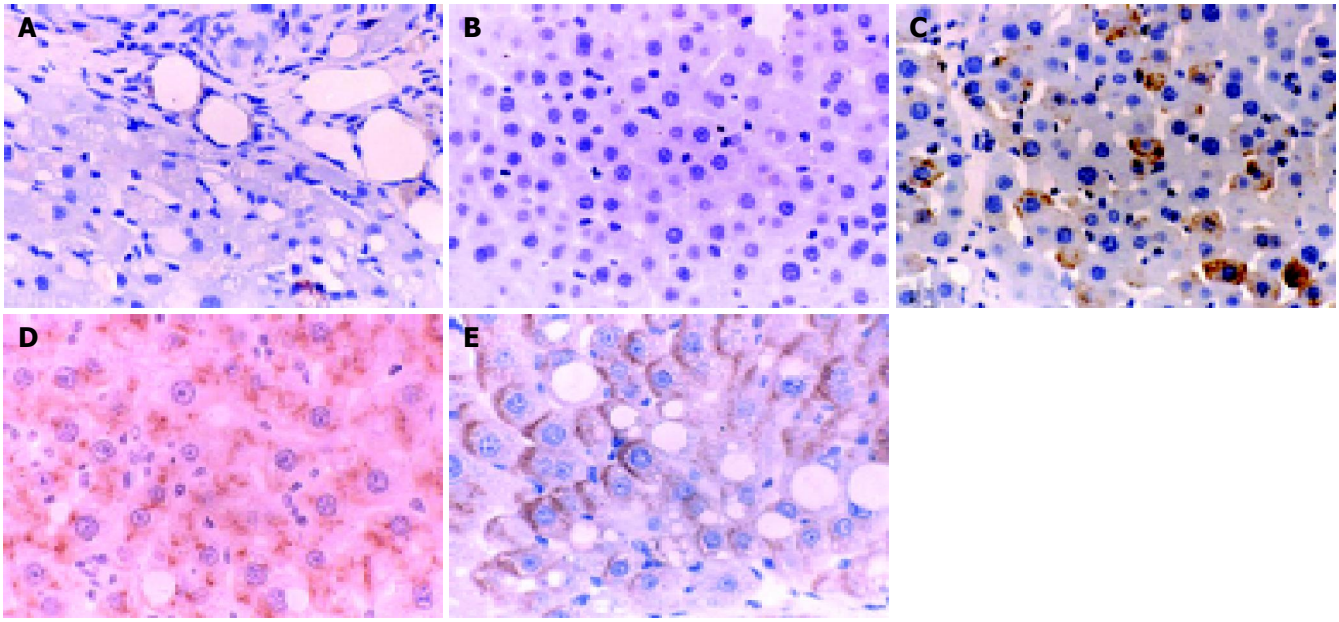

Figure 3 The expression of uPA in liver tissue (400×). A: In model group, there was very weak uPA expression; B: There was no expression of uPA in the normal group; C: Guiyuanfang group; D: Autologous BMSCs transplantation group; E: Guiyuanfang plus autologous BMSC transplantation group.

structures, including perivenular ballooning degeneration of hepatocytes. In Guiyuanfang group, mild fatty change and vacuolation of hepatocytes were observed. The fibrous septa were less well defined and discontinuous and fewer nodules of regenerative parenchyma were noted. In autologous BMSC group, there was evidence of early fibrosis with a number of cells with fibroblast-like morphology in some sections. The appearance of bridging collagen fibers was prevented almost completely in rats treated with Guiyuanfang plus autologous BMSCs. Only occasional short fibril fragments could be visualized. Most liver tissues were restored to normal organization (Figure 2). The χ^2 test was used to assess the fibrosis score, and there was significant difference among all treated groups and model group (Table 3).

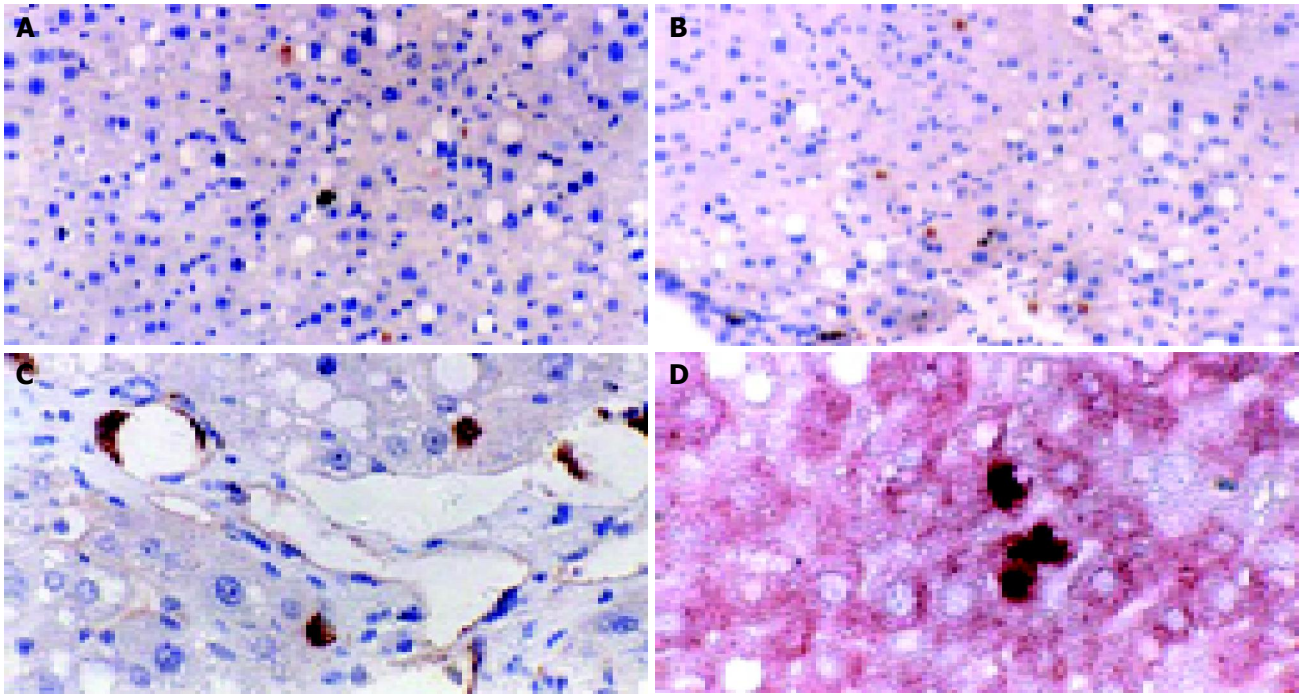

Figure 4 Fate of transplanted BMSCs 4 wk after transplantation. The differentiation of transplanted BMSCs in liver fibrosis environment. A: Some transplanted stem cells have migrated into parenchyma, exhibiting the morphology of hepatocyte (BMSCs group, 200×); B: Most transplanted cells were distributed at portal region (Guiyuanfang plus BMSC group, 200×); C: Some transplanted stem cells exhibited the morphology of bile epithelium cells or hepatocyte (Guiyuanfang plus BMSC group, 400×); D: Double immunohistochemical staining showed that the BrdU-labeled cells were fully integrated in the liver parenchyma, along with the expression of cytokeratin-18, the liver epithelial specific marker (Guiyuanfang plus BMSCs group, 400×).

Table 3 Effects of Guiyuanfang and BMSC transplantation on fibrosis score

Group	*n*	Grade of liver fibrosis				
		0	I	II	III	IV
Control	10	8	2	0	0	0
Model	10	0	0	0	2	8
Guiyuanfang	10	0	2	5	2	1
BMSCs	8	0	2	3	3	0
Guiyuanfang plus BMSCs	8	0	3	4	1	0

I = thickened perivenular collagen and a few thin collagen septa; II = thin septa with incomplete bridging between portal regions; III = thin septa and extensive bridging; IV = thickened septa with complete bridging of portal regions and a nodular appearance.

Expression of uPA and co-localization of BrdU and cytokeratin-18

The normal liver tissues showed very weak uPA expression, and Guiyuanfang caused a marked increase of uPA expression in the livers in a dose-dependent manner. The uPA expression in the liver tissues of autologous BMSC transplantation group and Guiyuanfang plus autologous BMSCs transplantation group was the strongest (Figure 3).

The transplanted cells were predominantly in clusters of 1-3 cells each. Double immunohistochemical staining showed that the BrdU-labeled cells were fully integrated in the liver parenchyma, showing the appearance of hepatocytes, along with the expression of cytokeratin-18, the liver epithelial specific marker. Some BMSCs have differentiated into hepatocytes or endothelial cells (Figure 4).

DISCUSSION

Chronic diseases and age-associated illness are major challenges in today's medicine. The pathogenesis of these diseases and symptoms may not only be multifactorial but also could vary from one individual to another. The complex, difficult and changing nature of these chronic diseases has certainly slowed western science's approach to finding treatments leaving today a large medical need that has not yet been met. The potential usefulness of Chinese medicine embodies the belief that maintaining healthy homeostasis of the body involves the balance of a mixture of chemicals at different organs or tissues. The liver fibrosis is one of these diseases. To find new therapies for liver diseases, the best approach is to integrate traditional and modern approaches. Now cell transplantation has been found to be promising for liver diseases. So integrating Chinese medicine with cell transplantation will provide us with new leads to understand the regulation of homeostasis and further advancement of human medicine.

To the best of our knowledge, this is the first experimental study, investigating TCM and BMSC transplantation on liver fibrosis. To ensure the therapeutic effect, we selected the empiristic formula, Guiyuanfang, which has been used for hundreds of years. Our work showed that Guiyuanfang could improve liver function, protect hepatocytes from toxicant, promote protein synthesis, maintain cytoplasm membrane stable, and provide a good environment for hepatocyte function. It also inhibits inflammatory response, reduces necrotic region, and promotes the phagocytosis of debris and fibrils. Guiyuanfang reverses the liver fibrosis

by neutralizing profibrogenic cytokines inhibiting the generation and accumulation of collagen, promoting the degradation of ECM, and improving microcirculation. It is possible that the protective effects of Guiyuanfang may be due to either enhanced collagen breakdown or diminished collagen synthesis. In the study, we observed the obvious increase of uPA expression in the fibrotic liver tissue, after administration of Guiyuanfang. The recovery from fibrosis was correlated with the uPA expression.

Previous work has shown that hepatocyte transplantation can correct liver-based metabolic disorders, prolong the survival of rodents with experimentally-induced acute liver failure, and provide significant hepatic support to animals with hypertension, liver fibrosis, and irreversible cirrhosis[14]. Recently accumulating evidence indicates that bone marrow can differentiate into specific cell types. Transplantation of bone marrow cells *in vivo* resulted in the appearance of hepatocyte of donor origin in recipient liver[15-18]. Transplanted bone marrow cells can repopulate hepatic and biliary duct epithelia under certain circumstances. Generally the patients with liver fibrosis are likely to have difficulty in producing healthy hepatocytes. There were a lot of solutions reported to enhance bone marrow cell differentiation and proliferation, however, all had their own shortage[19-21], so how to improve conditions to induce hepatocytes from bone marrow cells *in vivo* and *in vitro* is a great challenge for the medical scientists. In this study, Guiyuanfang could improve the liver microcirculation, reduce the toxic metabolic, and finally provide a good environment for the transplanted BMSCs to engraft and to proliferate in the fibrotic liver. Although we could not determine whether the initial survival of transplanted cells in the fibrotic liver was different from that in the normal liver, and we were still only able to propagate a small number of hepatocyte-like cells from BMSCs, the present study is a step further in such a direction, and this work still has important implications.

In conclusion, we found that transplanted BMSCs engrafted, survived, and proliferated in the fibrosis livers indefinitely. BMSCs in hepatic fibrogenic environment can differentiate into hepatocytes, endothelial cells. Guiyuanfang can synergize with the BMSCs to improve the recovery from liver fibrosis. Such a possibility will be of great interest in developing treatments for patients with liver fibrosis.

REFERENCES

1 **Schuppan D**, Jia JD, Brinkhaus B, Hahn EG. Herbal products for liver diseases: a therapeutic challenge for the new millennium. *Hepatology* 1999; **30**: 1099–1104
2 **Slehria S**, Rajvanshi P, Ito Y, Sokhi RP, Bhargava KK, Palestro CJ, McCuskey RS, Gupta S. Hepatic sinusoidal vasodilators improve transplanted cell engraftment and ameliorate microcirculatory perturbations in the liver. *Hepatology* 2002; **35**: 1320-1328
3 **Kobayashi N**, Ito M, Nakamura J, Cai J, Gao C, Hammel JM, Fox IJ. Hepatocyte transplantation in rats with decompensated cirrhosis. *Hepatology* 2000; **31**: 851–857
4 **Gagandeep S**, Rajvanshi P, Sokhi RP, Slehria S, Palestro CJ, Bhargava KK, Gupta S. Transplanted hepatocytes engraft, survive, and proliferate in the liver of rats with carbon tetrachloride-induced cirrhosis. *J Pathol* 2000; **191**: 78–85
5 **Chinzei R**, Tanaka Y, Shimizu-Saito K, Hara Y, Kakinuma S, Watanabe M, Teramoto K, Arii S, Takase K, Sato C, Terada N, Teraoka H. Embryoid-body cells derived from a mouse embryonic stem cell line show differentiation into functional hepatocytes. *Hepatology* 2002; **36**: 22–29
6 **Guha C**, Parashar B, Deb NJ, Garg M, Gorla GR, Singh A, Roy-Chowdhury N, Vikram B, Roy-Chowdhury J. Normal hepatocytes correct serum bilirubin after repopulation of Gunn rat liver subjected to irradiation/partial resection. *Hepatology* 2002; **36**: 354–362
7 **Fox IJ**, Chowdhury JR, Kaufman SS, Goertzen TC, Chowdhury NR, Warkentin PI, Dorko K, Sauter BV, Strom SC. Treatment of the Crigler-Najjar syndrome type I with hepatocyte transplantation. *N Engl J Med* 1998; **338**: 1422–1426
8 **Strom SC**, Fisher RA, Thompson MT, Sanyal AJ, Cole PE, Ham JM, Posner MP. Hepatocyte transplantation as a bridge to orthotopic liver transplantation in terminal liver failure. *Transplantation* 1997; **63**: 559–569
9 **Ott M**, Schmidt HH, Cichon G, Manns MP. Emerging therapies in hepatology: liver-directed gene transfer and hepatocyte transplantation. *Cells Tissues Organs* 2000; **167**: 81–87
10 **Dorshkind K**. Multilineage development from adult bone marrow cells. *Nat Immunol* 2002; **3**: 311–313
11 **Jiang Y**, Jahagirdar BN, Reinhardt RL, Schwartz RE, Keene CD, Ortiz-Gonzalez XR, Reyes M, Lenvik T, Lund T, Blackstad M, Du J, Aldrich S, Lisberg A, Low WC, Largaespada DA, Verfaillie CM. Pluripotency of mesenchymal stem cells derived from adult marrow. *Nature* 2002; **418**: 41–49
12 **Krause DS**, Theise ND, Collector MI, Henegariu O, Hwang S, Gardner R, Neutzel S, Sharkis SJ. Multi-organ, multi-lineage engraftment by a single bone marrow-derived stem cell. *Cell* 2001; **105**: 369–377
13 **Brunt EM**. Grading and staging the histopathological lesions of chronic hepatitis: the Knodell histology activity index and beyond. *Hepatology* 2000; **31**: 241–246
14 **Fox IJ**. Transplantation into and inside the liver. *Hepatology* 2002; **36**: 249–251
15 **Alison MR**, Poulsom R, Jeffery R, Dhillon AP, Quaglia A, Jacob J, Novelli M, Prentice G, Williamson J, Wright NA. Hepatocytes from non-hepatic adult stem cells. *Nature* 2000; **406**: 257
16 **Theise ND**, Nimmakayalu M, Gardner R, Illei PB, Morgan G, Teperman L, Henegariu O, Krause DS. Liver from bone marrow in humans. *Hepatology* 2000; **32**: 11–16
17 **Lagasse E**, Connors H, Al-Dhalimy M, Reitsma M, Dohse M, Osborne L, Wang X, Finegold M, Weissman IL, Grompe M. Purified hematopoietic stem cells can differentiate into hepatocytes *in vivo*. *Nat Med* 2000; **6**: 1229–1234
18 **Schwartz RE**, Reyes M, Koodie L, Jiang Y, Blackstad M, Lund T, Lenvik T, Johnson S, Hu WS, Verfaillie CM. Multipotent adult progenitor cells from bone marrow differentiate into functional hepatocyte-like cells. *J Clin Invest* 2002; **109**: 1291–1302
19 **Laconi S**, Pillai S, Porcu PP, Shafritz DA, Pani P, Laconi E. Massive liver replacement by transplanted hepatocytes in the absence of exogenous growth stimuli in rats treated with retrorsine. *Am J Pathol* 2001; **158**: 771–777
20 **Miyazaki M,** Akiyama I, Sakaguchi M, Nakashima E, Okada M, Kataoka K, Huh NH. Improved conditions to induce hepatocytes from rat bone marrow cells in culture. *Biochem Biophys Res Commun* 2002; **298**: 24–30
21 **Mallet VO**, Mitchell C, Mezey E, Fabre M, Guidotti JE, Renia L, Coulombel L, Kahn A, Gilgenkrantz H. Bone marrow transplantation in mice leads to a minor population of hepatocytes that can be selectively amplified *in vivo*. *Hepatology* 2002; **35**: 799–804

PO Box 2345, Beijing 100023, China
www.wjgnet.com
wjg@wjgnet.com

ELSEVIER

World J Gastroenterol 2005;11(8):1161-1166
World Journal of Gastroenterology ISSN 1007-9327

• *BASIC RESEARCH* •

Effect of operation-synchronizing transfusion of apoptotic spleen cells from donor rats on acute rejection of recipient rats after liver transplantation

Jing Liu, Yi Gao, Shuan Wang, Er-Wei Sun, Yu Wang, Zhi Zhang, Yi-Qiang Shan, Shi-Zheng Zhong

Jing Liu, Yi Gao, Shuan Wang, Er-Wei Sun, Yu Wang, Zhi Zhang, Yi-Qiang Shan, Department of Organ Transplantation, Zhujiang Hospital, First Military Medical University, Guangzhou 510282, Guangdong Province, China
Shi-Zheng Zhong, Institute of Clinical Anatomy, First Military Medical University, Guangzhou 510515, Guangdong Province, China
Supported by the National Natural Science Foundation of China, No. 39970705
Correspondence to: Dr. Er-Wei Sun, Department of Organ Transplantation, Zhujiang Hospital, 253, Gongye Highway, Guangzhou 510282, Guangdong Province, China. ewsun@263.net
Telephone: +86-20-61643402 Fax: +86-20-6164778
Received: 2004-3-31 Accepted: 2004-05-29

Abstract

AIM: To study effect of operation-synchronizing transfusion of apoptotic spleen cells from donor rats on acute rejection of recipient rats after liver transplantation.

METHODS: Two of Wistar rats were chosen randomly for normal liver pathology control and ten of SD rats chosen randomly for liver function control as blank group (no operation). The rest of Wistar and SD rats were divided into four groups: control group (only liver transplantation), Dex group (donors receiving intraperitoneal injection of dexamethasone), SpC group (recipients receiving infusion of spleen cells of donors), Dex-SpC group (recipients receiving infusion of apoptotic spleen cells of donors), with each group except blank group, containing 10 SD rats and 10 Wistar rats, respectively. Wistar rats received liver transplantation from SD rats, in the meantime they received infusion of spleen cells of donors, which were induced by an intraperitoneal injection of dexamethasone (3 mg/(d.kg)·b.w) for three days before liver transplantation. The serum alanine transaminase (ALT), total bilirubin (T bili), liver pathological changes and survival time were analysed. Statistical analysis was carried out using SPSS 10.0 for Windows. Differences of the parametric data of ALT in means were examined by one-way ANOVA. Differences of ALT between two groups were examined by LSD. Differences of the nonparametric data of T bili in means and scores of pathology classification for acute rejection were examined by Kruskal-Willis H test. The correlations between ALT and T bili were analysed by Bivariate. Kaplan-Meier curves were used to demonstrate survival distribution. The log-rank test was used to compare the survival data.

RESULTS: There were significant differences in ALT of the five groups ($F = 23.164$ $P = 0.000$), and ALT in Dex-SpC group was significantly higher than that in blank control, control, Dex, and SpC groups ($P = 0.000$), and ALT in SpC group was significantly higher than that in blank control ($P = 0.000$), control ($P = 0.004$), and Dex groups ($P = 0.02$). Results of nonparametric analysis of T bili showed that there were differences in T bili of the five groups ($\chi^2 = 33.265$ $P = 0.000$). T bili in Dex-SpC group was significantly higher than that in blank control, control, Dex, and SpC groups. T bili in SpC group was higher than that in blank control, control, and Dex groups. There were significant differences in scores of pathology classification for acute rejection in each of the groups ($\chi^2 = 25.933$, $P = 0.000$). The pathologically more serious acute rejection was found in Dex-SPC group than in other groups. No sign of acute rejection was observed in the blank control group. Slight acute rejection was observed in the control group. Slight-moderate acute rejection was observed in the Dex group. Moderate-acute rejection was observed in the SpC group. Severe-acute rejection was observed in the Dex-SpC group. The survival time in Dex-SpC group was shorter than in other groups (*statistic* = 11.13, $P = 0.011$). ALT and T bili were positively correlated ($r = 0.747$, $P = 0.000$, two-tailed).

CONCLUSION: In order to reduce quantity of blood loss from rats after liver transplantation, only one of ALT or T bili is needed for liver function measurement of rats. Simultaneous injection of apoptotic spleen cells from donors induced by dexamethasone to liver transplantation rats aggravates acute rejection. One important mechanism of aggravation of acute rejection may be that apoptotic cells are not removed in time and that dead cells including apoptotic cells release inflammatory factors.

Key words: Liver transplantation; Acute rejection; Dexamethasone

Liu J, Gao Y, Wang S, Sun EW, Wang Y, Zhang Z, Shan YQ, Zhong SZ. Effect of operation-synchronizing transfusion of apoptotic spleen cells from donor rats on acute rejection of recipient rats after liver transplantation. *World J Gastroenterol* 2005; 11(8): 1161-1166
http://www.wjgnet.com/1007-9327/11/1161.asp

INTRODUCTION

Rejection of recipients to organs of donors is a very important

issue. Particularity in liver transplantation[1-7], rejection of recipients to liver of donors is still a problem that has puzzled clinicians and immunologists. Induced immune tolerance is an effective way to resolve rejection. Therefore, immune tolerance of liver transplantation is one of the hot spots in the field of organ transplantation immunity. We carried out experimental study on tolerance induction of rat liver transplantation by transfusion of spleen cells from dexamethasone-treated donor rats before liver transplantation in our laboratory and found that such a treatment could prolong the survival time of grafts and that some recipients could live a long time. Thus we succeeded in tolerance induction of rat liver transplantation[8]. We also studied the mechanisms of apoptotic cells from donors to induce immune tolerance[9-12]. However, it is difficult to attain apoptotic cells of donors before clinical liver transplantation. If tolerance of rat liver transplantation can be induced by transfusion of spleen cells from dexamethasone-treated donor rats in the meantime of liver transplantation, it would be more practical.

MATERIALS AND METHODS

Equipments

Shanghai Medical Apparatus and Instruments Factory made packages of instruments showing minute points and Bull-Dog tongs; un-damaging suture of 7/0,8/0,9/0 was supplied by Shanghai Medical Apparatus and Instruments Suture Silk Factory. We made venous cannulas from cotton rods produced in Guandong Zhongshan Plastic Factory. Cage catheters of bile duct were made from segmental epidural catheter produced in Zhejiang Jiaxing Shujia Medical Apparatus and Instruments Factory. W-CJ-IF ultra-clean operating boar was made in Suzhou Purification Equipment Factory. High-speed hypothermia centrifugal machine UNIVERSAL 16R was made in Germany Hettich Company. CX7 automatic biochemistry analyzer was made by American Beckman Company. Olefin microtome was made by Germany Leica Company.

Reagents

Diethyl ether solutions were made in Guangdong Shantou Xilong Chemical Plant. Dexamethasone sodium phosphate parenteral solution (3 mg/(d.kg)b.w., made by Wuhan Binghuhe Pharmaceutical Co., Ltd,) was injected intraperitoneally into SD rats in corresponding groups at 8 a.m. for three days before liver transplantation. Atropine was made by Xuzhou Ryen pharmaceutical Co., Ltd. Heparin was made by Nanjing Xintian Biochemistry Pharmaceutical Co., Ltd.

Animals

Ninety-two male clean-closed colony Wistar and SD rats (weighing 220-280 g) were purchased from Experimental Animals Center of First Military Medical University and Zhongshan University, respectively. Body weight of donors was a little less than that of recipients. Two of Wistar rats were used randomly for normal liver pathology control and ten of SD rats were randomly used for liver function control. The rest of Wistar and SD rats were divided into four groups: control group (only liver transplantation), Dex group (donor received intraperitoneal injection of dexamethasone, three days before liver transplantation), SpC group (recipients received infusion of spleen cells of donors), Dex-SpC group (recipients received infusion of apoptotic spleen cells of donors treated with dexamethasone three days before liver transplantation). There were ten SD rats and ten Wistar rats in each group in which liver transplantations were carried out, and SD rats received livers from Wistar rats. As a rule, rats were fasted 12 h, restrained from water for 30 min before operation and subcutaneous injection of atropine (0.04 mg/kg b.w.) was done 15-30 min before operation.

Methods of operation and preparation of suspension fluid of spleen cells

Rats were put into an instrument filled with vapor of diethyl ether and taken out after they became motionless for 3-5 s. Then, their heads were covered with centrifuge tubes filled with vapor of diethyl ether. Spleens of rats in corresponding groups were removed. Suspension fluid of spleen cells (1 mL, concentration 5×10^7/mL) was fabricated by routine method; also, its vital force was more than 95%. Modified two-cuff method of Kamada[13] was used in the course of rat liver transplantation. Suspension fluid of spleen cells was injected into recipients through dorsal veins of penis 30 min after portal veins of recipients reopened.

Observation parameters

We observed general condition (body weight, appearance, activities, jaundice), liver function, liver histopathology, scores for acute rejection, and survival time after liver transplantation. ALT and T bili were assayed by CX7 automatic biochemistry analyzer with blood attained from tail veins on the seventh day after liver transplantation. Biopsy of livers of SD rats in each group were carried out by biopsy needle on the seventh day after liver transplantation. Liver tissue sample was fixed in 10% formaldehyde solution, embedded in paraffin, sliced up, stained in hematoxylin and eosin solution and observed under light microscopes. Scores of pathology classification for acute rejection were calculated according to Williams' method[14,15].

Statistical analysis

Data were expressed as mean±SE. Statistical analysis was carried out using SPSS 10.0 for Windows. Differences of the parametric data of ALT in means were examined by one-way ANOVA. Differences of ALT between two groups were examined by LSD. Differences of the nonparametric data of T bili on means and scores of pathology classification for acute rejection were examined by Kruskal-Wallis H test. The correlation between ALT and T bili was analysed by Bivariate. Kaplan-Meier curves were used to demonstrate survival distribution. The log-rank test was used to compare the survival data in the whole and between groups. A P value <0.05 was considered statistically significant.

RESULTS

General state

One rat died from bleeding of portal vein of donor post-operation in Dex-SpC group and blood could not be gained

from the tail vein of one rat in each of blank control, Dex, SpC, Dex-SpC groups. All the rats in each group awoke after operation, could crawl at once, were fed with sugar solution in 60 min and with food after a day of liver transplantation. The rats ate little, became depressed and emaciated; moreover, the color of pinna and urine became dark yellow in Dex-SpC group from the seventh to the ninth day after liver transplantation. The same phenomena could be found in SpC group from fifteenth to seventeenth day, in Dex group from the third week to the fourth week, and in a few rats the fifth week after post-operation.

Result of ALT

Results of ALT could meet the condition of analysis of variance (Figure 1, Table 1). Results of analysis of variance of ALT showed that there were significant differences in ALT of the five groups ($F = 23.164$ $P = 0.000$), and that ALT in Dex-SpC group was significantly higher than that in blank control, control, Dex, SpC groups($P = 0.000$), and that ALT in SpC group was significantly higher than that in blank control ($P = 0.000$), control ($P = 0.004$),and Dex groups ($P = 0.02$).

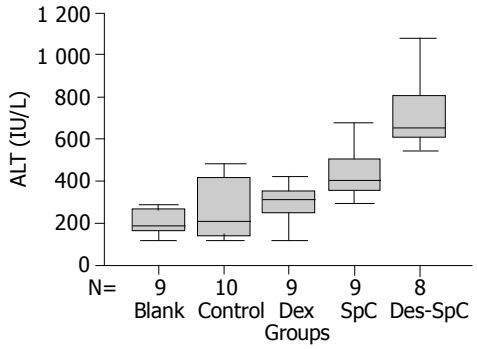

Figure 1 Boxplot of ALT one week after liver transplantation ALT: Alanine transaminase; Blank: The group without liver transplantation; Control: The group only with liver transplantation; Dex: The group treated with dexamethasone; SpC: The group treated with spleen cells; Dex-SpC: The group treated with dexamethasone and spleen cells.

Table 1 ALT and T bili in recipients in each group 1 wk after liver transplantation

Groups	*n*	ALT (IU/L)			T bili (μmol/L)
		mean±SE		95% Confidence interval	95% Confidence interval
Blank	9	201.1	60.3	154.8-247.5	1.2-4.8
Control	10	259.0	138.1	161.1-358.7	7.6-27.2
Dex	9	293.9	94.9	220.9-366.8	15.4-43.2
SpC	9	433.8	123.2	339.1-528.5[a]	33.7-69.7
Dex-SpC	8	717.0	178.5	567.8-866.2[b]	69.1-111.4

[a]$P<0.05$ *vs* Control, Dex; [b]$P<0.001$ *vs* Control, Dex, SpC. ALT: Alanine transaminase; T bili: Total bilirubin; Blank: The group without liver transplantation; Control: The group only with liver transplantation; Dex: The group treated with dexamethasone; SpC: The group treated with spleen cells; Dex-SpC: The group treated with dexamethasone and spleen cells.

Results of T bili

Results of T bili could not meet the condition of analysis of variance (Figure 2, Table 1). Result of nonparametric analysis of T bili showed that there were differences in TBil of the five groups ($\chi^2 = 33.265$ $P = 0.000$). T bili in Dex-SpC group was significantly higher than that in blank control, control, Dex group, and SpC groups and that T bili in SpC group was higher than that in blank control, control, and Dex groups.

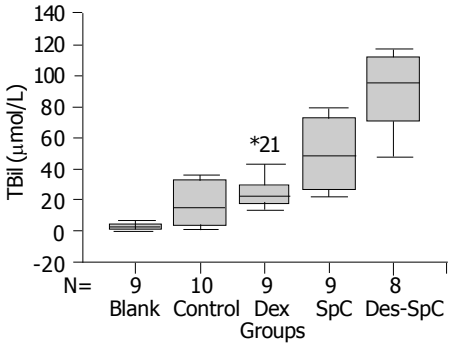

Figure 2 Boxplot of T bili one week after liver transplantation T bili: Total bilirubin; Blank: The group without liver transplantation; Control: The group with only liver transplantation; Dex: The group treated with dexamethasone; SpC: The group treated with spleen cells; Dex-SpC: The group treated with dexamethasone and spleen cells.

Correlation of ALT and T bili

Analysis of correlation of ALT and Tbili showed that there were significant positive correlations ($r = 0.747$, $P = 0.000$, two-tailed) between them.

Results of liver pathology about acute rejection

Scores of pathology classification for acute rejection in each of the groups were calculated according to Williams' method[14,15] (Table 2). The scores from zero to two, from four to five, from six to seven, and from eight to nine showed no acute rejection, light acute rejection, moderate acute rejection, and severe acute rejection, respectively[15]. There were significant differences in scores of pathology classification for acute rejection between the groups ($\chi^2 = 25.933$, $P = 0.000$). Pathological most severe-acute rejection was found in Dex-SPC group. No sign of acute rejection was observed in blank control group (Figure 3A). Slightly acute rejection was observed in control group (Figure 3B). Slight-moderate acute rejection was observed in Dex group (Figure 3D). Moderate-acute rejection was observed in SpC group (Figure 3C). Severe acute rejection was observed in Dex-SpC group (Figure 3E).

Table 2 Scores of pathology classification for acute rejection in each group

Group	*n*	Rejection active index						
		1	4	5	6	7	8	9
Blank	2	2						
Control	10		9	1				
Dex	10			1	9			
SpC	10				5	4	1	
Dex-SpC	9						2	7

Abbreviations as in Table 1.

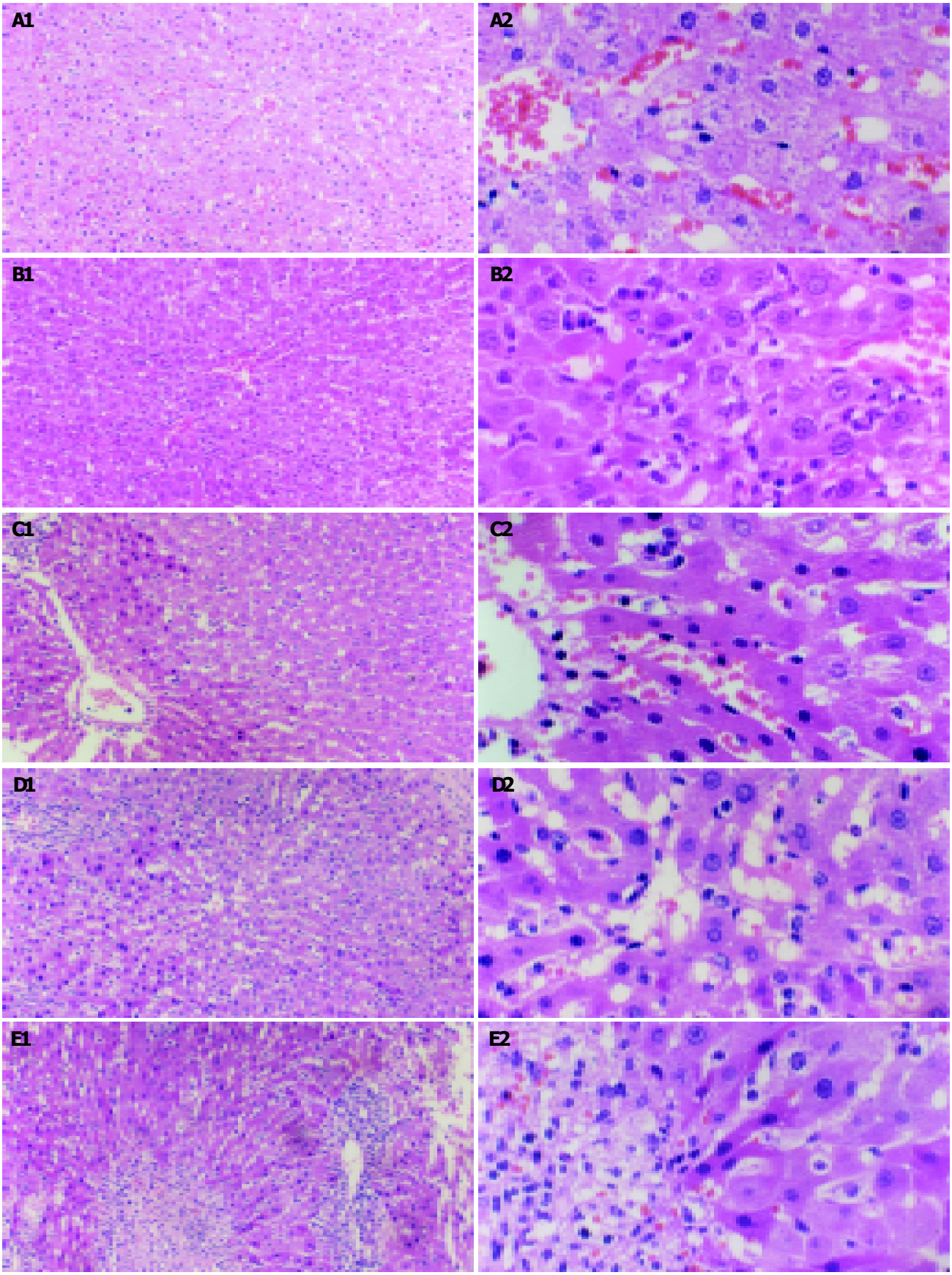

Figure 3 Histopathology in different groups. A: Histopathology in blank control group showing no acute rejection (HE, A1: original magnification: 33×; A2: original magnification: 132×); B: Histopathology in control group showing slightly acute rejection 1 wk after orthotopic liver transplantation (OLT) (HE, B1: original magnification: 33×; B2: original magnification: 132×); C: Histopathology in Dex group showing slight–moderate acute rejection 1 wk after OLT (HE, C1: original magnification: 33×; C2: original magnification: 132×); D: Histopathology in SpC group showing moderate–acute rejection 1 wk after OLT, with less extensive hepatocyte necrosis (HE, D1: original magnification: 33×; D2: original magnification: 132×); E: Histopathology in Dex-SpC group showing serious acute rejection 1 wk after OLT, with more extensive hepatocytes necrosis (HE, E1: original magnification: 33; E2: original magnification: 132×).

Survival period

Survival period after liver transplantation in each group are shown in Table 3 and Figure 4. There were significant differences in survival period between the groups (pooled over strata, *statistic* = 11.13, $P = 0.011$). The survival period in the Dex-SpC group was significantly shorter than that in the control group ($P = 0.0085$) and the Dex group ($P = 0.0326$).

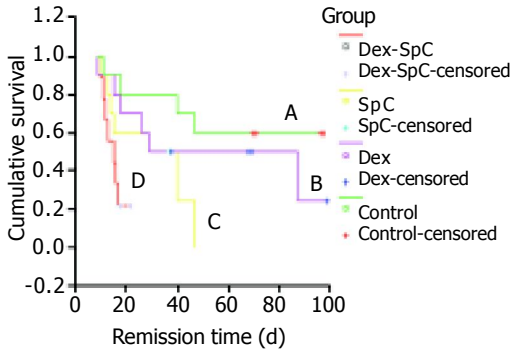

Figure 4 Curve of survival time after liver transplantation in each group. Pooled over strata (*statistic* = 11.13, *P* = 0.011), Pairwise over strata, D *vs* A (*statistic* = 6.93, *P* = 0.0085), B (*statistic* = 4.57, *P* = 0.0326), C (*statistic* = 2.24 , *P* = 0.1342). A: control group, B: Dex group, C: SpC group, D: Dex-SpC group.

Table 3 Survival period after liver transplantation in each group

Groups	*n*	Survival period (d)	Mean (d)
Control	10	11, 18, 40, 47, >70 (×2), >71 (×2), >96, >97	69.8
Dex	10	9, 15, 18, 26, 29, >38, >68,, >69, >87, >99	56.2
SpC	10	10, 13, 14, 15, 29, 40, 47, >37 (×2), >38	29.9
	1	0.5 (death from surgical reasons)	
Dex-SpC	+		15.3
	9	10, 11, 12, 13, 15, 16, 17, >18, >22	

Abbreviations as in Table 1.

DISCUSSION

As liver is an essential organ, once there is acute rejection after liver transplantation in a rat, which cannot be managed, the rat will die in a short time. The survival time of rats and grafts in orthotopic liver transplantation is the same. The loss of liver function can be an end-point of acute rejection. Therefore, survival period of recipients can indicate survival time of grafts. When acute rejection for liver occurs, ALT and bilirubin come out of cells. ALT and T bili in blood increase quickly. Assaying of liver function is helpful to determine grades of acute rejection. The results of ALT and T bili and survival time accord with the changes in pathology of liver.

Antigens of donors are injected into recipients, resulting in different outcomes from promoting immune response to immune tolerance. The survival time of grafts of pancreas, heart and skin were prolonged obviously after the dendritic cells from donors' livers were injected into recipients before transplantations[16]. The survival times of grafts were also prolonged obviously after marrow or spleen cells were injected into recipients before transplantations[17]. Starzl[18], using microchimerism believed that the graft was alive longer because the recipient had formed microchimerism by antigen of the donor injected before. There have been numerous studies on apoptosis[19]. Our experiment showed that transfusion of spleen cells from dexamethasone-treated donor to recipients before liver transplantation could prolong the survival time of grafts and that some recipients could live a long time, indicating successful tolerance induction of rat liver transplantation[8]. We speculate that liver is a special place where apoptotic cells are phagocytized. Apoptotic cells inhibit immunity in local places where they are accumulated. The antigen-presenting cells (APCs) that phagocytize apoptotic cells present to T cells in inhibited circumstance induce immune tolerance[4].

DCs can phagocytize apoptotic cells. But there is dispute about whether this phagocytosis could cause immune tolerance or response[20]. Hawiger *et al*[21], found that DCs' antigen-presenting could lead to immune tolerance. The results of liver function, pathology and survival time in this experiment showed that operation synchronizing transfusion of apoptotic spleen cells from donor rats accelerated acute rejection of rat liver transplantation. It is almost impossible that operation synchronizing transfusion of apoptotic lymphocytes from donor would induce immune tolerance. The reasons are, maybe as follows: First, though the phagocytes in livers account for 80% of the total in human bodies, the function of phagocytes have been damaged because of warm and cold ischemic/reperfusion injury. Therefore, the phagocytes cannot phagocytize apoptotic cells immediately, and the apoptotic cells, which cannot be phagocytized at once become necrotic and release inflammatory factors such as TNF-α, IL-1β, IL-6 and IL-8 that can activate DCs[22], and make them mature. The ability of antigen presenting of APCs become stronger[23]. So an acute rejection happens[24-27]. Second, according to the theory of danger signal[28], there have been plenty of danger signals that resulted from warm and cold ischemic-reperfusion injury. Though the number of necrotic cells is less than 5%, there are 35% apoptotic cells[8], necrotic cells and apoptotic cells, which cannot be phagocytized at once release danger signals. The danger signals were so strong that APCs in recipients including DCs phagocytized the spleen cells of donors including necrotic cells and apoptotic cells and presented with antigens of donors, produced co-stimulatory molecules, accelerated acute rejection of rat liver transplantation finally (Figure 5). Third, the results of this experiment showed the acute rejection in the groups with injected spleen cells of donors treated or untreated was more serious than the groups without injected spleen cells. The spleen cells solution including DCs distributed the whole body because of blood circulation, activated the lymph organs and caused immune responses. On the other hand, immune responses depended on lymphocytes of the donor circulating to the liver of the recipient or the graft of liver releasing soluble antigens to blood circulation when only liver transplantation was carried out.

Because there was positive correlation between ALT and T bili, we can sample blood as little as possible so as to reduce effects of blood loss on survival time. Only one of ALT and T bili is needed to measure the liver function.

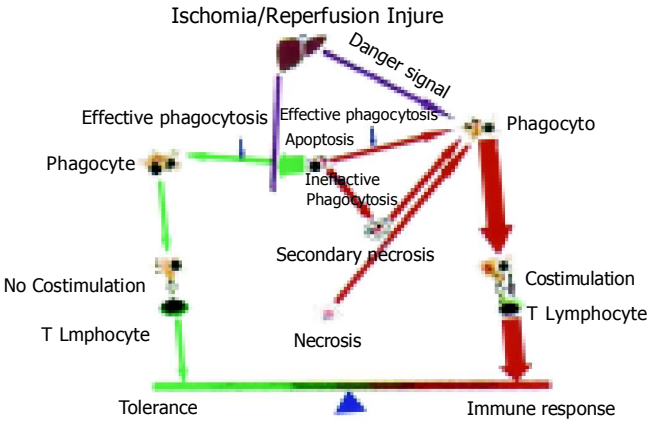

Figure 5 Diagram of synchronizing transfusion of apoptotic spleen cells accelerating acute rejection of rat liver transplantation.

Also, because the Wistar and SD rats were purchased from different units and grouped randomly, we excluded the effects of difference of rats on the whole results. In this experiment, the survival time in the control group was longer than that reported in literature[8,29]. In order to find out the reasons, liver transplantations were carried out seven times by the same method using Wistar and SD rats provided by the same unit. The mean survival time was 11.1 d, significantly shorter than that of the Control group ($P<0.01$). There were no differences compared to that of Wang[8]. Therefore, we suspect that the gene of the SD rats might have been mutated or added to the gene of Wistar rats in the control group[30].

REFERENCES

1 **Starzl TE,** Demetris AJ, Murase N, Ildstad S, Ricordi C, Trucco M. Cell migration, chimerism, and graft acceptance. *Lancet* 1992; **339:** 1579-1582
2 **Bishop GA,** Sun J, Sheil AG, McCaughan GW. High-dose/activation-associated tolerance: a mechanism for allograft tolerance. *Transplantation* 1997; **64:** 1377-1382
3 **Krams SM,** Martinez OM. Apoptosis as a mechanism of tissue injury in liver allograft rejection. *Semin Liver Dis* 1998; **18:** 153-167
4 **Sun EW,** Shi YF. Apoptosis: the quiet death silences the immune system. *Pharmacol Ther* 2001; **92:** 135-145
5 **Qian S,** Lu L, Fu F, Li Y, Li W, Starzl TE, Fung JJ, Thomson AW. Apoptosis within spontaneously accepted mouse liver allografts: evidence for deletion of cytotoxic T cells and implications for tolerance induction. *J Immunol* 1997; **158:** 4654-4661
6 **Thomson AW,** Drakes ML, Zahorchak AF, O'Connell PJ, Steptoe RJ, Qian S, Lu L. Hepatic dendritic cells: immunobiology and role in liver transplantation. *J Leukoc Biol* 1999; **66:** 322-330
7 **Thomson AW,** Lu L. Are dendritic cells the key to liver transplant tolerance? *Immunol Today* 1999; **20:** 27-32
8 **Wang S.** Experimental study on tolerance induction of rat liver transplantation by transfusion of spleen cells from *in vivo* dexamethasone-treated donor rats. Master academic degree papers of first military medical university. *Diyi Junyi Daxue* 2001: 21-32
9 **Chen JF,** Gao Y, Sun EW, Wang S. Immunosuppression of allotransplantation induced by transfusion of donor apoptotic cells. *Zhonghua Shiyan Waike Zazhi* 2003; **20:** 608-610
10 **Zhang L,** Sun EW, Ge Q, Zeng YY, Gao W. An *in vitro* study of the inhibition of T cell activation by apoptotic cells. *Zhongguo Mianyixue Zazhi* 2000; **16:** 407-411
11 **Sun EW,** Chen YF, Nakajima H. Tolerance induction in adult rats with normal immune status by spleen cell from dexamethasone-treated animals. *Diyi Junyi Daxue Xuebao* 2000; **20:** 380-382
12 **Zhang L,** Zhu T, Sun EW, Shen SQ, Guo H, Min ZL, Chen ZH. Study the mechanisms and inducing transplantation immune tolerance of FTY720. *Zhonghua Waike Zazhi* 2003; **41:** 773-777
13 **Kamada N,** Calne RY. Orthotopic liver transplantation in the rat. Technique using cuff for portal vein anastomosis and biliary drainage. *Transplantation* 1979; **28:** 47-50
14 **Williams JW,** Peters TG, Vera SR, Britt LG, van Voorst SJ, Haggitt RC. Biopsy-directed immunosuppression following hepatic transplantation in man. *Transplantation* 1985; **39:** 589-596
15 **Banff schema for grading liver allograft rejection: an international consensus document**. *Hepatology* 1997; **25:** 658-663
16 **Lu L,** Qian S, Hershberger PA, Rudert WA, Lynch DH, Thomson AW. Fas ligand (CD95L) and B7 expression on dendritic cells provide counter-regulatory signals for T cell survival and proliferation. *J Immunol* 1997; **158:** 5676-5684
17 **Valente JF,** Ogle CK, Alexander JW, Li BG, Custer DA, Noel JG, Ogle JD. Bone marrow and splenocyte coculture-generated cells enhance allograft survival. *Transplantation* 1997; **64:** 114-123
18 **Starzl TE,** Demetris AJ, Murase N, Trucco M, Thomson AW, Rao AS. The lost chord: microchimerism and allograft survival. *Immunol Today* 1996; **17:** 577-584; discussion 588
19 **Yang LQ,** Fang DC, Wang RQ, Yang SM. Effect of NF-kappaB, survivin, Bcl-2 and Caspase3 on apoptosis of gastric cancer cells induced by tumor necrosis factor related apoptosis inducing ligand. *World J Gastroenterol* 2004; **10:** 22-25
20 **Steinman RM,** Turley S, Mellman I, Inaba K. The induction of tolerance by dendritic cells that have captured apoptotic cells. *J Exp Med* 2000; **191:** 411-416
21 **Hawiger D,** Inaba K, Dorsett Y, Guo M, Mahnke K, Rivera M, Ravetch JV, Steinman RM, Nussenzweig MC. Dendritic cells induce peripheral T cell unresponsiveness under steady state conditions *in vivo*. *J Exp Med* 2001; **194:** 769-779
22 **Lau AH,** Thomson AW. Dendritic cells and immune regulation in the liver. *Gut* 2003; **52:** 307–314
23 **Iyoda T,** Shimoyama S, Liu K, Omatsu Y, Akiyama Y, Maeda Y, Takahara K, Steinman RM, Inaba K. The CD8+ dendritic cell subset selectively endocytoses dying cells in culture and *in vivo*. *J Exp Med* 2002; **195:** 1289–1302
24 **Rovere P,** Sabbadini MG, Vallinoto C, Fascio U, Zimmermann VS, Bondanza A, Ricciardi-Castagnoli P, Manfredi AA. Delayed clearance of apoptotic lymphoma cells allows cross-presentation of intracellular antigens by mature dendritic cells. *J Leukoc Biol* 1999; **66:** 345-349
25 **Gallucci S,** Lolkema M, Matzinger P. Natural adjuvants: endogenous activators of dendritic cells. *Nat Med* 1999; **5:** 1249-1255
26 **Nakamitsu A,** Hiyama E, Imamura Y, Matsuura Y, Yokoyama T. Kupffer cell function in ischemic and nonischemic livers after hepatic partial ischemia/reperfusion. *Surg Today* 2001; **31:** 140-148
27 **Stuart LM,** Lucas M, Simpson C, Lamb J, Savill J, Lacy-Hulbert A. Inhibitory effects of apoptotic cell ingestion upon endotoxin-driven myeloid dendritic cell maturation. *J Immunol* 2002; **168:** 1627-1635
28 **Matzinger P.** Tolerance, danger, and the extended family. Annu Rev *Immunol* 1994; **12:** 991-1045
29 **Du Z,** Song JC, Zhang ZX, Du B, Yang J. Hepatic allograft survival in rats without immunosuppressants after intrathymic splenocyte transplantation. *Zhonghua Qiguan Yizhi Zazhi* 1996; **17:** 80-82
30 **Shi XY,** Li LJ. The animals' factors effecting the experiment results. In: Shi XY, eds. Modern medicine experiment zoology. *Beijing: People's Surgeon Publishing Company* 2000: 30-34

PO Box 2345, Beijing 100023, China
www.wjgnet.com
wjg@wjgnet.com

ELSEVIER

World J Gastroenterol 2005;11(8):1167-1171
World Journal of Gastroenterology ISSN 1007-9327

• *CLINICAL RESEARCH* •

Clinical significance of serum levels of vascular endothelial growth factor and its receptor in biliary disease and carcinoma

Munechika Enjoji, Makoto Nakamuta, Koji Yamaguchi, Satoshi Ohta, Kazuhiro Kotoh, Marie Fukushima, Masami Kuniyoshi, Tomomi Yamada, Masao Tanaka, Hajime Nawata

Munechika Enjoji, Makoto Nakamuta, Satoshi Ohta, Kazuhiro Kotoh, Marie Fukushima, Masami Kuniyoshi, Hajime Nawata, Department of Medicine and Bioregulatory Science, Graduate School of Medical Sciences, Kyushu University, Fukuoka, Japan
Koji Yamaguchi, Masao Tanaka, Department of Surgery and Oncology, Graduate School of Medical Sciences, Kyushu University, Fukuoka, Japan
Tomomi Yamada, Medical Information Science, Graduate School of Medical Sciences, Kyushu University, Fukuoka, Japan
Correspondence to: Munechika Enjoji, M.D., Ph.D., Department of Medicine and Bioregulatory Science, Graduate School of Medical Sciences, Kyushu University, 3-1-1 Maidashi, Higashi-ku, Fukuoka 812-8582, Japan. enjoji@intmed3.med.kyushu-u.ac.jp
Telephone: +81-92-642-5282 Fax: +81-92-642-5287
Received: 2004-07-17 Accepted: 2004-08-30

Abstract

AIM: To investigate the clinical significance of serum vascular endothelial growth factor (VEGF) and soluble VEGF receptor-1 (VEGFR1/Flt-1) (sVEGFR1) levels in biliary diseases.

METHODS: We analyzed the serum levels of these proteins in patients with acute cholangitis (group 1), biliary malignancies (group 2), and primary biliary cirrhosis or primary sclerosing cholangitis (group 3), and in healthy donors (group 4). The influence of inflammation was also analyzed. Serum VEGF levels were expressed as VEGF per platelet (VEGF/PLT, pg/10^6) in order to exclude the influence of platelet counts.

RESULTS: sVEGFR1 levels were significantly higher in groups 1 and 2 than in the control group, but did not correlate with inflammatory markers. VEGF/PLT levels were generally higher in patients with active inflammation than in those with carcinoma. C-reactive protein strongly correlated with the levels of serum VEGF independently of platelet and leukocyte counts, even in cancer patients. In cancer patients, VEGF/PLT and sVEGFR1 levels might be indicators for evaluating the effect of medical treatment or the disease progression.

CONCLUSION: Serum VEGF and VEGFR1 might be useful markers for gauging the clinical effect of various treatments on patients.

Key words: VEGF; VEGFR1; Cholangiocarcinoma; Cholangitis

Enjoji M, Nakamuta M, Yamaguchi K, Ohta S, Kotoh K, Fukushima M, Kuniyoshi M, Yamada T, Tanaka M, Nawata H. Clinical significance of serum levels of vascular endothelial growth factor and its receptor in biliary disease and carcinoma. *World J Gastroenterol* 2005; 11(8): 1167-1171
http://www.wjgnet.com/1007-9327/11/1167.asp

INTRODUCTION

Angiogenic response occurs through the release of various angiogenic factors such as vascular endothelial growth factor (VEGF). VEGF is known to be synthesized by endothelial cells, leukocytes, and megakaryocytes[1]. Angiogenesis is essential for the growth and survival of solid tumors and VEGF plays a predominant role in inducing tumor-associated angiogenesis[2,3]. Generally, VEGF is detected in most malignant epithelial tumor cells and it has been reported that the level of VEGF expression in tumor tissue is of prognostic value[4,5]. Some groups reported that both serum and plasma VEGF concentrations correlate with tumor stage[6,7]. Megakaryocytes are an important source of VEGF, which is stored in the α granules of platelets[8]. A close correlation between platelet counts and serum VEGF has been reported in cancer patients and this phenomenon is presumably due to the release of VEGF following platelet activation during the clotting process[9,10].

A VEGF-specific tyrosine kinase receptor, VEGF receptor-1 (VEGFR1/Flt-1), is found in vascular endothelial cells of tumor vessels[2,3,11]. A naturally occurring soluble form of VEGFR1 (sVEGFR1) is an alternatively spliced variant of the VEGFR1 gene and can be secreted into the circulation[5,12]. VEGFR1 has a high affinity for VEGF, even in soluble form[12]. sVEGFR1 can be derived not only from vessels but also from tumor cells[13-15]. sVEGFR1 appears to be a crucial, intrinsic, negative regulator of VEGF and it may play a key role in tumor angiogenesis[16,17].

The expression of VEGF and VEGFR1 in tissues of cholangiocarcinoma has been examined histopathologically[18]. VEGF is strongly expressed in malignant cholangiocytes, whereas the surrounding mesenchymal and endothelial cells are consistently negative for VEGF. On the other hand, VEGFR1 is expressed exclusively by endothelial cells adjacent to tumor cells and rarely expressed in quiescent endothelial cells. Endothelial cells are demonstrated as the only cellular source of the receptor. However, little is known about the clinical significance of serum levels of VEGF and sVEGFR1 in biliary diseases, especially in benign disease. The current study was therefore, initiated to evaluate the serum values

of VEGF and sVEGFR1 in patients with biliary diseases.

MATERIALS AND METHODS

Sera were collected from patients with biliary disease at the Third Department of Internal Medicine and the First Department of Surgery, Kyushu University Hospital, between 2001 and 2003. Patients were divided into three groups: Group 1. Cholangitis with active inflammation (n = 42); Group 2. Biliary neoplasms including intrahepatic and extrahepatic cholangiocarcinoma (n = 44), gallbladder carcinoma (n = 7), and ampullary carcinoma (n = 8); Group 3. Vanishing bile duct disorder of autoimmune origin, primary sclerosing cholangitis (PSC: n = 12) or primary biliary cirrhosis (PBC: n = 13). For the control group (Group 4), serum samples from 31 healthy blood donors were assayed. Informed consent was obtained from each patient prior to their entering the study.

Serum concentrations of VEGF and sVEGFR1 were quantified using the high-sensitivity ELISA kits (R&D Systems, Minneapolis, MN) according to the manufacturer's specifications. The sensitivity of VEGF and sVEGFR1 assays was 9 pg/mL. C-reactive protein (CRP) was used as a laboratory marker of inflammation. The number of platelets and leukocytes in peripheral blood was routinely tested. Statistical analyses were performed using Spearman's correlation analysis, Kruskal-Wallis test with Bonferroni correlation for multiple comparisons, or Wilcoxon's signed rank test and the results were considered statistically significant if P was less than 0.05.

RESULTS

Correlation of VEGF levels with platelet counts

In this study, blood donors formed one of these four groups: Group 1. patients with acute cholangitis/cholecystitis; Group 2. patients with biliary carcinoma; Group 3. PBC or PSC; Group 4. healthy volunteers (see Materials and Methods). Correlations between pairs of parameters were tested by Spearman's correlation analysis. Overall, VEGF levels showed a close relationship with platelet counts: Group 1. r = 0.449, P = 0.0029; Group 2, r = 0.439, P = 0.0005; Group 3. r = 0.393, P = 0.0520; Group 4. r = 0.537, P = 0.0018 (Figure 1). On the other hand, VEGF levels were not significantly correlated with WBC counts in healthy donors and patients with benign biliary disease: Group 1 r = 0.166; Group 3 r = 0.325; Group 4, r = 0.312. However, the correlation was significant in patients with malignancy: Group 2, r = 0.487, P<0.0001. These results indicated that platelet counts could considerably control serum VEGF levels in patients. Therefore, the concentration of VEGF per platelet (VEGF/PLT, pg/10^6) was calculated by dividing the serum VEGF values (pg/mL) by the platelet counts ($\times 10^6$/mL) in order to standardize and accurately compare the VEGF levels between patients. When VEGF levels were expressed relative to platelet counts, WBC counts did not show a significant correlation: Group 1, r = -0.049; Group 2, r = 0.288; Group 3, r = -0.076; Group 4, r = 0.205. There was no significant correlation between platelet and leukocyte counts (data not shown). The correlation was not significant between serum levels of sVEGFR1 and platelet or leukocyte counts.

Serum levels of VEGF, sVEGFR1, and VEGF/PLT

Serum levels of VEGF, sVEGFR1, and VEGF/PLT were compared among groups by Kruskal-Wallis test (Bonferroni correlation for multiple comparisons). Data for each group were presented as (median [25th. percentile, 75th. percentile]; mean value). VEGF values were significantly higher in Group

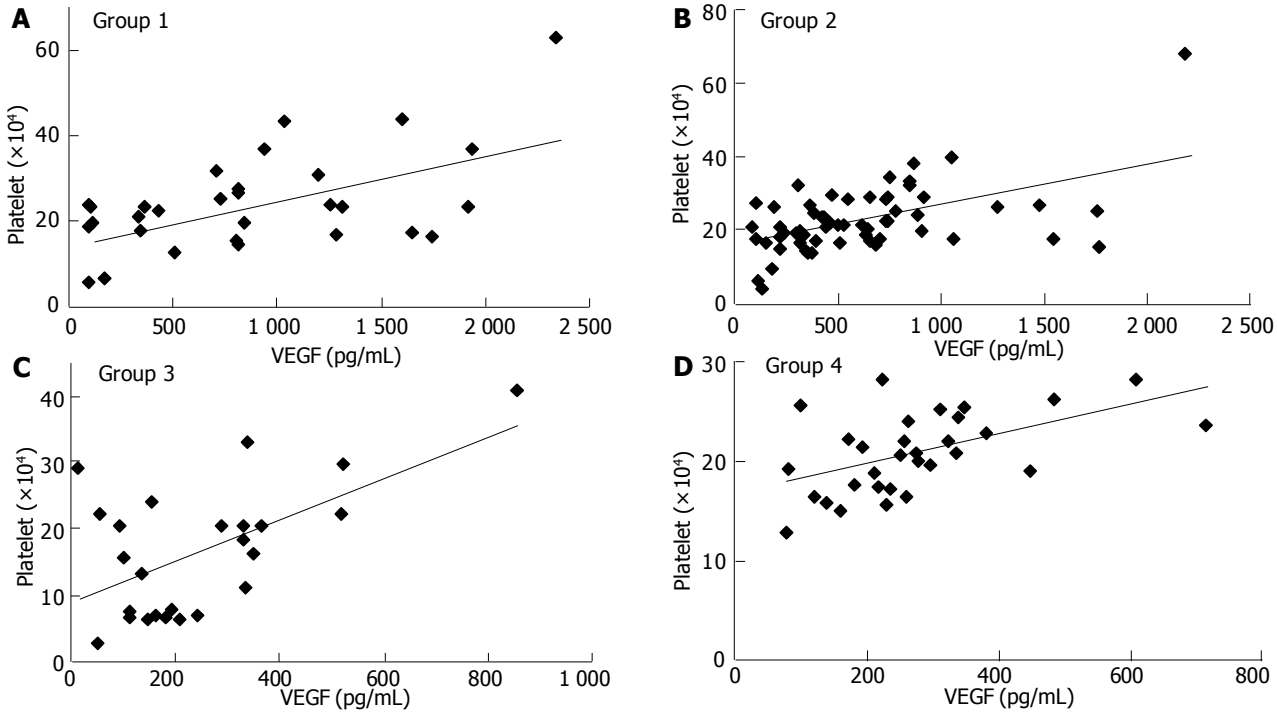

Figure 1 Correlation between serum VEGF levels and platelet counts. A: group 1; B: group 2; C: group 3; D: group 4.

1 (648.5 [390, 1066]; 805.6 pg/mL) and Group 2 (504 [347, 775]; 633.7 pg/mL) than in Group 3 (191 [113, 333]; 246.7 pg/mL) and Group 4 (261 [185, 338]; 278.2 pg/mL) (Figure 2A). VEGF/PLT levels showed the same pattern as VEGF, and were significantly higher in Group 1 (3.22 [2.33, 4.59]; 3.78 pg/10^6) and Group 2 (2.51 [1.84, 3.26]; 2.86 pg/10^6) than in Group 3 (1.78 [1.02, 2.35]; 1.74 pg/10^6) and Group 4 (1.26 [0.89, 1.52]; 1.28 pg/10^6) (Figure 2B). sVEGFR1 levels were significantly higher in Group 1 (72 [62, 88]; 81.2 pg/mL) and Group 2 (72 [59, 90]; 77.0 pg/mL) than in Group 4 (56 [47, 74]; 60.4 pg/mL) (Figure 2C).

Influence of inflammation

The correlation between CRP, a commonly used marker of inflammation, and VEGF/PLT or sVEGFR1 was analyzed in patients (groups 1-3) by Spearman's correlation analysis. CRP levels were normally distributed within each group. In acute inflammatory disease (group 1), CRP and VEGF/PLT were closely correlated ($r = 0.575$, $P<0.0001$) (Figure 3A), but there was no correlation between CRP and sVEGFR1 ($r = -0.067$). In patients with chronic autoimmune disease, the PBC and PSC group, no significant correlation was found between CRP and VEGF/PLT ($r = -0.084$) or sVEGFR1 ($r = 0.398$). In cancer patients, significant correlations were observed between CRP and VEGF/PLT ($r = 0.717$, $P<0.0001$) (Figure 3B), and also between CRP and sVEGFR1 ($r = 0.318$, $P = 0.018$).

Movement of serum VEGF/PLT and sVEGFR1 in cancer patients

In almost all our patients, biliary carcinoma was clinically detected and diagnosed at advanced stages (stage IV or III). Therefore, patients with cancer were divided into two groups for the convenience of clinical severity: Group A, patients treated by curative surgical resection ($n = 13$); Group B, patients with no effective treatment ($n = 14$). Significant difference was tested by Wilcoxon's signed-rank test. The levels of VEGF/PLT and sVEGFR1 were measured before and 4 wk after surgical operation in group A. In group B, the parameters were measured at intervals of 3 mo. At the time of admission to our hospital, there was no significant difference in the levels of VEGF/PLT and sVEGFR1 between Groups A and B. However, in Group A, the levels of VEGF/PLT ($P = 0.0001$) and sVEGFR1 ($P = 0.0024$) decreased significantly after surgical treatment (Figures 4A, B). By contrast, the levels of both significantly increased in Group B: VEGF/PLT, $P = 0.0134$; sVEGFR, $P = 0.0017$ (Figures 4C, D).

DISCUSSION

Recent studies have shown that serum VEGF levels are closely related to platelet counts in cancer patients[1,7,19,20]. It has been suggested that serum VEGF levels reflect platelet counts rather than VEGF secretion from tumor cells, or that platelets act as a scavenger through endocytosis and storage of VEGF secreted from the tumor[1,7,10,19-21]. We demonstrated,

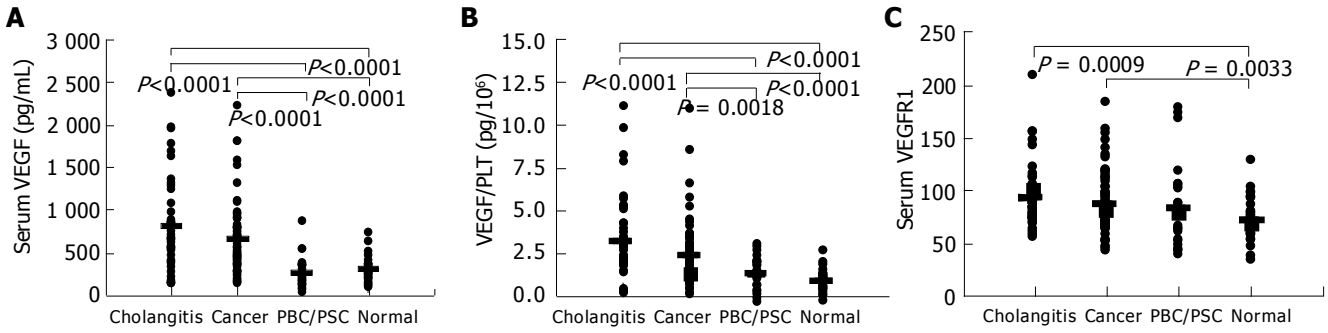

Figure 2 VEGF (A), VEGF/PLT (B), and VEGFR1 (C) levels in patients with biliary disease and healthy volunteers. The mean value of each group is presented as a bold line. VEGF/PLT: the calculated parameter by dividing the serum VEGF values (pg/mL) by the platelet counts (×10^6/mL); Cholangitis: patients with acute cholangitis or cholecystitis; Cancer: patients with biliary neoplasms; PBC/PSC: patients with primary biliary cirrhosis or primary sclerosing cholangitis; normal: healthy volunteers.

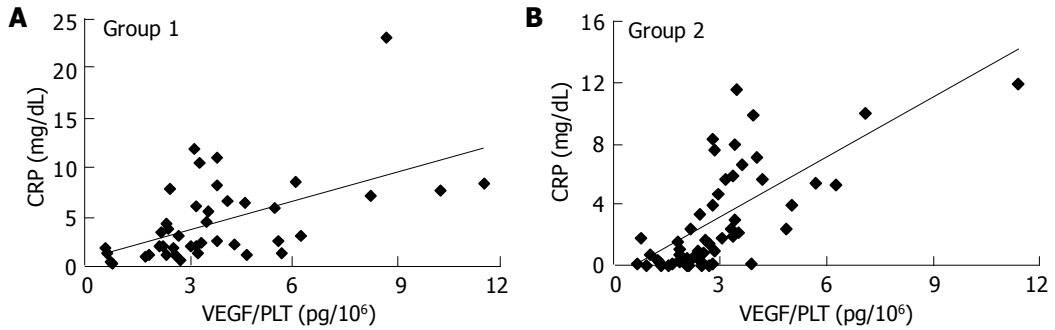

Figure 3 Correlation between C-reactive protein (CRP) and VEGF/PLT levels in group 1 (A) and group 2 (B). VEGF/PLT: the calculated parameter by dividing the serum VEGF values (pg/mL) by the platelet counts (×10^6/mL).

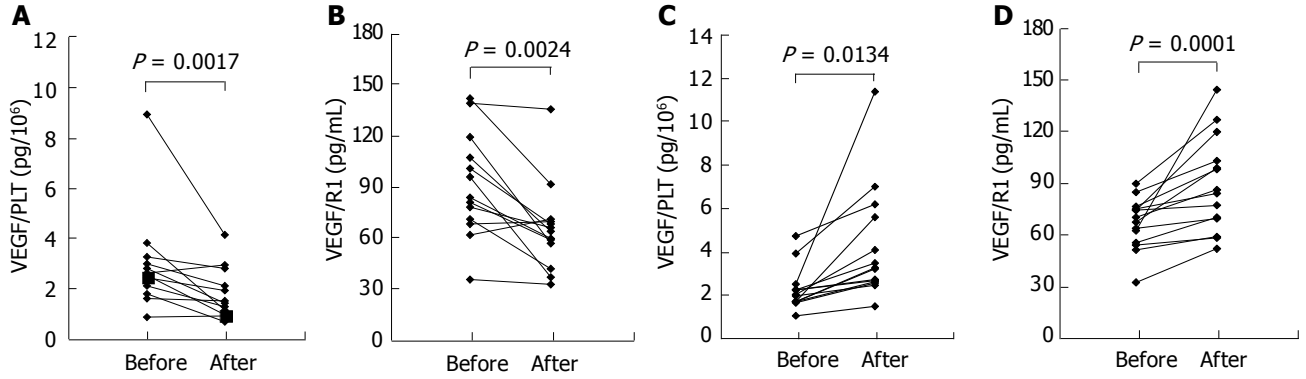

Figure 4 Time course of VEGF/PLT (A and C) and VEGFR1 (B and D) levels in patients with biliary cancer. The levels were measured in each patient before and after the curative operation (A and B) or before and after the progression of cancer in size without any effective treatments (C and D). VEGF/PLT: the calculated parameter by dividing the serum VEGF values (pg/mL) by the platelet counts (×10^6/mL).

in this study, the relationship between serum VEGF and platelet counts is also true in biliary cancer ($r = 0.439$, $P = 0.0005$). On the other hand, some groups have not found such a correlation between VEGF and platelet counts in benign disease and healthy controls[13,14]. However, in our study, a correlative trend was obvious in acute cholangitis ($r = 0.449$, $P = 0.0029$), autoimmune biliary disease ($r = 0.393$, $P = 0.052$), and normal controls ($r = 0.537$, $P = 0.0018$). Therefore, we reasoned that expressing VEGF levels relative to platelet counts is a more meaningful way to compare the clinical significance of VEGF among diseases. Leukocytes are another known producer of VEGF. However, when WBC counts were compared with VEGF/PLT, no correlation was found in any of the groups. This finding indicates that WBC counts in peripheral blood do not significantly influence the levels of VEGF.

In our study, the levels of VEGF/PLT were higher ($P = 0.0152$) in acute cholangitis patients (mean value: 3.78 pg/10^6) than in cancer patients (mean value: 2.86 pg/10^6) and closely correlated with serum CRP levels ($r = 0.575$, $P<0.0001$). Angiogenesis is a necessary process for inflammation and tissue regeneration. It has been reported that inflammation and hypoxic change with expression of various tissue factors, cytokines, and chemokines stimulate VEGF synthesizing cells such as platelets, immune cells, and inflammatory cells[22-24]. Acute cholangitis is a typical intensive infectious disease. Therefore, in the patients with the disease, the correlation between inflammation activity marker, CRP, and serum VEGF levels is expressed more significantly.

Surprisingly, in biliary cancer patients, VEGF/PLT is also closely correlated with CRP ($r = 0.717$, $P<0.0001$). The phenomenon raises the question whether cholangiocarcinoma cells really produce and secrete significant amounts of VEGF, since VEGF/PLT levels may be increased by the same mechanism as in cholangitis. In patients with hypervascular massive tumors like hepatocellular carcinoma, immunohistochemical VEGF expression in cancer cells and serum VEGF are quantitatively correlated[25]. These findings support the concept that VEGF production and neovascularization are absolutely needed for these tumors to survive. On the other hand, cholangiocarcinoma is a relatively hypovascular and invasive tumor, namely, inflammation may be a more significant clinical characteristic in cholangiocarcinoma than in HCC. Therefore, platelets and inflammatory cells may play an important role in VEGF production/secretion in cholangitis as well. If this hypothesis is true, then it is not surprising that, in view of the degree of inflammation, VEGF/PLT levels were higher in the cholangitis group than in the neoplasm group.

Among the patients with autoimmune biliary disease (PBC and PSC), those at advanced stages (i.e., liver cirrhosis) showed lower platelet counts (under 1×10^5/μL), and therefore, the mean serum VEGF level in this group was only 234.6 pg/mL. However, no correlation was found between VEGF/PLT and CRP. These autoimmune diseases are characterized by chronic inflammatory conditions. VEGF expression is thoroughly characterized in rheumatoid arthritis (RA), a well-known systemic autoimmune disease. Serum levels of VEGF have been reported to be elevated in patients with RA and to correlate with disease activity and inflammatory markers. However, over time, the correlation with VEGF levels is only seen in RA of early to median disease duration, but not of long duration[26-28]. Generally, in patients with PBC/PSC, the clinical state is relatively stable even at advanced stages and the inflammatory events are not pronounced. Therefore, serum VEGF and VEGF/PLT levels may be in a relatively low grade and independent of CRP levels.

In our study, serum sVEGFR1 levels did not correlate with platelet and WBC counts. sVEGFR1 levels were statistically higher in groups 1 and 2 than in the normal control group. This finding can be explained by previous evidence showing that endothelial sVEGFR1 is up-regulated by its ligand, VEGF[13]. Indeed sVEGFR1 levels tend to change with VEGF/PLT level.

We have investigated whether the levels of VEGF/PLT and sVEGFR1 reflect the effect of surgical treatment in patients with biliary carcinoma. If not treated, both levels were elevated with the lapse of time. However, the levels clearly declined as a consequence of curative surgical resection. The results indicate that these serum proteins might be useful markers for gauging the clinical effect of various treatments on patients.

REFERENCES

1 **Salven P,** Orpana A, Joensuu H. Leukocytes and platelets of

patients with cancer contain high levels of vascular endothelial growth factor. *Clin Cancer Res* 1999; **5:** 487-491
2 **Veikkola T,** Alitalo K. VEGFs, receptors and angiogenesis. *Semin Cancer Biol* 1999; **9:** 211-220
3 **Neufeld G,** Cohen T, Gengrinovitch S, Poltorak Z. Vascular endothelial growth factor (VEGF) and its receptors. *FASEB J* 1999; **13:** 9-22
4 **Linderholm B,** Lindh B, Tavelin B, Grankvist K, Henriksson R. p53 and vascular endothelial growth factor (VEGF) expression predicts outcome in 833 patients with primary breast carcinoma. *Int J Cancer* 2000; **89:** 51-62
5 **Toi M,** Bando H, Ogawa T, Muta M, Hornig C, Weich HA. Significance of vascular endothelial growth factor (VEGF)/soluble VEGF receptor-1 relationship in breast cancer. *Int J Cancer* 2002; **98:** 14-18
6 **Kumar H,** Heer K, Lee PW, Duthie GS, MacDonald AW, Greenman J, Kerin MJ, Monson JR. Preoperative serum vascular endothelial growth factor can predict stage in colorectal cancer. *Clin Cancer Res* 1998; **4:** 1279-1285
7 **George ML,** Eccles SA, Tutton MG, Abulafi AM, Swift RI. Correlation of plasma and serum vascular endothelial growth factor levels with platelet count in colorectal cancer: clinical evidence of platelet scavenging? *Clin Cancer Res* 2000; **6:** 3147-3152
8 **Wartiovaara U,** Salven P, Mikkola H, Lassila R, Kaukonen J, Joukov V, Orpana A, Ristimaki A, Heikinheimo M, Joensuu H, Alitalo K, Palotie A. Peripheral blood platelets express VEGF-C and VEGF which are released during platelet activation. *Thromb Haemost* 1998; **80:** 171-175
9 **Maloney JP,** Silliman CC, Ambruso DR, Wang J, Tuder RM, Voelkel NF. *In vitro* release of vascular endothelial growth factor during platelet aggregation. *Am J Physiol* 1998; **275**: H1054-H1061
10 **Webb NJ,** Bottomley MJ, Watson CJ, Brenchley PE. Vascular endothelial growth factor (VEGF) is released from platelets during blood clotting: implications for measurement of circulating VEGF levels in clinical disease. *Clin Sci (Lond)* 1998; **94:** 395-404
11 **Petrova TV,** Makinen T, Alitalo K. Signaling via vascular endothelial growth factor receptors. *Exp Cell Res* 1999; **253:** 117-130
12 **Kendall RL,** Thomas KA. Inhibition of vascular endothelial cell growth factor activity by an endogenously encoded soluble receptor. *Proc Natl Acad Sci USA* 1993; **90:** 10705-10709
13 **Hornig C,** Barleon B, Ahmad S, Vuorela P, Ahmed A, Weich HA. Release and complex formation of soluble VEGFR-1 from endothelial cells and biological fluids. *Lab Invest* 2000; **80:** 443-454
14 **Inoue T,** Kibata K, Suzuki M, Nakamura S, Motoda R, Orita K. Identification of a vascular endothelial growth factor (VEGF) antagonist, sFlt-1, from a human hematopoietic cell line NALM-16. *FEBS Lett* 2000; **469:** 14-18
15 **Lamszus K,** Ulbricht U, Matschke J, Brockmann MA, Fillbrandt R, Westphal M. Levels of soluble vascular endothelial growth factor (VEGF) receptor 1 in astrocytic tumors and its relation to malignancy, vascularity, and VEGF-A. *Clin Cancer Res* 2003; **9:** 1399-1405
16 **Hornig C,** Weich HA. Soluble VEGF receptors. *Angiogenesis* 1999; **3:** 33-39
17 **Shibuya M.** Structure and dual function of vascular endothelial growth factor receptor-1 (Flt-1). *Int J Biochem Cell Biol* 2001; **33:** 409-420
18 **Benckert C,** Jonas S, Cramer T, Von Marschall Z, Schafer G, Peters M, Wagner K, Radke C, Wiedenmann B, Neuhaus P, Hocker M, Rosewicz S. Transforming growth factor beta1 stimulates vascular endothelial growth factor gene transcription in human cholangiocellular carcinoma cells. *Cancer Res* 2003; **63:** 1083-1092
19 **Salgado R,** Vermeulen PB, Benoy I, Weytjens R, Huget P, Van Marck E, Dirix LY. Platelet number and interleukin-6 correlate with VEGF but not with bFGF serum levels of advanced cancer patients. *Br J Cancer* 1999; **80:** 892-897
20 **Benoy I,** Salgado R, Colpaert C, Weytjens R, Vermeulen PB, Dirix LY. Serum interleukin-6, plasma VEGF, serum VEGF, and VEGF platelet load in breast cancer patients. *Clin Breast Cancer* 2002; **2:** 311-315
21 **Vermeulen PB,** Salven P, Benoy I, Gasparini G, Dirix LY. Blood platelets and serum VEGF in cancer patients. *Br J Cancer* 1999; **79:** 370-373
22 **Tonnesen MG,** Feng X, Clark RA. Angiogenesis in wound healing. *J Investig Dermatol Symp Proc* 2000; **5:** 40-46
23 **Lingen MW.** Role of leukocytes and endothelial cells in the development of angiogenesis in inflammation and wound healing. *Arch Pathol Lab Med* 2001; **125:** 67-71
24 **Verheul HM,** Jorna AS, Hoekman K, Broxterman HJ, Gebbink MF, Pinedo HM. Vascular endothelial growth factor-stimulated endothelial cells promote adhesion and activation of platelets. *Blood* 2000; **96:** 4216-4221
25 **Poon RT,** Lau CP, Cheung ST, Yu WC, Fan ST. Quantitative correlation of serum levels and tumor expression of vascular endothelial growth factor in patients with hepatocellular carcinoma. *Cancer Res* 2003; **63:** 3121-3126
26 **Kikuchi K,** Kubo M, Kadono T, Yazawa N, Tamaki K. Serum concentration of vascular endothelial growth factor in collagen diseases. *Br J Dermatol* 1998; **139:** 1049-1051
27 **Harada M,** Mitsuyama K, Yoshida H, Sakisaka S, Taniguchi E, Kawaguchi T, Ariyoshi M, Saiki T, Sakamoto M, Nagata K, Sata M, Matsuo K, Tanikawa K. Vascular endothelial growth factor in patients with rheumatoid arthritis. *Scand J Rheumatol* 1998; **27:** 377-380
28 **Pinheiro GR,** Andrade CA, Gayer CR, Coelho MS, Freire SM, Scheinberg MA. Serum vascular endothelial growth factor in late rheumatoid arthritis. *Clin Exp Rheumatol* 2001; **19:** 721-723

PO Box 2345, Beijing 100023, China
www.wjgnet.com
wjg@wjgnet.com

ELSEVIER

World J Gastroenterol 2005;11(8):1172-1178
World Journal of Gastroenterology ISSN 1007-9327

• *CLINICAL RESEARCH* •

Synchronous electrogastrographic and manometric study of the stomach as an esophageal substitute

Ferenc Izbéki, Tibor Wittmann, Sándor Ódor, Balázs Botos, Áron Altorjay

Ferenc Izbéki, Tibor Wittmann, Department of Medicine, University of Szeged, Szeged, Korányi fasor 8-10, H-6720, Hungary
Sándor Ódor, Department of Medicine, Saint George University Teaching Hospital, Székesfehérvár, Seregélyesi u. 3., H-8000, Hungary
Balázs Botos, Áron Altorjay, Department of Surgery, Saint George University Teaching Hospital, Székesfehérvár, Seregélyesi u. 3., H-8000, Hungary
Correspondence to: Áron Altorjay M.D., Ph.D., Professor of Surgery, Department of Surgery, Saint George University Teaching Hospital, Seregélyesi u. 3., Székesfehérvár, H-8000, Hungary. altorjay@mail.fmkorhaz.hu
Telephone: +36-22-504-100 Fax: +36-22-504-100
Received: 2004-07-17 Accepted: 2004-09-19

Abstract

AIM: To investigate the electric and contractile mechanisms involved in the deranged function of the transposed stomach in relation to the course of the symptoms and the changes in contractile and electrical parameters over time.

METHODS: Twenty-one patients after subtotal esophagectomy and 18 healthy volunteers were studied. Complaints were compiled by using a questionnaire, and a symptom score was formed. Synchronous electrogastrography and gastric manometry were performed in the fasting state and postprandially.

RESULTS: Eight of the operated patients were symptom-free and 13 had symptoms. The durations of the postoperative periods for the symptomatic (9.1±6.5 mo) and the asymptomatic (28.3±8.8 mo) patients were significantly different. The symptom score correlated negatively with the time that had elapsed since the operation. The percentages of the dominant frequency in the normogastric, bradygastric and tachygastric ranges differed significantly between the controls and the patients. A significant difference was detected between the power ratio of the controls and that of the patients. The occurrence of tachygastria in the symptomatic and the symptom-free patients correlated negatively both with the time that had elapsed and with the symptom score. There was a significant increase in motility index after feeding in the controls, but not in the patients. The contractile activity of the stomach increased both in the controls and in the symptom-free patients. In contrast, in the group of symptomatic patients, the contractile activity decreased postprandially as compared with the fasting state.

CONCLUSION: The patients' post-operative complaints and symptoms change during the post-operative period and correlate with the parameters of the myoelectric and contractile activities of the stomach. Tachygastria seems to be the major pathogenetic factor involved in the contractile dysfunction.

Key words: Transposed stomach; Electrogastrography; Gastric manometry; Post-operative complaints; Contractile dysfunction; Tachygastria

Izbéki F, Wittmann T, Ódor S, Botos B, Altorjay Á. Synchronous electrogastrographic and manometric study of the stomach as an esophageal substitute. *World J Gastroenterol* 2005; 11(8): 1172-1178
http://www.wjgnet.com/1007-9327/11/1172.asp

INTRODUCTION

For reconstruction of the alimentary tract, gastric interposition is the most common procedure in patients with esophageal cancer[1]. Preparation of the stomach, as an esophageal substitute, is associated with substantial alterations: vagotomy is inevitable and the blood supply is reduced. Both truncal and highly selective vagotomy have been found to disrupt the gastric electric activity[2] and to delay the gastric emptying of solids[3]. Consequently, use of the stomach as an esophageal substitute involves multiple influences on the gastric secretion and motility, resulting in post-operative symptoms in both the short and the long-term[4,5]. These motility disorder seems to be a significant problem even in 10-year survivors, who are not satisfied with the daily food intake quantity, with no resulting gain in body weight after surgery[6]. Altered motility, including a gastroesophageal and a duodenogastric reflux, has been attributed to the development of these symptoms[4,7,8]. This complaint has been found to correlate with the weekly occurrence either of reflux or of heartburn, resulting in an increasing number of non-malignancy deaths[6]. However, controversial reports have been published on the functional properties of the stomach as an esophageal substitute after esophagectomy; when pulled up into the chest, the stomach has been claimed to act as an inert organ[7,9,10] whereas others have reported the detection of contractions in the gastric wall on radiological examination[11] and also via manometry and the use of a barostat[12-14]. The frequency and propagation of the gastric contractions are controlled by the myoelectric activities of the stomach, which can be measured by means of cutaneous

electrodes placed on the abdominal skin[15,16]. Synchronized activity has been demonstrated between the gastric contractions and the cutaneous or electromyographic activity[16-18], but this was not observed following total gastrectomy[19,20]. The ingestion of food has been associated with changes in the electromyographic activity that is reflected in both serosal and cutaneous recordings[21,22].

The primary aim of the present study was to investigate the electric and contractile mechanisms involved in the deranged function of the transposed stomach through the synchronous application of electrogastrography and gastric manometry. Secondary objectives were to find a possible correlation between the course of the symptoms and the development of the contractile and electric parameters during time.

MATERIALS AND METHODS

Subjects

Twenty-one patients, 14 men and 7 women, aged 24-72 years (median 56.5), who had undergone subtotal esophagectomy for either cancer (n = 15) or benign disease (n = 6).

All patients were operated on by the same surgeon (AA), as described by Akiyama *et al*[23]. Briefly, following a subtotal resection of the esophagus, gastric substitution was performed in one sitting. The extent of resection of the lesser curvature is determined by a line connecting the highest point in the fundus, points where the vessels of the lesser curvature enter the stomach wall, and the lesser curvature at the junction of the arterial arcades of the right and left gastric arteries. This permits the removal of all potentially-involved lymph nodes while preserving the arterial network to the fundus intact. Preservation of the venous system must be carefully ensured to allow normal venous drainage. The denervated stomach was pulled up into the posterior mediastinum. An esophagogastrostoma was created over the azygos vein in the thoracic dome. The gastric emptying may be impaired after this operation, and thus a pyloroplasty was routinely added in each case[24,25]. No patient had participated in radiotherapy or chemotherapy, which influence the gastrointestinal motility.

Patients, operated upon consecutively between 1997 and 2001, were investigated for a median of 11 (4-38) mo post-operatively. A detailed history of their complaints was taken by using a validated questionnaire adapted from the literature[26-28]. dysphagia, early satiety, postprandial epigastric fullness, retrosternal pain, epigastric pain, regurgitation, nausea and vomiting were scored with regard to severity (0 = not present, 1 = modest, 2 = moderate, 3 = severe and frequency (1 = 2-3 times a month, 2 = once a week, 3 = 2-3 times a week, 4 daily). The maximum sum of scores was 56. Anorexia, diarrhea and symptoms of the dumping syndrome were also recorded.

Control studies were performed on 18 healthy volunteers, 11 men and 7 women, aged 21-58 years (median 42), who had no previous foregut disease or operation.

Each of the subject enrolled into the study signed an informed consent form.

Prior to enrolment, as part of a scheduled follow-up examination, all patients underwent abdominal ultrasonography, thoraco-abdominal CT and upper gastrointestinal endoscopy in order to exclude the relapse of the malignancy and to visually assess the anastomoses.

Manometric study

Synchronous manometric and electrogastrographic examinations were carried out between 9 a.m., and 2 p.m. after overnight fasting.

Manometric studies were performed as described by Collard *et al*[13,14]. The contractile activity of the stomach in each subject was studied by using a six-channel polyvinyl catheter passed through a nostril and positioned in the stomach under fluoroscopic control, so that the recording side-holes were located at distances from the pylorus of 2, 4, 7, 12, 17 and 22 cm in all individuals. Each channel was perfused with distilled water at a rate of 0.6 mL/min. Electric impulses generated by external transducers were transmitted to a polygraphic system (PC Polygram Synectics Medical, Stockholm, Sweden) that was connected to a personal computer via an analogue-digital interface and the data were analyzed.

The subjects were investigated in a semi-supine position, with the upper part of the body elevated at an angle of 50° throughout the study. The fasting gastric motility was recorded for about 2 h; the subjects then consumed a standard semisolid test meal of 800 kcal, and the recording was continued for 2 h postprandially. Significant difference was not observed between the times required for consumption of the test meal by the patients and the controls (16±3 and 15±2.5 min, respectively).

Manometric recordings were evaluated as described by Collard *et al*[13,14]. The baseline was set by using both the manual and automatic baseline calculation systems of the software. The vertical axis was scaled up to reveal waves of <1.2 kPa in an amplitude that cannot be observed on the default scales. The scaled-up manometric recordings were inspected visually on screen and the ones with the most prominent microwaves were selected. As the contractile activities of the distal ports were more pronounced than those of the proximal ones, tracings recorded by one of the three distal ports were chosen. All the waves of the selected tracing were sorted into one of the different predefined classes. Waves were defined as macrowaves if the amplitude was ⩾1.2 kPa, and as microwaves if it was <1.2 kPa. Macrowaves were subclassified further according to amplitude (1.2-6.6 kPa, >6.6-26.6 kPa and >26.6 kPa) and the frequency distribution of both micro and macrowaves was determined for each subject. The numbers of each type of contraction were determined by reading the tracings on screen and the contraction rates were determined by dividing the number of total contractions by the duration of the recording in minutes. The beginnings and ends of the time frames of the different types of waves were recorded in order to select the corresponding electrogastrographic recordings.

A motility index was calculated by dividing the sum of the areas under the macrowaves by the duration of recording time in minutes in the best antral channel during both the fasting and postprandial periods, as described by Collard *et al*[13,14].

The contraction rates were also determined in all subjects, both in the fasting state and postprandially, by counting all

pressure waves in the selected recordings.

Electrogastrography

Electrogastrography was performed as described in Refs[15,29-31]. After the manometric catheter had been positioned, the skin was cleaned and two disposable electrocardiographic electrodes were placed 5-cm apart along the gastric corpus-antrum axis, determined by ultrasonography in the control subjects and localized by the preceding fluoroscopy in the patients. A third, reference electrode was placed on the chest over the liver. Electrogastrographic recordings were started, synchronized with the manometric recordings and performed with a Digitrapper electrogastrograph (Synectics Medical AB, Stockholm, Sweden). All recordings were made at a sampling frequency of 4 Hz. The internal low- and high-pass filters were set at 0.5 and 10 cpm, respectively. The recorded data were processed by a software program (ElectroGastroGram Version 6.3, Gastrosoft Inc., Synectics Medical), using a personal computer. Before the computer-assisted analysis, the total recordings were visually inspected onscreen so as to detect artefacts and to debug the data. The parts of the electrogastrographic recordings which corresponded to the time frame of the evaluated manometric recordings were then selected and were analyzed separately by the computer. The main component of the electrogastrographic recording is the gastric signal. The frequency believed to be of gastric origin and at which the power has a peak value is called the dominant frequency.

The following parameters were evaluated: *Dominant frequency* (*DF*): the frequency with the greatest amplitude within the normal range of gastric slow waves. *Dominant power* (*DP*): the power at the DF. *Power ratio* (*PR*): the ratio of the preprandial and the postprandial DPs. *Percentages of normogastria and dysrhythmia*: *Normogastria* is the percentage of time during which normal slow waves are observed between 2 and 4 cpm. Gastric dysrhythmias are classified as *bradygastria* when the DF peak is in the range 0.5-2 cpm, and as *tachygastria* when it is in the range 4-9 cpm. *Dominant frequency* and *dominant power instability coefficients* (*DFIC* and *DPIC*): the ratio of the standard deviation and the mean of the DF or DP.

Ethical approval

The investigation received prior ethical approval from the local Ethics Committee of Saint George Teaching Hospital. All subjects gave their written informed consent to participate in this study.

Statistical analysis

Normally distributed data are expressed as means and standard deviations while non-normally distributed data are given as medians and full ranges. The Kolmogorov-Smirnov test was used to determine the normal distribution of the data. Manometric data are expressed as medians. For the statistical evaluation of the manometric data, the Wilcoxon signed-rank sum test for paired comparisons and the Mann-Whitney *U*-test for unpaired comparisons were used. Electrogastrographic data are expressed as means and standard deviations. Statistical evaluation of the data was performed by the Independent Samples *t*-test used with between-subjects designs and the Paired Samples *t*-test with within-subjects designs. All the statistical computations were performed with an SPSS 8.0 for Windows software package.

RESULTS

The median of the symptom scores was 5, with a range of 0-39. Eight patients (38%) were totally free of symptoms. On the basis of the symptoms, the operated patients were sub-classified into symptomatic and symptom-free groups. A significant difference was observed between the symptomatic and the asymptomatic patients as concerns the duration of the post-operative period (9.1±6.5 and 28.3±8.8 mo, respectively; $P<0.0001$). Eleven (84.6%) of the symptomatic patients, but only one of the symptom free-patients, had been operated upon within the previous year.

The symptom score correlated negatively with the time that had elapsed since the operation (Pearson's correlation coefficient $r = -0.652$; $P = 0.01$) (Figure 1).

Seven of the symptomatic patients experienced postprandial fullness and 8 others early satiety. Mild early satiety and postprandial fullness occurred 1-3 times a week in 5 patients. The 3 most seriously symptomatic patients reported moderate early satiety and postprandial fullness daily. These symptoms were accompanied by regurgitation in 7 patients, with frequency 2-3 times a week in most cases. Nine patients had mostly mild epigastric pain 1-3 times a week. Seven patients complained of nausea, and in 2 of them it resulted in vomiting. The latter took place 2-3 times a week in the 2 most symptomatic patients. One patient

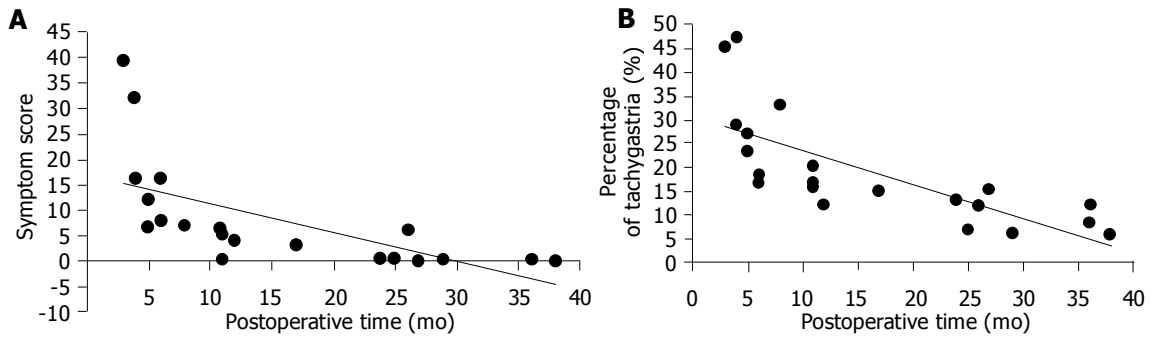

Figure 1 The correlation between the symptom score and the length of the postoperative period in patients after esophagectomy with the stomach as a substitute. A: Symptom score; B: Percentage of tachygastria.

complained of dysphagia. In general, the symptoms were mild or moderate in 85% of the symptomatic patients, and only 2 patients had serious complaints. Four patients (19%) had diarrhea, and 2 (9.5%) had the dumping syndrome; the latter was easily managed by dietary measures.

The results of electrogastrography are summarized in Table 1. The percentages of the DF in the normogastric, bradygastric and tachygastric ranges were significantly different in the healthy control subjects and the operated patients. Food ingestion did not have a significant effect on the percentages of normogastria, bradygastria and tachygastria in either the healthy or the operated group. The DF did not differ significantly between the healthy controls and the patients. The significant increase observed in the DF in the healthy controls in the fed state did not occur in the operated patients. The DFIC was significantly higher in the operated patients without significant postprandial changes. In the patients, the DP did not change significantly in the postprandial period, whereas it increased significantly in the control subjects; this resulted in a significant difference between the two groups. A significant difference in PR was detected between the healthy control subjects and the operated patients. Significant change in the DPIC was not observed between the two groups or after food ingestion.

Table 1 Comparison of fasting and postprandial electrogastrographic variables in healthy control (HC) volunteers and esophagectomized patients with the stomach as a substitute

		HC (n = 18)	Operated (n = 21)	*P* (*HC vs Operated*)
Normogastria (%)	preprandial	79.1±10.5	45.3±20.5	*P*<0.001
	postprandial	81.8±9.8	42.4±23.3	*P*<0.001
	P (*pre- vs postprandial*)	NS	NS	
Bradygastria (%)	preprandial	10.5±5.7	31.1±14.4	*P*<0.001
	postprandial	9.7±6.2	33.2±14.5	*P*<0.001
	P (*pre- vs postprandial*)	NS	NS	
Tachygastria (%)	preprandial	8.4±5.7	18.5±11.4	*P*<0.05
	postprandial	6.8±4.9	20.8±12.1	*P*<0.001
	P (*pre- vs postprandial*)	NS	NS	
DF (cpm)	preprandial	2.81±0.62	3.06±1.80	NS
	postprandial	3.04±0.46	3.51±2.00	NS
	P (*pre- vs postprandial*)	*P*<0.02	NS	
DFIC (%)	preprandial	31.2±12.8	53.6±25.9	*P*<0.001
	postprandial	32.3±14.9	55.0±27.9	*P*<0.001
	P (*pre- vs postprandial*)	NS	NS	
DP (μV^2)	preprandial	927±447	529±450	*P*<0.01
	postprandial	1 399±727	603±578	*P*<0.001
	P (*pre- vs postprandial*)	*P*<0.005	NS	
DPIC (%)	preprandial	80.1±30.0	82.2±36.9	NS
	postprandial	88.3±30.2	83.5±32.4	NS
	P (*pre- vs postprandial*)	NS	NS	
Power ratio		1.75±1.2	1.09±0.18	*P*<0.02

When the electrogastrographic parameters of the symptomatic and the symptom-free patients were analyzed separately, the percentages of tachygastria correlated negatively both with the time that had elapsed since the operation and the symptom score (Pearson's correlation coefficients of -0.652 and -0.740, respectively; $P = 0.01$ for both). The percentages of tachygastria for the symptomatic and the symptom-free patients differed significantly (23.9±11.7 *vs* 10.9±5.03, respectively; *P*<0.003) and similar values were observed in the fed state (24.9±11.7 *vs* 6.8±4.9). The tachygastric fraction in the asymptomatic patients was not significantly different from that in the healthy controls (10.9±5.03 *vs* 8.4±5.7; $P = 0.38$). A correlation could not be established between other electrogastrographic parameters and the time that had elapsed since the operation or the manometric parameters.

Table 2 presents the motility indices in the symptomatic and symptom-free groups of operated patients and in the control subjects during fasting and in the postprandial periods. The motility index increased significantly in the healthy control subjects, reflecting an increased motility after food ingestion, whereas it remained unchanged in both groups of operated patients. Although the motility indices of the symptomatic and asymptomatic groups of operated patients were significantly different, both were significantly lower than that for the healthy volunteers.

Table 2 Fasting and postprandial motility indices in healthy volunteers and in esophagectomized patients with the stomach as a substitute

	Operated (n = 21)				
	Symptomatic	Symptom free	*Significance Symptomatic vs Asymptomatic*	Healthy controls (n = 18)	*Significance Operated vs control*
Preprandial	1.39±0.51	2.38±0.82	*P*<0.01	3.03±0.79	*P*<0.001
Postprandial	1.28±0.81	2.44±1.05	*P*<0.006	7.39±1.90	*P*<0.001
Significance	NS	NS		*P*<0.001	

The rates of contraction are shown in Table 3. The frequency of the contractions detected by manometry is compared with the frequency of the electric activity and expressed as a percentage. The number of contractions per minute is less than the DF in each group of subjects, in both the fasting and the fed state. On an average, only about two-thirds of the electric control activity was detected as contractions. A significant postprandial increase in the contractile rate was seen only in the healthy control subjects.

The fasting and postprandial frequency distributions of the gastric contractions in the healthy volunteers and the two groups of operated patients are depicted in Figure 2.

Significant increases in the 1.2-6.6 kPa, >6.6-26.6 kPa and >26.6 kPa waves were observed in the healthy control subjects postprandially (*P*<0.004 for all). Similarly, significant increases in the >26.6 kPa and >6.6-26.6 kPa waves were observed in the symptom-free operated patients (*P*<0.02 and *P*<0.0001, respectively). Since the preprandial percentage of the waves of 1.2-6.6 kPa waves was significantly higher than that for the healthy controls (12.7% *vs* 27.1%; *P*<0.001), significant postprandial change was not observed. In contrast, in the symptomatic group of patients, the percentage of the waves of 1.2-6.6 kPa did not change postprandially, whereas the >6.6-26.6 kPa waves decreased significantly (*P*<0.002), as compared to the fasting percentage.

Table 3 The response to a test meal of mechanical activity in the stomach of healthy volunteers and of esophagectomized patients with a transposed stomach, expressed as the number of contractions per minute. The electromechanical fractions express the percentage of the dominant frequency that develops mechanical contractions

	Operated patients (n = 21)						Healthy controls (n = 18)	
	Preprandial			Postprandial			Preprandial	Postprandial
	Total	Symptomatic	Asymptomatic	Total	Symptomatic	Asymptomatic		
Contractions	2.16±1.66	2.24±2.01	2.03±0.93	2.19±1.85	2.14±2.28	2.26±0.97	2.2±0.71	2.36±0.73[1]
Electromechanical fraction	68.7±19.4	67.5±22.5	70.5±15.8	62.5±31.0	54.2±32.3	76.0±24.8	78.2±17.6	75.8±18.7

[1]P<0.02.

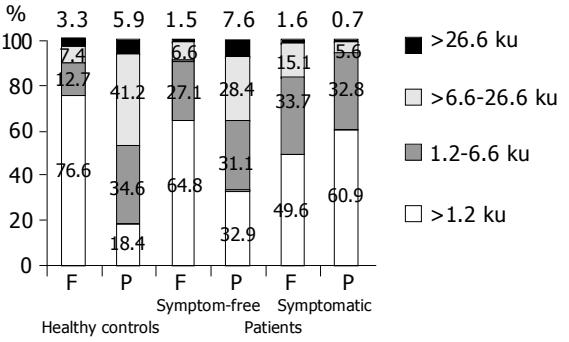

Figure 2 Distribution of intragastric pressure wave classes for healthy controls and operated patients in the fasting (F) and postprandial (P) states.

DISCUSSION

The origin of the complaints in patients, who have undergone oesophagectomy with the stomach substituting for the gullet, is not clearly understood. These symptoms were earlier attributed to the loss of contractility of the transposed stomach[7,9,10], although it has recently been demonstrated that the stomach as an esophageal substitute maintains its contractile activity[12-14,32]. Notwithstanding this preserved contractile activity of the transposed stomach, the patients frequently suffer from symptoms of disordered gastric emptying[33-36] and the pathogenesis remains unresolved. Accordingly, in the present study, we investigated the relationship between the symptoms and the functional properties of the transposed stomach, and also the temporal dimensions. Previous studies had investigated the stomach as an oesophageal replacement either by manometry[13,14,31-33,37] or by electrogastrography[7,19,38], and proved that the transposed stomach generates measurable contractile waves and displays detectable electric activity. In order to evaluate the association between the contractile and electric activities of the transposed stomach in relation to the complaints of the patients, we applied these diagnostic modalities synchronously.

The symptoms of our patients are similar to those reported for the late results of esophagectomy with the stomach as substitute[39-41]. Postprandial fullness and vomiting have been shown to be likely consequences of delayed gastric emptying[42,43]. Half of our symptomatic patients reported postprandial fullness, which, together with the disordered contractile activity and dysrhythmias detected, implies impaired gastric emptying. The dumping syndrome and diarrhea was less frequent than reported in Ref.[44]. All of our patients with symptoms of delayed gastric emptying had been operated on within a year of the assessment. The prevalence of symptoms in our patients operated on within the previous year corresponds to or is somewhat better than the literature data[41,44]. As concerns the severity of the symptoms in our patients, which were assessed semi-quantitatively by using a scoring system, the median score proved to be less than that reported in diabetic patients with dyspepsia[26].

Our results indicate that the changes in the distribution of the gastric wall contraction waves are most pronounced in the group of symptomatic patients. The mechanical activity of the transposed stomach was affected most, both in the fasting and in the postprandial state, and resulted in the most prominent symptoms. As regards the groups of patients in whom the stomach is utilized as a substitute after esophagectomy, the motility indices of the stomach remained lower and more pronounced in the symptomatic patients. Feeding normally induces increases in the gastric motility indices, but this did not occur in either group of our operated patients. The discrimination of different types of contraction waves on the basis of their amplitudes and analysis of the frequency and distribution demonstrated a lack of postprandial modification of the gastric motor patterns; moreover, a significant decrease in the percentage of >6.6-26.6 kPa wave contractions was observed in the symptomatic patients, as another manifestation of an insufficient gastric motor activity. In contrast, *Collard and Ramagnoli* reported a postprandial increase in contractile activity, but we observed this only in the healthy controls in our study, and not in the patients. This controversy might be explained by the longer post-operative period in the earlier study[14]. Indeed, after feeding, the higher-amplitude contractile activities were found to be lower in our symptomatic patients, whereas an improvement was observed in the patients free of symptoms. The combined application of manometry and electrogastrography demonstrated a good correlation between the changes in slow wave activity and the mechanical performance. This is characterized by bradygastria and decreased DP; additionally, the postprandial increase in myoelectric activity that occurred in the healthy persons was not observed in the operated patients. Nonetheless, the DFs in the healthy controls and the patients did not differ significantly, which points to a preserved gastric pacemaker activity. These observations provide further evidence that the changes in both electric and motor activities are results of vagotomy[2].

The postprandial increases in DF and DP that were observed

in our healthy control subjects are well known[16,30,31,45,46]. A postprandial increase in the DFIC did not occur either in the healthy controls or in the patients, though this instability was significantly greater in the patients in both the fasting and the postprandial states, which reveals a more unstable electric state. The postprandial change in the DP is thought to be a result of the spatial change in the position of the stomach[30]. The significant decrease in DP in the operated patients might therefore, reflect the transposition of the stomach rather than being a consequence of an altered function.

The frequency of contractions in our study was lower than that reported by *Collard and Ramagnoli*[14] and even the DF detected by electrogastrography. This could be a consequence of the methodological difference. We counted all the contractions in a selected tracing, while *Collard and Ramagnoli* counted the contractions in 3 different antral strips of 10 min each. On the other hand, a difference between the rate of the electrical control activity and contractile activity has also been detected by others in dogs by synchronous serosal electric recordings and intragastric manometry[47].

In the pathogenesis of the symptoms of esophagectomized patients, gastric vagal denervation has been shown to play a role[33,48-50]. Accordingly, a novel surgical technique was elaborated recently to spare the vagal nerves, especially in patients operated on with benign esophageal diseases[51]. After vagotomy, delayed gastric emptying of a solid meal was observed in the early postoperative period, but after a year the gastric emptying in patients with either truncal or selective vagotomy did not differ from that in controls[48]. Vagotomy has been shown to result in a disorganization of the basic electric rhythm in dogs[52], and tachygastria has been demonstrated by implanted gastric electrodes in patients with truncal vagotomy[50]. This is in accord with the relatively low prevalence and a diminishing tendency with time of the symptoms of delayed gastric emptying in our patients.

Our present data are consistent with reports on the denervated stomach as an esophageal replacement that has been shown to act as a contractile organ, this contractile activity being recovered postoperatively over time[13]. However, the recovery of the motor response is not complete, as indicated by the diminished response of the motility indices to a test meal even in the asymptomatic group of patients. A clear difference was observed in the lengths of post-operative periods of the symptomatic and the symptom-free patients: a majority of the symptomatic patients had been operated on within 1 year, whereas the symptom-free patients have had surgery more than 2 years previously. *Collard* reported recovery of the contractile activity over a 3-year period[13].

An important phenomenon is the tachygastria that occurs in the transposed stomach, which exhibits a tendency to return to normogastria in time. Tachygastria has been documented in patients with functional dyspepsia and delayed gastric emptying[39,52]. Tachygastria too has been shown to be accompanied by the absence of contractility in vagotomized dogs[52] and humans after vagotomy with[45] or without symptoms of altered gastric emptying. This might be a consequence of the disturbed proximal-distal coordination of pacemaker activity in the smooth muscle. The negative correlation between the symptoms of our patients and the postoperative time, together with the significant difference between the percentages of tachygastria in the symptomatic and asymptomatic patients suggests that tachygastria could be one of the important factors playing a role in the pathogenesis of the complaints. This is supported by the observation that significant tachygastria was not detected in the asymptomatic patients or the healthy controls. These data suggest that the complaints of patients with a transposed stomach are consequences of a decrease in the electromechanical activity of the stomach. Electrogastrography itself is a useful method with which to provide important information on the gastric motility in these patients.

The major new findings of our present study are the time dependency of the post-operative complaints and symptoms of the patients, and their correlation with the parameters of the myoelectric and contractile activities of the stomach, obtained by simultaneous electrogastrographic and manometric investigations. The processes of electromechanical adaptation in the transposed stomach result in decreases in time of the postoperative symptoms in patients after esophagectomy. Tachygastria seems to be the major pathogenetic factor involved in the contractile dysfunction.

REFERENCES

1 **Skinner DB.** Esophageal reconstruction. *Am J Surg* 1980; **139:** 810-814

2 **Geldof H,** van der Schee EJ, van Blankenstein M, Smout AJ, Akkermans LM. Effects of highly selective vagotomy on gastric myoelectrical activity. An electrogastrographic study. *Dig Dis Sci* 1990; **35:** 969-975

3 **Malagelada JR,** Rees WD, Mazzotta LJ, Go VL. Gastric motor abnormalities in diabetic and postvagotomy gastroparesis: effect of metoclopramide and bethanechol. *Gastroenterology* 1980; **78:** 286-293

4 **Hölscher AH,** Voit H, Buttermann G, Siewert JR. Function of the intrathoracic stomach as esophageal replacement. *World J Surg* 1988; **12:** 835-844

5 **Nishihira T,** Watanabe T, Ohmori N, Kitamura M, Toyoda T, Hirayama K, Kawachi S, Kuramoto J, Kanoh T, Akaishi T. Long-term evaluation of patients treated by radical operation for carcinoma of the thoracic esophagus. *World J Surg* 1984; **8:** 778-785

6 **Baba M,** Aikou T, Natsugoe S, Kusano C, Shimada M, Kimura S, Fukumoto T. Appraisal of ten-year survival following esophagectomy for carcinoma of the esophagus with emphasis on quality of life. *World J Surg* 1997; **21:** 282-285; discussion 286

7 **Bonavina L,** Anselmino M, Ruol A, Bardini R, Borsato N, Peracchia A. Functional evaluation of the intrathoracic stomach as an oesophageal substitute. *Br J Surg* 1992; **79:** 529-532

8 **Mannell A,** Hinder RA, San-Garde BA. The thoracic stomach: a study of gastric emptying, bile reflux and mucosal change. *Br J Surg* 1984; **71:** 438-441

9 **Moreno-Osset E,** Tomas-Ridocci M, Paris F, Mora F, Garcia-Zarza A, Molina R, Pastor J, Benages A. Motor activity of esophageal substitute (stomach, jejunal, and colon segments). *Ann Thorac Surg* 1986; **41:** 515-519

10 **Morton KA,** Karwande SV, Davis RK, Datz FL, Lynch RE. Gastric emptying after gastric interposition for cancer of the esophagus or hypopharynx. *Ann Thorac Surg* 1991; **51:** 759-763

11 **Huang GJ,** Wang LJ, Liu JS, Cheng GY, Zhang DW, Wang GQ, Zhang RG. Surgery of esophageal carcinoma. *Semin Surg*

Oncol 1985; **1:** 74-83
12 **Logeman F,** Roelofs JM, Obertop H, Akkermans LM. Tonic motor activity of the narrow gastric tube used as an oesophageal substitute. *Eur J Surg* 2000; **166:** 301-306
13 **Collard JM,** Romagnoli R, Otte JB, Kestens PJ. The denervated stomach as an esophageal substitute is a contractile organ. *Ann Surg* 1998; **227:** 33-39
14 **Collard JM,** Romagnoli R. Human stomach has a recordable mechanical activity at a rate of about three cycles/minute. *Eur J Surg* 2001; **167:** 188-194
15 **Chen JD,** Richards RD, McCallum RW. Identification of gastric contractions from the cutaneous electrogastrogram. *Am J Gastroenterol* 1994; **89:** 79-85
16 **Smout AJ,** van der Schee EJ, Grashuis JL. What is measured in electrogastrography? *Dig Dis Sci* 1980; **25:** 179-187
17 **Hamilton JW,** Bellahsene BE, Reichelderfer M, Webster JG, Bass P. Human electrogastrograms. Comparison of surface and mucosal recordings. *Dig Dis Sci* 1986; **31:** 33-39
18 **Mintchev MP,** Kingma YJ, Bowes KL. Accuracy of cutaneous recordings of gastric electrical activity. *Gastroenterology* 1993; **104:** 1273-1280
19 **Homma S,** Shimakage N, Yagi M, Hasegawa J, Sato K, Matsuo H, Tamiya Y, Tanaka O, Muto T, Hatakeyama K. Electrogastrography prior to and following total gastrectomy, subtotal gastrectomy, and gastric tube formation. *Dig Dis Sci* 1995; **40:** 893-900
20 **Kaiho T,** Shimoyama I, Nakajima Y, Ochiai T. Gastric and non-gastric signals in electrogastrography. *J Auton Nerv Syst* 2000; **79:** 60-66
21 **Kuhlbusch R,** Zacchi-Deutschbein P, Frieling T, Lubke HJ, Enck P. Postprandial changes of electrical activity of the stomach after different meals. *Z Gastroenterol* 1998; **36:** 885-886, 889-891
22 **Lin Z,** Chen JD, Schirmer BD, McCallum RW. Postprandial response of gastric slow waves: correlation of serosal recordings with the electrogastrogram. *Dig Dis Sci* 2000; **45:** 645-651
23 **Akiyama H,** Miyazono H, Tsurumaru M, Hashimoto C, Kawamura T. Use of the stomach as an esophageal substitute. *Ann Surg* 1978; **188:** 606-610
24 **Altorjay A,** Kiss J, Voros A, Sziranyi E. The role of esophagectomy in the management of esophageal perforations. *Ann Thorac Surg* 1998; **65:** 1433-1436
25 **Altorjay A,** Paszti I, Kiss J, Tasnadi G. Gastrojejunal interposition for esophageal replacement. *Pediatr Surg Int* 1999; **15:** 132-134
26 **Pfaffenbach B,** Wegener M, Adamek RJ, Schaffstein J, Lee YH, Ricken D. Antral myoelectric activity, gastric emptying, and dyspeptic symptoms in diabetics. *Scand J Gastroenterol* 1995; **30:** 1166-1171
27 **Keshavarzian A,** Iber FL, Vaeth J. Gastric emptying in patients with insulin-requiring diabetes mellitus. *Am J Gastroenterol* 1987; **82:** 29-35
28 **Horowitz M,** Harding PE, Maddox AF, Wishart JM, Akkermans LM, Chatterton BE, Shearman DJ. Gastric and oesophageal emptying in patients with type 2 (non-insulin-dependent) diabetes mellitus. *Diabetologia* 1989; **32:** 151-159
29 **Lindberg G,** Iwarzon M, Hammarlund B. 24-hour ambulatory electrogastrography in healthy volunteers. *Scand J Gastroenterol* 1996; **31:** 658-664
30 **Pfaffenbach B,** Adamek RJ, Kuhn K, Wegener M. Electrogastrography in healthy subjects. Evaluation of normal values, influence of age and gender. *Dig Dis Sci* 1995; **40:** 1445-1450
31 **Chen JZ,** McCallum RW. Electrogastrographic parameters and their clinical significance. In: Chen JZ and McCallum RW, eds. Electrogastrography: Principles and Applications. *New York: Raven Press, Ltd* 1994: 45-73
32 **Walsh TN,** Caldwell MT, Fallon C, McGeown G, Kidney D, Freyne P, Byrne PJ, Hennessy TP. Gastric motility following oesophagectomy. *Br J Surg* 1995; **82:** 91-94
33 **Nakabayashi T,** Mochiki E, Garcia M, Haga N, Kato H, Suzuki T, Asao T, Kuwano H. Gastropyloric motor activity and the effects of erythromycin given orally after esophagectomy. *Am J Surg* 2002; **183:** 317-323
34 **Hill AD,** Walsh TN, Hamilton D, Freyne P, O'Hare N, Byrne PJ, Hennessy TP. Erythromycin improves emptying of the denervated stomach after oesophagectomy. *Br J Surg* 1993; **80:** 879-881
35 **Mannell A,** McKnight A, Esser JD. Role of pyloroplasty in the retrosternal stomach: results of a prospective, randomized, controlled trial. *Br J Surg* 1990; **77:** 57-59
36 **Collard JM,** Romagnoli R, Otte JB, Kestens PJ. Erythromycin enhances early postoperative contractility of the denervated whole stomach as an esophageal substitute. *Ann Surg* 1999; **229:** 337-343
37 **Del Poli M,** Mioli P, Gasparri G, Casalegno PA, Camandona M, Bronda M, Albertino B, Cassolino P. Functional study of intestinal transplants after esophagectomy. *Minerva Chir* 1991; **46:** 241-245
38 **Ravelli AM,** Spitz L, Milla PJ. Gastric emptying in children with gastric transposition. *J Pediatr Gastroenterol Nutr* 1994; **19:** 403-409
39 **Labbe F,** Pradere B, Tap G, Bloom E, Gouzi JL. Late morbidity after esophagectomy for cancer: is partial esophagectomy preferred? *Chirurgie* 1998; **123:** 468-473
40 **Fok M,** Cheng SW, Wong J. Pyloroplasty versus no drainage in gastric replacement of the esophagus. *Am J Surg* 1991; **162:** 447-452
41 **De Leyn P,** Coosemans W, Lerut T. Early and late functional results in patients with intrathoracic gastric replacement after oesophagectomy for carcinoma. *Eur J Cardiothorac Surg* 1992; **6:** 79-84; discussion 85
42 **Sarnelli G,** Caenepeel P, Geypens B, Janssens J, Tack J. Symptoms associated with impaired gastric emptying of solids and liquids in functional dyspepsia. *Am J Gastroenterol* 2003; **98:** 783-788
43 **Stanghellini V,** Tosetti C, Paternic A, Barbara G, Morselli-Labate AM, Monetti N, Marengo M, Corinaldesi R. Risk indicators of delayed gastric emptying of solids in patients with functional dyspepsia. *Gastroenterology* 1996; **110:** 1036-1042
44 **McLarty AJ,** Deschamps C, Trastek VF, Allen MS, Pairolero PC, Harmsen WS. Esophageal resection for cancer of the esophagus: long-term function and quality of life. *Ann Thorac Surg* 1997; **63:** 1568-1572
45 **Gonlachanvit S,** Chey WD, Goodman KJ, Parkman HP. Effect of meal size and test duration on gastric emptying and gastric myoelectrical activity as determined with simultaneous [13C] octanoate breath test and electrogastrography in normal subjects using a muffin meal. *Dig Dis Sci* 2001; **46:** 2643-2650
46 **Geldof H,** van der Schee EJ, van Blankenstein M, Grashuis JL. Electrogastrographic study of gastric myoelectrical activity in patients with unexplained nausea and vomiting. *Gut* 1986; **27:** 799-808
47 **You CH,** Chey WY. Study of electromechanical activity of the stomach in humans and in dogs with particular attention to tachygastria. *Gastroenterology* 1984; **86:** 1460-1468
48 **Howlett PJ,** Sheiner HJ, Barber DC, Ward AS, Perez-Avila CA, Duthie HL. Gastric emptying in control subjects and patients with duodenal ulcer before and after vagotomy. *Gut* 1976; **17:** 542-550
49 **Aeberhard P,** Bedi BS. Effects of proximal gastric vagotomy (PGV) followed by total vagotomy (TV) on postprandial and fasting myoelectrical activity of the canine stomach and duodenum. *Gut* 1977; **18:** 515-523
50 **Hocking MP.** Postoperative gastroparesis and tachygastria-response to electric stimulation and erythromycin. *Surgery* 1993; **114:** 538-542
51 **Banki F,** Mason RJ, DeMeester SR, Hagen JA, Balaji NS, Crookes PF, Bremner CG, Peters JH, DeMeester TR. Vagal-sparing esophagectomy: a more physiologic alternative. *Ann Surg* 2002; **236:** 324-335; discussion 335-336
52 **Schippers E,** Vantrappen G, Braun J, Schumpelick V. Electromyographic and manometric studies of stomach motility after vagotomy. *Z Gastroenterol* 1991; **29:** 581-584

PO Box 2345, Beijing 100023, China
www.wjgnet.com
wjg@wjgnet.com

ELSEVIER

World J Gastroenterol 2005;11(8):1179-1181
World Journal of Gastroenterology ISSN 1007-9327

• *CLINICAL RESEARCH* •

An anomaly in persistent right umbilical vein of portal vein diagnosed by ultrasonography

Shigeo Nakanishi, Katsuya Shiraki, Kouji Yamamoto, Mutsumi Koyama, Takeshi Nakano

Shigeo Nakanishi, Katsuya Shiraki, Kouji Yamamoto, Takeshi Nakano, First Department of Internal Medicine, Mie University School of Medicine, Tsu, Mie 514-8507, Japan
Shigeo Nakanishi, Mutsumi Koyama, Matsusaka Central General Hospital of Medicine, Matsusaka, Mie 515-2161, Japan
Correspondence to: Katsuya Shiraki, M.D., Ph.D. First Department of Internal Medicine, 2-174, Edobashi, Tsu, Mie, 514-8507, Japan. katsuyas@clin.medic.mie-u.ac.jp
Telephone: +81-59-231-5015 Fax: +81-59-231-5201
Received: 2004-04-10 Accepted: 2004-07-17

Abstract

AIM: To detect the anomaly in the persistent right umbilical vein (PRUV) of portal vein (PV) with deviation of the ligamentum tere and left-sided gallbladder.

METHODS: A total of 5783 candidates for routine analysis were evaluated for hepatic vascular abnormalities by ultrasonography.

RESULTS: Ten candidates (0.17%) had a portal vein anomaly with a rightward-deviated ligamentum tere. The blood-flow velocity in the PRUV of the portal vein (17.7±3.0 cm/s) of the 10 cases was similar to that of the right anterior portal trunk (17.6±4.1 cm/s). However, the vessel diameter of the PRUV (φ12.4±4.4 mm) was larger than the right anterior portal trunk (j6.1±0.9 mm). Therefore, flow volume in the anomalous portion (0.97±0.30 L/min) was more than that in the right anterior portal trunk (0.18±0.05 L/min).

CONCLUSION: The anomaly plays an important role in intra-hepatic PV flow.

Key words: PV anomaly; Persistent right umbilical vein; Ultrasonography

Nakanishi S, Shiraki K, Yamamoto K, Koyama M, Nakano T. An anomaly in persistent right umbilical vein of portal vein diagnosed by ultrasonography. *World J Gastroenterol* 2005; 11(8): 1179-1181
http://www.wjgnet.com/1007-9327/11/1179.asp

INTRODUCTION

Abdominal ultrasonography (US) is a routine clinical method of examining the liver. The classification of Couinaud is used at present in order to divide the liver into 8 areas counter-clockwise from the caudate lobe. In this classification, the portal vein (PV) dominates an area, and the hepatic vein becomes a boundary in each area. Therefore, understanding the main root and branching of the PV is very important.

We observed an anomaly in the persistent right umbilical vein (PRUV) of PV first described by Matsumoto[1] in 1986, who noted the absence of the umbilical portion of the left PV from its normal site and deviation of the ligamentum teres to the right. Therefore, we investigated the prevalence of PRUV during routine ultrasonography screening.

MATERIALS AND METHODS

Between April 1995 and March 1996, 5 783 (3 227 men, 2 556 women) subjects underwent abdominal US at Matsusaka Central General Hospital. We had detected anomalous portal branching of PRUV in 10 persons. Ten men and 10 women were enrolled in this study.

An ALOKA SSD-650 ultrasound machine with 3.5 MHz convex array probes was used. Then we routinely assessed PV flow by duplex sonography (combined real-time and pulsed Doppler) employing an EUB-565A transducer with 3.5-5.0 MHz (Hitachi, Japan). The wall-filter was set at 50-100 Hz. Sample volume was maintained below 5 mm and located at the center of each vessel. The spectral waveform was angle-corrected and the Doppler angles of incidence were less than 60°. We observed anomalous portal vein branching system by B-mode method. Then we investigated blood vessel diameter, mean velocity and mean flow volume with pulse wave Doppler methods, and compared the left side umbilical portion with normal group of patients and trunk of the PRUV. Pulsed Doppler US was performed in the supine position, using mechanical ventilation or quiet breathing in a fasting state. The sample point of the pulsed Doppler US examination was placed at the center of the umbilical portion.

RESULTS

Anomaly of the PRUV of PV was incidentally detected during a routine abdominal US. The prevalence of this anomaly was 0.17% (10 of 5 783). Three men and 7 women aged 20-81 years (mean, 53.9 years) had the anomaly. In these patients with PRUV at the portal hepatis, the portal trunk first gave rise to a branch to the right posterior segment. The left PV which normally runs horizontally at this level was absent, and there was no major branch to the right anterior segment. The portal trunk then ran upward and gave off a branch to the left lobe. At this point, the PV

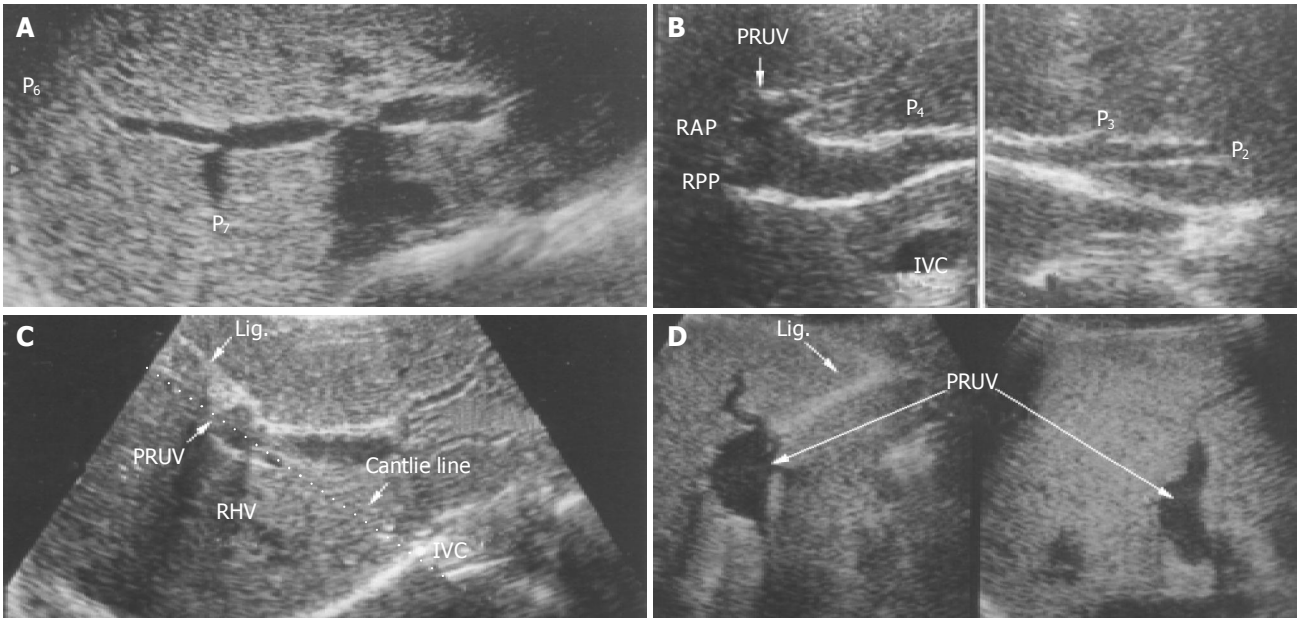

Figure 1 Persistent right umbilical vein shown on ultrasonogram. A: Right posterior portal branch originating from the main portal vein at the portal hepatis; B: Anterior portal branch and P_4 branch of the portal vein originating from the umbilical portion; C, D: Persistent right umbilical vein on the Cantlie line; PRUV: Persistent right umbilical vein; RAP: right anterior portal vein; RPP: right posterior portal vein; Lig: Ligamentum teres; RHV: Right hepatic vein.

made a U-turn in a right anterior direction and downward, giving off branches to the right anterior segment and small branches to the left lobe. The umbilical portion was not identified at its usual position (i.e., in the left PV between the medial and lateral segments of the liver). Instead, a U-shaped part resembling the umbilical portion was seen above the gallbladder fossa (i.e., on the Cantlie line). Right anterior segment and quadrate lobe of the liver were supplied from the entire part of the PRUV (Figure 1).

We then examined the blood vessel diameter of the PRUV and the right anterior portal trunk. The diameter of normal adult right anterior portal trunk was 6.1±0.9 mm (5.9±0.9 mm for men, 6.4±1.0 mm for women) and that of the PRUV was 12.4±4.4 mm (men 16.0±2.4 mm, women 10.1±3.8 mm). Therefore, the PRUV was significantly enlarged. The mean flow velocity in the PRUV was 17.7±3.0 cm/s (17.6±3.1 cm/s for men, 17.1±3.1 cm/s for women) and that of the right anterior portal trunk was 17.6±4.1 cm/s (16.0±3.2 cm/s for men, 18.9±3.4 cm/s for women) demonstrating no difference. However, the mean flow volume of right anterior portal trunk 0.20±0.06 L/min, 0.18±0.05 L/min for men, 21±0.06 L/min for women) was significantly lower than that of the PRUV 0.97±0.30 L/min (1.21±0.21 L/min for men (0.82±0.34 L/min for women) Table 1.

In patients with this anomaly, the PRUV lay astride the ligamentum teres, or on the left side of the ligamentum teres of the gallbladder (i.e., left-sided gallbladder) (Figure 2).

Only in 1 of these 10 cases, the neck of the gallbladder began diagonally opposite the main PV. The gallbladder body went in the direction of the left side and fundus was enlarged to the left side of the above mesenteric artery (Figure 3). In two patients, the left hepatic vein was shunted from the top of the PRUV to the portal branch to the inside of the left-lobe. Turbulent blood-flow together with portal venous shunt was observed at the PRUV (Figure 4). Two patients underwent hepatic resection because of an intra-hepatic bile duct stone in the right posterior segment. Furthermore, 1 patient showed malrotation of the intestine in the colon fiberscopic examination.

Table 1 Comparison of blood vessel diameter, blood flow velocity and volume comparison between normal persons (NP) and patients with PRPV (mean±SD)

	Patients with		
	NP	PRUV	*P*
Vessel diameter (φ^{mm})			
Male	5.9±0.9 (*n*=10)	16.0±2.4 (*n* = 4)	<0.01
Female	6.4±1.0 (*n* = 10)	10.1±3.8 (*n* = 6)	<0.01
Total	6.1±0.9 (*n* = 20)	12.4±4.4 (*n* = 10)	<0.01
Mean velocity (cm/s)			
Male	17.6±3.1 (*n* = 10)	16.0±3.2 (*n* = 4)	NS
Female	17.1±3.1 (*n* = 10)	18.9±3.4 (*n* = 6)	NS
Total	17.7±3.0 (*n* = 20)	17.6±4.1 (*n* = 10)	NS
Flow volume (L/min)			
Male	0.18±0.05 (*n* = 10)	1.21±0.21 (*n* = 4)	<0.01
Female	0.21±0.06 (*n* = 10)	0.82±0.34 (*n* = 6)	<0.01
Total	0.20±0.06 (*n* = 20)	0.97±0.30 (*n* = 10)	<0.01

Note: NP, Normal group of patient; PRUV, Persistent right umbilical vein.

DISCUSSION

The prevalence of PRUV ranges from 0.1% to 0.7%, according to previous reports[1,2,3,6]. The reported prevalence is almost equivalent to 0.17% (10 of 5 783) in our present study. Other studies have reported a higher prevalence, which is 1.2% in the computed tomography study of Maetani *et al*.[8]. This difference is probably due to the absence of an ultrasonographic examination. Infect, 4 of 10 cases in our study were not detected for this anomaly during a previous examination. Therefore, this anomaly should be kept in mind during ultrasonographic examination.

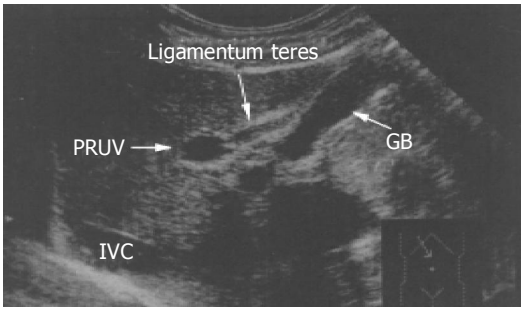

Figure 2 Persistent right umbilical vein of the portal vein astride the igamentum teres of the gallbladder. PRUV: persistent right umbilical vein; GB: gallbladder; IVC: inferior vena cava.

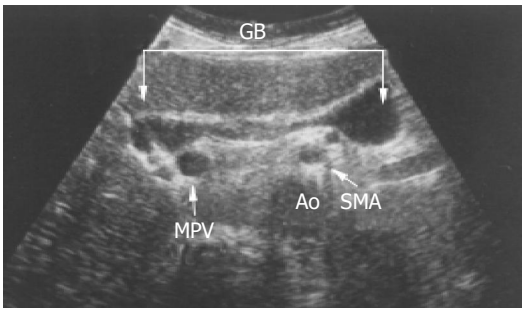

Figure 3 A case of persistent right umbilical vein with left-sided gallbladder. GB: gallbladder; MPV: main portal vein; Ao: abdominal aorta.

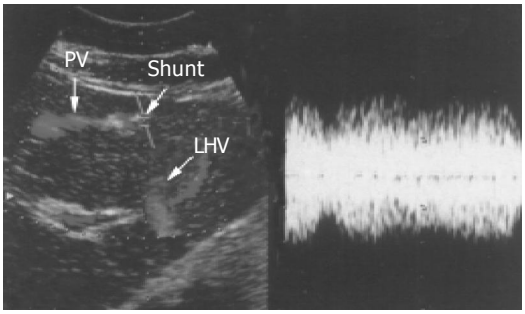

Figure 4 Persistent right umbilical vein with portal venous shunt of the P3 and left hepatic vein. LHV: left hepatic vein; PV: portal vein.

A striking feature of this anomaly is the deviation of the ligamentum teres to the right, accompanying a PRUV. Therefore, the PRUV becomes a decisive factor to confirm the position of this ligamentum teres. The male to female ratio of this anomaly is reported to be 2∶3 according to Yamasaki *et al*.[9]. Our study showed a 4∶6 ratio of male to female with this anomaly.

Blood vessel diameter and mean flow volume were clearly increased in the right umbilical portion compared to that of right anterior portal trunk. The reason is probably that right umbilical portion plays a role in the right anterior segment branch and the left lobe branch from main portal vein.

Ramification in some major branches at more distal levels is the most important clinical feature of this PV anomaly. A risk for hepatic necrosis increases in liver resection otherwise an anomalous portal trunk is well understood at the peripheral branch level. Dissection of the liver along the right side of the ligamentum teres, as is usually performed in the donor's liver during a partial liver transplantation, may cause a circulatory disturbance of a wide area of the right lobe. Therefore, it is important to understand the portal running by US before operation. In addition, this portal anomaly always accompanies the abnormal position of the left side of the gallbladder (left-sided gallbladder).

Gross[6] proposed two hypotheses for the origin of a left-sided gallbladder. The normal gallbladder migrates to the left lobe instead of the right and localizes at, the left side of the ligamentum teres. An accessory gallbladder may arise from the left hepatic duct while the normal gallbladder fails to develop.

However, Ozeki *et al*.[4] reported a case of left-sided gallbladder with a PV anomaly and proposed another origin. They suggested that the gallbladder is situated on the left side of the ligamentum teres simply because the latter deviates to the right. Furthermore, Kimura *et al*.[5] and Yamasaki *et al*.[9] reported a case of portal in front of the duodenum. Infrahepatic inferi should be looked for during routine US screening or vena cava defect[10], multiple spleens, malrotation of the intestine and annular pancreas with PRUV should be considered.

In conclusion, PV anomaly has important clinical implications in preoperative examination of the liver, and should be looked for during routine screening.

REFERENCES

1 **Matsumoto H**. A newer concept of the segments of the liver. *Jpn J Med Ultrasonics* 1986; **13**: 551-552
2 **Ozeki Y**, Onitsuka A, Hayasi K, Sasaki E. A case of left-sided gallbladder with anomalous branching of the intrahepatic portal vein. *J Jpn Surg Soc* 1987; **88**: 1644-1650
3 **Kuwayama M**, Takeuchi K, Tsuruoka N, Inoue S, Shiroyama M, Tsuru T, Nakanishi N. Ultrasonic evaluation of the different branching patterns of the portal vein in the hepatic hilum. *Jpn J Med Ultrasonics* 1989; **16**: 346-353
4 **Ozeki Y**, Onitsuka A, Hino A, Matsunami H, Nishida H, Saito K, Shimokawa K, Hirose H. Anomalous branching of the intrahepatic portal vein associated with anomalous position of round ligament: Report of cases. *Acta Hepatl Jpn* 1989; **30**: 372-377
5 **Kimura A**, Takayasu K, Yamada T, Makuuchi M, Yamazaki S, Hasegaya H. Congenital anomaly of the intrahepatic portal system complicated by intrahepatic cholangio cellular carcinoma: A case report. *Jpn J Gastroenterol Surg* 1990; **23**: 787-790
6 **Gross RE**. Congenital anomalies of the gallbladder: A review of one hundred and forty eight cases, with report of a double gallbladder. *Arch Surg* 1936; **32**: 131-162
7 **Couinaud C**. Surgical anatomy of the liver revisited: Embryology. C. Couinaud, Paris, pp 11-24
8 **Maetani Y**, Itoh K, Kojima N, Tabuchi T, Shibata T, Asonuma K, Tanaka K, Konishi J. Portal vein anomaly associated with deviation of the ligamentum teres to the right and malposition of the gallbladder. *Radiology* 1998; **207**: 723-728
9 **Yamasaki H**, Miyazaki S, Tanemura K, Morimoto Y, Kijima H, Sakamoto T, Yamasaki Y, Kuwata K, Hukuoka A, Kitada H. Clinical significance of anomalous Branching of intrahepatic portal vein. *Jpn J Med Ultrasonics* 1991; **18**: 436-443
10 **Kitamura T**, Takeuchi K, Murashima N, Hashimoto M, Yoshida Y, Kurosaki A, Kuwayama M. A case of an anomalous of the intrahepatic portal combined With Azygos continuation of the IVC. *Jpn J Med Ultrasonics* 1987; **51:** 845-846

PO Box 2345, Beijing 100023, China
www.wjgnet.com
wjg@wjgnet.com

ELSEVIER

World J Gastroenterol 2005;11(8):1182-1186
World Journal of Gastroenterology ISSN 1007-9327

• *BRIEF REPORTS* •

Long-term follow-up after complete ablation of Barrett's esophagus with argon plasma coagulation

Ahmed Madisch, Stephan Miehlke, Ekkehard Bayerdoerffer, Birgit Wiedemann, David Antos, Anke Sievert, Michael Vieth, Manfred Stolte, Heinrich Schulz

Ahmed Madisch, Stephan Miehlke, Medical Department I, Technical University Hospital, Dresden, Germany
Ekkehard Bayerdörffer, Department of Hematology and Oncology, University Hospital Marburg, Germany
Bärbel Wiedemann, Institute of Medical Statistics and Biometry, Technical University Hospital, Dresden, Germany
David Antos, Clinic for Pediatric Diseases, Ludwig-Maximilians-University-Hospital Munich, Germany
Heinrich Schulz, Anke Sievert, Gastroenterologist in private practice, Bremen, Germany
Michael Vieth, Institute of Pathology, Otto-von Guericke-University of Magdeburg, Germany
Manfred Stolte, Institute of Pathology, Klinikum Bayreuth, Bayreuth, Germany
Correspondence to: Ahmed Madisch, M.D., Medical Department I, Technical University Hospital, Fetscherstr. 74, D-01307 Dresden, Germany. madisch@mk1.med.tu-dresden.de
Telephone: +49-351-458-4702 Fax: +49-351-458-4394
Received: 2004-07-28 Accepted: 2004-09-09

Abstract

AIM: To report the long-term outcome of patients after complete ablation of non-neoplastic Barrett's esophagus (BE) with respect to BE relapse and development of intraepithelial neoplasia or esophageal adenocarcinoma.

METHODS: In 70 patients with histologically proven non-neoplastic BE, complete BE ablation was achieved by argon plasma coagulation (APC) and high-dose proton pump inhibitor therapy (120 mg omeprazole daily). Sixty-six patients (94.4%) underwent further surveillance endoscopy. At each surveillance endoscopy four-quadrant biopsies were taken from the neo-squamous epithelium at 2 cm intervals depending on the pre-treatment length of BE mucosa beginning at the neo-Z-line, and from any endoscopically suspicious lesion.

RESULTS: The median follow-up of 66 patients was 51 mo (range 9-85 mo) giving a total of 280.5 patient years. A mean of 6 biopsies were taken during surveillance endoscopies. In 13 patients (19.7%) tongues or islands suspicious for BE were found during endoscopy. In 8 of these patients (12.1%) non-neoplastic BE relapse was confirmed histologically giving a histological relapse rate of 3% per year. In none of the patients, intraepithelial neoplasia nor an esophageal adenocarcinoma was detected. Logistic regression analysis identified endoscopic detection of islands or tongues as the only positive predictor of BE relapse (P = 0.0004).

CONCLUSION: The long-term relapse rate of non-neoplastic BE following complete ablation with high-power APC is low (3% per year).

Key words: Barrett's esophagus; Argon plasma coagulation; Esophageal adenocarcinoma

Madisch A, Miehlke S, Bayerdörffer E, Wiedemann B, Antos D, Schulz H, Sievert A, Vieth M, Stolte M. Long-term follow-up after complete ablation of Barrett's esophagus with argon plasma coagulation. *World J Gastroenterol* 2005; 11(8): 1182-1186
http://www.wjgnet.com/1007-9327/11/1182.asp

INTRODUCTION

Barrett's esophagus (BE) is a metaplastic replacement of the normal squamous epithelium by specialized intestinal columnar epithelium. BE is considered as a premalignant condition arising in patients with chronic gastroesophageal reflux disease (GERD)[1,2]. Approximately 6-12% of patients with symptoms of GERD develop this condition[2,3]. Gerson *et al*[4] reported a BE prevalence of 25% in asymptomatic male veterans older than 50 years of age undergoing screening sigmoidoscopy for colorectal cancer. BE is a well-recognized risk factor for esophageal adenocarcinoma. Patients with BE have a 30- to 125-fold increased risk of developing adenocarcinoma compared to the general population[3,5,6]. Proton pump inhibitor (PPI) therapy, even at high doses, does not result in complete regression of BE[7-10]. Thus, there have been made many efforts to develop effective endoscopic treatments such as photodynamic therapy[11,12] and laser therapy[13] in order to ablate BE.

In recent years, argon plasma coagulation (APC) has been suggested as an effective technique for the ablation of BE[7,14-16]. APC is a thermal cautery device that involves the transmission of a high-frequency current via a constant flow of ionized argon gas. The depth of tissue destruction is limited to 2-3 mm. Short- and mid-term efficacy data of APC treatment are promising[15-17]. However, long-term follow-up studies investigating the risk of BE relapse or development of neoplasia after APC treatment are sparse. So far, only two studies have assessed the long-term outcome of patients with BE after APC treatment reporting a high endoscopic and histological relapse rate of 30 and 62% during a mean follow-up period of 3 years[18,19].

We have previously described a large cohort of patients with non-neoplastic BE who underwent ablation of BE by

high-power APC[16]. Here, we report the long-term outcome of patients after complete ablation of BE with respect to BE relapse and the development of intraepithelial neoplasia or esophageal adenocarcinoma.

MATERIALS AND METHODS

Patients

In an outpatient setting, consecutive patients undergoing endoscopy for the evaluation of GERD symptoms were evaluated between 1994 and 1998. Patients were eligible for the study if BE without intraepithelial neoplasia was histologically confirmed and written informed consent was given, particularly regarding the experimental nature of the APC procedure. Patients were excluded from the study if they were younger than 18 years of age and if any serious gastrointestinal or extraintestinal disease or BE with any kind of intraepithelial neoplasia was present.

Endoscopy and APC treatment

At baseline endoscopy the macroscopic extent of BE was determined by measuring the distance between the most proximal point of columnar mucosa and the proximal end of gastric folds as referenced to the distance from the incisions. For the APC procedure, patients received intravenous sedation with 10-mg midazolam. Circumferential areas of BE were ablated by using an argon beamer device (APC300, ERBOTOM ICC200; Erbe Medizintechnik, Tübingen, Germany), using a gas flow of 2 L/min at a power setting of 90 W. Ablation was initiated at the gastroesophageal transition zone and proceeded longitudinally toward the proximal epithelial junction with squamous epithelium. All APC treatments were carried out by a single experienced gastroenterologist (H.S.) at intervals of 2-3 wk and continued until macroscopic and histological complete reepithelialization with squamous epithelium.

Biopsy protocol and histological assessment

Before the APC procedure, four-quadrant biopsies were obtained every 2 cm along the visible length of BE by using a spiked biopsy forceps with an open diameter of 7 mm (MTW Endoskopie, Wesel, Germany). Additional specimens were obtained from any abnormal area as recommended by Levine *et al*[30].

After macroscopic complete ablation of BE, regeneration of squamous epithelium was confirmed by quadrant biopsies every 2 cm. Thereafter, during surveillance endoscopies, two to four biopsies were routinely taken from the neo-squamous epithelium and additional biopsies from any endoscopically suspected BE or other suspicious lesions.

The histological examination included staining with hematoxillin and eosin, and PAS-alcian-blue at pH 2.5. The histologic diagnosis of BE was established only when specialized intestinal columnar epithelium was detected. Complete intestinal metaplasia of normal or inflammatory cardia mucosa was not classified as BE. All biopsies were examined by two experienced pathologists (M.S. and M.V.).

BE relapse was defined either as endoscopically suspected and histologically confirmed BE, or as random detection of BE by biopsies from exactly below the Z-line and/or underneath neosquamous epithelium (buried glands).

Antireflux therapy during follow-up

During the entire APC treatment period, 40 mg omeprazole was given three times daily in order to achieve maximum acid suppression. After completion of APC treatment the omeprazole dose was reduced to 20 mg or continued with 40 mg daily as maintenance therapy depending on the results of pH monitoring and reflux symptoms (cumulative reflux time [pH less than 4] less than 7% per 24 h). After 12 mo of follow-up, PPI therapy was continued depending on the presence of reflux symptoms or if esophagitis was detected during surveillance endoscopy. Antireflux surgery was considered in eligible patients.

RESULTS

APC treatment

Seventy-three patients (45 men, mean age 55±12 years, range 28-77 years) with histologically proven non-neoplastic BE and at least moderate to severe gastroesophageal reflux symptoms for more than one year were enrolled in the initial study[16]. The median length of BE was 4 cm (range 1-12 cm), 56 patients (76.7%) had a BE longer than 2 cm. Three patients were lost during APC treatment due to unwillingness to continue and therefore, excluded from this analysis. In 69 of 70 patients complete squamous regeneration was achieved after a median of two APC sessions. In one patient (extent of BE 8 cm) 6 sessions of APC were necessary during the first 12 mo to achieve complete ablation except for a persistent small island of residual BE without intraepithelial neoplasia. After repeated sessions of APC treatment, this patient also achieved complete ablation and was included in the long-term follow-up study.

The APC procedures were generally well tolerated[22]. No severe complications such as bleeding or perforation occurred. Three patients developed mild esophageal strictures that were successfully treated by a single bougie dilatation.

Long-term follow-up

Sixty-six out of 70 patients (94.3%) underwent further surveillance endoscopy approximately every 12 mo. The clinical characteristics of these 66 patients are summarized in Table 1. In these patients, the median follow-up period ranged from 9 to 85 mo with a median of 51 mo giving a total of 280.5 patient years. During the entire follow-up period, 220 endoscopies were performed (mean 3.3 endoscopies per patient) with a mean of six biopsies taken during endoscopy.

The remaining four patients who did not undergo further surveillance endoscopy after the initial follow-up of 12 mo were interviewed (M.A.) by telephone at mo 84, 75, 61 and 78, respectively, after complete APC ablation of BE. None of them reported having any symptoms of dysphagia or having a diagnosis of upper gastrointestinal tract carcinoma.

Thirty-three patients (50%) received further PPI therapy with symptom-adjusted doses. Based upon patients' willingness, 22 patients (33.3%) underwent laparoscopic fundoplication after complete BE ablation. Eight patients who underwent laparoscopic fundoplication required further PPI therapy. Eleven patients were free of reflux symptoms and had no further antireflux therapy.

Table 1 Baseline characteristics of patients with continuous surveillance endoscopy

Variable	
Patients (*n*)	66
Length of BE >3 cm, *n* (%)	37 (56)
APC applications (mean)	2[1]
APC energy (W)	90[1]
Median follow-up (mo)	51
Hiatal hernia, *n* (%)	26 (39)
Sustained PPI-therapy, *n* (%)	33 (50)
Laparoscopic fundoplicatio, *n* (%)	22 (33)

[1]Initial study[16].

BE relapse

In 13 of the 66 patients (19.7%) islands or tongues of BE was identified during surveillance endoscopy. The macroscopic features of suspicious BE are summarized in Table 2. In 8 of the 13 patients, BE was histologically confirmed. Therefore, the cumulative relapse rate of histologically confirmed BE during the entire long-term follow-up was 12.1% giving an annual relapse rate of approximately 3%. The probability of sustained absence of BE after complete ablation by APC is shown in Figure 1.

Table 2 Endoscopically suspicious and histologically confirmed BE relapse rates for 66 patients

	Endoscopically suspicious BE Number of patients (%)	Histologically confirmed BE Number of patients (%)
Endoscopic finding	13 (19.7)	8 (12.1)
Tongues >3 cm	1 (1.6)	1 (1.6)
Tongues >1 cm	5 (7.5)	3 (4.5)
Tongues <1 cm	4 (6.1)	2 (3)
Small islands	3 (4.5)	2 (3)

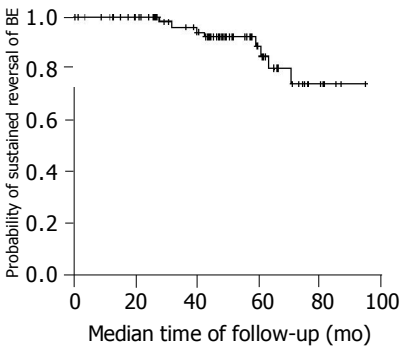

Figure 1 Probability of sustained absence of BE after complete ablation by APC.

Seven of the 8 patients with BE relapse received antireflux therapy during follow-up (laparoscopic fundoplication, $n = 3$; PPI therapy, $n = 4$). One BE relapse occurred in a patient without further antireflux therapy. All patients with histologically confirmed BE relapse were retreated with one session of high-power APC treatment.

Logistic regression analysis identified the endoscopic detection suspicious for BE as the only predictor of histological BE relapse. Other potential factors such as hiatal hernia, antireflux therapy or initial length of BE were not predictive for BE relapse (Table 3).

Table 3 Variables as predictors of BE relapse in 66 patients treated with APC and analyzed using logistic regression analysis

Variable	Multivariate analysis *P*
Age (yr)	0.57
Gender	0.11
Hiatal hernia	0.15
Number of APC sessions	0.22
Length of BE	0.10
Endoscopically islands or tongues of suspicious BE	0.0004
PPI therapy	0.96
Antireflux surgery	0.73

Importantly, neither intraepithelial neoplasia nor esophageal adenocarcinoma was detected in our patient cohort during the entire follow-up period.

DISCUSSION

The presence of BE as the most serious complication of GERD is associated with an increased risk of developing adenocarcinoma of the esophagus[1-6]. Thus, besides surveillance strategies many efforts have been made to develop new effective therapeutic endoscopic therapy for the ablation of BE such as thermal laser ablation or photodynamic therapy and APC[8,11-13,20].

The results of our long-term follow-up study suggest that endoscopic APC is effective and safe for the ablation of BE without neoplasia. To our knowledge the present study currently represents the largest series with the longest follow-up of patients. During a median follow-up of 51 mo we observed a low BE relapse rate of 12.1% after a complete BE ablation, which represents a BE relapse rate of approximately 3% per year. In our patient population neither intraepithelial neoplasia nor esophageal adenocarcinoma was detected.

Since the use of APC was described in a case report[21], several controlled studies with a larger number of patients have been fully published with a short- and mid-term follow-up[14,15,18,17,22,23,25]. The results of these studies are contradictory regarding both the initial success rate of complete ablation and relapse rate of BE. In four studies a complete ablation of BE between 87 and 100% is achieved[15-17,22]. Other studies showed only complete reversal of BE in 61-70% of patients[14,18,23,25]. The reported number of APC sessions (range 2-4) and the mean length of BE (4-6 cm) prior to the treatment were comparable in all studies. In contrast to all other published studies, in our study the highest level of energy (90 W) was applied during the APC treatment. This difference might be one reason for the higher rate of squamous reepithelialization in our study. Pereira-Lima *et al*[15] and Tigges *et al*[22] used APC at a power setting of up to 70 W and achieved a complete BE reversal in 96 and 91% of patients, respectively. We also used a higher dose of

omeprazole (40 mg three times daily) to suppress acid during the APC treatment period than all other studies.

Since most studies reported a low complication rate, APC can be regarded as a safe endoscopic method[24]. However, severe complications have been reported in four patients suffering from perforation[18,25], two patients died due to these complications. Although we used a high energy level in our study, only three patients (4.3%) developed a mild esophageal stricture, that was resolved after a single session of bougie dilatation. Since the long-term benefit of this procedure has not been sufficiently investigated, APC treatment should be still used primarily in experienced centers and within controlled trials.

Based upon the incidence of adenocarcinoma in patients with BE (estimated 0.5-1% per year)[1] we would have expected to observe up to three adenocarcinomas in our cohort. However, our data are certainly underpowered for valid incidence rates of adenocarcinoma after APC ablation of BE, or for the assessment of possible risk reduction of carcinoma development. In contrast to other studies we did not include patients with any kind of intraepithelial neoplasia in our study. Others have shown that in some cases adenocarcinoma might develop under the new regenerated squamous epithelium after APC treatment[26,27] although that was not the case in our study. This fact supports the current hypothesis that BE arises from pluripotential stem cells present in the basal layer of esophageal mucosa[28-34]. There are concerns that buried glands could remain beneath the new regenerated squamous epithelium after APC treatment and would not be detected by biopsies. However, it is still unknown whether buried glands relapse or still remain in BE due to incomplete ablation. Based upon our long-term follow-up data, this phenomenon appears not to be a clinically relevant problem, since we did not detect any buried glands in our cohort. Nevertheless, sampling cannot definitely rule out BE.

There are only two studies with long-term follow-up data after APC treatment of BE (Table 2). Kahaleh *et al*[19] published a study of 39 patients with BE, 7 of them with low-grade intraepithelial neoplasia and received APC treatment. After a complete ablation rate, they demonstrated a high BE relapse rate of 62% during a median follow-up period of 36 mo. Five out of seven patients with a low-grade intraepithelial neoplasia at baseline had recurrence of BE, one developed low-grade intraepithelial neoplasia again. In two patients of this cohort an esophageal adenocarcinoma was detected after a follow-up of 12 and 18 mo, respectively. Based upon these results, Kahaleh *et al*[19] concluded that APC cannot be recommended as an effective ablation method for BE. There are, however, some limitations in this study. First, it has to be considered that Kahaleh *et al*[19] showed a short-term relapse rate of 44% after 1 mo, thus it appears that in their study about 44% were incompletely ablated rather than relapsed. Weinstein[35] suggested that the reason for the low rate of complete ablation at baseline may be due to technical factors such as use of energy or acid suppression agents and demand of more vigorous ablation especially in longer-segment BE coupled with more potent acid suppression. Morris *et al*[18] described a cohort of 55 patients undergoing APC treatment of BE followed up a mean period of 36 mo. After a complete ablation rate of 70% no BE relapse was observed during the long-term follow-up. As in our initial report[16], we speculate that incomplete acid suppression and the lower level of energy may be the main reasons for the lower success rates of APC and remaining BE.

Several studies suggested short length of BE (<3 cm) and the normalization of acid exposure can be used as positive predictors of long-term reversal of BE[14,19]. Our regression analysis only identified the endoscopically detected suspicious BE as a positive predictor of histological BE relapse, whereas other factors such as the length of BE, hiatal hernia or previous antireflux therapy had no statistical impact on the sustained reversal of BE. In contrast to other studies[18,19] in which endoscopically suspicious BE was always confirmed histologically, we found endoscopically suspicious but not histologically confirmed BE in five patients. That means minimal endoscopic findings may not be equivalent to BE unless histologically confirmed.

In conclusion this study suggests that endoscopic APC is an effective method for the ablation of BE without neoplasia. The long-term relapse rate of BE is low. Nevertheless, APC treatment of BE does not replace surveillance endoscopy at present although cost-utility analysis has shown that subsequent surveillance of patients with BE but no neoplasia, even at 5-year intervals, is an expensive practice[36].

Although the present cohort was followed up for over 4 years without any evidence for intraepithelial neoplasia or adenocarcinoma, further long-term studies are warranted to determine whether risk reduction of malignancy can be achieved by APC ablation of BE.

REFERENCES

1 **Falk GW.** Barrett's esophagus. *Gastroenterology* 2002; **122:** 1569–1591
2 **Haag S,** Holtmann G. Reflux disease and Barrett's esophagus. *Endoscopy* 2003; **35:** 112–117
3 **Spechler SJ,** Goyal RK. Barrett's esophagus. *N Engl J Med* 1986; **315:** 362–371
4 **Gerson LB,** Shetler K, Triadafilopoulos G. Prevalence of Barrett's esophagus in asymptomatic individuals. *Gastroenterology* 2002; **123:** 461–467
5 **Hameeteman W,** Tytgat GN, Houthoff HJ, van den Tweel JG. Barrett's esophagus: development of dysplasia and adenocarcinoma. *Gastroenterology* 1989; **96**: 1249–1256
6 **Cameron AJ,** Ott BJ, Payne WS. The incidence of adenocarcinoma in columnar-lined (Barrett's) esophagus. *N Engl J Med* 1985; **313:** 857–859
7 **Deviere J.** Argon plasma coagulation therapy for ablation of Barrett's oesophagus. *Gut* 2002; **51:** 763–764
8 **Haringsma J.** Barrett's oesophagus: new diagnostic and therapeutic techniques. *Scand J Gastroenterol Suppl* 2002; **236:** 9–14
9 **Gore S,** Healey CJ, Sutton R, Eyre-Brook IA, Gear MW, Shepherd NA, Wilkinson SP. Regression of columnar lined (Barrett's) oesophagus with continuous omeprazole therapy. *Aliment Pharmacol Ther* 1993; **7:** 623–628
10 **Malesci A,** Savarino V, Zentilin P, Belicchi M, Mela GS, Lapertosa G, Bocchia P, Ronchi G, Franceschi M. Partial regression of Barrett's esophagus by long-term therapy with high-dose omeprazole. *Gastrointest Endosc* 1996; **44:** 700–705
11 **Dougherty T.** Photodynamic therapy for early esophageal cancer. *Photodynamic Therapy Association Meeting* 1990. Buffalo, NY: 1990
12 **Overholt BF,** Panjehpour M, Haydek JM. Photodynamic

therapy for Barrett's esophagus: follow-up in 100 patients. *Gastrointest Endosc* 1999; **49:** 1–7

13 **Gossner L,** May A, Stolte M, Seitz G, Hahn EG, Ell C. KTP laser destruction of dysplasia and early cancer in columnar-lined Barrett's esophagus. *Gastrointest Endosc* 1999; **49:** 8–12

14 **Basu KK,** Pick B, Bale R, West KP, de Caestecker JS. Efficacy and one year follow up of argon plasma coagulation therapy for ablation of Barrett's oesophagus: factors determining persistence and recurrence of Barrett's epithelium. *Gut* 2002; **51:** 776–780

15 **Pereira-Lima JC,** Busnello JV, Saul C, Toneloto EB, Lopes CV, Rynkowski CB, Blaya C. High power setting argon plasma coagulation for the eradication of Barrett's esophagus. *Am J Gastroenterol* 2000; **95:** 1661–1668

16 **Schulz H,** Miehlke S, Antos D, Schentke KU, Vieth M, Stolte M, Bayerdörffer E. Ablation of Barrett's epithelium by endoscopic argon plasma coagulation in combination with high-dose omeprazole. *Gastrointest Endosc* 2000; **51:** 659–663

17 **Mork H,** Barth T, Kreipe HH, Kraus M, Al-Taie O, Jakob F, Scheurlen M. Reconstitution of squamous epithelium in Barrett's oesophagus with endoscopic argon plasma coagulation: a prospective study. *Scand J Gastroenterol* 1998; **33:** 1130–1134

18 **Morris CD,** Byrne JP, Armstrong GR, Attwood SE. Prevention of the neoplastic progression of Barrett's oesophagus by endoscopic argon beam plasma ablation. *Br J Surg* 2001; **88:** 1357–1362

19 **Kahaleh M,** Van Laethem JL, Nagy N, Cremer M, Deviere J. Long-term follow-up and factors predictive of recurrence in Barrett's esophagus treated by argon plasma coagulation and acid suppression. *Endoscopy* 2002; **34:** 950–955

20 **Walker SJ,** Selvasekar CR, Birbeck N. Mucosal ablation in Barrett's esophagus. *Dis Esophagus* 2002; **15:** 22–29

21 **Dumoulin FL,** Terjung B, Neubrand M, Scheurlen C, Fischer HP, Sauerbruch T. Treatment of Barrett's esophagus by endoscopic argon plasma coagulation. *Endoscopy* 1997; **29:** 751–753

22 **Tigges H,** Fuchs KH, Maroske J, Fein M, Freys SM, Muller J, Thiede A. Combination of endoscopic argon plasma coagulation and antireflux surgery for treatment of Barrett's esophagus. *J Gastrointest Surg* 2001; **5:** 251–259

23 **Van Laethem JL,** Cremer M, Peny MO, Delhaye M, Deviere J. Eradication of Barrett's mucosa with argon plasma coagulation and acid suppression: immediate and mid term results. *Gut* 1998; **43:** 747–751

24 **Grade AJ,** Shah IA, Medlin SM, Ramirez FC. The efficacy and safety of argon plasma coagulation therapy in Barrett's esophagus. *Gastrointest Endosc* 1999; **50:** 18–22

25 **Byrne JP,** Armstrong GR, Attwood SE. Restoration of the normal squamous lining in Barrett's esophagus by argon beam plasma coagulation. *Am J Gastroenterol* 1998; **93:** 1810–1815

26 **Shand A,** Dallal H, Palmer K, Ghosh S, MacIntyre M. Adenocarcinoma arising in columnar lined oesophagus following treatment with argon plasma coagulation. *Gut* 2001; **48:** 580–581

27 **Van Laethem JL**, Peny MO, Salmon I, Cremer M, Devi¨¨re J. Intramucosal adenocarcinoma arising under squamous re-epithelialisation of Barrett's oesophagus. *Gut* 2000; **46:** 574–577

28 **Jankowski JA,** Harrison RF, Perry I, Balkwill F, Tselepis C. Barrett's metaplasia. *Lancet* 2000; **356:** 2079–2085

29 **Cameron AJ,** Lomboy CT, Pera M, Carpenter HA. Adenocarcinoma of the esophagogastric junction and Barrett's esophagus. *Gastroenterology* 1995; **109:** 1541–1546

30 **Levine DS,** Haggitt RC, Blount PL, Rabinovitch PS, Rusch VW, Reid BJ. An endoscopic biopsy protocol can differentiate high-grade dysplasia from early adenocarcinoma in Barrett's esophagus. *Gastroenterology* 1993; **105:** 40–50

31 **Eisendrath P,** Van Laethem JL, Deviere J. Follow-up of Barrett's epithelium after ablation by endoscopic argon plasma coagulation. *Gastrointest Endosc* 2001; **54:** 137–138

32 **Pech O,** Gossner L, May A, Ell C. Management of Barrett's oesophagus, dysplasia and early adenocarcinoma. *Best Pract Res Clin Gastroenterol* 2001; **15:** 267–284

33 **Wang KK,** Sampliner RE. Mucosal ablation therapy of barrett esophagus. *Mayo Clin Proc* 2001; **76:** 433–437

34 **Van Laethem JL,** Jagodzinski R, Peny MO, Cremer M, Deviere J. Argon plasma coagulation in the treatment of Barrett's high-grade dysplasia and *in situ* adenocarcinoma. *Endoscopy* 2001; **33:** 257–261

35 **Weinstein WM.** Is Barrett's esophagus dangerous? *Endoscopy* 2002; **34:** 1007–1009

36 **Inadomi JM,** Sampliner R, Lagergren J, Lieberman D, Fendrick AM, Vakil N. Screening and surveillance for Barrett esophagus in high-risk groups: A cost-utility analysis. *Ann Intern Med* 2003; **138:** 176–186

PO Box 2345, Beijing 100023, China
www.wjgnet.com
wjg@wjgnet.com

ELSEVIER

World J Gastroenterol 2005;11(8):1187-1192
World Journal of Gastroenterology ISSN 1007-9327

• *BRIEF REPORTS* •

IBD5 polymorphisms in inflammatory bowel disease: Association with response to infliximab

Elena Urcelay, Juan Luis Mendoza, Alfonso Martínez, Laura Fernández, Carlos Taxonera, Manuel Díaz-Rubio, Emilio G. de la Concha

Elena Urcelay, Alfonso Martínez, Laura Fernández, Emilio G. de la Concha, Immunology Department, Hospital Universitario San Carlos, Madrid, Spain
Juan Luis Mendoza, Carlos Taxonera, Manuel Díaz-Rubio, Gastroenterology Department, Hospital Universitario San Carlos, Madrid, Spain
Supported by grant from MCYT SAF 2003-08522. Elena Urcelay is recipient of a "Ramon y Cajal" contract of the MCYT. Alfonso Martinez is a recipient of a "Post-MIR" contract of the Spanish Health Ministry (01/F011)
Correspondence to: Dr. Elena Urcelay, Immunology Department, Hospital Universitario San Carlos, Martin Lagos s/n, Madrid 28040, Spain. eurcelay@hcsc.es
Telephone: +34-913303347 Fax: +34-913303344
Received: 2004-09-07 Accepted: 2004-10-27

Abstract

AIM: Inflammatory bowel diseases (IBD) are multifactorial pathologies of unknown etiology. One susceptibility locus, *IBD5*, has been mapped to chromosome 5q31. We analyzed our Spanish cohorts of Crohn's disease (CD) and ulcerative colitis (UC) patients to determine whether this locus is associated with IBD, and to ascertain the main clinical phenotype influenced by this risk factor. The kind of interaction, either genetic heterogeneity or epistasis, between this *IBD5* susceptibility region and the *NOD2/CARD15* gene mutations was studied as well. Finally, we assessed whether this locus can predict response to infliximab therapy.

METHODS: A case control study was performed with 274 CD and 211 UC patients recruited from a single center and 511 healthy ethnically matched controls. Two polymorphisms were genotyped in the *IBD5* locus and three in the *CARD15/NOD2* gene.

RESULTS: Our results evidence association only with CD especially with the fistulizing phenotype and in the absence of *NOD2/CARD15* variants (mutant allele frequency in patients *vs* controls: OR = 2.03, 95% CI = 1.35-3.06, $P<0.01$). The frequency of the *IBD5* homozygous mutant genotype significantly increased in CD patients lacking response to infliximab (RR = 3.88, 95% CI = 1.18-12.0, $P<0.05$). UC patients overall do not show association with 5q31 polymorphisms, although a similar trend to the one observed in CD is found within the worse prognosis group.

CONCLUSION: The *IBD5* variants may enhance an individual carrier's risk for CD, mainly in the absence of the *NOD2/CARD15* mutations and in fistulizing patients. The data presented suggest the potential role of the 5q31 polymorphisms as markers of response to infliximab.

Key words: Crohn's disease; Ulcerative colitis; 5q31 polymorphisms; Infliximab

Urcelay E, Mendoza JL, Martínez A, Fernández L, Taxonera C, Díaz-Rubio M, de la Concha EG. IBD5 polymorphisms in inflammatory bowel disease: Association with response to infliximab. *World J Gastroenterol* 2005; 11(8): 1187-1192
http://www.wjgnet.com/1007-9327/11/1187.asp

INTRODUCTION

Most patients with inflammatory bowel disease (IBD) are diagnosed as having Crohn's disease (CD) or ulcerative colitis (UC) according to clinical, endoscopic, radiological and pathological criteria[1]. Epidemiological studies claim significant contribution of genetics to the IBD etiology[2,3]. Even though differences are present between the two clinical forms of these autoimmune disorders of the gastrointestinal tract, relatives of patients with CD or UC are at increased risk of developing any form of IBD[4]. Therefore, it seems plausible that both CD and UC patients will share some susceptibility genes, while others will be phenotype-specific loci. A 250-kb haplotype in the 5q31 cytokine gene cluster was first described to confer CD risk in a Canadian population[5], and recently mapping to the OCTN cation transporter in the same population has been reported[6]. *IBD5* association with UC has also been found in a German cohort, in addition to the replication of the association of this region with CD[7]. The so-called *IBD5* locus might therefore be regarded as a general risk factor for IBD, at least in some populations. Simultaneously, a British study in a large European cohort of patients did not detect association with UC, and reported that the risk conferred by the 5q31 locus to CD patients was dependent on the presence of at least one of the *NOD2/CARD15* disease susceptibility alleles[8]. The *NOD2/CARD15* gene is an established CD risk locus, *IBD1*[9-11]. It encodes a protein with affinity for bacterial components that defectively activates the NF-κB pathway[12]. Therefore, whether the 5q31 region is a general risk factor for both intestinal diseases or for CD exclusively is open to debate, together with the putative epistatic interaction with the *NOD2/CARD15* predisposition gene. Further evidence from independent populations will aid in clarifying the importance of this locus in IBD.

Replication of the initial Canadian study associating the cytokine cluster region in 5q31 with CD has been obtained

in British and German populations, whereas the extremely low frequency of these polymorphisms in Japan precluded the analysis[13,14]. We aimed at replicating this finding in a Mediterranean population and we sought to determine the clinical forms showing the strongest impact of this risk factor.

Th1 cells are critical in the pathogenesis of CD and the release of Th1 cytokines increases during CD relapses. Tumor necrosis factor alpha (TNF-α) mediates mucosal inflammation and the efficiency of the TNF-α neutralizing agents has been proven. The infusion of chimeric anti-TNF-α antibodies (infliximab) has been shown to exert a pro-apoptotic effect on T-cells[15] and to inhibit the production of both Th1 type cytokines and granulocyte-macrophage colony stimulating factor (GM-CSF[16]). Given that the GM-CSF gene maps to the 5q31 cytokine cluster, we were interested in ascertaining whether this *IBD5* susceptibility locus had any influence on the response to infliximab treatment. Moreover, this 5q31 locus is a cluster of genes with relevance in the immune response, including several cytokine genes that map to this chromosomal region, and this alone may justify the approach.

MATERIALS AND METHODS

Patients and controls

The study group consisted of 274 unrelated adult white Spanish CD patients (53% women) with median follow-up 10.5 years (95% percentile values range from 3.4 to 26.9 years), recruited after informed consent from a single center. Diagnosis of CD was based on Lennard-Jones criteria[17]. Phenotypic details were obtained with the clinical history and personal interviews with patients. Disease phenotype was determined following the Vienna Classification[18]. Location: L_1 (Terminal ileum), L_2 (Colonic), L_3 (Ileocolonic) and L_4 (Upper Gastrointestinal). Behavior: B_1 (Inflammatory, Non-stricturing and non-fistulizing), B_2 (Stricturing) and B_3 (Fistulizing). Perianal disease was defined by the presence of perianal abscesses, fistulae and/or ulcers. In addition, 211 unrelated adult white Spanish UC patients (38% women) were recruited after informed consent from the same center. Their diagnosis was documented by conventional endoscopic, histologic, and clinical criteria. The median follow-up period was 8.5 years (95% percentile values range from 2.7 to 19.4 years). Disease was classified as extensive (inflammation proximal to the splenic flexure) or distal. Patients and data are regularly followed up in the Inflammatory Bowel Disease Unit at Hospital Clínico San Carlos, Madrid. A group of 511 healthy white, unrelated subjects (61% women) from the Madrid region (mainly hospital employees and blood donors) were used as controls.

Genotyping

***5q31* locus** Two variants, IGR2060a_1 and IGR3081a_1, were independently analyzed by using the SYBR Green Master Mix of Applied Biosystems, under conditions recommended by the manufacturer. Allelic genotyping was achieved in an ABI 7700 Sequence Detector (Applied Biosystems, Foster City, CA) with the following set of primers: IGR2060a_1: sense 5'-CTC ATT ACA TCC TTG CAA CCC T(G/C)-3' and antisense 5'-GAC ACA TGG TGT GAG CTC AGT CA-3'. IGR3081a_1: sense 5'-TCG CGT GAG TCC TAT TCT TTC T(T/G)-3' and antisense 5'-TTC ATA CTT CCA GCA GCG GG-3'.

***NOD2/CARD15* polymorphisms** Primers and probes used were previously described[19], in summary: Leu1007fsinsC was genotyped using a TaqMan assay (Applied Biosystems, Foster City, CA) and PCR products were analyzed in an ABI 7700 Sequence Detector (Applied Biosystems). Arg702Trp (sense, 5'-CAT CTG AGA AGG CCC TGC TC (C/T)-3'; antisense, 5'-CAG ACA CCA GCG GGC ACA-3') and Gly908Arg (sense, 5'-TTG GCC TTT TCA GAT TCT GG (G/C)-3'; antisense, 5'-CCC CTC GTC ACC CAC TCT G-3') were typed by allele-specific PCR. Wild-type/mutant genotype was assessed in an ABI 7700 Sequence Detector by SYBR Green assay. Previously sequenced samples were used as controls.

Treatments

Crohn's disease Forty patients received an intravenous infusion of infliximab at a dose of 5 mg/kg of body weight at wk 0, 2 and 6. The physicians assessing clinical response to infliximab were blinded for the genotype information. Clinical response was divided into two categories: response or non-response. Patients with active luminal (non-fistulizing) disease were considered responders if the CD activity index (CDAI) decreased below 150 or if a decrease of 70 points in CDAI after 4 wk was observed[20]. Patients with fistulizing disease were considered responders in case of complete fistulae healing or 50% decrease in the number of draining fistulae within two consecutive visits, i.e., if a response was observed at both weeks 10 and 14[21].

Ulcerative colitis Medical treatments (steroids, immunosuppressant agents and surgical intervention) were related to the severity of the disease. Immunosuppressant agents (azathioprine, 6-mercaptopurine and cyclosporine) were used in UC patients to induce remission in steroid refractory disease and as steroid-sparing agent in patients who were steroid-dependent. Procedures considered as surgical therapy were colonic resections.

Statistical analysis

Case-control analyses were performed with the χ^2 statistics or Fisher exact test. The association between genotypic and phenotypic characteristics of CD and UC was estimated by the odds ratio (OR) with 95% confidence interval (CI). The χ^2 test or Fisher exact test was used to compare responders and non-responders and association was expressed as relative risk (RR) with 95% CI. The statistical power considering a RR = 1.5 for the 5q31 polymorphisms is 84.38% for CD and 79.51% for UC. Logistic regression analysis was performed to assess whether 5q31 homozygous mutants were correlated with baseline characteristics of patients treated with infliximab. Statistical analysis was performed using the Statistical Package for the Social Sciences (SPSS) version 10.07 for Windows (SPSS Inc., Chicago, IL).

RESULTS

Eleven SNPs significantly associated with CD initially defined

the 250-kb *IBD5* locus. Due to the strong linkage disequilibrium (LD) among them, any of those 11 polymorphisms would be equally informative once LD was confirmed in one specific population. We genotyped two of those 11 SNPs, IGR2060a_1 and IGR3081a_1 from the 5' and 3' ends of the *IBD5* haplotype, to verify whether the extent of linkage disequilibrium was similar in our population and in those previously described. The rate of LD observed between these two SNPs was confirmed to be almost complete, in keeping with literature (data not shown).

In a case-control study with 274 CD and 211 UC Spanish patients and 511 unrelated healthy controls, we first examined the CD cohort to determine whether there was any evidence of association with the two above-mentioned *IBD5* SNPs. The comparison of the frequencies of the mutant allele carriage in CD patients overall with healthy controls nearly reached significant levels (200/341 *vs* 74/170, OR [CI] = 1.35 [0.96-1.89], $P = 0.07$). Due to clinical heterogeneity of the disease, it seemed interesting to clarify in which group of patients *IBD5* had the strongest impact on susceptibility. According to the Vienna Classification, dealing with anatomical localization and behavior of the lesions, the analysis revealed that some unique clinical characteristics were correlated with the genotype. The extended follow-up of the patients allowed us to confidently describe the localization and behavior of their lesions. The patients were classified in three groups: terminal ileum (L_1, 48.6%), colonic (L_2, 16.5%) and ileocolonic (L_3, 34.9%). In terms of the behavior their distribution was inflammatory (B_1, 43.3%), stricturing (B_2, 16.1%) and fistulizing (B_3, 40.6%). The ileocolonic L_3 and fistulizing B_3 clinical forms were both significantly associated with *IBD5* when compared to control subjects in the Spanish sample (Table 1). Data supported a dominant model of inheritance. When allelic frequencies were studied, the fistulizing patients were also significantly different from the group formed by the inflammatory plus stricturing patients (B_3 (119/101) *vs* B_1+B_2 (141/179), OR [CI] = 1.5 [1.04-2.14], $P<0.05$). Moreover, the homozygous mutant genotype was significantly more abundant in fistulizing patients than that in the inflammatory and stricturing clinical groups (Table 1, B_3 (33/77) *vs* B_1+B_2 (31/132), OR [CI] = 1.82 [1-3.34], $P<0.05$).

Table 1 Genotype frequencies of the *IBD5* SNPs in Crohn's disease patients and controls

	TT (%)	GT (%)	GG (%)
Controls ($n = 511$)	170 (33.3)	236 (46.2)	105 (20.5)
CD patients ($n = 274$)	74 (27)	136 (49.6)	64 (23.4)
CD-L_1 ($n = 133$) terminal ileum + UG	41 (30.8)	66 (49.6)	26 (19.6)
CD-L_2 ($n = 46$) colon	12 (26.1)	23 (50)	11 (23.9)
CD-L_3 ($n = 95$) ileocolon	21 (22.1)	47 (49.5)	27 (28.4)[a]
CD-B_1 ($n = 119$) inflammatory	36 (30.2)	60 (50.4)	23 (19.3)
CD-B_2 ($n = 44$) stricturing	14 (31.8)	22 (50)	8 (18.2)
CD-B_3 ($n = 110$) fistulizing	24 (21.3)	53 (48.9)	33 (30)[c]
CD-perianal ($n = 47$)	10 (21.3)	23 (48.9)	14 (29.8)
CD-non perianal ($n = 227$)	64 (28.2)	113 (49.8)	50 (22)

(GG+ GT) *vs* TT: [a]$P<0.05$; OR (CI) = 1.76 (1.02-3.05) compared to controls. (GG+ GT) *vs* TT: [c]$P<0.05$; OR (CI) = 1.79 (1.07-3.00) compared to controls.

Since the *IBD1* locus in chromosome 16 is a well-known genetic factor conferring susceptibility to CD we searched for epistatic effects with the *IBD5* region. Three *NOD2/CARD15* variants (R702W, G908R and L1007fs) act cooperatively to increase risk in CD: in the presence of any one of them, risk rises 2-6-fold and when homozygotes or compound heterozygotes appear, risk reaches up to 40-fold. We found that 31.4% of the Spanish CD patients present at least one of those three polymorphisms compared to 9.3% controls. To assess whether there was a different association of the *IBD5* locus on stratification by the *NOD2/CARD15* genotype, we studied the allele distribution of both polymorphisms IGR2060a_1 and IGR3081a_1 in the *NOD2/CARD15*-negative and *NOD2/CARD15*-positive populations. In the *NOD2/CARD15*-positive group, no *IBD5*-association could be detected (data not shown). Interestingly, we could observe that the association with *IBD5* was present in the *NOD2/CARD15*-negative individuals (Table 2). In this case, the genotype distribution in *NOD2/CARD15*-negative CD patients was significantly different from the one displayed for the healthy controls (OR [CI] = 1.68 [1.07-2.66], $P<0.05$). Again, as seen in the overall CD cohort, in the *NOD2/CARD15*-negative population the L_3 and B_3 subtypes were associated with the 5q31 polymorphisms (Table 2).

Table 2 Genotype frequencies of the *IBD5* SNPs in *NOD2/CARD15*-negative Crohn's disease patients and ethnically-matched controls

	TT (%)	GT (%)	GG (%)
Controls ($n = 511$)	170 (33.3)	236 (46.2)	105 (20.5)
CD patients ($n = 140$)	32 (22.9)	69 (49.3)	39 (27.9)[a]
CD-L_1 ($n = 55$) terminal ileum + UG	16 (29.1)	25 (45.5)	14 (25.5)
CD-L_2 ($n = 31$) colon	8 (25.8)	15 (48.4)	8 (25.8)
CD-L_3 ($n = 54$) ileocolon	8 (14.8)	29 (53.7)	17 (31.5)[b]
CD-B_1 ($n = 65$) inflammatory	17 (26.1)	33 (50.8)	15 (23.1)
CD-B_2 ($n = 15$) stricturing	6 (40)	7 (46.7)	2 (13.3)
CD-B_3 ($n = 59$) fistulizing	9 (15.25)	28 (47.5)	22 (37.3)[d]
CD-perianal ($n = 34$)	6 (17.7)	19 (55.9)	9 (26.5)
CD-non perianal ($n = 106$)	26 (24.5)	50 (47.2)	30 (28.3)

(GG+GT) *vs* TT: [a]$P<0.05$; OR (CI) = 1.68 (1.07-2.66) compared to controls. (GG+GT) *vs* TT: [b]$P<0.01$; OR (CI) = 2.87 (1.27-6.73) compared to controls. (GG+GT) *vs* TT: [d]$P<0.01$; OR (CI) = 2.77 (1.28-6.2) compared to controls.

Forty CD patients were treated with infliximab, and only 25 of them responded to treatment (see Methods), while the remaining 37.5% were non-responders. This means that infliximab was effective in around two-third of the CD patients, concordant with the previously reported efficiency of this therapy[21]. This overall response rate did not differ among the patient groups, regardless of the fistulizing or luminal phenotype. We pursued checking whether the polymorphisms located in the 5q31 locus could act as markers of response to this monoclonal antibody. No distorted distribution of the 5q31 phenotype among treated and non-treated CD patients was observed (homozygous mutant: 24.4% non-treated *vs* 25% treated). However, when the response to the monoclonal antibody was studied in those 40 CD patients (Table 3), the homozygous mutant

genotype was significantly associated with lack of response to infliximab treatment (RR [CI] = 3.88 [1.18-12.8], $P<0.05$). Patients' demographics and characteristics did not differ significantly between responders and non-responders. We only found significant association between homozygous mutant carriers and lack of response to infliximab treatment, which was independent of demographics, disease phenotype and concomitant medications. The frequency of the homozygous mutant genotype in the non-responders group was 46.7%, more than twice the frequency found for the healthy control cohort (20.3%) (OR [CI] = 3.42 [1.09-10.68], $P<0.05$). Moreover, significant difference was maintained when responders and non-responders to infliximab were compared (Table 3).

Table 3 Patients' characteristics at the time of infliximab treatment: the differential response to infliximab therapy in CD patients depends on their 5q31 genotype

	Responder (n = 25)	Non-responder (n = 15)	P
Demographics			
Mean age, yr (range)	35 (21-66)	40 (17-68)	0.21
Mean duration of disease, yr (range)	10 (1-27)	12 (1-31)	0.37
Male:Female	13:12	6:9	0.46
Smoker, n (%)	13 (52)	8 (53.3)	0.93
Extraintestinal manifestations, n (%)	13 (52)	7 (46)	0.92
Previous surgery, n (%)	14 (56)	9 (60)	0.80
Disease distribution			
Small bowel only, n (%)	9 (36)	4 (26.7)	0.54
Colon only, n (%)	3 (12)	2 (13.3)	1
Colon and small bowel, n (%)	13 (52)	9 (66)	0.62
Indication for infliximab			
Inflammatory disease only, n (%)	7 (28)	6 (40)	0.62
Fistulizing disease only, n (%)	10 (40)	7 (46.7)	1
Inflammatory and fistulizing disease, n (%)	8 (32)	2 (13.3)	0.27
Concomitant medication			
6-mercaptopurine, azathioprine, methotrexate, n (%)	17 (68)	13 (86.7)	0.27
Mesalamine, n (%)	7 (28)	4 (26.7)	0.52
Corticosteroid, n (%)	6 (24)	5 (33.3)	1
5q31 genotype			
Homozygous wild type, n (%)	6 (24)	3 (20)	1
Heterozygous, n (%)	16 (64)	5 (33.3)	0.1
Homozygous mutant, n (%)	3 (12)	7 (46.7)	0.024[a]

[a]$P<0.05$, RR (CI) = 3.88 (1.18-12.8).

The UC cohort was then analyzed and no evidence of association with this pathology in the Spanish sample was found. No significant difference was observed when comparing the two clinical forms, extensive and distal, to healthy controls. The main genetic determinant of UC susceptibility and extension within the Major Histocompatibility Complex (MHC) in our population is DRB1*0103. Stratifying by this MHC factor did not yield any difference either. Although UC disease can be treated with steroids in order to control symptoms, some patients eventually become resistant to or dependent on this therapy. To treat disease exacerbation in those cases, immunosuppressive therapy or even surgery is performed. If immunosuppressive drugs and/or surgical therapy were used at least once during the disease, it was considered as severe colitis. When the distribution of the 5q31 alleles was compared between these severe colitis patients and the healthy controls, a trend for association was seen (56/48 *vs* 440/572, OR [CI] = 1.52 [0.99-2.32], $P = 0.05$). These results could point to clinical heterogeneity of the UC samples tested as the cause underlying the variability reported in the association with the 5q31 haplotype. Others[22] have already observed the different UC incidence rate between sexes present in our population. The gender distribution of the *IBD5* genotype was compared to discern the male predominance in UC as a factor altering our results and no difference was found between men and women (TT: 39/22; GT: 73/42 and GG: 26/22, respectively).

DISCUSSION

A haplotype spanning 250 kb in the cytokine gene cluster on chromosome 5q31 was originally reported to be associated with Crohn's disease in a Canadian population[5,23]. Moreover, functional variants of OCTN cation transporter genes have been recently found in association with CD in this population, probably affecting the uptake of physiologic compounds and toxins[6]. Replication trials have been performed in order to verify the association of the 5q31 locus in independent cohorts. There are important disagreements in the literature regarding the relevance of this chromosome 5-risk locus in IBD. The influence of this locus in UC has been reported only once[7]. The primary purpose of this work was testing the involvement of the *IBD5* risk alleles in IBD disease susceptibility in the Spanish population. We have been able to replicate the association previously found in CD, but not in our UC cohort, although both seem to share a similar trend. This difference could be due either to a lesser effect of this locus on UC susceptibility or to an association with a yet-unidentified specific subgroup of UC patients or to the combination of both.

The complex genetic background of IBD has been revealed by the identified locus to locus interactions. A previous study stated that the *IBD5* association was present only in individuals with at least one of the known *NOD2/CARD15* susceptibility alleles, but was not significantly elevated in CD patients who had no *NOD2/CARD15* mutation[8]. The present work shows that the association found with *IBD5* in the Spanish CD cohort was due to the predisposition conferred to the *NOD2/CARD15*-negative subpopulation, and no influence was detected in the *NOD2/CARD15*-positive group. Our results agree with others reporting a contribution of the 5q31 variants in CD independently of the presence of *NOD2/CARD15* susceptibility alleles[7,14]. Moreover, our group has already determined that *NOD2/CARD15* and the Major Histocompatibility Complex locus are also independent genetic risk factors for CD[24]. The data presented suggest that one CD susceptibility locus affect a definite patient subgroup. Therefore, IBD predisposition would not always

be conferred by the presence of the same polymorphisms in many susceptibility genes, each with a small effect. Most probably, few variants would be enough to increase risk to one specific clinical form, and a different combination of risk factors would lend susceptibility to another clinical form. Thus, the genetic background determines which pathways are preferentially activated during tissue damage.

To assess the repercussion at the clinical subtypes of the disease, a detailed analysis following the Vienna Classification was performed. The CD perianal phenotype has been reported essential in the association with *IBD5*[14]. In contrast, the fistulizing phenotype is more strongly associated in the Spanish cohort tested in the present study, and in our patients, perianal lesions do not seem to be so crucial. It is interesting that both the interactions with the *IBD1* locus and the relationship with the clinical phenotype are not unequivocally reproduced in all the populations studied, probably indicating that the underlying different clinical composition of the cohorts tested sometimes preclude from detecting an effect. One could postulate that something similar occurs within the UC cohort, i.e., the different clinical composition may explain the apparently contradictory results reported in terms of association with the 5q31 locus.

Infliximab is a chimerical monoclonal antibody that inhibits the action of TNF-α. Although both infliximab and etanercept show powerful TNF-α neutralization, only infliximab (the only one effective in CD) binds to peripheral blood lymphocytes and lamina propria T cells to induce apoptosis of activated lymphocytes[15]. This provides a biological basis for the difference in CD effect of both drugs. It has been recently demonstrated that T cells from CD patients produce increased amounts of GM-CSF and that this increase significantly correlates with CD activity[16]. Moreover, the same study shows that infliximab inhibits the production of GM-CSF by mucosal T cells. Therefore, given the location of the GM-CSF gene in the *IBD5* risk locus, we were interested in exploring these 5q31 variants as potential markers of infliximab response. In clinical trials in CD, infliximab significantly decreased the CD activity index compared to placebo in treatment-resistant disease. However, this agent is expensive and at least one-third of the eligible patients fail to show any useful response. Lack of response seems a stable trait even after repeated infusions, suggesting that it might be genetically determined. Identifying predictors of response to infliximab may lead to better selection of patients for this maintenance therapy for individuals with CD. Several genes have been studied for this purpose: the TNF-α gene polymorphisms show conflicting results as predictors of response. Polymorphisms in the TNF-α receptors and the three mutations in the *NOD2/CARD15* gene have been reported not to be associated with infliximab response[16]. Our results showed that chromosome 5 polymorphisms associated with susceptibility to CD could be considered as good markers for response to infliximab therapy. The homozygous mutant patients for these IBD5 variants present a significantly worse response to infliximab. However, as the number of patients recruited is small, this preliminary interesting finding should be further confirmed in a larger cohort of treated CD patients before making any definite conclusion.

ACKNOWLEDGEMENTS

We thank Carmen Martínez for expert technical assistance.

REFERENCES

1 **Satsangi J**, Grootscholten C, Holt H, Jewell DP. Clinical patterns of familial inflammatory bowel disease. *Gut* 1996; **38**: 738-741
2 **Orholm M**, Munkholm P, Langholz E, Nielsen OH, Sorensen TI, Binder V. Familial occurrence of inflammatory bowel disease. *N Engl J Med* 1991; **324**: 84-88
3 **Bayless TM**, Tokayer AZ, Polito JM, Quaskey SA, Mellits ED, Harris ML. Crohn's disease: concordance for site and clinical type in affected family members-potential hereditary influences. *Gastroenterology* 1996; **111**: 573-579
4 **Bonen DK**, Cho JH. The genetics of inflammatory bowel disease. *Gastroenterology* 2003; **124**: 521-536
5 **Rioux JD**, Daly MJ, Silverberg MS, Lindblad K, Steinhart H, Cohen Z, Delmonte T, Kocher K, Miller K, Guschwan S, Kulbokas EJ, O'Leary S, Winchester E, Dewar K, Green T, Stone V, Chow C, Cohen A, Langelier D, Lapointe G, Gaudet D, Faith J, Branco N, Bull SB, McLeod RS, Griffiths AM, Bitton A, Greenberg GR, Lander ES, Siminovitch KA, Hudson TJ. Genetic variation in the 5q31 cytokine gene cluster confers susceptibility to Crohn disease. *Nat Genet* 2001; **29**: 223-228
6 **Peltekova VD**, Wintle RF, Rubin LA, Amos CI, Huang Q, Gu X, Newman B, Van Oene M, Cescon D, Greenberg G, Griffiths AM, St George-Hyslop PH, Siminovitch KA. Functional variants of OCTN cation transporter genes are associated with Crohn disease. *Nat Genet* 2004; **36**: 471-475
7 **Giallourakis C**, Stoll M, Miller K, Hampe J, Lander ES, Daly MJ, Schreiber S, Rioux JD. IBD5 is a general risk factor for inflammatory bowel disease: replication of association with Crohn disease and identification of a novel association with ulcerative colitis. *Am J Hum Genet* 2003; **73**: 205-211
8 **Mirza MM**, Fisher SA, King K, Cuthbert AP, Hampe J, Sanderson J, Mansfield J, Donaldson P, Macpherson AJ, Forbes A, Schreiber S, Lewis CM, Mathew CG. Genetic evidence for interaction of the 5q31 cytokine locus and the CARD15 gene in Crohn disease. *Am J Hum Genet* 2003; **72**: 1018-1022
9 **Inohara N**, Ogura Y, Chen FF, Muto A, Nunez G. Human Nod1 confers responsiveness to bacterial lipopolysaccharides. *J Biol Chem* 2001; **276**: 2551-2554
10 **Hugot JP**, Chamaillard M, Zouali H, Lesage S, Cezard JP, Belaiche J, Almer S, Tysk C, O'Morain CA, Gassull M, Binder V, Finkel Y, Cortot A, Modigliani R, Laurent-Puig P, Gower-Rousseau C, Macry J, Colombel JF, Sahbatou M, Thomas G. Association of NOD2 leucine-rich repeat variants with susceptibility to Crohn's disease. *Nature* 2001; **411**: 599-603
11 **Ogura Y**, Bonen DK, Inohara N, Nicolae DL, Chen FF, Ramos R, Britton H, Moran T, Karaliuskas R, Duerr RH, Achkar JP, Brant SR, Bayless TM, Kirschner BS, Hanauer SB, Nunez G, Cho JH. A frameshift mutation in NOD2 associated with susceptibility to Crohn's disease. *Nature* 2001; **411**: 603-606
12 **Watanabe T**, Kitani A, Murray PJ, Strober W. NOD2 is a negative regulator of Toll-like receptor 2-mediated T helper type 1 responses. *Nat Immunol* 2004; **5**: 800-808
13 **Negoro K**, McGovern DP, Kinouchi Y, Takahashi S, Lench NJ, Shimosegawa T, Carey A, Cardon LR, Jewell DP, van Heel DA. Analysis of the IBD5 locus and potential gene-gene interactions in Crohn's disease. *Gut* 2003; **52**: 541-546
14 **Armuzzi A**, Ahmad T, Ling KL, de Silva A, Cullen S, van Heel D, Orchard TR, Welsh KI, Marshall SE, Jewell DP. Genotype-phenotype analysis of the Crohn's disease susceptibility haplotype on chromosome 5q31. *Gut* 2003; **52**: 1133-1139
15 **Van den Brande JM**, Braat H, van den Brink GR, Versteeg HH, Bauer CA, Hoedemaeker I, van Montfrans C, Hommes DW, Peppelenbosch MP, van Deventer SJ. Infliximab but not

etanercept induces apoptosis in lamina propria T-lymphocytes from patients with Crohn's disease. *Gastroenterology* 2003; **124**: 1774-1785

16 **Agnholt J**, Kelsen J, Brandsborg B, Jakobsen NO, Dahlerup JF. Increased production of granulocyte-macrophage colony-stimulating factor in Crohn's disease-a possible target for infliximab treatment. *Eur J Gastroenterol Hepatol* 2004; **16**: 649-655

17 **Lennard-Jones JE**. Classification of inflammatory bowel disease. *Scand J Gastroenterol Suppl* 1989; **170**: 2-6; discussion 16-19

18 **Gasche C**, Scholmerich J, Brynskov J, D'Haens G, Hanauer SB, Irvine EJ, Jewell DP, Rachmilewitz D, Sachar DB, Sandborn WJ, Sutherland LR. A simple classification of Crohn's disease: report of the Working Party for the World Congresses of Gastroenterology, Vienna 1998. *Inflamm Bowel Dis* 2000; **6**: 8-15

19 **Hampe J**, Cuthbert A, Croucher PJ, Mirza MM, Mascheretti S, Fisher S, Frenzel H, King K, Hasselmeyer A, MacPherson AJ, Bridger S, van Deventer S, Forbes A, Nikolaus S, Lennard-Jones JE, Foelsch UR, Krawczak M, Lewis C, Schreiber S, Mathew CG. Association between insertion mutation in NOD2 gene and Crohn's disease in German and British populations. *Lancet* 2001; **357**: 1925-1928

20 **Hanauer SB**, Feagan BG, Lichtenstein GR, Mayer LF, Schreiber S, Colombel JF, Rachmilewitz D, Wolf DC, Olson A, Bao W, Rutgeerts P. Maintenance infliximab for Crohn's disease: the ACCENT I randomised trial. *Lancet* 2002; **359**: 1541-1549

21 **Sands BE**, Anderson FH, Bernstein CN, Chey WY, Feagan BG, Fedorak RN, Kamm MA, Korzenik JR, Lashner BA, Onken JE, Rachmilewitz D, Rutgeerts P, Wild G, Wolf DC, Marsters PA, Travers SB, Blank MA, van Deventer SJ. Infliximab maintenance therapy for fistulizing Crohn's disease. *N Engl J Med* 2004; **350**: 876-885

22 **Loftus EV**, Silverstein MD, Sandborn WJ, Tremaine WJ, Harmsen WS, Zinsmeister AR. Ulcerative colitis in Olmsted County, Minnesota, 1940-1993: incidence, prevalence, and survival. *Gut* 2000; **46**: 336-343

23 **Rioux JD**, Silverberg MS, Daly MJ, Steinhart AH, McLeod RS, Griffiths AM, Green T, Brettin TS, Stone V, Bull SB, Bitton A, Williams CN, Greenberg GR, Cohen Z, Lander ES, Hudson TJ, Siminovitch KA. Genomewide search in Canadian families with inflammatory bowel disease reveals two novel susceptibility loci. *Am J Hum Genet* 2000; **66**: 1863-1870

24 **Fernandez L**, Mendoza JL, Martinez A, Urcelay E, Fernandez-Arquero M, Garcia-Paredes J, Peña AS, Diaz-Rubio M, de la Concha EG. IBD1 and IBD3 determine location of Crohn's disease in the Spanish population. *Inflamm Bowel Dis* 2004; **10**: 715-722

PO Box 2345, Beijing 100023, China
www.wjgnet.com
wjg@wjgnet.com

ELSEVIER

World J Gastroenterol 2005;11(8):1193-1195
World Journal of Gastroenterology ISSN 1007-9327

• *BRIEF REPORTS* •

Transforming growth factor beta can be a parameter of aggressiveness of pT1 colorectal cancer

Katarzyna Guzinska-Ustymowicz, Andrzej Kemona

Katarzyna Guzinska-Ustymowicz, Andrzej Kemona, Department of General Pathomorphology, Affiliated Medical University of Białystok, ul.Waszyngtona 13, 15-889 Białystok, Poland
Correspondence to: Katarzyna Guzinska-Ustymowicz M.D., Department of General Pathomorphology, Medical University of Białystok, ul.Waszyngtona 13, 15-269 Białystok, Poland. kguzinska@poczta.onet.pl
Telephone: +48-85-7485942 Fax: +48-85-7485990
Received: 2004-06-24 Accepted: 2004-07-27

Abstract

AIM: To evaluate the significance of transforming growth factor beta (TGF β) expression, in correlation with histopathological parameters, at the front of invasion in T1 colorectal cancer (CRC) and presence of metastases.

METHODS: TGF β immunohistochemical expression was studied in 34 specimens of colorectal adenocarcinomas (pT1). A three-step avidin-biotinylated immuno-peroxidase (ABCu-NCL) staining technique was performed on 4-μm paraffin-embedded tissue sections with a monoclonal antibody to TGF β (Novocastra, NCL-TGFB, clone TGFB 17, dilution 1:40).

RESULTS: Seventeen (50%) out of 34 lesions were positive for TGF β expression. The TGF β-positive rate in patients with vascular invasion was significantly higher than in those without vascular invasion (11/14 cases, $P<0.01$, $P = 0.005$). The TGF β-positive rate was observed in 91.7% of patients with presence of tumor budding at the front of invasion (11/12 cases, $P<0.01$, $P = 0.0003$). A statistically significant correlation was found between the presence of lymph node metastases and positive expression of TGF β (14/16 cases, $P<0.01$, $P = 0.0001$). We also observed that the TGF β-positive rates in groups with distant and non-distant metastases were 92.8% and 20% respectively, and a significant correlation between TGF β expression and distant metastasis was shown ($P<0.01$, $P = 0.00003$).

CONCLUSION: The evaluation of TGF β expression of protein in association with histological parameters can be used as a parameter of the aggressiveness of pT1 CRC.

Key words: TGFβ; Tumor budding; Colorectal cancer

Guzinska-Ustymowicz K, Kemona A. Transforming growth factor beta can be a parameter of aggressiveness of pT1 colorectal cancer. *World J Gastroenterol* 2005; 11(8): 1193-1195
http://www.wjgnet.com/1007-9327/11/1193.asp

INTRODUCTION

Colorectal cancer (CRC) is one of the most common types of cancer in Poland and other western countries. According to statistics, the mortality of CRC is ranking second in western countries and third in Poland amongst all cancers. That is why its biology is still being investigated by researchers[1-3]. Transforming growth factor β (TGF β) is a multifunctional cytokine that can induce growth inhibition, apoptosis, and differentiation of intestinal epithelial cells[4,5].

Generally, TGF β inhibits the growth of normal intestinal epithelial cells but can switch to a growth stimulator with tumor progression and enhance malignant transformation[6,7].

Until now, the number of potential prognostic factors for CRC is continually increasing, which is associated with its biologically diverse malignancy, given the same stage of advancement. Some histological parameters such as vascular invasion and tumor budding at the front of invasion seem to give very important information about invasive potential and metastasis of CRC. A few published studies have associated tumor- budding with metastatic changes[8-12]. These results seem to confirm that tumor- budding can play a crucial role as a prognostic factor in CRC. Also, the observed presence of neoplastic cells and nets of cells in lymphatic and venous vessels (vascular invasion) is an important feature of invasiveness in CRC. On the other hand, the presence of lymph node and distant metastasis is a recognized parameter of metastatic potential. This is why the aims of the study were, to evaluate the vascular invasion and tumor-budding in CRC growth zone, to analyze its relationship with the expression of TGF β protein in tumors, and to find any correlation between the expression of TGF β and the presence of metastases.

MATERIALS AND METHODS

Collection of samples

Thirty-four T1 colorectal carcinoma specimens from 34 patients, treated by radical surgery at the Department of Surgery, J. Śniadecki Hospital, Białystok, Poland, between 1999 and 2003, were examined retrospectively. Patients' clinical records and pathological reports were reviewed with special attention paid to the presence or absence of lymph node metastasis, local recurrence, and distant metastasis. Tissue specimens were collected immediately after tumor

removal, fixed in 100 g/L formaldehyde, embedded in paraffin, and then histopathologically examined using standard hematoxylin-eosin staining according to the TNM classification.

Vascular invasion, lymphatic and venous invasion were examined and grouped. Tumor budding was examined according to the criteria of Morodomi *et al*[1].

Immunohistochemistry

Slides of 4-μm-thick serial sections of the primary tumor were prepared. A standard avidin-biotin immunoperoxidase (Novostain Super ABC Kit (universal), No. NCL-ABCu, Biokom, Poland) method was used for the detection of TGF β expression. Briefly, the slides were dewaxed using xylene, transferred to alcohol, placed in citric acid buffer (10 mmol/L) and heated in a microwave oven (700 W) for 15 min to expose antigens. Endogenous peroxidase activity was inhibited by incubating the section with 3% hydrogen peroxide in methanol for 5 min. The slides were then washed three times with phosphate-buffered saline (PBS) and incubated in 10 g/L normal horse serum for 20 min to reduce nonspecific antibody binding. After washing with PBS, the slides were incubated overnight at 4 ℃ with monoclonal antibodies. Anti-human TGF β protein monoclonal antibody (Novocastra, NCL-TGFB, clone TGFB 17, dilution 1:40, Biokom, Poland) was used. Nonspecific mouse IgG was used as a negative control. The reaction products were visualized with diaminobenzidine DAB (DAKO S3000, Dako, Poland). The sections were counterstained with hematoxylin, dehydrated, and mounted. The tissue sections known to be positive were used as positive controls.

Evaluation of samples

The immunostaining of cytoplasm was observed under a light microscope for TGF β. TGF β expression was semi-quantitatively assessed in neoplastic cells of primary tumors. Cases were considered positive when >20% of cancerous cells was stained with TGF β and negative when <20% of cancerous cells was stained with TGF β. The percentage of TGF β-positive cells was calculated in at least 500 neoplastic cells per sample, under light microscope (×400). The overall results of immunohistochemical examinations are presented in Tables 1-4.

Table 1 TGF β expression in main mass of CRC with and without vascular invasion

Parameter	*n*	Expression of TGF β, *n* (%)		Total (%)
		Negative	Positive	
With vascular invasion	14	3 (21.4)	11 (78.6)	41.2
Without vascular invasion	20	14 (70)	6 (30)	58.8

$P = 0.005$, $P<0.01$.

Table 2 TGF β expression in main mass of CRC with and without lymph node metastasis

Parameter	*n*	Expression of TGF β, *n* (%)		Total (%)
		Negative	Positive	
With lymph node metastasis	16	2 (12.5)	14 (87.5)	47.1
Without lymph node metastasis	18	15 (83.3)	3 (16.7)	52.9

$P = 0.0001$, $P<0.01$.

Table 3 TGF β expression in main mass of CRC with and without distant metastasis

Parameter	*n*	Expression of TGF β, *n* (%)		Total (%)
		Negative	Positive	
With distant metastasis	14	1 (7.2)	13 (92.8)	41.2
Without distant metastasis	20	16 (80.0)	4 (20.0)	58.8

$P = 0.00003$, $P<0.01$.

Table 4 TGF β expression in main mass of CRC with and without tumor budding

Parameter	*n*	Expression of TGF β, *n* (%)		Total (%)
		Negative	Positive	
With tumor budding	12	1 (8.3)	11 (91.7)	35.3
Without tumor budding	22	16 (72.7)	6 (27.3)	64.7

$P = 0.00003$, $P<0.01$.

Statistical analysis

The association between TGF β expression and clinicopathological parameters was examined using χ^2 test. Fisher's exact test was used for statistical analysis. $P<0.05$ was considered statistically significant.

RESULTS

In our study, 17 (50%) out of 34 colorectal carcinomas displayed positive cytoplasmatic TGF β protein reactivity (Figure 1). There was a significant difference between the expression of TGF β in patients with and without vascular invasion (78.6% and 30% respectively, $P<0.01$). A significant difference also existed between the expression of TGF β in primary tumor and lymph node metastases (87.5%, $P<0.01$) and distant metastases (92.8%, $P<0.01$). The presence of tumor- budding at the front of invasion showed a statistically significant correlation with the expression of TGF β in the primary tumor ($P<0.01$).

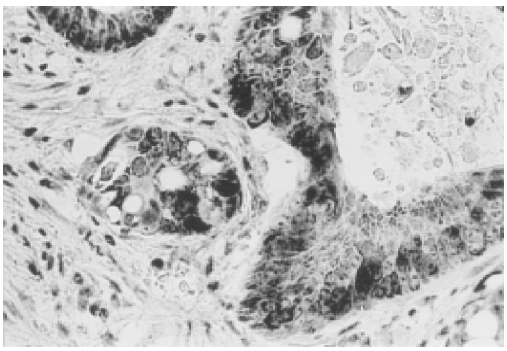

Figure 1 Strong cytoplasmic expression of TGF β in neoplastic cells ×200.

DISCUSSION

Recent studies reported that many tumor cells, including colon cancer cells, can secrete TGF β[13,14]. It has been shown that elevated levels of human TGF β protein in colorectal

cancer correlate with an increased metastatic potential[15]. There is a significant correlation between tumor expression of TGF β 1 and a shorter post-operative survival[16]. It has been reported that plasma concentrations of active total TGF β1 are significantly higher in patients with CRC than in healthy volunteers[17]. Patients with CRC in stages C-D have significantly higher expressions of TGF β1 in tumors [16]. Some authors observed that the expression of TGF β1 is closely related to a higher rate of lymph node metastases in gastric cancer[18]. Our results also showed that the expression of TGF β in CRC pT1 with lymph node and distant metastasis was higher. All these findings are consistent with the results from Robson *et al*[19] who reported a positive expression in 58% of tumors. Similarly, Bellone *et al*[20] reported that colon carcinoma progression is associated with gradual and significant increases in the expression of TGF-β1, TGF-β2 mRNA and proteins. Tsushima *et al*[21] showed that preoperative TGF β1 level is a predictive factor for liver metastasis after curative resection.

The novel histopathological parameter in CRC associated with invasion is known as 'tumor- budding'. Recent studies of the prognostic factors for CRC have paid attention to tumor-budding as a potential prognostic factor[1,8-12]. We found a statistically significant correlation between the intensity of tumor- budding and lymph node involvement[2]. Hase *et al*[8] examined 663 patients with CRC for tumor-budding, and suggested that tumor- budding is an important prognostic factor in patients with CRC. Morodomi *et al*[1] reported that tumor- budding represents the neoplastic cells that are directly involved in host tissue invasion. According to these authors, if the degree of differentiation in colorectal adenocarcinoma is moderate (G2), lymph node involvement is highly probable. However, even in these moderately differentiated tumors, lymphatic involvement is probable but less likely. In well-differentiated adenocarcinomas (G1), tumor-budding and lymphatic invasion are usually not observed. If tumor-budding occurs in such cases, then lymph node involvement is highly probable.

We found that the expression of TGF β in investigated tumors (T1) was strongly correlated with the presence of tumor -budding, vascular invasion at the front of invasion and presence of lymph node and distant metastases. These results suggest that TGF seems to be closely related to the aggressiveness of CRC.

REFERENCES

1 **Morodomi T,** Isomoto H, Shirouzu K, Kakegawa K, Irie K, Morimatsu M. An index for estimating the probability of lymph node metastasis in rectal cancers. Lymph node metastasis and the histopathology of actively invasive regions of cancer. *Cancer* 1989; **63:** 539-543

2 **Guzi ska-Ustymowicz K,** Sulkowska M, Famulski W, Sulkowski S. Tumour 'budding' and its relationship to p53 and Bcl-2 expression in colorectal cancer. *Anticancer Res* 2003; **23:** 649-653

3 **Famulski W,** Guzi ska-Ustymowicz K, Sulkowska M, Chabowski A, Zalewski B, Piotrowski Z, Stasiak-Barmuta A, Sulkowski S. Tumour budding intensity in relation to cathepsin D expression and some clinicopathological features of colorectal cancer. *Folia Histochem Cytobiol* 2001; **39** Suppl 2: 171-172

4 **Fujiwara T,** Stolker JM, Watanabe T, Rashid A, Longo P, Eshleman JR, Booker S, Lynch HT, Jass JR, Green JS, Kim H, Jen J, Vogelstein B, Hamilton SR. Accumulated clonal genetic alterations in familial and sporadic colorectal carcinomas with widespread instability in microsatellite sequences. *Am J Pathol* 1998; **153:** 1063-1078

5 **Markowitz SD,** Roberts AB. Tumor suppressor activity of the TGF β pathway in human cancers. *Cytokine Growth Factor Rev* 1996; **7:** 93-102

6 **Polyak K.** Negative regulation of cell growth by TGF beta. *Biochim Biophys Acta* 1996; **1242:** 185-199

7 **Hsu S,** Huang F, Hafez M, Winawer S, Friedman E. Colon carcinoma cells switch their response to transforming growth factor beta 1 with tumor progression. *Cell Growth Differ* 1994; **5:** 267-275

8 **Hase K,** Shatney C, Johnson D, Trollope M, Vierra M. Prognostic value of tumor budding in patients with colorectal cancer. *Dis Colon Rectum* 1993; **36:** 627-635

9 **Ueno H,** Murphy J, Jass JR, Mochizuki H, Talbot IC. Tumor 'budding' as an index to estimate the potential of aggressiveness in rectal cancer. *Histopathology* 2002; **40:** 127-132

10 **Okuyama T,** Oya M, Ishikawa H. Budding as a risk factor for lymph node metastasis in pT1 or pT2 well-differentiated colorectal adenocarcinoma. *Dis Colon Rectum* 2002; **45:** 628-634

11 **Okuyama T,** Oya M, Yamaguchi M. Budding (sprouting) as a useful prognostic marker in colorectal mucinous carcinoma. *Jpn J Clin Oncol* 2002; **32:** 412-416

12 **Tanaka M,** Hashiguchi Y, Ueno H, Hase K, Mochizuki H. Tumor budding at the invasive margin can predict patients at high risk of recurrence after curative surgery for stage II, T3 colon cancer. *Dis Colon Rectum* 2003; **46:** 1054-1059

13 **Gregoire M,** Garrigue L, Blottiere H, Denis MG, Meflah K. Possible involvement of TGF beta 1 in the distinct tumorigenic properties of two rat colon carcinoma clones. *Invasion Metastasis* 1992; **12:** 185-196

14 **Fischer JR,** Darjes H, Lahm H, Schindel M, Drings P, Krammer PH. Constitutive secretion of bioactive transforming growth factor beta 1 by small cell lung cancer cell lines. *Eur J Cancer* 1994; **30A:** 2125-2129

15 **Narai S,** Watanabe M, Hasegawa H, Nishibori H, Endo T, Kubota T, Kitajima M. Significance of transforming growth factor beta1 as a new tumor marker for colorectal cancer. *Int J Cancer* 2002; **97:** 508-511

16 **Shim KS,** Kim KH, Han WS, Park EB. Elevated serum levels of transforming growth factor-beta1 in patients with colorectal carcinoma: its association with tumor progression and its significant decrease after curative surgical resection. *Cancer* 1999; **85:** 554-561

17 **Xiong B,** Yuan HY, Hu MB, Zhang F, Wei ZZ, Gong LL, Yang GL. Transforming growth factor-beta1 in invasion and metastasis in colorectal cancer. *World J Gastroenterol* 2002; **8:** 674-678

18 **Maehara Y,** Kakeji Y, Kabashima A, Emi Y, Watanabe A, Akazawa K, Baba H, Kohnoe S, Sugimachi K. Role of transforming growth factor-beta 1 in invasion and metastasis in gastric carcinoma. *J Clin Oncol* 1999; **17:** 607-614

19 **Robson H,** Anderson E, James RD, Schofield PF. Transforming growth factor beta 1 expression in human colorectal tumours: an independent prognostic marker in a subgroup of poor prognosis patients. *Br J Cancer* 1996; **74:** 753-758

20 **Bellone G,** Carbone A, Tibaudi D, Mauri F, Ferrero I, Smirne C, Suman F, Rivetti C, Migliaretti G, Camandona M, Palestro G, Emanuelli G, Rodeck U. Differential expression of transforming growth factors-beta1, -beta2 and -beta3 in human colon carcinoma. *Eur J Cancer* 2001; **37:** 224-233

21 **Tsushima H,** Ito N, Tamura S, Matsuda Y, Inada M, Yabuuchi I, Imai Y, Nagashima R, Misawa H, Takeda H, Matsuzawa Y, Kawata S. Circulating transforming growth factor beta1 as a predictor of liver metastasis after resection in colorectal cancer. *Clin Cancer Res* 2001; **7:** 1258-1262

PO Box 2345, Beijing 100023, China
www.wjgnet.com
wjg@wjgnet.com

ELSEVIER

World J Gastroenterol 2005;11(8):1196-1199
World Journal of Gastroenterology ISSN 1007-9327

• *BRIEF REPORTS* •

Role of the intracellular receptor domain of gp130 (exon 17) in human inflammatory bowel disease

Christoph J. Auernhammer, Kathrin Zitzmann, Fabian Schnitzler, Julia Seiderer, Peter Lohse, George Vlotides, Dieter Engelhardt, Michael Sackmann, Burkhard Göke, Thomas Ochsenkühn

Christoph J. Auernhammer, Kathrin Zitzmann, Fabian Schnitzler, Julia Seiderer, George Vlotides, Dieter Engelhardt, Michael Sackmann, Burkhard Göke, Thomas Ochsenkühn, Department of Internal Medicine II - Grosshadern, Ludwig-Maximilians-University, D-81377 Munich, Germany
Peter Lohse, Department of Clinical Chemistry - Grosshadern, Ludwig-Maximilians-University, D-81377 Munich, Germany
Supported by the Department of Clinical Chemistry - Grosshadern, Ludwig-Maximilians-University
Co-first-authors: Christoph J. Auernhammer and Kathrin Zitzmann
Correspondence to: Christoph Auernhammer, M.D., Department of Internal Medicine II, Klinikum Grosshadern, Ludwig-Maximilians-University, Marchioninistr 15, D-81377 Munich, Germany. christoph.auernhammer@med.uni-muenchen.de
Telephone: +49-89-7095-0 Fax: +49-89-700-4418
Received: 2004-06-08 Accepted: 2004-07-27

Abstract

AIM: To study the role of the intracellular receptor domain of gp130 in human inflammatory bowel disease (IBD).

METHODS: We amplified and sequenced the complete exon 17 of the human gp130 gene in 146 patients with IBD. According to clinical and histopathological signs, the 146 patients with IBD were classified as having Crohn's disease (n = 73) or ulcerative colitis (n = 63), or as indeterminate status (n = 10).

RESULTS: No mutations in exon 17 of the gp130 gene could be detected in any of the 146 patients with IBD examined.

CONCLUSION: There is no evidence that mutations in exon 17 of the gp130 gene are involved in the pathogenesis of human IBD.

Key words: Exon 17; Inflammatory bowel disease; gp130 gene

Auernhammer CJ, Zitzmann K, Schnitzler F, Seiderer J, Lohse P, Vlotides G, Engelhardt D, Sackmann M, Göke B, Ochsenkühn T. Role of the intracellular receptor domain of gp130 (exon 17) in human inflammatory bowel disease. *World J Gastroenterol* 2005; 11(8): 1196-1199
http://www.wjgnet.com/1007-9327/11/1196.asp

INTRODUCTION

The gp130 cytokine family includes interleukin (IL)-6, IL-11, leukemia inhibitory factor, oncostatin M, ciliary neurotrophic factor, novel-neurotrophin-1/B-cell stimulating factor-3, neuropoietin and cardiotrophin (CT)-1. Signal transduction of gp130 cytokines involves activation of the Janus kinases and signal transducer and activator of transcription (Jak-STAT) signaling cascade pathway as well as the src-homology tyrosine phosphatase 2 (SHP2)-Ras-Erk pathway. Briefly, ligand binding to the gp130 receptor complex induces autophosphorylation of Jaks, followed by the phosphorylation of specific tyrosine residues in the cytoplasmatic receptor domain and subsequent tyrosine phosphorylation of STAT proteins. Phosphorylated STAT proteins (pSTATs) translocate as homo- or heterodimeric complexes to the nuclei and act as specific transcription factors by binding to regulatory promoter elements of various genes[1-3].

The intracellular domain of the common gp130 receptor subunit harbors several essential motifs involved in signal transduction of gp130 cytokines (Figure 1). The membrane proximal homology region of the intracellular gp130 domain containing the box1 and box2 motifs is important for Jak association[1,4]. The tyrosine residue $Y_{757/759\ (murine/human)}$ in the cytoplasmic domain of activated gp130 is essential for the association of gp130 with src-homology 2 domain-bearing protein tyrosine phosphatase (SHP)-2 and suppressor of cytokine signaling (SOCS)-3[1,4]. SHP-2 down-regulates STAT signaling and links the Jak-STAT cascade to the ras-dependent mitogen-activated protein kinase pathway. SOCS-3 inhibits the Jak-STAT signaling cascade by directly inhibiting Jak kinase activity as well as by binding to activated intracellular cytokine receptor domains and inhibiting further protein association[1,3,4]. Finally, the tyrosines $Y_{765/767\ (murine/human)}$, $Y_{812/814\ (murine/human)}$, $Y_{904/905\ (murine/human)}$, and $Y_{914/915\ (murine/human)}$ in the cytoplasmic domain of activated gp130 are required for the association of STAT proteins with gp130. This association is essential for STAT phosphorylation and activation[1,4].

$Gp130^{\Delta STAT}$ mice harboring a mutated (Y765F and Q768A) and truncated (769stop) intracellular gp130 receptor domain, thus lacking the four specific STAT-binding site motifs YxxQ at tyrosines $Y_{765/812/904/914}$ in murine gp130, display abrogated STAT3 phosphorylation but elevated activation of SHP2 and Erk1/2 following IL-6 stimulation. $Gp130^{\Delta STAT}$ mice show impaired colonic mucosal wound healing, mucosal ulcers in the gastric pylorus and coecum, and exaggerated sodium dextran sulfate (DSS)-induced colitis[5-7].

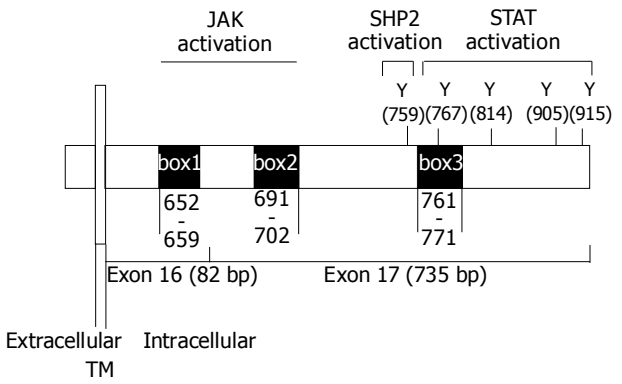

Figure 1 Schematic diagram of the intracellular receptor domain of human gp130 (adapted from Refs.[1-5]).

Crohn's disease and ulcerative colitis are classified as chronic inflammatory bowel diseases (IBDs) characterized by chronic inflammation and the inability to maintain mucosal integrity in the large and/or small intestine. The human gp130 gene is located on chromosome 5q11[4]. Until now, linkage studies have not reported the gp130-corresponding loci on chromosome 5q11 to be susceptible loci for IBD[8], whereas there have been considered susceptible loci for IBD on chromosome 5q31 and 5q13[8]. Nevertheless, data obtained from $Gp130^{\Delta STAT}$ mice strongly suggest that mutations in the intracellular binding sites of gp130 might play a role in the pathophysiology of IBD[5-7]. Therefore, we performed a candidate gene study, searching for mutations in exon 17 of the gp130 gene in 146 patients with IBD.

MATERIALS AND METHODS

Patients

A total of 146 patients with Crohn's disease (n = 73), ulcerative colitis (n = 63) or indeterminate colitis (n = 10) were recruited through the IBD in-patient and out-patient clinics at our university hospital in Munich. Patient data were obtained by chart review and patient questionnaire and recorded by a senior gastroenterologist. Inclusion criteria were based on homogenous diagnostic parameters including clinical data (physical examination, CDAI[9]/Lichtiger score[10]), laboratory findings, endoscopic criteria (location and degree of inflammation, stenosis, fistulas, transmural involvement in colonoscopy) and radiological findings (CT and/or MRT). At inclusion, all patients had duration of IBD of more than one year. An infectious pathogenesis of gastrointestinal symptoms was excluded in all patients by biopsy and stool culture. EDTA blood samples for molecular genetic studies were taken, after written informed consents were obtained from the patients and/or their parents. The study protocol followed ethical guidelines and was approved by the Institutional Ethical Committee.

DNA isolation and sequencing

Genomic DNA was isolated from the peripheral blood leukocytes with the DNA blood mini kit (QIAGEN, Hilden, Germany). Exon 17 of the gp130 gene (GeneBank Accession M57230; Ref.[4]) was amplified by PCR using the intron-specific primer pair 5'-AGTTTCAGAGATGCATTA GCTCTGTG-3' (sense) and 5'-GGCAAATGATCATCTT CAGAGAGTG-3' (antisense; nt 68781 to nt 69703 in GeneBank Accession AC016596) in order to avoid amplification of an intronless pseudogene of gp130[4]. Each 50-μL reaction contained approximately 300 ng of genomic DNA, 0.4 μmol/L of each primer, 1.5 mmol/L $MgCl_2$, 5 μL Thermo Start reaction buffer (ABgene, Epsom, UK), 125 μmol/L dNTPs, and 0.25 μL of Thermo Start Taq DNA polymerase (ABgene). PCR was performed for 40 amplification cycles (denaturation at 95 ℃ for 30 s, annealing at 62 ℃ for 30 s and extension at 72 ℃ for 30 s). PCR products were purified using the QIAquick PCR purification kit (QIAGEN, Hilden, Germany) and sequenced with the Big Dye terminator v3.1 ready reaction cycle sequencing kit (Applied Biosystems, Foster City, USA). Data analysis was performed on an ABI Prism 377 DNA sequencer (Applied Biosystems).

RESULTS

Patient characteristics

Seventy-three patients with Crohn's disease (39 males, 34 females), 63 patients with ulcerative colitis (24 males, 39 females) and 10 patients with indeterminate IBD (4 males, 6 females) were examined. The median age at inclusion was 39±10 years in the CD group, 41±15 years in the UC group and 47±19 years in the indeterminate group (mean±SD). All patients included in this study had a history of at least one episode with an elevated CDAI[9] of more than 150 points in Crohn's disease or a Lichtiger[10] score of more than 10 points in ulcerative colitis in combination with characteristic endoscopical and radiological findings.

gp130 exon 17 sequencing

The genomic DNA of the 146 patients with IBD, who were classified as Crohn's disease (n = 73), ulcerative colitis (n = 63) and indeterminate IBD (n = 10), was sequenced for mutations in exon 17 of the gp130 gene. None of these 146 patients carried a mutation or a polymorphism in this region of the gp130 receptor gene. Therefore, we could exclude mutations in exon 17 of the gp130 receptor gene being involved in the etiology of Crohn's disease in more than 5% of patients (P<0.05). Likewise, we did not find any evidence that mutations in exon 17 of the gp130 receptor gene might be involved in the etiology of ulcerative colitis.

DISCUSSION

The current study demonstrated a lack of mutations in exon 17 of the human gp130 gene in 146 patients with IBD, e.g., Crohn's disease and ulcerative colitis. Exon 17 of the gp130 gene[4] is spanning most of the intracellular region of the gp130 receptor (Figure 1) and harbors several important signal transduction regions such as the membrane proximal box2 motif for Jak association, the tyrosine residue $Y_{757/759\ (murine/human)}$ for SHP2 and SOCS-3 association, and the tyrosine residues $Y_{765/767\ (murine/human)}$, $Y_{812/814\ (murine/human)}$,

$Y_{904/905\ (murine/human)}$, and $Y_{914/915\ (murine/human)}$ for STAT association[1,4].

The animal model of gp130$^{\Delta STAT}$ mice demonstrated impaired STAT activation due to a truncated intracytoplasmatic gp130 receptor domain lacking the tyrosine residues $Y_{765/812/904/914}$ associated with impaired mucosal healing, mucosal ulcers in the gastric pylorus and caecum, and exaggerated DSS-induced colitis[5-7]. On the other hand, gp130 (757F) mice harboring a mutated (Y757F and V760A) YxxV motif for SHP-2 and SOCS-3 binding displayed enhanced tissue STAT3 phosphorylation, but abrogated SHP2-Ras-ERK signaling following IL-6 stimulation. Gp130 (757F) mice developed gastric adenomas by 3 mo of age[6]. These two gastrointestinal phenotypes are highly similar to the phenotypes exhibited by mice deficient in trefoil factor 1 (pS2/TFF1) and in intestinal trefoil factor (ITF)/TFF3, respectively. TFF1 and TFF3 are members of the trefoil factor (TFF) family; each of them bears a characteristic three-looped structure known as the trefoil domain. TFF1 is primarily expressed in gastric-pit mucus cells. TFF3 is expressed at its highest level in the mucous-secreting goblet cells of the small and large intestine. TFFs are supposed to be involved in the process of healing or restitution, since they are upregulated after injury to the gastrointestinal epithelium. TFF1 knock-out mice could develop gastric hyperplasia, whereas deletion of TFF3 might become visible in an exaggerated response to DSS-mediated epithelial damage. Regulation of TFF1 and TFF3 in the gastrointestinal tract seems to be dependent on SHP2/Erk and STAT1/3 signaling, as reduced gastric levels of TFF1 can be seen in gp130 (757F) mice, while reduced colonic levels of TFF3 are observed in gp130D^{STAT} mice[6,7]. Taken together, it seems that the integrity of the gastrointestinal mucosa can be maintained by a balanced activation of both pathways (leading to a certain ratio of TFF1 *vs* TFF3). According to this model, the imbalance in favor of STAT1/3 signaling leads to excessive antral proliferation, presumably caused by unhindered effects of STAT signaling. An exaggerated activation of the SHP2/Erk signaling cascade results in mucosal healing defects due to a lack of phosphorylated STAT3. Either the decreased level of phosphorylated STAT3 itself or down-regulation of TFF3 leads to impaired epithelial cell migration after the injury of the intestinal epithelium. However, our current study has demonstrated that impaired STAT activation due to a mutated or truncated intracellular gp130 receptor domain is not involved in the pathogenesis of IBD in humans. Nevertheless, mutations at this site might be involved in the pathogenesis of other human diseases, e.g., degenerative joint disease or blastocyst implantation failure[5].

Other studies suggest IBD to be associated with increased rather than decreased STAT activation. Increased STAT1 phosphorylation[11], STAT3 phosphorylation[12], and STAT-dependent SOCS-3 expression[11,12] have been observed in human colon samples from patients with IBD.. Phosphorylated STAT proteins are primarily expressed in inflammatory cells infiltrating the mucosa[11,12] and STAT activation is probably due to IL-6-mediated stimulation of these cells[13]. Suzuki *et al*[14] reported that a mutant SOCS-1 protein (F59D-JAB) inhibits the negative regulatory effects of endogenous SOCS-1 and SOCS-3. F59D-JAB transgenic mice demonstrate exaggerated DSS-induced colitis and hyperactivated STAT3 activation, probably due to lack of the negative regulatory role of SOCS-3[12]. Loss of SOCS-3 has recently been shown to result in prolonged STAT3 and STAT1 activation after IL-6 stimulation[15,16].

In summary, dysbalance of the Jak-STAT pathway seems to be involved in the pathogenesis of colitis[6,8,12,14]. In the current study, however, we found no evidence that mutations in exon 17 of the gp130 gene, encoding all functionally essential intracellular tyrosine residues of the gp130 receptor (Figure 1), are involved in the pathogenesis of human IBD. Our data suggest that other mechanisms are important for the dysbalance of the Jak-STAT pathway in IBD. The role of STAT protein activation and negative regulation of Jak-STAT signaling merits further investigation. Studies on the putative role of SOCS-3 mutations in the pathogenesis of IBD are currently underway.

ACKNOWLEDGEMENTS

We gratefully acknowledge the skilful technical assistance by Pia Lohse and Heike Rübsamen, Department of Clinical Chemistry - Grosshadern, Ludwig-Maximilians-University, D-81377 Munich, Germany.

This work contains parts of the unpublished doctoral thesis of K. Zitzmann at the Ludwig-Maximilians-University of Munich, Germany.

REFERENCES

1 **Heinrich PC**, Behrmann I, Haan S, Hermanns HM, Muller-Newen G, Schaper F. Principles of interleukin (IL)-6-type cytokine signalling and its regulation. *Biochem J* 2003; **374**: 1-20

2 **Vlotides G**, Zitzmann K, Stalla GK, Auernhammer CJ. Novel neurotrophin-1/B cell-stimulating factor-3 (NNT-1/BSF-3)/cardiotrophin-like cytokine (CLC) – a novel gp130 cytokine with pleiotropic functions. *Cytokine Growth Factor Rev* 2004; **15**: 325-336

3 **Auernhammer CJ**, Melmed S. The central role of SOCS-3 in integrating the neuro-immunoendocrine interface. *J Clin Invest* 2001; **108**: 1735-1740

4 **Szalai C**, Toth S, Falus A. Exon-intron organization of the human gp130 gene. *Gene* 2000; **243**: 161-166

5 **Ernst M**, Inglese M, Waring P, Campbell IK, Bao S, Clay FJ, Alexander WS, Wicks IP, Tarlinton DM, Novak U, Heath JK, Dunn AR. Defective gp130-mediated signal transducer and activator of transcription (STAT) signaling results in degenerative joint disease, gastrointestinal ulceration, and failure of uterine implantation. *J Exp Med* 2001; **194**: 189-203

6 **Tebbutt NC**, Giraud AS, Inglese M, Jenkins B, Waring P, Clay FJ, Malki S, Alderman BM, Grail D, Hollande F, Heath JK, Ernst M. Reciprocal regulation of gastrointestinal homeostasis by SHP2 and STAT-mediated trefoil gene activation in gp130 mutant mice. *Nat Med* 2002; **8**: 1089-1097

7 **Wang TC**, Goldenring JR. Inflammation intersection: gp130 balances gut irritation and stomach cancer. *Nat Med* 2002; **8**: 1080-1082

8 **van Heel DA**, Fisher SA, Kirby A, Daly MJ, Rioux JD, Lewis CM. Inflammatory bowel disease susceptibility loci defined by genome scan meta-analysis of 1952 affected relative pairs. *Hum Mol Genet* 2004; **13**: 763-770

9 **Best WR**, Becktel JM, Singleton JW, Kern F. Development of a Crohn's disease activity index. National Cooperative Crohn's Disease Study. *Gastroenterology* 1976; 70: 439-444

10 **Lichtiger S**, Present DH, Kornbluth A, Gelernt I, Bauer J, Galler G, Michelassi F, Hanauer S. Cyclosporine in severe ulcerative colitis refractory to steroid therapy. *N Engl J Med* 1994; **330**: 1841-1845

11 **Schreiber S**, Rosenstiel P, Hampe J, Nikolaus S, Groessner B, Schottelius A, Kuhbacher T, Hamling J, Folsch UR, Seegert D. Activation of signal transducer and activator of transcription (STAT) 1 in human chronic inflammatory bowel disease. *Gut* 2002; **51**: 379-385

12 **Lovato P**, Brender C, Agnholt J, Kelsen J, Kaltoft K, Svejgaard A, Eriksen KW, Woetmann A, Odum N. Constitutive STAT3 activation in intestinal T cells from patients with Crohn's disease. *J Biol Chem* 2003; **278**: 16777-16781

13 **Atreya R**, Mudter J, Finotto S, Mullberg J, Jostock T, Wirtz S, Schutz M, Bartsch B, Holtmann M, Becker C, Strand D, Czaja J, Schlaak JF, Lehr HA, Autschbach F, Schurmann G, Nishimoto N, Yoshizaki K, Ito H, Kishimoto T, Galle PR, Rose-John S, Neurath MF. Blockade of interleukin 6 trans signaling suppresses T-cell resistance against apoptosis in chronic intestinal inflammation: evidence in crohn disease and experimental colitis *in vivo*. *Nat Med* 2000; **6**: 583-588

14 **Suzuki A**, Hanada T, Mitsuyama K, Yoshida T, Kamizono S, Hoshino T, Kubo M, Yamashita A, Okabe M, Takeda K, Akira S, Matsumoto S, Toyonaga A, Sata M, Yoshimura A. CIS3/SOCS3/SSI3 plays a negative regulatory role in STAT3 activation and intestinal inflammation. *J Exp Med* 2001; **193**: 471-481

15 **Croker BA**, Krebs DL, Zhang JG, Wormald S, Willson TA, Stanley EG, Robb L, Greenhalgh CJ, Forster I, Clausen BE, Nicola NA, Metcalf D, Hilton DJ, Roberts AW, Alexander WS. SOCS3 negatively regulates IL-6 signaling *in vivo*. *Nat Immunol* 2003; **4**: 540-545

16 **Lang R**, Pauleau AL, Parganas E, Takahashi Y, Mages J, Ihle JN, Rutschman R, Murray PJ. SOCS3 regulates the plasticity of gp130 signaling. *Nat Immunol* 2003; **4**: 546-550

PO Box 2345, Beijing 100023, China
www.wjgnet.com
wjg@wjgnet.com

ELSEVIER

World J Gastroenterol 2005;11(8):1200-1203
World Journal of Gastroenterology ISSN 1007-9327

• *BRIEF REPORTS* •

Human papillomavirus in squamous cell carcinoma of esophagus in a high-risk population

Mohammad Farhadi, Zahra Tahmasebi, Shahin Merat, Farin Kamangar, Dariush Nasrollahzadeh, Reza Malekzadeh

Mohammad Farhadi, Shahin Merat, Dariush Nasrollahzadeh, Reza Malekzadeh, Digestive Disease Research Center, Tehran University of Medical Sciences, Tehran, Iran
Zahra Tahmasebi, Department of Molecular Biology, Khatam Postgraduate Faculty, Tehran, Iran
Farin Kamangar, Cancer Prevention Studies Branch, US National Cancer Institute, Bethesda, MD, USA
Supported by the Digestive Disease Research Center, Tehran University of Medical Sciences
Correspondence to: Professor Reza Malekzadeh, Digestive Disease Research Center, Shariati Hospital, North Kargar Avenue, Tehran 14114, Iran. malek@ams.ac.ir
Telephone: +98-21-8012992 Fax: +98-21-2253635
Received: 2004-02-11 Accepted: 2004-03-13

Abstract

AIM: To investigate the relation of human papillomavirus (HPV) and esophageal squamous cell carcinoma (ESCC) in Iranian patients as compared to normal controls.

METHODS: Using MY09/MY11 consensus primers, we compared the prevalence of a HPV *L1* gene in tumor tissues from 38 ESCC cases and biopsied tissues from 38 endoscopically normal Iranian individuals. We also compared the presence of HPV16 and HPV18 in the same samples using type-specific E6/E7 primers.

RESULTS: Fourteen (36.8%) of the 38 ESCC samples but only 5 (13.2%) of the 38 control samples were positive for the HPV *L1* gene ($P = 0.02$). Five (13.2%) of the ESCC samples but none of the control samples were positive for the HPV16 *E6/E7* gene ($P = 0.05$). Three (7.9%) of the ESCC samples and 5 (13.2%) of the control samples were positive for the HPV18 *E6/E7* gene ($P = 0.71$).

CONCLUSION: Our data are consistent with HPV DNA studies conducted in other high-risk areas for ESCC. HPV should be considered as a potential factor contributing to the high incidence of ESCC in Iran and other high-incidence areas of the world.

Key words: Papillomavirus; Squamous cell carcinoma of esophagus; Population

Farhadi M, Tahmasebi Z, Merat S, Kamangar F, Nasrollahzadeh D, Malekzadeh R. Human papillomavirus in squamous cell carcinoma of esophagus in a high-risk population. *World J Gastroenterol* 2005; 11(8): 1200-1203
http://www.wjgnet.com/1007-9327/11/1200.asp

INTRODUCTION

The role of human papillomavirus (HPV) in the etiology of esophageal squamous cell carcinoma (ESCC) has been debated in the past 20 years. Oncogenic types of HPV, most notably HPV 16 and HPV 18, are recognized as the most significant risk factors of cervical cancer[1]. A role of HPV in the etiology of cancers of vulva, anus, penis, and oropharyngeal cavity has also been established[2]. However, the role of HPV in the causation of ESCC remains controversial. Syrjanen first suggested a role of HPV in the etiology of ESCC in 1982, based on the observation of characteristic histological findings suggesting the presence of HPV in benign esophageal epithelia and malignant esophageal tumors[3]. Since then several studies have used a variety of techniques, including detection of HPV DNA in esophageal tumor tissues and serological methods, to examine the association between exposure to HPV and risk of ESCC[4]. The results of these studies are not consistent. Case series using polymerase chain reaction have found evidence of HPV in tumor tissues varying from 0 to 67%[4].

It has been suggested that the high variation in HPV DNA results may partly be explained by geographic variation. Most studies, that did not detect HPV DNA in esophageal tumors, were conducted in low-risk areas of USA or Europe. However most studies in high-risk areas for ESCC (such as China, South Africa, and Japan) found that HPV had significantly higher percentages in esophageal tumors[4].

Iran is a very high-risk area for esophageal cancer[5-8]. In some parts of northeastern Iran, the incidence rate of ESCC is reportedly over 100/100 000 person/year[5].

In order to investigate the prevalence of HPV infection in ESCC in Iran, a country with high rates of ESCC, we evaluated the tumor tissues from patients with ESCC and normal esophageal tissues from age-matched controls for the presence of HPV DNA.

MATERIALS AND METHODS

Formalin-fixed paraffin-embedded tissue samples were collected from the patients undergoing surgery for ESCC in two hospitals in Tehran (Shariati, Mehr) from 1996 to 2001. One control per case was selected from consecutive patients referred to a private gastroenterology clinic in Tehran for symptoms of dyspepsia. Only subjects who had normal endoscopy (non-ulcer dyspepsia) and matched on age (±5 years) with one of the case subjects were eligible to be controls. In the controls, two biopsies were taken from the middle third of the esophagus, about 30 cm from the incisor teeth.

The presence of the representative tumor in selected paraffin blocks was confirmed by at least two pathologists before the blocks were further processed for HPV DNA.

One block from each tumor and one block containing both biopsies from each control patient were evaluated for the presence of HPV *L1* gene using MY09/MY11 consensus (general) primers. MY09/MY11 primers are complementary to 450-bp-conserved sequences in the *L1* gene of HPV, and are able to amplify the *L1* gene from a broad range of HPV types. In samples where the *L1* gene could be amplified, further examination was performed to explore the presence of HPV16- and HPV18-specific *E6/E7* genes.

DNA extraction

Serial tissue sections (3-5 sections, each 10-20-μm thick) were cut from each paraffin block using disposable microtome blades. After rehydration, DNA was extracted using a lysis buffer containing 10 mmol/L Tris–HCl (pH 8), 100 mmol/L NaCl, 1% sodium docecyl sulfate, 200 μg/mL proteinase K, and 0.01% EDTA at 56 ℃ for 4 h and then incubated overnight at 37 ℃ in a lytic solution. After proteinase K digestion of the tissue, proteinase K was inactivated by incubation at 95 ℃ for 8-10 min. After vortex with phenol and 150 μL chloroform-isoamylalcohol and spun for 2 min at high speed, the upper phase was transferred to a new tube.

Sample suitability

Suitability of samples for PCR amplification was ascertained by testing for the beta-globin gene. Successful amplification of the beta-globin gene fragments indicated that the DNA sample was adequate for PCR analysis and that no PCR inhibitors were present.

Primers

To examine for the presence of any HPV DNA in the tissue, MY09/MY11 primer pairs were used to amplify the *L1* gene. To look for HPV types 16 and 18, the type-specific primer pairs for the *E6/E7* gene were used (Table 1). Distilled water was used as a negative control. This control was necessary to determine if any of the reagents was contaminated with HPV DNA.

Table 1 Primer sequences used for the amplification of HPV *L1*, HPV16 *E6/E7*, and HPV18 *E6/E7* genes

Target	Primer sequence	Approximate size (bp)
HPV *L1* gene (MY09)	5′ CGTCC{C/A}A{G/A}{G/A}GGA{T /A}ACTGATC 3′	450
HPV *L1* gene (MY11)	5′ GC{C/A}CAGGG {T/A} CAT AA {T/C}AATGG 3′	450
HPV16 *E6/E7* gene (sense)	5′ GAACAGCAATACAACAAACCCG 3′	240
HPV16 *E6/E7* gene (antisense)	5′ CCATGCATGATTACAGCTGG 3′	240
HPV18 *E6/E7* gene (sense)	5′ TGCCAGAAACCGTTGAATCC 3′	250
HPV18 *E6/E7* gene (antisense)	5′ CAATGTCTTGCAATGTTGCC 3′	250

Amplification

Master mixtures contained PCR buffer, 10 mmol/L Tris-HCl (pH 8.4), 50 mmol/L KCl, 2.5 mmol/L $MgCl_2$, 0.01% gelatin, 0.2 mmol/L of each dNTP (dATP, dCTP, dGTP and dTTP), 0.5 mmol/L of each primer and 2.5 units of Taq polymerase (Amp Taq). The PCR mixture was subjected to 30 cycles of amplification (using Genius thermal cycler) each consisting of an initial denaturing step at 94 ℃ for 1 min, annealing at 60 ℃ for 30 s and extension at 72 ℃ for 1 min.

The PCR products were then detected by 2% agarose gel electrophoresis and visualized by ethidium bromide staining. Results were saved by a documentation system along with a transilluminator.

Statistical methods

We used the χ^2 test or the Fisher exact test, wherever appropriate, to compare the proportions of cases and controls that were positive for HPV *L1* gene and HPV16 and HPV18 (type-specific *E6/E7* genes).

The study protocol was approved by the Ethics Committee of the Digestive Disease Research Center, Tehran University of Medical Sciences, and informed consent was obtained from all controls before endoscopy.

RESULTS

Tissue samples were available from 40 cases of ESCC operated between 1996 and 2001. After DNA extraction, two samples were found unsuitable for PCR and excluded. The other 38 samples (22 males and 16 females) were included in the study as cases. Thirty-eight control subjects (16 males and 22 females), age-matched to cases, were selected from patients who were endoscopied for dyspepsia and had normal endoscopies. Mean ± SD age was 54.2±13 years in cases (range 25-75 years), and 51.6±11.3 years in controls (range 22-78 years).

Fourteen (36.8%) out of the 38 ESCC samples but only 5 (13.2%) of the 38 control samples were positive for HPV *L1* gene ($P = 0.02$). Five (13.2%) of the ESCC samples but none of the control samples were positive for HPV16 *E6/E7* gene ($P = 0.05$). Three (7.9%) of the ESCC samples and 5 (13.2%) of the control samples were positive for HPV18 *E6/E7* gene ($P = 0.71$). No sample was positive for both HPV16 and HPV18.

DISCUSSION

ESCC has become the sixth most common cause of cancer death worldwide[9]. In western countries, where the risk of ESCC is generally low, consumption of tobacco and alcohol could explain more than 90% of the cases of ESCC[6,10]. However, in countries with the highest rates of ESCC, such as Iran and China, only a small proportion of ESCC cases could be attributed to smoking or alcohol consumption[6,11]. So other risk factors must be responsible for the high incidence of ESCC in these areas. Microbial agents, especially HPV, may be one of the factors that explain part of this high incidence of ESCC.

The etiologic role of oncogenic HPV types has been

established in many epithelial cancers, most notably cervical cancer[1,2]. Previous studies have shown that HPV16 and HPV18 are the most important risk factors for cervical cancer[1]. The mechanisms through which HPV can induce epithelial neoplasia have been extensively studied[12-15]. Some of the proteins produced by HPV, notably E6 and E7, are oncoproteins that could immortalize various human cell types, inactivate host proteins (such as p53 or pRb), and induce mutations in the host cell DNA[14,16,17].

The role of HPV in ESCC has been studied in many high-risk and low-risk areas of the world[4,18]. Most studies from high-risk areas, such as China and South Africa, have suggested a role of HPV in ESCC, while most studies from low-risk areas have failed to find any association[4,19-21]. To the best of our knowledge, this is the first study that reports the association between DNA markers of HPV and the risk of ESCC in Iran, a high-risk area for ESCC.

Our results imply that HPV is not a predominant risk factor for ESCC in Iran because only 14 (36.8%) of 38 samples of ESCC were positive for the common indicator of HPV (*L1* gene). However, this was higher than the percentage of positive samples in controls (13.2%) and the difference was statistically significant ($P = 0.02$). Higher prevalence of this HPV marker in ESCC cases than in controls may be confounded by other factors. But in the light of known mechanisms of carcinogenicity established for HPV and previous studies associating HPV with epithelial cancers, it is unlikely that the virus is a mere innocent bystander, and HPV should be considered as a potential factor contributing to high incidence of ESCC in Iran.

The prevalence of HPV16 was significantly higher in ESCC cases than that in controls ($P = 0.05$), but there was no statistically significant difference in the prevalence of HPV18 between cases and controls. This implies that only HPV16, but not HPV18, may be a risk factor for ESCC in Iran. A similar Chinese study by Zhou *et al* found a similar result. We found markers for HPV16 and HPV18 in only 8 out of 14 ESCC samples in which HPV *L1* gene was present. Therefore, it is possible that other HPV types, not tested in this study, may also be associated with the risk of ESCC in this area. Another line of evidence that argues against high exposure of the Iranian population to HPV16 and HPV18, and hence against these two types of HPV being major risk factors for ESCC in Iran, is the low prevalence of cervical cancer in Iran[7]. Low exposure to HPV16 and HPV18 in Iran is possibly related to the lifestyle and sexual behaviors in this religious society.

A potential shortcoming of this study, as well as other retrospective studies, is their limited ability to find an association between HPV and ESCC, if HPV has a "hit-and-run" mechanism for inducing ESCC, as some studies in a bovine model have suggested[22]. These studies have found that bovine papillomavirus is essential in the early stages of carcinogenesis of the bovine foregut, but is not needed for progression to the malignant state. Therefore, although we found evidence for the presence of HPV in only 38% of our case samples, it is possible that such evidence in other cases has disappeared. This hypothesis can only be tested in prospective studies with tissue or serum samples. So far, no prospective studies using tissue samples have examined this hypothesis, but two small prospective serologic studies have found a strong association between serologic HPV markers and the risk of ESCC[23,24].

In summary, our data are consistent with HPV DNA studies conducted in other high-risk areas for ESCC which showed evidence of HPV in tumor tissues from 20% to 50% of ESCC cases. We think that HPV should be considered as a potential factor contributing to the high incidence of ESCC in Iran and other high-incidence areas of the world. Further prospective studies are needed to test the hypothesis of a "hit-and-run" phenomenon, the hypothetical mechanism suggested for the disappearance of HPV from tumors after initial DNA damage.

REFERENCES

1 **Munoz N,** Bosch FX, de Sanjose S, Herrero R, Castellsague X, Shah KV, Snijders PJ, Meijer CJ. Epidemiologic classification of human papillomavirus types associated with cervical cancer. *N Engl J Med* 2003; **348:** 518-527

2 **Gillison ML,** Shah KV. Chapter 9: Role of mucosal human papillomavirus in nongenital cancers. *J Natl Cancer Inst Monogr* 2003; **31**: 57-65

3 **Syrjanen K,** Pyrhonen S, Aukee S, Koskela E. Squamous cell papilloma of the esophagus: a tumour probably caused by human papilloma virus (HPV). *Diagn Histopathol* 1982; **5:** 291-296

4 **Syrjanen KJ.** HPV infections and oesophageal cancer. *J Clin Pathol* 2002; **55:** 721-728

5 **Mahboubi E,** Kmet J, Cook PJ, Day NE, Ghadirian P, Salmasizadeh S. Oesophageal cancer studies in the Caspian Littoral of Iran: the Caspian cancer registry. *Br J Cancer* 1973; **28:** 197-214

6 **Munoz N,** Day NE. Esophageal cancer In: Schottenfeld D, Fraumeni JF, eds. Cancer Epidemiology and Prevention. *New York: Oxford University Press* 1996: 681-706

7 **Sadjadi A,** Malekzadeh R, Derakhshan MH, Sepehr A, Nouraie M, Sotoudeh M, Yazdanbod A, Shokoohi B, Mashayekhi A, Arshi S, Majidpour A, Babaei M, Mosavi A, Mohagheghi MA, Alimohammadian M. Cancer occurrence in Ardabil: results of a population-based cancer registry from Iran. *Int J Cancer* 2003; **107:** 113-118

8 **Saidi F,** Sepehr A, Fahimi S, Farahvash MJ, Salehian P, Esmailzadeh A, Keshoofy M, Pirmoazen N, Yazdanbod M, Roshan MK. Oesophageal cancer among the Turkomans of northeast Iran. *Br J Cancer* 2000; **83:** 1249-1254

9 **Parkin DM,** Bray F, Ferlay J, Pisani P. Estimating the world cancer burden: Globocan 2000. *Int J Cancer* 2001; **94:** 153-156

10 **Brown LM,** Hoover R, Silverman D, Baris D, Hayes R, Swanson GM, Schoenberg J, Greenberg R, Liff J, Schwartz A, Dosemeci M, Pottern L, Fraumeni JF. Excess incidence of squamous cell esophageal cancer among US Black men: role of social class and other risk factors. *Am J Epidemiol* 2001; **153:** 114-122

11 **Cook-Mozaffari PJ,** Azordegan F, Day NE, Ressicaud A, Sabai C, Aramesh B. Oesophageal cancer studies in the Caspian Littoral of Iran: results of a case-control study. *Br J Cancer* 1979; **39:** 293-309

12 **zur Hausen H,** de Villiers EM. Human papillomaviruses. *Annu Rev Microbiol* 1994; **48:** 427-447

13 **zur Hausen H.** Papillomaviruses in human cancers. *Proc Assoc Am Physicians* 1999; **111:** 581-587

14 **zur Hausen H.** Immortalization of human cells and their malignant conversion by high risk human papillomavirus genotypes. *Semin Cancer Biol* 1999; **9:** 405-411

15 **Chen HB,** Chen L, Zhang JK, Shen ZY, Su ZJ, Cheng SB, Chew EC. Human papillomavirus 16 E6 is associated with the nuclear matrix of esophageal carcinoma cells. *World J Gastroenterol* 2001; **7:** 788-791

16 **Mantovani F,** Banks L. The interaction between p53 and papillomaviruses. *Semin Cancer Biol* 1999; **9:** 387-395
17 **Caldeira S,** de Villiers EM, Tommasino M. Human papillomavirus E7 proteins stimulate proliferation independently of their ability to associate with retinoblastoma protein. *Oncogene* 2000; **19:** 821-826
18 **Lavergne D,** de Villiers EM. Papillomavirus in esophageal papillomas and carcinomas. *Int J Cancer* 1999; **80:** 681-684
19 **Kok TC,** Nooter K, Tjong-A-Hung SP, Smits HL, Ter Schegget JT. No evidence of known types of human papillomavirus in squamous cell cancer of the oesophagus in a low-risk area. Rotterdam Oesophageal Tumour Study Group. *Eur J Cancer* 1997; **33:** 1865-1868
20 **Chen B,** Yin H, Dhurandhar N. Detection of human papillomavirus DNA in esophageal squamous cell carcinomas by the polymerase chain reaction using general consensus primers. *Hum Pathol* 1994; **25:** 920-923
21 **Chang F,** Syrjanen S, Shen Q, Cintorino M, Santopietro R, Tosi P, Syrjanen K. Human papillomavirus involvement in esophageal carcinogenesis in the high-incidence area of China. A study of 700 cases by screening and type-specific *in situ* hybridization. *Scand J Gastroenterol* 2000; **35:** 123-130
22 **Campo MS.** Papillomas and cancer in cattle. *Cancer Surv* 1987; **6:** 39-54
23 **Dillner J,** Knekt P, Schiller JT, Hakulinen T. Prospective seroepidemiological evidence that human papillomavirus type 16 infection is a risk factor for oesophageal squamous cell carcinoma. *BMJ* 1995; **311:** 1346
24 **Bjorge T,** Hakulinen T, Engeland A, Jellum E, Koskela P, Lehtinen M, Luostarinen T, Paavonen J, Sapp M, Schiller J, Thoresen S, Wang Z, Youngman L, Dillner J. A prospective, seroepidemiological study of the role of human papillomavirus in esophageal cancer in Norway. *Cancer Res* 1997; **57:** 3989-3992

PO Box 2345, Beijing 100023, China
www.wjgnet.com
wjg@wjgnet.com

ELSEVIER

World J Gastroenterol 2005;11(8):1204-1209
World Journal of Gastroenterology ISSN 1007-9327

• *BRIEF REPORTS* •

Protective effect of Weikang decoction and partial ingredients on model rat with gastric mucosa ulcer

Tuo-Ying Fan, Qing-Qing Feng, Chun-Rong Jia, Qun Fan, Chun-An Li, Xue-Lian Bai

Tuo-Ying Fan, Qing-Qing Feng, Qun Fan, Chun-An Li, Xue-Lian Bai, 94 Hospital of PLA, Nanchang 330002, Jiangxi Province, China
Chun-Rong Jia, People's Hospital of Wuhan University, Wuhan 430060, Hubei Province, China
Qun Fan, Shenzhen Donghu Hospital, Shenzhen 518020, Guangdong Province, China
Supported by the Education Commission of Hubei Province, No. (1996)028
Co-first-authors: Tuo-Ying Fang and Qing-Qing Feng
Co-correspondence: Tuo-Ying Fang
Correspondence to: Dr. Qun Fan, Shenzhen Donghu Hospital, Shenzhen 518020, Guangdong Province, China. fqng1008@163.com
Telephone: +86-755-25634729 Fax: +86-755-25604034
Received: 2004-03-20 Accepted: 2004-06-11

Abstract

AIM: To investigate the protective mechanisms of Weikang (WK) decoction on gastric mucosae.

METHODS: Ninety rats were randomly divided into nine groups of 10 each, namely group, model group, group with large WK dosage, group with medium WK dosage, group with small WK dosage, group with herbs of jianpiyiqi (strengthening the spleen and replenishing qi), group with herbs of yangxuehuoxue (invigorating the circulation of and nourishing the blood), group with herbs of qingrejiedu (clearing away the heat-evils and toxic materials), group with colloidal bismuth pectin (CBP) capsules. According to the method adopted by Yang Xuesong, except normal control group, chronic gastric ulcer was induced with 100% acetic acid. On the sixth day after moldmaking, WK decoction was administered, respectively at doses of 20, 10 and 5 g/kg to rats of the WK groups, or the groups with herbs of jianpiyiqi, yangxuehuoxue and qingrejiedu, 10 mL/kg was separately administered to each group every day. For the group with CBP capsules, medicine was dissolved with water and doses 15 times of human therapeutic dose were administered (10 mL/kg solution containing 0.35% CBP). Rats of other groups were fed with physiological saline (10 mL/kg every day). Administration lasted for 16 d. Rats were killed on d 22 after mold making to observe changes of gastric mucosa. The mucus thickness of gastric mucosa surface was measured. Levels of epidermal growth factor (EGF) in gastric juice, nitric oxide (NO) in gastric tissue, endothelin (ET) in plasma, superoxide dismutase (SOD) in plasma, malondialdehyde (MDA) in plasma and prostaglandin I_2 (PGI_2) were examined.

RESULTS: Compared with control group, ulceration was found in gastric mucosa of model group rats. The mucus thickness of gastric mucosa surface, the levels of EGF, NO, 6-K-$PGF_1\alpha$ and SOD decreased significantly in the model group (EGF: 0.818±0.18 *vs* 2.168±0.375, NO: 0.213±0.049 *vs* 0.601±0.081, 6-K-$PGF_1\alpha$: 59.7±6.3 *vs* 96.6±8.30, SOD: 128.6±15.0 *vs* 196.6±35.3, $P<0.01$), the levels of ET (179.96±37.40 *vs* 46.64±21.20, $P<0.01$) and MDA (48.2±4.5 *vs* 15.7±4.8, $P<0.01$) increased. Compared with model group, the thickness of regenerative mucosa increased, glandular arrangement was in order, and cystic dilative glands decreased, while the mucus thickness of gastric mucosa surface increased (20 g/kg WK: 51.3±2.9 *vs* 23.2±8.4, 10 g/kg WK: 43.3±2.9 *vs* 23.2±8.4, 5 g/kg WK: 36.1±7.2 *vs* 23.2±8.4, jianpiyiqi: 35.4±5.6 *vs* 23.2±8.4, yangxuehuoxue: 33.1±8.9 *vs* 23.2±8.4, qingrejiedu: 31.0±8.0 *vs* 23.2±8.4 and CBP: 38.2±3.5 *vs* 23.2±8.4, $P<0.05$-0.01). The levels of EGF (20 g/kg WK: 1.364±0.12 *vs* 0.818±0.18, 10 g/kg WK: 1.359±0.24 *vs* 0.818±0.18, 5 g/kg WK: 1.245±0.31 *vs* 0.818±0.18, jianpiyiqi: 1.025±0.45 *vs* 0.818±0.18, yangxuehuoxue: 1.03±0.29 *vs* 0.818±0.18, qingrejiedu: 1.02±0.47 *vs* 0.818±0.18 and CBP: 1.237±0.20 *vs* 0.818±0.18, $P<0.05$-0.01), NO (20 g/kg WK: 0.480±0.026 *vs* 0.213±0.049, 10 g/kg WK: 0.390±0.055 *vs* 0.213±0.049, 5 g/kg WK: 0.394±0.026 *vs* 0.213±0.049, jianpiyiqi: 0.393±0.123 *vs* 0.213±0.049, yangxuehuoxue: 0.463±0.077 *vs* 0.213±0.049, qingrejiedu: 0.382±0.082 *vs* 0.213±0.049 and CBP: 0.395±0.053 *vs* 0.213±0.049, $P<0.05$-0.01), 6-K-$PGF_1\alpha$ (20 g/kg WK: 86.8±7.6 *vs* 59.7±6.3, 10 g/kg WK: 77.9±7.0 *vs* 59.7±6.3, 5 g/kg WK: 70.0±5.4 *vs* 59.7±6.3, jianpiyiqi: 73.5±12.2 *vs* 59.7±6.3, yangxuehuoxue: 65.1±5.3 *vs* 59.7±6.3, qingrejiedu: 76.9±14.6 *vs* 59.7±6.3, and CBP: 93.7±10.7 *vs* 59.7±6.3, $P<0.05$-0.01) and SOD (20 g/kg WK: 186.4±19.9 *vs* 128.6±15.0, 10 g/kg WK: 168.2±21.7 *vs* 128.6±15.0, 5 g/kg WK: 155.6±21.6 *vs* 128.6±15.0, jianpiyiqi: 168.0±85.3 *vs* 128.6±15.0, yangxuehuoxue: 165.0±34.0 *vs* 128.6±15.0, qingrejiedu: 168.2±24.9 *vs* 128.6±15.0, and CBP: 156.3±18.1 *vs* 128.6±15.0, $P<0.05$-0.01) significantly increased. The levels of ET (20 g/kg WK: 81.30±17.20 *vs* 179.96±37.40, 10 g/kg WK: 83.40±25.90 *vs* 179.96±37.40, 5 g/kg WK: 93.87±20.70 *vs* 179.96±37.40, jianpiyiqi: 130.67±43.66 *vs* 179.96±37.40, yangxuehuoxue: 115.88±34.09 *vs* 179.96±37.40, qingrejiedu: 108.22±36.97 *vs* 179.96±37.40, and CBP: 91.96±19.0 *vs* 179.96±37.40, $P<0.01$) and MDA (20 g/kg WK: 21.6±7.4 *vs* 48.2±4.5, 10 g/kg WK: 32.2±7.3 *vs* 48.2±4.5, 5 g/kg WK: 34.2±6.2 *vs* 48.2±4.5, jianpiyiqi: 34.9±13.8 *vs* 48.2±4.5, yangxuehuoxue: 35.5±16.7 *vs* 48.2±4.5, qingrejiedu: 42.2±17.6 *vs* 48.2±4.5, and CBP: 30.1±6.1 *vs* 48.2±4.5, $P<0.05$-0.01) obviously decreased. The 20 g/kg WK group was better than 10 g/kg (the mucus thickness: 51.3±2.9 *vs* 43.3±2.9, NO: 0.480±0.026 *vs* 0.390±0.055, SOD: 186.4±19.9 *vs*

168.2±21.7, $P<0.01$) and 5 g/kg (the mucus thickness: 51.3±2.9 *vs* 36.1±7.2, NO: 0.480±0.026 *vs* 0.394±0.026, SOD: 186.4±19.9 *vs* 155.6±21.6, $P<0.01$) groups and CBP group (the mucus thickness: 51.3±2.9 *vs* 38.2±3.5, NO: 0.480±0.026 *vs* 0.395±0.053, SOD: 186.4±19.9 *vs* 156.3±18.1, $P<0.01$) in the mucus thickness, NO and SOD levels and better than 10 g/kg (86.8±7.6 *vs* 77.9±7.0, $P<0.05$) and 5 g/kg (86.8±7.6 *vs* 70.0±5.4, $P<0.05$) groups in 6-K-$PGF_1\alpha$ level, 10 g/kg WK group was better than 5 g/kg WK (the mucus thickness: 43.3±2.9 *vs* 36.1±7.2, $P<0.01$, SOD: 168.2±21.7 *vs* 155.6±21.6, $P<0.05$) and CBP groups (the mucus thickness: 43.3±2.9 *vs* 38.2±3.5, $P<0.01$, SOD: 168.2±21.7 *vs* 156.3±18.1, $P<0.05$) in the mucus thickness and SOD level. In compound group, jianpiyiqi group, yangxuehuoxue group, qingrejiedu group, the level of ET was decreased, NO contents were increased in gastric tissue of ulcers in rats.

CONCLUSION: WK decoction and separated recipes have significantly protective effect on ethanol-induced gastric mucosal injury. They can increase the content of EGF in gastric juice, PGI_2 SOD in plasma and NO in gastric tissues, thicken the mucus on the gastric mucosa, and decrease the impairing factor MDA, ET in plasma.

Key words: Gastric mucosa/drug effects; Gastric ulcer; Epidermal growth factor; Nitric oxide

Fan TY, Feng QQ, Jia CR, Fan Q, Li CA, Bai XL. Protective effect of Weikang decoction and partial ingredients on model rat with gastric mucosa ulcer. *World J Gastroenterol* 2005; 11(8): 1204-1209

http://www.wjgnet.com/1007-9327/11/1204.asp

INTRODUCTION

PU is a common disease with a high clinical incidence, which features predicted curative ratio up to 95%, but high relapse rate at about 65-80% one year after withdrawal and up to nearly 100% within two years. Such being the case, treatment of PU and prevention of its relapse still is a problem in the medical field[1-5]. When the gastric mucosa is normal, the gastric wall can prevent digestion in the stomach by the mucus with hydrogen ion's consistence being 3-4 million times higher than that in the blood. Furthermore, most of the ulcerations are caused by the weakening of the protective ability of mucosa than by the increasing of the attacking factors[6-8]. In recent years, many experts have proved, by virtue of modern approaches, that herbs for strengthening the spleen can remove the damage to gastric mucosa in experiments, and can withstand ulcerations by way of consolidating the barrier of gastric mucus, speeding up the mucosal blood flow, quickening the reproduction of PGI_2, and holding back the damage by free radicals[9,10]. Protective effects of traditional Chinese medicine on gastric and intestinal mucosa offer a new method. WK decoction can treat PU and prevent relapse of PU according to clinical research[9-13]. The experiment was carried out to investigate the possible mechanisms and find a new traditional Chinese medical recipe on mucosal protection.

MATERIALS AND METHODS

Materials

Ninety pure wistar rats of either sex (180-250 g), provided by Tongji Medical University Experimental Animal Center, were caged by layer, male and female separated. After 1 wk of feeding, if no unfavorable reaction was inspected, the experiment would begin. Entire herbs consisting of huangqi and pugongying 30 g each, guizhi, zhiganchao and sanqi 6 g each, baishao, yuanhu 15 g each, dahuang 12 g, jianpiyiqi herbs consisting of huangqi 30 g, guizhi and zhiganchao 6 g each, yangxuehuoxue herbs consisting of yuanhu and bansho 15 g each, sanqi 6 g, qingrejiedu herbs consisting of dahuang 12 g and pugongying 30 g. The above herbs were boiled with 400 mL deionized water twice, 30 min each, then, the filtrate was condensed to a concentration of 1 g/mL and was put in a 500-mL glass bottle kept at low temperature. The CBP capsules were produced by Shanxi Ante Biological Pharmaceutical Co., Ltd., 92 Wei Yao Zhun Zi X-47-1.

Methods

Ninety rats were randomly divided into nine groups of 10 each, respectively marked with control group, model group, group with large WK dosage, group with medium WK dosage, group with small WK dosage, jianpiyiqi group, yangxuehuoxue group, qingrejiedu group and group with CBP capsules. According to the method adopted by Yang Xuesong[14], except for the control group, food was withheld for 24 h before modeling while water was allowed. Anesthetized with ether, these rats had their furs cut. Then, along the middle line under the xiphoid process, they were cut open from the belly (the cut was about 2 cm long). The stomach was exposed. Subsequently, filter paper with a diameter of 5 mm immersed in 100% acetic acid was pasted at the serosa at the intersection of antrum phlori and the stomach body twice of 30 s each. After that, new filter paper was used to absorb extra acetic acid on the surface of the stomach. This part was covered with omentum. The stomach was resumed to normal shape. Finally, cuts were sutured by layers, and coated with a layer of diluted ceiba acid for protection purpose. Administration was made to lavage the stomach from the sixth day after modeling. The doses of WK decoction were calculated by extrapolating the human therapeutic dose. Medium dosage was 15 times of human dose (10 mL/kg every d), large dosage was twice as much (20 mL/kg every d) while small dosage of one second (5 mL/kg every d), jianpiyiqi group, yangxuehuoxue group, qingrejiedu group (10 mL/kg every d) was administered to each group, for the group with CBP capsules, medicine was dissolved with water and doses 15 times of human therapeutic dose were administered (10 mL/kg solution containing 0.35% pectin bismuth), rats of other groups were fed with physiological saline (10 mL/kg every d). Administration lasted 16 d. From the 17 d, these rats were fasted for 24 h, water allowed. Before the experiment, the animals received 1 mL physiological saline. Two hours later, they were anesthetized with 1% sodium pentobarbital at a dose of 40-50 mg/kg on the

abdomen. Then, the rats were killed by removing their heads. Blood was sampled into two test tubes, one added with 30 μL EDTA disodium and 40 μL aprotinin to measure the concentration of endothelin (ET), and the another with 30 μL EDTA, disodium to measure the thickness of 6-K-$PGF_1\alpha$, MDA and serum superoxide dismutases (SOD). After the stomachs were removed, gastric juice was collected to measure epidermal growth factor (EGF). At the corpus and fundus ventriculus and antrum phlori each, one-third of stomach tissue was sampled, 200 mg in all, to measure the concentration of nitric oxide (NO). And, the ulcerations along the maximum diameter parallel to the longer axis of the stomach were selected and soaked with 10% formalin for 24 h. Pathological sections were taken to observe ulcerations and measure the thickness of mucus on the mucosa surfaces. All the kits for EGF, NO, 6-K-$PGF_1\alpha$, ET, MDA and SOD were provided by Nanjing Juli Biological Co., Ltd. For more details about measurements, please refer to their instruction manuals. Statistical disposition: all data were expressed in mean±SD. Means of specimens were compared by Q test and *t* test in the analysis of variance.

RESULTS

Overview

When coming around after modeling, the rats began to eat but lost their appetite dramatically. They were not as active as before, their furs and skins were dry and urine volume also decreased. About 5-7 d after modeling, they became active gradually, with appetite getting better, their skins and furs resumed lustrousness and the urine volume also rose. During the experiments, four rats died, three from the jianpiyiqi group, and one from the qingrejiedu group.

Pathological observations

Compared with the control group, rats in the model group suffered from damaged gastric mucosa. Ulcerations were deep into the muscular layer. Additionally, the holes were covered only with little reproduced mucosa, and glands were arranged disorderly, presenting a cystic dilatation. For the rats in the groups respectively with large, medium and small WK dosage, as well as the group with CBP capsules, the mucosa reproduced at the holes of gastric mucosa was thicker than the model group, and the damage area in the muscular layer was smaller. Glands tended to arrange orderly, with those of cystic dilation decreased.

Effect on the thickness of mucus on gastric mucosa

If arranged by the thickness of mucus on the gastric mucosa in ascending order, then the sequence is as follows: model group ($P<0.01$), group with small WK dosage and group with CBP capsules ($P<0.01$), group with medium WK dosage ($P<0.05$), group with large WK dosage ($P<0.01$), and the control group. There is little difference between the group with small WK dosage and the group with CBP capsules. Moreover, the mucus of the groups with partial ingredients is thicker than the model group ($P<0.05$-0.01) but thinner than the group with entire ingredients. The results are summarized in Table 1.

Table 1 Thickness of mucus on gastric mucosa surface and the content of EGF in gastric juice (mean±SD)

Group	Specimens	Thickness of mucus (μm)	EGF (ng/g)
Control	10	64.1±9.3[b,d]	2.168±0.375[b]
Model	10	23.2±8.4	0.818±0.18
WK (20 g/kg)	10	51.3±2.9[b,d]	1.364±0.12[a]
WK (10 g/kg)	10	43.3±2.9[b,c]	1.359±0.24[a]
WK (5 g/kg)	9	36.1±7.2[b]	1.245±0.31[a]
Jianpiyiqi	7	35.4±5.6[b]	1.025±0.45[c]
Yangxuehuoxue	10	33.1±8.9[b]	1.03±0.29[c]
Qingrejiedu	9	31.0±8.0	1.02±0.47[c]
CBP capsules	10	38.2±3.5[b]	1.237±0.20[a]

[a]$P<0.05$, [b]$P<0.01$ *vs* the model group, [c]$P<0.05$, [d]$P<0.01$ *vs* CBP capsules.

Effect on EGF

As shown in Table 1, in terms of the content of EGF in gastric juice, the model group is much lower than the control group ($P<0.01$), while the groups with large, medium and small WK dosage and the group with CBP capsules, between which there is no dramatic difference, are considerably higher than the model group ($P<0.05$). In general, groups with partial ingredients are lower than those with entire ingredients ($P<0.05$) but higher than the model group. The averages of all groups with partial ingredients are very close, with little remarkable difference.

Effect on the content of NO in gastric tissue

As regards the content of NO in gastric tissue, the model group is much lower than the control group ($P<0.01$), while the groups with large, medium and small WK dosage and the group with CBP capsules are considerably higher than the model group ($P<0.05$-0.01). The group with large WK dosage and the yangxuehuoxue group are greatly higher than the jianpiyiqi group, qingrejiedu group, group with medium and small WK dosage, the group with CBP capsules. See Table 2.

Table 2 Content of NO in gastric tissue and the content of ET in plasma (mean±SD)

Group	Specimens	NO (μmol/g)	ET (pg/mL)
Control	10	0.601±0.081[b,d]	46.64±21.20[bd]
Model	10	0.213±0.049	179.96±37.40
WK 20 g/kg	10	0.480±0.026[b,c]	81.30±17.20[b]
WK 10 g/kg	10	0.390±0.055[a]	83.40±25.90[b]
WK 5 g/kg	9	0.394±0.026[a]	93.87±20.70[b]
Jianpiyiqi	7	0.393±0.123[a]	130.67±43.66[bc]
Yangxuehuoxue	10	0.463±0.077[b,c]	115.88±34.09[bc]
Qingrejiedu	9	0.382±0.082[a]	108.22±36.97[b]
CBP capsules	10	0.395±0.053[a]	91.96±19.0[b]

[a]$P<0.05$, [b]$P<0.01$ *vs* the model group, [c]$P<0.05$, [d]$P<0.01$ *vs* CBP capsules.

Effect on the content of ET in plasma

As shown in Table 2, in regard to the content of ET in plasma, the model group is much higher than the control group ($P<0.01$), while the groups with herbs and the group with CBP capsules are considerably lower than the model group ($P<0.01$). For the groups with large, medium and

small WK dosage and the group with CBP capsules, there is no dramatic difference among them. The jianpiyiqi group, yangxuehuoxue group, qingrejiedu group are substantially higher than the groups with entire ingredients and with CBP capsules ($P<0.05$).

Effect on SOD and MDA in plasma

Compared with the control group, the model group is much lower in terms of SOD content ($P<0.01$), but higher in terms of MDA content ($P<0.01$). As regards SOD content, the groups with small WK dosage and with CBP capsules are substantially higher than the model group ($P<0.05$), but much lower than the group with medium WK dosage ($P<0.05$). The group with large WK dosage is higher than the group with medium WK dosage ($P<0.05$). In terms of MDA content, the groups with large, medium and small WK dosage and the group with CBP capsules, between which there is no dramatic difference, are hugely lower than the model group ($P<0.05$-$P<0.01$). See Table 3.

Table 3 Content of SOD and MDA in plasma of each group (mean±SD)

Group	Specimens	SOD (NU/mL)	f MDA (NM/mL)
Control	10	196.6±35.3[b,d]	15.7±4.8[b,d]
Model	10	128.6±15.0	48.2±4.5
WK 20 g/kg	10	186.4±19.9[b,d]	21.6±7.4[b,c]
WK 10 g/kg	10	168.2±21.7[a,c]	32.2±7.3[a]
WK 5 g/kg	9	155.6±21.6[a]	34.2±6.2[a]
Jianpiyiqi	7	168.0±85.3[a,c]	34.9±13.8[a]
Yangxuehuoxue	10	165.0±34.0[a,c]	35.5±16.7[a]
Qingrejiedu	9	168.2±24.9[a,c]	42.2±17.6[a,c]
CBP capsules	10	156.3±18.1[a]	30.1±6.1[a]

[a]$P<0.05$, [b]$P<0.01$ *vs* the model group, [c]$P<0.05$, [d]$P<0.01$ *vs* CBP capsules.

Effect on the content of 6-K-PGF$_1\alpha$ in plasma

In terms of 6-K-PGF$_1\alpha$ content, the model group is much lower than the control group ($P<0.01$), but higher than the groups with large, medium and small WK dosage and the group with CBP capsules ($P<0.05$). Between the groups with large, medium and small WK dosage and the group with CBP capsules, there is no dramatic difference ($P>0.05$), but the group with large WK dosage is greatly higher than the groups with medium and small dosage ($P<0.05$). See Table 4.

Table 4 Effect of WK on the content of 6-K-PGF$_1\alpha$ in plasma in rats (mean±SD)

Group	Specimens	6-K-PGF$_1\alpha$ (pg/mL)
Control	10	96.6±8.3[b]
Model	10	59.7±6.3
WK 20 g/kg	10	86.8±7.6[b]
WK 10 g/kg	10	77.9±7.0[a]
WK 5 g/kg	9	70.0±5.4[a]
Jianpiyiqi	7	73.5±12.2[a]
Yangxuehuoxue	10	65.1±5.3
Qingrejiedu	9	76.9±14.6[a]
CBP capsules	10	93.7±10.7[b]

[a]$P<0.05$, [b]$P<0.01$ *vs* the model group.

DISCUSSION

To the present day, major anti-PU medicines aim at fighting against mucosa-attacking factor. Such medicines include H_2 receptor antagonism, H^+-K^+ATP enzyme inhibitor, anti-cholin drugs, *Helicobacter pylori* (*Hp*) counteractant[15], *etc*. When the gastric mucosa is normal, the gastric wall can prevent digestion in the stomach by the mucus with hydrogenion's consistence 3-4 million times higher than that in the blood. However, when in PU, secretion of gastric acid generally stays low in the normal range, while in duodenal ulcer, the secretion is only 1/3 more than the normal level. Furthermore, not all PU are related with HP, which indicates that most ulcerations are caused by the weakening protective ability of mucosa and not by the increasing of the attacking factor. In clinically traditional Chinese herbs have good effect for PU[16-20]. The WK decoction derives from Jianzhong Astragalus Root Soup, with some herbs added or removed. This recipe mainly functions for strengthening the spleen and replenishing qi, complemented with other effects, such as invigorating the circulation of and nourishing the blood, and clearing away the heat-evils and expelling superficial evils. In recent years, by virtue of modern approaches, many experts have proved, strengthening the spleen can remove the damage to gastric mucosa in experiments, and can withstand ulcerations by way of consolidating the barrier of gastric mucus, speeding up the mucosal blood flow, quickening the reproduction of PGI_2, and holding back the damage by free radicals. For mucus, perfect structure is the foundation of its protecting function[21]. It is revealed by our experiments that, regardless of doses, WK in solid state can shrink ulcerations, build up the mucosa barrier, straighten up the arrangement of glands and better the structure. Additionally, dependent on its dosage, WK decoction also can thicken the mucus on the surface of gastric mucosa, which indicates that it can facilitate mucosa to secrete mucus. EGF of the human body can stimulate the mitosis of cells, improve the proliferation and differentiation of epithelium, and speed up the production of DNA and proteins in the gastric mucosa, all of which are of great importance to regenerate and repair the tissue[22-26]. Our experiments show that after modeling the content of EGF of the model group dropped greatly, but that of the groups with large, medium and small WK dosage and with CBP capsules climbed up. Comparatively, large doses of WK exerted more influence on the content of EGF than CBP capsules, which indicates that WK decoction has the function of protecting gastric mucus by enhancing the EGF content and its effect is dependent on dosage. NO protects the stomach by speeding up the circulation of blood in the gastric mucosa. Also, it plays an important role in defending the gastric mucosa as an antioxidant[26,27]. Our experiments reveal that the content of NO in the model group is much lower than that in the control group ($P<0.01$), indicating a decreased content of NO protective factor in the event of gastric ulceration. The content of NO in the groups with large, medium and small WK dosage and with CBP capsules are dramatically higher than that in the model group. Comparatively, large doses of WK exerted more influence on the content of NO than CBP capsules, which indicates that WK decoction can protect the gastric mucosa by enhancing NO content after treatment

but its effect is dependent on dosage. ET may antagonize the effect of NO, leading to an imbalanced NO/ET. As it may slow down the mucosal blood flow, gastric mucosa may be impaired[28-30]. Our experiments show that the content of ET in the model group is much higher than that in the control group, indicating increase of ET in the event of gastric ulceration. The content of NO in the groups with large, medium and small WK dosage and with CBP capsules are dramatically lower than that in the model group, which means that WK decoction can lower the content of ET in plasma by slowing down the production and secretion of ET. In general, to lower ET content and enhance the content of NO can keep NO/ET in balance, maintain normal mucosal blood flow and thus protect the gastric mucosa.

When stimulated by chemicals or in shortage of blood, the gastric and intestinal mucosa will produce tremendous free radicals, which impair mucosa. Through experimental results, we can see that the model group is much higher than the control group ($P<0.01$) in terms of MDA content but much lower than the latter in terms of SOD content ($P<0.01$). These data indicate that oxygen-derived free radicals will take part in ulceration and meanwhile oxygen-derived free radical scavengers that have protective function decrease. The groups with large, medium and small WK dosage and with CBP capsules are considerably lower than the model group in terms of MDA content but higher than the latter in terms of SOD content. Furthermore, the groups with medium and small WK dosage are higher than the group with CBP capsules in terms of SOD content ($P<0.05$), which shows that WK has better effect in increasing SOD contents, removing oxygen-derived free radicals and protecting the gastric mucosa. Its effect is dependent on dosage.

PGI_2 can restrain the secretion of gastric acid, enhance the mucosal blood flow and protect the cells and TXB_2. However, it has a short half-life period. Within two minutes, it can hydrolyze into stable 6-K-$PGF_1\alpha$. Our experiments show that the content of 6-K-$PGF_1\alpha$ in the model group is much lower than that in the control group ($P<0.01$), indicating that in case of ulceration protective factor 6-K-$PGF_1\alpha$ will decrease. But, the groups with large, medium and small WK dosage and with CBP capsules are considerably higher than the model group ($P<0.01$), which indicates that WK can protect the gastric mucosa and further repair ulcerations by increasing 6-K-$PGF_1\alpha$.

The WK decoction derives from huangqijianzhong decoction[31], with some herbs added or removed. However, huangqijianzhong decoction is mainly used for restoring qi by virtue of warm herbs. In consideration of the pathogenesis of ulcer diseases, such as deficiency of vital energy, blood stasis and tremendous heat toxins[32], we add some herbs for activating blood circulation to dissipate blood stasis[33], such as xuanhu (rhizomacorydalis) and sanqi (pseudoginseng), some herbs dahuang (rhubarbs) and pugongying (dandelion)[34] for clearing away the heat-evils and toxic materials. This recipe mainly functions for strengthening the spleen and replenishing qi, complemented with other effects, such as invigorating the circulation of and nourishing the blood, and clearing away the heat-evils. These experiments show that all the groups with partial ingredients have favorable effect of curing gastric ulcer for rats. These ingredients can increase contents of PGI2, EGF, SOD and NO, thicken the mucus on the gastric mucosa, and decrease the impairing factor MDA and ET. Through comparison, we find out that partial ingredients do not have as good effect as the entirety. In some cases, they show some dramatic statistical difference, while in other cases although there is no such difference, the group with entire ingredients has better figures. Therefore, the entire ingredients have better comprehensive effect in curing ulcerations. All medical herbs have their own substantial foundation supporting their activity and effect in treatment. Since the medicine has so many ingredients that may produce many complicated chemical reactions, its treatment effect is not equal to the aggregate effects of each ingredient. As for its effective substantial foundation, it is to be explored in further researches.

REFERENCES

1 **Fan Q**. Improve the healing quality and treatment of Chinese herbs. *Zhongyi Yanjiu* 1995; **8**: 46-47
2 **Zhou DQ**. Treatment of difficult digestive diseases with intergrated traditional and western medicine. *Beijing: China Medicine* Technical Publishing House, 1998: 94-127
3 **Fan Q,** Zhang HY. Ideology of improving the healing quality of ulcer with Chinese medicine. *Zhongguo Zhongxiyi Jiehe Piwei Zazhi* 1996; **4**: 186
4 **Liu JP**, Wang WZ, Bai JL, Bu T, Zhong QH. Recent circumstance on improving healing quality of peptic ulcer with Chinese medicine. *Shandong Zhongyi Zazhi* 2003; **22**: 381-383
5 **Deng C,** Luo WS. Research progress of healing quality of peptic ulcer with Chinese medicine. *Guangxi Zhongyiyao* 2003; **26**: 1-3
6 **Qu ZW**, Zhang DJ, Liu YP. Protective effect of weiyanling on gastric mucosa of rats. *Zhongguo Zhongxiyi Jiehe Xiaohua Zazhi* 2003; **11**: 276-276
7 **Li J**, Tang FA. Evaluation of clinical application of gastroduodcnal mucosal protutive agcnts. *Zhongguo Yiyuan Yongyao Pingjia Yu Fenxi* 2003; **3**: 133-137
8 **Qi HJ**, Hu MQ, Sun GJ. Experimental research of Chinese medicine on protective effect of gastric mucosa. *J Southcast Univ* 2003; **22**: 129-132
9 **Fan Q**, Fan TY, Jia CR, Den LQ. Protective effect of WK granule on gastric mucosa of rats. *Zhongguo Zhongxiyi Jiehe Xiaohua Zazhi* 2001; **9**: 223
10 **Zhang WN**, Li JB, Wang X. Clinical Study on Jianweiyuyang Granules for Treating the Relapse of Peptic Ulcer. *Hunan Zhongyiyao Daobao* 2003; **9**: 15-16
11 **Xia JQ**, Jia XB, Shen MQ, Xi ZH, Wang DM. Clinical research of preventive recurrence effect of weiyangping granule on peptic ulcer. *Zhongguo Zhongxiyi Jiehe Xiaohua Zazhi* 2003; **11**: 229-230
12 **Wang B**, Yao BT, Wu M. Research progress of preventive recurrence effect of traditional Chinese medicine on peptic ulcer. *Jilin Zhongyiyao* 2003; **23**: 51-53
13 **Zheng Y,** Hua H, Han HG, Song XM. Regulating effect of pugongying capsule for peripheral circulation T lymphocyte subpopulation and preventive recurrence effect on peptic ulcer. *Gansu Zhongyi Xueyuan Xuebao* 2003; **20**: 14-15
14 **Yang XS,** Li YN, Ye CM, Dong XY. Experimental study of correlation of gastric ulcer healing quality with risistance to reinjury by prednisone in rats. *Beijing Yike Daxue Xuebao* 1996; **28**: 454-456
15 **Shen YG**, Liu JC, Chen SB. Etiological and pharmacological treatment of peptic ulcer. *Zhongguo Xinyao Yu Linchuang Zazhi* 2003; **22**: 620-624

16 **Li G**, Wang JZ, Jiu FX. Research progress of therapeutic mechanism on traditional Chinese medicine for peptic ulcer. *Hebei Zhongyi* 2003; **25**: 391-392
17 **Zhao Y**, Wang QG, Li YH, Niu X, Jia YS, Zhang DM, Zhong XG. Effect of banxiaxiexing decoction and partial ingredient on shape change of peptic ulcer in rats. *Zhongguo Zhongyi Jichu Yixue Zazhi* 2003; **1**: 16-20
18 **Gao Y**, Yu H. Research and application of peptic ulcer treated by yanweikang powder. *Zhongyi Yaoxuekan* 2003; **21**: 377-378
19 **Dong MG**, He SD, Ye XH, Zou ZH. Preventing effect of kangerwei granule on rats with laiboratory gastric ulcer. *Zhongguo Zhongxiyi Jiehe Piwei Zazhi* 2003; **4**: 117
20 **Wang JW**, Qu L, Cheng R, Guo LJ. Pharmacological effect of weikexing capsual in the treatment of peptic ulcer. *Zhongguo Zhongxiyi Jiehe Xiaohua Zazhi* 2003; **11**: 30-32
21 **Zhan XB**, Li ZS, Cui ZM, Duan YM, Nie SN, Liu J, Xu GM. Changes of rat gastric mucosal barrier under stress conditions. *Zhonghua Neike Zazhi* 2002; 41: 374-377
22 **Li G**, Wang JZ, Jiang FB, Li SM. Relationship of platelet active factor, tumor necrosia-a, epidermal growth factor, prostaglandin E2 and peptic ulcer. *Hebei Zhongyi* 2003; **25**: 475-477
23 **Hu YT**, Zhen CE, Xing GZ, Zhang ML, Zhang JS, Wang DX, Lu YM. Relationship of transformation growth factor-alpha, epidermal growth factor, prostaglandin E2 in peptic ulcer patients. *Shijie Huaren Xiaohua Zazhi* 2002; **10**: 43-47
24 **He JH**, Luo HS. Effect of growth factor for healing of peptic ulcer. *Guowai Yixue Xiaohua xi Jibin Fence* 2003; **1**: 12-15
25 **Wang FW**, Li J, Hu ZL, Xie YY. Preventive effect of exogenetic nitride oxide on gastric movement in rat irritable gastric mucosa injury. *Shijie Huaren Xiaohua Zazhi* 2003; **12**: 2036-2038
26 **Liu XY**, Zhou ZG. Influence of yuyang powder on nitride oxide and prostacycli of rats with gastric ulcer by acetic acid. *Jiangxi Zhongyi Xueyuan Xuebao* 2003; **15**: 68-69
27 **Yu Y**, Huo XH. The function of nitride oxide in the cause injury of gastric and intestinal mucosa. *Weichangbingxue He Ganbingxue Zazhi* 1997; **6**: 376-378
28 **Duan YM**, Li ZS, Zhan XB, Gong YF, Xu GM. Protective effect of endothelin-1 specific antibody on irritable gastric mucosa injury. *Shijie Huaren Xiaohua Zazhi* 2003; **11**: 990-993
29 **Cheng S**, Xiao FY, Li GC, Zhang LH. Effect of XiaoKuiLing on endothelin and epidermal growth fastor receptor in rats with acetic gastric uleer. *Zhejian Zhongxiyi Jihe Zazhi* 2003; **3**: 4-6
30 **Zhang GF**, Chen YR, Zhang MX. Relationship between nitride oxide, epidermal growth factor and the injury of gastric mucosa. *Weichangbingxue He Ganbingxue Zazhi* 1999; **8**: 293-296
31 **He YY**, He ZF. 45 Patients with peptic ulcer treated by huangqijiangzhong decoction. *Nanhua Daxue Xuebao Yixueban* 2003; **31**: 234
32 **Ping ZKS**, Du X. Antibacterial effect of huanglianjiedu decoction on *Helicobactor pylori*. *Guowai Yixue Zhongyi Zhongyao Fenche* 2003; **25**: 97-98
33 **Zhang B**, Cai MQ, Yu M, Liu YJ, Zhang WY. Clinical observation of replenishing qi and dissipate blood stasis on 48 patients with peptic ulcer. *Zhongguo Zhonyi Jizheng* 2003; **2**: 22
34 **Zheng Y**. Regulating effect of pugongying capsule for peripheral circulation T lymphocyte subpopulation and preventive recurrence effect on peptic ulcer. *Zhongguo Zhongyiyao Xinxi Zazhi* 2003; **10**: 14-15

PO Box 2345, Beijing 100023, China
www.wjgnet.com
wjg@wjgnet.com

ELSEVIER

World J Gastroenterol 2005;11(8):1210-1214
World Journal of Gastroenterology ISSN 1007-9327

• *BRIEF REPORTS* •

Prognostic significance of cell infiltrations of immunosurveillance in colorectal cancer

Shi-Yun Tan, Yan Fan, He-Sheng Luo, Zhi-Xiang Shen, Yi Guo, Liang-Jia Zhao

Shi-Yun Tan, Yan Fan, He-Sheng Luo, Zhi-Xiang Shen, Department of Gastroenterology, Renmin Hospital of Wuhan University, Wuhan 430060, Hubei Province, China
Yi Guo, Department of Pharmacal Instrument, General Hospital for Wuhan Iron and Steel Corporation Staff, Wuhan 430080, Hubei Province, China
Liang-Jia Zhao, Department of Respiration, Traditional Chinese Medicine Hospital of Jingzhou, Jingzhou 434000, Hubei Province, China
Supported by "Tenth Five-Year" Key Project of Scientific and Technological Bureau of Hubei Province, No. 2002AA301C59
Co-first-authors: Shi-Yun Tan and Yan Fan
Correspondence to: Shi-Yun Tan, Department of Gastroenterology, Renmin Hospital of Wuhan University, Wuhan 430060, Hubei Province, China. tanshiyun@medmail.com.cn
Telephone: +86-27-88041919-2135
Received: 2004-06-15 Accepted: 2004-07-22

Abstract

AIM: To determine whether the mast cell (MCs) and tumor-associated macrophage (TAMs) counts have any correlation with clinical outcome in colorectal cancer, and to investigate whether MCs undergo phenotypic changes in colorectal cancer.

METHODS: The MC and TAM counts were determined immunohistochemically in 60 patients with colorectal cancer and the depth of invasion, lymph node metastasis rate, distant metastasis rates, and survival rates were compared between patients with low (less than the mean number of positive cells) and high (more than the mean number of positive cells) cell counts.

RESULTS: Both patients with a low MC count and patients with a low TAM count had significantly deeper depth of invasion than those with a high MC count and those with a high TAM count ($P<0.01$ and $P<0.01$ respectively). Patients with a high MC count and patients with a high TAM count were significantly higher showing significantly lower rates of lymph node metastasis, distant metastasis than those with a low MC count and those with a low TAM count. There were significant positive correlation between MC counts and TAM counts ($r = 0.852$, $P<0.01$). In both cancerous tissue and normal colorectal tissue, the predominant MC phenotype was MC_{TC}. The 5-year survival rate estimated was significantly lower in both patients with a low MC count and patients with a low TAM count than in those with a high MC count and those with a high TAM count ($P<0.05$ and $P<0.01$ respectively).

CONCLUSION: There appears to be a direct relationship between the number of MCs and clinical outcome in patients with colorectal cancer, even though MCs exhibited no significant phenotypic changes. TAM count is of value to predict the clinical outcome or prognosis. It is more beneficial for estimating biological character of colorectal carcinoma to combine MC and TAM counts.

Key words: Mast cells; Phenotype; Macrophages; Colorectal cancer; Prognosis

Tan SY, Fan Y, Luo HS, Shen ZX, Guo Y, Zhao LJ. Prognostic significance of cell infiltrations of immunosurveillance in colorectal cancer. *World J Gastroenterol* 2005; 11(8): 1210-1214
http://www.wjgnet.com/1007-9327/11/1210.asp

INTRODUCTION

Numerous cells of immunosurveillance are known to microscopically infiltrate in cancers. These infiltrating immunosurveillance cells, including mast cell (MCs) and tumor associated macrophages (TAMs), have been found to reflect a tumor-related immune response[1-4].

In the fight against cancer, MCs have been shown to play several roles. While some studies report on the antitumor functions of MCs including natural cytotoxicity[1] and the release of antitumor compounds[2], in addition to the enhancement of the cytotoxic activation of mainly peritumoral eosinophils and macrophages[5-8], others suggest a direct relationship between MCs and tumor angiogenesis[9,10]. Many theories have been advanced as to the reasons for the antitumor functions of MCs, in particular as to whether phenotypic changes occur in the presence of cancer cells[11-13]. It is well known that human MCs are conventionally divided into two types depending on the expression of different proteases in their granules: MCs positive only for tryptase (MC_T) and MCs positive for both tryptase and chymase (MC_{TC}). Phenotypic changes have been reported in pathological conditions including helminth infections, sarcoidosis and allergic alveolitis[14,15]. Unlike the definitive studies already mentioned, however, few researches have demonstrated a clear correlation between MCs and tumor toxicity in colorectal cancer, and, as yet, the MC phenotype in lung cancer has not been characterized.

Although TAMs have the potential to mediate tumor cytotoxicity and to stimulate antitumor lymphocytes[3], it is still unclear whether TAMs can predict tumor prognosis.

The purpose of this study was to determine: (1) whether a direct correlation exists between the number of these

inflammatory cells (MCs and TAMs) and the clinical outcome of patients with colorectal cancer, and (2) whether these MCs undergo phenotypic changes in colorectal cancer.

MATERIALS AND METHODS

Materials

A total of 60 carcinomas of the colon and rectum (35 men and 25 women, mean age: 67.9 years, range 48-80 years) were selected from our department and affiliated hospitals between 1995 and 2002. We also obtained 20 "normal" colon and rectum specimens (mean age = 59 years, age range 41-86 years, male:female = 12:8) from the biopsy and autopsy files of our department. Depth of invasion was graded according to the standard TNM classification.

All specimens were immediately fixed in neutral-buffered formalin and embedded in paraffin wax. Several 4-μm serial sections were obtained from each case. They were subjected to immunohistochemical analysis.

Methods

Mast cell immunohistochemical staining and estimation of mast cell phenotype[19] To distinguish MC_T and MC_{TC}, two serial sections were stained for both chymase and tryptase, both of which were known to be contained in the granules of MC cytoplasm, using the EnVision method and the streptavidin-peroxidase conjugated method (S-P) methods[14].

After deparaffinization and rehydration, for antigen retrieval the sections were microwaved at 750 W for 10 min. the specimens were incubated with 3% H_20_2, for 10 min to quench endogenous peroxidase activity, and incubated with 1.5% non-immune goat serum for 20 min to suppress nonspecific binding of subsequent reagents. Then they were incubated with two primary antibodies, namely primary antibody CC1 (monoclonal mouse anti-human MC chymase, Novocastra, dilution = 1:500), and primary antibody AA1 (monoclonal mouse anti-human MC tryptase, Novocastra, dilution = 1:1 000) for 60 min at 25 ℃. After washing with PBS, the slides were subsequently incubated respectively with Polymer Helper (PV9000 kits, Zhongshan Bio Corp., Beijing, China) for 20 min and biotin-conjugated goat anti-mouse IgG antibody for 15 min. Then, after washing again with PBS, the sections were incubated respectively with poly peroxidase-goat-anti-mouse IgG antibody for 30 min and streptavidin-peroxidase complex (SP kits, Zhongshan Bio Corp., Beijing, China) for 15 min. Diaminobenzidine was used as chromogen to yield brown reaction products. Nuclei were counterstained with Harris hematoxylin.

Using light microscopy, the mean number of chymase-positive MCs/total MCs per 5 fields with the most abundant infiltration at a magnification of 400× was counted, and the ratio was calculated. Chymase-positive MCs were considered to be MC_{TC}, all others, MC_T.

TAMs immunohistochemical staining

After deparaffinization, for antigen retrieval, the sections were microwaved at 750 W for 10 min and the sections were incubated in 3% hydrogen peroxide for 10 min in order to devitalize endogenous peroxidase. Deparaffinized and rehydrated specimens were heated in 10 mmol/L citrate buffer, pH 6.0, for 10 min in an autoclave at 120 ℃. After cooling to room temperature for 30 min, the specimens were incubated with normal goat serum for 15 min at 37 ℃. Then they were incubated with monoclonal antibody against CD68 (Zhongshan Bio Corp.) for 60 min at 37 ℃, followed by the S-P technique using an S-P kit (Zhongshan Bio Corp., Beijing, China) and diaminobenzidine as the chromogen. Nuclei were counterstained with Harris hematoxylin.

The mean number of TAMs per 5 fields with the most abundant infiltration at a magnification of 400× was counted.

Statistical analysis

Correlation between the degree of infiltration by each cell type and the various clinicopathologic factors was analyzed using the Student's *t*-test, Mann-Whitney *U* test, χ^2 test, and Pearson correlation was performed for correlation analysis between MCs and TAMs. Survival curves were constructed using the Kaplan-Meier method and differences were tested using log-rank statistics. The level of critical significance was assigned at $P<0.05$.

RESULTS

Immunohistochemical staining of MCs (tryptase, chymase) and TAM (CD68)

Immunohistochemical staining indicated that tryptase, chymase and CD68 were localized in the cytoplasm. Infiltrating MCs and TAMs were distributed primarily in the invasive area of the cancers (Figure 1). At ×400 magnification, the

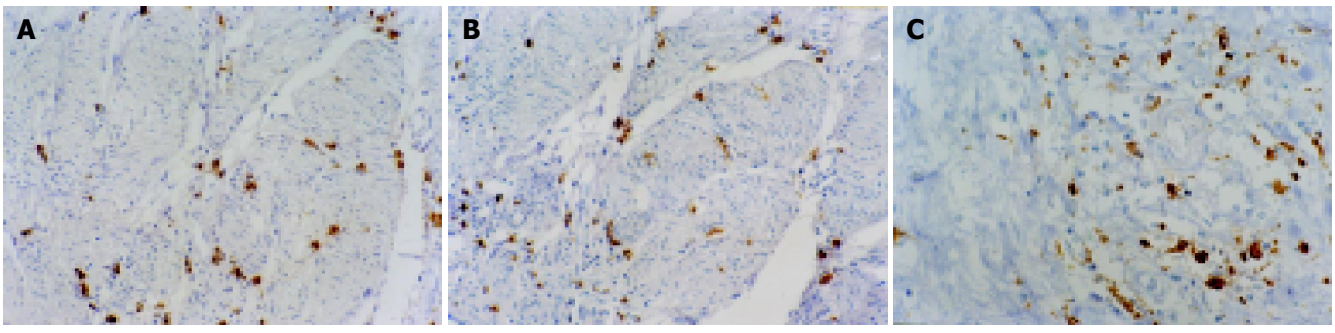

Figure 1 Immunohistochemical staining of MCs phenotype and TAMs A: Immunostaining for MC tryptase, ×200; B: Immunostaining for MC chymase, ×200; C: Immunostaining for macrophages (CD68), ×400.

mean number of total MCs was 59.2, and of TAM 81.2. Of the 60 patients, 27 had 59 or more MCs and were ascribed to the high level of MCs infiltration group, while the remaining 33 patients had 58 or less MCs and were put into the low level of MCs infiltration group. Twenty-nine patients had 81 or more TAMs and were denoted by the high level of TAM infiltration group, while the remaining 31 patients had 80 or less TAMs and were denoted by the low level of TAM infiltration group.

Correlation between the expression of each antigen and various clinicopathologic factors

Table 1 shows the correlation between the expression of each antigen and the various clinicopathologic factors. Patients with a low level of MC infiltration had significantly deeper depth of invasion than those with a high level of MC infiltration ($P<0.01$). The percentage of patients with a high level of MC infiltration was significantly higher in lymph node metastasis-negative cases (59.3%) than those with a low MC count in lymph node metastasis-negative cases (27.3%, $P<0.05$), and higher in distant metastasis-negative cases (74.1%) than in distant metastasis-negative cases (48.5%, $P<0.05$).

Table 1 Correlations between MC and macrophages infiltration and the various clinicopathologic factors

	MCs		TAMs	
	High[1]	Low[2]	High[3]	Low[4]
Age (yr)[5]	61.2	57.2	58.3	59.7
Sex[7]				
Male	13	22	16	19
Female	14	11	13	12
Histological grade of carcinoma[6]				
Well	12	9	14	10
Moderate	11	14	12	12
Poor	4	10	3	9
Depth of invasion[7]				
Superficial Ta-T1	19[b]	10	19[d]	9
Invasive T2-T4	8[b]	23	10[d]	22
Lymph node metastasis[7]				
Positive	11[a]	24	12[c]	22
Negative	16[a]	9	17[c]	9
Distant metastasis[7]				
Positive	7[a]	17	8[c]	18
Negative	20[a]	16	21[c]	13

[1]Patients with a high level of MCs infiltration. [2]Patients with a low level of MCs infiltration. [3]Patients with a high level of TAMs infiltration. [4]Patients with a low level of TAMs infiltration. [5]Student's *t*-test. [6]Mann-Whitney test. [7]χ^2 test. [a]$P<0.05$, [b]$P<0.01$, [c]$P<0.05$, [d]$P<0.01$.

Patients with a low TAM count had significantly deeper depth of invasion than those with a high TAM count ($P<0.01$). The percentage of patients with a low TAM count was significantly higher in lymph node metastasis-positive cases (71.0%) than those with a high TAM count in lymph node metastasis-positive cases (41.4%, $P<0.05$), and in lymph node metastasis-positive cases (58.1%) than in lymph node metastasis-positive cases (27.6%, $P<0.05$).

Estimation of MC phenotype

With regard to mast cell subpopulations, MC_{TC} always predominated over MC_T in each group. The percentage of MC_T and MC_{TC} in colorectal cancer group and normal group is shown in Table 2. The percentage of MC_T was 22.6%, and that of MC_{TC} was 77.4% in colorectal cancer. Although the quantities of MC_T and MC_{TC} were significantly higher in the tissue of colorectal carcinoma than in normal colorectal tissue, there were no significant differences in this percentage between normal groups and colorectal cancer groups (Table 2).

Table 2 Proportion of MC_T and MC_{TC} in colorectal cancer and normal

	MC_{TC} (mean±SD)	MC_T (mean±SD)	Total
Normal group ($n = 20$)	10.1±3.2 (74.3%)	3.5±0.9 (25.7%)	13.6±2.1 (100%)
Colorectal cancer group ($n=60$)	45.8±10.6 (77.4%)	13.4±4.9 (22.6%)	59.2±9.3 (100%)

MC_T, mast cell positive for tryptase. MC_{TC}, mast cell positive for tryptase and chymase. The percentage of MCr and MCrc was not significant in both groups ($P>0.05$, χ^2 test).

The percentage of MC_T and MC_{TC} in colorectal cancer with various histological grades was all approximately 25% and 75% respectively. There were no differences in the percentage of MC_T and MC_{TC} among well, moderately and poorly differentiated tumors (Table 3).

Table 3 Proportion of MC_T and MC_{TC} in colorectal cancer with various histological grades

Histological grade of carcinoma	MC_{TC} (mean±SD)	MC_T (mean±SD)	Total
Well ($n = 21$)	50.8±12.5 (80.5%)	12.3±5.1 (19.5%)	63.1±10.1 (100%)
Moderate ($n = 25$)	42.2±9.1 (73.0%)	15.6±3.3 (27.0%)	57.8±8.2 (100%)
Poor ($n = 14$)	44.7±8.5 (80.0%)	11.2±4.7 (20.0%)	55.9±5.3 (100%)

MC_T, mast cell positive for tryptase. MC_{TC}, mast cell positive for tryptase and chymase. The percentage of MCr and MCrc was not significant in every group ($P>0.05$. χ^2 test).

Correlation between MCs and TAMs

There was significant positive correlation between MC and TAM counts (Figure 2. $r = 0.852$, $P<0.0001$).

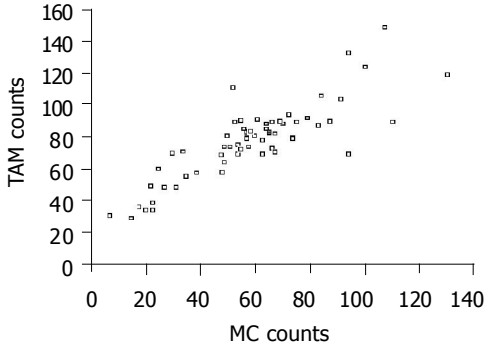

Figure 2 Correlation between MCs and TAMs.

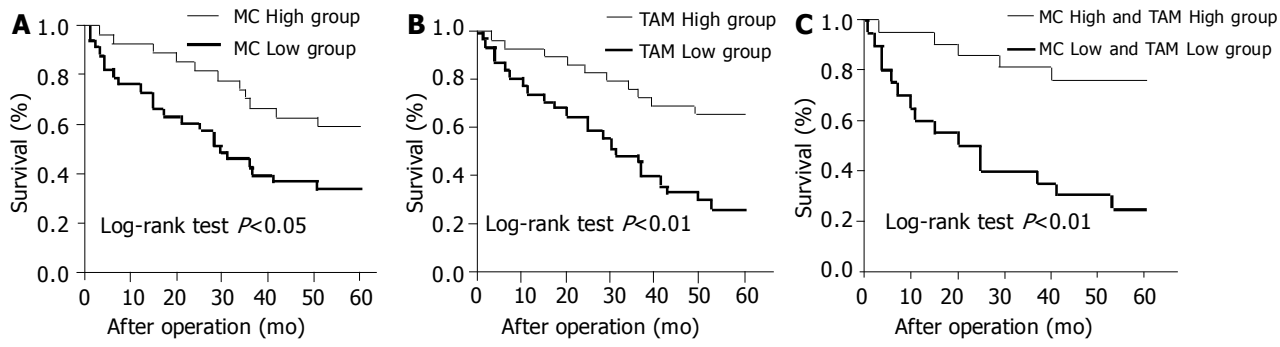

Figure 3 Survival analysis. A: Survival comparison between patients with a high level of MC infiltration and those with a low level of MC infiltration (Kaplan-Meier method); B: Survival comparison between patients with a high level of TAM infiltration and those with a low level of TAM infiltration (Kaplan-Meier method); C: Survival comparison between patients with a high level of both MC and TAM infiltration and those with a low level of both MC and TAM infiltration (Kaplan-Meier method).

Survival analysis

Survival at 5 years was 59.3% in patients with a high MC count compared to 33.3% in those patients with a low MC count. Overall survival was significantly shorter for patients with a low MC count than those with a high MC count (Figure 3A, log-rank test, $P<0.01$).

Survival at 5 years was 65.5% in patients with a high TAM count and 25.8% in patients with a low TAM count. There is a significant difference observed between the two groups (Figure 3B, log-rank test, $P<0.01$).

Twenty-one patients had a high level of both MC and TAM infiltrations. This group's survival rate at 5 years (76.2%) was higher than the patients with a low level of both MC and TAM infiltrations (25.0%, Figure 3C).

DISCUSSION

In this study, we evaluated the relationship between MCs and the clinical outcome in 60 randomly selected patients with colorectal cancer, and found a significant correlation between MC count and patient prognosis. Similar observations have been reported in lung cancer[16] as well as breast cancer[17]. These results suggest that MCs may exert a cytotoxic effect on cancer cells.

The effector components in the MC granules that suppress tumor cell activity have not been clearly identified. MCs contain the serine proteases, tryptase and chymase[18]. One study indicates that MC proteases may kill tumor cells directly by destroying surface structures on tumor cells and indirectly by altering the medium in a fashion analogous to the effect of arginase[19].

In addition to these effector components, experimental studies have shown that MC chymase induces the accumulation of macrophages, neutrophils and other inflammatory cells *in vivo*[8]. Furthermore, MC enhances the cytotoxic activation of mainly peritumoral macrophages and eosinophils[5-8] and may indirectly exert a cytotoxic effect on cancer cells. These suggestions that MCs may inhibit the malignant progression of carcinomas are supported in our study by the higher number of MCs in High Group, which had a better prognosis than Low Group, which had fewer MCs.

Other studies, however, have reported on the relationship between MCs and tumor angiogenesis[9,10,20]. Secreting MCs are able to induce and enhance angiogenesis via multiple, in part, interacting pathways[20]. As has been demonstrated, MC secreting products such as basic fibroblast growth factor[21] and histamine[22] may act directly on endothelial cells by stimulating their migration and proliferation. VEGF, a well-demonstrated mediator secreted by MCs, may contribute to angiogenesis[23]. Recently, MC tryptase was found to be a novel and potent angiogenic factor[24]. On account of this information, MCs may be seen to play a role in promoting tumor growth. However, our results, in addition to other studies, indicate that MCs are cytotoxic to cancer cells. Because of these conflicting reports, further studies are required to ascertain whether MCs enhance host immunity against cancer cells or accelerate tumor growth.

Several studies have focused on MC phenotypes in order to identify the effector components of MCs and their particular roles. Because phenotypic changes have been reported in pathological conditions including helminth infections, sarcoidosis and allergic alveolitis[14,15], we were interested in determining whether MCs might undergo phenotypic changes in colorectal cancer. The present study revealed: while there was significant difference in the quantities of MC_T and MC_{TC} between colorectal cancer and normal colorectal tissue, no difference was found in the proportion of MC_T and MC_{TC} between colorectal cancer and normal colorectal tissues. This finding suggests that both MC_T and MC_{TC} may equally proliferate or infiltrate in colorectal cancer.

It is well known that TAMs have numerous functions and, when activated, TAMs inhibit cancer growth and destroy cancer cells[25]. To date, a significant difference in the degree of TAM infiltration has been reported with regard to human bladder cancer[26]. However, whether correlation exists between the degree of TAM infiltration and cancer progression and prognosis remains unclear. Our results demonstrate that TAMs may exert a suppressive function against cancer progression and occurrence of regional lymph node metastasis and distant metastasis. Furthermore, a high level of TAM infiltration had some impact on prognosis. Therefore, TAM infiltration may manifest sufficient systemic anti-tumoral effect.

In the present study, there was significant positive correlation

between MC counts and TAM counts, and 16 patients with a high level of both MC and TAM infiltration (76.2%) survived for 5 years after surgery. MC secreting product-chymase induces the accumulation of macrophages, neutrophils and other inflammatory cells *in vivo*[8]. Furthermore, MC also enhances the cytotoxic activation of TAMs and eosinophils[5-8]. Our findings support those results by showing that the cooperative interaction of TAMs and MCs is important for anti-tumoral immunoreaction.

In conclusion, MC and TAM count were found to have a direct relationship with clinical outcome in patients with colorectal cancer. From these results, we presume that MCs and TAMs may play an important role in the enhancement of host immunity against cancer cells and that an increase in MCs and TAMs may improve the postoperative prognosis of patients with colorectal cancer. It is beneficial for estimating biological character of colorectal carcinoma to combine MC and TAM counts. Further studies are required with respect to MC phenotyping to confirm whether or not changes do indeed occur in the presence of colorectal cancer.

REFERENCES

1 **Ghiara P,** Boraschi D, Villa L, Scapigliati G, Taddei C, Tagliabue A. *In vitro* generated mast cells express natural cytotoxicity against tumour cells. *Immunology* 1985; **55:** 317–324
2 **Henderson WR,** Chi EY, Jong EC, Klebanoff SJ. Mast cell-mediated tumor-cell cytotoxicity. Role of the peroxidase system. *J Exp Med* 1981; **153:** 520–533
3 **Alleva DG,** Askew D, Burger CJ, Elgert KD. Fibrosarcoma-induced increase in macrophage tumor necrosis factor alpha synthesis suppresses T cell responses. *J Leukoc Biol* 1993; **54:** 152-160
4 **Tani K,** Ogushi F, Shimizu T, Sone S. Protease-induced leukocyte chemotaxis and activation: roles in host defense and inflammation. *J Med Invest* 2001; **48:** 133-141
5 **Coussens LM,** Werb Z. Inflammatory cells and cancer: think different! *J Exp Med* 2001; **193:** F23-F26
6 **Montemurro P,** Nishioka H, Dundon WG, de Bernard M, Del Giudice G, Rappuoli R, Montecucco C. The neutrophil-activating protein (HP-NAP) of *Helicobacter pylori* is a potent stimulant of mast cells. *Eur J Immunol* 2002; **32:** 671-676
7 **Dimitriadou V,** Koutsilieris M. Mast cell-tumor cell interactions: for or against tumour growth and metastasis? *Anticancer Res* 1997; **17:** 1541-1549
8 **He S,** Walls AF. Human mast cell chymase induces the accumulation of neutrophils, eosinophils and other inflammatory cells *in vivo*. *Br J Pharmacol* 1998; **125:** 1491-1500
9 **Roche WR.** Mast cells and tumors. The specific enhancement of tumor proliferation *in vitro*. *Am J Pathol* 1985; **119:** 57–64
10 **Marks RM,** Roche WR, Czerniecki M, Penny R, Nelson DS. Mast cell granules cause proliferation of human microvascular endothelial cells. *Lab Invest* 1986; **55:** 289–294
11 **Matsunaga Y,** Terada T. Mast cell subpopulations in chronic inflammatory hepatobiliary diseases. *Liver* 2000; **20:** 152-156
12 **Terada T,** Matsunaga Y. Increased mast cells in hepatocellular carcinoma and intrahepatic cholangiocarcinoma. *J Hepatol* 2000; **33:** 961-966
13 **Nagata M,** Shijubo N, Walls AF, Ichimiya S, Abe S, Sato N. Chymase-positive mast cells in small sized adenocarcinoma of the lung. *Virchows Arch* 2003; **443:** 565-573
14 **Arizono N,** Koreto O, Nakao S, Iwai Y, Kushima R, Takeoka O. Phenotypic changes in mast cells proliferating in the rat lung following infection with Nippostrongylus brasiliensis. *Virchows Arch B Cell Pathol Incl Mol Pathol* 1987; **54:** 1–7
15 **Walls AF,** Roberts JA, Godfrey RC, Church MK, Holgate ST. Histochemical heterogeneity of human mast cells: disease-related differences in mast cell subsets recovered by bronchoalveolar lavage. *Int Arch Allergy Appl Immunol* 1990; **92:** 233–241
16 **Tomita M,** Matsuzaki Y, Onitsuka T. Correlation between mast cells and survival rates in patients with pulmonary adenocarcinoma. *Lung Cancer* 1999; **26:** 103-108
17 **Aaltomaa S,** Lipponen P, Papinaho S, Kosma VM. Mast cells in breast cancer. *Anticancer Res* 1993; **13:** 785–788
18 **Irani AA,** Schechter NM, Craig SS, DeBlois G, Schwartz LB. Two types of human mast cells that have distinct neutral protease compositions. *Proc Natl Acad Sci USA* 1986; **83:** 4464–4468
19 **Farram E,** Nelson DS. Mouse mast cells as anti-tumor effector cells. *Cell Immunol* 1980; **55:** 294–301
20 **Norrby K.** Mast cells and angiogenesis. *APMIS* 2002; **110:** 355-371
21 **Qu Z,** Liebler JM, Powers MR, Galey T, Ahmadi P, Huang XN, Ansel JC, Butterfield JH, Planck SR, Rosenbaum JT. Mast cells are a major source of basic fibroblast growth factor in chronic inflammation and cutaneous hemangioma. *Am J Pathol* 1995; **147:** 564–573
22 **Meininger CJ,** Zetter BR. Mast cells and angiogenesis. *Semin Cancer Biol* 1992; **3:** 73–79
23 **Grizzi F,** Franceschini B, Chiriva-Internati M, Liu Y, Hermonat PL, Dioguardi N. Mast cells and human hepatocellular carcinoma. *World J Gastroenterol* 2003; **9:** 1469-1473
24 **Blair RJ,** Meng H, Marchese MJ, Ren S, Schwartz LB, Tonnesen MG, Gruber BL. Human mast cells stimulate vascular tube formation. Tryptase is a novel, potent angiogenic factor. *J Clin Invest* 1997; **99:** 2691–2700
25 **Mantovani A,** Bottazzi B, Colotta F, Sozzani S, Ruco L. The origin and function of tumor-associated macrophages. *Immunol Today* 1992; **13:** 265-270
26 **Hanada T,** Nakagawa M, Emoto A, Nomura T, Nasu N, Nomura Y. Prognostic value of tumor-associated macrophage count in human bladder cancer. *Int J Urol* 2000; **7**: 263-269

PO Box 2345, Beijing 100023, China
www.wjgnet.com
wjg@wjgnet.com

ELSEVIER

World J Gastroenterol 2005;11(8):1215-1219
World Journal of Gastroenterology ISSN 1007-9327

• *BRIEF REPORTS* •

Efficacy of different treatment strategies for hepatocellular carcinoma with portal vein tumor thrombosis

Jia Fan, Jian Zhou, Zhi-Quan Wu, Shuang-Jian Qiu, Xiao-Ying Wang, Ying-Hong Shi, Zhao-You Tang

Jia Fan, Jian Zhou, Zhi-Quan Wu, Shuang-Jian Qiu, Xiao-Ying Wang, Ying-Hong Shi, Zhao-You Tang, Liver Cancer Institute, Zhongshan Hospital, Fudan University, Shanghai 200032, China
Supported by the Foundation of Hundred Outstanding Scholars Project of Shanghai, No. 97BR029 and the Science and Technology Development Foundation of Shanghai, No. 984419067
Correspondence to: Professor Jia Fan, Liver Cancer Institute, Zhongshan Hospital, Fudan University, 136 Yixueyuan Road, Shanghai 200032, China. jiafan99@yahoo.com
Telephone: +86-21-64037181 Fax: +86-21-64037181
Received: 2004-07-28 Accepted: 2004-09-04

Key words: Hepatocellular carcinoma; Portal vein tumor thrombosis; Surgical resection; Chemotherapy; Chemoembolization

Fan J, Zhou J, Wu ZQ, Qiu SJ, Wang XY, Shi YH, Tang ZY. Efficacy of different treatment strategies for hepatocellular carcinoma with portal vein tumor thrombosis. *World J Gastroenterol* 2005; 11(8): 1215-1219
http://www.wjgnet.com/1007-9327/11/1215.asp

Abstract

AIM: To evaluate the efficacy of different treatment strategies for hepatocellular carcinoma (HCC) with portal vein tumor thrombosis (PVTT) and investigate factors influencing prognosis.

METHODS: One hundred and seventy-nine HCC patients with macroscopic PVTT were enrolled in this study. They were divided into four groups and underwent different treatments: conservative treatment group (n = 18), chemotherapy group (n = 53), surgical resection group (n = 24) and surgical resection with postoperative chemotherapy group (n = 84). Survival rates of the patients were analyzed by the Kaplan-Meier method. A log-rank analysis was performed to identify group differences. Cox's proportional hazards model was used to analyze variables associated with survival.

RESULTS: The mean survival periods of the patients in four groups were 3.6, 7.3, 10.1, and 15.1 mo respectively. There were significant differences in the survival rates among the groups. The survival rates at 0.5-, 1-, 2-, and 3-year in surgical resection with postoperative chemotherapy group were 55.8%, 39.3%, 30.4%, and 15.6% respectively, which were significantly higher than those of other groups (P<0.001). Multivariate analysis revealed that the strategy of treatment (P<0.001) and the number of chemotherapy cycles (P = 0.012) were independent survival predictors for patients with HCC and PVTT.

CONCLUSION: Surgical resection of HCC and PVTT combined with postoperative chemotherapy or chemoembolization is the most effective therapeutic strategy for the patients who can tolerate operation. Multiple chemotherapeutic courses should be given postoperatively to the patients with good hepatic function reserve.

INTRODUCTION

Hepatocellular carcinoma (HCC) is the fifth most common cancer worldwide, with the highest incidence in Asia and Africa[1]. HCC tends to invade the intrahepatic vasculature, especially the portal vein. Portal vein tumor thrombosis (PVTT) can be detected in 30.0% to 62.2% of patients with HCC[2-4]. Macroscopic tumor thrombus in portal vein appears to be the terminal stage of HCC, and is associated with the threat of bleeding of the esophageal varices, or liver failure[5,6]. The natural history of untreated HCC with PVTT is very poor. The median survival of such patients was reported to be 2.7 mo, whereas survival in those without PVTT was 24.4 mo[7,8]. Furthermore, it has been proved that portal vein invasion is correlated with intrahepatic metastasis and recurrence after treatment. The presence of tumor thrombus is correlated with poor prognosis[9-11]. The management of HCC with portal vein tumor thrombosis is complicated and controversial. PVTT was considered a relative or absolute contraindication to surgical resection. Only conservative and palliative treatments were available. With the improvement of surgical techniques and chemotherapy, many strategies have been used to treat HCC with PVTT. Some therapies have been reported to achieve promising results[3,12-16]. However, little has been done to assess the efficacy of different therapeutic strategies. In this study, we compared the clinical outcomes of different treatment strategies and investigate prognostic factors of patients with HCC and PVTT at our institution.

MATERIALS AND METHODS

Patients

The eligibility criteria were: (1) HCC with tumor thrombus in the first branch and/or main trunk of the portal vein confirmed by preoperative investigations or intraoperative exploration; (2) solitary or multiple tumors mainly located

in one lobe of the liver, and the PVTT can be removed together with the tumors in preoperative assessment; (3) no distant metastasis; (4) good or moderate hepatic function (Child-Pugh A or B); and (5) no contraindication to laparotomy.

From January 1997 to December 2002, 198 HCC patients with PVTT who met the eligibility criteria were treated at the Liver Cancer Institute, Digestive and Interventional Department of Zhongshan Hospital, Fudan University, China. Nineteen patients who were lost to follow-up were excluded. The remaining 179 were enrolled in the current study. There were 160 men and 19 women with a mean age of 47.46±10.8 years (range, 26-75 years). Serum hepatitis B surface antigen (HBsAg) was positive in 146 patients (81.6%), and hepatitis C antibody was positive in 5 patients. The α-fetoprotein (AFP) level was elevated in 149 cases (83.2%). Most of the patients had underlying cirrhosis (87.6%). According to the Child-Pugh classification, 135 patients (75.4%) were Child-Pugh A, 44 patients (24.6%) were Child-Pugh B. The tumor size was 10.5±3.2 cm (range, 3.0-22.0 cm) in diameter. Tumor thrombi involved in the first branch or extended to main trunk of portal vein. Written informed consent was obtained from all of the patients. Patients were followed until January 2004, or until the time of death.

Study design

One hundred and seventy-nine patients were divided into four groups and received different strategies of treatment: (1) conservative treatment group: traditional Chinese medicine or combined with immunotherapy was prescribed in 18 patients; (2) chemotherapy group: TACE or intraoperative hepatic artery ligation (HAL) combined with hepatic artery infusion (HAI) or portal vein infusion (PVI) were performed in 53 patients. Postoperative chemotherapy was performed through the hepatic artery or portal vein, and periodical chemoembolization through hepatic artery; (3) surgical resection group: tumors and PVTT were resected en bloc or thrombi were extracted from the portal vein after removal of the tumors in 24 patients; and (4) surgical resection combined with adjunctive chemotherapy group: hepatic arterial infusion chemotherapy (HAIC) and/or portal vein infusion chemotherapy (PVIC), transcatheter hepatic arterial chemoembolization (TACE), or selective percutaneous portal vein chemotherapy (SPVC) were performed in 84 patients after hepatectomy and thrombectomy.

Surgical procedure

Left lateral segmentectomy was performed in 7 patients, left hemi-hepatectomy in 20, left trilobectomy in 3, right partial hepatectomy in 43, right hemi-hepatectomy in 13, right trilobectomy in 2, partial median lobectomy in 5, combined left and right partial hepatectomy in 6, combined hepatic segmentectomy in 7, and complete caudate lobe resection and extended left lateral segmentectomy in 2 patients. PVTT was taken out in all cases underwent resection. Extrahepatic bile duct tumor thrombus was removed simultaneously in 6 patients, hepatic vein tumor thrombus in 5, the inferior vena cava tumor thrombus in 3, and superior mesenteric vein tumor thrombus in 1. The technique for tumor thrombus removal was as described previously[17].

Chemotherapy regimen

Each course of chemotherapy consisted of 1 000-1 500 mg 5-fluorouracil (5-FU), 80-100 mg cisplatin (CDDP), 8-20 mg mitomycin (MMC) or 40-60 mg epiadriamycin and 5-20 mL lipiodol. For TACE or SPVC, the drugs were administered in bolus injection. For HAIC and/or PVIC, they were administered via a subcutaneously implanted injection port either by intermittent injection or by a continuous infusion pump. Lipiodol was administered through hepatic artery. This procedure was repeated at one-month intervals according to patients' liver function and response to treatment. The number of chemotherapy cycles varied from 1 to 7.

Statistical analysis

Differences in clinicopathologic variables among the four groups were compared by the χ^2 test. Survival of the patients was analyzed by the Kaplan-Meier method, and comparison of the group differences was made by the log-rank test. Cox's proportional hazards model was used to analyze the variables associated with survival. Statistical analysis was carried out with SPSS software. $P<0.05$ was considered significant.

RESULTS

The clinical characteristics of 179 HCC patients with PVTT are summarized in Table 1. The clinicopathologic variables of the four groups were not statistically significant in terms of gender, age, Child-Pugh classification, tumor location, tumor size, tumor number, or location of tumor thrombus ($P>0.05$).

Survival periods

The survival of the four groups is presented in Table 2. The mean survival times of patients in conservative treatment group, chemotherapy group, surgical resection group, and surgical resection combined with adjunctive chemotherapy group were 3.6, 7.3, 10.1, and 15.1 mo respectively. The overall 0.5-, 1-, 2- and 3- year survival rates of the patients in the surgical resection combined with adjunctive chemotherapy group were 55.8%, 39.3%, 30.4%, and 15.6% respectively, which were the highest among the four groups ($P<0.001$). Survival periods of surgical resection group were significantly longer than those of conservative treatment group ($P = 0.001$). In addition, a statistically significant difference was found between surgical resection group and chemotherapy group ($P = 0.019$).

Factors influencing the survival after surgical resection

In the univariate analysis, variables that showed significant differences in survival for 108 patients who underwent surgical resection were tumor size and number of chemotherapy cycles (Table 3). None of the other variables, including number of tumors, tumor capsules, and location of tumor thrombus were significantly associated with

survival. Multivariate analysis with Cox's proportional hazards model identified only number of chemotherapy cycles was an independent prognostic factor for a favorable prognosis ($P = 0.008$), while tumor size was not.

Table 1 Clinical characteristics of 179 HCC patients with PVTT

Clinical characteristics	Conservative treatment ($n = 18$)	Chemo-therapy ($n = 53$)	Surgical resection ($n = 24$)	Surgical resection with chemotherapy ($n = 84$)	P
Gender					0.522
Male	15	49	20	76	
Female	3	4	4	8	
Age (yr)					0.510
<45	8	28	9	45	
⩾45	10	25	15	39	
Child-Pugh Class					0.731
A	12	39	18	66	
B	6	14	6	18	
Tumor location					0.351
Left lobe	3	6	5	22	
Right lobe	10	33	13	51	
Left and right lobe	4	13	6	9	
Caudate lobe	1	1	0	2	
Tumor size					0.430
<10 cm	6	25	13	45	
⩾10 cm	12	28	11	39	
Tumor number					0.715
1	11	33	14	58	
⩾2	7	20	10	26	
Tumor thrombus location					0.639
Left branch	3	7	4	18	
Left branch extending to main trunk	1	2	2	7	
Right branch	6	23	12	41	
Right branch extending to main trunk	4	10	4	11	
Left, right branch and main trunk	4	11	2	7	

Table 2 Survival periods and rates of different groups

Groups	Mean survival periods (mo)	0.5-yr survival rate (%)	1-yr survival rate (%)	2-yr survival rate (%)	3-yr survival rate (%)
Conservative treatment	3.6	5.5	0	0	0
Chemotherapy	7.3	34.6	11.8	0	0
Surgical resection	10.1	46.8	22.7	9.8	0
Surgical resection with chemotherapy	15.1	55.8	39.3	30.4	15.6

Table 3 Variables influencing postoperative survival of patients with HCC and PVTT

Influent variables	Survival periods (mo) mean±SD	P
Tumor size		
<10 cm	19.2±3.26	0.037
⩾10 cm	12.8±2.47	
Number of chemotherapy cycles		
0	8.6±1.68	0.006
1	11.9±2.24	
2	16.7±2.98	
⩾3	23.1±4.32	

Prognostic factors for PVTT patients

Pretreatment and treatment variables of all 179 patients with PVTT were analyzed by the Cox's proportional hazards model. Multivariate analysis showed that the strategy of treatment ($P<0.001$) and the number of chemotherapy cycles ($P = 0.012$) were independent survival predictors for patients with HCC and PVTT.

DISCUSSION

Efficacy of surgical resection for HCC with PVTT

Prognosis is extremely poor in patients with HCC complicated with PVTT[7,8]. Different treatments have been tried, to improve the survival of those patients. Some investigators reported the safety and efficacy of TACE for HCC with portal vein tumor thrombosis; however, the 5-year survival rate of the patients was only 0-16.8%[18,19]. These data indicate that TACE is not effective in treating portal vein tumor thrombosis. It was suggested that surgical resection provided more satisfactory results. Ohkubo *et al*[3] presented the report of surgical resection for 47 patients with PVTT. The postoperative 1-, 3-, and 5-year survival rates were 53.9%, 33.2%, 23.9% respectively. The prognosis was better if the tumor was less than 10 cm and had no intrahepatic metastases. Minagawa *et al*[20] also reported the efficacy of surgical treatment in HCC patients with PVTT. The mean survival time of the 18 patients who underwent surgical resection was 3.4±2.7 years, and postoperative 1-, 3- and 5-year survival rates were 82.0%, 42.0% and 42.0% respectively, whereas the mean survival time of 27 patients of chemotherapy group was 0.36±0.26 years. Multivariate analysis indicated that surgical resection is a positive prognostic factor. We previously reported that hepatic resection combined with thrombectomy was performed in 79 patients with HCC and PVTT at our institute, and the median survival time was 12 mo, while the median survival time of 18 patients in HAI or TACE group was 5 mo. The postoperative 1-, 3-, and 5-year survival rates were 53.9%, 26.9% and 16.6% in surgical resection group *vs* 22.2%, 5.6% and 0% in the HAI or TACE group respectively[17]. These results were in agreement with those of others. In this study, patients of surgical resection group and surgical resection combined with adjunctive chemotherapy group had higher survival rates than those of conservative treatment group or chemotherapy group. Cox's multivariate analysis also showed that the strategy of treatment was an independent survival predictor for patients with HCC and PVTT. We believe that the benefits of tumor and thrombus resection en bloc or hepatectomy plus thrombectomy are as follows: (1) decrease of portal vein pressure and prevention of intractable ascites and esophageal varices bleeding; (2) recovery of blood flow of portal vein and improvement of liver function; (3) reducing the tumor burden and increasing the efficacy of postoperative multimodality treatments such as HAI, PVI, TACE and biotherapy; and (4) improvement of quality of life and survival rate of the patients[13,21,22]. Therefore, surgical resection is an effective therapy for HCC with PVTT.

Necessity of postoperative chemotherapy

The major cause of postoperative death in the patients with

PVTT was cancer recurrence in the remnant liver[3,20,23]. The possible causes of HCC recurrence after surgical resection include invisible intrahepatic metastases present preoperatively in the remnant liver, dissemination of tumor cells during surgical manipulation, and multicentric origin of the tumor. It is widely accepted that intrahepatic metastasis, by the portal venous system, is an important mechanism for intrahepatic recurrence[9,24,25]. Adjuvant chemotherapy after hepatic resection may effectively kill residual microscopic tumor cells in the remnant liver and circulation. Lipiodol was also used because of its selective accumulation in tumors when delivered intraarterially and being a carrier for anticancer drugs[10,18,26]. Recent reports have presented favorable results of using adjunctive chemotherapy or chemoembolization after operation for PVTT patients. In our previous study, we reported that 58 patients with HCC with tumor thrombus in the first branch of portal vein underwent surgical resection and 24 patients received operation combined with periodical PVI and/or HAI, chemoembolization or TACE. The median survival time of the first group was 13 mo, and the postoperative 1-, 3- and 5-year survival rates were 59.7%, 27.4%, 8.8% respectively, whereas the median survival time of the second group was 16.5 mo and 1-, 3- and 5-year survival rates were 79.2%, 54.6% and 42.0% respectively; the difference between the two groups was significant[27]. Similar results have been published by Fukuda *et al*[23]. He reported that the overall 3-year survival rate was 48.5% for 19 HCC patients with tumor thrombi in the main portal vein, inferior vena cava and extrahepatic bile duct, who had received postoperative hepatic arterial infusion chemotherapy, and 5 patients survived more than 5 years after the operation. In the present study, the overall 0.5-, 1-, 2- and 3-year survival rates of the patients in the surgical resection combined with adjunctive chemotherapy group were 55.8%, 39.3%, 30.4% and 15.6% respectively. However, the overall 0.5-, 1-, 2- and 3- year survival rates of patients underwent surgical resection alone were 46.8%, 22.7%, 9.8% and 0% respectively. Our results indicate that postoperative adjunctive chemotherapy can reduce recurrence and is indispensable to prolonging survival. Thus, adjunctive chemotherapy should be recommended after operation in attempts to eliminate micrometastases that might be present at the time of operation or malignant cells shed during surgical manipulation of the tumor.

Prognostic factors related to survival of patients with HCC and PVTT

In this study, multivariate analysis with Cox's proportional hazards model identified the strategy of treatment and the number of postoperative chemotherapy cycles were independent prognostic factors for a favorable prognosis of patients with HCC and PVTT. The strategy of treatment influencing the survival had been well discussed above. Multiple chemotherapy courses also prolonged the survival of the patients with HCC and PVTT. We believe that the explanation for this phenomenon is that the cytotoxic effects of chemotherapy drugs usually follow log cell kill kinetics[28]. Cell killing, therefore, is proportional. Tumor cells cannot be eliminated by only one course of chemotherapy. If multiple treatments cycles are given, the opportunity to kill the residual tumor cells will increase, and the better prognosis may achieve. However, chemotherapy or chemoembolization may damage the remnant liver parenchyma, especially in cirrhotic patients, which result in impairment or deterioration of liver function[29,30]. Consequently, the number of the chemotherapy cycles will be decided according to patients' hepatic function and response to the treatment. With careful monitoring, repeated chemotherapy or chemoembolization is safe and effective.

In conclusion, surgical resection combined with postoperative adjunctive chemotherapy is the most effective therapeutic strategy for HCC patients with PVTT when liver function is compensative. If hepatic reserve is permitted, repeated adjunctive chemotherapy or chemoembolization after operation could be recommended to prolong the survival of the patients. Further prospective randomized controlled studies with large case numbers are required to support our findings.

REFERENCES

1 **Llovet JM**, Burroughs A, Bruix J. Hepatocellular carcinoma. *Lancet* 2003; **362**: 1907-1917

2 **Esnaola NF**, Mirza N, Lauwers GY, Ikai I, Regimbeau JM, Belghiti J, Yamaoka Y, Curley SA, Ellis LM, Nagorney DM, Vauthey JN. Comparison of clinicopathologic characteristics and outcomes after resection in patients with hepatocellular carcinoma treated in the United States, France, and Japan. *Ann Surg* 2003; **238**: 711-719

3 **Ohkubo T**, Yamamoto J, Sugawara Y, Shimada K, Yamasaki S, Makuuchi M, Kosuge T. Surgical results for hepatocellular carcinoma with macroscopic portal vein tumor thrombosis. *J Am Coll Surg* 2000; **191**: 657-660

4 **Tsai TJ**, Chau GY, Lui WY, Tsay SH, King KL, Loong CC, Hsia CY, Wu CW. Clinical significance of microscopic tumor venous invasion in patients with resectable hepatocellular carcinoma. *Surgery* 2000; **127**: 603-608

5 **Poon RT**, Fan ST. Evaluation of the new AJCC/UICC staging system for hepatocellular carcinoma after hepatic resection in Chinese patients. *Surg Oncol Clin N Am* 2003; **12**: 35-50, viii

6 **Yeh JL**, Peng YC, Tung CF, Chen GH, Chow WK, Chang CS, Yeh HZ, Poon SK. Clinical predictors of large esophagogastric varices in patients with hepatocellular carcinoma. *Dig Dis Sci* 2002; **47**: 723-729

7 **Llovet JM**, Bustamante J, Castells A, Vilana R, Ayuso Mdel C, Sala M, Bru C, Rodes J, Bruix J. Natural history of untreated nonsurgical hepatocellular carcinoma: rationale for the design and evaluation of therapeutic trials. *Hepatology* 1999; **29**: 62-67

8 **Pawarode A**, Voravud N, Sriuranpong V, Kullavanijaya P, Patt YZ. Natural history of untreated primary hepatocellular carcinoma: a retrospective study of 157 patients. *Am J Clin Oncol* 1998; **21**: 386-391

9 **Nagasue N**, Ono T, Yamanoi A, Kohno H, El-Assal ON, Taniura H, Uchida M. Prognostic factors and survival after hepatic resection for hepatocellular carcinoma without cirrhosis. *Br J Surg* 2001; **88**: 515-522

10 **Roayaie S**, Frischer JS, Emre SH, Fishbein TM, Sheiner PA, Sung M, Miller CM, Schwartz ME. Long-term results with multimodal adjuvant therapy and liver transplantation for the treatment of hepatocellular carcinomas larger than 5 centimeters. *Ann Surg* 2002; **235**: 533-539

11 **Poon RT**, Fan ST, Ng IO, Wong J. Prognosis after hepatic resection for stage IVA hepatocellular carcinoma: a need for reclassification. *Ann Surg* 2003; **237**: 376-383

12 **Yu AS**, Keeffe EB. Management of hepatocellular carcinoma.

Rev Gastroenterol Disord 2003; **3**: 8-24
13 **Tazawa J**, Maeda M, Sakai Y, Yamane M, Ohbayashi H, Kakinuma S, Miyasaka Y, Nagayama K, Enomoto N, Sato C. Radiation therapy in combination with transcatheter arterial chemoembolization for hepatocellular carcinoma with extensive portal vein involvement. *J Gastroenterol Hepatol* 2001; **16**: 660-665
14 **Ando E**, Tanaka M, Yamashita F, Kuromatsu R, Yutani S, Fukumori K, Sumie S, Yano Y, Okuda K, Sata M. Hepatic arterial infusion chemotherapy for advanced hepatocellular carcinoma with portal vein tumor thrombosis: analysis of 48 cases. *Cancer* 2002; **95**: 588-595
15 **Kaneko S**, Urabe T, Kobayashi K. Combination chemotherapy for advanced hepatocellular carcinoma complicated by major portal vein thrombosis. *Oncology* 2002; **62** Suppl 1: 69-73
16 **Neeman Z**, Libutti SK, Patti JW, Wood BJ. Percutaneous radiofrequency ablation of hepatocellular carcinoma in the presence of portal vein thrombosis. *Clin Imaging* 2003; **27**: 417-420
17 **Fan J**, Wu Z, Tang Z, Yu Y, Zhou J, Qiu S, Zhang B. Hepatic resection with removal of tumor thrombi for hepatocellular carcinoma with tumor thrombi in portal vein and curative analysis. *Zhonghua Waike Zazhi* 1999; **37**: 8-11
18 **Ueno K**, Miyazono N, Inoue H, Nishida H, Kanetsuki I, Nakajo M. Transcatheter arterial chemoembolization therapy using iodized oil for patients with unresectable hepatocellular carcinoma: evaluation of three kinds of regimens and analysis of prognostic factors. *Cancer* 2000; **88**: 1574-1581
19 **O'Suilleabhain CB**, Poon RT, Yong JL, Ooi GC, Tso WK, Fan ST. Factors predictive of 5-year survival after transarterial chemoembolization for inoperable hepatocellular carcinoma. *Br J Surg* 2003; **90**: 325-331
20 **Minagawa M**, Makuuchi M, Takayama T, Ohtomo K. Selection criteria for hepatectomy in patients with hepatocellular carcinoma and portal vein tumor thrombus. *Ann Surg* 2001; **233**: 379-384
21 **Ando E**, Tanaka M, Yamashita F, Fukumori K, Sumie S, Yano Y, Sata M. Chemotherapy for hepatocellular carcinoma with portal hypertension due to tumor thrombus. *J Clin Gastroenterol* 2000; **31**: 247-249
22 **Inoue K**, Nakamura T, Kinoshita T, Konishi M, Nakagohri T, Oda T, Takahashi S, Gotohda N, Hayashi T, Nawano S. Volume reduction surgery for advanced hepatocellular carcinoma. *J Cancer Res Clin Oncol* 2004; **130**: 362-366
23 **Fukuda S**, Okuda K, Imamura M, Imamura I, Eriguchi N, Aoyagi S. Surgical resection combined with chemotherapy for advanced hepatocellular carcinoma with tumor thrombus: report of 19 cases. *Surgery* 2002; **131**: 300-310
24 **Tung-Ping Poon R**, Fan ST, Wong J. Risk factors, prevention, and management of postoperative recurrence after resection of hepatocellular carcinoma. *Ann Surg* 2000; **232**: 10-24
25 **Cha C**, Fong Y, Jarnagin WR, Blumgart LH, DeMatteo RP. Predictors and patterns of recurrence after resection of hepatocellular carcinoma. *J Am Coll Surg* 2003; **197**: 753-758
26 **Huang YH**, Wu JC, Lui WY, Chau GY, Tsay SH, Chiang JH, King KL, Huo TI, Chang FY, Lee SD. Prospective case-controlled trial of adjuvant chemotherapy after resection of hepatocellular carcinoma. *World J Surg* 2000; **24**: 551-555
27 **Fan J**, Wu ZQ, Tang ZY, Zhou J, Qiu SJ, Ma ZC, Zhou XD, Ye SL. Multimodality treatment in hepatocellular carcinoma patients with tumor thrombi in portal vein. *World J Gastroenterol* 2001; **7**: 28-32
28 **Norton L**. Adjuvant breast cancer therapy: current status and future strategies-growth kinetics and the improved drug therapy of breast cancer. *Semin Oncol* 1999; **26**: 1-4
29 **Ono T**, Yamanoi A, Nazmy El Assal O, Kohno H, Nagasue N. Adjuvant chemotherapy after resection of hepatocellular carcinoma causes deterioration of long-term prognosis in cirrhotic patients: metaanalysis of three randomized controlled trials. *Cancer* 2001; **91**: 2378-2385
30 **Chan AO**, Yuen MF, Hui CK, Tso WK, Lai CL. A prospective study regarding the complications of transcatheter intraarterial lipiodol chemoembolization in patients with hepatocellular carcinoma. *Cancer* 2002; **94**: 1747-1752

PO Box 2345, Beijing 100023, China
www.wjgnet.com
wjg@wjgnet.com

ELSEVIER

World J Gastroenterol 2005;11(8):1220-1224
World Journal of Gastroenterology ISSN 1007-9327

• *BRIEF REPORTS* •

CpG oligodeoxynucleotides inhibit tumor growth and reverse the immunosuppression caused by the therapy with 5-fluorouracil in murine hepatoma

Xian-Song Wang, Zhen Sheng, You-Bing Ruan, Yang Guang, Mu-Lan Yang

Xian-Song Wang, Zhen Sheng, You-Bing Ruan, Yang Guang, Mu-Lan Yang, Department of Pathology, Tongji Medical College, Huazhong University of Technology and Science, Wuhan 430030, Hubei Province, China
Supported by the Natural Science Foundation of Hubei Province, No. 2000J006
Correspondence to: Dr. Xian-Song Wang, Department of Pathology, Tongji Medical College, Huazhong University of Technology and Science, Wuhan 430030, Hubei Province, China. xiansongw@yahoo.com
Telephone: +86-27-83692639
Received: 2004-07-05 Accepted: 2004-08-30

Abstract

AIM: To investigate the effect of CpG-containing oligodeoxynucleotides (CpG ODN) alone or in combination with the chemotherapeutic agent 5-fluorouracil (5-FU) on tumor growth and whether CpG ODN can reverse the immunosuppression caused by the chemotherapy with 5-FU in murine hepatoma model.

METHODS: Hepatoma model was established by subcutaneous inoculation with hepatoma-22 (H_{22}) cells into the right flank of BALB/c mice. Mice with tumor were treated by peritumoral injection of CpG ODN alone or in combination with subcutaneous injection of 5-FU. Tumor size was quantified regularly. Serum levels of IL-12 and IFN-γ in mice were assayed by enzyme-linked immunosorbent assay (ELISA). The lytic capacity of splenic NK cells was tested by lactate dehydrogenase release assay.

RESULTS: Peritumoral injection of CpG ODN alone or in combination with subcutaneous injection of 5-FU, and the treatment with 5-FU alone all led to significant inhibition of hepatoma growth. The mean tumor volumes fell by 46.66% in mice injected with CpG ODN, 68.34% in the 5-FU treated mice, and 70.23% in mice treated with the combination of CpG ODN and 5-FU than in controls. There was no significant difference in tumor size between 5-FU-treated mice and mice treated with the combination of 5-FU and CpG ODN ($P>0.05$). The serum levels of IL-12 and IFN-γ of mice treated with CpG ODN alone (IL-12: 464.50±24.37 pg/mL; IFN-γ: 134.20±25.76 pg/mL) or with the co-administration of CpG ODN and 5-FU (IL-12: 335.83±28.74 pg/mL; IFN-γ: 111.00±5.33 pg/mL) were significantly higher than that of controls (IL-12: 237.50±45.31 pg/mL; IFN-γ: 56.75±8.22 pg/mL). The production of IL-12 and IFN-γ was suppressed moderately in 5-FU-treated mice (IL-12: 166.67±53.22 pg/mL; 53.33±16.98 pg/mL) compared to control mice ($P>0.05$), whereas the combination of CpG ODN and 5-FU significantly increased the serum levels of IL-12 and IFN-γ compared to 5-FU alone ($P<0.05$). The NK cell killing activity in CpG ODN-treated mice (44.04±1.38%) or the mice treated with CpG ODN combined with 5-FU (30.67±1.28%) was significantly potentiated compared to controls (19.22±0.95%, $P<0.05$). The co-administration of CpG ODN and 5-FU also significantly enhanced the lytic activity of NK cells when compared with the treatment with 5-FU alone (12.03±1.42%, $P<0.05$).

CONCLUSION: The present data suggests that CpG ODN used as single therapeutic agent triggers anti-tumor immune response to inhibit the growth of implanted hepatoma and reverses the immunosuppression caused by the chemotherapy with 5-FU.

Key words: CpG-oligodeoxynucleotides; Hepatoma 22; Immunotherapy; 5-fluorouracil; Mice

Wang XS, Sheng Z, Ruan YB, Guang Y, Yang ML. CpG oligodeoxynucleotides inhibit tumor growth and reverse the immunosuppression caused by the therapy with 5-fluorouracil in murine hepatoma. *World J Gastroenterol* 2005; 11(8): 1220-1224

http://www.wjgnet.com/1007-9327/11/1220.asp

INTRODUCTION

CpG is a dinucleotide containing cytosine (C) and guanine (G). Bacterial DNA and synthetic oligodeoxynucleotides containing the CpG motifs (CpG ODN) have been shown to be potent activators of immune system, which can provoke various immune cells and induce the production of a wide variety of T helper-1 (Th1)-promoting cytokines, such as interleukin 12 (IL-12), interferon-γ (IFN-γ), tumor necrosis factor-α (TNF-α) and IL-6[1-4]. As a strong immunostimulatory agent, CpG ODN is able to prevent effectively against bacterial, viral and parasitic infections[5-7]. CpG ODN also enhances the anti-tumor efficacy of monoclonal antibodies or cancer vaccines when used as immune adjuvants in animal tumor models[8,9]. The administration of CpG ODN alone is also capable of triggering potent anti-tumor immune responses against

various experimental tumors, for example, lymphoma, leukemia, melanoma, colon tumor, glioma, cervical cancer, neuroblastoma[8,10-14].

Among the available approaches used for the treatment of hepatocellular carcinoma (HCC), chemotherapy is still a major alternative for the majority of cases. However, a single chemotherapeutic agent usually was shown to be poor in suppressing HCC and improving the overall survival rate of patients with HCC[15]. Immunotherapy, as a novel option for tumor management, has offered some clinical benefits for improvement of the survival patients with HCC[16]. In particular, the combination therapy with chemotherapeutic agents and immunostimulators, such as 5-fluorouracil (5-FU) and IFN, has been found to be effective in enhancing the HCC-inhibitory effect of chemotherapy alone[16,17]. In the present study, we investigated the therapeutic potential of CpG ODN by peritumoral injection in murine hepatoma model and the possibility that the combination CpG ODN with 5-FU promotes the inhibitory efficacy of 5-FU alone.

The production of large amounts of IL-12 and IFN-γ, and the activation of natural killer (NK) cells has been thought to be an important property of the CpG ODN-elicited immune response[5-7,18]. In this study, we evaluated the effects of CpG ODN on immune cells by examining the serum levels of IL-12 and IFN-γ and cytotoxicity of splenic NK cells in mice with tumor to further understand the possible mechanism responsible for CpG ODN action. The chemotherapeutic drug 5-FU usually causes severe bone marrow suppression leading to immunosuppression; in contrast, CpG ODN is a potent immune activator; hence we also explored whether or not CpG ODN used in combination with 5-FU could improve the immunosuppressive condition in 5-FU-treated mice in terms of IL-12 and IFN-γ contents in murine sera and NK cell killing activity.

MATERIALS AND METHODS

Mice

BALB/c mice were obtained from the Animal Center of Tongji Medical College (Wuhan, China) and used for studies at ages of 6 to 8 wk with an average body weight of 20 g.

Cell lines and cell culture

Mouse hepatoma cell line, hepatoma-22 (H_{22}) and murine lymphoma YAC-1 cell line were provided by China Center for Type Culture Collection (Wuhan, China). H_{22} cells were maintained in our laboratory by injecting intraperitoneally 1×10^6 cells into the above-mentioned BALB/c mice. YAC-1 cells were cultured in RPMI 1640 medium supplemented with 10% heat-inactivated fetal bovine serum, 100 IU/mL of penicillin, 100 μg/mL of streptomycin and 2 mmol/L L-glutamine at 37 ℃, 50 mL/L CO_2. All culture reagents were purchased from Gibco BRL, UK.

Oligodeoxynucleotides

The ODNs used in the present study included CpG ODN 1826 and the non-CpG control ODN 1982[19]. Both of the purified ODNs were purchased from Shanghai Sangon Biological Engineering Technology Service Co. Ltd. (Shanghai, China). The sequence of CpG ODN 1826 was: 5'-TCCATGACGTTCCTGACGTT-3', which contains two CpG dinucleotides. The non-CpG ODN 1982 sequence was: 5'-TCCAGGACTTCTCTCAGGTT-3'. Before *in vivo* use, ODNs were dissolved in sterile isotonic sodium chloride.

Tumor implantation and tumor treatments

H_{22} cells harvested from the peritoneal cavity of the mice bearing hepatoma-22 were washed three times with cold PBS. 1×10^6 of cells with a viability of >95%, as determined by trypan blue exclusion, were inoculated subcutaneously at the right hind flank of BALB/c mice. The implanted tumors exhibited 100% survival. When the subcutaneous tumor diameter had reached 4-5 mm (5 d after tumor inoculation), treatment with ODNs alone or in combination with 5-FU was started. Mice were injected peritumorally with 50 μL of sodium chloride per day (control) or 50 μg of ODNs dissolved in 50 μL of saline (once per day) on d 5, 10, 15 and 17 after tumor inoculation. From the first day of treatment, 5-FU (25 mg/kg) dissolved in 50 μL of saline was given at the back of mice per day subcutaneously for 12 consecutive days with or without peritumoral injection of ODN (CpG ODN) as described above. Tumor diameter were measured every third day with a caliper and tumor volume was calculated according to the following formula: V = (largest diameter)×(smallest diameter)^2/2. For each experiment, groups of 5-8 mice were used.

In vitro assay for IL-12 and IFN-γ levels

Peripheral blood was collected from mice with tumor 24 h after the final injection of ODNs. Sera were separated and frozen at -70 ℃. Serum levels of IL-12 (p40) and IFN-γ were measured using enzyme-linked immunosorbent assay (ELISA) kits (BioSource International, Inc., CA, USA) according to the manufacturer's instructions. The results were expressed as pg/mL.

Assay of splenic NK cell activity

After collection of blood, mice were killed by cervical dislocation. Spleen was freshly removed and smashed in cold RPMI 1640 media; a single-cell suspension was obtained by passing the material through a sterile nylon mesh of 100 and 200 gauge in turn. Lymphocytes were separated from suspension by gradient centrifugation with Ficoll-Hypaque with a specific gravity of 1.09. NK cell activity was determined by the lactate dehydrogenase (LDH) release assay[20]. Briefly, purified lymphocytes were incubated with the NK-sensitive target cell YAC-1 at E:T ratios of 100 for 4 h in triplicates at 37 ℃ in a 50 mL/L CO_2 incubator. The spontaneous and maximum release of LDH was determined by culturing YAC-1 cells in culture medium alone or with 1% sodium lauryl sulfate. After incubation, the enzymatic reactions were carried out in the dark over a period of 15 min according to the methods described by Konjevic *et al*[20]. All reagents were purchased from Sigma (St. Louis, MO). The absorbances were read at 570 nm and NK cell lytic activity was calculated by the following formula: lytic activity (%) = (experimental release - spontaneous release) / (maximum release - spontaneous release) ×100%.

Statistical analysis

All results were expressed as mean±SE of individual animal values in each group. Statistical analyses were performed by the unpaired Student's *t* test. Results were considered significant at $P<0.05$.

RESULTS

Inhibition of tumor growth by CpG ODN and 5-FU

The average survival duration of mice, bearing hepatoma without any treatment was 23 d. Considering that chemotherapeutic or immunostimulatory agents would lose their therapeutic efficacy with the progress of tumor, we killed all mice 18 d after tumor inoculation to compare the effects of different therapeutic agents on tumor growth. Eight days after tumor cell inoculation (3 d after the initial treatments), subcutaneous injection of 5-FU or peritumoral injection of CpG ODNs, but not non-CpG ODN, led to greater reduction of tumor volumes compared to controls injected with sodium chloride (Figure 1). By 17 d of post-tumor implantation, the mean tumor volumes fell by 46.66% in mice injected with CpG ODN ($n = 8$), which is greater than that seen in controls ($n = 5$; 3579.38±480.72 *vs* 6710.40±909.80 mm^3; $P<0.005$). A stronger tumor inhibition occurred in 5-FU-treated mice ($n = 8$), with tumor volumes 68.34% smaller than controls (2124.56±434.04 *vs* 6710.40±909.80 mm^3, $P<0.001$). The tumor growth inhibition was not observed in non-CpG ODN-treated mice (6780.70±656.41 mm^3, $n = 5$). The results suggest that the antitumoral effect of CpG ODN was dependent on the CpG motifs within the ODN.

Inhibition of tumor growth by the co-administration with CpG ODN and 5-FU

Treatment with the combination of CpG ODN and 5-FU ($n = 8$) resulted in a 70.23% reduction of mean tumor volumes compared to controls (1997.78±474.56 *vs* 6710.40±909.80 mm^3, $P<0.001$). There was no significant difference in the tumor inhibition between mice treated with 5-FU alone and combined use of CpG ODN and 5-FU (Figure 1). The result showed that CpG ODN did not produce a cooperative inhibition of hepatoma growth with 5-FU.

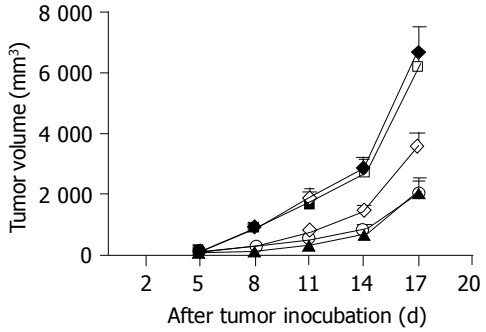

Figure 1 Tumor volumes (mean±SE) in BALB/c mice with hepatoma treated with sodium chloride (control, ◆, $n = 5$), non-CpG ODN (□, $n = 5$), CpG ODN (◇, $n = 8$), 5-FU (▲, $n = 8$) and 5-FU combined with CpG ODN (○, $n = 8$).

CpG ODN stimulates IL-12 and IFN-γ production

To assess the effects of CpG ODN on immune cell activity in mice with hepatoma, we examined and compared the serum levels of IL-12 and IFN-γ in all mice after different treatments. As shown in Figure 2, concentrations of IL-12 and IFN-γ in sera of mice treated with CpG ODN were significantly higher than those in sera of controls (IL-12: 464.50±24.37 *vs* 237.50±45.31 pg/mL, $P<0.01$; IFN-γ: 134.20±25.76 *vs* 56.75±8.22 pg/mL, $P<0.05$). There was also a significant increase in serum levels of IL-12 and IFN-γ of mice treated with the co-administration of CpG ODN and 5-FU compared to controls (IL-12: 335.83±28.74 *vs* 237.50±45.31 pg/mL, $P<0.05$; IFN-γ: 111.00±5.33 *vs* 56.75±8.22 pg/mL, $P<0.05$), whereas non-CpG ODN treatment did not affect the levels of IL-12 and IFN-γ. The results indicated that CpG ODN could induce the production of IL-12 and IFN-γ in mice bearing tumor and the stimulatory effects were dependent on the CpG motifs containing ODN. The production of IL-12 and IFN-γ was suppressed moderately in 5-FU-treated mice compared to control mice, whereas the combination of CpG ODN and 5-FU significantly increased serum levels of IL-12 and IFN-γ compared to 5-FU alone (IL-12: 335.83±28.74 *vs* 166.67±53.22 pg/mL, $P<0.05$; IFN-γ: 111.00±5.33 *vs* 53.33±16.98 pg/mL, $P<0.05$). The data suggest that CpG ODN can reverse the inhibition of immune cells resulting from the 5-FU therapy.

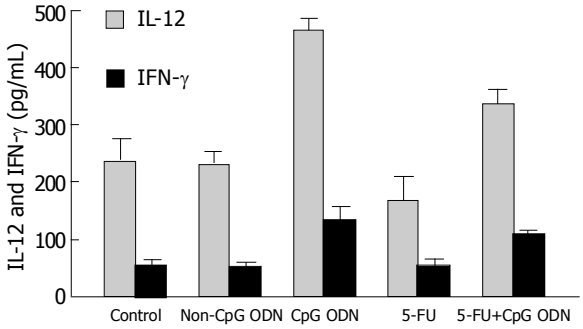

Figure 2 The serum levels of IL-12 and IFN-γ (mean±SE) in BALB/c mice with hepatoma after different treatments. Peripheral blood was collected from mice with tumor 24 h after the final injection of sodium chloride (control, $n = 5$), non-CpG ODN ($n = 5$), CpG ODN ($n = 8$), 5-FU ($n = 8$) and 5-FU combined with CpG ODN ($n = 8$). ODNs IL-12 and IFN-γ contents in sera were assayed with ELISA.

Effects of CpG ODN on cytotoxicity of splenic NK cells

To evaluate the effect of CpG ODN on the activity of splenic NK cells, we detected the lytic activity of NK cells against YAC1 tumor target cells (Table 1). NK cell killing activity in CpG ODN-treated mice and the mice treated with CpG ODN combined with 5-FU was significantly higher than those in controls, whereas the potentiation of NK cell activity was not seen in non-CpG ODN-treated mice. This observation showed the ability of CpG ODN to activate NK cells and augment their cytotoxicity, and the CpG motifs were necessary for the immunostimulatory activity of CpG ODN. Injection with 5-FU alone caused a relatively mild

but no significant inhibition of NK cell compared to control animals. However, the lytic activity of NK cells in mice treated with the combination of CpG ODN and 5-FU is significantly higher than those in 5-FU-treated mice ($P<0.05$), which suggests that CpG ODN is capable of eliminating the inhibition of NK cell function induced by 5-FU.

Table 1 NK cell activity of hepatoma-bearing mice receiving different treatments

Groups	*n*	NK activity (%)
Control	4	19.22±0.95
Non-CpGODN	5	19.33±1.95
CpGODN	6	44.04±1.38[a]
5-FU	6	12.03±1.42
5-FU+CpGODN	6	30.67±1.28[a]

[a]$P<0.05$ *vs* the control group.

DISCUSSION

CpG ODN 1826 is known as a strong immune activator and induces protective and curative Th1 responses against infections and tumor *in vivo*, and the immunostimulatory effects of CpG ODN 1826 are dependent on the CpG motifs within oligodeoxynucleotides[5-7,21]. Our studies here first showed that peritumoral injection of CpG ODN 1826 as a single therapeutic agent suppressed the growth of implanted hepatoma in mice, but the oligodeoxynucleotide without CpG motifs was ineffective. The findings are consistent with the previous observations obtained in several tumor models treated with CpG ODN 1826[11,19,21].

The most important immunostimulatory property of CpG ODN is to activate directly antigen-presenting cells (APCs), including macrophages, monocytes and dendritic cells (DCs), to produce a large amount of Th1-promoting cytokines especially IL-12 and IFN-γ[13,14,22]. IL-12 and IFN-γ are critical cytokines in the induction of cellular immunity. IL-12 can promote Th1 cell immune response and stimulate T cells and NK cells to secrete IFN-γ[23]. The activated NK cells also release IL-12, which together with IFN-γ, in turn further activate NK cells, APCs and T cells and enhance their immune activity[18,24]. It has been reported that the IL-12 and IFN-γ-dependent immunological mechanisms are responsible for the CpG ODN-triggered protective response to infections[5-7]. The immunological activity of CpG ODN in the antitumoral response varies with the ODN sequence and backbone as well as tumor models. For example, CpG ODN 1585 was ineffective in lymphoma model but induced a significant regression of tumor in melanoma via NK cells, whereas the inhibition of CpG ODN 1826 in lymphoma model was dependent on both NK and T cells[23]. In the present study, CpG ODN induced production of IL-12 and IFN-γ and potentiated NK cell lytic activity, which exhibited the ability of CpG ODN to activate various immune cells of the mice with hepatoma and to elicit the anti-tumor response. The results also suggest that the production of IL-12 and IFN-γ as well as NK cell activation may play a role in the CpG ODN 1826-induced inhibition of hepatoma growth.

So far, the efficacy of chemotherapeutic agents remains superior to single immune modulators in the management of HCC, which was also confirmed in the present result that 5-FU showed stronger inhibitory effect on hepatoma growth than CpG ODN. Unfortunately, 5-FU inhibits cancer cell growth but also damages normal cells, especially the hemopoietic cells within bone marrow, which can cause bone marrow suppression leading to immunosuppression. CpG ODN is a potent immunostimulator; besides the activation of various immune cells, it has been shown to trigger extramedullary hematopoiesis and enhance cytotoxic T cell function in the irradiated mice[25]. IL-12 derived from activated APCs has been reported to promote maturation of primitive bone marrow precursors and proliferation of DCs synergistically with other hemopoietic growth factors[23]. Theoretically the co-administration of 5-FU and CpG ODN 1826 in mice with hepatoma should be able to reverse the depressed immune function resulting from 5-FU therapy, thereby enhancing the anti-tumor efficacy of 5-FU alone. Our results that the treated mice with CpG ODN combined with 5-FU had higher serum levels of IL-12 and IFN-γ and stronger NK cell lytic activity than the 5-FU-treated mice suggest that CpG ODN indeed reconstitutes immune function of mice treated with 5-FU. However, no significant difference in mean tumor volumes was observed between the two treatments. The results reflected the possibility that the combined use of CpG ODN with 5-FU did not increase the tumor-inhibitory effect of 5-FU. But it is mostly possible that the dose of 5-FU used here is enough to inhibit cancer cells, which cannot be exceeded by the addition of CpG ODN. Even if the combination of CpG ODN with 5-FU failed to produce synergistic inhibition of tumor growth, the immune-potentiating effect induced by CpG ODN undoubtedly contributes to the anti-tumor response in mice, and increases the toleration to the chemotherapeutic agents, thereby bringing about positive effect on tumor control.

In this study, peritumoral injection of CpG ODN did not produce any adverse effects showing that CpG ODN is safer than chemotherapeutic drugs or other immunostimulatory agents such as IL-2 and IFN in tumor treatment. Furthermore, CpG ODN is cheaper and easily available. Therefore, the present findings that CpG ODN inhibited hepatoma growth and triggered an immune response to reverse the immunosuppression caused by 5-FU therapy give rise to the interest that CpG ODN may also be a useful agent in human HCC management.

REFERENCES

1 **Krieg AM**, Yi AK, Matson S, Waldschmidt TJ, Bishop GA, Teasdale R, Koretzky GA, Klinman DM. CpG motifs in bacterial DNA trigger direct B-cell activation. *Nature* 1995; **374**: 546-549

2 **Jakob T**, Walker PS, Krieg AM, Udey MC, Vogel JC. Activation of cutaneous dendritic cells by CpG-containing oligodeoxynucleotides: a role for dendritic cells in the augmentation of Th1 responses by immunostimulatory DNA. *J Immunol* 1998; **161**: 3042-3049

3 **Häcker H**, Mischak H, Miethke T, Liptay S, Schmid R, Sparwasser T, Heeg K, Lipford GB, Wagner H. CpG-DNA-specific activation of antigen-presenting cells requires stress kinase activity and is preceded by non-specific endocytosis and endosomal maturation. *EMBO J* 1998; **17**: 6230-6240

4 **Sun S**, Zhang X, Tough DF, Sprent J. Type I interferon-mediated stimulation of T cells by CpG DNA. *J Exp Med* 1998; **188**: 2335-2342

5 **Walker PS**, Scharton-Kersten T, Krieg AM, Love-Homan L, Rowton ED, Udey MC, Vogel JC. Immunostimulatory oligodeoxynucleotides promote protective immunity and provide systemic therapy for leishmaniasis via IL-12- and IFN-gamma-dependent mechanisms. *Proc Natl Acad Sci USA* 1999; **96**: 6970–6975

6 **Harandi AM**, Eriksson K, Holmgren J. A protective role of locally administered immunostimulatory CpG oligodeoxynucleotide in a mouse model of genital herpes infection. *J Virol* 2003; **77**: 953-962

7 **Gramzinski RA**, Doolan DL, Sedegah M, Davis HL, Krieg AM, Hoffman SL. Interleukin-12- and gamma interferon-dependent protection against malaria conferred by CpG oligodeoxynucleotide in mice. *Infect Immun* 2001; **69**: 1643-1649

8 **Wooldridge JE**, Ballas Z, Krieg AM, Weiner GJ. Immunostimulatory oligodeoxynucleotides containing CpG motifs enhance the efficacy of monoclonal antibody therapy of lymphoma. *Blood* 1997; **89**: 2994-2998

9 **Davila E**, Celis E. Repeated administration of cytosine-phosphorothiolated guanine-containing oligonucleotides together with peptide/protein immunization results in enhanced CTL responses with anti-tumor activity. *J Immunol* 2000; **165**: 539-547

10 **Blazar BR**, Krieg AM, Taylor PA. Synthetic unmethylated cytosine-phosphate-guanosine oligodeoxynucleotides are potent stimulators of antileukemia responses in naive and bone marrow transplant recipients. *Blood* 2001; **98**: 1217-1225

11 **Sharma S**, Karakousis CP, Takita H, Shin K, Brooks SP. Intra-tumoral injection of CpG results in the inhibition of tumor growth in murine Colon-26 and B-16 tumors. *Biotechnol Lett* 2003; **25**: 149-153

12 **Carpentier AF**, Xie J, Mokhtari K, Delattre JY. Successful treatment of intracranial gliomas in rat by oligodeoxynucleotides containing CpG motifs. *Clin Cancer Res* 2000; **6**: 2469-2473

13 **Baines J**, Celis E. Immune-mediated tumor regression induced by CpG-containing oligodeoxynucleotides. *Clin Cancer Res* 2003; **9**: 2693-2700

14 **Carpentier AF**, Chen L, Maltonti F, Delattre JY. Oligodeoxynucleotides containing CpG motifs can induce rejection of a neuroblastoma in mice. *Cancer Res* 1999; **59**: 5429-5432

15 **Lin DY**, Lin SM, Liaw YF. Non-surgical treatment of hepatocellular carcinoma. *J Gastroenterol Hepatol* 1997; **12**: S319-S328

16 **Patt YZ**, Hassan MM, Lozano RD, Brown TD, Vauthey JN, Curley SA, Ellis LM. Phase II trial of systemic continuous fluorouracil and subcutaneous recombinant interferon Alfa-2b for treatment of hepatocellular carcinoma. *J Clin Oncol* 2003; **21**: 421-427

17 **Leung TW**, Patt YZ, Lau WY, Ho SK, Yu SC, Chan AT, Mok TS, Yeo W, Liew CT, Leung NW, Tang AM, Johnson PJ. Complete pathological remission is possible with systemic combination chemotherapy for inoperable hepatocellular carcinoma. *Clin Cancer Res* 1999; **5**: 1676-1681

18 **Ballas ZK**, Rasmussen WL, Krieg AM. Induction of NK activity in murine and human cells by CpG motifs in oligodeoxynucleotides and bacterial DNA. *J Immunol* 1996; **157**: 1840-1845

19 **Heckelsmiller K**, Rall K, Beck S, Schlamp A, Seiderer J, Jahrsdörfer B, Krug A, Rothenfusser S, Endres S, Hartmann G. Peritumoral CpG DNA elicits a coordinated response of CD8 T cells and innate effectors to cure established tumors in a murine colon carcinoma model. *J Immunol* 2002; **169**: 3892-3899

20 **Konjević G**, Jurišić V, Banićević B, Spužić I. The difference in NK-cell activity between patients with non-Hodgkin's lymphomas and Hodgkin's disease. *Br J Haematol* 1999; **104**: 144-151

21 **Ballas ZK**, Krieg AM, Warren T, Rasmussen W, Davis HL, Waldschmidt M, Weiner GJ. Divergent therapeutic and immunologic effects of oligodeoxynucleotides with distinct CpG motifs. *J Immunol* 2001; **167**: 4878-4886

22 **Chu RS**, Targoni OS, Krieg AM, Lehmann PV, Harding CV. CpG oligodeoxynucleotides act as adjuvants that switch on T helper 1 (Th1) immunity. *J Exp Med* 1997; **186**: 1623-1631

23 **Lamont AG**, Adorini L. IL-12: a key cytokine in immune regulation. *Immunol Today* 1996; **17**: 214-217

24 **Chace JH**, Hooker NA, Mildenstein KL, Krieg AM, Cowdery JS. Bacterial DNA-induced NK cell IFN-gamma production is dependent on macrophage secretion of IL-12. *Clin Immunol Immunopathol* 1997; **84**: 185-193

25 **Sparwasser T**, Hültner L, Koch ES, Luz A, Lipford GB, Wagner H. Immunostimulatory CpG-oligodeoxynucleotides cause extramedullary murine hemopoiesis. *J Immunol* 1999; **162**: 2368-2374

PO Box 2345, Beijing 100023, China
www.wjgnet.com
wjg@wjgnet.com

ELSEVIER

World J Gastroenterol 2005;11(8):1225-1227
World Journal of Gastroenterology ISSN 1007-9327

• *BRIEF REPORTS* •

Effect of fermented soy milk on the intestinal bacterial ecosystem

I-Chi Cheng, Huey-Fang Shang, Tzann-Feng Lin, Tseng-Hsing Wang, Hao-Sheng Lin, Shyh-Hsiang Lin

I-Chi Cheng, Shyh-Hsiang Lin, Graduate Institute of Nutrition and Health Sciences, Taipei Medical University, Taipei, Taiwan, China
Huey-Fang Shang, Department of Microbiology, College of Medicine, Taipei Medical University, Taipei, Taiwan, China
Tzann-Feng Lin, Tseng-Hsing Wang, Hao-Sheng Lin, Taiwan Tobacco and Liquor Company (TTL), Taiwan, China
Supported by the Taiwan Tobacco and Liquor Company, No. 0930001444
Correspondence to: Shyh-Hsiang Lin, Graduate Institute of Nutrition and Health Sciences, Taipei Medical University, (110) 250 Wu-Hsing Street, Taipei, Taiwan, China. lin5611@tmu.edu.tw
Telephone: +886-2-27361661-6551-126 Fax: +886-2-27373112
Received: 2004-09-08 Accepted: 2004-10-07

Abstract

AIM: To investigate the effect of fermented soy milk on human ecosystem in the intestinal tract by way of examining the population of different microorganisms isolated from fecal samples.

METHODS: A crossover experimental design was applied. Twenty-eight healthy adults completed this experiment. Each subject consumed 250 mL, twice a day between meals, of either fermented soy milk or regular soy milk first for 2 wk, then switched to the other drink after 2 wk. Fecal samples were collected from all subjects every week starting from the second week to the end of the experiment. The microorganisms analyzed were *Bifidobacterium* spp., *Lactobacillus* spp., *Clostridium perfringens*, coliform organisms, and total anaerobic organisms.

RESULTS: In the period of fermented soy milk consumption, the populations of *Bifidobacterium* spp. and *Lactobacillus* spp. increased ($P<0.05$) as well as the ratios of *Bifidobacterium* spp. and *Lactobacillus* spp. to *Clostridium perfringens* ($P<0.05$). The population of coliform organisms decreased ($P<0.05$) when subjects were in the period of fermented soy milk consumption.

CONCLUSION: Intake of fermented soy milk significantly improved the ecosystem of the intestinal tract in the body by increasing the amount of probiotics.

Key words: Fermented; Soy; Intestinal; Bacterial; Ecosystem

Cheng IC, Shang HF, Lin TF, Wang TH, Lin HS, Lin SH. Effect of fermented soy milk on the intestinal bacterial ecosystem. *World J Gastroenterol* 2005; 11(8): 1225-1227
http://www.wjgnet.com/1007-9327/11/1225.asp

INTRODUCTION

Probiotics are bacteria with health-benefits that live in the intestinal tract. Probiotics reduce lactose-intolerance symptoms, increase the resistance of the intestines to diseases, inhibit cancer cells from proliferating, modulate the concentration of plasma cholesterol, improve digestive functions, and stimulate the immune system[1,2]. On the other hand, prebiotics are the food ingredients that can be utilized by or can enhance the growth of probiotics. Some commonly mentioned prebiotics are lactose, fructooligosaccharides, and galactooligosaccharides[3-6]. Soybeans and soy products have been well known for their health benefits. In soybeans, oligosaccharides were also proven to be prebiotics[7]. The combination of probiotics and prebiotics is called synbiotics[1]. Fermented soy milk, according to previous statements, can be considered as a synbiotic product. Thus, our objective was to investigate the effect of fermented soy milk on the ecosystem in the intestinal tract of human subjects.

MATERIALS AND METHODS

Subjects

This study was approved by the Human Ethics Committee of Taipei Medical University (Taipei, Taiwan). Subjects were recruited mostly from the campus of Taipei Medical University and had no acute or chronic diseases, gastrointestinal problems, or a recent history of taking antibiotics. Before executing this study, written informed consents were acquired from all subjects. Totally 36 subjects participated at the beginning. Subjects were advised to maintain their normal life style during the experiment.

Study design

A crossover design was used in this study. Subjects were randomly assigned to two groups, A and B. In group A, subjects consumed fermented soy milk first, and then switched to regular soy milk, while regular soy milk was consumed first in group B. The total experimental time was 9 wk. A 2-wk adjustment period was carried out, followed by consumption of experimental drinks for 2 wk. Before switching to the other experiment drink, there was another 2-wk period for washout. After all subjects had completed consuming the two kinds of experimental drink, there was a 1-wk washout period before the experiment formally ended. The drink consisted of 250 mL each time given 30 min after a meal, twice a day (500 mL/d). A 3-d (Sunday, Monday and Tuesday) dietary record was completed by subjects every week during the experiment.

Sample collection and microorganism analyses

About 1 g of fecal samples from each subject was collected

in wk 2, 3, 4, 6, 7, 8, and 9 for microorganism analyses. Samples were stored at -20 ℃ for less than 24 h before analysis. For the analyses, 0.5 g of the inner part of a fecal sample (to retrieve anaerobic material) was mixed well with 15 mL of an anaerobic solution (Table 1), followed by serial dilutions to acquire different concentrations (10^{-1} to 10^{-8}). Certain microorganisms were isolated from fecal samples using the media and methods developed by Molly *et al*[8]. The bacteria, media and incubation times are listed in Table 2. Starting from the lowest concentration, 50 μL of the solution was then inoculated on different media using the spread plate method. For incubating *Clostridium perfringens*, 1 mL of solutions with suitable concentrations, determined by the result of a pre-experiment, was mixed well with TSC medium (without egg-yolk) using the pour plate method, followed by mixing with the regular TSC medium. After the liquid medium solidified, the plate was placed in an anaerobic chamber.

When counting colonies, plates with 30-300 colonies were included. The number of bacteria was presented as log CFU/g of wet weight of feces. The calculation formulae are listed as follows and are based on the FDA Bacteriological Analytical Manual: *Bifidobacterium* spp., *Lactobacillus* spp., coliform organisms, and total anaerobic organisms: CFU/plate ×20 (50 μL/plate)×dilution factor×15 mL/sample (g); and *Clostridium perfringens*: CFU/plate×dilution factor×15 mL/sample (g).

Table 1 Composition of the anaerobic solution

Chemicals	Weight
KH_2PO_4	4.5 g
Na_2HPO_4	6.0 g
L-cysteine HCl·H_2O	0.5 g
Tween 20	1 g
Galtin	2 g
Distilled water	1 L

Statistical analysis

All data are presented as the mean±SD. One-way analysis of variance (ANOVA), unpaired and paired *t*-tests were performed using SAS version 8.1. $P<0.05$ was the level of significance.

RESULTS

Before the experiment started, 8 people withdrew from the study due to personal reasons. Thus, totally 28 people participated and completed two experimental periods. As shown in Table 3, there were no significant changes in weight, height, or BMI between before and after the study.

Group A (fermented soy milk first, regular soy milk second)

In this group (Figure 1A), we found that during the first period of fermented soy milk consumption, the populations of coliform organisms and *Clostridium perfringens* significantly decreased ($P<0.05$). In the same period, the populations of both *Lactobacillus* spp. and *Bifidobacterium* spp. increased ($P<0.05$). The ratios of *Lactobacillus* spp. and *Bifidobacterium* spp. to *Clostridium perfringens* also increased in the first period. In the second period of regular soy milk consumption, the populations of coliform organisms and *Clostridium perfringens* and the ratios of *Lactobacillus* spp. and *Bifidobacterium* spp. to *Clostridium perfringens* did not change.

Group B (regular soy milk first, fermented soy milk second)

In this group (Figure 1B), in the first and second periods, the population of *Lactobacillus* spp. significantly increased ($P<0.05$). In the second period, the populations of coliform organisms and *Clostridium perfringens* significantly decreased ($P<0.05$), while the population of *Bifidobacterium* spp. significantly increased ($P<0.05$). At the end of the first and second periods, the ratios of *Lactobacillus* spp. and *Bifidobacterium* spp. to *Clostridium perfringens* had significantly increased ($P<0.05$). The population of total anaerobic bacteria did not change in either group.

DISCUSSION

The population of microorganisms in the intestine is in a balanced phase[9]. When the number of probiotics increases, the number of harmful bacteria decreases. As seen in the results, we found that when subjects were in the period of fermented soy milk consumption, their intestinal ecosystem

Table 2 Microorganisms analyzed and incubating media, times and temperatures

Medium	Microorganism	Color of the colony	Incubation conditions
Bifidobacteria iodoacetate medium–25 (BIM-25)	*Bifidobacterium* spp.	Green	48 h, 35-37 ℃
Lactobacillus anaerobic MRS with bromocresol green (MRS-modified)	*Lactobacillus* spp.	Reddish orange	48 h, 35-37 ℃
Tryptose-sulfite-D-cycloserine agar (TSC)	*Clostridium perfringens*	White with black center	24 h, 35-37 ℃
Endo agar plates (Endo)	Coliform organisms	Metallic red	24 h, 35-37 ℃
CDC anaerobe blood agar plates (CDC)	Total anaerobic organisms	White	48 h, 35-37 ℃

Table 3 Background information of subjects before and after the study

Group	*n*		Wk 0			Wk 8		
		Age (yr)	Weight (kg)	Height (cm)	BMI	Weight (kg)	Height (cm)	BMI
A	14	23.1±1.1	56.4±10.6	162.0±7.9	21.3±2.3	56.1±10.2	162.0±7.9	21.2±2.2
B	14	22.6±1.8	55.9±8.3	162.6±8.2	21.1±1.5	56.1±9.5	163.1±8.8	21.1±3.5

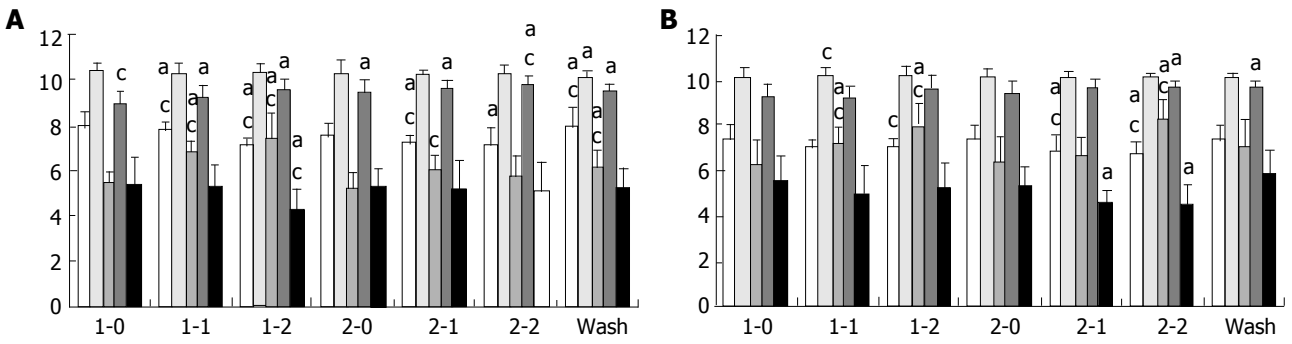

Figure 1 Changes in the number (log) of different microorganisms during the experiment. A: the group in which fermented soy milk was consumed in the first period; B: the group in which regular soy milk was consumed in the first period. Data presented as the mean±SD, n=13; □: coliform organisms,□: *total anaerobic organisms*,■: *lactobacillus* spp.,■: *Bifidobacterium* spp.,■: *Clostridium* to wk 2-0, $^aP<0.05$ *vs* total anaerobic organisms; $^cP<0.05$ *vs* total anaerobic organisms.

tended to be improved by an increase in the populations of the so-called "good bacteria". The effect could be maintained even 3 wk after cessation of fermented soy milk consumption. On the other hand, results showed that regular soy milk also had some effect on increasing the population of *Lactobacillus* spp. This may have been because soybeans contain certain types of oligosaccharides such as raffinose and stachyose that can be utilized by *Lactobacillus* spp. as energy sources[10,11]; this reduces the beany odor and gas production in the intestines[12]. It was found that, by culturing different probiotics in soy milk, the amounts of raffinose and stachyose that caused reduction of gas production in the stomach while the amounts of sucrose, glucose, galactose, acetic acid, and free amino acids increased[13]. The increase in probiotics lowers the risk of GI tract dysfunction from bacterial invasion and hence, maintains one of the major functions of GI tract, the barrier function[14]. Beside the effects of consuming fermented soy milk determined in this experiment, soy products are well known for their health benefits. It has been found that the intake of soy products reduces the risk of various cancers, lowers the levels of blood lipid and cholesterol, and prevents oxidation of VLDL and LDL, and hence lowering the risk of cardiovascular diseases[15-17].

In conclusion, consumption of fermented soy milk is beneficial to the ecosystem of the intestinal tract by increasing the populations of probiotics and reducing the populations of unwanted bacteria. In addition, fermented soy milk may also provide other exclusive ingredients such as isoflavone and saponin that do not exist in dairy products.

REFERENCES

1 **Gibson GR**, Roberfroid MB. Dietary modulation of the human colonic microbiota: introducing the concept of prebiotics. *J Nutr* 1995; **125**: 1401–1412
2 **Gonzalez SN**, Cardozo R, Apella MC, Oliver G. Biotherapeutic role of fermented milk. *Biotherapy* 1994; 8: 129–134
3 **Buddington RK**, Williams CH, Chen SC, Witherly SA. Dietary supplement of neosugar alters the fecal flora and decreases activities of some reductive enzymes in human subjects. *Am J Clin Nutr* 1996; **63**: 709-716
4 **Gibson GR**, Beatty ER, Wang X, Cummings JH. Selective stimulation of bifidobacteria in the human colon by oligofructose and inulin. *Gastroenterology* 1995; **108**: 975-982
5 **Rowland IR**, Tanaka R. The effects of transgalactosylated oligosaccharides on gut flora metabolism in rats associated with a human faecal microflora. *J Appl Bacteriol* 1993; **74**: 667–674
6 **MacGillivray PC**, Finlay HVL, Binns TB. Use of lactulose to create a preponderance of Lactobacilli in the intestine of bottle-fed infants. *Scott Med J* 1959; **4**: 182–189
7 **Chow J**. Probiotics and prebiotics: A brief overview. *J Ren Nutr* 2002; **12**: 76-86
8 **Molly K**, Vande Woestyne M, De Smet I, Verstraete W. Validation of the simulator of the human intestinal microbial ecosystem (SHIME) reactor using microorganism-associated activities. *Microb Ecol Health Dis* 1994; **7**: 191-200
9 **Todar K**. The bacterial flora of humans. Todar's Online Textbook of Bacteriology. 2002. Available from: URL: http://textbookofbacteriology.net/normalflora.html
10 **Hang YD**, Jackson H. Preparation of soybean cheese using lactic starterorganisms I. General characteristics of the finished cheese. *Food Technol* 1967; **21**: 1967-1995
11 **Yamanaka Y**, Okumura S, Mitsugi K, Hasagawa Y. Process for preparing a sour milk beverage or yoghurt. *Food Sci Technol Abstr* 1969; **1**: 1308-1310
12 **Thananunkul D**, Tanaka M, Chichester CO, Lee TC. Degradation of raffinose and stachyose in soybean milk by α-galactosidase from *Mortierella vinacea*. Entrapment of α-galactosidase within polyacrylamide gel. *J Food Sci* 1976; **41**: 173-175
13 **Wang YC**, Yu RC, Yang HY, Chou CC. Sugar and acid contents in soymilk fermented with lactic acid bacteria alone or simultaneously with bifidobacteria. *Food Microbiol* 2003; **20**: 333-338
14 **Ding LA**, Li JS. Intestinal failure: pathophysiological elements and clinical diseases. *World J Gastroenterol* 2004; **10**: 930-933
15 **Samman S**, Khosla P, Carroll KK. Intermediate density lipoprotein-apolipoprotein B turnover in rabbits fed semipurified diets containing casein or soy protein. *Ann Nutr Metab* 1990; **34**: 98-103
16 **Vahouny GV**, Adamson I, Chalcarz W, Satchithanandam S, Muesing R, Klurfeld DM, Tepper SA, Sanghvi A, Kritchevsky D. Effects of casein and soy protein on hepatic and serum lipids and lipoprotein lipid distributions in the rat. *Atherosclerosis* 1985; **56**: 127-137
17 **Sirtori CR**, Galli G, Lovati MR, Carrara P, Bosisio E, Kienle MG. Effects of dietary proteins on the regulation of liver lipoprotein receptors in rats. *J Nutr* 1984; 114: 1493-1500

PO Box 2345, Beijing 100023, China
www.wjgnet.com
wjg@wjgnet.com

ELSEVIER

World J Gastroenterol 2005;11(8):1228-1231
World Journal of Gastroenterology ISSN 1007-9327

• *BRIEF REPORTS* •

Relationship between expression and distribution of cyclooxygenase-2 and bcl-2 in human gastric adenocarcinoma

Xiao-Li Chen, Bao-Shan Su, Run-Qin Sun, Jun Zhang, Yi-Li Wang

Xiao-Li Chen, Bao-Shan Su, Run-Qin Sun, Department of Pathology, Second Hospital of Xi'an Jiaotong University, Xi'an 710004, Shaanxi Province, China
Jun Zhang, Section of Gastroenterology, Department of Medicine, Second Hospital of Xi'an, Jiaotong University, Xi'an 710004, Shaanxi Province, China
Yi-Li Wang, Institute for Cancer Research, Xi'an Jiaotong University, Xi'an 710061, Shaanxi Province, China
Co-correspondents: Yi-Li Wang
Correspondence to: Dr. Xiao-Li Chen, Department of Pathology, Second Hospital of Xi'an Jiaotong University, Xi'an 710004, Shaanxi Province, China. chenxiaoli64.student@sina.com
Telephone: +86-29-88546322
Received: 2004-06-15 Accepted: 2004-07-22

Abstract

AIM: To explore expression and distribution features of COX-2 and bcl-2 in human gastric adenocarcinoma tissues and to study its biological significance.

METHODS: Totally 36 human gastric carcinoma samples were enrolled in this study (cardiac adenocarcinoma 16 cases, distal gastric adenocarcinoma 20 cases). The expressions of COX-2 and bcl-2 in cancerous tissues and corresponding para-cancerous tissues were investigated by immunohistochemistry using COX-2 polyclonal antibody and bcl-2 monoclonal antibody. The normal gastric mucosa tissues were used as control.

RESULTS: The expressions of COX-2 and bcl-2 in gastric carcinoma were significantly higher than that in the para-cancerous tissues (77.8% *vs* 47.2%, $P<0.01$, 80.56% *vs* 58.33%, $P<0.05$). The expression of COX-2 in cardiac adenocarcinoma was remarkably higher than that in the distal gastric carcinoma (93.8% *vs* 65.0%, $P<0.01$). The expression of COX-2 was mainly localized in the cytoplasm of tumor cells and partly in the nucleus. There is a transition of the COX-2 cytoplasmic positivity to nucleic in tumor cells with the increase of gastric carcinoma pathological grade. Interstitial macrophages, fibroblasts and vascular endothelial cells also expressed COX-2. The tissues with higher expression of COX-2 also expressed high level of bcl-2 protein.

CONCLUSION: Abnormal expression pattern of COX-2 within the tissues of human gastric cancer is correlated with tumor location and lymph node metastasis. COX-2 may regulate expression of apoptosis suppressor gene (bcl-2) through interaction of tumor cells and stromal cells and play an important role in the generation and development of tumors, which will be of great help in developing new methods for antitumor therapy.

Key words: Gastric adenocarcinoma; Apoptosis suppressor gene (bcl-2); Cyclooxygenase (COX-2)

Chen XL, Su BS, Sun RQ, Zhang J, Wang YL. Relationship between expression and distribution of cyclooxygenase-2 and bcl-2 in human gastric adenocarcinoma. *World J Gastroenterol* 2005; 11(8): 1228-1231
http://www.wjgnet.com/1007-9327/11/1228.asp

INTRODUCTION

Cyclooxygenases (COXes), which are the key enzymes in prostaglandin (PG) biosynthesis, are thought to be important in maintaining the normal physiological functions and certain pathological process. Currently, cyclooxygenases have at least 2 isoenzymes in the mammal, namely COX-1 and COX-2. COX-1 is expressed in most tissues and is thought to be important in maintaining the normal physiological functions. COX-2 may be involved in the repairment of peptic ulcer and colitis, development and progression of tumor by promoting proliferation of cells and tumor angiogenesis, and inhibition of apoptosis[1,2]. Recently, the relationship between COX-2 and human gastric cancer has been emphasized. The increased expression of COX-2 mRNA or protein has been demonstrated in human tumors of digestive system[3-10], such as esophageal cancer, colorectal cancer, liver cancer and pancreas cancer. The expression of COX-2 protein in human gastric carcinoma has also been reported. However, distribution features of COX-2 protein in human gastric carcinoma and the relationship between COX-2 and bcl-2 are still not clear. To clarify the contribution of COX-2 and bcl-2 in gastric carcinoma, it is essential to examine the expression of COX-2 and bcl-2 within tissues of human gastric carcinoma.

In this study, we used immunohistochemistry method to detect the expression of COX-2 and bcl-2 protein in human gastric adenocarcinoma and their corresponding para-cancerous tissues, and to explore the distribution features of COX-2 and bcl-2 in human gastric adenocarcinoma and the biological significance, and to provide rational foundation for designing effective schemes of antitumor therapy.

MATERIALS AND METHODS

Materials

A total of 36 human gastric adenocarcinoma (including 16

cardiac adenocarcinomas and 20 distal gastric adenocarcinomas) cases were investigated. All tissues were surgically resected. Cancerous tissue and para-cancerous gastric mucosa were all from the same specimens. Morphologically normal gastric mucosa tissues were used as control. Each specimen was fixed in 10% phosphate-buffered formalin immediately after resection, embedded in paraffin and sectioned into 4 μm for immunohistochemical study and routine histological examination.

The study was approved by the Ethics Committee of our hospital and all patients gave written informed consent prior to enrollment.

Reagents and methods

Polyclonal mouse anti-human COX-2 antibody was purchased from Santa Cruz Biotechnology Co. Mouse anti-human monoclonal antibody bcl-2 was purchased from Danmark Co. The SP staining kit was purchased from Zymed Co. The procedures of immunohistochemical staining were performed according to the manufacturer's instructions. The known positive colorectal cancer tissues were used as positive control. As negative control, PBS was used to replace primary antibody.

Assessment of staining

Under the light microscope, the immunoreactivity was evaluated both qualitatively and quantitatively. Intensity and percentage of positive cells were used to evaluate each tissue section. The immunostaining intensity was scored as 0 (achromatic), 1 (light yellow), 2 (yellow), and 3 (brown). Immunostaining quantity was scored as follows: 1 = <25%, 2 = 26-50%, 3 = 51-75% and 4 = >75% of tumor cell showing positivity. The combined score, based on both qualitative and quantitative immunostaining, was determined by multiplying the qualitative and quantitative scores. Based on the combined score, the samples were grouped as follows: negative (-) 0-1, weak (+) 2-3, moderate (++) 4-6, strong (+++) >6.

Statistical analysis

With statistical analysis package (SPSS) version 10.0 for Windows, difference between groups was evaluated by using chi-square test and Student's *t* test. The *P* value less than 0.05 was considered statistically significant. All reported *P* values were two-sided.

RESULTS

Expression of COX-2 and bcl-2 in normal gastric mucosa

In the normal gastric mucosa, the expression of COX-2 was mostly negative. Smattering deep glandular epithelia cells showed weak-positive expression of COX-2. The expression of bcl-2 was negative or focus weak-positive reaction in the normal gastric mucosa.

Distribution of COX-2 within tissues of human gastric carcinomas (Table 1)

The expression of COX-2 was mainly localized in the cytoplasm of tumor cells, partly in the nucleus (Figure 1). The expressions of COX-2 were detected in the para-cancerous tissues (Figure 2), including gastric mucosal

Table 1 Pathological characteristics of gastric adenocarcinoma and immunohistochemical COX-2 staining

Pathological characteristics	*n*	Expression of COX-2				Positive rate (%)	*P*
		-	+	++	+++		
Gastric carcinomas	36	8	12	10	6	77.8	<0.01[b]
Para-cancerous tissues	36	19	10	7	0	47.2	
Location of tumor							
Cardiac carcinoma	16	1	4	8	3	93.8	<0.01[b]
Non-cardiac carcinoma	20	7	8	2	3	65.0	
Histological type							
Intestinal carcinoma	17	3	5	5	4	82.3	
Diffuse carcinoma	19	5	7	4	3	74.1	
Metastatic lymph node							
Positive	22	1	10	5	6	95.5	<0.005[b]
Negative	14	7	2	5	0	50.0	

[b]*P*<0.01 *vs* the expression of COX-2 was significant between gastric carcinoma and para-cancerous tissues, location of tumor, and metastatic lymph node.

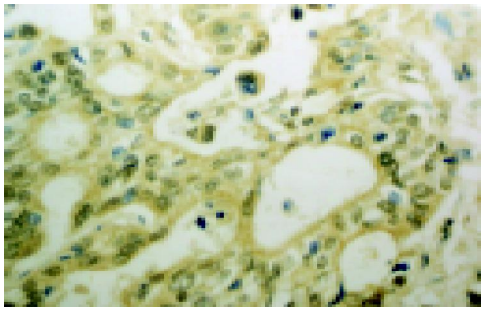

Figure 1 Expression of COX-2 in tissue of human gastric adenocarcinoma. Some stromal cells showed positive stains. Immunohistochemical staining, ×400.

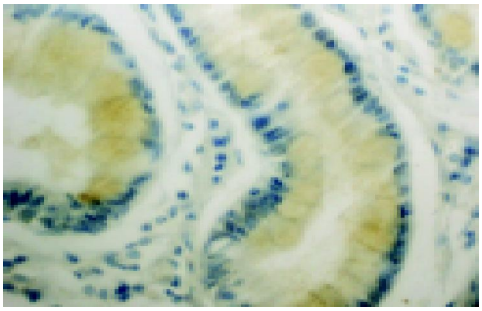

Figure 2 Expression of COX-2 in the para-cancerous tissue. Intestinal metaplasia epithelia and goblet cells showed plasmatic stain. Immunohistochemical staining, ×400.

epithelia, intestinal metaplasia epithelia, goblet cells and a few glandular epithelia, but with lower intensity. The COX-2 expression was also observed on interstitial macrophages, fibroblasts and endothelial cells. The expression of COX-2 in cancerous tissues was significantly higher than that in the para-cancerous tissues (77.8% *vs* 47.2%). Compared to the distal gastric adenocarcinoma, the rate of COX-2 expression was dramatically higher in cardiac adenocarcinoma (93.8% *vs* 65%). There was no significant difference in the expression of COX-2 based on the tumor differentiation. However, the cytoplasmic positivity of COX-2 was transformed to nucleic positivity with the increase of pathological grade of gastric carcinoma. Meanwhile, we observed that the expression of COX-2 in metastatic cases was higher than that in non-metastatic one ($P<0.005$), which suggested that the expression of COX-2 may contribute to infiltrating metastasis potential of cancer cells.

The expression of bcl-2 protein in gastric cancer tissues (see Table 2)

The expression of bcl-2 protein in gastric cancer tissues was located in cytoplasm of tumor cells and stromal lymphocytes. In para-cancerous tissues, only a few deep glandular epithelium cells and intestinal metaplasia cells expressed bcl-2 protein. The positive rate and intensity of bcl-2 expression in gastric cancer tissues were higher than that in para-cancerous tissues. The expression of bcl-2 protein was not correlated with location and histological type of tumor and lymph node metastasis (data was not shown).

Table 2 Expression of bcl-2 in gastric cancer and para-cancerous tissues

Type of tissue	*n*	Expression of bcl-2				Positive rate (%)	*P*
		-	+	++	+++		
Gastric cancer tissue	36	7	9	12	8	80.56	<0.025[a]
Para-cancerous tissues	36	15	14	4	3	58.33	

[a]$P<0.05$ *vs* the expression of bcl-2 was significant between gastric carcinoma and para-cancerous tissues.

DISCUSSION

COXes are thought to be important in maintaining the normal physiological and pathological functions. COX-2 may be involved in the development and progress of tumor by promoting proliferation of cells and tumor angiogenesis and inhibiting apoptosis of cells[1,2].

The increased expression of COX-2 mRNA or protein has been demonstrated in human tumors of digestive system[3-8], such as esophageal cancer, colorectal cancer, liver cancer and pancreas cancer. The expression of COX-2 protein in human gastric cancer tissues has also been reported. However, distribution features of COX-2 protein in human gastric cancer tissues, relationship between COX-2 and bcl-2 are not completely clear. In the present study, we demonstrated that COX-2 protein was overexpressed in human gastric cancer tissues. The location of COX-2 products varied with difference of tumor differentiation. In intestinal adenocarcinoma, COX-2 protein was present in the cytoplasm of tumor cells with moderate staining intensity. But in diffuse adenocarcinoma, COX-2 protein was localized in nucleus of tumor cells and stained with brown granules. Sometimes, COX-2 protein simultaneously appeared in nucleus and cytoplasm of tumor cells. Interestingly, the positive rate of COX-2 expression and stained intensity in cardiac carcinoma were significantly higher than that in gastric distal carcinomas. These findings differed from other reports[9] in which similar rate of positivity was evident in intestinal-type cardiac carcinoma (52%) when compared to the noncardiac ones (64%). However, there was a trend of lower incidence of strong COX-2 positivity in cardiac than in noncardiac tumors (14% *vs* 41%). This difference of COX-2 distribution may be associated with specificity and sensitivity related to different COX-2 antibodies and staining protocols or procedures. There may be ethnic difference between different peoples. Recent studies[11] indicated that genesis of cardiac cancer was related to reflux esophagitis, intestinal metaplasia in the junction of stomach and esophagus and atypical hyperplasia. Incidence of cardiac adenocarcinoma was increasing in Chinese, which may be one of the factors that lead to high-level expression of COX-2 in cardiac cancer.

Our results showed that COX-2 protein was not only expressed in neoplastic epithelial cells, but also in interstitial macrophages and fibroblasts, which might be an incidental phenomenon in the progression of diseases unrelated to carcinogenesis itself or might be a reaction to mucosal lesion. The stromal cells expressing COX-2 can stimulate proliferation of epithelium cells and promote tumorigenesis through paracrine ways[12]. Williams and his colleagues[13] found that the growth of a lung carcinoma cell line is markedly attenuated in COX-2 $^{-/-}$ mice or mice treated with a COX-2-selective inhibitor. In sporadic colorectal adenomas, COX-2 was localized on superficial interstitial macrophages and dysplastic epithelial cells. The mechanism to induce epithelial carcinogenesis may be COX-2-mediated paracrine signaling between the macrophages and epithelial cells within tumors[14].

The development and progression of stomach cancer is a pathological process involving many factors, stages and oncogenes, in which imbalance between apoptosis and proliferation of cells plays an important role. Bcl-2 gene is a well-known apoptosis suppressor gene leading to increase of abnormal cells by inhibiting cell apoptosis and prolonging life span of cells, but not promoting cell proliferation, so it will make way for the development of tumors[15]. Our results showed that the positive rate and intensity of bcl-2 protein expression in tissues of gastric adenocarcinomas was higher than that in para-cancerous tissues, suggesting that epithelial cells might have overexpression of bcl-2 protein during malignancy transformation of gastric mucosa, which makes regulatory mechanism of cells changeable. Therefore, the balance between apoptosis and proliferation of cell was destroyed, which will conduce to development of tumors. The expression of bcl-2 protein was not related to differentiation and location of gastric adenocarcinoma.

Recent studies[16-19] suggest that COX-2 was involved in the development of tumors through following ways: (1) COX-2 can increase products of prostaglandin; (2) COX-2

can transform pre-carcinogen to carcinogen; (3) COX-2 can inhibit apoptosis of cells and promote adhesion of cells; (4) COX-2 can promote angiogenesis of tumor; (5) COX-2 can regulate inflammation and immune functions; (6) COX-2 can enhance invasive ability of tumor cells. We also found in the present experiment that the tissues with a high-level expression of COX-2 expressed simultaneously high-level of bcl-2 protein, indicating the COX-2 can promote expression of bcl-2 and decrease cell apoptosis. Therefore, we suppose COX-2 plays an important regulatory role in bcl-2 expression. Further study of interaction between COX-2 and bcl-2 in the gastric cancer is warranted.

REFERENCES

1 **Uefuji K,** Ichikura T, Mochizuki H. Expression of cyclooxygenase-2 in human gastric adenomas and adenocarcinomas. *J Surg Oncol* 2001; **76:** 26-30

2 **Wu AW,** Gu J, Ji JF, Li ZF, Xu GW. Role of COX-2 in carcinogenesis of colorectal cancer and its relationship with tumor biological characteristics and patients' prognosis. *World J Gastroenterol* 2003; **9:** 1990-1994

3 **Fournier DB,** Gordon GB. COX-2 and colon cancer: potential targets for chemoprevention. *J Cell Biochem Suppl* 2000; **34:** 97-102

4 **Lim HY,** Joo HJ, Choi JH, Yi JW, Yang MS, Cho DY, Kim HS, Nam DK, Lee KB, Kim HC. Increased expression of cyclooxygenase-2 protein in human gastric carcinoma. *Clin Cancer Res* 2000; **6:** 519-525

5 **Tucker ON,** Dannenberg AJ, Yang EK, Zhang F, Teng L, Daly JM, Soslow RA, Masferrer JL, Woerner BM, Koki AT, Fahey TJ. Cyclooxygenase-2 expression is up-regulated in human pancreatic cancer. *Cancer Res* 1999; **59:** 987-990

6 **Yu J,** Leung WK, Lee TL, Tse PC, To KF, Sung JJ. Promoter hypermethylation of cyclooxygenase-2 in gastric carcinoma. *Int J Oncol* 2003; **22:** 1025-1031

7 **Shiota G,** Okubo M, Noumi T, Noguchi N, Oyama K, Takano Y, Yashima K, Kishimoto Y, Kawasaki H. Cyclooxygenase-2 expression in hepatocellular carcinoma. *Hepatogastroenterology* 1999; **46:** 407-412

8 **Zimmermann KC,** Sarbia M, Weber AA, Borchard F, Gabbert HE, Schror K. Cyclooxygenase-2 expression in human esophageal carcinoma. *Cancer Res* 1999; **59:** 198-204

9 **Saukkonen K,** Nieminen O, van Rees B, Vilkki S, Harkonen M, Juhola M, Mecklin JP, Sipponen P, Ristimaki A. Expression of cyclooxygenase-2 in dysplasia of the stomach and in intestinal-type gastric adenocarcinoma. *Clin Cancer Res* 2001; **7:** 1923-1931

10 **Zhang J,** Liu Y, Cao ZL, Chen XL, Wang KM, Guo XD, Zuo AL, Gong J. Analysis pathological lesions at distal esophagus and esophagogastric junction. *Zhonghua Xiaohua Neijing Zazhi* 2002; **19:** 214-217

11 **van Rees BP,** Saukkonen K, Ristimaki A, Polkowski W, Tytgat GN, Drillenburg P, Offerhaus GJ. Cyclooxygenase-2 expression during carcinogenesis in the human stomach. *J Pathol* 2002; **196:** 171-179

12 **Williams CS,** Tsujii M, Reese J, Dey SK, DuBois RN. Host cyclooxygenase-2 modulates carcinoma growth. *J Clin Invest* 2000; **105:** 1589-1594

13 **Chapple KS,** Cartwright EJ, Hawcroft G, Tisbury A, Bonifer C, Scott N, Windsor AC, Guillou PJ, Markham AF, Coletta PL, Hull MA. Localization of cyclooxygenase-2 in human sporadic colorectal adenomas. *Am J Pathol* 2000; **156:** 545-553

14 **Lauwers GY,** Scott GV, Karpeh MS. Immunohistochemical evaluation of bcl-2 protein expression in gastric adenocarcinomas. *Cancer* 1995; **75:** 2209-2213

15 **Sung JJ,** Leung WK, Go MY, To KF, Cheng AS, Ng EK, Chan FK. Cyclooxygenase-2 expression in *Helicobacter pylori*-associated premalignant and malignant gastric lesions. *Am J Pathol* 2000; **157:** 729-735

16 **Kelly LM,** Hill AD, Kennedy S, Connolly EM, Ramanath R, Teh S, Dijkstra B, Purcell R, McDermott EW, O'Higgins N. Lack of prognostic effect of Cox-2 expression in primary breast cancer on short-term follow-up. *Eur J Surg Oncol* 2003; **29:** 707-710

17 **Howe LR,** Dannenberg AJ. COX-2 inhibitors for the prevention of breast cancer. *J Mammary Gland Biol Neoplasia* 2003; **8:** 31-43

18 **Zang T,** Sun F, Li Y. Expression of COX-2 in prostatic cancer and benign prostatic hyperplasia *Zhonghua WaiKe Zazhi* 2001; **39:** 702-703

19 **Higashi Y,** Kanekura T, Kanzaki T. Enhanced expression of cyclooxygenase (COX)-2 in human skin epidermal cancer cells: evidence for growth suppression by inhibiting COX-2 expression. *Int J Cancer* 2000; **86**: 667-671

PO Box 2345, Beijing 100023, China
www.wjgnet.com
wjg@wjgnet.com

ELSEVIER

World J Gastroenterol 2005;11(8):1232-1236
World Journal of Gastroenterology ISSN 1007-9327

• *BRIEF REPORTS* •

Expression of TNF-α and VEGF in the esophagus of portal hypertensive rats

Zhao-Hui Yin, Xun-Yang Liu, Rang-Lang Huang, Shu-Ping Ren

Zhao-Hui Yin, Xun-Yang Liu, Rang-Lang Huang, Shu-Ping Ren, Department of General Surgery, Third Xiangya Hospital, Central South University, Changsha 410013, Hunan Province, China
Co-correspondence: Rang-Lang Huang
Correspondence to: Dr. Zhao-Hui Yin, Division of Transplantation Surgery, Center for Surgical Sciences, Karolinska University Hospital, Huddinge B56, S-141 86 Stockholm, Sweden. yinzhaohui0451@hotmail.com
Telephone: +46-8-58582568
Received: 2004-01-15 Accepted: 2004-08-21

Abstract

AIM: To investigate the expression of tumor necrosis factor-alpha (TNF-α) and vascular endothelial growth factor (VEGF) in the development of esophageal varices in portal hypertensive rats.

METHODS: Thirty male Sprague-Dawley (SD) rats in the model group in which a two-stage ligation of portal vein plus ligation of the left adrenal vein was performed, were divided into three subgroups (M_7, M_{14}, and M_{21}) in which the rats were kiued on the seventh day, the 14th d and the 21 d after the complete portal ligation. Thirty male SD rats, which underwent the sham operation in the control group, were also separated into three subgroups (C_7, C_{14} and C_{21}) corresponding to the models. The expression of TNF-α and VEGF in the esophagus of all the six subgroups of rats were measured with immunohistochemical SP technique.

RESULTS: The portal pressure in the three model subgroups was significantly higher than that in the corresponding control subgroups (23.82±1.83 *vs* 11.61±0.86 cmH_2O, 20.90±3.27 *vs* 11.43±1.55 cmH_2O and 20.68±2.27 *vs* 11.87±0.79 cmH_2O respectively, $P<0.01$), as well as the number (9.3±1.6 *vs* 5.1±0.8, 11.1±0.8 *vs* 5.4±1.3 and 11.7±1.5 *vs* 5.2±1.1 respectively, $P<0.01$) and the total vascular area (78 972.6±3 527.8 *vs* 12 993.5±4 994.8 μm^2, 107 207.5±4 6461.4 *vs* 11 862.6±5 423.2 μm^2 and 110 241.4±49 262.2 *vs* 11 973.7±3 968.5 μm^2 respectively, $P<0.01$) of submucosal veins in esophagus. Compared to the corresponding controls, the expression of TNF-α and VEGF in M_{21} was significantly higher (2.23±0.30 *vs* 1.13±0.28 and 1.65±0.38 *vs* 0.56±0.30 for TNF-α and VEGF respectively, $P<0.01$), whereas there was no difference in M_7 (1.14±0.38 *vs* 1.06±0.27 and 0.67±0.35 *vs* 0.50±0.24 for TNF-α and VEGF respectively, $P>0.05$) and M_{14} (1.20±0.25 *vs* 1.04±0.26 and 0.65±0.18 *vs* 0.53±0.25 for TNF-α and VEGF respectively, $P>0.05$). And the expression of TNF-α and VEGF in M_{21} was significantly higher than that in M_7 (2.23±0.30 *vs* 1.14±0.38 and 1.65±0.38 *vs* 0.67±0.35 for TNF-α and VEGF respectively, $P<0.01$) and M_{14} (2.23±0.30 *vs* 1.20±0.25 and 1.65±0.38 *vs* 0.65±0.18 for TNF-α and VEGF respectively, $P<0.01$), but there was no difference between M_7 and M_{14} (1.14±0.38 *vs* 1.20±0.25 and 0.67±0.35 *vs* 0.65±0.18 for TNF-α and VEGF respectively, $P>0.05$).

CONCLUSION: In the development of esophageal varices in portal hypertensive rats, increased TNF-α and VEGF may be not an early event, and probably play a role in weakening the esophageal wall and the rupture of esophageal varices.

Key words: Portal hypertension; Esophageal varices; Tumor necrosis factor-alpha; Vascular endothelial growth factor

Yin ZH, Liu XY, Huang RL, Ren SP. Expression of TNF-α and VEGF in the esophagus of portal hypertensive rats. *World J Gastroenterol* 2005; 11(8): 1232-1236
http://www.wjgnet.com/1007-9327/11/1232.asp

INTRODUCTION

It has been known that portal hypertension is responsible for the opening and dilatation of relative collateral vessels, which can lead to the development of varices at various locations. Esophageal varices are one of its most common and sometimes lethal complications. The studies on esophageal varices have been going on for more than one century, and have gained great achievements especially in the treatment, but the mechanism of their development remains to be clarified.

The functions of humoral substances in portal hypertension had been studied for a long time; however, most of the research was on their changes in the circulation. Recent studies suggested that the changes of humoral substances in portal hypertensive esophagus may be responsible for the development and rupture of esophageal varices[1-4].

Tumor necrosis factor-alpha (TNF-α), a 17 ku mononuclear-derived cytotoxic protein, plays an important role in the pathogenesis of multiple diseases[5-8]. The evidences indicate that the increased production of TNF-α has been implicated in the vasodilatation associated with portal hypertension, which mainly mediated through an increased release of nitric oxide[9-12]. And further studies showed that TNF-α may activate not only the nitric oxide

synthase (NOS) gene but also the ET-1 gene[13-16]. Furthermore, recent studies suggested that the overexpression of NOS and ET-1 in portal hypertensive esophagus may be responsible for the development and rupture of esophageal varices[1-3], but the expression and function of TNF-α in portal hypertensive esophagus remain unclear.

Vascular endothelial growth factor (VEGF), termed on its ability to promote growth of vascular endothelial cells, is a glycoprotein that selectively induces endothelial proliferation, angiogenesis, and capillary hyperpermeability, and is known as a key regulator of blood vessel growth[17,18]. Several studies showed that the VEGF gene is expressed in a wide variety of normal animals and human tissue[19,20], and it also plays an important role in some pathological conditions, which related to vessel changes[21-25]. Though the serum VEGF levels in cirrhotic patients was significantly lower than that in the control[26-28], the expression of VEGF in portal hypertensive gastric mucosa, whether in patients or in animal models, had significantly increased[29,30]. As to esophageal varices, another complication of portal hypertension, Genesca *et al*[27] observed that the serum VEGF levels in cirrhotic patients without gastroesophageal varices was higher than that in patients with them, but how it is expressed in portal hypertensive esophagus remains unknown.

Since esophageal varices are characterized by the pathological changes of esophageal submucosal vein, and are also components during the progress of portal hypertension, we hypothesized that TNF and VEGF may be involved in the etiopathology of esophageal varices. So in the present study, we established a rat model of esophageal varices by a two-stage ligation of portal vein plus ligation of the left adrenal vein, then investigated the dynamic expression of TNF-α and VEGF in the development of esophageal varices in portal hypertensive rats.

MATERIALS AND METHODS

Preparation of esophageal variceal rat model

Sixty male Sprague-Dawley rats weighing 225-275 g, obtained from the Laboratory Animals Center of Xiangya Medical College, were divided into the model group and the control randomly. Modified from Tanoue's method[31], a two-stage ligation of portal vein plus ligation of the left adrenal vein was performed in the model group. In brief, with the rats under ether anesthesia, the portal vein was isolated after median laparotomy. A ligature was tied by a 3-0 silk around both an 18-gauge hypodermic needle lying alongside the portal vein and the portal vein, and then removal of the needle yielded a partial ligation of the portal vein. Subsequently, both ends of silk were drawn out through the abdominal wall after a round the portal vein, and placed hypodermically in the flank. In addition, the left kidney, adrenal gland, and adrenal veins were exposed, and the left adrenal vein was ligated, but no devascularization was conducted at the circumference of the left renal vein except removal of the retroperitoneal fat around the top of left kidney. Seven days after the operation, the ends of the silk in the flank were pulled simultaneously to make a complete portal ligation.

Thirty rats in model group were divided into three subgroups (M_7, M_{14}, and M_{21}, $n = 10$), which were kiued on the seventh day, the 14th d and the 21 d after the complete portal ligation. The rats in the control group, which underwent a sham operation, were also separated into three subgroups (C_7, C_{14}, and C_{21}, $n = 10$), corresponded to the model group.

The rats fed with rat chow and water ad libitum before and after surgery. All procedures are under the animal protection council.

Measurement of the portal pressure

After the rats were anesthetized with ether and the superior mesenteric vein was exposed. A catheter perfused with heparin saline solution (200 units of heparin diluted in 1 mL of 0.9% saline solution) was inserted through the superior mesenteric vein into the portal vein. The portal pressure was measured from the height of the column of saline within the catheter, with the right atrium as the zero reference.

Tissue preparation

After portal pressure measurement, the rats were killed with a bolus of 0.5 mL potassium chloride via the mesenteric catheter. The lower esophagus (0.5 cm in length from esophagogastric junction) was excised, fixed in 10% buffered formalin, and embedded in paraffin. Serial transverse sections were cut at 4 μm, some stained with hematoxylin and eosin (HE) for pathological study and others for immunohistochemistry.

Immunohistochemical procedure

TNF-α and VEGF were detected by the immunohistochemical SP technique according to the manufacturer's instructions. In TNF-α staining, the antigen enhancement was performed by immersing the slides in boiling 10 mmol/L citric acid buffer (pH 6.0) for 20 min. In VEGF staining, sections were treated with boiling EDTA solution for 20 min. After immersing in 0.3% H_2O_2 in methanol for 10 min and incubating with normal goat serum for 10 min at room temperature, sections were incubated with the primary antibody of either anti-TNFα (goat polyclonal antibody, Santa Cruz, diluted 1∶50) or anti-VEGF antibody (mouse monoclonal antibody, Santa Cruz, diluted 1∶50) at 4 ℃ overnight. Then, sections were incubated with biotinylated second antibody of either anti-mouse or anti-goat IgG for 10 min at room temperature, followed by 10-min incubation in an S-P complex solution. Finally, the peroxidase activity was visualized with 0.4% diaminobenzidine (DAB). Sections were rinsed in 0.01 mol/L phosphate buffer solution (PBS, pH 7.4) between every two steps. We used PBS instead of the primary antibody as negative control.

Morphometric analysis

With the computer software HPIAS-1000, the number of vessels and the total vascular area (diameter >20 μm) in the esophageal submucosa were calculated.

Immunohistochemical expression of TNF-α and VEGF were detected with the corrected optical density (COD) values. Briefly, the optical density of immunoreactive

products in five randomly selected fields of each different esophageal section was measured by an image-based analysis system, and the measurement was standardized by subtracting the background intensity of each section.

Statistical analysis

All data were analyzed using the *SPSS10.0* for *Windows*. The results were expressed as the mean±SD. Mann-Whitney *U* test was used to determine any significance between groups. $P<0.05$ was considered to be significant.

RESULTS

Portal pressure

The mean portal pressure in all three model subgroups (M_7, M_{14}, and M_{21}) was significantly higher than that in the corresponding control subgroups (C_7, C_{14}, and C_{21}) ($P<0.01$). There was no difference in portal pressure between M_{14} and M_{21} ($P>0.05$), and it had significantly decreased in both than in M_7 ($P<0.05$) (Table 1).

Table 1 Portal venous pressure (cmH_2O, $n = 10$) (mean±SD)

Group	7 d	14 d	21 d
Model	23.82±1.83	20.90±3.27	20.68±2.27
Control	11.61±0.86	11.43±1.55	11.87±0.79

Esophageal morphometric analysis

Number of veins in submucosa The number of submucosal veins in the three model subgroups (M_7, M_{14}, and M_{21}) was significantly higher than that in the corresponding control subgroups (C_7, C_{14}, and C_{21}) ($P<0.01$), but there was no difference between model subgroups ($P>0.05$) (Table 2).

Table 2 Number of veins in the esophageal submucosa ($n = 10$) (mean±SD)

Group	7 d	14 d	21 d
Model	9.3±1.6	11.1±0.8	11.7±1.5
Control	5.1±0.8	5.4±1.3	5.2±1.1

Total vascular area in submucosa The total vascular area in the three model subgroups (M_7, M_{14}, and M_{21}) was significantly higher than in the corresponding control subgroups (C_7, C_{14}, and C_{21}) ($P<0.01$). There was no difference in total vascular area between M_{14} and M_{21} ($P>0.05$), and it was significantly higher in both than that in M_7 ($P<0.05$) (Figure 1, Table 3).

Table 3 Total vascular area in the esophageal submucosa (μm^2, $n = 10$) (mean±SD)

Group	7 d	14 d	21 d
Model	78 972.6±3 527.8	107 207.5±4 6461.4	110 241.4±49 262.2
Control	12 993.5±4 994.8	11 862.6±5 423.2	11 973.7±3 968.5

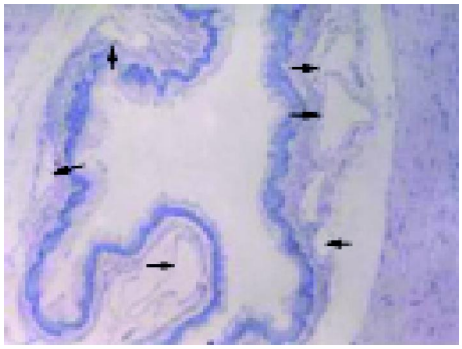

Figure 1 Markedly dilated esophageal submucosal veins (*arrow*) in the lower esophagus in M_{14} group. (H & E, 40).

Expression of TNF-α

Positive TNF-α-immunoreactive products (brown-colored) were mainly observed on the surface of esophageal mucosa (Figure 2). The immunoreactivity for TNF-α in M_{21} group was stronger than that in M_7, M_{14} and the control subgroups ($P<0.01$), but there was no difference between M_7 and M_{14} ($P>0.05$) (Table 4).

Table 4 COD value of TNFα -positive products in the lower esophagus (mean±SD)

Group	7 d	14 d	21 d
Model	1.14±0.38	1.20±0.25	2.23±0.30
Control	1.06±0.27	1.04±0.26	1.13±0.28

Expression of VEGF

The VEGF-immunoreactive brown-colored deposits were mainly located in the endothelia of submucosal vessels, and were also seen in the muscularis mucosa and propria (Figure 2). The immunohistochemistry staining intensity for VEGF in M_{21} group was stronger than that in M_7, M_{14} and the control subgroups ($P<0.01$), but there was no difference between M_7 and M_{14} ($P>0.05$) (Table 5).

Table 5 COD value of VEGF-positive products in the lower esophagus (mean±SD)

Group	7 d	14 d	21 d
Model	0.67±0.35	0.65±0.18	1.65±0.38
Control	0.50±0.24	0.53±0.25	0.56±0.30

DISCUSSION

In our study, a prehepatic portal hypertensive rat model was created, and the rats in model group developed more submucosal vessels than in the control. On the 14th d and the 21 d after the complete portal ligation, the portal pressure and the vascular area were stabilized basically; so we conclude that 7 d after the complete portal ligation should be considered the early stage, whereas 14 and 21 d, the persistent stage, in the development of esophageal varices.

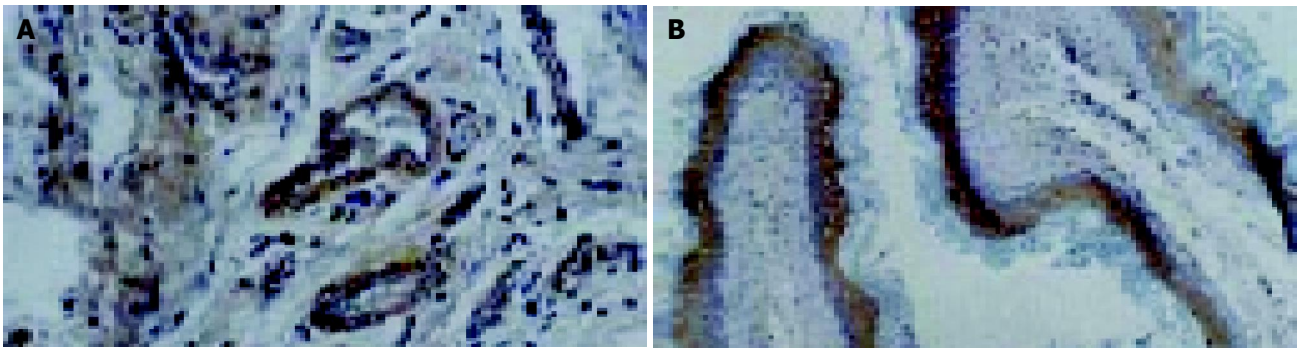

Figure 2 VEGF and TNF-α immunoreactive staining in the lower esophagus of portal hypertensive rats. A: VEGF-immunoreactive staining in M_{21} group, and positive staining mainly located in the endothelia of submucosal vessels of the lower esophagus. (× 200); B: TNF-α immunoreactive staining in M_{21} group, and positive staining mainly located on the surface of the lower esophageal mucosa. (×100).

TNF-α was first identified as an endotoxin-induced serum factor that can cause necrosis of tumors, by Carswell *et al*[31] in 1975, and this multifunctional cytokine can increase vascular permeability and cause both structural and metabolic changes in vascular endothelial cells[33]. Our results showed that overexpression of TNF-α was only detected in M_{21} group, and the positive immunostaining areas were mainly in the surface of esophageal mucosa rather than submucosal vessels. Though other studies suggested that TNF-α can cause the overexpression of NOS and ET-1 in portal hypertensive gastric mucosa, our results showed that the overexpression of NOS and ET-1 was even earlier than TNF-α (data not shown). All findings indicated that TNF-α produced in local esophagus may play an important role at the persistent stage in the development of esophageal varices via other pathway instead of NOS and ET-1 pathway, and the pathogenesis of esophageal varices may be different from the portal hypertensive gastropathy (PHG). On the other hand, as an inflammatory factor, the overexpression of TNF-α in the surface of esophageal mucosa may increase mucosal susceptibility to injury, but its function in local portal hypertensive esophagus remains to be clarified.

VEGF was first described by Senger[34] in 1983 who partially purified a factor secreted by hepatocarcinoma cell lines that increased dye extravasation into the skin of guinea pigs. This peptide was also termed vascular *permeability factor* (VPF) since it can increase interstitial accumulation of intravenously injected dye and stimulate the production of ascites[34,35], or termed *vasculotropin* based on its ability to stimulate endothelial cell migration[36], and now this peptide is referred to as VEGF. VEGF can stimulate endothelial mitosis, migration and increase permeability of endothelial monolayers by binding to the three different receptors[18]. In our study, its expression in M_{21} group was stronger than in other groups, which suggested that the synthesis of VEGF was not an early accident in the development of esophageal varices. Kroll *et al*[36] observed that the activation of VEGF receptor-2 leads to an up-regulation of NOS protein. Though we did not detect the expression of VEGF receptor-2 in our study, our data showed the overexpression of NOS in portal hypertensive esophagus, which seems not to be activated by VEGF produced at local esophagus indicating that the overexpression of NOS was earlier than VEGF (data not shown). The late-stage increased VEGF can probably cause edema of submucosal layer and lead varices losing their surrounding support, consequently resulting in the weakness of the esophageal wall and predisposes varices to the rupture by inducing vascular hyperpermeability.

Interestingly, we also noticed the controversy that whether a dilated submucosal vein plexus resulted from passive opening of pre-existent vascular channels or from the newly formed vessels. In our study, the model rats developed more submucosal vessels than the control. However, we only counted the vessels with diameter over 20 μm; there is always the possibility that the higher vessel number could be attributed to the dilatation of pre-existent veins not counted in the control group due to their small size. Nevertheless, the total vascular area in M_{14} and M_{21} was significantly higher than M_{7}, but there is no significant difference in the number of vessels, which indicated the majority of the dilatation of pre-existent veins in the early stage of esophageal varices. In addition, whether the overexpression of VEGF indicates the formation of new vessels at late stage of esophageal varices, our acute model cannot answer the question yet; however, it is more likely there is the passive opening of pre-existent vascular channels at early stage in the development of esophageal varices, and de novo synthesis of new vascular channels may appear at late stage.

REFERENCES

1 **Tanoue K**, Tarnawski AS, Santos AM, Hanke S, Sugimachi K, Sarfeh IJ. Reduced expression of basic fibroblast growth factor and its receptor mRNAs and proteins in portal hypertensive esophageal mucosa: a mechanism responsible for muscularis mucosae thinning and variceal rupture. *Surgery* 1996; **119**: 424-430

2 **Ohta M**, Pai R, Kawanaka H, Ma T, Sugimachi K, Sarfeh IJ, Tarnawski AS. Expression of endothelin-1, and endothelin A and B receptors in portal hypertensive esophagus of rats. *J Physiol Pharmacol* 2000; **51**: 57-67

3 **Tanoue K**, Ohta M, Tarnawski AS, Wahlstrom KJ, Sugimachi K, Sarfeh IJ. Portal hypertension activates the nitric oxide synthase genes in the esophageal mucosa of rats. *Gastroenterology* 1996; **110**: 549-557

4 **Huang YQ**, Xiao SD, Zhang DZ, Mo JZ. Nitric oxide synthase distribution in esophageal mucosa and hemodynamic changes in rats with cirrhosis. *World J Gastroenterol* 1999; **5**: 213-216

5 **Mitsiades CS**, Poulaki V, Mitsiades N. The role of apoptosis-inducing receptors of the tumor necrosis factor family in thy-

roid cancer. *J Endocrinol* 2003; **178**: 205-216
6 **Vassalli P**. The pathophysiology of tumor necrosis factors. *Annu Rev Immunol* 1992; **10**: 411-452
7 **Feldman AM**, Combes A, Wagner D, Kadakomi T, Kubota T, Li YY, McTiernan C. The role of tumor necrosis factor in the pathophysiology of heart failure. *J Am Coll Cardiol* 2000; **35**: 537-544
8 **Ruiz-del-Arbol L**, Urman J, Fernandez J, Gonzalez M, Navasa M, Monescillo A, Albillos A, Jimenez W, Arroyo V. Systemic, renal, and hepatic hemodynamic derangement in cirrhotic patients with spontaneous bacterial peritonitis. *Hepatology* 2003; **38**: 1210-1218
9 **Mookerjee RP**, Sen S, Davies NA, Hodges SJ, Williams R, Jalan R. Tumour necrosis factor alpha is an important mediator of portal and systemic haemodynamic derangements in alcoholic hepatitis. *Gut* 2003; **52**: 1182-1187
10 **Munoz J**, Albillos A, Perez-Paramo M, Rossi I, Alvarez-Mon M. Factors mediating the hemodynamic effects of tumor necrosis factor-alpha in portal hypertensive rats. *Am J Physiol* 1999; **276**: G687–G693
11 **Lopez-Talavera JC**, Cadelina G, Olchowski J, Merrill W, Groszmann RJ. Thalidomide inhibits tumor necrosis factor alpha, decreases nitric oxide synthesis, and ameliorates the hyperdynamic circulatory syndrome in portal-hypertensive rats. *Hepatology* 1996; **23**: 1616-1621
12 **Fernando B**, Marley R, Holt S, Anand R, Harry D, Sanderson P, Smith R, Hamilton G, Moore K. *N*-acetylcysteine prevents development of the hyperdynamic circulation in the portal hypertensive rat. *Hepatology* 1998; **28**: 689-694
13 **Marsden PA**, Brenner BM. Transcriptional regulation of the endothelin-1 gene by TNF-alpha. *Am J Physiol* 1992; **262**: C854-C861
14 **Ohta M**, Tarnawski AS, Itani R, Pai R, Tomikawa M, Sugimachi K, Sarfeh IJ. Tumor necrosis factor alpha regulates nitric oxide synthase expression in portal hypertensive gastric mucosa of rats. *Hepatology* 1998; **27**: 906-913
15 **Kaviani A**, Ohta M, Itani R, Sander F, Tarnawski AS, Sarfeh IJ. Tumor necrosis factor-alpha regulates inducible nitric oxide synthase gene expression in the portal hypertensive gastric mucosa of the rat. *J Gastrointest Surg* 1997; **1**: 371-376
16 **Kawanaka H**, Jones MK, Szabo IL, Baatar D, Pai R, Tsugawa K, Sugimachi K, Sarfeh IJ, Tarnawski AS. Activation of eNOS in rat portal hypertensive gastric mucosa is mediated by TNF-alpha via the PI 3-kinase-Akt signaling pathway. *Hepatology* 2002; **35**: 393-402
17 **Ferrara N**, Henzel WJ. Pituitary follicular cells secrete a novel heparin-binding growth factor specific for vascular endothelial cells. *Biochem Biophys Res Commun* 1989; **161**: 851-858
18 **Ferrara N**, Gerber HP, LeCouter J. The biology of VEGF and its receptors. *Nat Med* 2003; **9**: 669-676
19 **Berse B**, Brown LF, Van de Water L, Dvorak HF, Senger DR. Vascular permeability factor (vascular endothelial growth factor) gene is expressed differentially in normal tissues, macrophages, and tumors. *Mol Biol Cell* 1992; **3**: 211-220
20 **Monacci WT**, Merrill MJ, Oldfield EH. Expression of vascular permeability factor/vascular endothelial growth factor in normal rat tissues. *Am J Physiol* 1993; **264**: C995- C1002
21 **Brown LF**, Yeo KT, Berse B, Yeo TK, Senger DR, Dvorak HF, van de Water L. Expression of vascular permeability factor (vascular endothelial growth factor) by epidermal keratinocytes during wound healing. *J Exp Med* 1992; **176**: 1375-1379
22 **Pierce EA**, Avery RL, Foley ED, Aiello LP, Smith LE. Vascular endothelial growth factor/vascular permeability factor expression in a mouse model of retinal neovascularization. *Proc Natl Acad Sci USA* 1995; **92**: 905-909
23 **Hashimoto E**, Ogita T, Nakaoka T, Matsuoka R, Takao A, Kira Y. Rapid induction of vascular endothelial growth factor expression by transient ischemia in rat heart. *Am J Physiol* 1994; **267**: H1948-H1954
24 Banai S, Shweiki D, Pinson A, Chandra M, Lazarovici G, Keshet E. Upregulation of vascular endothelial growth factor expression induced by myocardial ischaemia: implications for coronary angiogenesis. *Cardiovasc Res* 1994; **28**: 1176 - 1179
25 **Suzuki K**, Hayashi N, Miyamoto Y, Yamamoto M, Ohkawa K, Ito Y, Sasaki Y, Yamaguchi Y, Nakase H, Noda K, Enomoto N, Arai K, Yamada Y, Yoshihara H, Tujimura T, Kawano K, Yoshikawa K, Kamada T. Expression of vascular permeability factor/vascular endothelial growth factor in human hepatocellular carcinoma. *Cancer Res* 1996; **56**: 3004-3009
26 **Akiyoshi F**, Sata M, Suzuki H, Uchimura Y, Mitsuyama K, Matsuo K, Tanikawa K. Serum vascular endothelial growth factor levels in various liver diseases. *Dig Dis Sci* 1998; **43**: 41-45
27 **Genesca J**, Gonzalez A, Mujal A, Cereto F, Segura R. Vascular endothelial growth factor levels in liver cirrhosis. *Dig Dis Sci* 1999; **44**: 1261-1262
28 **Tsugawa K**, Hashizume M, Migou S, Kishihara F, Kawanaka H, Tomikawa M, Sugimachi K. Role of vascular endothelial growth factor in portal hypertensive gastropathy. *Digestion* 2000; **61**: 98-106
29 **Tsugawa K**, Hashizume M, Tomikawa M, Migou S, Kawanaka H, Shiraishi S, Sueishi K, Sugimachi K. Immunohistochemical localization of vascular endothelial growth factor in the rat portal hypertensive gastropathy. *J Gastroenterol Hepatol* 2001; **16**: 429-437
30 **Tanoue K**, Kitano S, Hashizume M, Wada H, Sugimachi K. A rat model of esophageal varices. *Hepatology* 1991; **13**: 353-358
31 **Carswell EA**, Old LJ, Kassel RL, Green S, Fiore N, Williamson B. An endotoxin-induced serum factor that causes necrosis of tumors. *Proc Natl Acad Sci USA* 1975; **72**: 3666-3670
32 **Stephens KE**, Ishizaka A, Larrick JW, Raffin TA. Tumor necrosis factor causes increased pulmonary permeability and edema. Comparison to septic acute lung injury. *Am Rev Respir Dis* 1988; **137**: 1364-1370
33 **Senger DR**, Galli SJ, Dvorak AM, Perruzzi CA, Harvey VS, Dvorak HF. Tumor cells secrete a vascular permeability factor that promotes accumulation of ascites fluid. *Science* 1983; **219**: 983-985
34 **Senger DR**, Connolly DT, Van de Water L, Feder J, Dvorak HF. Purification and NH2-terminal amino acid sequence of guinea pig tumor-secreted vascular permeability factor. *Cancer Res* 1990; **50**: 1774-1778
35 **Favard C**, Moukadiri H, Dorey C, Praloran V, Plouet J. Purification and biological properties of vasculotropin, a new angiogenic cytokine. *Biol Cell* 1991; **73**: 1-6
36 **Kroll J**, Waltenberger J. VEGF-A induces expression of eNOS and iNOS in endothelial cells via VEGF receptor-2 (KDR). *Biochem Biophys Res Commun* 1998; **252**: 743-746

PO Box 2345, Beijing 100023, China
www.wjgnet.com
wjg@wjgnet.com

ELSEVIER

World J Gastroenterol 2005;11(8):1237-1240
World Journal of Gastroenterology ISSN 1007-9327

• *BRIEF REPORTS* •

Expression of p57^{kip2} and its relationship with clinicopathology, PCNA and p53 in primary hepatocellular carcinoma

Ke-Jun Nan, Hui Guo, Zhi-Ping Ruan, Zhao Jing, Shaan-Xi Liu

Ke-Jun Nan, Hui Guo, Zhi-Ping Ruan, Zhao Jing, Department of Oncology, First Hospital of Xi'an Jiaotong University, Xi'an 710061, Shaanxi Province, China
Shaan-Xi Liu, Department of Hematology, First Hospital of Xi'an Jiaotong University, Xi'an 710061, Shaanxi Province, China
Correspondence to: Ke-Jun Nan, Department of Oncology, First Hospital of Xi'an Jiaotong University, Xi'an 710061, Shaanxi Province, China. guoguo79_79@163.com
Fax: +86-29-85324086
Received: 2004-02-14 Accepted: 2004-03-02

Abstract

AIM: To investigate the expression of p57^{kip2} and its relationship with clinicopathology, PCNA and p53 in primary hepatocellular carcinoma (HCC).

METHODS: Expression of p57^{kip2}, PCNA and p53 in tumor tissues from 32 patients with HCC and 10 liver tissues of normal persons was detected with Elivision immunohistochemical technique.

RESULTS: The p57^{kip2} protein positive-expression rate in HCC was 56.25%, lower than that in normal tissues (100%, P<0.05). The reduced expression of p57^{kip2} protein correlated significantly with moderate or low differentiation of tumor cells (P = 0.007 <0.05), high clinical stage (P = 0.041 <0.05) and poor prognosis (P = 0.036 <0.05), but did not correlate significantly with metastasis, tumor size, level of AFP and age (P>0.05). The PCNA positive-expression rate was 56.25%, which was correlated significantly with the expression of p57^{kip2} (P = 0.025<0.05). The p53 positive-expression rate was 46.88%, which was not correlated significantly with the expression of p57^{kip2} (P>0.05).

CONCLUSION: There is a marked loss or absence of p57^{kip2} expression and high expression of PCNA in HCC, which are involved in carcinogenesis and development of HCC. The p57^{kip2} and p53 may induce apoptosis via different mechanisms.

Key words: p57^{kip2}; PCNA; p53; Hepatocellular carcinoma

Nan KJ, Guo H, Ruan ZP, Jing Z, Liu SX. Expression of p57^{kip2} and its relationship with clinicopathology, PCNA and p53 in primary hepatocellular carcinoma. *World J Gastroenterol* 2005; 11(8): 1237-1240
http://www.wjgnet.com/1007-9327/11/1237.asp

INTRODUCTION

The damage of cell cycle is the crucial point in carcinogenesis and development of HCC. Orderly progression of cell cycle is controlled by the families of cyclins and cyclin-dependent kinas (CDKs), which are restrictively counterbalanced by CDK inhibitors (CDKIs). The p57^{kip2} was found by Matsuoka and located at 11p11.5, which is included in the CIP-KIP families. The structure of p57^{kip2} has partial homology with p21 and p27, which harbors homologous CDK binding domains or function of cyclin-CDK complexes and makes cell cycle to arrest in G_1 phase[1]. The p57^{kip2} has the function of a tumor suppressor gene. The expression of PCNA has an intimate relationship with cell proliferation[2]. The p53 is an important gene to induce cell apoptosis and may have osculation with p57^{kip2} in function[3]. In this study, the expression of p57^{kip2}, PCNA protein and p53 in tissues of HCC as detected with immunohistochemical Elivision technique to investigate the roles of p57^{kip2}, PCNA and p53 in the genesis and progression of HCC.

MATERIALS AND METHODS

Materials

Thirty-two specimens of HCC and 10 normal liver tissues as controls were collected from surgical resections performed in the First Hospital of Xi'an Jiaotong University from 2000 to 2002. Of the patients, 26 (81.25%) were males and 6 (18.75%) were females and the mean age was 49.19±12.32 years (range, 29-77 years). All the patients were confirmed to have HCC by the clinicopathological diagnosis. According to the histological grading, three were at grade I, 14 were at grade II, 11 were at grade III and 4 were at grade IV. All the specimens of HCC and normal liver tissues were fixed in 100 mL/L buffered formalin, processed routinely, embedded in paraffin and cut into 4-μm-thick sections, which were placed on poly-L-lysine-coated slides for immunohistochemistry. In each case, all available hematoxylin and eosin-stained sections were reviewed, and representative blocks were chosen for further studies. Anti-human p57^{kip2} monoclonal antibody (57P06), anti-human PCNA monoclonal antibody (PC10), anti-human p53 monoclonal antibody (MAB-0226) and Elivision kit were supplied by Maixin-Bio Co., Fuzhou, China.

Immunohistochemical study (Elivision)

Slides were deparaffinized in xylene twice for 10 min, dehydrated through graded ethanol to distilled water for 5 min, respectively. Endogenous peroxidase activity was blocked with 3% hydrogen peroxidase for 20 min. Slides

were heated in 0.01 mol/L citrate buffer (pH 6.0) at a high temperature and high pressure for 7 min for antigen retrieval. After cooled to room temperature, the sections were incubated for 20 min in a blocking solution containing 10% normal goat serum in PBS [0.01 mol/L phosphate (pH 7.4)] and incubated with anti-human $p57^{kip2}$ monoclonal antibody (work quality) in a humidified chamber at 4 ℃ overnight. While the sections with anti-human PCNA monoclonal antibody and anti-human p53 monoclonal antibody (1:50, Santa Cruz Biotechnology, CA, USA) were incubated for 1 h at 37 ℃, incubated for 40 min with goat anti-rabbit IgG conjugated to horseradish peroxidase (Santa Cruz Biotechnology). The 3,3'-diaminobenzidine was used as chromogen for 3 min. Slides were counterstained for 2 min with hematoxylin solution and differentiated for 3 s with hydrochloric acid alcohol, then dehydrated and cover slipped. Normal liver tissue was regarded as a positive control, whereas the primary antibody was replaced by PBS as a negative control.

Value of score

The cells with brown-yellow granules in the nuclei or cytoplasm were taken as $p57^{kip2}$ positive cells, and the mean of 10 visual fields on each slide was counted. The extent of positivity was graded as follows: 0, <10%; 1, 10-25%; 2, 25-50%; 3, 50-75%; 4, >75% of the hepatocytes. The intensity was evaluated as follows: 0, negative; 1, weak; 2, moderate; 3, strong. The score was obtained by multiplying the extent and the intensity of positivity. The slides were distinguished as negative (-), positive (+), strong positive (++) and strongest positive (+++) when the score was <2, between 3 and 5, 6 and 8, and >9, respectively. The cells with brown-yellow granules in the nuclei were taken as PCNA and p53 positive cells. The slides were distinguished as negative (-), and positive (+) when the count of positive cells was less than 50% and over 50% for PCNA and p53, respectively.

Statistical analysis

Fisher's exact test and Spearman correlation (SPSS 11.0 for Windows) were adopted to assess the association between $p57^{kip2}$ expression and clinicopathology, PCNA and p53. $P<0.05$ was considered statistically significant.

RESULTS

$p57^{kip2}$ expression in HCC and normal tissues

The $p57^{kip2}$ protein was located in the nuclei or cytoplasm of normal liver cells and the HCC cells with brown-yellow granules (Figures 1, 2). The $p57^{kip2}$ protein positive-expression rate in tumor tissues of HCC was 56.25% (18/32), which was lower than that (100.0%) in the normal liver tissues ($P<0.05$).

Relationship between $p57^{kip2}$ and clinicopathology

The $p57^{kip2}$ protein positive-expression rate in moderate or poorly differentiated group was 20.0%, being lower than that (88.24%) in well-differentiated group ($P = 0.007$). In a word, the lower the cancer cells were differentiated, the higher the rate of $p57^{kip2}$ protein was reduced. In addition, the reduced $p57^{kip2}$ expression showed a significant relationship with higher clinical stages (stages III and IV, $P = 0.041$) and poor prognosis (<1 year, $P = 0.036$). However, no relationship was found between $p57^{kip2}$ and age, level of AFP, tumor size and local metastasis (Table 1).

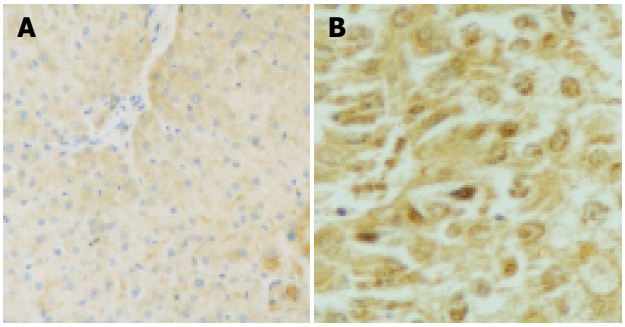

Figure 1 Positive $p57^{kip2}$ expression in normal hepatocytes and well-differentiated carcinomas. A: Positive $p57^{kip2}$ expression in normal hepatocytes (20×); B: Positive $p57^{kip2}$ expression in well-differentiated carcinomas (40×).

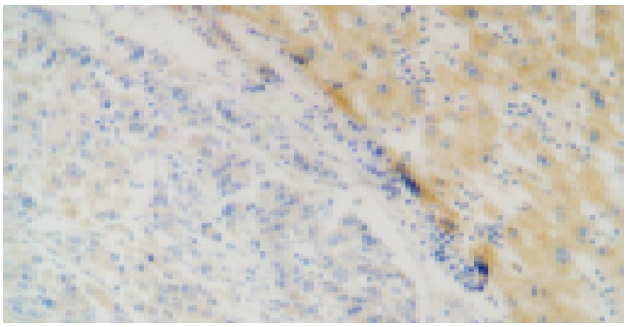

Figure 2 Negative $p57^{kip2}$ expression in moderately or poorly differentiated carcinomas and positive expression of $p57^{kip2}$ in adjacent liver tissues (20×).

Table 1 Relationship between $p57^{kip2}$ and pathological indexes

Characters	$p57^{kip2}$ protein expression				Positive rate (%)
	–	+	++	+++	
Histological grade					
I-II	2	4	5	6	88.24[a]
III-IV	12	0	3	0	20.00[a]
Clinical stage					
I-II	5	2	6	5	72.22[c]
III-IV	9	2	2	1	35.71[c]
Age (yr)					
<45	2	2	5	3	83.33
⩾45	12	2	3	3	40.00
AFP (μg/L)					
<400	7	3	5	6	66.67
⩾400	7	1	3	0	36.36
Tumor size					
<5 cm	4	3	3	3	69.23
⩾5 cm	10	1	5	3	47.37
Local metastasis					
Yes	7	2	4	4	58.82
No	7	2	4	2	53.33
Survival time					
<1 year	11	0	4	3	38.89[e]
⩾1 year	3	4	4	3	78.57[e]

[a]$P<0.05$ *vs* poorly differentiated group; [c]$P<0.05$ *vs* high clinical stages; [e]$P<0.05$ *vs* poor prognosis.

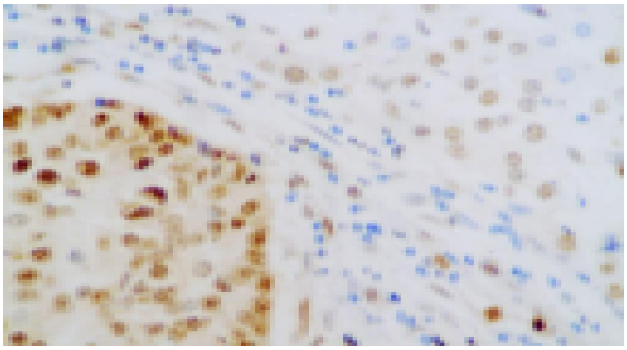

Figure 3 Highly positive expression of PCNA in tumor tissue of HCC and low expression of PCNA in adjacent liver tissues (40×).

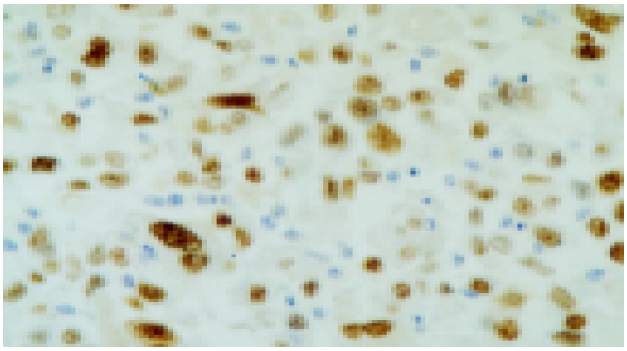

Figure 4 Positive expression of p53 in HCC tissue (40×).

Relationship of p57^{kip2}, PCNA and p53

PCNA was located in nuclei of HCC cells with brown-yellow granules (Figure 3). The p53 was located in nuclei of positive HCC cells with brown-yellow granules (Figure 4).

The results suggested that the PCNA positive-expression rate was higher in HCC tissue (56.25%) than that in the normal liver tissues (30%) and the p53 positive-expression rate was lower in HCC tissue (46.88%) compared with that in the normal liver tissues (80%, $P<0.05$).

The p57^{kip} protein positive-expression rate in tumor tissues of PCNA positive-expression group was 38.39%, and was 78.39% in tumor tissues of PCNA negative-expression group. There was a significant relationship between the two groups ($r = 0.397$, $P = 0.025$). The p57^{kip2} protein positive-expression rate in tumor tissues of p53 positive-expression group (66.67%) was higher than that in tumor tissues of p53 negative-expression group (47.03%). But there was no significant relationship between the two groups ($r = 0.197$, $P = 0.279$) (Table 2).

Table 2 Relationship between p57^{kip2}, PCNA and p53

Characters	p57^{kip2} Protein expression			
	-	+	++	+++
PCNA				
–	3	3	3	5
+	11	1	5	1
p53				
–	9	1	5	2
+	5	3	3	4

DISCUSSION

The G_1-phase regulation of cell cycle was a complex process in which multiple factors took part, and abnormality of cell cycle regulation was significantly correlated with the genesis and progression of tumors[4].

The p57^{kip2} gene is located on chromosome 11p15.5 and p57^{kip2} protein is a cell cycle inhibitor with a molecular weight of 57 kDa, which is included in the CIP/KIP family and similar to p21 and p27 protein in functions. The p57^{kip2} contains three structural domains: N-terminal region bearing homology with CDK-inhibitors p21 (CIP1) and p27 (KIP1), a central proline-rich domain, and a C-terminal region (QT domain) shared with p27^{KIP1}. The proline-rich domain included clusters of alternating proline-alanine residues (PAPA-repeats) that were hypothesized to mediate specific protein-protein interactions required for the p57^{kip2} function[5,6]. The tumor suppressor mechanism of p57^{kip2} protein might be integrated with cyclin-CDK complexes including E-CDK2, D2-CDK2 and A-CDK2, making cell cycle to arrest in the G_1 phase[7]. In many CDKIs, only p57^{kip2} was essential for the embryo formation and played an important role in proliferation, movement, transfiguration, differentiation and other complicated processes[8]. The mice of p57^{kip2} knockout developed a series of abnormalities, high rate of tumor occurrence and high mortality, suggesting that p57^{kip2} might participate in cell proliferation and differentiation[9].

Paternal alleles of p57^{kip2} were imprinted, maternal alleles of p57^{kip2} were normally expressed and loss of imprinting and imprinting mistakes of p57^{kip2} led to decreased level of gene expression leading to carcinogenesis and development of tumors[10]. It is the first gene that is regulated through imprinting. As a tumor suppressor and regulator of growth, this expression mode of p57^{kip2} increased the risk of abnormalities and cancers[11]. Several types of childhood tumors, including Wilms' tumor, adrenocortical carcinoma, rhabdomyosarcoma and hepatocellular carcinoma, display a specific loss of maternal 11p15 alleles, suggesting that genomic imprinting plays an important part[8]. A few studies about p57^{kip2} protein expression in human esophageal cancer, gastric cancer, colorectal carcinoma, epithelial ovarian tumor, breast cancer, neoplastic thyroid tissues and extra hepatic bile duct carcinoma and intrahepatic cholangiocellular carcinoma have been reported[12-19], but the relationship between p57^{kip2} protein expression and HCC was less reported. In this study, we found that the p57^{kip2} protein positive-expression rate in HCC tissues was significantly lower than that in normal liver tissues, suggesting that loss of p57^{kip2} expression correlated with malignant transformation of hepatocytes. The high loss rate of p57^{kip2} was also found by Nakai[20] and the occurrence rate of tumor was increased after p57^{kip2} gene was knocked out. There was a significant correlation between the p57^{kip2} positive-expression and histological grade of HCC ($P = 0.007$), the poorer the cancer cells were differentiated, the lower the expression of p57^{kip2} in tumor tissues was. There was a significant correlation between well-differentiated and poorly differentiated HCC ($P<0.05$), showing that the inactivation of p57^{kip2} could occur at early stage of hepatocytes transformation, leading to decrease of p57^{kip2} protein expression, and p57^{kip2} negative-regulation function and resulting in hepatocytes over-proliferation. It suggested that

expression of $p57^{kip2}$ was negatively correlated with clinical stage and that $p57^{kip2}$ protein negative-expression may indicate a poor prognosis. In our statistical analysis, we found that there was a significant relationship between $p57^{kip2}$ protein expression and prognosis. The $p57^{kip2}$ protein was more highly expressed in tumors with a good prognosis, compared with tumors with a poor prognosis.

PCNA was an assistant factor of DNA synthetase delta, it took part in DNA biological synthesis and regulated cell cycle and cell proliferation by a tetramer with cyclin, CDK and p21. The amount of PCNA could reflect the proliferating activity of cancer cells, and could be regarded as the index of proliferation[21]. Over-expression of PCNA was associated with a variety of tumors of the digestive system. Our results showed that the PCNA positive-expression rate was higher in HCC tissue than that in normal liver tissues and the $p57^{kip2}$ protein positive-expression rate was lower in PCNA positive tissues than that in PCNA negative tissues ($P<0.05$), suggesting that PCNA had a high positive-expression in HCC and cell proliferating activity was high in tumor tissues with negative or reduced expression of $p57^{kip2}$ protein. It was proved that $p57^{kip2}$ could interact with PCNA, and $p57^{kip2}$ could block by DNA replication via suppressing the function of PCNA as a tumor suppressor.

It has been found that p53 is an important apoptosis gene and its mutation induces cell-cycle dysregulation. Fifty percent of human tumors with p53 mutation had abnormality of DNA check. The HCCs with p53 mutation had a high malignant potential, and p53 mutation in the primary lesion could be used as an indicator for the biological behavior of recurrent HCCs, and as an independent prognostic factor affecting survival after recurrence, but DNA check had no p53-dependent mechanism. Our results showed a positive relationship between $p57^{kip2}$ and p53, but without statistical significance. Hong stimulated hepatocytes with low-dose thioacetamide (TA) and found $p57^{kip2}$ increased to a peak level at d 2 but p53 increased to a peak level at d 3, showing that $p57^{kip2}$ arrested cell cycle in the S phase but p53 arrested cells in G1 phase. It has been proved that p53 expression is reduced in HCC, but $p57^{kip2}$ can directly combine with CDK-cyclins via non-p53-dependent mechanism to suppress CDKs and differs from p21 which blocks cell cycle via p53-p21-CDKs-cyclins path.

In summary, the reduced expression of $p57^{kip2}$ and the high expression of PCNA are involved in carcinogenesis and development of HCC. The $p57^{kip2}$ and p53 can induce apoptosis by different mechanisms.

REFERENCES

1 **Matsuoka S**, Edwards MC, Bai C, Parker S, Zhang P, Baldini A, Harper JW, Elledge SJ. p57KIP2, a structurally distinct member of the $p21^{CIP1}$ Cdk inhibitor family, is a candidate tumor suppressor gene. *Genes Dev* 1995; **9**: 650-662

2 **Yue H**, Na YL, Feng XL, Ma SR, Song FL, Yang B. Expression of p57kip2, Rb protein and PCNA and their relationships with clinicopathology in human pancreatic cancer. *World J Gastroenterol* 2003; **9**: 377–380

3 **Zhu MH**, Ni CR, Zhu Z, Li FM, Zhang SM. Determination of expression of eight p53-related genes in hepatocellular carcinoma with tissue microarrays. *Aizheng* 2003; **22**: 680-685

4 **Lee MH**, Yang HY. Negative regulators of cyclin-dependent kinases and their roles in cancers. *Cell Mol Life Sci* 2001; **58**: 1907-1922

5 **Li Y**, Millikan RC, Newman B, Conway K, Tse CK, Liu ET. P57 (KIP2) polymorphisms and breast cancer risk. *Hum Genet* 1999; **104**: 83–88

6 **Lee MH**, Reynisdottir I, Massague J. Cloning of p57 KIP2, a cyclin-dependent kinase inhibitor with unique domain structure and tissue distribution. *Genes Dev* 1995; **9**: 639–649

7 **Leibovitch MP,** Kannengiesser C, Leibovitch SA. Signal-induced ubiquitination of p57(Kip2) is independent of the C-terminal consensus Cdk phosphorylation site. *FEBS Lett* 2003; **543**: 125-128

8 **Hatada I,** Inazawa J, Abe T, Nakayama M, Kaneko Y, Jinno Y, Niikawa N, Ohashi H, Fukushima Y, Iida K, Yutani C, Takahashi S, Chiba Y, Ohishi S, Mukai T. Genomic imprinting of human p57KIP2 and its reduced expression in Wilms' tumors. *Hum Mol Genet* 1996; **5**: 783–788

9 **Zhang P**, Liegeois NJ, Wong C, Finegold M, Hou H, Thompson JC, Silverman A, Harper JW, DePinho RA, Elledge SJ. Altered cell differentiation and proliferation in mice lacking $p57^{KIP2}$ indicates a role in Beckwith–Wiedemann syndrome. *Nature* 1997; **387**: 151-158

10 **Yokoo T**, Toyoshima H, Miura M, Wang Y, Iida KT, Suzuki H, Sone H, Shimano H, Gotoda T, Nishimori S, Tanaka K, Yamada N. p57Kip2 regulates actin dynamics by binding and translocating LIM-kinase 1 to the nucleus. *J Biol Chem* 2003; **278**: 52919-52923

11 **Yan Y**, Frisen J, Lee MH, Massague J, Barbacid M. Ablation of the CDK inhibitor p57Kip2 results in increased apoptosis and delayed differentiation during mouse development. *Genes Dev* 1997; **11**: 973-983

12 **Matsumoto M**, Furihata M, Ohtsuki Y, Sasaguri S, Ogoshi S. Immunohistochemical characterization of p57KIP2 expression in human esophageal squamous cell carcinoma. *Anticancer Res* 2000; **20**: 1947-1952

13 **Liang B**, Wang S, Yang X, Ye Y, Yu Y, Cui Z. Expressions of cyclin E, cyclin dependent kinase 2 and p57 (KIP2) in human gastric cancer. *Chin Med J (Engl)* 2003; **116**: 20-23

14 **Yaswen P**, Stampfer MR. Molecular changes accompanying senescence and immortalization of cultured human mammary epithelial cells. *Int J Biochem Cell Biol* 2002; **34**: 1382–1394

15 **Noura S**, Yamamoto H, Sekimoto M, Takemasa I, Miyake Y, Ikenaga M, Matsuura N, Monden M. Expression of second class of KIP protein p57KIP2 in human colorectal carcinoma. *Int J Oncol* 2001; **19**: 39–47

16 **Rosenberg E**, Demopoulos RI, Zeleniuch-Jacquotte A, Yee H, Sorich J, Speyer JL, Newcomb EW. Expression of cell cycle regulators p57(KIP2), cyclin D1, and cyclin E in epithelial ovarian tumors and survival. *Hum Pathol* 2001; **32**: 808-813

17 **Ito Y**, Yoshida H, Nakano K, Kobayashi K, Yokozawa T, Hirai K, Matsuzuka F, Matsuura N, Kuma K, Miyauchi A. Expression of p57/Kip2 protein in normal and neoplastic thyroid tissues. *Int J Mol Med* 2002; **9**: 373–376

18 **Schwarze SR**, Shi Y, Fu VX, Watson PA, Jarrard DF. Role of cyclin-dependent kinase inhibitors in the growth arrest at senescence in human prostate epithelial and uroepithelial cells. *Oncogene* 2001; **20**: 8184-8192

19 **Ito Y**, Takeda T, Sasaki Y, Sakon M, Yamada T, Ishiguro S, Imaoka S, Tsujimoto M, Monden M, Matsuura N. Expression of p57/Kip2 protein in extrahepatic bile duct carcinoma and intrahepatic cholangiocellular carcinoma. *Liver* 2002; **22**: 145–149

20 **Nakai S**, Masaki T, Shiratori Y, Ohgi T, Morishita A, Kurokohchi K, Watanabe S, Kuriyama S. Expression of p57(KIP2) in hepatocellular carcinoma: relationship between tumor differentiation and patient survival. *Int J Oncol* 2002; **20**: 769–775

21 **Saftoiu A**, Ciurea T, Georgescu C, Banita M, Comanescu V, Rogoveanu I, Gorunescu F, Georgescu I. Immunohistochemical assessment of proliferating cell nuclear antigen in primary hepatocellular carcinoma and dysplastic nodules. *J Cell Mol Med* 2003; **7**: 436–446

PO Box 2345, Beijing 100023, China
www.wjgnet.com
wjg@wjgnet.com

ELSEVIER

World J Gastroenterol 2005;11(8):1241-1244
World Journal of Gastroenterology ISSN 1007-9327

• *CASE REPORT* •

Liver cirrhosis as a consequence of iron overload caused by hereditary nonspherocytic hemolytic anemia

Philip Hilgard, Guido Gerken

Philip Hilgard, Guido Gerken, Department of Gastroenterology and Hepatology, University Hospital Essen, Essen, Germany
Correspondence to: Dr. Philip Hilgard, Universitätsklinikum Essen, Klinik für Gastroenterologie and Hepatologie, Hufelandstraße 55, 45122 Essen, Germany. philip.hilgard@uni-essen.de
Telephone: +49-201-723-2390 Fax: +49-201-723-5971
Received: 2004-05-10 Accepted: 2004-08-12

Abstract

Nonspherocytic hereditary anemias are occasionally accompanied by significant iron overload but the significance for the development of chronic liver disease is not clear. We described two cases of patients with chronic liver disease and severe iron overload due to chronic hereditary hemolysis. Both patients have had signs of liver cirrhosis and severe hemolysis since childhood. A hereditary pyruvate kinase deficiency (PKD) was discovered as the underlying reason for the hemolysis. Sequencing of the pyruvate kinase gene showed a mutation within exon 11. Liver histology in both patients revealed cirrhosis and a severe iron overload but primary hemochromatosis was excluded by HFE-gene analysis. An iron reduction therapy with desferrioxamine led to significant decrease of serum ferritin and sustained clinical improvement. PKD-induced hemolysis may cause severe iron overload even in the absence of HFE-genotype abnormalities. This secondary iron overload can lead to chronic liver disease and cirrhosis. Therefore, the iron metabolism of PKD patients has to be closely monitored and iron overload should be consequently treated.

Key words: Hemochromatosis; Pyruvate kinase deficiency; Liver cirrhosis; Iron overload; Desferrioxamine

Hilgard P, Gerken G. Liver cirrhosis as a consequence of iron overload caused by hereditary nonspherocytic hemolytic anemia. *World J Gastroenterol* 2005; 11(8): 1241-1244
http://www.wjgnet.com/1007-9327/11/1241.asp

INTRODUCTION

Hereditary hemolytic anemia is classified as spherocytic anemia and nonspherocytic anemia. Spherocytic hemolytic anemia is based on an impairment of the erythrocyte membrane or mutations of integral compounds or the hemoglobin molecule. Nonspherocytic hemolytic anemia is caused by a functional defect of particular enzymes of the erythrocellular glucose metabolism, namely the glycolytic cascade. Since, glycolysis is the only way for mature erythrocytes to generate ATP, inhibition of this pathway results in disturbance of the erythrocellular energy metabolism and, ultimately, hemolysis[1].

Here, we report two cases of patients with severe, nonspherocytic hemolytic anemia caused by hereditary pyruvate kinase deficiency (PKD). The chronic hemolysis led to secondary hepatocellular iron overload and subsequently liver cirrhosis. These results suggest a consequent control of the iron metabolism and the liver function in patients with PK deficiency and, if necessary, an iron reducing therapy.

CASE REPORT

Case 1

A 56-year-old male patient (patient 1) with severe abdominal pain, fever, nausea and emesis was admitted to the emergency room. In addition, the patient had stigmata of chronic liver disease such as icterus, spider naevi, dilated abdominal subcutaneous veins and ascites. The clinical picture and an abdominal ultrasound examination suggested advanced liver cirrhosis and acute cholecystitis in the presence of gallstones. Laboratory parameters at admission confirmed severe inflammation. A significant iron overload, as indicated by high serum iron and ferritin and siderinuria, was found. Bilirubin was high and the liver function parameters (cholinesterase, prothrombin time and albumin) were significantly altered. However, further differentiation of the elevated bilirubin revealed that the major proportion was indirect bilirubin (>70%). In conjunction with an elevated lactat-dehydrogenase (LDH 450 U/L) this was suggestive for hemolysis. Concomitantly, the patient had anemia (hemoglobin 9.4 mg/dL) with significantly stimulated erythropoiesis, as demonstrated by the elevated reticulocyte count of 21% (Table 1).

The patient reported the first onset of icterus at the age of 12. At that time the spleen was removed and he had significant and long-term improvement of the clinical situation. Importantly, the patient revealed a positive family history with a brother (patient 2) who suffered from chronic hemolysis as well. Therefore, further efforts attempting to clarify the etiology of the hemolytic anemia focused on the hereditary hemolytic syndromes. Normal hemoglobin electrophoresis and negative testing for sickle cell disease excluded hemoglobin abnormalities and no sphero or elliptocytosis was found. Osmotic resistance of the red blood cells was normal. However, examination of intracellular erythrocyte enzymes revealed a massively decreased activity of pyruvate kinase

(3.5 U/10^{11} erythrocytes; normal: 17.1-26.5), while the activities of glucose-6-phosphate dehydrogenase, hexokinase and glutation reductase were normal. This finding led to the diagnosis of hereditary PKD.

After the antibiotic pretreatment, open cholecystectomy was performed. The gallbladder was severely inflamed and the intraoperative inspection and palpation of the liver were suggestive for liver cirrhosis. The liver was biopsied and histology confirmed advanced periportal bridging. Furthermore, a severe iron overload of hepatocytes and biliary epithelial cells was present, suggestive for genetic hemochromatosis (Figure 1). However, analysis of the *HFE*-genotype revealed no mutations and other chronic liver diseases, such as alcohol, viral, or autoimmune-related hepatitis and biliary diseases were excluded. Since a causal treatment of PKD is at present not available, an iron-chelating therapy with subcutaneous administration of desferrioxamine twice a day[2] was initiated. Despite a significant stabilization of the clinical condition under therapy (no ascites was found in follow-up visits after 3, 6 and 12 mo) and in view of the advanced stage of the liver cirrhosis (Child-Pugh Score 9), the patient was evaluated and recommended for liver transplantation. Unfortunately, he refused transplantation and conservative therapy with desferrioxamine was continued. Unexpectedly, liver function is to date stable for more than 3 years.

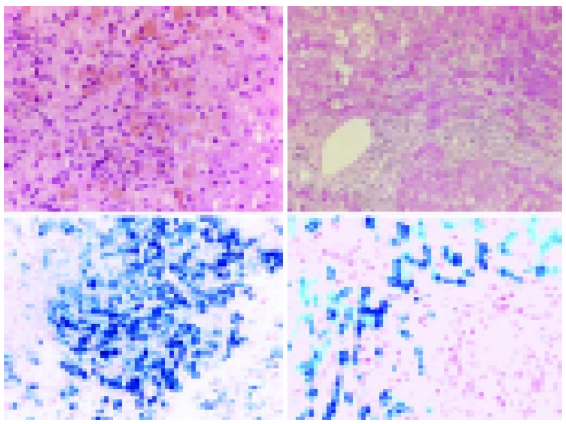

Figure 1 Liver histology of two patients with hereditary corpuscular hemolysis. Liver biopsies from patient 1 and 2 were fixed in formaldehyde and embedded in paraffin following standard protocols. Sections of 4-μm thickness were stained either with hematoxylin–eosin (HE-stain) or Perls Prussian Blue. Hepatic iron deposition was graded according to DiBisceglie.

Case 2

The diagnosis of PKD prompted us to examine the younger brother of the patient, who had a very similar medical history of the development of icterus and concomitant splenectomy during childhood. His actual laboratory parameters are shown in Table 1 (patient 2). The bilirubin elevation in this patient was caused solely by hemolysis, since direct bilirubin proportion was within the normal range (0.7 mg/dL). Correspondingly, all other hemolysis parameters were elevated and erythropoiesis was significantly stimulated (reticulocyte count of 22‰). Pyruvate kinase activity was even lower in this patient than in the older brother. The definitive confirmation of the congenital defect in both patients was now performed by sequence analysis of the pyruvate kinase gene within chromosome 5. A mutation of a single base at position 1 529 within exon 11 of this gene, with substitution of guanine (G) by adenosin (A) was evident (Figure 2). On the amino acid level this mutation could cause an exchange of arginine 510 into glutamate. This patient also had elevated liver enzymes but, in contrast to the older brother, he had no clinical signs of cirrhosis and his liver function was completely normal. There was no evidence for alcoholtoxic, viral or autoimmune hepatitis or an underlying biliary disease. However, iron metabolism parameters with high serum iron and ferritin were in a similar range as in his older brother, indicating massive iron overload. Liver biopsy confirmed the severe hepatocellular iron overload, and revealed furthermore advanced periportal bridging (Figure 1). This patient showed a markedly reduced ejection fraction in echocardiography, indicating iron-induced toxic cardiomyopathy. An iron chelating therapy with desferrioxamine was initiated and complemented by phlebotomy with a bimonthly withdrawal of 500-mL blood. In both patients, the iron reducing therapy led to a significant reduction of iron and ferritin over the next 12 mo (Figure 3).

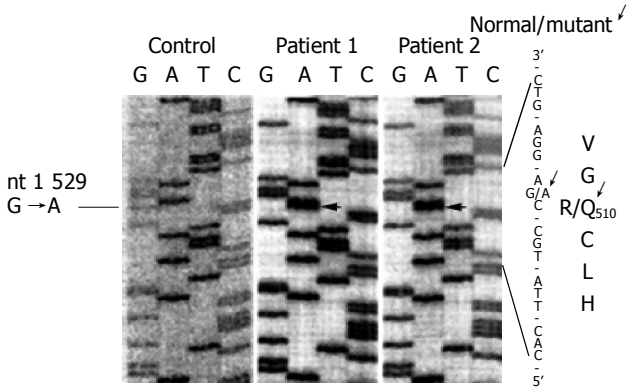

Figure 2 Partial sequence analysis of the pyruvate kinase gene (exon 11) in the patients described. Genomic DNA was prepared from peripheral blood mononuclear cells (PBMC) and sequenced according to standard protocols, applying [α^{35}S] dATP during the termination reaction and subsequent fluorography.

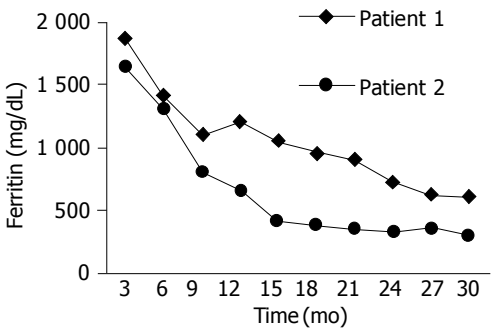

Figure 3 Decrease of iron overload in the patients under desferrioxamine therapy. Iron metabolism was assessed by serum ferritin concentration over a period of time of 30 mo.

Table 1 Laboratory parameters of the described patients at admission

Liver inflammation and function	*Normal*	*Patient 1*	*Patient 2*
ALT (GOT),	5–20 U/L	30 U/L	31 U/L
AST (GPT)	5–25 U/L	39 U/L	41 U/L
γ-GT	5–30 U/L	41 U/L	61 U/L
Alkaline phosphatase	<180 U/L	224 U/L	219 U/L
Prothrombin time	70–110%	48%	102%
INR		1.43	0.99
Albumin	(3.6–5.0 g/dL)	2.9 mg/dL	4.4 mg/dL
Cholinesterase	(3.5–7.0 kU/L)	2.1 kU/L	4.8 kU/L
C-reactive protein	<0.7 mg/dL	10 mg/dL	0.5 mg/dL
Erythrocyte morphology		anisocytosis, poikilocytosis, acanthocytosis	macrocytosis, anisocytosis, poikiLocytosis
Blood count, parameters of hemolysis and iron metabolism			
· WBC	(3–10/nL)	24 /nL	13 /nL
· Hemoglobin	(13.5--16 g/dL)	9.2 g/dL	11.5 g/dL
· Free hemoglobin	(35--65 mg/dL)	150 mg/L	115 mg/L
· Total bilirubin	(0.4--1.0 mg/dL)	8.3 mg/dL	7.6 mg/dL
· Direct bilirubin	(0.2--0.5 mg/dL)	1.7 mg/dL	0.8 mg/dL
· Haptoglobin	(<0.23 g/L)	< 0.233 g/L	< 0.233 g/L
· Lactat-dehydrogenase	(10--150 U/L)	450 U/L	375 U/L
· Reticulocytes	(<1%)	21 %	22 %
· Ferritin	(15–630 ng/mL)	1850 ng/mL	1620 ng/mL
· Urine iron excretion		0.5 mg/24 h	0.3 mg/24 h

DISCUSSION

The diagnosis of PKD in both cases was confirmed by sequence analysis of the PK gene, which revealed a single nucleotide mutation (G to A) in the PK gene within exon 11 at position 1 529. Together with the glucose-6-phosphate-dehydrogenase (G6PD) deficiency, PK deficiency is the most common type of hereditary enzyme defect within the glycolytic pathway causing nonspherocytic anemia[3,4]. The point mutation detected in our 2 patients (G1529A) is one of the most frequent mutations within the western European population[5-7]. The remaining activity of PK in patients carrying this mutation has been reported to be 10-25% and reticulocytosis varies from 5% to 66%[7]. The disease shows a broad range of clinical severity, which is loosely correlated to the impairment of hematological parameters: The lower the residual PK activity and the higher the reticulocyte count, the more the patients are affected[7,3]. Since PK catalyzes the final step within the glycolytic pathway (phosphoenol-pyruvate→pyruvate), a decreased activity results in alterations of the erythrocellular energy metabolism. Subsequently, the activity of the membrane associated sodium-potassium ATPase is impaired, leading to instability of red blood cells[8].

A main clinical feature in the two PKD patients, examined in this study, is a considerable iron overload. The iron overload is independent of transfusion therapy. In the liver tissue, the iron overload includes hepatocytes and even biliary epithelial cells. Since this histological pattern correlates to genetic hemochromatosis, the HLA phenotype and the commonly known mutations in the hereditary hemochromatosis (*HFE*)-gene (C282Y and H63D) were examined. The possibility of a coincidence of both diseases seems not unlikely, since 2-20% of the European population have mild alterations of the iron status associated with heterozygosity for the main hemochromatosis mutation (C282Y), while a much higher proportion carry the H63D mutation. A recent study revealed abnormalities of the *HFE*-gene in 35% of nontransfused patients with PKD and these abnormalities coincide with increased serum iron and ferritin[9]. However, in our patients heterozygosity for genetic hemochromatosis was ruled out by a normal *HFE*-genotype.

In addition to heterozygosity for hemochromatosis, splenectomy has been reported to be an independent risk factor for iron overload in hemolytic diseases[10,11]. While the increased iron turnover is the basis for the iron overload in PKD[9,12], it alone is not sufficient to cause iron accumulation in this disease[9,12]. Since both of our patients underwent splenectomy during childhood, this circumstance was considered as a main contribution to the significant iron overload they had. It is well accepted, that primary and secondary iron overloads have prefibrogenic effects within the liver tissue, by sustained induction of oxidative stress[13,14]. As in our patients, the level of the liver transaminases may only be marginally elevated, since the iron-induced chronic inflammation is often of very low activity, but nevertheless results in progressive fibrosis[13]. Independent of the pathogenesis, liver iron concentration must exceed a critical threshold, which has been suggested to be around 350-400 μmol/L/g, in order to cause hepatocellular damage[15,16]. Above this threshold, the secondary iron overload (e.g.,due to hemolytic disease) may have the same deleterious effects as the primary iron overload in genetic hemochromatosis.

Taken together, it becomes obvious that the clinical symptoms of the patients described in this study, are all based on the PKD in association with the splenectomy. Under this circumstance, chronic hemolysis is capable of causing significant iron overload, which in turn is responsible for the liver and cardiac disease of both patients. The pathophysiological importance of iron overload in these patients was also demonstrated by the effectiveness of the iron chelating therapy, which led to a significant decrease of serum ferritin and a stable liver function for more than 3 years. In addition to the iron overload, PKD-induced hemolysis is responsible for the abdominal symptoms of the elder patient (case 1). The chronic excess of bilirubin obviously altered the solvent properties of the bile, resulting in cholelithiasis, presumably consisting of bilirubin stones. The stones caused cholecystitis, perhaps combined with acute or chronic cholangitis. After cholecystectomy, these associated symptoms such as fever and abdominal pain relieved completely. Histological examination of gallbladder and the gallstones after surgery confirmed these clinical suspicions.

In summary, this study demonstrates that PKD-induced hemolysis in conjunction with splenectomy may cause severe iron overload even in the absence of *HFE*-genotype abnormalities. The secondary iron overload may lead to chronic liver disease and cirrhosis. Unfortunately, a sufficient causal therapy for PKD is at present not available, although new therapeutic strategies are under evaluation. The most promising gene therapeutic approaches may be either transplantation of heterologous hematopoietic stem cells[17] or the reinfusion of autologous stem cells after correction

of the PK gene sequence in the stem cell DNA *in vitro*[18]. Until such therapies become available, we suggest a close monitoring of the iron metabolism of PKD patients and a consequent treatment of iron overload.

ACKNOWLEDGEMENTS

The authors thank Peter Nuernberg, Institute of Medical Genetics, Charité Universitiy Hospital, Humboldt University, Berlin, Germany for sequencing the pyruvate kinase gene and Peter Schirmacher, Institute for Pathology, University of Cologne for staining of the liver tissue.

REFERENCES

1 **Miwa S,** Fujii H. Molecular basis of erythroenzymopathies associated with hereditary hemolytic anemia: tabulation of mutant enzymes. *Am J Hematol* 1996; **51:** 122-132
2 **Jensen PD,** Jensen FT, Christensen T, Ellegaard J. Evaluation of transfusional iron overload before and during iron chelation by magnetic resonance imaging of the liver and determination of serum ferritin in adult non-thalassaemic patients. *Br J Haematol* 1995; **89:** 880-889
3 **Demina A,** Varughese KI, Barbot J, Forman L, Beutler E. Six previously undescribed pyruvate kinase mutations causing enzyme deficiency. *Blood* 1998; **92:** 647-652
4 **Beutler E,** Miwa S, Palek J. Hemolytic anemias. *Rev Invest Clin* 1994; Suppl: 162-168
5 **Baronciani L,** Beutler E. Molecular study of pyruvate kinase deficient patients with hereditary nonspherocytic hemolytic anemia. *J Clin Invest* 1995; **95:** 1702-1709
6 **Kanno H,** Fujii H, Hirono A, Omine M, Miwa S. Identical point mutations of the R-type pyruvate kinase (PK) cDNA found in unrelated PK variants associated with hereditary hemolytic anemia. *Blood* 1992; **79:** 1347-1350
7 **Lenzner C,** Nurnberg P, Jacobasch G, Gerth C, Thiele BJ. Molecular analysis of 29 pyruvate kinase-deficient patients from central Europe with hereditary hemolytic anemia. *Blood* 1997; **89:** 1793-1799
8 **Zanella A,** Rebulla P, Vullo C, Izzo C, Tedesco F, Sirchia G. Hereditary pyruvate kinase deficiency: role of the abnormal enzyme in red cell pathophysiology. *Br J Haematol* 1978; **40:** 551-562
9 **Zanella A,** Bianchi P, Iurlo A, Boschetti C, Taioli E, Vercellati C, Zappa M, Fermo E, Tavazzi D, Sampietro M. Iron status and HFE genotype in erythrocyte pyruvate kinase deficiency: study of Italian cases. *Blood Cells Mol Dis* 2001; **27:** 653-661
10 **Piperno A,** Sampietro M, Taddei MT, Fiorelli G. Factors affecting erythrocyte ferritin content in thalassaemia intermedia. *Br J Haematol* 1984; **56:** 173-174
11 **Pootrakul P,** Rugkiatsakul R, Wasi P. Increased transferrin iron saturation in splenectomized thalassaemic patients. *Br J Haematol* 1980; **46:** 143-145
12 **Salem HH,** Van Der Weyden MB, Firkin BG. Iron overload in congenital erythrocyte pyruvate kinase deficiency. *Med J Aust* 1980; **1:** 531-532
13 **Poli G.** Pathogenesis of liver fibrosis: role of oxidative stress. *Mol Aspects Med* 2000; **21:** 49-98
14 **Lesnefsky EJ.** Tissue iron overload and mechanisms of iron-catalyzed oxidative injury. *Adv Exp Med Biol* 1994; **366:** 129-146
15 **Jensen PD,** Jensen FT, Christensen T, Nielsen JL, Ellegaard J. Relationship between hepatocellular injury and transfusional iron overload prior to and during iron chelation with desferrioxamine: a study in adult patients with acquired anemias. *Blood* 2003; **101:** 91-96
16 **Bassett ML,** Halliday JW, Powell LW. Value of hepatic iron measurements in early hemochromatosis and determination of the critical iron level associated with fibrosis. *Hepatology* 1986; **6:** 24-29
17 **Takatu A,** Nash RA, Zaucha JM, Little MT, Georges GE, Sale GE, Zellmer E, Kuhr CS, Lothrop CD Jr, Storb R. Adoptive immunotherapy to increase the level of donor hematopoietic chimerism after nonmyeloablative marrow transplantation for severe canine hereditary hemolytic anemia. *Biol Blood Marrow Transplant* 2003; **9:** 674-682
18 **Tani K,** Yoshikubo T, Ikebuchi K, Takahashi K, Tsuchiya T, Takahashi S, Shimane M, Ogura H, Tojo A, Ozawa K. Retrovirus-mediated gene transfer of human pyruvate kinase (PK) cDNA into murine hematopoietic cells: implications for gene therapy of human PK deficiency. *Blood* 1994; **83:** 2305-2310

PO Box 2345, Beijing 100023, China
www.wjgnet.com
wjg@wjgnet.com

ELSEVIER

World J Gastroenterol 2005;11(8):1245-1247
World Journal of Gastroenterology ISSN 1007-9327

• *CASE REPORT* •

Clostridium difficile causing acute renal failure: Case presentation and review

Jasmin Arrich, Gottfried H. Sodeck, Gürkan Sengölge, Christoforos Konnaris, Marcus Müllner, Anton N. Laggner, Hans Domanovits

Jasmin Arrich, Gottfried H. Sodeck, Marcus Müllner, Anton N. Laggner, Hans Domanovits, Department of Emergency Medicine, Medical University Vienna, General Hospital, Währinger Gürtel 18-20, A-1090, Austria
Christoforos Konnaris, Department of Internal Medicine IV, Division of Occupational Medicine, Medical University Vienna, General Hospital, Währinger Gürtel 18-20, A-1090, Austria
Gürkan Sengölge, Department of Medicine III, Division of Nephrology and Dialysis, Medical University Vienna, General Hospital, Währinger Gürtel 18-20, A-1090, Austria
Correspondence to: Professor Hans Domanovits, Department of Emergency Medicine, Medical University Vienna, General Hospital, Währinger Gürtel 18-20, A-1090, Austria, Europe
Telephone: +43-1-40400-1964 Fax: +43-1-40400-1965
Received: 2004-07-23 Accepted: 2004-09-19

Abstract

AIM: *Clostridium difficile* infection is primarily a nosocomial infection but asymptomatic carriers of *Clostridium difficile* can be found in up to 5% of the general population. Ampicillin, cephalosporins and clindamycin are the antibiotics that are most frequently associated with *Clostridium difficile*-associated diarrhea or colitis. Little is known about acute renal failure as a consequence of *Clostridium difficile*-associated diarrhea.

METHODS: In this case report, we describe the course of *Clostridium difficile*-associated diarrhea in an 82-year-old patient developing acute renal failure. Stopping the offending agent and symptomatic therapy brought a rapid improvement of diarrhea and acute renal failure, full recovery was gained 18 d after admission. In a systematic review we looked for links between the two conditions.

RESULTS: The link between *Clostridium difficile*-associated diarrhea and acute renal failure in our patient was most likely volume depletion. However, in experimental studies a direct influence of *Clostridium difficile* toxins on renal duct cells could be shown.

CONCLUSION: Rapid diagnosis, nonspecific supportive treatment and specific antibiotic treatment, especially in the elderly, may lower excess mortality *Clostridium difficile*-associated diarrhea and renal failure being possible complications.

Key words: Acute renal failure; *Clostridium difficile*; Diarrhea

Arrich J, Sodeck GH, Sengölge G, Konnaris C, Müllner M, Laggner AN, Domanovits H. *Clostridium difficile* causing acute renal failure: Case presentation and review. *World J Gastroenterol* 2005; 11(8): 1245-1247
http://www.wjgnet.com/1007-9327/11/1245.asp

INTRODUCTION

Clostridium difficile-associated diarrhea is more common in the hospital setting. A recent study found toxins of *Clostridium difficile* in 18% of inpatients and in 58% of inpatients with unexplained leukocytosis[1,2]. Overall mortality of patients with hospital-acquired *Clostridium difficile*-associated diarrhea was reported to be 15%[1]. However, toxins of *Clostridium difficile* have also been found out of hospital in 5% of fecal specimens of the asymptomatic general population[3]. Overall mortality of elderly patients admitted to an intensive care unit with the diagnosis of acute renal failure was reported to be 61%[4]. *Clostridium difficile*-associated diarrhea and acute renal failure are both well-recognized conditions but rarely occur together. The clinical course may be more severe and mortality increased particularly in the elderly population. Both conditions are reversible by relatively simple measures provided an early diagnosis is made. The clinical work-up and outcome of an 82-year-old man, suffering from acute renal failure due to preclinical-acquired *Clostridium difficile*-associated diarrhea, is presented. Epidemiology, diagnostics and standards of treatment are critically reviewed in line with current literature.

CASE REPORT

An 82-year-old man presented, in poor but stable general condition, to the local emergency department of a tertiary care university hospital with typical signs of gastroenteritis lasting for 5 d. His medical history included non-insulin-dependent diabetes mellitus since 10 years, two myocardial infarctions 1 year ago, cerebrovascular occlusive disease treated with carotid endarterectomy 2 years ago and pulmonary embolism 4 years ago. Initially, he had presented to his general practitioner with abdominal pain lasting for a few days. Considering his complex medical history his general practitioner put him on amoxicillin/clavulanate potassium. Because the symptoms did not improve during the following days and his general condition started to deteriorate, the patient called the ambulance and he was brought to the hospital. On examination the patient's blood-pressure was 115/85 mmHg (15/11 kPa), his pulse rate 60 beats/min, he was dehydrated but afebrile. Laboratory examinations showed highly elevated

plasma urea (41 mmol/L, normal range 2.5-6.7 mmol/L) and creatinine levels (1149.2 μmol/L, normal range 70-150 μmol/L) (Figure 1). Serum levels of electrolytes, white blood cell count and CRP were within normal range (CRP under 1 mg/dL, WBC 4.3-10.8×10^9/L) (Figure 2), and fibrinogen was only slightly increased (6 g/L, normal range 1.80-3.90 g/L). Prerenal acute renal failure was assumed as primary working diagnosis because of dehydration due to prolonged diarrhea and the patient's long-term therapy with furosemide. Diuretics were stopped; under continuous intravenous and oral fluid replacement the patient's general condition improved. Prior to referral to a medical ward, stool cultures were requested. During the following days white blood cell count and acute phase proteins increased, indicating an ongoing infection. Chest x-rays showed no signs of pneumonia and blood cultures did not reveal bacteremia. Stool specimen was positive for *Clostridium difficile*. The patient was started on intravenous metronidazole 1.5 g/d. Three days after onset of specific therapy, inflammatory markers reached maximum levels (WBC 12 g/L, CRP 6 mg/dL) and decreased in the further course (Figure 2), while plasma urea and creatinine levels returned to normal (Figure 1). *Clostridium difficile* toxins could not be detected in any subsequent stool samples. Fully recovered, the patient could be discharged from hospital, 18 d after initial presentation.

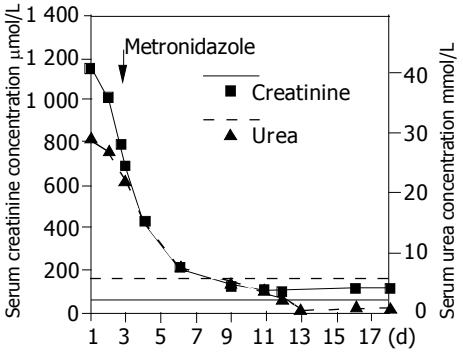

Figure 1 Serum urea (---) and creatinine (—) levels over time of hospital stay with the horizontal lines representing normal ranges of urea (---) and creatinine (—). The arrow indicates start of specific antibiotic treatment.

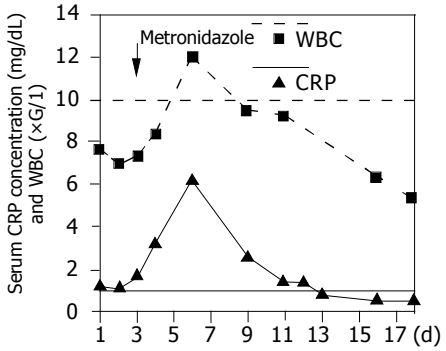

Figure 2 White blood cell count (---) and serum CRP levels (—) over time of hospital stay with horizontal lines representing normal ranges of white blood cell count (---) and CRP (—). The arrow indicates start of specific antibiotic treatment.

DISCUSSION

Risk factors

Considering the high prevalence of *Clostridium difficile* infections in the hospital setting, our patient may have been infected during a previous hospital stay. But an acquisition of infection out of hospital is not excluded. Because of his old age and his comorbidities including non-insulin-dependent diabetes mellitus, ischaemic heart disease, cerebrovascular occlusive disease and pulmonary embolism, he certainly was at risk to develop *Clostridium difficile*-associated diarrhea as well as acute renal failure. Antibiotic-associated diarrhea as a common course of infection with *Clostridium difficile* has a broad spectrum of clinical manifestations ranging from mild diarrhea to pseudomembranous colitis and fulminant colitis[5]. The risk factors that could be identified as associated with severe disease (defined by a hospital stay of greater than 14 d, colectomy, intensive care unit admission or death of patient) were age over 70 years, comorbid illnesses, and recurrence of *Clostridium difficile*-associated diarrhea[6]. Acute renal failure is characterized by an abrupt decline in renal function resulting in an inability to excrete metabolic wastes and maintain proper fluid and electrolyte imbalance[7]. Prerenal acute renal failure together with intrarenal acute renal failure due to ischaemia and nephrotoxins are responsible for most episodes of acute renal failure[8]. Common causes of prerenal failure are volume depletion as a result of diarrhea, reduced fluid intake, fever, diuretics, or heart failure. Elderly patients are particularly susceptible to prerenal failure because of their predisposition to hypovolaemia and high prevalence of renal-artery atherosclerotic disease[9].

Developments of the diagnosis of Clostridium difficile-associated diarrhea

The diagnosis of *Clostridium difficile*-associated diarrhea was confirmed by ELISA testing for enterotoxin A and B. The diagnosis of an infection with *Clostridium difficile* can be made either by testing for toxin A or B (ELISA and cytotoxin assay), bacterial enzymes (Latex agglutination test) or by bacterial culture. Bacterial culture is highly sensitive and allows bacterial strain typing, but also takes 2-5 d to perform[5]. Latex agglutination tests are fast and inexpensive and have improved in sensitivity in the past few years[10].

Treatment

For our patient, intravenous and oral fluid replacement therapy in addition to the appropriate antibiotic agent brought a rapid improvement in his condition. In fact both diseases share the same principles of nonspecific treatment (Table 1, 2). Reversing the underlying cause is the first and most beneficial measure. In *Clostridium difficile* infection it is discontinuation of offending antibiotic treatment, in acute renal failure it may be stopping a nephrotoxic agent or treating diarrhea. Further important measures in both diseases are replacing intravascular volume and correcting electrolyte abnormalities.

Clostridium difficile and antibiotics

In our case, amoxicillin/clavulanate potassium seemed to have initiated deterioration of first mild gastrointestinal symptoms. The development of *Clostridium difficile*-associated diarrhea and pseudomembranous colitis, however, is not

restricted to certain antibiotics. The ones that are most frequently associated are ampicillin, cephalosporins and clindamycin. If patients require antibiotics, another way of treating them is changing to an agent that has less frequently been associated with the disease[5]. First line agents for the treatment of symptomatic *Clostridium difficile* infection include oral vancomycin or metronidazole. A recent study, investigating resistance of *Clostridium difficile* strains to different antibiotics found no evidence that the most common human strains were resistant to vancomycin or metronidazole while all strains were resistant to cefoxitin and most strains resistant to ceftriaxon[11].

Table 1 Treatment of acute renal failure[7]

Reverse underlying causes
Return intravascular volume and mean arterial pressure to normal
Correct electrolyte imbalances
Treat hyperkalaemia and acidosis with inhaled beta-agonists, insulin/glucose, sodium bicarbonate, binding resins (sodium polystyrene sulfonate)
Discontinue or avoid nephrotoxins
Adjust doses of medications that are eliminated by the kidney or by dialysis
Initiate renal replacement therapy in case of volume overload, hyperkalaemia, metabolic acidosis refractory to medical treatment
Obtain nephrologic consultation as soon as possible

Table 2 Treatment of infections with toxigenic *C. difficile*[5]

Discontinuation of offending antibiotic
Correction of fluid loss and electrolyte imbalance
Antimicrobial agents if symptoms are severe or persistent
Oral agents (preferred)
Metronidazole: 250 mg, four times daily to 500 mg 3 times daily for 7–14 d
Vancomycin: 125 mg, four times daily, 7–14 d
Parenteral agent
Metronidazole: 500 mg, given intravenously every 6 h

More than volume depletion?

In our case the most likely link between *Clostridium difficile* colitis and acute renal failure was volume depletion due to prolonged diarrhea. Dramatic improvement of the patient's general condition and rapidly decreasing serum creatinine and urea levels after initiation of fluid therapy support this hypothesis. A medline search retrieved three articles dealing with acute renal failure in patients with *Clostridium difficile*-associated diarrhea. Two articles reported on hospitalized patients with acute and chronic renal failure developing *Clostridium difficile*-associated diarrhea[12,13], another one described a case of IgA nephropathy after out of hospital acquired antibiotic-associated *Clostridium difficile* colitis[14]. As potential cause the authors discuss an immunologic perturbation, culminating in mesangial IgA deposition. In our case no renal biopsy was taken, however, an IgA nephropathy as underlying cause of acute renal failure was not likely. Mere experimental are influences of *Clostridium difficile* toxins on renal duct cells. Klussmann and Maric reported that *Clostridium difficile* toxin B increases water permeability in primary cultured collecting duct cells by translocating aquaporin-2 water channel carrying vesicles into the cell membrane[15]. Cell death cells plays a major role in acute renal failure and it could be observed that toxins of *Clostridium difficile* initiate. Whether these mechanisms contribute to acute renal failure remain to be investigated.

In conclusion, our patient presented with a course of *Clostridium difficile*-associated diarrhea followed by acute renal failure. Under continuous volume replacement therapy and specific antibiotics the patient's general condition improved, inflammatory markers, serum urea and creatinine rapidly returned to normal and the patient could be discharged after full recovery 18 d after admission. Both acute renal failure and *Clostridium difficile*-associated diarrhea are potentially life-threatening diseases in the elderly but may be reversed using appropriate therapy. Keeping in mind a possible direct link between these two serious diseases, this report once more stresses the need for rapid diagnosis and specific treatment, especially in the elderly, to prevent fatal outcome.

REFERENCES

1 **Miller MA,** Hyland M, Ofner-Agostini M, Gourdeau M, Ishak M. Morbidity, mortality, and healthcare burden of nosocomial *Clostridium difficile*-associated diarrhea in Canadian hospitals. *Infect Control Hosp Epidemiol* 2002; **23:** 137-140

2 **Wanahita A,** Goldsmith EA, Marino BJ, Musher DM. *Clostridium difficile* infection in patients with unexplained leukocytosis. *Am J Med* 2003; **115:** 543-546

3 **Rivera EV,** Woods S. Prevalence of asymptomatic *Clostridium difficile* colonization in a nursing home population: a cross-sectional study. *J Gend Specif Med* 2003; **6:** 27-30

4 **Druml W.** Prognosis of acute renal failure 1975-1995. *Nephron* 1996; **73:** 8-15

5 **Hurley BW,** Nguyen CC. The spectrum of pseudomembranous enterocolitis and antibiotic-associated diarrhea. *Arch Intern Med* 2002; **162:** 2177-2184

6 **Andrews CN,** Raboud J, Kassen BO, Enns R. *Clostridium difficile*-associated diarrhea: predictors of severity in patients presenting to the emergency department. *Can J Gastroenterol* 2003; **17:** 369-373

7 **Singri N,** Ahya SN, Levin ML. Acute renal failure. *JAMA* 2003; **289:** 747-751

8 **Thadhani R,** Pascual M, Bonventre JV. Acute renal failure. *N Engl J Med* 1996; **334:** 1448-1460

9 **Pascual J,** Liano F, Ortuno J. The elderly patient with acute renal failure. *J Am Soc Nephrol* 1995; **6:** 144-153

10 **Turgeon DK,** Novicki TJ, Quick J, Carlson L, Miller P, Ulness B, Cent A, Ashley R, Larson A, Coyle M, Limaye AP, Cookson BT, Fritsche TR. Six rapid tests for direct detection of *Clostridium difficile* and its toxins in fecal samples compared with the fibroblast cytotoxicity assay. *J Clin Microbiol* 2003; **41:** 667-670

11 **Drummond LJ,** McCoubrey J, Smith DG, Starr JM, Poxton IR. Changes in sensitivity patterns to selected antibiotics in *Clostridium difficile* in geriatric in-patients over an 18-month period. *J Med Microbiol* 2003; **52:** 259-263

12 **Barany P,** Stenvinkel P, Nord CE, Bergstrom J. *Clostridium difficile* infection-a poor prognostic sign in uremic patients? *Clin Nephrol* 1992; **38:** 53-57

13 **Arning M,** Gehrt A, Wolf M, Aul C, Chlebowski H, Hadding U, Schneider W. A lethal course in pseudomembranous enterocolitis during the parenteral administration of vancomycin and imipenem. *Dtsch Med Wochenschr* 1992; **117:** 91-95

14 **Gaughan WJ,** Hassan MH, McCue PA, Burke JF, Sharma K. Association of IgA nephropathy with *Clostridium difficile* colitis. *Am J Kidney Dis* 1999; **34:** e16

15 **Klussmann E,** Maric K, Rosenthal W. The mechanisms of aquaporin control in the renal collecting duct. *Rev Physiol Biochem Pharmacol* 2000; **141:** 33-95

PO Box 2345, Beijing 100023, China
www.wjgnet.com
wjg@wjgnet.com

ELSEVIER

World J Gastroenterol 2005;11(8):1248-1249
World Journal of Gastroenterology ISSN 1007-9327

• *CASE REPORT* •

Report of gossypiboma from the standpoint in medicine and law

Li-Rung Shyung, Wen-Hsiung Chang, Shee-Chan Lin, Shou-Chuan Shih, Chin-Roa Kao, Sun-Yen Chou

Li-Rung Shyung, Division of Gastroenterology, Department of Internal Medicine, Mackay Memorial Hospital, Mackay Junior College of Nursing, Taipei, Taiwan, China; L.L.B., Department of Law, National Taiwan University, China
Wen-Hsiung Chang, Shee-Chan Lin, Shou-Chuan Shih, Chin-Roa Kao, Sun-Yen Chou, Division of Gastroenterology, Department of Internal Medicine, Mackay Memorial Hospital, Mackay Junior College of Nursing, Taipei, Taiwan, China
Correspondence to: Dr. Wen-Hsiung Chang, Division of Gastroenterology, Department of Internal Medicine, Mackay Memorial Hospital, No. 92, Sec. 2, Chung-Shan North Road, Taipei 104, Taiwan, China. luke.skywalk@msa.hinet.net
Telephone: +886-914042363
Received: 2004-07-12 Accepted: 2004-08-31

Abstract

We report on a case of gossypiboma. A 78-year-old man was admitted to our hospital with acute abdomen. He had undergone an operation for colon cancer 4 mo previously. Abdominal ultrasonography revealed an echogenic lesion with a hypoechoic rim and strong posterior acoustic shadowing in the lower abdomen. Diagnosis of gossypiboma can be made by ultrasonography to avoid loss-of-chance of survival. We reviewed the English literature briefly of gossypiboma from the medical and juridical view. According to the theory of loss-of-chance, the damage of plaintiff is the loss of the chance of survival or recovery, rather than the final harm. The victim would allow recovery for the loss of the chance from the defendant. But the plaintiff would show by a preponderance that he was deprived of a betterchance of a cure. Under the proposed rule, the compensable value of the victim would be the plaintiff's compensation for the loss of the victim's chance of survival.

Key words: Gossypiboma; Loss-of-chance; Preponderance

Shyung LR, Chang WH, Lin SC, Shih SC, Kao CR, Chou SY. Report of gossypiboma from the standpoint in medicine and law. *World J Gastroenterol* 2005; 11(8): 1248-1249
http://www.wjgnet.com/1007-9327/11/1248.asp

INTRODUCTION

Retained gauzes in the abdominal cavity are infrequent nowadays, but they present a diagnostic problem even if radiopaque threads and gauze double counts are used in the operation room[1]. It can cause loss-of-chance of survival or recovery.

We will present an acute abdomen occurring 4 mo after a gauze was left in the abdomen. Ultrasound examinations proved helpful, and they are described in this report.

CASE REPORT

A 78-year-old man with a history of previous operation for colon cancer was admitted with the chief complaints of acute epigastric pain for several days. He was rather well until several days before this admission when he experienced acute epigastric pain and poor appetite intermittently. On arrival, his consciousness was clear and vital signs were stable (blood pressure: 120/60 mmHg, pulse rate: 72/min, respiratory rate: 18/min, and body temperature: 36.5 ℃). Physical examination revealed no abdominal mass was felt. Results of rectal examination were normal. An ultrasound scan of the abdomen revealed an echogenic lesion with a hypoechoic rim and strong posterior acoustic shadowing in the lower abdomen (Figure 1). A plain x-ray of the abdomen revealed a long and fine opacity over the right lower quadrant abdomen, some mottled small air densities were superimposed on this area (Figure 2). Under the impression of intraabdominal abscess, exploratory laparotomy was performed. At laparotomy there was a focal abscess in the right lower quadrant abdomen containing a laparotomy gauze. The abscess cavity was irrigated and the retained gauze was resected. The abdomen was drained and closed. The postoperative period was uneventful.

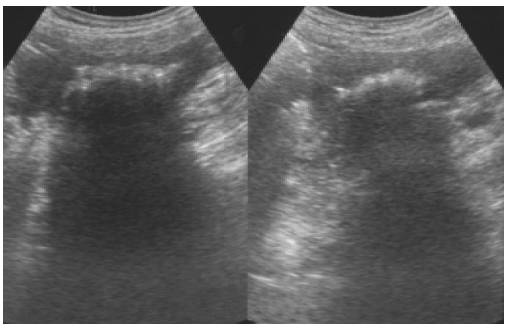

Figure 1 Right intercostal sonogram obtained 4 mo after surgery show a cystic mass with irregular internal components. Posteriorly, the mass has strong acoustic shadowing.

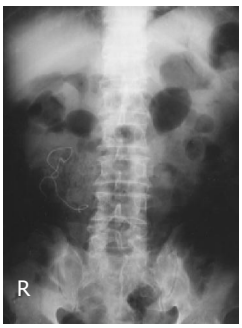

Figure 2 Plain roentgenogram of abdomen after abdominal sonogram. Notice serpentine linear opacity over the right portion of abdomen, some mottled hyperdensities are adjacent to this linear opacity- all diagnostic features of a retained gauze.

DISCUSSION

Radiopaque threads impregnated into surgical gauzes were first introduced by Cahn in 1929, but were not come into general use in the United States until about 1940[2]. A retained gauze left in the abdomen must be considered in the differential diagnosis of patients with a history of laparotomy, and thus one needs a careful review of the patient's past history. During the first two months of retained gauze, there was a little reaction, death being unrelated to the presence of the gauze. From 2 mo to 2 years, infective inflammation and abscess were found. During that period, extrusion of the gauze occurred through an externally fistulous tract or internally into the rectum, vagina, bladder, or intestinal lumen[3].

There are surgeons who recommend the routine postoperative abdominal film after abdominal operation[4]. On abdominal films, a whirl-like appearance is characteristic of retained gauzes. This appearance is considered to be due to gas trapped in the fibers of the gauze[5]. The ultrasound is very useful in the diagnosis of abdominal retained gauze[6]. The ultrasound feature is usually a well-delineated mass containing wavy internal echo with a hypoechoic rim and a strong posterior acoustic shadowing[7]. Ultrasonography images can be classified into two groups, a cystic type and a solid type. The former showed a cystic lesion with zigzag echogenic bundle. The latter showed a complex mass with hyper- and hypoechoic regions. A postoperative diagnosis of retained gauze can be made from the characteristic appearance on ultrasonography images. This can avoid delayed diagnosis and medical errors.

A doctor may negligently fail to diagnoses a preexisting disease, allowing it to progress, with harmful effects. The disease was obviously a cause of harm. The doctor's negligence in allowing the disease to progress may also have caused the harm. In assessing the value of that loss-of-chance of gossypiboma, the disease should be deemed a preexisting condition and be taken into account. To illustrate, consider the case in which a doctor negligently fails to diagnose a patient's cancerous condition until it has become inoperable. Assume further that even with a timely diagnosis the patient would have had only a 30% chance of recovering from the disease. A rational approach would allow recovery from the loss of the chance of cure even though the chance was not better than even. While the plaintiff here could not prove by a preponderance of the evidence that he was denied a cure by the defendant's negligence, he would show by a preponderance that he was deprived of a 30% chance of a cure.

In our case, the preexisting condition and the effect of the doctor's tortuous conduct attach within a relatively short time, the burden of providing the extent to which the preexisting condition reduced the value of the interest in question should be shifted to the doctor. Shifting the burden of proof is not a completely satisfactory solution, this shift simply realigns the scale[8,9].

REFERENCES

1 **Gencosmanoglu R,** Inceoglu R. An unusual cause of small bowel obstruction: gossypiboma--case report. *BMC Surg* 2003; **3:** 6

2 **Rymer CA,** McCarthy JD. A silent sponge speaks. *Am J Surg* 1974; **128:** 103-104

3 **Lin SC,** Huang F, Kao CR, Yang KC, Chou SY, Shih SC, Lin DC, Huang CH. Ultrasonographic appearance of retained surgical sponges-3 cases report. *Chinese J Gastroenterol* 1984; **1:** 218-222

4 **Jones SA.** The foreign body problem after laparotomy. Personal experiences. *Am J Surg* 1971; **122:** 785-786

5 **Kokubo T,** Itai Y, Ohtomo K, Yoshikawa K, Iio M, Atomi Y. Retained surgical sponges: CT and US appearance. *Radiology* 1987; **165:** 415-418

6 **Sekiba K,** Akamatsu N, Niwa K. Ultrasound characteristics of abdominal abscesses involving foreign bodies (gauze). *J Clin Ultrasound* 1979; **7:** 284-286

7 **Chau WK,** Lai KH, Lo KJ. Sonographic findings of intraabdominal foreign bodies due to retained gauze. *Gastrointest Radiol* 1984; **9:** 61-63

8 **Todd SA.** Identifying and valuing the injury in lost chance cases. *Mich L Rev* 1998; **96:** 1335-1361

9 **Lori RE.** Loss of chance as technique: Toeing the line at fifty percent. *Texas L Rev* 1993; **27:** 369-402

PO Box 2345, Beijing 100023, China
www.wjgnet.com
wjg@wjgnet.com

ELSEVIER

World J Gastroenterol 2005;11(8):1250
World Journal of Gastroenterology ISSN 1007-9327

Acknowledgements to Reviewers of *World Journal of Gastroenterology*

Many reviewers have contributed their expertise and time to the peer review, a critical process to ensure the quality of *World Journal of Gastroenterology*. The editors and authors of the articles submitted to the journal are grateful to the following reviewers for evaluating the articles (including those were published and those were rejected in this issue) during the last editing period of time.

Francis K.L Chan, Professor
Department of Medicine and Therapeutics, Prince of Wales Hospital, The Chinese University of Hong Kong, 30-32 Ngan Shing Street, Shatin, Hong Kong, China

Pelayo Correa, Boyd Professor
Department of Pathology, Louisiana State University Health Science Center, 1901 Perdido St., New Orleans La 70112, United States

Jun Cheng, Professor
Dean Assistant, Beijing Earth Altar Hospital Dean 13 Earth Altar Park, Anwai Avenue, East District, Beijing 100011, China

Da-Jun Deng, Professor
Department of Cancer Etiology, Peking University School of Oncology, 1 Da-Hong-Luo-Chang Street, Western District, Beijing 100034, China

Sheung-Tat Fan, Professor
Department of Surgery, The University of Hong Kong, Queen Mary Hospital, 102 Pokfulam Road, Hong Kong, China

Xue-Gong Fan, Professor
Xiangya Hospital, Changsha 410008, China

Anna S Gukovskaya, Professor
Department of Medicine, UCLA, 11301 Wilshire Blvd, Los Angeles 91301, United States

Jin Gu, Professor
Peking University School of Oncology, Beijing Cancer Hospital, Beijing 100036, China

De-Wu Han, Professor
Shanxi Medical University, 86 Xinjian South Road, Taiyuan 030001, China

Zhi-Qiang Huang, Professor
Abdominal Surgery Institute of General Hospital of PLA, Fuxing Road, Beijing 100853, China

Hiromi Ishibashi, Professor
Director General, Clinical Research Center, National Hospital Organization (NHO) Nagasaki Medical Center, Professor, Department of Hepatology, Nagasaki University Graduate School of Biomedical Sciences, Kubara 2-1001-1 Kubara Omura, Nagasaki 856-8562, Japan

John P Neoptolemos, Professor
Divison of Surgery and Oncology, University of Liverpool, Divison of Surgery and Oncology, Royal Liverpool University Hospital, Daulby Street, Liverpool L9 3GA, United Kingdom

Vasiliy Ivanovich Reshetnyak, Professor
Institute of General Reanimatology, 25-2, Petrovka Str., Moscow 107031, Russian Federation

Yu-Gang Song, Professor
Department of Training, The First Military Medicine University, The First Military Medicine University, Guangzhou 510515, China

Qin Su, Professor
Department of Pathology, Cancer Hospital and Cancer Institute, Chinese Academy of Medical Sciences and Peking Medical College, PO Box 2258, Beijing 100021, China

Peng Shang, Professor
Department of Cell Biology, Faculty of Life Sciences, 127 Western Youyi Road, Northwestern Polytechnological University, Xi'an , 710072, China

Jian-Ying Wang, Professor
University of Maryland School of Medicine, Baltimore VA Medical Center (112), 10N. Greene St, Baltimore, MD 21201, United States

Yuan Wang, Professor
Institute of Biochemistry and Cell Biology, Shanghai Institutes for Biological Sciences, Chinese Academy of Sciences, Shanghai 200031, China

Chun-Yang Wen, M.D.
Department of Molecular Pathology, Atomic Bomb Disease Institute, Nagasaki University Graduate School of Biomedical Sciences. 1-12-4 Sakamoto, Nagasaki 852-8523, Japan

Jian-Zhong Zhang, Professor
Department of Pathology and Laboratory Medicine, Beijing 306 Hospital, 9 North Anxiang Road, PO Box 9720, Beijing 100101, China

Zhi-Rong Zhang, Professor
West China School of Pharmacy, Sichuan University, 17 South Renmin Road, Chengdu 610041, Sichuan Povince, China

Mu-Jun Zhao, M.D.
Institute of Biochemistry and Cell Biology, Chinese Academy of Sciences, 320 Yueyang Road, Shanghai 200031, China

PO Box 2345, Beijing 100023, China
www.wjgnet.com
wjg@wjgnet.com

ELSEVIER

World J Gastroenterol 2005;11(8):Appendix 1
World Journal of Gastroenterology ISSN 1007-9327

Meetings

Major meetings coming up

Digestive Disease Week
106th Annual Meeting of AGA, The American Gastroenterology Association
May 14-19, 2005
www.ddw.org/
Chicago, Illinois

13th World Congress of Gastroenterology
September 10-14, 2005
www.wcog2005.org/
Montreal, Canada

13th United European Gastroenterology Week, UEGW
October 15-20, 2005
www.uegf.org/
Copenhagen, Denmark

American College of Gastroenterology Annual Scientific Meeting
October 28-November 2, 2005
www.acg.gi.org/
Honolulu Convention Center, Honolulu, Hawaii

Events and Meetings in the upcoming 6 months

Canadian Digestive Disease Week Conference
February 26-March 6, 2005
www.cag-acg.org
Banff, AB

International Colorectal Disease Symposium 2005
February 3–5, 2005
info@icds-hk.org
Hong Kong

EASL 2005 the 40th annual meeting
April 13–17, 2005
www.easl.ch/easl2005/
Paris, France

Pediatric Gastroenterology, Hepatology and Nutrition
March 13, 2005
Jakarta, Indonesia

21st annual international congress *of Pakistan society of Gastroenterology & GI Endoscopy*
March 25–27, 2005
www.psgc2005.com
Peshawar

8th Congress of the Asian Society of HepatoBiliary Pancreatic Surgery
February 10–13, 2005
Mandaluyong, Philippines

World Congress on Gastrointestinal Cancer
June 15–18, 2005
Barcelona

British Society of Gastroenterology Conference (BSG)
March 14–17, 2005
www.bsg.org.uk
Birmingham

Digestive Disease Week *DDW 106th Annual Meeting*
May 15–18, 2005
www.ddw.org
Chicago, Illinois

Events and meetings in 2005

Canadian Digestive Disease Week Conference
February 26-March 6, 2005
www.cag-acg.org
Banff, AB

2005 World Congress of Gastroenterology
September 12–14, 2005
Montreal, Canada

International Colorectal Disease Symposium 2005
February 3–5, 2005
Hong Kong

13th UEGW meeting *United European Gastroenterology Week*
October 15–20, 2005
www.webasistent.cz/guarant/uegw2005/
Copenhagen-Malmoe

7th International Workshop on Therapeutic Endoscopy
September 10–12, 2005
www.alfamedical.com
Theodor Bilharz Research Institute

EASL 2005 the 40th annual meeting
April 13–17, 2005
www.easl.ch/easl2005/
Paris, France

Pediatric Gastroenterology, Hepatology and Nutrition
March 13, 2005
Jakarta, Indonesia

21st annual international congress *of Pakistan society of Gastroenterology & GI Endoscopy*
March 25–27, 2005
www.psgc2005.com
Peshawar

8th Congress of the Asian Society of HepatoBiliary Pancreatic Surgery
February 10–13, 2005
Mandaluyong, Philippines

APDW 2005 - Asia Pacific Digestive Week 2005
September 25–28, 2005
www.apdw2005.org
Seoul, Korea

World Congress on Gastrointestinal Cancer
June 15–18, 2005
Barcelona

British Society of Gastroenterology Conference (BSG)
March 14–17, 2005
www.bsg.org.uk
Birmingham

Digestive Disease Week *DDW 106th Annual Meeting*
May 15–18, 2005
www.ddw.org
Chicago, Illinois

70th ACG Annual Scientific Meeting and Postgraduate Course
October 28-November 2, 2005
Honolulu Convention Center, Honolulu, Hawaii

Events and Meetings in 2006

EASL 2006 - THE 41ST ANNUAL MEETING
April 26–30, 2006
Vienna, Austria

Canadian Digestive Disease Week Conference
March 4–12, 2006
www.cag-acg.org
Quebec City

XXX pan-american congress of digestive diseases *XXX congreso panamericano de anfermedades digestivas*
November 25-December 1, 2006
www.gastro.org.mx
Cancun

World Congress on Gastrointestinal Cancer
June 14–17, 2006
Barcelona, Spain

7th World Congress of the International Hepato-Pancreato-Biliary Association
September 3–7, 2006
www.edinburgh.org/conference
Edinburgh

71st ACG Annual Scientific Meeting and Postgraduate Course
October 20–25, 2006
Venetian Hotel, Las Vegas, Neveda

PO Box 2345, Beijing 100023, China
www.wjgnet.com
wjg@wjgnet.com

ELSEVIER

World J Gastroenterol 2005;11(8):Appendix 2-3
World Journal of Gastroenterology ISSN 1007-9327

Instructions to authors

GENERAL INFORMATION

World Journal of Gastroenterology (*WJG,* ISSN 1007-9327) is a weekly journal of more than 48 000 circulation, published on the 7th, 14th, 21st and 28th of every month.

Original Research, Clinical Trials, Reviews, Comments, and Case Reports in esophageal cancer, gastric cancer, colon cancer, liver cancer, viral liver diseases, *etc*., from all over the world are welcome on the condition that they have not been published previously and have not been submitted simultaneously elsewhere.

Published jointly by
The WJG Press and Elsevier Inc.

SUBMISSION OF MANUSCRIPTS

Manuscripts should be typed double-spaced on A4 (297×210 mm) white paper with outer margins of 2.5 cm. Number all pages consecutively, and start each of the following sections on a new page: Title Page , Abstract, Introduction, Materials and Methods, Results, Discussion, Acknowledgements, References, Tables, Figures and Figure Legends. Neither the Editors nor the Publisher is responsible for the opinions expressed by contributors. Manuscripts formally accepted for publication become the permanent property of The WJG Press and Elsevier Inc., and may not be reproduced by any means, in whole or in part without the written permission of both the Authors and the Publisher. We reserve the right to put onto our website and copy-edit accepted manuscripts. Authors should also follow the guidelines for the care and use of laboratory animals of their institution or national animal welfare committee.

Authors should retain one copy of the text, tables, photographs and illustrations, as rejected manuscripts will not be returned to the author(s) and the editors will not be responsible for the loss or damage to photographs and illustrations.

Online submission
Online submission is strongly advised. Manuscripts should be submitted through the Online Submission System at: http://www.wjgnet.com/index.jsp. Authors are highly recommended to consult the ONLINE INSTRUCTIONS TO AUTHORS (http://www.wjgnet.com/wjg/help/instructions.jsp) before attempting to submit online. Authors encountering problems with the Online Submission System may send an email describing the problem to wjg@wjgnet.com for assistance. If you submit manuscript online, do not make a postal contribution. A repeated online submission for the same manuscript is strictly prohibited.

Postal submission
Send 3 duplicate hard copies of the full-text manuscript typed double-spaced on A4(297×210 mm) white paper together with any original photographs or illustrations and a 3.5 inch computer diskette or CD-ROM containing an electronic copy of the manuscript including all the figures, graphs and tables in native Microsoft Word format or *.rtf format to:

World Journal of Gastroenterology
Room 1066, Yishou Garden,
No.58, North Langxinzhuang Road,
PO Box 2345, Beijing 100023, China
E-mail: wjg@wjgnet.com
http: //www.wjgnet.com

MANUSCRIPT PREPARATION

All contributions should be written in English. All articles must be submitted using a word-processing software. All submissions must be typed in 1.5 line spacing and in word size 12 with ample margins. The letter font is Tahoma. For authors originating from China, one copy of the Chinese translation of the manuscript is also required (excluding references). Style should conform to our house format. Required information for each of the manuscript sections is as follows:

Title page
Full manuscript title, running title, all author(s) name(s), affiliations, institution(s) and/or department(s) where the work was accomplished, disclosure of any financial support for the research, and the name, full address, telephone and fax numbers and email address of the corresponding author should be involved. Titles should be concise and informative (removing all unnecessary words), emphasize what is NEW, and avoid abbreviations. A short running title of less than 40 letters should be provided. List the author(s)' name(s) as follows: initials and/or first name, middle name or initial(s) and full family name.

Abstract
An informative, structured abstract of no more than 250 words should accompany each manuscript. Abstracts for original contributions should be structured into the following sections: AIM: Only the purpose should be included. METHODS: The materials, techniques, instruments and equipments, and the experimental procedures should be included. RESULTS: The observatory and experimental results, including data, effects, outcome, *etc*. should be included. Authors should present *P* value where necessary, and the significant data should accompany. CONCLUSION: Accurate view and the value of the results should be included.

The format of structured abstracts is at: http://www.wjgnet.com/wjg/help/11.doc

Key words
Please list 3-10 key words that could reflect content of the study.

Text
For most article types, the main text should be structured into the following sections: INTRODUCTION, MATERIALS AND METHODS, RESULTS and DISCUSSION, and should include appropriate Figures and Tables. Data should be presented in the body text or Figures and Tables, not both.

Illustrations
Figures should be numbered as 1, 2, 3 and so on, and mentioned clearly in the main text. Provide a brief title for each figure on a separate page. No detailed legend should be involved under the figures. This part should add into the text where the figures are applicable. Digital images: black and white photographs should be scanned and saved in TIFF format at a resolution of 300 dpi; color images should be saved as CMYK (print files) and not RGB (screen-viewing files). Place each photograph in a separate file. Print images: supply images of size no smaller than 126×76 mm printed on smooth surface paper; label the image by writing the Figure number and orientation using an arrow. Photomicrographs: indicate the original magnification and stain in the legend. Digital Drawings: supply files in EPS if created by Freehand and Illustrator, or TIFF from Photoshop. EPS files must be accompanied by a version in native file format for editing purposes. Scans of existing line drawings should be scanned at a resolution of 1200 dpi and as close as possible to the size at which they will appear when printed, not smaller. Please use uniform legends for the same subjects. For example: Figure 1 Pathological changes of atrophic gastritis after treatment. A: ...; B: ...;C: ...; D: ...; E: ...; F: ...; G: ...

Tables
Three-line tables should be numbered as 1, 2, 3 and so on, and mentioned clearly in the main text. Provide a brief title for each table. No detailed legend should be involved under the tables. This part should add into the text where the tables are applicable. The information should complement but not duplicate that contained in the text. Use one horizontal line under the title, a second under the column heads, and a third below the Table, above any footnotes. Vertical and italic lines should be omitted.

Notes in tables and illustrations
Data which is not statistically significant should not be noted. $^{a}P<0.05$, $^{b}P<0.01$ ($P>0.05$ should not be noted). If there are other series of *P* values, $^{c}P<0.05$ and $^{d}P<0.01$ are used; Third series of *P* values can be expressed as $^{e}P<0.05$ and $^{f}P<0.01$. Other notes in tables or under

illustrations should be expressed as ^1F, ^2F, ^3F; or some other symbols with a superscript (Arabic numerals) in the upper left corner. In a multi-curve illustration, each curve should be labeled with ●, ○, ■, □, ▲, △, *etc*. in a certain sequence.

Acknowledgments

Brief acknowledgments of persons who have made genuine contributions to the manuscripts and who endorse the data and conclusions are included. Authors are responsible for obtaining written permission to use any copyrighted text and/or illustrations.

References

Cited references should mainly be drawn from journals covered in the Science Citation Index (http://www.isinet.com) and/or Index Medicus (http://www.ncbi.nlm.nih.gov/PubMed) databases. Mention all references in the text, tables and figure legends, and set off by consecutive, superscripted Arabic numerals. References should be numbered consecutively in the order in which they appear in the text. Abbreviate journal title names according to the Index Medicus style (http://www.ncbi.nlm.nih.gov/entrez/query.fcgi?db=journals). Unpublished observations and personal communications are not listed as references. The style and punctuation of the references conform to ISO standard and the Vancouver style (5th edition); see examples below. Reference lists not conforming to this style could lead to delayed or even rejected publication status. Examples:

Standard jounal article (list all authors and include the PubMed ID [PMID] where applicable)

1 **Das KM,** Farag SA. Current medical therapy of inflammatory bowel disease. *World J Gastroenterol* 2000; 6: 483-489 [PMID: 11819634]

2 **Pan BR**, Hodgson HJF, Kalsi J. Hyperglobulinemia in chronic liver disease: Relationships between *in vitro* immunoglobulin synthesis, short lived suppressor cell activity and serum immunoglobulin levels. *Clin Exp Immunol* 1984; 55: 546-551 [PMID: 6231144]

3 **Lin GZ,** Wang XZ, Wang P, Lin J, Yang FD. Immunologic effect of Jianpi Yishen decoction in treatment of Pixu-diarrhoea. *Shijie Huaren Xiaohua Zazhi* 1999; 7: 285-287 [CMFAID:1082371101835979]

Books and other monographs (list all authors)

4 **Sherlock S,** Dooley J. Diseases of the liver and billiary system. 9th ed. Oxford: Blackwell Sci Pub, 1993: 258-296

Chapter in a book (list all authors)

5 **Lam SK.** Academic investigator's perspectives of medical treatment for peptic ulcer. In: Swabb EA, Azabo S. Ulcer disease: investigation and basis for therapy. New York: Marcel Dekker, 1991: 431-450

Electronic journal (list all authors)

6 **Morse SS.** Factors in the emergence of infectious diseases. Emerg Infect Dis serial online, 1995-01-03, cited 1996-06-05; 1(1):24 screens. Available from: URL: http//www.cdc.gov/ncidod/EID/eid.htm

PMID requirement

From the full reference list, please submit a separate list of those references embodied in PubMed, keeping the same order as in the full reference list, with the following information only: (1) abbreviated journal name and citation (e.g. *World J Gastroenterol* 2003;9(11): 2400-2403; (2) article title (e.g. Epidemiology of gastroenterologic cancer in Henan Province, China; (3) full author list (e.g. Lu JB, Sun XB, Dai DX, Zhu SK, Chang QL, Liu SZ, Duan WJ; (4) PMID (e.g. 14606064). Provide the full abstracts of these references, as quoted from PubMed on a 3.5 inch disk or CD-ROM in Microsoft Word format and send by post to the *WJG* Press. For those references taken from journals not indexed by *Index Medicus*, a printed copy of the first page of the full reference should be submitted. Attach these references to the end of the manuscript in their order of appearance in the text.

Inappropriate references

Authors should always cite references that are relevant to their article, and avoid any inappropriate references. Inappropriate references include those that are linked with a hyphen and the difference between the two numbers at two sides of the hyphen is more than 5. For example, [1-6], [2-14] and [1,3,4-10,22] are all considered as inappropriate references. Authors should not cite their own unrelated published articles.

Statistical data

Present as mean±SD and mean±SE.

Statistical expression

Express *t* test as *t*(in italics), *F* test as *F*(in italics), chi square test as χ^2 (in Greek), related coefficient as *r*(in italics), degree of freedom as γ(in Greek), sample number as *n*(in italics), and probability as *P*(in italics).

Units

Use SI units. For example: body mass, m(B) = 78 kg; blood pressure, p (B)=16.2/12.3 kPa; incubation time, t(incubation)=96 h, blood glucose concentration, c(glucose) 6.4±2.1 mmol/L; blood CEA mass concentration, p(CEA) = 8.6 24.5 μg/L; CO_2 volume fraction, 50 mL/L CO_2 not 5% CO_2; likewise for 40 g/L formaldehyde, not 10% formalin; and mass fraction, 8 ng/g, *etc*. Arabic numerals such as 23,243,641 should be read 23 243 641.

The format about how to accurately write common units and quantum is at: http://www.wjgnet.com/wjg/help/15.doc

Abbreviations

Standard abbreviations should be defined in the abstract and on first mention in the text. In general, terms should not be abbreviated unless they are used repeatedly and the abbreviation is helpful to the reader. Permissible abbreviations are listed in Units, Symbols and Abbreviations: A Guide for Biological and Medical Editors and Authors (Ed. Baron DN, 1988) published by The Royal Society of Medicine, London. Certain commonly used abbreviations, such as DNA, RNA, HIV, LD50, PCR, HBV, ECG, WBC, RBC, CT, ESR, CSF, IgG, ELISA, PBS, ATP, EDTA, mAb, can be used directly without further mention.

Italicization

Quantities: *t* time or temperature, *c* concentration, *A* area, *l* length, *m* mass, *V* volume.
Genotypes: *gyr*A, *arg* 1, *c myc*, *c fos*, *etc*.
Restriction enzymes: *Eco*RI, *Hin*dI, *Bam*HI, *Kbo* I, *Kpn* I, *etc*.
Biology: *Helicobacter pylori, H pylori, E coli, etc*.

SUBMISSION OF THE REVISED MANUSCRIPTS AFTER ACCEPTED

Please revise your article according to the revision policies of *WJG*. The revised version including manuscript and high-resolution image figures (if any) should be copied on a floppy or compact disk. Author should send the revised manuscript, along with printed high-resolution color or black and white photos, copyright transfer letter, the final check list for authors, and responses to reviewers by a courier (such as EMS) (submission of revised manuscript by e-mail or on the WJG Editorial Office Online System is NOT available at present).

Language evaluation

The language of a manuscript will be graded before sending for revision. (1) Grade A: priority publishing; (2) Grade B: minor language polishing; (3) Grade C: a great deal of language polishing; (4) Grade D: rejected. The revised articles should be in grade B or grade A.

Copyright assignment form

It is the policy of WJG to acquire copyright in all contributions. Papers accepted for publication become the copyright of WJG and authors will be asked to sign a transfer of copyright form. All authors must read and agree to the conditions outlined in the Copyright Assignment Form (which can be downloaded from http://www.wjgnet.com/wjg/help/9.doc).

Final check list for authors

The format is at: http://www.wjgnet.com/wjg/help/13.doc

Responses to reviewers

Please revise your article according to the comments/suggestions of reviewers. The format for responses to the reviewers' comments is at: http://www.wjgnet.com/wjg/help/10.doc

Proof of financial support

For paper supported by a foundation, authors should provide a copy of the document and serial number of the foundation.

Publication fee

Authors of accepted articles must pay publication fee.

PO Box 2345, Beijing 100023, China
www.wjgnet.com
wjg@wjgnet.com

ELSEVIER

World J Gastroenterol 2005;11(8):Appendix 4
World Journal of Gastroenterology ISSN 1007-9327

World Journal of Gastroenterology standard of quantities and units

Number	Nonstandard	Standard	Notice
1	4 days	4 d	In figures, tables and numerical narration
2	4 days	four days	In text narration
3	day	d	After Arabic numerals
4	Four d	Four days	At the beginning of a sentence
5	2 hours	2 h	After Arabic numerals
6	2 hs	2 h	After Arabic numerals
7	hr, hrs,	h	After Arabic numerals
8	10 seconds	10 s	After Arabic numerals
9	10 year	10 years	In text narration
10	Ten yr	Ten years	At the beginning of a sentence
11	0,1,2 years	0,1,2 yr	In figures and tables
12	0,1,2 year	0,1,2 yr	In figures and tables
13	4 weeks	4 wk	
14	Four wk	Four weeks	At the beginning of a sentence
15	2 months	2 mo	In figures and tables
16	Two mo	Two months	At the beginning of a sentence
17	10 minutes	10 min	
18	Ten min	Ten minutes	At the beginning of a sentence
19	50% (*V/V*)	500 mL/L	
20	50% (m/*V*)	500 g/L	
21	1 M	1 mol/L	
22	10 μM	10 μmol/L	
23	1N HCl	1 mol/L HCl	
24	1N H_2SO_4	0.5 mol/L H_2SO_4	
25	4rd edition	4th edition	
26	15 year experience	15- year experience	
27	18.5 kDa	18.5 ku,18 500u or M_r18 500	
28	25 g.kg^{-1}/d^{-1}	25 g/(kg·d) or 25 g/kg per day	
29	6900	6 900	
30	1000 rpm	1 000 r/min	
31	sec	s	After Arabic numerals
32	1 pg·L^{-1}	1 pg/L	
33	10 kilograms	10 kg	
34	13 000 rpm	13 000 *g*	High speed; *g* should be in italic and suitable conversion.
35	1000 *g*	1 000 r/min	Low speed. *g* cannot be used.
36	Gene bank	GenBank	International classified genetic materials collection bank
37	Ten L	Ten liters	At the beginning of a sentence
38	Ten mL	Ten milliliters	At the beginning of a sentence
39	umol	μmol	
40	30 sec	30 s	
41	1 g/dl	10 g/L	10-fold conversion
42	OD_{260}	A_{260}	"OD" has been abandoned.
43	One g/L	One microgram per liter	At the beginning of a sentence
44	*A*260 nm	$A_{260\,nm}$	*A* should be in italic.
	^{b}P<0.05	^{a}P<0.05	In Table, no note is needed if there is no significance in statistics: ^{a}P<0.05, ^{b}P<0.01 (no note if P>0.05). If there is a second set of P value in the same table, ^{c}P<0.05 and ^{d}P<0.01 are used for a third set: ^{e}P<0.05, ^{f}P<0.01.
45	**F*=9.87, §*F*=25.9, #*F*=67.4	^{1}F=9.87,^{2}F=25.9, ^{3}F=67.4	Notices in or under a table
46	KM	km	kilometer
47	CM	cm	centimeter
48	MM	mm	millimeter
49	Kg, KG	kg	kilogram
50	Gm, gr	g	gram
51	nt	N	newton
52	l	L	liter
53	db	dB	decibel
54	rpm	r/min	rotation per minute
55	bq	Bq	becquerel, a unit symbol
56	amp	A	ampere
57	coul	C	coulomb
57	HZ	Hz	
59	w	W	watt
60	KPa	kPa	kilo-pascal
61	p	Pa	pascal
62	ev	EV	volt (electronic unit)
63	Jonle	J	joule
64	J/mmol	kJ/mol	kilojoule per mole
65	10×10×10cm^3	10 cm×10 cm×10 cm	
66	N·km	KN·m	moment
67	$\bar{x}$±s	mean±SD	In figures, tables or text narration
68	Mean±SEM	mean±SE	In figures, tables or text narration
69	*im*	im	intramuscular injection
70	*iv* iv	intravenous	injection
71	Wang et al	Wang *et al*	
72	EcoRI	*Eco*RI	*Eco* in italic and RI in positive. Restriction endonuclease has its prescript form of writing.
73	Ecoli	*E.coli*	Bacteria and other biologic terms have their specific expression.
74	Hp	*H pylori*	
75	Iga	*Iga*	writing form of genes
76	*igA*	IgA	writing form of proteins
77	-70 kDa	~70 ku	